DEVELOPMENTS IN PETROLEUM SCIENCE 40 A
ADVISORY EDITOR: G.V. CHILINGARIAN

asphalthenes and asphalts, 1

T.F. YEN and G.V. CHILINGARIAN
(editors)

ELSEVIER

Developments in Petroleum Science, 40 A

asphalthenes and asphalts, 1

DEVELOPMENTS IN PETROLEUM SCIENCE

Advisory Editor: G.V. Chilingarian

Volumes 1, 3, 4, 7 and 13 are out of print

2. W.H. FERTL – Abnormal Formation Pressures
5. T.F. YEN and G.V. CHILINGARIAN (Editors) – Oil Shale
6. D.W. PEACEMAN – Fundamentals of Numerical Reservoir Simulation
8. L.P. Dake – Fundamentals of Reservoir Engineering
9. K. MAGARA – Compaction and Fluid Migration
10. M.T. SILVIA and E.A. ROBINSON – Deconvolution of Geophysical Time Series in the Exploration for Oil and Natural Gas
11. G.V. CHILINGARIAN and P. VORABUTR – Drilling and Drilling Fluids
12. T.D. VAN GOLF-RACHT – Fundamentals of Fractured Reservoir Engeneering
14. G. MÓZES (Editor) – Paraffin Products
15A. O. SERRA – Fundamentals of Well-log Interpretation, 1. The acquisition of logging data
15B. O. SERRA – Fundamentals of Well-log Interpretation, 1. The interpretation of logging data
16. R.E. CHAPMAN – Petroleum Geology
17A. E.C. DONALDSON, G.V. CHILINGARIAN and T.F. Yen (Editors) – Enhanced Oil Recovery, I. Fundamentals and analyses
17B. E.C. DONALDSON, G.V. CHILINGARIAN and T.F. Yen (Editors) – Enhanced Oil Recovery, II. Processes and operations
18A. A.P. SZILAS – Production and Transport of Oil and Gas, A. Flow mechanics and production (second completely revised edition)
18B. A.P. SZILAS – Production and Transport of Oil and Gas, B. Gathering and Transport (second completely revised edition)
19A. G.V. CHILINGARIAN, J.O. ROBERTSON Jr. and S. KUMAR – Surface Operations in Petroleum Production, I
19B. G.V. CHILINGARIAN, J.O. ROBERTSON Jr. and S. KUMAR – Surface Operations in Petroleum Production, II
20. A.J. DIKKERS – Geology in Petroleum Production
21. F. RAMIREZ – Application of Optimal Control Theory to Enhanced Oil Recovery
22. E.C. DONALDSON, G.V. CHILINGARIAN and T.F. Yen – Microbial Enhanced Oil Recovery
23. J. HAGOORT – Fundamentals of Gas Reservoir Engineering
24. W. LITTMANN – Polymer Flooding
25. N.K. BAIBAKOV and A.R. GARUSHEV – Thermal Methods of Petroleum Production
26. D. MADER – Hydraulic Proppant Farcturing and Gravel Packing
27. G. DA PRAT – Well Test Analysis for Naturally Fractured Reservoirs
28. E.B. NELSON (Editor) – Well Cementing
29. R.W. ZIMMERMAN – Compressibility of Sandstones
30. G.V. CHILINGARIAN, S.J. MAZZULLO and H.H. RIEKE – Carbonate Reservoir Characterization: A Geologic-Engineering Analysis, Part I
31. E.C. DONALDSON (Editor) – Microbial Enhancement of Oil Recovery - Recent Advances
32. E. BOBOK – Fluid Mechanics for Petroleum Engineers
33. E. FJÆR, R.M. HOLT, P. HORSRUD, A.M. RAAEN and R. RISNES – Petroleum Related Rock Mechanics
34. M.J. ECONOMIDES – A Practical Companion to Reservoir Stimulation
35. J.M. VERWEIJ – Hydrocarbon Migration Systems Analysis
36. L. DAKE – The Practice of Reservoir Engineering
37. W.H. SOMERTON – Thermal Properties and Temperature related Behavior of Rock/fluid Systems
38. W.H. FERTL, R.E. CHAPMAN and R.F. HOTZ (Editors) – Studies in Abnormal Pressures
39. E. PREMUZIC and A. WOODHEAD (Editors) – Microbial Enhancement of Oil Recovery - Recent Advances – Proceedings of the 1992 International Conference on Microbial Enhanced Oil Recovery

Developments in Petroleum Science, 40 A

asphaltenes and asphalts, 1

Edited by

T.F. YEN
School of Engineering, Program of Environmental Engineering,
University of Southern California, Los Angeles, California, USA

and

G.V. CHILINGARIAN
School of Engineering, University of Southern California, Los Angeles, California, USA

ELSEVIER SCIENCE
Amsterdam — Lausanne — New York — Oxford — Shannon — Tokyo 1994

ELSEVIER SCIENCE B.V.
Sara Burgerhartstraat 25
P.O. Box 211, 1000 AE Amsterdam, The Netherlands

Library of Congress Cataloging-in-Publication Data

Asphaltenes and asphalts / edited by T.F. Yen and G.V. Chilingarian.
p. cm. -- (Developments in petroleum science ; 40)
Includes bibliographical references and indexes.
ISBN 0-444-88291-X (v. 1 : acid-free)
1. Asphaltene. 2. Asphalt. I. Yen, Teh Fu, 1927-
II. Chilingarian, George V., 1929- . III. Series.
TP692.4.A8A74 1994
665.5'388--dc20 94-3116
CIP

ISBN: 0-444-88291-X

This book is printed on acid-free paper.

Printed in The Netherlands

DEDICATED TO OUR FATHERS

Rev. Guang Pu Yen, B.D.
Tungchan, Yunnan, China (1893–1989)

Dr. Varos Chilingarian, M.D.
Batum, Georgia (1896–1993)

for their contributions to humanity

This page intentionally left blank

PREFACE

This volume is dealing directly with the science and technology of a very important topic — asphaltenes. Asphaltene is invariably present in asphalt or bitumen and other fossil fuel-derived liquids such as coal tar, coal liquefaction products, pyrolyzed shale oil from oil shales, source rock extracts, and numerous naturally occurring bituminous substances. The latter include asphaltites, asphaltoids, waxes, and carbonaceous deposits having composition between that of petroleum and coal. In the United States the term asphalt is used, which is equivalent to bitumen, a term adopted in Europe: thus, in this volume both terms are used interchangeably.

The editors have invited a group of internationally known scientists and engineers, who have devoted a great portion of their life career to this specialty, to contribute to this volume. Inasmuch as this field often requires more than one discipline to yield only a meagre information, the chapters cover a variety of subjects. This book will conveniently serve as a learning guide for beginners as well as a reference book for experts.

At this time, the entire picture of the asphaltenes is still not completely understood. Some experts only see part of the "elephant", when he or she "touches" the "animal". This book offers a glimpse of the entire "body of elephant" or the entire field of asphaltenes. The objective of this book is also to link the asphaltenes and asphalts in a broad sense, often ignored by the paving technologists.

The editors would like to express their gratitude to all contributors for their patience to make this book a reality. In some cases, it required more than four years. In the mean time, one of the contributors, Dr. M.A. Bestougeff of France, deceased. The editors would like to convey their deep sympathy to his friends and associates, who lost a very energetic and capable worker in the asphaltene field. Elsevier Science and Dr. Herman Frank also must be commended for promoting international good will in the technical horizons of the coming century. The help extended by Jacques Kiebert and Dawood Momeni was indeed invaluable.

TEH FU YEN and GEORGE V. CHILINGARIAN

This page intentionally left blank

LIST OF CONTRIBUTORS

M.A. BESTOUGEFF	*12 rue Jean Thoman, 95600 Eaubonne, France (deceased)*
B. BRÛLÉ	*Jean Lefebvre, 11 Bd. Jean Mermoz, 92202 Neuilly sur Seine Cedex, France*
L.A. BURYAKOVSKIY	*Institute of Deep Oil and Gas Deposits, Azerbaijan Academy of Sciences, Baku, 370143 Azerbaijan*
R. BYRAMJEE	*Chemin Creux, 84200 Carpentras, France (formerly: Total – Compagnie Française des Pétrole)*
G.V. CHILINGARIAN	*Department of Civil Engineering, University of Southern California, Los Angeles, CA 90089-1211, USA*
R.D. DJEVANSHIR	*Institute of Deep Oil and Gas Deposits, Azerbaijan Academy of Sciences, Baku, 370143 Azerbaijan*
E.K. ENSLEY	*Western Research Institute, P.O. Box 3395, Laramie, WY 82071-3395, USA*
J. ESCOBEDA	*Department of Chemical Engineering, University of Illinois, Box 4348, Chicago, IL 60680, USA*
C. GIAVARINI	*Dipartimento di Ingegneria Chimica, dei Materiali delle Materie Prime e Metallurgia, Università degli Studi di Roma "La Sapienza", Via Eudossiana, 18-00184 Rome, Italy*
G. GONZÁLEZ	*Petrobrás Research Center, Cidade Universitária, Q. 7, Ilha do Fundão, CEP 21949-900, Rio de Janeiro, RJ, Brazil*
M.R. ISLAM	*Department of Geology and Geological Engineering, South Dakota School of Mines and Technology, Rapid City, SD 57701-3995, USA*
L.J. LIU	*Daqing Petroleum Institute, Petrochemical Engineering Department, Anda, Helongjiang 151400, People's Republic of China*
G.A. MANSOORI	*Department of Chemical Engineering, University of Illinois, Box 4348, Chicago, IL 60680, USA*
M.B.C. MOREIRA	*Petrobrás Research Center, Cidade Universitária, Q. 7, Ilha do Fundão, CEP 21949-900, Rio de Janeiro, RJ, Brazil*
S.J. PARK	*Department of Chemical Engineering, University of Illinois, Box 4348, Chicago, IL 60680, USA*
G. RAYMOND	*Laboratoire Central des Ponts et Chaussées, 58, Bd. Lefebvre, 75015 Paris, France*
V.S. RAVI-KUMAR	*Department of Chemical Engineering, University of Southern California, Los Angeles, CA 90089-1211, USA*
J.G. REYNOLDS	*Lawrence Livermore National Laboratory, University of California, L-365, P.O. Box 808, Livermore, CA 94551, USA*

R.C. SANE	*Jacobs Engineering Group Inc., 251 South Lake Avenue, Pasadena, CA 91101, USA*
M.M. SHARMA	*Department of Petroleum Engineering, University of Texas, Austin, TX 78712, USA*
E.Y. SHEU	*Texaco Research and Development Inc., P.O. Box 509, Beacon, NY 12508, USA*
J.G. SPEIGHT	*Western Research Institute, P.O. Box 3395, Laramie, WY 82071-3395, USA*
D.A. STORM	*Texaco Research and Development Inc., P.O. Box 509, Beacon, NY 12508, USA*
C. SUCH	*Laboratoire Central des Ponts et Chaussées, 58, Bd. Lefebvre, 75015 Paris, France*
T.T. TSOTSIS	*Department of Chemical Engineering, University of Southern California, Los Angeles, CA 90089-1211, USA*
I.A. WEBSTER	*Unocal Corporation, 1201 West 5th Street, P.O. Box 7600, Los Angeles, CA 90051, USA*
E.V. WHITEHEAD	*3, Howard Close, Hampton, Middlesex TW12 2UB, UK*
T.F. YEN	*Program of Environmental Engineering, University of Southern California, Los Angeles, CA 90089-2531, USA*
R.J. ZOU	*Hebei Academy of Science, Shijiazhuang, People's Republic of China (deceased)*

CONTENTS

Asphaltenes and Asphalts, 1. Developments in Petroleum Science, 40
edited by T.F. Yen and G.V. Chilingarian

Chapter 1

INTRODUCTION

T.F. YEN and G.V. CHILINGARIAN

INTRODUCTORY REMARKS

Asphaltene is an essential constituent of asphalt and the two substances are closely related. Inasmuch as the structure of asphaltenes is complex and not precisely understood, their thorough investigation is commonly avoided. Furthermore, research in the field of asphaltenes is not monetarily rewarding, as a consequence of which very little basic research was being done as pointed out by M.A. Bestougeff, author of Chapter 3. According to him, asphaltene science is not deemed a worthwhile endeavor, with asphaltene being considered an "ignorable" substance by the scientific community [1].

Due to their complex nature, a multidisciplinary approach is necessary to ascertain the precise nature of asphaltenes. Organic chemistry alone is not sufficient; physics, mathematics, and engineering are also necessary in studying asphaltenes. Researchers, however, normally employ only one approach.

Further compounding the above difficulties is the fact that researchers often use the wrong substance for their study, despite the superb quality of their equipment and impeccability of their methodology. Asphaltenes are generally known as substances insoluble in *n*-pentane or *n*-hexane, or soluble in benzene or toluene. This definition encompasses numerous materials that are not characterized very well, and often are contaminated.

The validity or the early asphaltene model proposed by Yen [2,3] has been questioned by some investigators. They do not realize that this model is applicable to the native petroleum asphaltene and not to the refinery or coal-derived ones. They also claim that asphaltenes are not peri-condensed. Different asphaltenes have different aromatic structures that are not identical. It is true that refinery asphaltenes are kata-condensed, coal-derived ones have very small aromatic cluster, and asphaltenes derived from biodegradable oil often contain only linked aromatic system [4,5]. A researcher should report accurately on the structure of his or her asphaltene sample, which could be readily weathered, or have a different source material. They should not criticize the generalized structure of native asphaltene from crude oil at the wellhead, which is the original Yen's model.

Research findings must be validated by different experimental methods. A model should not be proposed without experimental corroboration using a multiplicity of techniques, both chemical and physical. A model is only a working tool for any given investigation, so that improvements can be implemented in future investigations.

BITUMENS

Great confusion exits in the literature on the definition of the term *bitumen*. It occurs in the earth's crust in various forms: (1) dispersed state, in trace quantities; and (2) accumulations, where bitumen either impregnates the rock or occurs in a pure or nearly pure form (see Eremenko [6]).

In the first half of the 20th century, the term bitumen continued to be applied to the crude oil and its natural derivatives (maltha, asphalt, ozokerite, etc.). In this original meaning, bitumens are called naphthides. The term bitumen is also used for asphalts and asphalt-like manufactured substances utilized in road construction, including products from the processing of coals and/or oil shales.

The term bitumen also denotes substances that can be extracted from coals (lignites and hard coals). In addition, it is used as a general term for organic matter (OM) in sediments and rocks. The soluble part of dispersed organic matter (DOM) is referred to in Russia as *bitumoid* (bitumen-like substance).

The term bitumoid is applied in Russia, for example, to the organic matter (OM) that can be extracted from the sediments or rocks by the relatively mild organic solvents that do not produce any significant breakdown of the OM [6].

There are great differences in the content (yield) of bitumoid when different solvents are used. For example, the yield of chloroform extract on the average is lower by a factor of 2.6 than the yield of bitumoid extracted with a mixture of benzene (70%), acetone (15%), and ethanol (15%).

In studying bitumoids, the C, H, S, and N contents are determined with oxygen content usually being determined by difference. To determine the group composition of bitumoids, the following three fractions are commonly segregated: oils, resins, and asphaltenes.

In nature, bitumoids are formed mainly at the expense of panlipoidins during various stages of lithogenesis. During sedimentogenesis the primary sources of bitumoids are the lipid and lipoid components of living matter — fats, fatty acids, waxes, resins, and isoprenoid compounds.

Diagenetic [7] bitumoids are mainly biogenic and are free or almost free of the light hydrocarbons that are characteristic for the naphtha and kerosene fractions of crude oil. The writers have discussed bitumen in detail in previous books [8,9] and publications [10]. They considered bitumen as the carbon disulfide-soluble portion of bituminous substances; the insoluble portion consists of kerogen and pyrobitumen. In Europe, both asphaltic bitumen and bitumen terms are often used, whereas in America, asphalt is commonly used. In the literature, asphalt and bitumen are often used interchangeably.

RESINS AND ASPHALTENES

The sapropelic OM has the greatest capacity to form bitumoids, whereas the humic OM has the lowest capacity. In crude oils, in distillate cuts beginning with kerosene, and in distillation residues, there is a group of high-molecular-weight heteroorganic compounds that are lumped under the name of resins and asphaltenes

besides gas oil. Their content may be as large as 40% in heavy, high-resin (asphaltic) crudes. Carbon and hydrogen constitute 80–95% of the resin and asphaltene molecules, with oxygen always present. Sulfur, nitrogen and metals are also usually present.

The content of resins in crude oils (2–40%) exceeds by far (approximately 3 to 40 times) the content of asphaltenes (trace to 6%; usually <1%). Carboids and carbenes, which resemble asphaltenes, differ from them by having higher oxygen content. They, however, are absent in crude oils and distillate cuts. In small quantities, they are found in residues from vacuum distillation, in cracked tars, and in native and petroleum asphalts. Resins are semiliquid (sometimes almost solid) dark brown to black substances, have specific gravity around 1 and molecular weight of 500 to 2000 (usually 600–1000). Asphaltenes, on the other hand, are dark, amorphous powders, have specific gravity greater than 1 and molecular weights of 1000 to 10,000 (average = 5000).

A decisive role in determining the constitution of resins and asphaltenes is played by the condensed cyclic structural systems. A number of reviews have been published previously in this regard [11,12,13].

Resins are classified as acidic and neutral, the former consisting of asphaltogenic (polynaphthenic) acids and their anhydrides.

As pointed out by Eremenko [6], the methods of recovery, separation, and classification of resins and asphaltenes are based on differences in solubility of the components in various solvents: (1) carboids — insoluble in carbon disulfide, (2) carbenes — soluble in carbonic disulfide but insoluble in carbon tetrachloride; (3) asphaltenes — soluble in carbon disulfide and carbon tetrachloride, but insoluble in the low-boiling saturated hydrocarbons, such as petroleum ether; and (4) malthenes — soluble in low-boiling saturated hydrocarbons (malthenes include resins and oils). One classification scheme on the basis of solubility parameters is presented in Table 1-1 [14].

A conceptual structural model of asphaltenes is presented in Chapter 15. This model is based on prior literature data and the results of experimental studies on the diffusion of asphaltenes through model porous systems. During diffusion experiments, the writers were able to determine the distribution of various heteroatoms within the different molecular weight/size ranges of the asphaltene species. Asphaltenes are viewed as a "complex colloidal mixture in a state of dynamic interexchange."

In Chapter 11, M. Rafiq Islam presented a critical review of many field and laboratory observations of asphaltene problems. He reviewed mathematical models and physicochemical descriptions of asphaltenes and asphaltic crude oils. Besides being inaccurate except for a small range of variables, most models rely on the experimentally-determined parameters or adjustable coefficients. Owing to the complexity and inexactness of asphaltene properties, such a problem can be expected.

Asphaltene precipitation or the presence of asphaltenes may have many implications in the recovery of crude oils. Asphaltene precipitation may occur on application of various thermal and other enhanced oil recovery techniques or even at primary production conditions.

TABLE 1-1

Classification of asphalts based on solubility in solvents and solubility parameter [a] (after Yen [14]).

Fraction		Solubility	Solubility parameter δ in Hildebrands [b]	Remarks
number	designation			
1	gas oil	propane soluble	<6	saturated and aromatic hydrocarbons
2	resin	propane insoluble pentane soluble	6–7	combined 1 and 2 are also called maltene or petrolene
3	asphaltene	pentane insoluble benzene soluble	7–9	ASTM uses CCl_4 instead of benzene
4	carbene	benzene insoluble CS_2 soluble [c]	9–10	ASTM uses CCl_4 instead of benzene
5	carboid	CS_2 insoluble [c] pyridine soluble	10–11	combined 4 and 5 are referred to as preasphaltene or asphatol
6	mesophase	pyridine insoluble	>11	

[a] Volatile-free basis.
[b] 1 Hildebrand = 2.04 $J^{1/2}/cm^{3/2}$ = 1 $cal^{1/2}/cm^{3/2}$.
[c] Because of the flammability of CS_2, pyridine is preferred; fractions 4 and 5 can be combined.

The mere presence of asphaltenes in solution may have major effects on rheology of crude oils. In many cases, the presence and precipitation of asphaltene lead to near-wellbore plugging and many other production problems. Asphaltenes, however, may have some beneficial effects in oil production owing to the formation of microbubbles with asphaltenes acting as nucleation sites. In addition, the asphaltenes alter the rock wettability and, thus increase the relative permeability to oil, which leads to improved oil recovery.

Many questions of asphaltene properties under primary and thermal recovery conditions in the reservoirs remain unanswered. Owing to the complex nature of asphaltene, much more research work is necessary to identify all governing factors which influence the asphaltene precipitation and its impact on crude oil rheology. The existing models have not been able to accurately predict the asphaltene precipitation.

G.A. Mansoori et al. (Chapter 8) also pointed out that deposition of complex and heavy organic compounds, which exist in petroleum fluids, can cause a number of severe problems. To prevent deposition inside the reservoir, at the wellhead, and inside the transmission lines, it is necessary to be able to predict the onset and amount of deposition owing to various factors. In Chapter 8, the mechanisms of asphaltene deposition are modeled on the basis of different theories. The continuous thermodynamic (CT) model and the steric colloidal (SC) model, and their predictive capabilities are discussed. The chromatographic characterization of asphaltene deposits from different crude oils is also presented. Utilization of kinetic theory of aggregation enables one to develop a fractal aggregation (FA) model, which combines the ideas of the two proposed CT and SC models. The FA model is capable of

describing several situations, such as the phenomenon of organic deposition, growing mechanism of heavy organic aggregates, the geometric aspects of aggregates, the size distribution of precipitated organic materials, and the solubility of heavy organic material in petroleum fluids under the influence of miscible solvents.

The adsorption of asphaltenes and resins extracted from filtered and recovered shale oil on various minerals and the effect of this process on the properties of the mineral-aqueous solution interface was investigated by Casper Gonzalez and M.B.C. Moreira (Chapter 9). For all the minerals studied, the adsorption of asphaltenes was greater than the adsorption of resins, presenting a plateau in the case of recovered shale oil. There was evidence of surface saturation in the case of filtered shale oil.

For neutral or intermediate pH, the electrophoretic mobility of the mineral particles was not affected to a great extent by the presence of absorbed resins or asphaltenes below pH 3 or above pH 12. Relatively important changes were observed, however, in the pH range of 3 to 12, indicating the presence of very weak basic and acidic groups in the asphaltene molecules.

The adsorption produced important changes in the wettability of the mineral particles. The equilibrium contact angle for silica, quartz and clays was above 90° when asphaltenes were the absorbed species. In the experience of the editors, resins and asphaltenes appear to render rock more oil-wet.

In Chapter 10, J.G. Reynolds examines the effects that the asphaltene precipitation has on the size of vanadium-, nickel- and sulfur-containing compounds in heavy crude oils and residue through size exclusion chromatographic data, and discusses the effects in terms of characterization and processing. In some cases, the metal-containing compounds appear to partially agglomerate upon precipitation, rendering compounds of sizes larger than those detected in the whole feed. For the sulfur-containing compounds, this agglomeration upon the precipitation does not appear. The precipitation appears to adequately separate the largest of the sulfur-containing compounds from the whole feed.

The interrelationship of asphaltene and asphalt has been emphasized in the last three chapters of the book. Without a thorough understanding of the asphaltene behavior, it is hard to properly evaluate asphalt either for paving or other uses.

CONCLUDING REMARKS

The writers feel that basic research in the field of asphaltenes is inadequately funded. Investigators, who are concerned with the practical aspects of asphalt, have more status than those who are concerned with its theoretical aspects. The former need to open their minds to advances in the latter field. It is regretful that the most recent findings are targeted toward establishing specifications with inadequate attention allotted to the basic research [15]. Finally, the writers recommend the creation of an international repository of asphaltene samples.

REFERENCES

[1] Bestougeff, M.A., Justice for asphaltenes, *L'actualite Chim.*, Sept., pp. 7–9 (1981).
[2] Yen, T.F., Present status of the structure of petroleum heavy ends and its significance to various technical applications, *Am. Chem. Soc., Div. Petrol. Chem. Preprints*, 17(1): 102–104 (1972).
[3] Yen, T.F., Structure of petroleum asphaltene and its significance, *Energy Sources*, 1(4): 447–463 (1974).
[4] Yen, T.F., *The Role of Trace Metals in Petroleum*. Ann Arbor Science Publishers, Ann Arbor, Mich, 221 pp. (1975)
[5] Yen, T.F., The role of asphaltenes in heavy crude and tar sands. In: R.F. Meyer and C.T. Steele (Editors), *The Future of Heavy Crude and Tar Sands*. McGraw-Hill, New York, N.Y., pp. 174–179 (1980).
[6] Eremenko, N.A., *Petroleum Geology Handbook*. OSI Publ., Los Angeles, Calif., 600 pp. (1990).
[7] Larsen, G. and Chilingar, G.V. (Editors), *Diagenesis in Sediments and Sedimentary Rocks, Developments in Sedimentology, 25A*. Elsevier, Amsterdam, 579 pp. (1979).
[8] Chilingarian, G.V. and Yen, T.F. (Editors), *Bitumens, Asphalts and Tar Sands*. Elsevier, Amsterdam, 331 pp. (1978).
[9] Yen, T.F. and Chilingarian, G.V. (Editors), *Oil Shale. Developments in Petroleum Science 5*. Elsevier, Amsterdam, 292 pp. (1976).
[10] Wen, C.S., Chilingarian, G.V. and Yen T.F., Properties and structures of bitumens. In: T.F. Yen and G.V. Chilingarian (Editors), *Bitumens, Asphalts and Tar Sands. Developments in Petroleum Science 5*. Elsevier, Amsterdam, pp. 155–190 (1978).
[11] Bunger, J.W. and Li, N.C., *Chemistry of Asphaltenes. Advances in Chemistry Series 195*. American Chemical Society, Washington, D.C., 260 pp. (1981).
[12] Tissot, B., *Characterization of Heavy Crude Oils and Petroleum Residues*. Editions Technip, Paris, 524 pp. (1984).
[13] Giavarini, C. and Speight, J.G. (Editors), *Proceedings, International Conference on Bitumen Chemistry, Rome*. Western Research Institute, Laramie, Wyo. (1991).
[14] Yen, T.F., Asphaltenic materials. In: *Encyclopedia of Polymer Science and Engineering*. Index Volume, John Wiley and Sons, New York, N.Y., 2nd ed., pp. 1–10 (1990).
[15] Giavarini, C., Concluding Remarks. In: C. Giavarini and J.G. Speight (Editors), *Proceedings, International Conference on Bitumen Chemistry, Rome*. Western Research Institute, Laramie, Wyo., pp. 1033–1034 (1991).

Asphaltenes and Asphalts, 1. Developments in Petroleum Science, 40
edited by T.F. Yen and G.V. Chilingarian

Chapter 2

CHEMICAL AND PHYSICAL STUDIES OF PETROLEUM ASPHALTENES

JAMES G. SPEIGHT

INTRODUCTION

Crude petroleum is a mixture of compounds boiling at different temperatures that can be separated into a variety of generic fractions by distillation (Table 2-1) and by fractionation (Fig. 2-1). In fact, it is by such methods that the molecular boundaries of petroleum can be defined (Figs. 2-2 and 2-3) to provide a better sense of the overall composition of petroleum and how it might behave during refining. These boundaries cover a wide range of boiling points and carbon numbers of hydrocarbon compounds. Other compounds containing nitrogen, oxygen, and sulfur as well as trace metals, are also included within the petroleum "boundary".

Petroleums from different sources exhibit different boundary limits and it is not surprising that petroleum is difficult to define with any degree of precision. Inasmuch as there is a wide variation in the properties of petroleum, the proportions in which the different constituents occur will also vary widely [1,2]. Thus, some crude oils have higher proportions of the lower boiling constituents, whereas others (such as the bitumens or natural asphalts) have higher proportions of the higher boiling constituents (often called the "asphaltic components" or "residuum").

TABLE 2-1

Boiling point ranges of various fractions of crude oil (after Speight [3, p. 280])

Fraction	Boiling point range [a]	
	(°C)	(°F)
Light naphtha	−1–150	30– 300
Gasoline	−1–180	30– 355
Heavy naphtha	150–205	300– 400
Kerosene	205–260	400– 500
Stove oil	205–290	400– 550
Light gas oil	260–315	400– 600
Heavy gas oil	315–425	600– 800
Lubricating oil	>400	>750
Vacuum gas oil	425–600	800–1100
Residuum	>600	1100

[a] For convenience, boiling point ranges are interconverted to the nearest 5°.

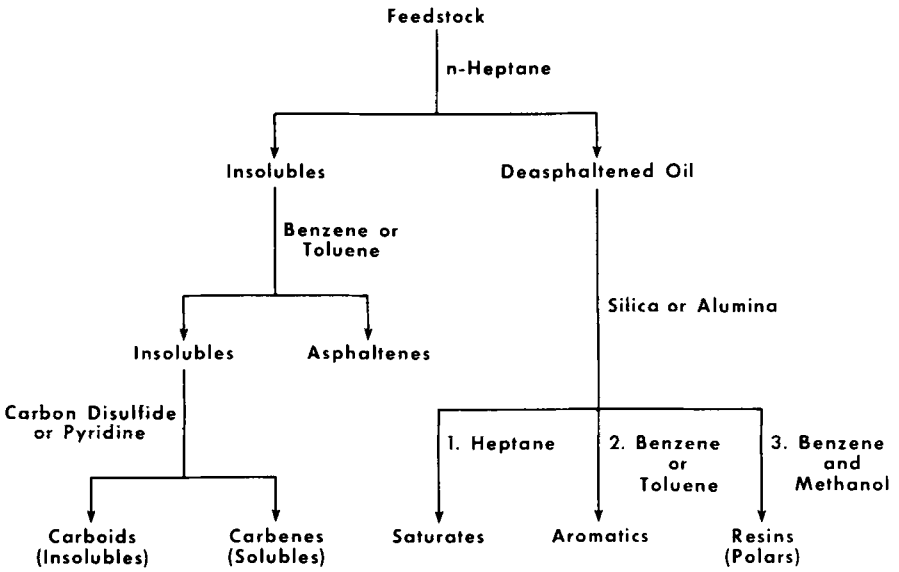

Fig. 2-1. Simplified representation of the separation of petroleum into six major fractions.

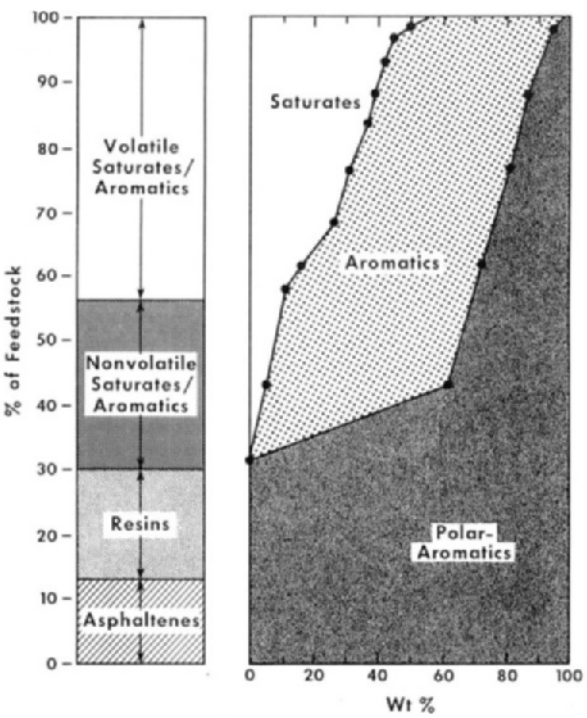

Fig. 2-2. General "map" of petroleum derived by fractionation using solvent techniques and adsorption techniques. (After Speight [4, p. 145].)

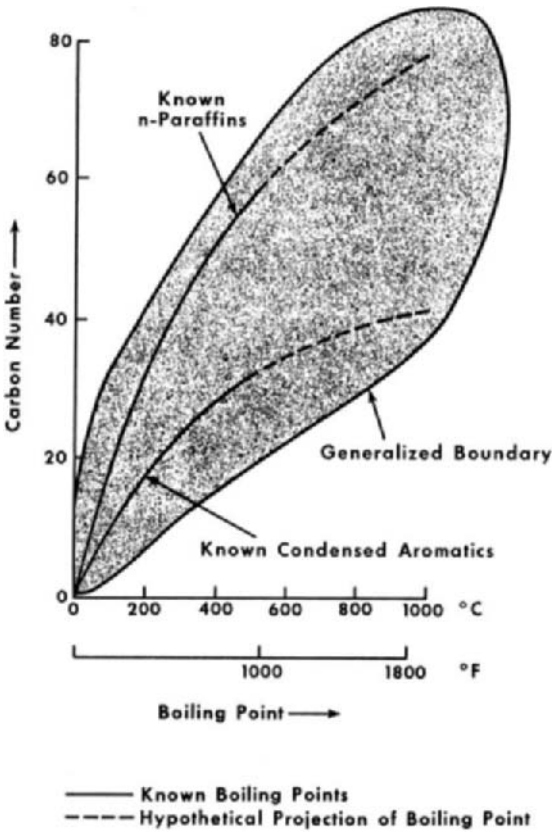

Fig. 2-3. Arbitrarily defined physical boundaries for petroleum using carbon number and boiling point data. (After Speight [4, p. 123].)

For the purposes of terminology it is preferable to subdivide petroleum and related materials into three major classes: (a) materials of natural origin; (b) materials that are manufactured, i.e., petroleum products; and (c) materials that are derived from natural or manufactured materials by fractionation (Table 2-2) [3,5].

Finally, no attempt, other than passing reference where required, is made in this chapter to deal with the metal constituents of petroleum. This is a complex subject and there are several works available that deal with metals in petroleum [6–8].

SEPARATION

Hydrocarbon solvents

The determination of the asphaltene content of petroleum and asphalt has been investigated for the most part of this century [9–14] and the art is not new. It is

TABLE 2-2

Various class/subgroups of petroleum and related materials (after Speight [15, p. 4])

Natural materials	Manufactured materials	Derived materials
Petroleum	Wax	Oils
Heavy oil	Residuum [a]	Resins
Mineral wax	Asphalt [b]	Asphaltenes
Bitumen (native asphalt)	Tar	Carbenes
Asphaltite	Pitch	Carboids
Asphaltoid	Coke	
Migrabitumen	Synthetic crude oil	
Bituminous rock		
Bituminous sand [c]		
Kerogen		
Natural gas		
Tar sands [d]		
Oil sands [e]		

[a] Residuum — the nonvolatile portion of petroleum and often further defined as "atmospheric" (b.p. > 350°C/660°F) or vacuum (b.p. > 565°C/1050°F).
[b] Asphalt — a product of a refinery operation; usually made from a residuum.
[c] Bituminous sands — more correct; bitumen is a naturally occurring asphalt.
[d] Tar sands — a misnomer, tar is a product of coal processing.
[e] Oil sands — also a misnomer but equivalent to usage of "'oil shale".

now generally accepted that asphaltenes are, by definition, a solubility class that is precipitated from petroleum, heavy oil, and bitumen by the addition of an excess of the liquid hydrocarbon [16].

The procedure by which asphaltenes are separated not only dictates asphaltene yield but can also dictate the "quality" of the fraction. For example, the use of different hydrocarbons influences the yield by a considerable factor [17–21], and the technique employed dictates whether or not the asphaltene contains co-precipitated resins.

Thus, use of insufficient proportions of the precipitating medium will cause the resins, a fraction isolated at a later stage of the separation procedure by adsorption chromatography (Fig. 2-1), to be separated with the asphaltene fraction either by inclusion within the asphaltene fraction or by adsorption onto the asphaltenes from the supernatant liquid [22]. The resins can be released by reprecipitation of the asphaltene fraction from toluene using the liquid hydrocarbon (i.e. pentane or heptane that was used for the original separation [23]. The supernatant liquid, however, should be inspected for any asphaltene material that has remained soluble. Failure to perform the separation technique correctly, and leaving the isolation procedure open to question, can throw serious doubt on any conclusions drawn from subsequent work done on the isolated material.

In fact, to ensure "stable" asphaltene yields from heavy oils, it is necessary to employ: (a) >30 ml hydrocarbon per g feedstock; (b) pentane or heptane, which are the preferable liquid hydrocarbons, although volatility constraints and stability of

asphaltene-type are tending to favor the use of *n*-heptane; and (c) 8–10 hour contact time, which is the preferable period.

The final aspect of the deasphalting is a reprecipitation sequence to remove any adsorbed or occluded resin material. This procedure involves dissolution of the asphaltenes in benzene or toluene (10 ml per g asphaltene) followed by the addition of the hydrocarbon (50 ml of the precipitant per ml toluene or benzene) to the solution. This sequence should be repeated three times to remove any of the lower-molecular-weight soluble material and to provide consistency of the asphaltene fraction [20,23].

Different feedstocks will have different amounts of asphaltenes (Table 2-3), which can also influence feedstock properties. This is particularly true of different feedstocks from any one crude oil (Fig. 2-4) where the nonvolatile asphaltenes are

TABLE 2-3

Generalized compositional ranges for the bulk fractions in crude petroleum, heavy oil, and residua

	Range of composition (w/w %)			Carbon residue (w/w %)
	asphaltenes	resins	oils	
Petroleum	<0.1–12	3–22	67–97	0.2–10.0
Heavy oil	11 –45	14–39	24–64	10.0–22.0
Residua	11 –29	29–39	?–49	18.0–32.0

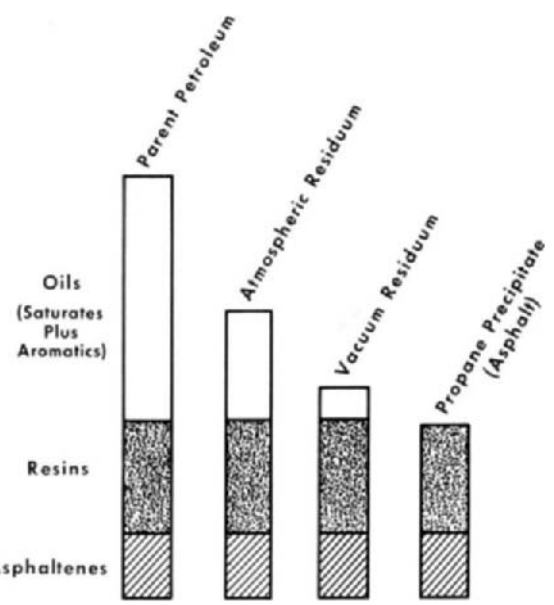

Fig. 2-4. Schematic representation of the relationship between a crude oil, two residua from crude oil, and the propane asphalt. (After Speight [24, p. 260].)

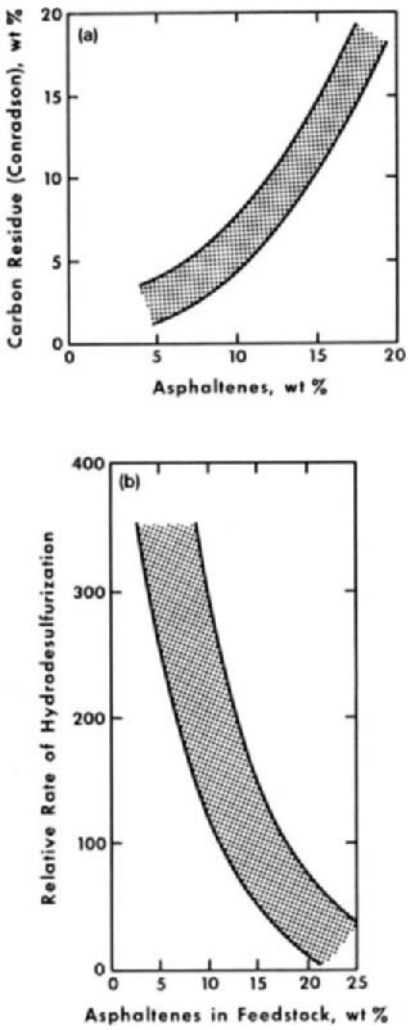

Fig. 2-5. Relationship of asphaltene content to (a) carbon residue and (b) rate of catalytic hydrodesulfurization. (After Speight [4, p. 143].)

concentrated in the residue or in the propane asphalt. In addition, differing asphaltenes contents lead to variations in the amount of thermal coke (Fig. 2-5a) [3,25–27] as produced by the various carbon residue tests [28]. Asphaltene content also causes variations in the relative rates of catalytic reactions such as hydrodesulfurization (Fig. 2-5b) [16,26]. Thus, differences in asphaltene content of feedstocks will be reflected in the methods chosen for refining the different feedstocks [4].

It must always be remembered that the definition of the nonvolatile constituents of petroleum (i.e., the asphaltenes, the resins, and, to some extent, part of the oils

fraction insofar as nonvolatile oils do occur in residua and other heavy feedstocks) (Fig. 2-4) is an operational aid. Such materials pass through the refining sequence by virtue of their volatility (or lack thereof) and it is difficult to base such separations on chemical or structural features [19,23].

NONHYDROCARBON SOLVENTS

It is well established the asphaltene fraction can be removed from petroleum using a wide variety of solvents [20]. Little is known, however, about the nature of another aspect of the laboratory deasphalting process, namely the use of non-hydrocarbon solvents as deasphalting media and their influence on asphaltene solubility.

There had been some attention paid to this aspect of asphaltene removal [5,29,30] with the aim of determining the efficiency of the concept and of what factors, if any, affect the ability of asphaltenes to remain in solution. The results of such studies (Table 2-4 and Fig. 2-6) [29] strongly suggest that the solubility of asphaltenes in various solvents is related to the surface tension, δ, of the solvent [12,31].

For any one series of organic solvents, the relationship between the solubility of the asphaltenes and the solubility parameter, δ, of the solvent is quite regular but the general relationship between asphaltene solubility and δ only appears to hold for the hydrocarbon solvents, as noted earlier [20]. In fact, comparison of the data obtained with the non-hydrocarbon solvents shows that there is severe variance of asphaltene solubility from series to series and the results are only comparable within any particular solvent series.

Of the non-hydrocarbon solvents (Table 2-4), only the ethers had a solvent power approaching that of the hydrocarbons, and non-aromatic ethers have superior solvent power to the non-aromatic ketones, esters and alcohols irrespective of the value of δ. This general trend of an increasing solvent power from lower to higher members of a series, however, is reversed in the ester series, where solvent power decreases with increasing molecular weight of the alkoxy radical. Apparently this also applies when the molecular weight of the acid radical is increased; for example, ethyl propionate ($\delta = 4.8$) dissolves less asphaltenes than ethyl acetate ($\delta = 4.9$).

Obviously, asphaltene solubility is complex and is dependent upon several factors. This phenomenon is unpredictable when different series of solvents are considered, and varies markedly from solvent to solvent. Within any one particular series, however, the relationship between asphaltene solubility and the surface tension or, for that matter, the molar volume is evident. It is interesting that in these tests neither a low spatial requirement of the solvent nor an increased electron availability in the solvent (which allows electronic interactions between the solvent and the asphaltenes), appreciably affected the solvent power.

In summary, the separation of asphaltenes from petroleum is not only a function of the amount of diluent added but also a function of the type and composition of the precipitant [20,29,32].

TABLE 2-4

Solubility of asphaltenes in various solvents (after Speight [29])

Solvent	$\delta = \gamma V^{-1/3}$	Solubility (wt%)
Normal hydrocarbons		
Pentane	3.2	0
Hexane	3.5	18.3 (20.1)[a]
Heptane	3.8	30.1 (32.5)
Octane	3.9	38.9 (42.0)
Nonane	4.0	40.3 (44.4)
Decane	4.1	43.2 (46.7)
2-Methyl hydrocarbons		
Isohexane	3.4	7.6 (9.5)
Isoheptane	3.7	22.1 (24.3)
Isooctane	3.8	29.9 (32.0)
Osononane	3.9	38.3 (40.8)
Isodecane	3.9	39.8 (42.0)
Terminal olefins		
Pentene	3.4	2.8 (4.1)
Hexene	3.6	21.3 (23.1)
Heptene	3.8	32.9 (35.5)
Octene	4.0	43.9 (46.7)
Nonene	4.1	47.2 (49.1)
Decene	4.1	47.7 (49.7)
Ethers		
Ethyl ether	3.5	15.3
n-Propyl ether	3.8	22.9
n-Butyl ether	4.0	30.0
n-Amyl ether	4.2	36.5
Ethyl-*t*-butyl ether	3.5	19.5
Ketones		
Acetone	5.3	4.7
3-Pentanone	5.2	17.8
Acetophenone	7.8	100.0
2-Pentamone	5.1	27.0
Methylethyl ketone	5.4	18.2
Methylisobutyl ketone	4.7	11.5
Esters		
Methyl acetate	5.6	37.7
Ethyl acetate	4.9	15.3
Propyl acetate	4.8	12.4
Ethyl propionate	4.8	13.2
Alcohols		
n-amyl alcohol	5.2	3.3
Ethylene glycol	12.2	4.2

[a] Figures in parentheses are calculated using the data presented in Mitchell and Speight [20]; where δ = solubility parameter, γ = surface tension, and V = molar volume.

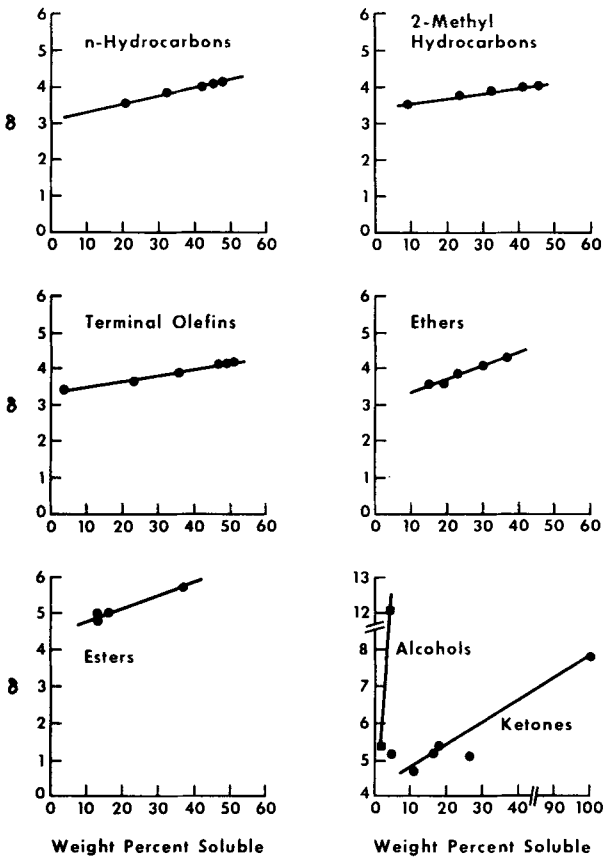

Fig. 2-6. Asphaltene solubility in relation to the solubility parameter, δ, of the solvent. (After Speight [29].)

COMPOSITION

Ultimate (elemental) composition

The elemental compositions of asphaltenes isolated by use of excess (greater than 30 volumes per g of feedstock) *n*-pentane as the precipitant shows that the amounts of carbon and hydrogen usually vary over only a narrow range (Tables 2-5 and 2-6) corresponding to H/C ratios of $1.15 \pm 0.05\%$, although values outside of this range sometimes are found.

The near constancy of the H/C ratio is surprising when the number of possible molecular and elemental combinations involving the heteroelements are considered. In fact, this property, more than any other, is the cause for the general belief that unaltered asphaltenes from virgin petroleum have a definite composition. Furthermore, it is still widely believed that asphaltenes are precipitated from petroleum by

TABLE 2-5

Properties of asphaltenes from Alberta conventional crude oils (after Speight [15], p. 408)

Source	Elemental composition (daf)					Molecular weight [a]	Spin No. ($\times 10^{18}$)	Atomic ratios			
	C	H	N	O	S			H/C	N/C	O/C	S/C
Upper Cretaceous											
Pembina (Belly River J)	87.91	8.29	1.00	1.84	0.95		2.9	1.13	0.010	0.016	0.004
Pembina (Keystone Belly River H)	87.80	8.03	1.20	1.97	1.00		3.6	1.10	0.012	0.017	0.004
Ferrier (Belly River A)	88.95	8.23	1.14	1.20	1.47		4.6	1.11	0.011	0.010	0.006
Pembina (Cardium)	88.42	8.01	1.30	1.27	1.01		2.7	1.09	0.013	0.011	0.004
Gilby (Cardium A)	84.14	10.66	1.11	3.03	1.06		1.2	1.52	0.011	0.027	0.005
Crossfield (Cardium A)	89.39	7.63	1.12	1.34	0.51		5.4	1.02	0.011	0.011	0.002
Barons (Colorado)	89.28	7.49	1.17	1.13	0.92	5890	3.5	1.01	0.011	0.009	0.004
Crossfield (Cardium B)	88.49	8.21	1.61	1.38	0.31	4250		1.11	0.016	0.012	0.001
Cyn-Pem (Cardium A)	86.84	10.21	1.29	1.10	0.56	4120		1.41	0.013	0.009	0.002
Carrington (Cardium B)	85.14	11.10	0.66	2.51	0.59	2090		1.56	0.007	0.022	0.003
Lower Cretaceous — Lower Colorado Group											
Giroux Lake (Viking A)	89.22	7.64	0.93	1.61	0.60	7100	3.6	1.03	0.008	0.014	0.003
Legal (Viking)	89.01	7.66	1.25	1.11	0.98		3.5	1.03	0.012	0.009	0.004
Joarcam (Viking)	87.08	7.79	1.16	2.98	0.99		3.3	1.07	0.011	0.026	0.004
Crossfield (Viking A)	89.40	8.07	0.99	1.36	0.18		5.6	1.08	0.009	0.011	0.001
Provost (Viking A)	88.13	7.96	1.14	1.43	1.08		2.9	1.08	0.014	0.012	0.005
Cessford (Basal Colorado A)	84.70	7.78	1.23	1.08	5.20	6690	2.5	1.10	0.012	0.010	0.023
Joarcam (Viking)	85.48	7.88	1.44	4.31	0.89	5060		1.11	0.014	0.038	0.004
Lower Cretaceous — Mannville Group											
Willesden Green (Glauconitic A)	87.02	7.11	1.43	1.03	3.41	6800	3.5	0.98	0.014	0.009	0.015
Medicine River (Ostracod A)	86.29	7.54	1.16	1.02	4.00		3.4	1.05	0.012	0.009	0.017
Kaybob (Cadomin B)	86.01	7.34	0.89	0.70	5.06	6880	3.3	1.02	0.009	0.006	0.022
Niton (Basal Quartz B)	84.12	8.35	0.73	4.12	2.68		2.2	1.19	0.007	0.037	0.012
Pembina (Keystone Ellerslie A)	85.72	7.45	1.31	1.04	4.48		2.3	1.04	0.013	0.009	0.020
Gilby Alexander (Basal Quartz D)	82.31	7.72	2.33	1.27	6.37	6580		1.13	0.024	0.012	0.029
Jurassic											
Gilby (Jurassic B)	86.05	6.65	1.15	0.53	5.63	6700	4.5	0.93	0.011	0.005	0.024
Medicine River (Jurassic A)	86.10	6.90	1.11	0.56	5.33	7280	4.4	0.96	0.011	0.005	0.023
Medicine River (Jurassic C)	84.30	7.43	1.34	2.06	4.87	4070		1.06	0.014	0.018	0.022
Triassic											
Boundary Lake South (Triassic E)	86.26	7.89	1.49	0.83	3.52	5050	3.1	1.10	0.015	0.007	0.015
Worsley (Triassic A)	82.90	7.68	1.36	1.13	6.92		1.8	1.11	0.014	0.010	0.031
Sturgeon Lake South (Triassic A)	84.08	7.41	1.33	1.05	6.12		5.0	1.06	0.014	0.009	0.027

Carboniferous											
Eaglesham (Debolt C)	87.62	7.49	1.14	1.65	2.09		3.2	1.03	0.011	0.014	0.009
Crossfield (Rundle C)	87.53	8.05	0.07	0.95	2.76		2.4	1.10	0.007	0.008	0.012
Del Sonita (Rundle)	84.87	8.41	0.63	1.86	4.23		2.8	1.19	0.006	0.016	0.019
Sylvan Lake (Pekisko B)	86.31	7.50	1.36	1.46	3.37		2.0	1.04	0.014	0.013	0.015
Twining North (Rundle)	86.29	7.11	0.99	0.64	4.97	6290	3.7	0.99	0.010	0.006	0.022
Cherhill (Banff A)	82.32	8.06	1.69	1.40	6.53	5800	2.0	1.17	0.018	0.013	0.030
Swalwell (Pekisko A)	85.64	7.55	1.11	1.87	3.83	4850	3.3	1.06	0.011	0.016	0.017
Princess (Pekisko A)	84.47	7.62	1.28	1.13	5.50	4580		1.08	0.013	0.010	0.024
Upper Devonian — Wabumum Group											
Leduc-Woodbend (D-1B)	85.57	7.86	1.42	3.86	1.29	4270	1.3	0.10	0.014	0.034	0.006
Upper Devonian — Winterburn Group											
Maimo (D-2A)	85.65	7.73	1.40	1.02	4.21		2.2	1.08	0.014	0.009	0.018
Alix (D-2A)	82.85	9.14	2.04	4.41	1.53		0.2	1.32	0.021	0.040	0.007
Youngstown (Arcs)	85.29	7.44	1.88	0.82	4.57	4075		1.05	0.019	0.007	0.020
Joffre (D-2)	85.72	7.90	0.83	2.96	2.59		0.9	1.11	0.008	0.026	0.011
Fenn-Big Valley (D-2A)	86.21	8.07	1.56	0.52	3.64		2.9	1.12	0.016	0.005	0.016
Youngstown (Arcs)	85.74	7.23	1.15	0.96	4.92	5310	2.4	1.01	0.011	0.008	0.022
Bonnie Glen (D-3A)	89.09	7.60	0.73	1.37	1.22		1.5	1.02	0.007	0.016	0.005
Westerose (D-3)	86.97	7.75	1.23	2.04	2.00		0.9	1.07	0.012	0.018	0.009
Maimo (D-3A)	87.05	7.62	1.59	0.45	3.29		3.6	1.05	0.016	0.004	0.014
Erskine (D-3)	84.60	6.46	1.24	0.92	6.78	7750	4.4	0.92	0.013	0.008	0.030
Upper Devonian — Beaverhill Lake											
Loon (Slave Point A)	89.53	7.43	1.04	0.79	1.21		3.3	1.00	0.010	0.007	0.005
Loon (Slave Point A)	87.07	9.45	1.02	1.70	0.76	3525		1.30	0.010	0.015	0.003
Swan Hills (Beaverhill Lake A)	89.70	6.84	0.92	1.64	0.90		5.2	0.92	0.009	0.014	0.004
Goose River (Beaverhill Lake A)	89.71	7.00	1.02	1.52	0.75		2.4	0.94	0.010	0.013	0.003
Middle Devonian — Elk Point											
Zama (Keg River C)	86.46	8.52	0.91	0.54	3.57	2010	2.3	1.18	0.009	0.005	0.015
Zama (Keg River WWW)	84.49	7.45	2.37	1.23	4.46	3695		1.06	0.024	0.011	0.020
Zama (Muskeg B)	86.83	7.86	0.92	0.56	3.82	4270	4.0	1.09	0.009	0.005	0.016
Zama (Muskeg V)	85.71	7.81	1.36	1.30	5.82	3600		1.09	0.014	0.011	0.025
Nipisi (Keg River Sandstone A)	89.59	7.49	1.00	0.63	1.29		3.5	1.00	0.010	0.005	0.005
Zama (Muskeg W)	86.40	9.03	1.66	2.13	0.78	4125		1.25	0.016	0.019	0.003
Nipisi (Gilwood A)	89.62	7.34	1.02	0.84	1.18		2.8	0.98	0.010	0.007	0.005
Gilwood (Gilwood A)	87.94	7.61	2.21	1.77	0.47	4455		1.04	0.022	0.015	0.002
Granite Wash											
Loon (Granite Eash)	89.79	7.40	0.96	0.62	1.22		3.1	0.99	0.009	0.005	0.005
Red Earth (Granite Wash E)	86.50	7.74	1.30	3.05	1.41	2670		1.07	0.013	0.026	0.006

[a] Vapor pressure osmometry (vpo): benzene.

TABLE 2-6

Properties of asphaltenes from Alberta heavy oils and bitumens (after Speight [15], p. 411)

Source	Elemental composition (daf)					Molecular weight [a]	Spin No. ($\times 10^{18}$)	Atomic ratios			
	C	H	N	O	S			H/C	N/C	O/C	S/C
Lower Cretaceous — Mannville Group											
Lloydminster (Sparky J)	81.94	7.96	1.00	1.14	7.96	7360	2.9	1.17	0.010	0.010	0.036
Wildmere (Sparky)	82.18	8.18	1.59	0.44	7.61	6415		1.19	0.017	0.004	0.035
Lloydminster (Blairmore)	81.91	8.11	1.18	1.00	7.80	6670		1.19	0.012	0.009	0.036
Chauvin (Mannville A)	82.81	7.87	1.22	1.38	6.72		1.2	1.14	0.013	0.013	0.030
Inland (Colony)	80.42	7.81	2.59	1.99	7.19	5770	1.6	1.17	0.028	0.019	0.034
South Taber (Mannville A)	82.73	7.75	2.82	0.95	5.75	3980	2.0	1.12	0.029	0.009	0.026
Alderson (Lower Mannville B)	82.79	7.52	2.14	1.58	5.97	3780	2.4	1.09	0.022	0.011	0.025
Bantry (Mannville A)	83.30	7.79	1.48	1.88	5.55	4900	2.0	1.12	0.015	0.017	0.025
Chauvin South (Sparky C)	82.64	8.21	1.36	1.56	6.23	5890		1.19	0.014	0.014	0.028
Athabasca	80.31	8.37	1.09	2.45	7.77	3850	1.2	1.25	0.012	0.023	0.036
Athabasca	80.47	8.45	1.25	1.88	7.95	5100	1.2	1.26	0.013	0.018	0.037
Athabasca	82.63	8.35	1.43	1.85	5.75	8500	1.6	1.21	0.015	0.017	0.026
Athabasca	80.62	8.31	1.24	1.61	8.21	6320	1.6	1.24	0.013	0.015	0.038
Wabasca	81.00	8.32	0.99	2.11	7.57	6740	1.2	1.23	0.010	0.020	0.035
Wabasca	80.13	8.29	1.58	1.91	8.09	3700	1.2	1.24	0.017	0.018	0.038
Wabasca	81.01	8.13	0.94	2.21	7.70	6680	1.6	1.20	0.010	0.020	0.036
Wabasca	80.06	8.23	1.20	2.58	7.93	7370	1.4	1.23	0.013	0.024	0.037
Cold Lake	83.33	8.41	1.23	1.64	5.39	6870	2.2	1.21	0.013	0.015	0.024
Cold Lake	80.76	8.25	1.14	2.61	7.21	6860	1.4	1.23	0.012	0.024	0.033
Cold Lake	81.04	8.35	1.24	2.24	7.14	5320	1.5	1.24	0.013	0.021	0.033
Peace River	81.04	8.33	1.07	1.83	7.73	7800	1.0	1.23	0.011	0.017	0.036
Jurassic											
Conrad (Ellis)	86.61	7.64	1.32	0.96	3.47		0.9	1.06	0.013	0.008	0.015
Carboniferous											
Glenevis (Banff)	83.18	7.73	1.01	1.37	6.71	9040	0.6	1.12	0.010	0.012	0.030
Glenevis (Banff)	82.91	8.23	1.50	0.52	6.84	4765		1.19	0.015	0.005	0.031
Matziwin (Pekisko A)	84.38	7.90	1.64	1.06	5.02	6670	2.5	1.12	0.017	0.009	0.022
Blue Ridge (Pekisko A)	84.83	6.93	1.82	0.88	5.54	4175		0.98	0.018	0.008	0.024

[a] vpo: benzene.

hydrocarbon solvents because of this composition and not only because of solubility properties.

In contrast to the carbon and hydrogen contents of asphaltenes, notable variations do occur in the proportions of the heteroelements, in particular in the proportions of oxygen and sulfur. Oxygen content varies from 0.3% to 4.9% and sulfur content varies from 0.3% to 10.3%. On the other hand, the nitrogen content of the asphaltenes has a somewhat lesser degree of variation (0.6% to 3.3% at the extremes). Exposing asphaltenes to atmospheric oxygen, however, can substantially alter the oxygen content, and exposing a crude oil to elemental sulfur, or even to sulfur-containing minerals, can result in excessive sulfur uptake. It is not unreasonable to suggest that oxygen and sulfur contents vary more markedly than does nitrogen content because of the potential for reaction between the petroleum material and oxygen or sulfur (and sulfur-containing minerals).

The nature of the source material and regional variations in maturation conditions will serve to differentiate one crude oil (and hence one asphaltene) from another. In the simplest sense, it might be suggested that the maturation process tends to be a "great equalizer", insofar as most chemical reactions may be close to the equilibrium state, over the time periods involved. In addition, differences between the asphaltenes reflect the differences in the relative amounts of the functional molecular types present and the way in which the structural types are combined in the various asphaltenes.

The use of heptane as the precipitant yields an asphaltene fraction that is substantially different from the pentane-insoluble material (Table 2-7). For example, the H/C ratios of the heptane precipitate are markedly lower than those of the pentane precipitate, indicating a higher degree of aromaticity in the heptane precipitate. The N/C, O/C, and S/C ratios are usually higher in the heptane precipitate, indicating higher proportions of the heteroelements in this material [33].

There are also some interesting compositional relationships that can be derived from the data. These data confirm the general consistency of asphaltene compo-

TABLE 2-7

Elemental compositions of various asphaltenes (after Speight [34])

Source	Precipitating medium	Composition (wt%)					Atomic ratios			
		C	H	N	O	S	H/C	N/C	O/C	S/C
Canada	*n*-pentane	79.5	8.0	1.2	3.8	7.5	1.21	0.013	0.036	0.035
	n-heptane	78.4	7.6	1.4	4.6	8.0	1.16	0.015	0.044	0.038
Iran	*n*-pentane	83.8	7.5	1.4	2.3	5.0	1.07	0.014	0.021	0.022
	n-heptane	84.2	7.0	1.6	1.4	5.8	1.00	0.016	0.012	0.026
Iraq	*n*-pentane	81.7	7.9	0.8	1.1	8.5	1.16	0.008	0.010	0.039
	n-heptane	80.7	7.1	0.9	1.5	9.8	1.06	0.010	0.014	0.016
Kuwait	*n*-pentane	82.4	7.9	0.9	1.4	7.4	1.14	0.009	0.014	0.034
	n-heptane	82.0	7.3	1.0	1.9	7.8	1.07	0.010	0.017	0.036

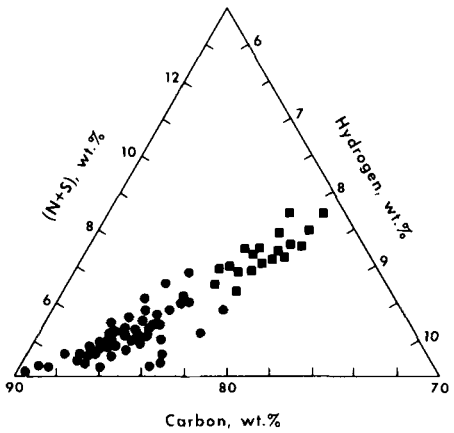

Fig. 2-7. Compositional relationships of asphaltenes. (After Speight [15, p. 413].)

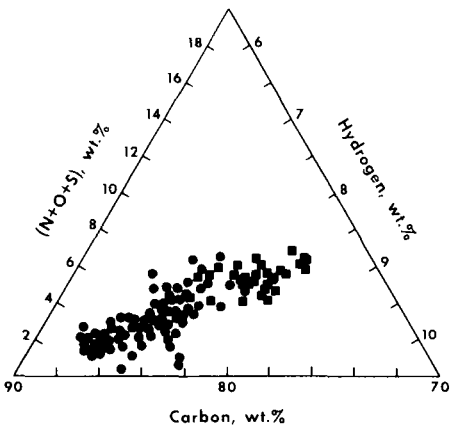

Fig. 2-8. Compositional relationships of asphaltenes. (After Speight [15, p. 414].)

sition but the data also show that where composition varies, it is usually due to heteroatom content (Figs. 2-7 and 2-8). It is also possible to show from these data where the asphaltenes fit into the kerogen maturation diagram (Fig. 2-9) as well as compare the elemental data with those data obtained for different kerogens (Table 2-8). It should be noted, however, that the data are for kerogen samples, like the asphaltenes, are not from the same locale and are at different stages of maturity.

On this point, the role of kerogen in the petroleum maturation process is worthy of comment. It has been suggested by many workers that kerogen is first formed from the organic debris and then acts as the direct precursor to petroleum. The suggestion is that geothermal effects and geological time are responsible for the generation of oil from the kerogen.

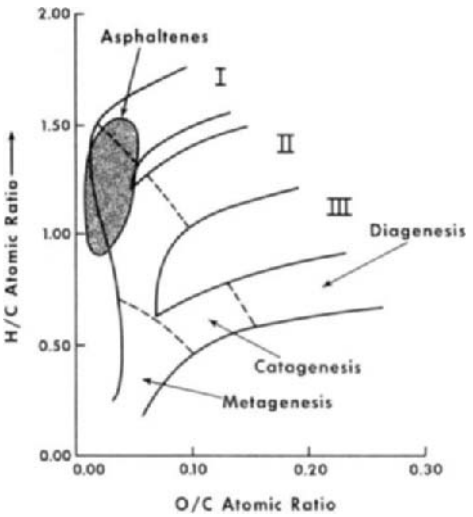

Fig. 2-9. Positioning of H/C–O/C ratios on the H/C vs. O/C maturation diagram. (After Speight [15, p. 418].)

An alternate suggestion is that kerogen may be formed simultaneously with a "protopetroleum". There is also a subsequent stage of kerogen formation in which the more polar constituents of the "protopetroleum" participate (Fig. 2-10). Indeed they may even be the driving force in the formation of the second "batch" of kerogen. As the "protopetroleum" becomes more paraffinic, the insoluble polar constituents separate and remain in the formation to form kerogen. The separation of the polar constituents in the formation is analogous to the deasphalting process (q.v.) but it must be recognized that not all of the polar constituents will react to form kerogen. Some may/will be carried by the maturing oil into the reservoir.

At this time, there is also the potential for interaction of the liquid with minerals in the strata. Any heteroatom material in the maturing liquid could then form asphaltenes during the maturation process. Thus, the origin of the asphaltene is just

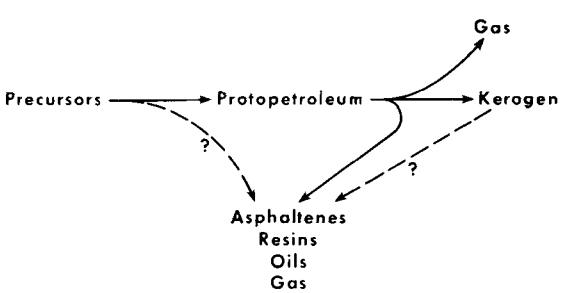

Fig. 2-10. Simplified representation of petroleum formation without the formation of kerogen as an intermediate.

TABLE 2-8

Elemental composition of various kerogen samples (after Speight [15, p. 77])

Locale	Elemental composition (wt%)					Atomic ratios			
	C	H	O	N	S	H/C	O/C	N/C	S/C
Australia									
Alpha	80.8	9.8	7.3	1.1	1.0	1.45	0.068	0.012	0.005
Byfield	66.8	5.8	25.2	2.2	0.5	1.05	0.283	0.028	0.003
	67.9	5.7	23.5	2.1	0.8	1.00	0.260	0.027	0.004
	65.6	5.8	25.6	2.3	0.5	1.07	0.292	0.030	0.003
	75.3	9.1	11.9	2.2	1.5	1.44	0.119	0.025	0.007
	72.5	9.2	14.0	2.2	?	1.52	0.144	0.026	0.011
	76.2	8.6	11.0	2.7	1.4	1.36	0.109	0.030	0.007
Camooweal	78.0	8.1	8.3	2.8	2.8	1.25	0.080	0.031	0.013
Condor	77.5	9.1	8.3	2.3	2.5	1.41	0.081	0.025	0.012
	78.9	9.0	9.1	2.8	0.4	1.38	0.087	0.030	0.022
	70.0	8.2	9.4	1.9	4.2	1.41	0.101	0.023	0.022
	70.2	7.9	15.1	1.9	5.1	1.34	0.161	0.023	0.027
	68.9	6.7	15.4	2.7	6.6	1.17	0.168	0.033	0.036
	72.4	5.7	16.1	2.9	1.4	0.95	0.169	0.034	0.007
	78.8	9.5	9.0	2.4	0.3	1.44	0.086	0.026	0.001
Coorongite	77.5	10.8	9.3	0.4	2.0	1.67	0.90	0.004	0.010
	77.1	11.0	11.3	0.4	0.2	1.72	0.110	0.004	0.001
Duaringa	71.6	9.5	14.2	1.4	1.4	1.60	0.149	0.017	0.007
	60.6	7.7	14.2	1.0	4.8	1.53	0.176	0.014	0.030
	71.3	9.4	15.5	1.0	1.4	1.58	0.166	0.012	0.007
	69.1	9.4	12.3	1.2	3.8	1.63	0.133	0.015	0.021
	68.8	8.6	14.9	1.3	1.2	1.50	0.163	0.016	0.006
	50.4	6.1	11.1	1.3	5.9	1.44	0.165	0.022	0.044
	78.3	10.0	9.5	1.7	0.5	1.54	0.091	0.019	0.002
	74.1	9.6	13.8	1.6	0.9	1.55	0.140	0.019	0.005
	71.5	7.3	17.3	2.4	1.5	1.22	0.192	0.029	0.008
Glen Davis	85.5	10.4	0.2	1.1	0.6	1.46	0.022	0.011	0.003
Joadja	84.8	9.8	3.1	1.2	1.1	1.39	0.028	0.012	0.005
Julia Creek	74.2	7.5	11.3	2.4	4.6	1.21	0.115	0.028	0.023
Lowmead	73.0	8.4	15.6	2.2	0.8	1.38	0.161	0.026	0.004
Mersey River	78.4	10.0	7.4	1.2	3.1	1.53	0.070	0.013	0.015
Mt. Coolon	69.0	6.5	21.3	0.9	1.9	1.12	0.236	0.011	0.010
Nagoorin	72.9	7.1	15.3	3.3	1.4	1.17	0.157	0.039	0.007
	77.6	10.6	9.6	1.0	1.2	1.63	0.093	0.011	0.006
	77.0	9.8	10.5	1.5	1.2	1.52	0.100	0.017	0.006
	75.3	9.9	11.8	1.8	1.2	1.57	0.118	0.020	0.006
	74.9	10.2	12.7	1.6	0.6	1.64	0.127	0.018	0.003
Stuart	69.0	6.0	20.9	2.8	0.9	1.04	0.228	0.035	0.005
	75.9	10.4	10.8	1.7	1.2	1.64	0.107	0.019	0.006
	74.7	9.9	11.6	1.7	0.2	1.59	0.116	0.019	0.001
	72.3	8.6	17.8	1.2	0.3	1.43	0.118	0.014	0.0010
	85.3	12.6	0.5	1.1	0.5	1.77	0.004	0.011	0.002
	85.6	12.3	0.3	1.2	0.5	1.73	0.003	0.012	0.002
Tasmanite	75.9	9.4	8.8	2.1	3.8	1.39	0.087	0.024	0.019
	82.7	10.7	6.6			1.55	0.059		
Yaamba	77.3	10.4	9.6	2.0	0.7	1.61	0.093	0.022	0.003

TABLE 2-8 (continued)

Locale	Elemental composition (wt%)					Atomic ratios			
	C	H	O	N	S	H/C	O/C	N/C	S/C
Brazil									
Cypris	80.2	11.8	8.0			1.77	0.075		
Irati	82.9	9.0	5.7	2.4		1.31	0.052	0.025	
	78.8	9.5	7.8	3.9		1.44	0.074	0.042	
Burma									
Amherst	79.0	11.2	9.8			1.70	0.93		
Canada									
Alberta	86.7	9.0	4.3			1.25	0.37		
Colombia									
La Luna	89.6	7.2	3.2			0.96	0.027		
Czechoslovakia									
Kounova	82.5	9.5	8.0			1.38	0.073		
Pilzen	86.1	7.8	6.1			1.09	0.059		
England									
Kimmeridge	77.0	8.0	15.0			1.25	0.0146		
Estonia									
Kukersite	79.3	10.0	10.7			1.51	0.101		
France									
Wurtemberg	83.1	9.0	7.9			1.30	0.71		
St. Hillaire	87.2	7.9	4.9			1.09	0.042		
Autun	84.3	8.4	7.3			1.19	0.065		
Aleksinac	71.9	8.7	16.2			1.46	0.169	0.038	
Scotland									
Lothian	82.0	8.5	9.5			1.24	0.087		
	75.7	10.4	9.8	4.2		1.64	0.097	0.047	
South Africa									
Ermelo	82.0	8.2	9.8			1.20	0.089		
United States									
Arkansas	95.8	2.7	1.5			0.34	0.012		
California	83.0	8.4	8.6			1.22	0.078		
Colorado	76.5	10.0	10.3	0.6	2.6	1.57	0.100	0.007	0.013
Green River	82.2	10.1	7.8			1.47	0.071		
	87.5	8.7	3.8			1.19	0.033		
	77.4	10.3	9.3	3.1		1.59	0.090	0.034	
	79.9	10.2	6.2	2.5	1.2	1.53	0.058	0.027	0.006
	79.8	10.2	6.7	2.4	1.0	1.53	0.063	0.026	0.005
	80.8	10.3	5.6	2.4	1.0	1.53	0.052	0.025	0.005
	80.6	10.3	5.8	2.3	1.0	1.53	0.054	0.024	0.005
	81.0	10.3	5.3	2.5	0.9	1.53	0.050	0.026	0.004
	80.9	10.5	4.8	2.6	1.2	1.56	0.045	0.028	0.006
	81.4	10.4	4.8	2.3	1.0	1.53	0.044	0.024	0.005
	80.0	10.4	6.4	2.3	0.9	1.56	0.060	0.025	0.004
	80.1	10.2	6.5	2.1	1.1	1.53	0.061	0.022	0.005
	80.7	10.4	5.3	2.6	1.0	1.55	0.049	0.028	0.005

TABLE 2-8 (continued)

Locale	Elemental composition (wt%)					Atomic ratios			
	C	H	O	N	S	H/C	O/C	N/C	S/C
United States (continued)									
Kansas	88.2	5.1	6.7			0.69	0.057		
Kentucky	80.9	7.1	7.9	2.8	1.4	1.06	0.073	0.029	0.006
	80.7	6.9	8.1	2.7	1.7	1.03	0.075	0.029	0.008
	81.9	6.5	11.6			0.95	0.106		
	82.6	8.7	8.7			1.26	0.079		
	81.8	7.6	6.4	2.3	1.9	1.11	0.059	0.024	0.009
	82.7	7.3	5.8	2.2	2.0	1.06	0.053	0.022	0.009
	81.4	7.4	6.8	2.3	2.1	1.09	0.063	0.024	0.009
	82.0	7.4	6.3	2.3	2.0	1.08	0.058	0.024	0.009
Louisiana	80.3	5.4	14.3			0.81	0.133		
Michigan	86.2	8.2	5.6			1.14	0.049		
Oklahoma	80.1	7.0	12.9			1.05	0.121		
	88.3	6.7	5.0			0.91	0.042		
Texas	93.2	3.0	3.8			0.39	0.031		
Utah	75.9	9.1	8.4	3.9	2.6	1.44	0.083	0.044	0.013
	80.9	8.6	4.4	3.8		1.28	0.041	0.040	0.011
	82.7	4.1	8.3	1.7	3.2	0.60	0.075	0.017	0.015

as likely to occur within the oil rather than as a breakdown of kerogen during the maturation process.

That an asphaltene-type material occurs as part of a kerogen matrix is beyond question [35]. By definition, this should be anticipated. Many kerogens contain a toluene-soluble "bitumen" and, thus, bitumen should be anticipated to contain an asphaltene fraction. But it must be remembered that asphaltenes are not a specific chemical class but are a solubility class. As such, there may be considerable differences between asphaltenes separated from kerogen "bitumen" and those separated from petroleum.

Fractional composition

One aspect of asphaltene characterization that has provided strong evidence for the complexity of petroleum asphaltenes arises from composition studies using fractionation techniques [36–40]. It is unfortunate, however, that such studies have not received more recognition as they provide valuable information about the character of petroleum asphaltenes.

Fractionation of asphaltenes by solvent techniques allows asphaltenes, in the simplest sense, to be regarded as mixtures of aromatic types and nitrogen types. There is evidence (Fig. 2-11) that in the more aromatic species (i.e., lower H/C-types) the nitrogen content predominates. There is also fragmentary evidence, which is not conclusive yet [41] that the more aromatic asphaltene molecules contain a higher proportion of basic (i.e., pyridinic) nitrogen, whereas the less aromatic asphaltene molecules contain a higher proportion of non-basic (i.e., pyrrolic) nitrogen.

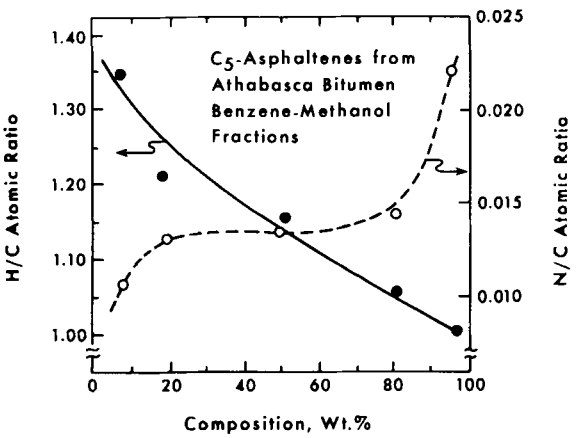

Fig. 2-11. Representation of an asphaltene as a collection of different H/C and N/C types. (After Speight [42, p. 38].)

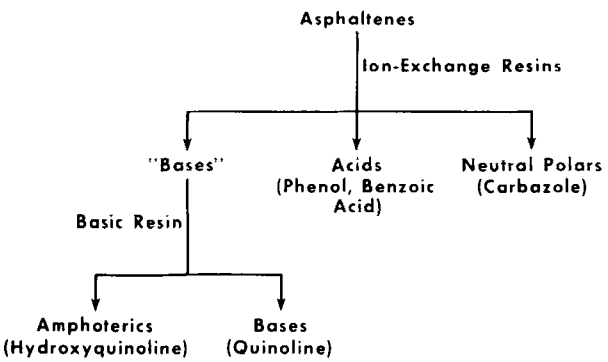

Fig. 2-12. Schematic representation of the fractionation of asphaltenes into functional classes with examples of the functional types.

Asphaltene fractionation using solid adsorbents has not enjoyed the popularity of fractionation using solvents. Retention of material on the adsorbent has always been cited as a disadvantage of such studies. Indeed, if there is any heat of adsorption at the initial admixture of the adsorbent with the asphaltene solution, there is also the potential for irreversible chemical changes which leaves questions about the true nature of the asphaltene eluate.

Nevertheless, there has been some success in defining asphaltenes as acidic and basic materials on the basis of separation using gel permeation chromatography [43], a transition metal oxide solid acid catalyst [45], silica gel chromatography [46], and ion exchange resins (Fig. 2-12) [40,47]. Analytical data also show that these fractions contain several heteroatoms per molecule and reinforce the concept of asphaltenes being complex mixtures of molecular sizes and various functional types (Fig. 2-13) [48].

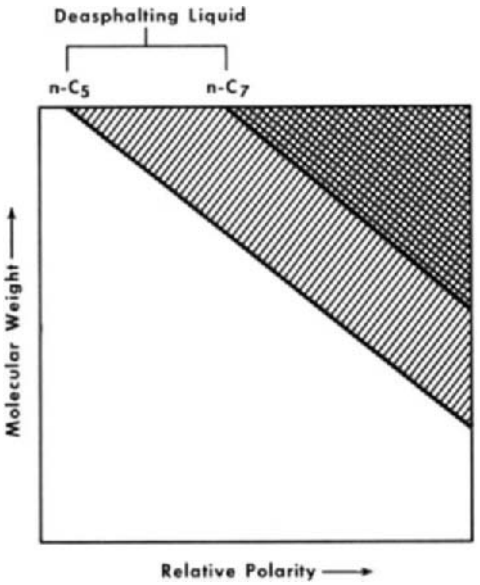

Fig. 2-13. Schematic representation of asphaltene composition based on molecular weight and polarity. (After Long [44].)

STRUCTURAL STUDIES

The molecular nature of the nonvolatile fractions of petroleum has been the subject of numerous investigations [49–54], but determining the actual structures of the constituents of the asphaltene fraction has proved to be difficult. It is, no doubt, the great complexity of the asphaltene fraction that has hindered the formulation of the individual molecular structures.

Nevertheless, the various investigations have brought to light some significant facts about asphaltene structure.

Hydrocarbon structures

Early postulates of asphaltene structure centered around a variety of polymer structures based on aromatic systems [3,55,56]. Much of the information available on the structural parameters and carbon skeleton of petroleum fractions and asphaltenes has been derived from spectroscopic studies of asphaltenes isolated from various petroleums and natural asphalts [52,53,57–62]. The data from these studies support the hypothesis that asphaltenes, viewed structurally, contain condensed polynuclear aromatic ring systems bearing alkyl side chains.

There are also indications that asphaltenes consist of condensed aromatic nuclei that carry alkyl and alicyclic systems with heteroelements (i.e., nitrogen, oxygen, and sulfur) scattered throughout in various, including heterocyclic, locations. With increasing molecular weight of the asphaltene fraction, both aromaticity and the

proportion of heteroelements increase [2,63,64]. In addition, the proportion of asphaltenes in petroleum varies with source, depth of burial, the specific (or API) gravity of the crude oil, and the sulfur content of the crude oil as well as a nonasphaltene sulfur [2].

These later attempts invoked the concept of large polynuclear aromatic systems and efforts were made to describe the total structures of asphaltenes (Fig. 2-14) in accordance with magnetic resonance data and results of other spectroscopic and analytical techniques [52,53,65,66].

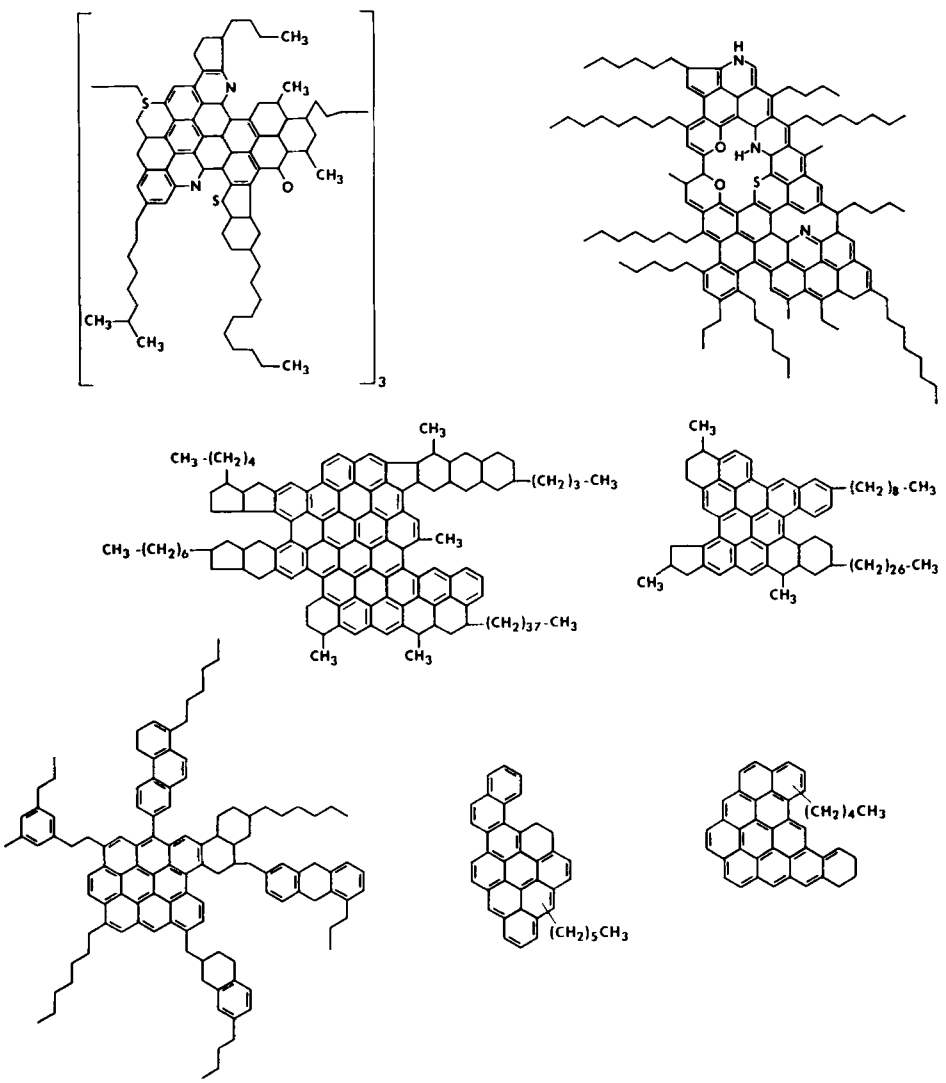

Fig. 2-14. Examples of asphaltene formulae based on large polynuclear aromatic systems.

In spite of these generalities, many facets of asphaltene structure still remain unknown and it is this overall lack of structural detail which indicates that current, and future, chemical research should focus on (a) skeletal structure; (b) the size of the polynuclear aromatic systems; (c) the internuclear bonds that need to be thermally or catalytically cleaved to produce more "manageable" lower-molecular-weight fragments; (d) the heteroatom types and subsequent ease, or difficulty of removal; (e) the metallic constituents and their occurrence in porphyrinic or non porphyrinic locations; and (f) the actual physicochemical relationships that exist between the asphaltenes and the other constituents of the oil.

More than anything else, however, it is the number of rings in such systems that is open to question. The number of rings apparently varies from as low as six in smaller systems to fifteen to twenty in more complex systems. It is difficult to visualize these postulated structures as part of the asphaltene molecule. Such complex structures as derived in the early studies may have several shortcomings that do not fully explain asphaltene behavior. Nevertheless, the early studies did serve as pioneering efforts by which later studies were stimulated.

These early studies did serve to show that asphaltenes could be considered as chemical entities rather than a diffuse nondescript fraction. The true complexity of the asphaltene fraction, however, needed further definition. In fact, all methods employed for structural analysis involve, at some stage or another, assumptions that (although based on data that may have been derived from studies of the more volatile fractions of petroleum) may be of questionable validity when applied to asphaltenes [67,68]. But start must be made at some point and, when dealing with an unknown, assumptions are always necessary. One can only hope that the assumptions used in the derivation of model structures are valid and explain asphaltene behavior.

Thus, a question is raised as to the ability of such structures being able to explain the behavior of asphaltenes. Indeed, this question will persist even as postulated structures evolve to those that are, supposedly, more "acceptable". The relationship of the highly condensed structures to the proposed maturation paths of petroleum is also open to question. In fact, the writer considers that the structures of asphaltenes are more closely related to the structural moieties found in a variety of natural products.

The thermal decomposition of asphaltenes provides an excellent example of the inconsistencies that can arise in the derivation of structural types from spectroscopic methods (i.e., magnetic resonance), where alkyl side chains are deduced to contain approximately four carbon atoms [69–73].

Asphaltene pyrolysis (350–800°C; 660–1470°F) produces substantial amounts of alkanes (having up to forty carbon atoms in the molecule) in the distillate, which can only be presumed to reflect the presence of such chains in the original asphaltene. Transalkylation studies [74] also provide evidence for longer alkyl side chains in the asphaltene molecules.

Obviously, recognition of the inconsistencies of the spectroscopic method with respect to the paraffinic moieties must lead to recognition of similar inconsistencies when considering the aromatic nucleus.

TABLE 2-9

Some of the molecular types produced from asphaltene fractions by pyrolysis (after Speight [40, p. 820])

HOMOLOGOUS SERIES	MOLECULAR TYPES	
Alkylbenzene	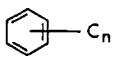	n = 1 - 7
Alkylnaphthalene	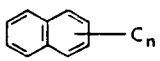	n = 1 - 4
Benzothiophene	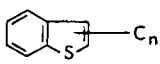	n = 1 - 3
Dibenzothiophene	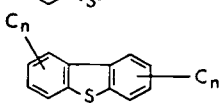	n = 1
Phenanthrene	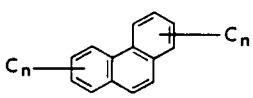	n = 1
Chrysene	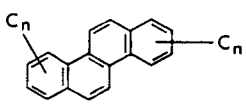	n = 1

TABLE 2-10

Production of aromatics, nonaromatics, and carbon residue from various asphaltene subfractions (after Speight [40, p. 820])

Fraction	H/C atomic	Molecular weight[a]	Volatiles		Residue (wt%)
			aromatics	nonaromatics	
Amphoterics	1.04	2350	51	49	63
Bases	1.06	2250	48	52	60
Acids	1.23	1910	40	60	43
Neutral polars	1.29	1420	33	65	38

[a] Vapor pressure osmometry in pyridine at 65, 75 and 85°C and extrapolated to room temperature. Data are for Athabasca asphaltenes.

The application of thermal techniques to study the nature of the volatile thermal fragments from petroleum asphaltenes has produced some interesting data relating to the polynuclear aromatic systems [69,70,73,75–77]. These thermal techniques have produced strong evidence for the presence of small (1–4 ring) polynuclear aromatic systems (Tables 2-9 and 2-10) [23,78]. There was an overall preponderance of single ring (cycloparaffin and alkylbenzene) species as well as the domination of saturated material over aromatic material.

The preponderance of the low-molecular-weight material in the volatile products is to be anticipated on the basis that more complex systems remain as nonvolatile material and, in fact, are converted to coke. One other point worthy of note is that the py/gc/ms program does not accommodate nitrogen and oxygen species. This matter is resolved, in part, by the concentration of nitrogen and oxygen in the nonvolatile material (coke) and the overall low proportions of these heteroatoms originally present in the asphaltenes.

The major drawback to the application of a pyrolysis–gas chromatography–mass spectrometry (py/gc/ms) technique to study of the polynuclear aromatic systems in petroleum asphaltenes is the small amount of material that remains as a nonvolatile residue (Table 2-10). Aside from speculation about the polynuclear aromatic systems in the residue, it should be noted that the majority of the nitrogen (>90%), oxygen (>50%) and sulfur (>60%) in the natural asphaltene remains in the coke [23,73].

All these data detract from the prior structural studies, which focused on a large central polynuclear system having pendant alkyl side chains (Fig. 2-14).

Some years ago, a novel concept was brought forth in which asphaltenes were regarded as a regular hydrocarbon polymer or even a sulfur-hydrocarbon polymer. Both polymers invoked the concept of the hydrocarbon portion being based on the sterane/hopane-type systems [79]. This concept arose because of the nature of the products obtained by reacting an asphaltene with potassium naphthalide [79]. But it was erroneously assumed that this particular organometallic reagent, one of several known to participate in rapid, complex reactions with organic substrates, cleaved only specific bonds. Potassium naphthalide, however, is less specific in terms of bond cleavage than was proposed [80]. In fact, the reaction of potassium naphthalide with tetrahydrofuran alone, under conditions that are identical to those reported where asphaltenes were also present, produces a light brown amorphous powder [81] that could erroneously be identified as a major product had any asphaltene been present.

The macromolecular structure of asphaltenes has also been subject to investigation insofar as the means by which the molecules can form a micelle is of importance to geochemists and to process chemists. X-ray analyses and molecular weight determination (see below) were the methods chosen to investigate the macromolecular structure of asphaltenes [82]. The X-ray method is well documented in its use for carbon and graphites and yields information about the dimension of the unit cell such as interlamellar distance ($c/2$), layer diameter (L_a), height of unit cell (L_c), and number of lamellae (N_c) contributing to the micelle (Fig. 2-15).

Application of another X-ray procedure, an X-ray diffraction matrix method, to the problem of determining asphaltene structure produced some novel results [83]. For example, asphaltenes (precipitated by *n*-pentane) that are soluble in decane gave histograms completely different from those obtained with the decane-insoluble material (Fig. 2-16). This suggested the existence of at least two different hydrocarbon structural types within the asphaltene fraction. Of particular interest was the more complex decane-insoluble fraction. It contained aromatic systems of much greater complexity, which actually appeared to be collections of simpler units that were actually similar to those in the lower molecular weight material, but linked head-to-tail in a cyclic system.

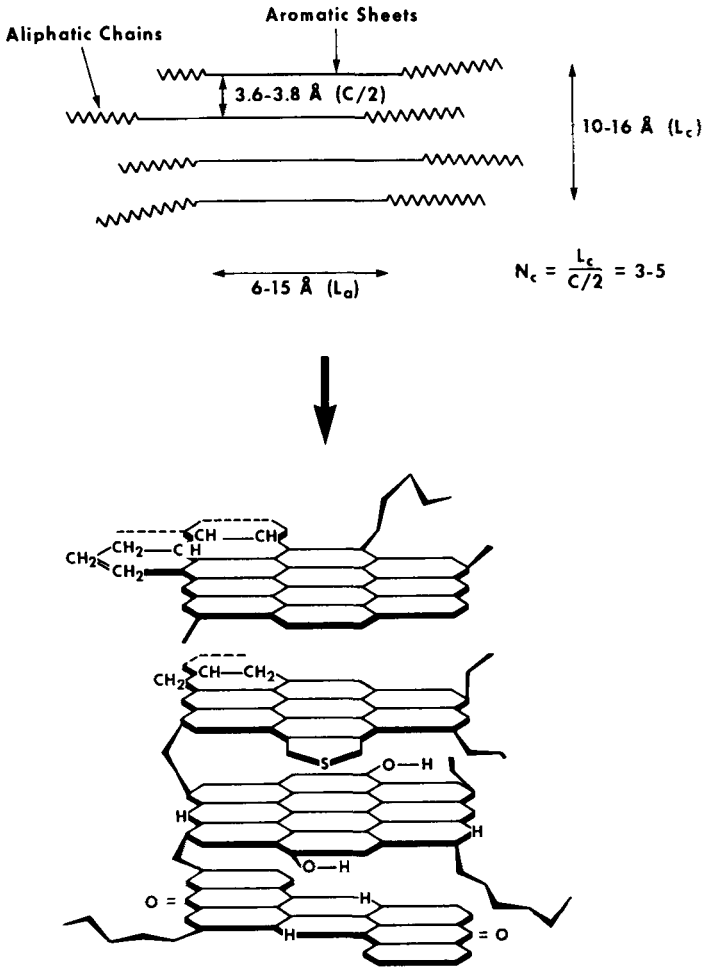

Fig. 2-15. Schematic representation of an asphaltene cluster as deduced from X-ray diffraction patterns.

This gave rise to a suggestion, similar to those of the very early studies [55, 56], that asphaltenes may actually contain smaller polynuclear systems than those derived by procedures such as nuclear magnetic resonance.

Of all of the methods applied to determining the types of polynuclear aromatic hydrocarbon systems in petroleum asphaltenes [84,85], one with considerable potential, but given the least attention, is ultraviolet spectroscopy [86].

Typically, the ultraviolet spectrum of a petroleum asphaltene shows two major regions, both with very little fine structure. Interpretation of such a spectrum can only be made in general terms. What is often not realized is that the technique can add valuable information about the degree of condensation of polynuclear aromatic ring systems through the auspices of high-performance liquid chromatography [30,

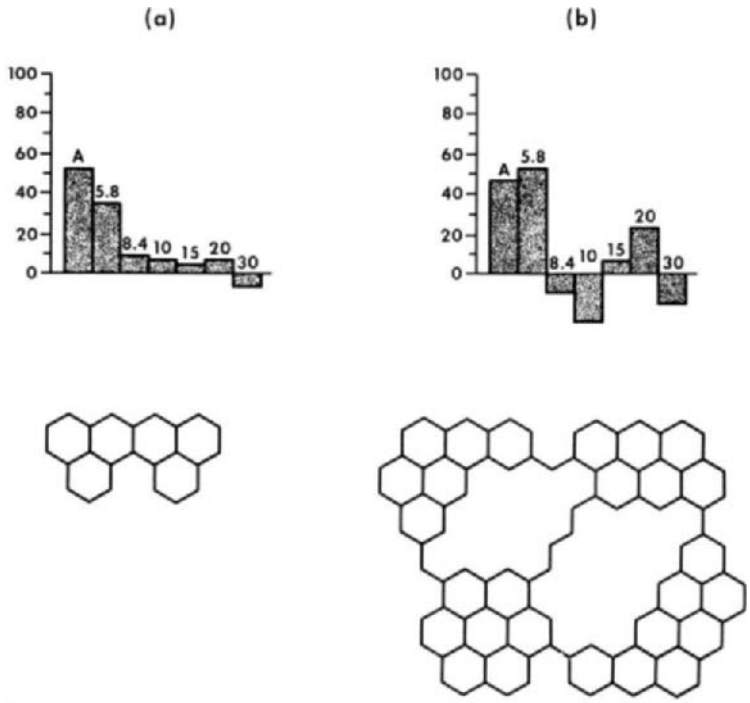

Fig. 2-16. Histograms and hypothetical aromatic units for (a) decane-soluble asphaltenes and (b) decane-insoluble asphaltenes from Athabasca bitumen. (After Speight and Moschopedis [33]; Speight [83].)

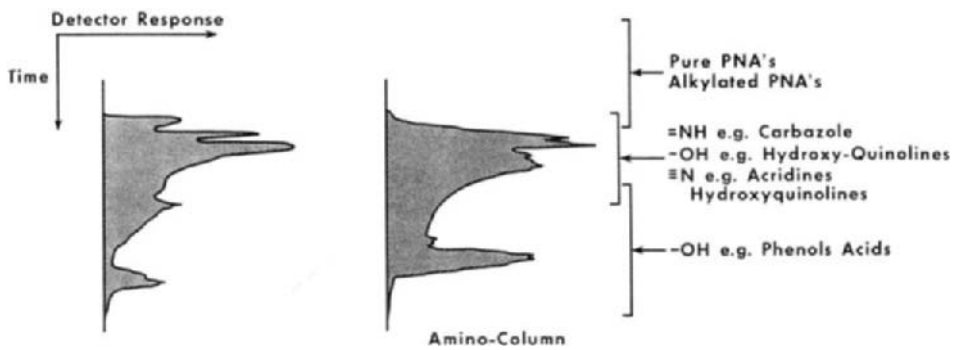

Fig. 2-17. Simplified chromatograms of two different asphaltenes by high-performance liquid chromatography.

40,86,87]. Indeed, when this approach is taken the technique not only confirms the complex nature of the asphaltene fraction (Fig. 2-17) and also allows further detailed identifications to be made of the individual functional constituents of asphaltenes.

For example, amphoteric species and basic nitrogen species contain polynuclear aromatic systems having two-to-six rings per system. On the other hand, the

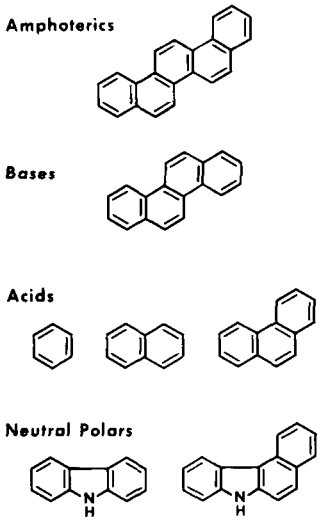

Fig. 2-18. Simplified illustration of the various ring-types in asphaltenes.

acidic subfractions (phenolic/carboxylic functions) and the neutral polar subfractions (amides/imino functions) contain few if any polynuclear aromatic systems having more than three rings per system (Fig. 2-18). In all cases, the evidence favored the preponderance of the smaller (one-to-four) ring systems [40]. But, perhaps what is more important about the results of these investigations is that the data confirm that asphaltenes are, indeed, a complex mixture of compound types (Figs. 2-11, 2-12, and 2-13). This confirms the fractionation studies and, thus, asphaltenes cannot be represented by any particular formula that is construed to be "average".

Heteroatom structures

Unfortunately, in many studies, too little emphasis has been placed on determining the nature and location of the nitrogen, oxygen, and sulfur atoms in the asphaltene structure. Proton magnetic resonance did not take into account the heteroatoms, which had to be accommodated by convenient incorporation into the hydrocarbon systems. In fact, in order to place the heteroatoms into the structures derived by proton magnetic resonance would require significant modifications of the molecular models to, perhaps, much larger structures. Indeed, this may be cited as a major disadvantage of many of the models that have been derived to date.

Studies on the disposition of nitrogen in petroleum asphaltenes indicated the existence of nitrogen as various heterocyclic types [88–97]. The more conventional types of nitrogen (from the organic chemist's viewpoint), i.e., primary, secondary, and tertiary aromatic amines, have not been established as being present in petroleum asphaltenes. There are also reports where the organic nitrogen in petroleum asphaltenes has been defined in terms of basic and nonbasic types [95]. There is evidence for the occurrence of carbazolic nitrogen in asphaltenes [90,93].

More recent assumptions include nitrogen in asphaltenes on the basis of not more than one nitrogen atom per molecule [98]. Such an assumption may be difficult to justify on a natural product basis where molecules with two or more nitrogen atoms are known. It would, however, serve as a reasonable guide for molecular studies where generalizations are often necessary.

Thermal studies have shown that only 1% of the nitrogen is lost during the thermal treatment, whereas substantially more sulfur (23%) and more of the oxygen (>40%) are lost as a result of this treatment. The tendency for nitrogen and sulfur to remain in the nonvolatile residue produced during thermal decomposition, as opposed to the relatively easy elimination of oxygen, supports the concept that nitrogen and sulfur are stable because of their location in ring systems. More recent studies [99] have brought to light the occurrence of four-ring aromatic nitrogen species in petroleum (Fig. 2-19). These findings are of particular interest because they correspond to the ring systems that have been tentatively identified by application of high performance liquid chromatography (HPLC) to the basic nitrogen fraction of asphaltenes.

Of the heteroelements in petroleum, there are more data pertaining to the locations of the oxygen atoms than to the sulfur and nitrogen atoms. The majority of the data, however, relates to the oxygen functions in blown (oxidized) asphalts and residua, which may be of little relevance to the oxygen functions in the native materials.

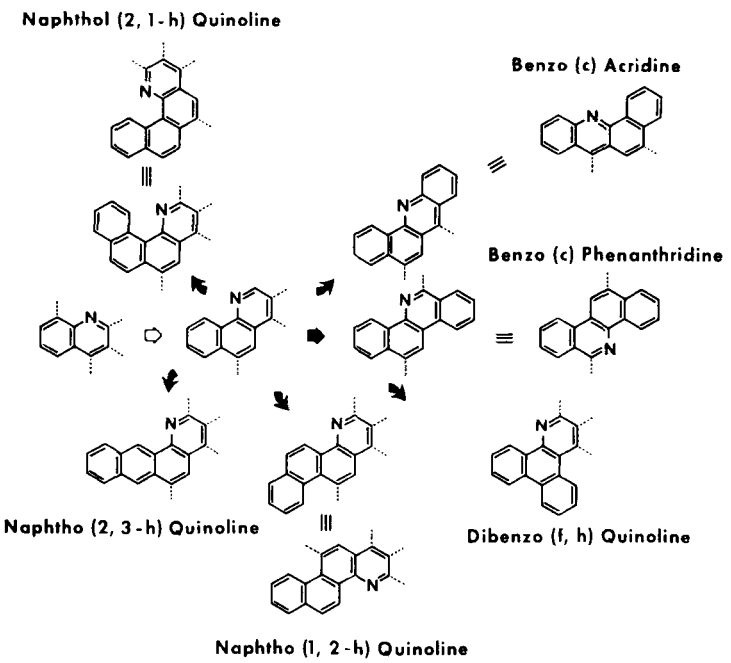

Fig. 2-19. Representative four-ring aromatic nitrogen species which occur in petroleum. (After Schmitter et al. [99].)

Oxygen has been identified in carboxylic, phenolic and ketonic locations [69,70, 95,100–103], but is not usually regarded as being located primarily in heteroaromatic ring systems. In the context of polyhydroxy aromatic nuclei existing in Athabasca asphaltenes, it is of interest to note that pyrolysis at 800°C results in the formation of resorcinols [69] implying that such functions may indeed exist in the asphaltenes.

Sulfur occurs as benzothiophenes, dibenzothiophenes and naphthenebenzothiophenes [23,54,90,95,104–108]. More highly condensed thiophene-types may also exist, but are precluded from identification by low volatility. Other forms of sulfur that occur in asphaltenes include the alkyl-alkyl sulfides, alkyl-aryl sulfides, and aryl-aryl sulfides [54].

Investigations of the size distribution of the sulfur species indicates an increase in the size of the sulfur species from aromatics to resins to asphaltenes [109].

Metals (i.e., nickel and vanadium) are much more difficult to integrate into the asphaltene system. The nickel and vanadium occur as porphyrins [8,110], but whether or not these are an integral part of the asphaltene structure is not known. Some of the porphyrins can be isolated as a separate stream from petroleum [6].

In summary, asphaltenes contain similar functionalities, but with some variation in degree [26]. For example, asphaltenes from the more paraffinic crude oils appeared (through this cursory examination) to contain less quinone and amide systems than those from the "heavy" oils.

MOLECULAR WEIGHT

Determining the molecular weights of asphaltenes is a problem, because they have a low solubility in the liquids often used for the determination. Also adsorbed resin material leads to discrepancies in molecular weight determination and precipitated asphaltenes should be reprecipitated several times prior to the determination. Thus careful precipitation and careful choice of the determination method are both very important for obtaining meaningful results [111].

A fairly comprehensive study of asphaltene molecular weights by vapor pressure osmometry has been reported and shows that the molecular weights of various asphaltenes are dependent not only on the nature of the solvent, but also on the solution temperature at which the determinations were performed (Table 2-11) [100]. Data from later work involving molecular weight determinations by the cryoscopic method [112], however, indicate that the molecular nature of asphaltenes is not conducive to the determination of absolute molecular weights by any one method.

For any one particular method, the observed molecular weights suggest that asphaltenes form molecular aggregates, even in dilute solution [114] and this association is influenced by solvent polarity, asphaltene concentration, and the temperature of the determination (Fig. 2-20) [111,112]. In fact, it is strongly recommended that, to negate the concentration effects and the temperature effects, the molecular weight determinations be carried out at each of three different concentrations at each of three different temperatures. The data for each temperature are then extrap-

TABLE 2-11

Molecular weights of petroleum asphaltenes by vapor pressure osmometry (after Moschopedis et al. [113, p. 228])

Sample era	Molecular weight						
	C_6H_6	CH_2Br_2	C_5H_5N	$C_6H_5NO_2$			
Solvent temperature (°C):	37	37	37	37[a]	100	115	130
Upper Cretaceous	2092	2010	2103	2000	1990	2050	1940
Lower Cretaceous	4850	3430	2655	2050	1890	1820	1825
	6669	4719	4221	3590	2470	2220	1920
	6415	4562	2687	1650	1550	1410	1500
	5768	4952	2736	2040	2020	1970	2060
	3977	3456	2400	2150	1860	1740	1660
	3782	3483	2829	2350	2030	1900	1990
	4904	4068	2551	2070	1790	1700	1630
	6583	5512	3179	1300	1250	1260	1220
	5886	4589	2439	1830	1700	1670	1650
Carboniferous	4766	3907	2721	2010	1880	1870	1830
	6672	3999	2898	2500	2250	2970	1960
	4174	3667	2683	2170	2090	2140	2160
Lower Devonian	4125	3864	2541	1900	1830	1890	1810

[a] Extrapolated value.

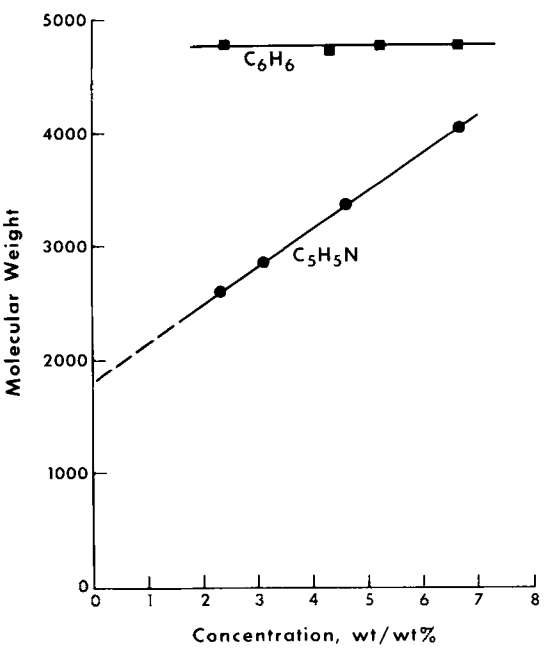

Fig. 2-20. Variation of asphaltene molecular weights with concentration. (After Moschopedis et al. [113].)

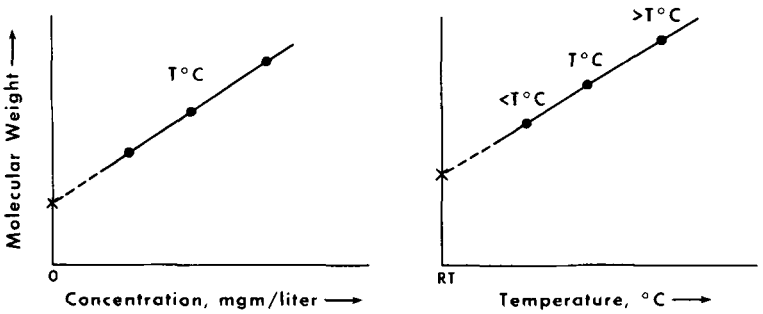

Fig. 2-21. Determination of asphaltene molecular weights to negate concentration and temperature effects.

olated to zero concentration and the zero concentration data at each temperature are then extrapolated to room temperature (Fig. 2-21) [78].

The precise mechanism of the association has not been conclusively established, but hydrogen bonding [54,115,116] and the formation of charge-transfer complexes [54] have been cited as the causative mechanisms. There is evidence that asphaltenes participate in such complexes [117,118], but the exact chemical or physical manner in which they would form in petroleum is still open to discussion. Intermolecular hydrogen-bonding could also be involved in asphaltene association and may have a significant effect on observed molecular weights [116].

The formation of strong intermolecular hydrogen bonds between amphoteric species (Fig. 2-22) is known [119]. The presence of such species in petroleum is proven [47] and must be considered a highly probable option for intermolecular bonding between asphaltene molecules.

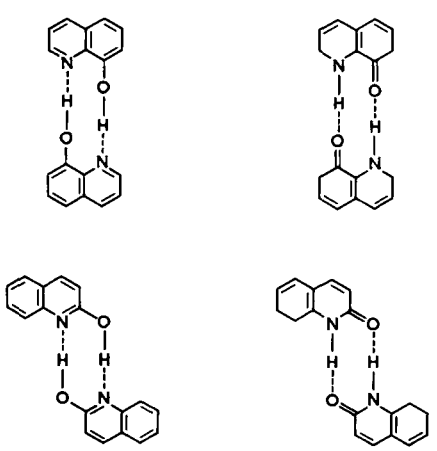

Fig. 2-22. Representation of hydrogen bonding of the amphoteric part of an asphaltene which produces stronger-than-usual hydrogen bonds.

TABLE 2-12

Variation of molecular weight of pentane-precipitated and heptane-precipitated asphaltenes

Asphaltenes	Solvent[a] (wt%)	Molecular weight			
		C_6H_6	CH_2Br_2	C_5H_5N	$C_6H_5NO_2$[b]
A. Pentane	100	4050	2730	2310	1610
Reprecipitated (×1)	93	5120	3380	2590	2010
Resin (C_5-solubles)	7	710			
Reprecipitated (×3)	89	8710	5810	–	2640
Resin (C_5-solubles)	13	797			
Pentane extracted	90	8450	6740		2820
Resin (C_5-solubles)	10	845			
B. Heptane	100	6850	4320	3580	2670
Reprecipitated (×3)	92	8560	6890	4310	2880
Resin (C_7-solubles)	8	1050			

[a] Asphaltene concentration: 2.5% w/w; temperature: 37°C.
[b] Extrapolated values from data derived at 100, 115 and 130°C.

Data from a series of asphaltene molecular weight determinations (Table 2-12) present strong evidence to support the contention that "resin" material (i.e., precipitant-soluble material) is occluded within the asphaltene matrix during the precipitation procedure. In each case, removal of this resin material gives rise to higher observed molecular weights of the "purified" asphaltenes. In addition, and as noted previously for the whole asphaltenes [113], the molecular weights of the "purified" asphaltenes also varied with the solvent used for the determination (Table 2-12); i.e., solvents of high dielectric constant decrease the observed molecular weights.

In addition, when the freshly-precipitated asphaltenes were extracted continuously (Soxhlet) with different solvents and molecular weight determinations were carried out on the insoluble material, a decrease in asphaltene molecular weight with dielectric constant of the solvent was noted (Table 2-13).

Thus, the tendency of asphaltenes to undergo association and/or dissociation depending upon the nature of the solvent also appears true for the series of higher-molecular-weight fractions. It should be noted, however, that although the results with these particular asphaltenes and with asphaltenes available from other crude oils [113,120] suggest that molecular weight varies with dielectric constant of the solvent, there may be other factors not yet investigated, which may, in part, also be responsible for this phenomenon. The final phenomenon reported here to influence the molecular weight of the asphaltene is the relative polarity of the solvent used in the precipitation technique (Table 2-14).

It is of interest to speculate at this point about the means by which the resin material is retained by the asphaltenes. For example, asphaltenes and resins have been suggested to have points of structural similarity [2,100], which is responsible

TABLE 2-13

Variation of molecular weight of insoluble fractions (Soxhlet) of pentane-precipitated asphaltenes

Asphaltenes	Solvent [a] (wt%)	Molecular weight			
		C_6H_6	CH_2Br_2	C_5H_5N	$C_6H_5NO_2$ [b]
Untreated	100	4050	2730	2310	1610
Pentane-extracted	90	8450	6740		2820
Extract	10	845			
Heptane-extracted	72	8940	7120	4380	2980
Extract	28	2310			
Hexadecane-extracted [c]	58	12490	8800		3510
Extract	42	2530			
Methylethyl ketone-extracted	93	15650		5980	3060
Extract	7	983			
3-Pentanone-extracted	65	18000		12410	6380
Extract	35	1352			
Ether-extracted	93	11370	8730		2910
Extract	7	1822			
Ethyl acetate-extracted	95	12000	8260	4270	2880
Extract	5	728			

[a] Asphaltene concentration: 2.5% w/w; temperature: 37°C.
[b] Extrapolated values from data derived at 100, 115 and 130°C.
[c] Stirred at 85°C for 24 h; insolubles separated by filtration; solubles separated by removal of the solvent in vacuo.

TABLE 2-14

Variation of asphaltene molecular weight with the dispersing solvent

Solvent	Precipitant	Asphaltene [a] molecular weight
Benzene	*n*-pentane	5120
Carbon tetrachloride	*n*-pentane	5080
Tetrahydrofuran	*n*-pentane	8840
Pyridine	*n*-pentane	13390

[a] Reprecipitated once from the solvent used for the initial precipitation.

for their affinity to each other in solution and in petroleum. As noted above, in the case of amphoteric species, there is potential for strong bonding to occur (Fig. 2-22), thereby increasing the intensity by which the resins are held to the asphaltenes and, also, by which the asphaltene molecules associate with each other thereby requiring stronger dispersing solvents to release the resins (Table 2-14).

On the other hand, asphaltenes may be analogous to coal insofar as it appears that asphaltenes have adsorption characteristics and may even exhibit a distinct physical structure or participate in clathrate-type systems. If this is the case, swelling

by a solvent such as pyridine would undoubtedly free resin material from the asphaltenes. There is the additional possibility that, if the resin material is retained purely by a surface adsorption phenomenon, it may be expected to be cleaned from the asphaltenes by the repetitive precipitation. All three effects could play a part in the retention of resin (i.e., precipitant-soluble) material by the asphaltenes.

Obviously, there are other facets of asphaltene precipitation that need to be investigated, but it is obvious from these data that it is extremely difficult to obtain "clean" (resin-free) asphaltenes without a multiple precipitation technique. Whereas the amount of resin may have some influence on the asphaltene yield (and, therefore, on an estimation of crude oil composition), the resin occluded within (or adsorbed on to) the asphaltene during the separation procedure have a considerable effect on the observed molecular weight and, presumably, on the degree of association of the asphaltenes. Indeed, the speculative concept that asphaltenes release the final vestiges of this resin only upon swelling by a solvent such as pyridine is also worthy of consideration.

If this subsection were to be summarized succinctly, it could be stated that asphaltene molecular weights are truly variable. Data produced from the determinations using highly polar solvents, however, indicate that the molecular weights, in solvents that prevent association, usually fall into the range 2000 ± 500! There is some support for this conclusion from mass spectrometry studies [121], but caution is advised when using mass spectrometry especially where the volatility of the sample is critical to the conclusions. Failure to recover all of the material and the formation of a thermal residue in the system [23] can remove not only the more polar species, but also the higher-molecular-weight species.

MOLECULAR MODELS

Some researchers, in addition to deriving broad generalities from the use of various analytical techniques, are attempting to assign specific molecular configurations to the asphaltene constituents. It must be remembered, however, that, within any one petroleum, a variety of structures exist in the asphaltene fraction (in which there is a decided hydrogen deficiency), but the close relationships of the various hydrocarbon series comprising the asphaltenes, resins, and oils give rise to much overlapping of fractions into neighboring series, both in molecular weight and in the H/C atomic ratio.

Nevertheless, the overall goal of the structural studies, by which the molecular models are derived, should not be merely the derivation of a model for asphaltenes, but should be the use of the model to predict the behavior of asphaltenes in processing. The model then fills a very useful function, that of being able to predict conversion chemistry and physics, which is, perhaps, the sole reason for the existence of the model.

A major constraint in the acceptance of a variety of hypothetical, or average, structures for asphaltenes is the validity of the proposed structures in terms of the complex maturation process (Fig. 2-23). During this maturation process, original

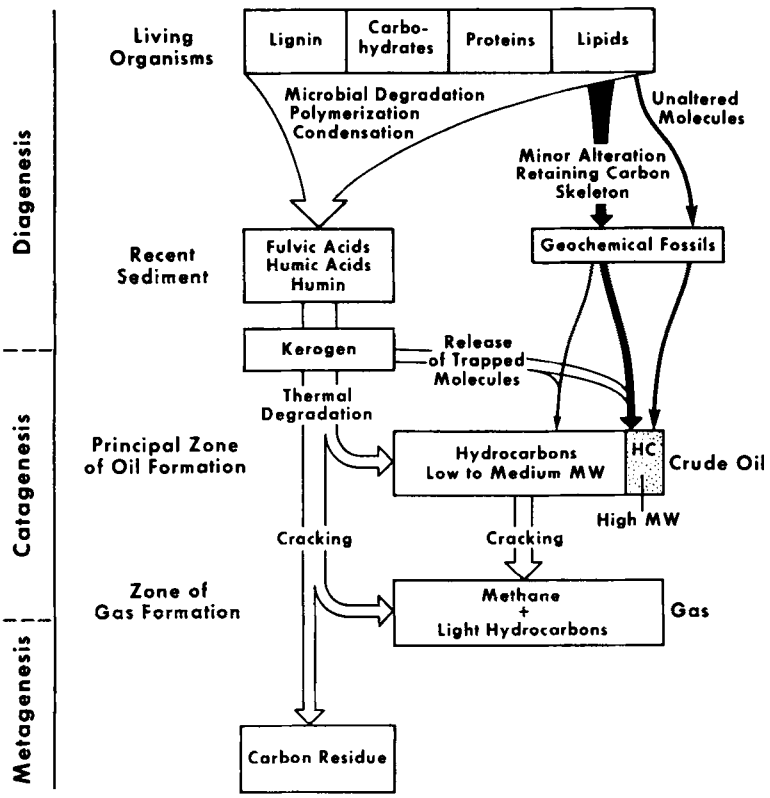

Fig. 2-23. Schematic representation of the petroleum maturation process. (After Tissot and Welte [122].)

molecules may remain unchanged or may be modified as they become part of petroleum (Fig. 2-24) [122]. In addition, the character of the volatile fragments produced during a thermal assay as well as the character of the heteroatoms (nitrogen, oxygen and sulfur) casts serious doubts upon the authenticity of the hypothetical large polynuclear aromatic systems that have been postulated as being a truly representative of the asphaltene structure.

Highly-condensed polynuclear aromatic structures, that have been used to explain the high yields of thermal coke from asphaltenes, are not consistent with the natural product origins of petroleum asphaltenes. Such entities would require conditions of temperature and pressure for their formation that are more extreme than those currently recognized as being responsible for petroleum maturation. On this note, it must be remembered that many natural products contain small polynuclear aromatic systems and that large polynuclear aromatic systems are not usually found in nature in the types of source materials that were considered [123–125].

The concept of an asphaltene model that uses smaller polynuclear aromatic systems would be more in keeping with the types of polynuclear aromatic systems that occur in nature. This assumes that there have not been any severe changes

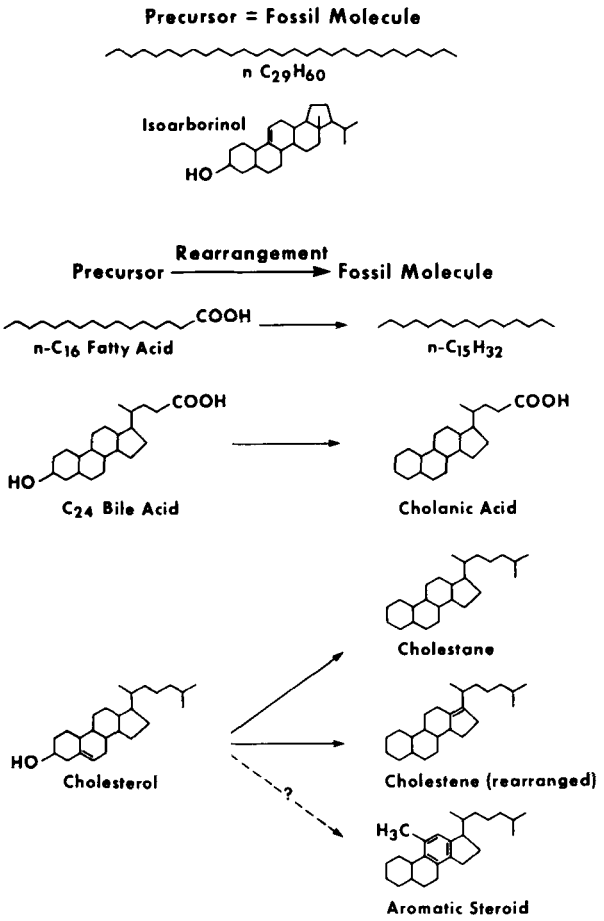

Fig. 2-24. Illustration of the chemical changes that can occur in the maturation process. (After Tissot and Welte [122].)

to the skeletal structures of these systems during geologic time and under geologic conditions [122]. Any changes are presumed to involve reaction of the aromatic ring systems with each other. This is not achieved by condensation to form the large polynuclear aromatic ring systems, but by coupling directly through the agency of ring-to-ring carbon bonds or by the involvement of sulfur, oxygen, and aliphatic hydrocarbon moieties. This type of model also allows for the incorporation of hydroaromatic systems into the asphaltene molecule. Hydroaromatic systems might not be expected to exist under the conditions that produce large polynuclear aromatic systems and justification of their existence in such a model might be difficult.

Every attempt should also be made to design a model that is in agreement with the chemical and physical effects that exist in the natural product field [126,127]. Acceptance of any other premises may be self-defeating.

It is pertinent here to recognize that the simpler aromatic systems that are known to exist in nature and have been identified in unpolluted sediments [122]. Indeed, the sterane ring system, which can aromatize to polynuclear aromatic systems, is well known. Considering the sterane ring systems, it is preferable that the asphaltene polynuclear aromatic systems are based on the angular (i.e., phenanthrene) system than on the linear (i.e., anthracene) system [128].

If functionality is a requirement, polyhydroxyaromatics, such as gallic acid and ellagic acid, as well as polyhydroxyquinones are also common in nature [125]. Amide and carbazole types have also been recognized in natural product systems [125] as has nitrogen in many alkaloid systems [123].

Sulfur (as thiophene-type sulfur) is more difficult to identify and its presence in the biological systems (other than the sulfur in the amino acids cysteine and methionine) is still speculative, although there are means by which inorganic (mineral) sulfur can be incorporated into petroleum as organic sulfur [129–131].

It is also worthy of note here that asphaltenes have been postulated to contain charged species within their structure [95], which, of course, may be analogous to the occurrence of zwitterion structures in proteins and peptides [119].

On this basis, perhaps it is preferable to define asphaltenes in terms of natural product systems (Table 2-15) that have undergone some chemical change over the geologic time and under the prevailing local conditions where the burial occurred. Such systems support more the "recognized" maturation pathways than any of the structures heretofore conceived.

These observations require some adjustments to the previous postulates of the asphaltene structure. Thus, previously conceived structures where the sole aromatic system is a large polynuclear alkylated system are considered to be unlikely in view of the aforementioned data and reasoning in spite of their frequent occurrence in the literature. Actually, the current evidence is indicative of a much more "open"

TABLE 2-15

Speculative vestiges of natural product molecules that are present in petroleum asphaltenes

1. Hydrocarbons
   - paraffinic chains
   - aromatic ring systems
   - inter-ring alkyl chains
2. Heteroatoms
   - pyridinic nitrogen
   - carbazolic nitrogen
   - phenolic oxygen
   - carbonyl oxygen
   - sulfidic sulfur
   - thiophenic sulfur
3. Metals
   - porphyrinic
   - nonporphyrinic

(rather than highly condensed) structure. On this basis, a key structural feature of petroleum asphaltenes is the occurrence of small polynuclear aromatic systems, thiophenic systems, and paraffinic moieties within the asphaltene "molecule".

The manner in which these moieties appear within the asphaltene "molecule" must for the present remain largely speculative but, above all, it must be remembered that asphaltenes are a solubility class and, as such, may be assumed to be an accumulation of (literally) thousands of structural entities. But caution is advised against combining a variety of identified products into one (albeit hypothetical) structure.

One area where the large polynuclear aromatic systems have been assumed to be essential in the models is the high yields of coke formed from the asphaltenes. In support of the formation of a nonvolatile residue (coke) being formed from small condensed ($\leq$6) ring systems rather than requiring a large condensed aromatic ring system, it is worthy of note that heat-resistant polymers containing aromatic and heterocyclic units such as polyquinolines and polyquinoxalines have a strong tendency to form large condensed systems during pyrolysis that will finally carbonize [132]. Obviously, there are a series of, as yet, undefined primary and secondary reactions that play a role in the formation of coke!

The thermal decomposition of organic species has been the subject of many studies [133–140]. The technique usually requires sealing the compound in a tube followed by heating for a required period of time. By this means, a valuable series of thermal characteristics were derived for a variety of compounds.

In general, the data show that polynuclear aromatic systems produce high yields of coke or carbon residue. The occurrence of heteroatoms in the aromatic rings can have a variable effect. There are general indications, however, that most heteroatom species, especially nitrogen compounds, show an increase in the coke yield relative to the corresponding hydrocarbons.

More recent work over a period of years [41] has attempted to bring the coke formation from aromatic species, as it relates to petroleum, into the correct perspective, i.e., by actual use of the carbon residue test equipment and conditions. In the smaller polynuclear aromatic systems, volatility of the model compound is a major factor in determining the yield of the carbon residue. Hydrocarbons of low-molecular-weight, say less than 350, tend to distill, or even sublime, and fail to produce a significant amount of a carbon residue. By suitable and cautious choice of a range of aromatic systems, however, it was possible to investigate the factors that influence the formation and yield of carbon residue as it is produced in the test.

In general, and in agreement with the previous work, the lower volatility of the polynuclear heterocyclic systems caused the production of higher yields of coke in the carbon residue test [41], relative to their hydrocarbon analogs. In addition, various porphyrins gave carbon residues in the 35–90% w/w range. It was also noted that when mixtures of model compounds were treated in the carbon residue test, the potential for interaction between the components, e.g., hydrogen bonding, had a beneficial effect on the yield of the carbon residue. That is, increases in the yield of the carbon residue were noted over the predicted values.

Carbon residue formation, as evidenced by the carbon residue test, is not only a

function of molecular size but also a function of aromaticity, heteroatom content, and intermolecular interactions.

Thus, in more complex molecules such as asphaltenes, where secondary reactions could, in part, negate the volatility effect, it is evident that large polynuclear aromatic systems are not necessary to produce the high yields of coke from asphaltenes. Therefore, asphaltene formulae that are designed around smaller polynuclear aromatic hydrocarbon systems, which are more in greater agreement with the natural product origins of petroleum, are also consistent with the formation of high yields of carbon residue.

The danger in all of these studies is in attempting to link together fragmented molecules produced during, and identified as products of, thermal investigations into a structure that is believed to be real. Functionality and polynuclear aromatic ring systems are real, but combination of these parameters into one or even several structures can be misleading.

Molecular models can be an excellent aid to understanding process chemistry and physics. As long as the model allows predictability of process behavior, use of the model is warranted; however, caution is advised. Because of the complexity of the asphaltene fraction, there is no one method that will guarantee the development of a suitable molecular model.

The effort must be multidimensional taking into account all of the properties and characteristics of the material. Extreme caution is advised when average structures are used. Averages can be misleading especially when molecular weight data can be a major limitation to the development of the average structure [89].

Indeed, even when a multidimensional approach is employed for derivation of a model, there is no guarantee that the model is a true reflection of the molecular types in the asphaltene fraction. It must also be recognized that any model developed may not be the only, or final, answer to the problem. As techniques improve and knowledge evolves, so must the model.

Recognition of the fact that it is not possible to compose a model that represents all of the properties of asphaltenes is a major achievement. The molecular size, as deduced from molecular weight measurements, prohibits this. It is more preferable to design models that are representative of the various constituent fractions of an asphaltene.

For example, models that could better explain the asphaltene behavior should be selected from the various parts of the molecular weight-polarity diagram. The easiest would be to select the two extremes of this diagram and design highly polar and neutral species. This would be the amphoteric and substantially less polar (or near neutral) constituents of asphaltenes [44,48,84].

On the basis of the above concept, the constituents would have smaller polynuclear aromatic systems and would also span the range of functional types as well as molecular sizes (Figs. 2-25 and 2-26). It must be emphasized, however, that these models are mere representations of molecular configurations and are to be used here for discussion only. Similar models can be derived for different asphaltenes that are more in agreement with the elemental and molecular parameters derived by any of the aforementioned physical methods.

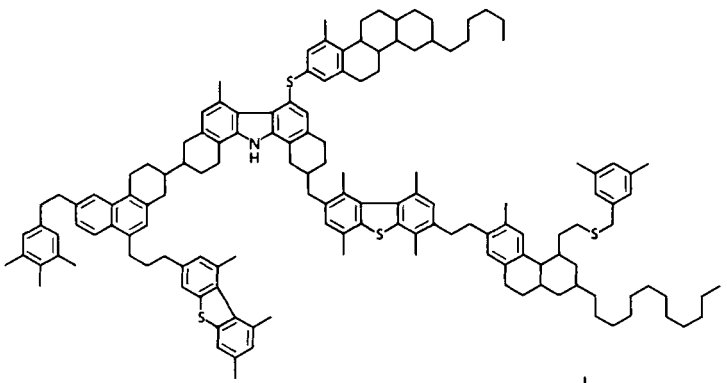

C: 84.5%
H: 8.6%
N: 0.7%
O: <0.1%
S: 6.2%
Mol. Wt.: 2060
Carbon Residue (Calc.) ≈ 45-50%
H/C: 1.22

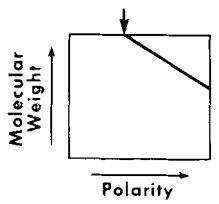

Fig. 2-25. Schematic representation of an alternate model for a neutral polar asphaltene.

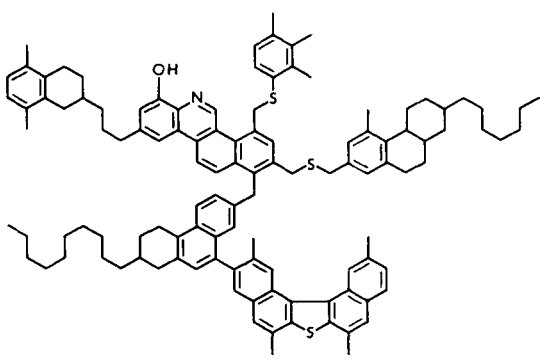

C: 84.3%
H: 8.0%
N: 0.8%
O: 0.9%
S: 8.0%
Mol. Wt.: 1637
Carbon Residue (Calc.) ≈ 50-55%
H/C: 1.14

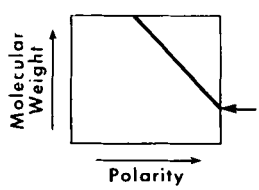

Fig. 2-26. Schematic representation of an alternate model for an amphoteric asphaltene.

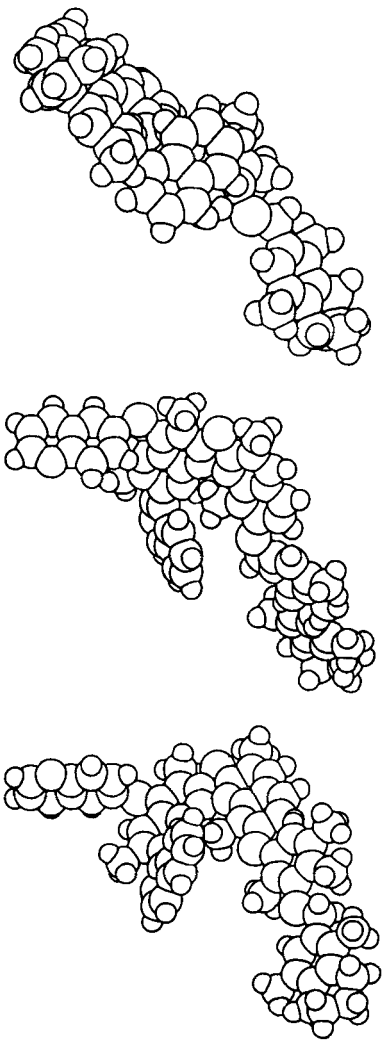

Fig. 2-27. Molecular model of the structure shown in Fig. 2-26 looking at the model from different angles.

Such models would not only have to be compatible with the other constituents of petroleum but also be able to represent the thermal chemistry and other process operations. It must also be recognized that although such models can have the large size dimensions that have been proposed for asphaltenes, they can also be "molecular chameleons" insofar as they can vary in dimensions depending upon the angle of rotation about an axis (Fig. 2-27) and/or the freedom of rotation about one, or more, of the bonds. This type of knowledge could be very important in the design of process catalysts [16].

The models also allow an "open structure" not previously conceived for models

of petroleum asphaltenes. Such a structure also promotes the idea of a three-dimensional system for asphaltenes rather than a large, polynuclear aromatic system which, excluding the side chains, is predominantly planar. Parallel with the development of these models for petroleum asphaltenes, came the suggestion that asphaltenes separated from kerogen bitumen have a much more "open" structure, consisting of smaller polynuclear systems (Fig. 2-28) than previously believed, as is the structure of kerogen itself [35,141,142].

Finally, preliminary data from the investigation of the resin fraction supports the concept of such systems throughout the nonvolatile portion of petroleum. The data were strongly indicative of similar polynuclear aromatic systems as found in the asphaltenes. This would certainly support the suggestion of Koots and Speight [2] that asphaltenes and resins, from a particular crude oil, have several structural and/or functional similarities that allow preferential association in solution and in petroleum [100].

The manner in which these moieties occur within the asphaltene fraction must, for the present, remain largely speculative. Above all, it must be remembered that asphaltenes are a solubility class and, as such, may be an accumulation of thousands of (similar/dissimilar) structural entities. Hence, caution is advised against combining a range of identified products into one (albeit hypothetical) structure. For example, it would be presumptuous to suggest, on the basis of thermal studies, that petroleum asphaltenes are a polymeric analogue of alkyl benzenes and/or naphthalenes, and/or phenanthrenes, and/or benzothiophenes, and/or dibenzothiophenes, and/or, etc.

ASPHALTENES IN PETROLEUM

The means by which the asphaltenes remain dispersed in the oil medium has been the subject of much speculation, not only by geochemists but also by process chemists and engineers. Molecular interaction of the type cited above (i.e., hydrogen bonding and charge-transfer complexation) could have a potentially significant effect on the yields of coke that are formed during thermal processing [41].

An early hypothesis of the physical structure of petroleum (Fig. 2-29) [143] suggested that asphaltenes are the centers of micelles formed by adsorption, or even by absorption of part of the maltenes, that is, resin material, onto the surfaces or into the interiors of the asphaltene particles. Thus, most of those substances with greater molecular weight and with the most pronounced aromatic nature are situated closest to the nucleus and are surrounded by lighter constituents of lesser aromatic nature. The transition of the intermicellular (dispersed or oil) phase is gradual and almost continuous. Continued attention to this aspect of asphaltene chemistry has led to the assumption that asphaltenes exist as clusters within the micelle. This arises mainly because of the tendency for asphaltenes to associate in dilute solution in solvents of low polarity and from possible misinterpretation of viscosity data [113]. The presence of asphaltene "stacks" in the solid phase, as deduced from X-ray diffraction patterns [50] also seemed to support the concept of widespread existence of asphaltene clusters in the micelle.

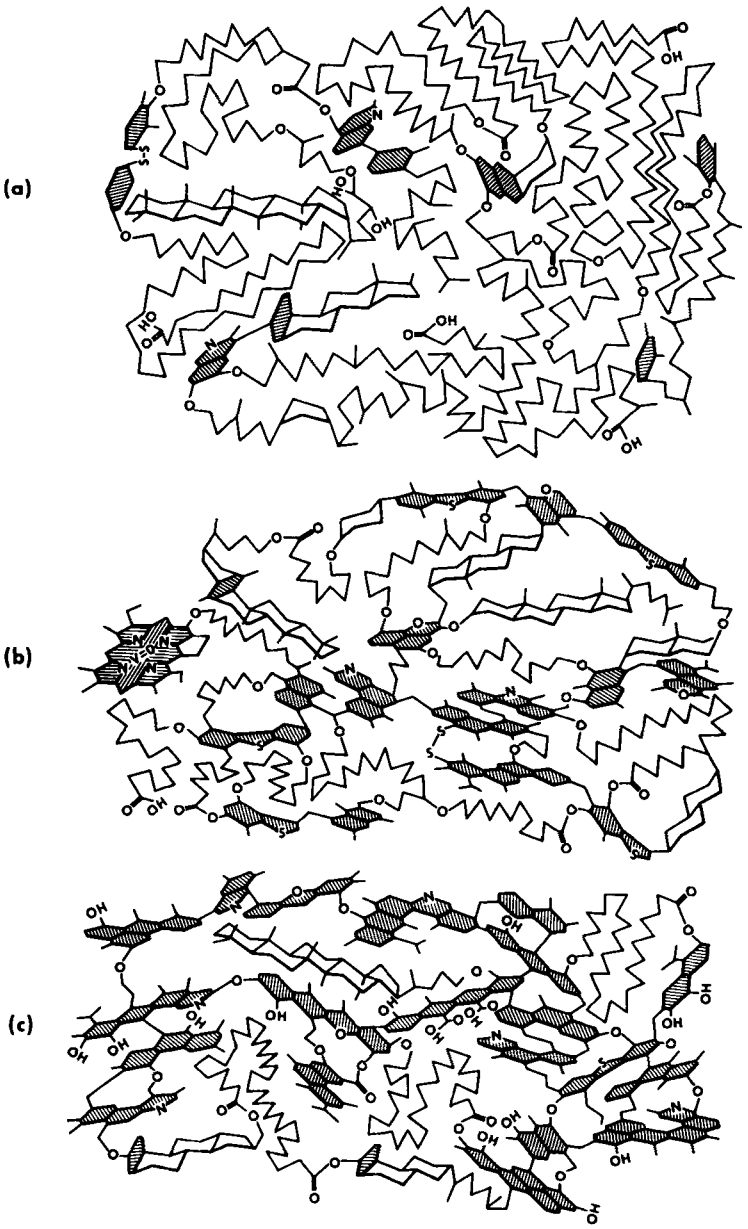

Fig. 2-28. Generalized models of the asphaltenes from (a) Type I kerogen, (b) Type II kerogen, and (c) Type III kerogen. (From Behar and Vandenbroucke [35].)

Asphaltenes are, in fact, insoluble in the oil fraction [2,144], but it is now clear that the asphaltene dispersion is mainly attributable to the resins. In fact, it is possible to bring about dispersion of asphaltenes in their corresponding oil fractions only by addition of resins. The general indications are that the degree of aromaticity of,

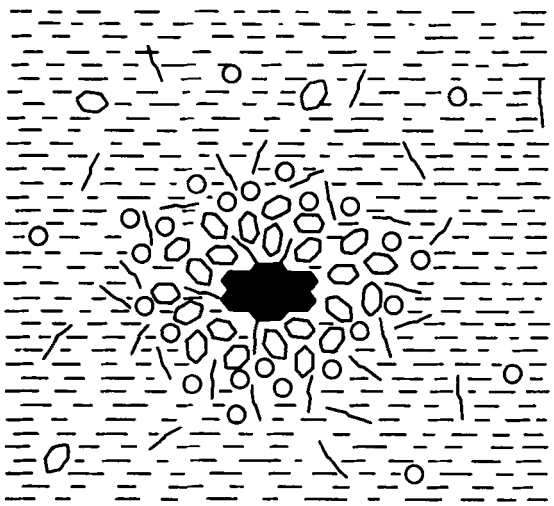

Fig. 2-29. Schematic representation of the physical structure of petroleum. (After Pfeiffer and Saal [143].)

and the proportion of heteroelements in, the resins appear to play an important part in the ability of these materials to bring about solubility of the asphaltenes in an oil. Furthermore, if the added resins are less aromatic than the natural resins, asphaltenes will not disperse. For resins where the aromaticity is equal to that of the natural resins, those having higher heteroelement content are better for dispersion purposes.

The evidence available in the literature appears to indicate that the hydrocarbon structures and some features, such as the various condensed ring systems, in different petroleums are similar (from the asphaltenes and resins to the constituents of the oil fraction). The variety of source materials involved in petroleum genesis, however, implies that, on an individual molecular scale, there may be substantial structural differences among the constituents of the various crude oils and bitumens.

Furthermore, the difficulty with which resins from one crude oil peptize (as in the case of a colloid, the terms peptization, dispersion, and solubilization are often used interchangeably to describe the means by which asphaltenes exist within petroleum) asphaltenes from a different crude oil, and the instability of the "blend" [2] can be construed as evidence for the occurrence of significant structural differences among the asphaltenes and resins of various crude oils.

The asphaltenes appear to be the final (excluding carbenes and carboids, those organic fractions of petroleum that are insoluble in toluene or benzene) condensation product as indicated from oxidation where the scheme of reaction is [116]:

oils $\longrightarrow$ resins $\longrightarrow$ asphaltenes

A relatively high degree of aromaticity is generally prevalent in the asphaltenes

and the resins. But in some resins, the hydrocarbons show an increase in aliphatic material (more side chains, for example) until, with considerable saturation, the oils, which contain numerous alkyl chains of varying length, are reached. The degree of aromaticity is important when the resins are desorbed. High aromaticity of the maltenes (i.e., that part of petroleum remaining after the asphaltenes have been removed, often referred to as the deasphalted oil) indicates good solvency for the asphaltenes, and the solvent power of the maltenes is one of the most important factors in determining the physicochemical behavior of the petroleum colloid system.

Petroleum is a complex system, therefore, with each fraction being dependent upon other systems for complete mobility and solubility [2]. It is presumed that the resins associate with the asphaltenes in the manner of an electron donor-acceptor. Also there could well be several structural similarities between the asphaltenes and resins that would have an adverse effect on the ability of the resins to associate with asphaltenes from a different crude oil [2,100].

The concept of hydrogen-bonding interactions being one of the means of association between the asphaltenes and resins has, however, led to a reconsideration of the assumed cluster as part of the micelle. Indeed, it appears that when resins and asphaltenes are present together, hydrogen-bonding may be one of the mechanisms by which resin-asphaltene interactions are achieved. Resin-asphaltene interactions are preferred over asphaltene-asphaltene interactions [100]. If the same intermolecular forces are projected to petroleum, it would perhaps not be surprising that asphaltenes exist not as larger agglomerations, but as single entities that are peptized, and effectively dispersed, by the resins.

It is now considered more likely, therefore, that the micelle in petroleum consists of a single asphaltene molecule, rather than a stack of asphaltene molecules, surrounded (peptized, dispersed) by resin molecules.

PROCESS CHEMISTRY

There have been many attempts to react asphaltenes to produce a variety of nonfuel products [145,146]. But perhaps the most important reactions in the current context are thermal reactions and the manner in which they relate to thermal and catalytic refining options [24]. It is known that asphaltenes will produce significant quantities of distillable liquids in thermal processes (Table 2-16) but the presence of significant quantities of thermal coke in the products has always been an issue.

Understanding the refining chemistry from the behavior of model compounds, however, under refining conditions is not as straight forward as it may appear [68]. There have been several attempts to generalize the nature of the reaction (Fig. 2-30) but none have been totally adequate.

The individual reactions occurring in an extremely complex mixture and the "interference" of the products from some of the constituents with those from other constituents of the mixture is unpredictable. Hence, caution is advised when applying the data from model compound studies to the behavior of petroleum and,

TABLE 2-16

Thermal decomposition of Athabasca asphaltenes (after Speight [147, p. 57])

Products	Heating rate	
	rapid (20°C min^{-1})	slow (2°C min^{-1})
Light oil (yield, wt%)	35.2	43.9
Resins (yield, wt%)	4.5	4.5
Coke (yield, wt%)	48.4	49.0
Gases (wt% — by difference)	11.9	2.9
(wt% — found)	11.2	2.3

Loss of heteroelements during cracking

	Loss (% w/w)	
	rapid heating	slow heating
Oxygen	81.3	80.1
Nitrogen	1.0	1.0
Sulfur	23.4	17.1

especially, the molecularly complex heavy oils. These latter have few, if any, parallels in organic chemistry.

The limitations of processing heavy oils and residua depend, to a large extent, on the amount of higher-molecular-weight constituents (in the present context, the asphaltenes) present in the feedstock [16,148–150] which are responsible for high yields of thermal and catalytic coke (Fig. 2-31).

The thermal decomposition of petroleum asphaltenes has received some attention [69,70,77,151–155], but special attention has been given to the nature of the volatile products of asphaltene decomposition mainly because of the difficulty of characterizing the nonvolatile coke. It has been noted that the organic nitrogen in the asphaltenes invariably undergoes thermal reaction to concentrate in the nonvolatile coke (Fig. 2-32) [72,156].

Thus, although asphaltenes produce high yields of thermal coke, little is known of the actual chemistry of coke formation. In a more general scheme, the chemistry of asphaltene coking has been suggested to involve the thermolysis of thermally-labile bonds to form reactive species, which then react with each other (condensation) to form coke (Fig. 2-33).

In a mixture as complex as a residuum or heavy oil, the reaction processes can only be generalized because of difficulties in analyzing the products and the feedstock, molecules of which have an intricate and complex nature. The formation of coke from the higher-molecular-weight and polar constituents of a given feedstock is detrimental to process efficiency and to catalyst performance. A key to increasing the conversion efficiency is to develop a better understanding of the principal coke-formers, the asphaltenes [78].

It has been generally assumed that the chemistry of coke formation has involved immediate condensation reactions to produce higher-molecular-weight, condensed

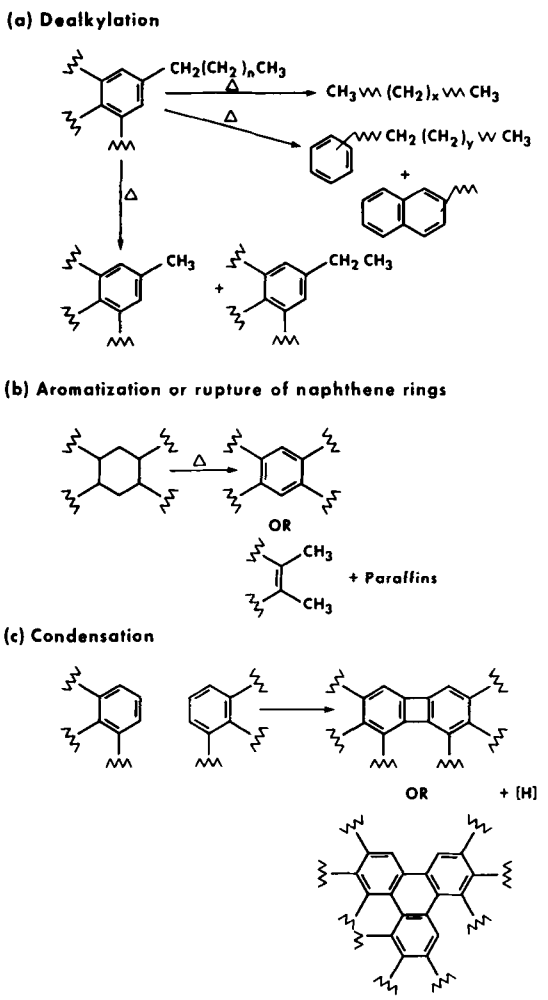

Fig. 2-30. Generalized (until lately!) representation of the thermal decomposition of asphaltenes. (After Speight [3, p. 220].)

aromatic species. The initial reactions in the coking of petroleum feedstocks that contain asphaltenes involve the thermolysis of aromatic-alkyl systems to produce volatile species (paraffins, olefins) and nonvolatile species (aromatics) [78].

It is also known that nitrogen species not only concentrate in the coke [72,158] but also contribute to the pattern of the thermolysis [78]. For example, the presence of nitrogen in ring systems appears to enhance the activity of adjacent carbon-hydrogen or carbon-carbon bonds to thermolysis [133].

If it can be assumed that heterocyclic nitrogen will play a similar role in the thermolysis of asphaltenes, the initial reactions will, therefore, involve thermolysis of aromatic-alkyl bonds that are enhanced by the presence of heterocyclic nitrogen. An

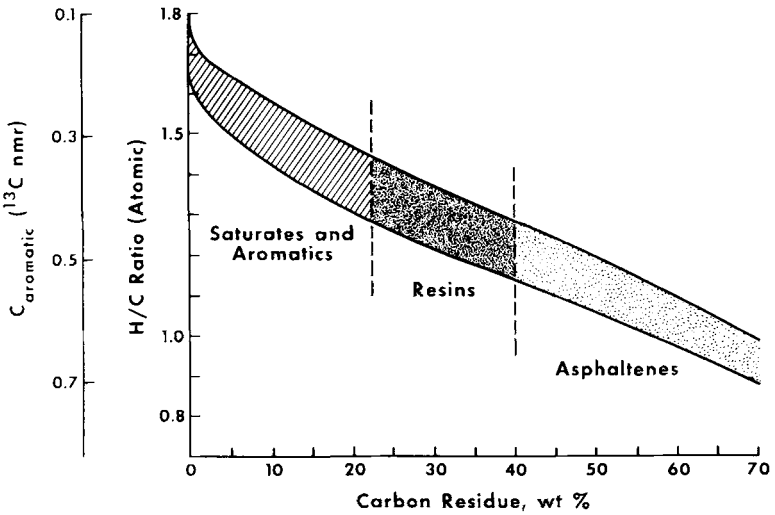

Fig. 2-31. Relationship of H/C atomic ratio to carbon residue for a range of petroleum fractions. (After Speight [157].)

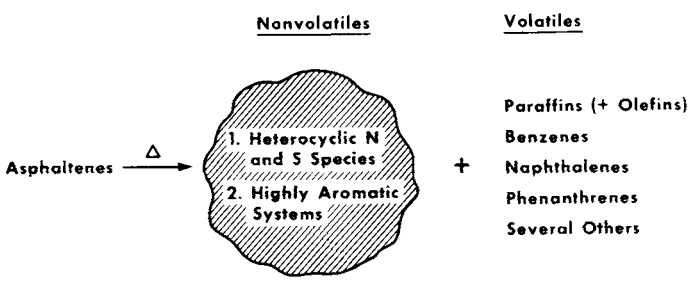

Fig. 2-32. Generalized representation of asphaltene decomposition.

ensuing series of secondary reactions such as aromatization of naphthenic species and condensation of the aromatic ring systems will then lead to the production of coke.

Thus, the initial step in the formation of coke from asphaltenes (and the resins) is the formation of volatile and nonvolatile hydrocarbon fragments and nonvolatile heteroatom-containing systems. In short, it is the polar species that react preferentially to initiate the thermal decomposition process. The highly aromatic, highly polar (refractory) products then separate from the surrounding oil medium as an insoluble phase and proceed to form coke [152–154].

This situation may be likened to the deasphalting process in which a paraffinic liquid is added to the petroleum to cause the asphaltenes to separate. Only in this case, the liquid hydrocarbon is the result of the thermal decomposition of the asphaltene molecules and is formed in situ. At the same time, the asphaltene nuclear fragments become progressively more polar as the paraffinic fragments are stripped from the

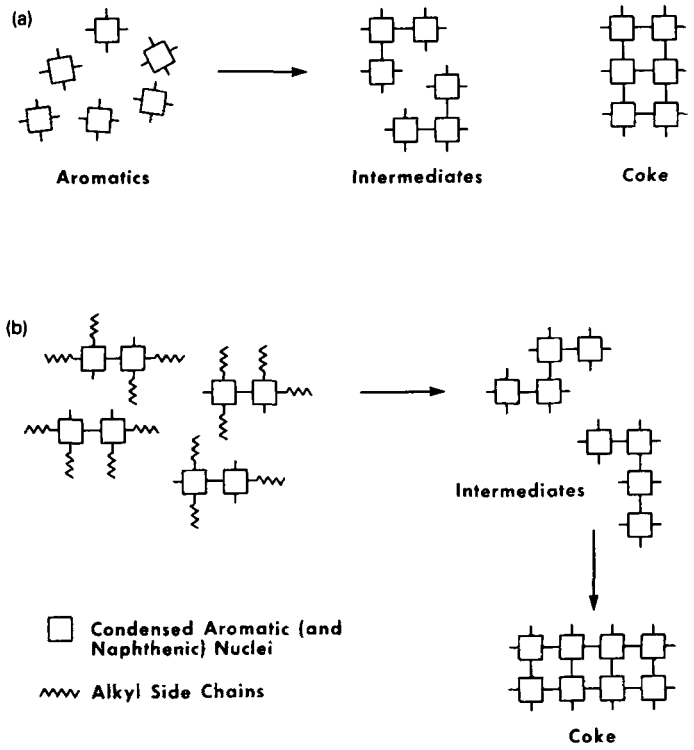

Fig. 2-33. Simplified representation of the formation of coke from (a) simpler aromatics and (b) more complex aromatics such as asphaltenes.

ring systems by scission of the bonds (preferentially) between the carbon atoms alpha and beta to the aromatic rings. In summary, the solubility parameter of the liquid medium is decreased whereas, at the same time, the solubility parameter of the polar aromatic species is increased. Hence, insolubility of the polar aromatics ensues.

Petroleum may be visualized as a three-phase system (Fig. 2-34). In this system, the two liquid phases are aromatics and saturates, whereas the asphaltenes exist as a soluble phase. As the liquid becomes progressively more paraffinic (i.e., less aromatic) in nature, the asphaltenes become progressively less soluble. Finally, insolubility, or separation of the polar species from the liquid phase, occurs and coking ensues.

Another point is worthy of consideration is the solubility parameter of petroleum fractions. Little is known about the solubility parameter data for petroleum. There has been a noteworthy attempt to define the solubility parameter ranges for different fossil fuel liquids (Fig. 2-35) [159]. As an extension of this concept, there is now sufficient fragmented data in the literature to draw an approximate correlation between H/C atomic ratio and the solubility parameter, δ, for hydrocarbons and the constituents of the lower-boiling fractions of petroleum (Fig. 2-36).

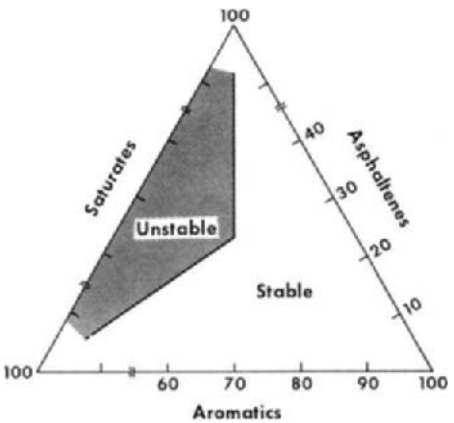

Fig. 2-34. Simplified representation of petroleum as a three-phase system; asphaltene cracking produces saturate products, whereas the asphaltene itself becomes more aromatic and more polar. The "stable" zone is decreased and the "unstable" zone is increased on a relative basis. The aromatic products are "encouraged" to precipitate.

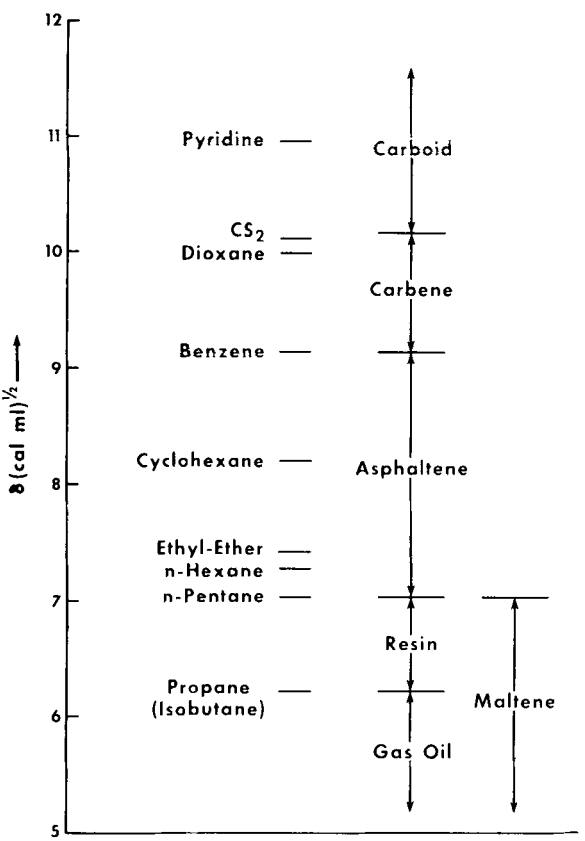

Fig. 2-35. Representation of the solubility parameters for organic solvents and various petroleum fractions. (After Yen [159].)

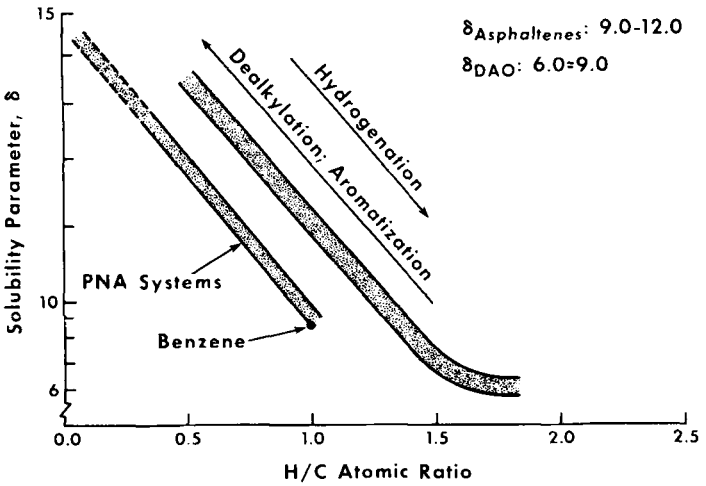

Fig. 2-36. Relationship of the solubility parameter, δ, to the H/C atomic ratio.

It is also known [41] that hydrocarbon solvents can dissolve polynuclear hydrocarbons where there is, usually, less than a three-point difference between the lower-solubility parameter of the solvent and the higher-solubility parameter of the solute. From these data, a parallel, or near parallel, line can be assumed that allows the solubility parameters of the asphaltenes and resins to be estimated (Fig. 2-36).

Thus, the solubility parameter of asphaltenes can be estimated to fall in the 9–12 range which is in agreement with the asphaltenes being composed of a mixture of different compounds types with the accompanying variation in polarity. Removal of alkyl side chains from the asphaltenes will decrease the H/C ratio and increase the solubility parameter thereby bringing about a concurrent decrease of the solubility of the asphaltene product in the hydrocarbon solvent.

If the models, used as examples in this work, can be used as a guide to the process chemistry, it should be anticipated that there might be some initial fragmentation and aromatization (Figs. 2-37 and 2-38). Indeed, data available (Table 2-17) suggest that this does occur. The isolatable products from the early stages of asphaltene decomposition are more aromatic than the original asphaltenes and have a slightly reduced molecular weight. By definition and character [78], these are carbenes. The next step will be the more complete fragmentation of the asphaltenes to produce the carboids which are, by definition through solubility, the true precursors to coke.

There is also the distinct possibility that there will be some reactions that occur almost immediately with the onset of heating. Such reactions will most certainly include the elimination of carbon dioxide from carboxylic fragments and, perhaps, even intermolecular coupling through phenolic moieties. There may even be "prompt" reactions that occur almost immediately. In other words, these are reactions that are an inevitable consequence of the nature of the asphaltene. Example of such reactions are the rapid aromatization of selected hydroaromatic rings to create a more aromatic asphaltene.

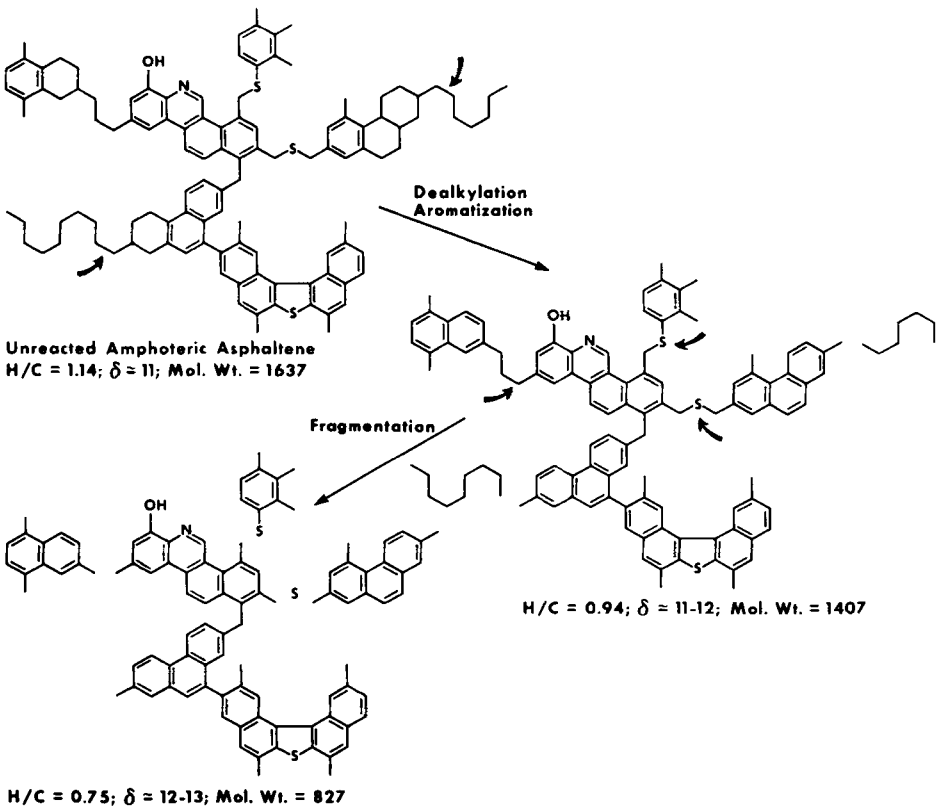

Fig. 2-37. Schematic representation of the use of an amphoteric molecule to study the chemistry of coking.

TABLE 2-17

Atomic H/C ratios and molecular weights of the pyridine-soluble products (carbenes) from the thermolysis of asphaltenes at various temperatures (after Speight [78, p. 414])

Temperature (°C)	H/C atomic	C_A [a]	Molecular weight
untreated	1.237	0.45	1890
300	1.114	0.52	1700
350	1.109	0.55	1650
400	1.009	0.61	1580
500	0.987	0.66	1610
600	0.913	0.70	1640

[a] Fraction of carbon in aromatic locations as deduced by ^{13}C NMR.

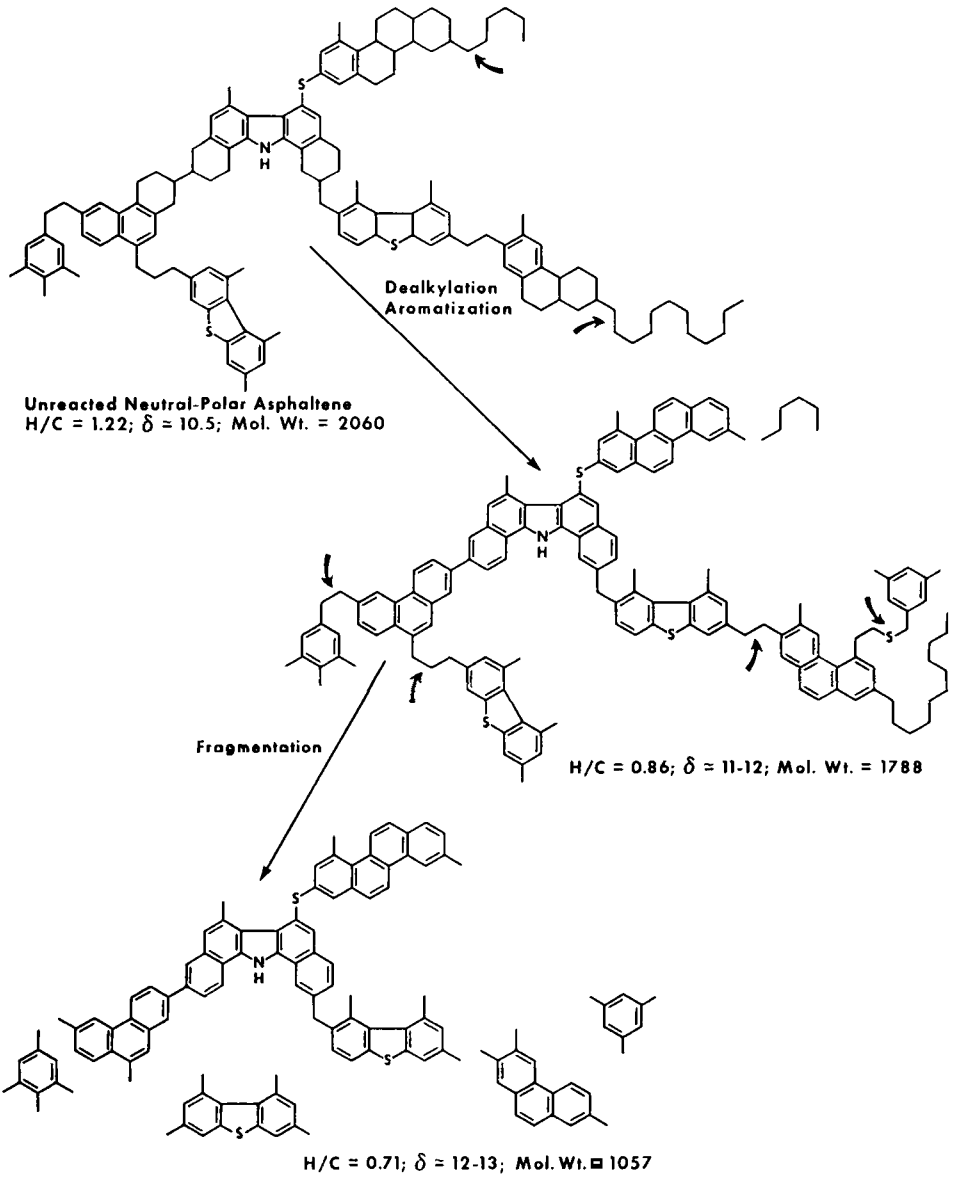

Fig. 2-38. Schematic representation of the use of a neutral polar molecule to study the chemistry of coking.

Whereas such reactions will, obviously, play a role in coking, the precise role is difficult to define. Decarboxylation and the reactions of phenol moieties are not believed to be a major force in the coking chemistry. Perhaps, it is the immediate aromatization of selected, or all of the, hydroaromatic systems that renders inter-

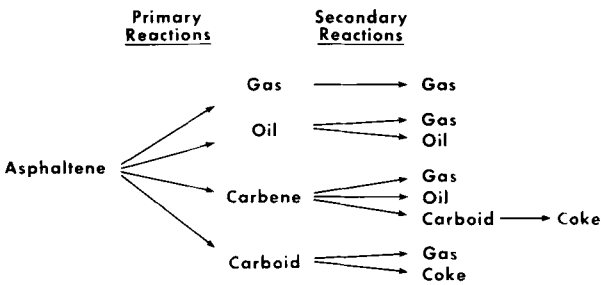

Fig. 2-39. Schematic representation of the formation of thermal products form asphaltenes. Other tertiary reactions such as the formation of naphthas, middle distillates, and gas oils from the "oil" fraction are not included in this model.

and intramolecular hydrogen management difficult and coke formation a relatively simple operation.

Many of these reactions (Fig. 2-39) may occur simultaneously and it may be difficult to factor the driving force in the coking reaction. What does appear to be certain, is that true formation of coke, insofar as a product is produced that is at least 90% by weight carbon, does not occur until insolubility has ensued!

One additional corollary to this work is that conventional models of petroleum asphaltenes (which, in spite of evidence to the contrary, invoked the concept of a large polynuclear aromatic system) offer little, if any, explanation of the intimate events involved in the chemistry of coking. Models, which invoke the concept of asphaltenes being a complex solubility class with molecular entities being composed of smaller polynuclear aromatic systems, are more in agreement with the present data.

It is also interesting to note that whereas the aromaticity of the asphaltenes is approximately equivalent to the yield of thermal coke (Fig. 2-31), not all of the original aromatic carbon in the asphaltenes form coke. Volatile aromatic species are eliminated during thermal decomposition and it must be assumed that some of the original aliphatic carbon plays a role in coke formation. The precise nature of this is to be determined but the process can be represented as involving multichemical reactions (Fig. 2-39). Little has been acknowledged here of the role of low-molecular-weight polar species (resins) in coke formation. It is worthy of note, however, that the resins are presumed to be lower-molecular-weight analogues of the asphaltenes. This being the case, similar reaction pathways may apply.

Thus, it is now considered more likely that molecular species within the asphaltene fraction, which contain nitrogen and other heteroatoms (and have lower volatility than the pure hydrocarbons), are the prime movers in the production of coke [78]. Such species, containing various polynuclear aromatic systems, would be denuded of the attendant hydrocarbon moieties and would undoubtedly be insoluble [86,160,161] in the surrounding hydrocarbon medium. The next step would be gradual carbonization of such entities to form coke [152,153,154].

The use of a catalytic process for the conversion of high-asphaltene feedstocks adds another dimension to asphaltene science. Asphaltenes will interact with cata-

lysts, especially acidic support catalysts through the basic nitrogen, just as they will interact with adsorbents. The means by which they do so is another issue, but evidence is available for interaction at a single functional group in which the remainder of the asphaltene molecule remains in the liquid phase. There is also a less desirable option in which the asphaltene reacts with the catalyst at several points of contact causing a more massive lay-down of coke on the catalyst surface [16].

REFERENCES

[1] Gruse, W.A. and Stephens, D.R., *The Chemical Technology of Petroleum*. McGraw-Hill, New York, N.Y., 675 pp. (1960).
[2] Koots, J.A. and Speight, J.G. *Fuel*, 54: 179 (1975).
[3] Speight, J.G., *The Chemistry and Technology of Petroleum*. Marcel Dekker, New York, N.Y. (1980).
[4] Speight, J.G., *Fuel Science and Technology Handbook*. Marcel Dekker, New York, N.Y., 1193 pp. (1990).
[5] Pfeiffer, J.H., *The Properties of Asphaltic Bitumen*. Elsevier, Amsterdam, 285 pp. (1950).
[6] Branthaver, J.F., in: J.G. Speight (Editor), *Fuel Science and Technology Handbook*. Marcel Dekker, New York, N.Y., p. 83 (1990).
[7] Filby, R.H. and Branthaver, J.F., *Complexes in Fossil Fuels, ACS Symposium Series 344*. American Chemical Society, Washington, D.C., 436 pp. (1987).
[8] Yen, T.F., *The Role of Trace Metals in Petroleum*. Ann Arbor Science Publishers, Ann Arbor, Mich., 221 pp. (1975).
[9] Eisma, E. and Krom, C.J., *J. Inst. Pet., London*, 37: 582 (1951).
[10] Hubbard, R.L. and Stanfield, K.E., *Anal. Chem.*, 20: 460 (1948).
[11] Marcusson, J., *Mitt. Materialprufungsant.*, 36: 209 (1918).
[12] Nellensteyn, F.J., *Chem. Weekblad*, 28: 313 (1931).
[13] Nellensteyn, F.J. and Roodenburg, N.M., *Chem.-Zeitung*, 545: 819 (1930).
[14] Sachanen, A., *Pet. Zeitung*, 21: 1441 (1925).
[15] Speight, J.G., *The Chemistry and Technology of Petroleum*. Marcel Dekker, 2nd ed., New York, N.Y., 760 pp. (1991).
[16] Speight, J.G., in: S. Kaliaguine and A. Mahay (Editors), *Catalysis on the Energy Scene*. Elsevier, Amsterdam, p. 515 (1984).
[17] Ali, L.H. and Al-Ghannan, K.A., *Fuel*, 60: 1043 (1981).
[18] Andersen, S.I. and Birdi, K.S., *Fuel Sci. Technol. Int.*, 8: 593 (1990).
[19] Girdler, R.B., *Proc. Assoc. Asphalt Paving Technol.*, 34: 45 (1965).
[20] Mitchell, D.L. and Speight, J.G., *Fuel*, 52: 149 (1973).
[21] van Nes, K. and van Westen, H.A., *Aspects of the Constitution of Mineral Oils*. Elsevier, Amsterdam, 484 pp. (1951).
[22] Ali, L.H., Al-Ghannam, K.A. and Al-Rawi, J.M., *Iraqi J. Sci.*, 26: 41 (1985).
[23] Speight, J.G. and Pancirov, R.J., *Liq. Fuels Technol.*, 2: 287 (1984).
[24] Speight, J.G., *Annu. Rev. Energy*, 11: 253 (1986).
[25] Roberts, I., *Am. Chem. Soc., Div. Petrol. Chem., Prepr.*, 34(2): 251 (1989).
[26] Speight, J.G., Paper presented at the Am. Chem. Soc. Meet., Div. Geochem., New York, August 23–28 (1981).
[27] Yan, T.Y., *Fuel*, 69: 1062 (1990).
[28] *Annual Book of ASTM Standards, Standards D-189 and D-524, Vol. 05.01*. American Society for Testing and Materials, Philadelphia, Pa. (1991).
[29] Speight, J.G., *Alberta Res. Counc., Inf. Ser.*, No. 84 (1979).
[30] Monin, J.C. and Pelet, R., in: M. Bjoroey (Editor), *Advances in Organic Geochemistry*. John Wiley and Sons, New York, N.Y. (1983).

[31] Nellensteyn, F.J., in: A.E. Dunstan, A.W. Nash, B.T. Brooks and H.T. Tizzard (Editors), *The Science of Petroleum, Vol. IV*. Oxford University Press, Oxford, p. 2760 (1938).
[32] Hotier, B. and Robin, M., *C.R. Acad. Sci. Paris, Sér. 2*, 292: 39 (1981).
[33] Speight, J.G. and Moschopedis, S.E., in: J.W. Bunger and N.C. Li (Editors). *Chemistry of Asphaltenes*. American Chemical Society, Washington, D.C., p. 1 (1981).
[34] Speight, J.G., *Alberta Res. Counc., Inf. Ser.*, No. 81 (1978).
[35] Behar, F. and Vandenbroucke, M., *Rev. Inst. Fr. Pét.*, 41: 173 (1986).
[36] Bestougeff, M.A. and Darmois, R., *C.R. Acad. Sci. Paris*, 224: 1365 (1947).
[37] Bestougeff, M.A. and Darmois, R., *C.R. Acad. Sci. Paris*, 227: 129 (1948).
[38] Bestougeff, M.A. and Mouton, Y., *Bull. Liaison Lab. Pont. Chaus.*, Spec. Vol., 79 pp. (1977).
[39] Dron, R., Bestougeff, M.A. and Voinovitch, I.A., *Laboratoire Central des Ponts et Chaussées, Rapp. Rech., LPC No. 75*. Ministère de l'Equipement et de l'Amengement du Territoire, Paris (1978).
[40] Speight, J.G., *Am. Chem. Soc., Div. Pet. Chem., Prepr.*, 31(4): 818 (1986).
[41] Speight, J.G., Unpublished data (1978) and continuing investigations.
[42] Speight, J.G., in: B.P. Tissot (Editor), *Characterization of Heavy Crude Oils and Petroleum Residues*. Editions Technip, Paris, p. 32 (1984).
[43] Altgelt, K.H., *J. Appl. Polymer Sci.*, 9: 3389 (1965).
[44] Long, R.B., in: J.W. Bunger and N. Li (Editors), *The Chemistry of Asphaltenes. Advances in Chemistry Series 195*. American Chemical Society, Washington, D.C., p. 17 (1981).
[45] Gould, K.A., Grenoble, D.C., Murrell, L.L. and Peters, W.J.M., *U.S. Patent 4,422,929* (December 27, 1983).
[46] Selucky, M.L., Kim, S.S., Skinner, F. and Strausz, O.P., in: J.W. Bunger and N.C. Li (Editors), *The Chemistry of Asphaltenes. Advances in Chemistry Series 195*. American Chemical Society, Washington, D.C., p. 83 (1981).
[47] Francisco, M.A. and Speight, J.G., *Am. Chem. Soc., Div. Fuel. Chem., Prepr.*, 29(1): 36 (1984).
[48] Long, R.B., *Am. Chem. Soc., Div. Pet. Chem., Prepr.*, 24(4): 891 (1979).
[49] Bestougeff, M.A., *Chem. Ind.*, 60: 137 (1948).
[50] Dickie, J.P. and Yen, T.F., *Anal. Chem.*, 39: 1847 (1967).
[51] Erdman, J.G., *ASTM, Spec. Publ.* 389: 259 (1965).
[52] Speight, J.G., *Appl. Spectrosc. Rev.*, 5: 211 (1972).
[53] Yen, T.F., *Am. Chem. Soc., Div. Pet. Chem., Prepr.*, 17(4): F102 (1972).
[54] Yen, T.F., *Energy Sources*, 1: 447 (1974).
[55] Hillman, E. and Barnett, B., *Proc. 4th Annu. Meet. ASTM*, 37(2): 558 (1937).
[56] Murphy, B., *J. Inst. Pet., London*, 31: 475 (1945).
[57] Ali, L.H., Al-Ghannam, K.A. and Al-Rawi, J.M., *Fuel*, 69: 519 (1990).
[58] Bandurski, E., *Energy Sources*, 6: 47 (1982).
[59] Dickinson, E.M., *Fuel*, 59: 290 (1980).
[60] Haley, G.A., *Anal. Chem.*, 44: 580 (1972).
[61] Sadeghi, K.M., Sadeghi, M.A., Wu, W.H. and Yen, T.F., *Fuel*, 68: 782 (1989).
[62] Yen, T.F. and Erdman, J.G., *Am. Chem. Soc., Div. Pet. Chem., Prepr.*, 7(3): 99 (1962).
[63] Yen, T.F., *Fuel*, 49: 134 (1970).
[64] Yen, T.F., *Am. Chem. Soc., Div. Fuel. Chem., Prepr.*, 15(1): 57 (1971).
[65] Sawatsky, H., Boyd, M.L. and Montgomery, D.S., *J. Inst. Pet., London*, 53: 162 (1967).
[66] Witherspoon, P.A. and Winniford, R.S., in: B. Nagy and U. Colombo (Editors), *Fundamental Aspects of Petroleum Geochemistry*. Elsevier, New York, N.Y., p. 261 (1967).
[67] Ebert, L.B., *Fuel Sci. Technol. Int.*, 8: 563 (1990).
[68] Ebert, L.B., Mills, D.R. and Scanlon, J.C., *Am. Chem. Soc., Div. Pet. Chem., Prepr.*, 32(2): 419 (1987).
[69] Ritchie, R.G.S., Roche, R.S. and Steedman, W., *Fuel*, 58: 523 (1979).
[70] Ritchie, R.G.S., Roche, R.S. and Steedman, W., *Chem. Ind.*, 25 (1979).
[71] Simm, I. and Steedman, W., *Fuel*, 59: 669 (1980).
[72] Speight, J.G., *Fuel*, 49: 76 (1970).
[73] Speight, J.G., *Fuel*, 50: 102 (1971).

[74] Farcasiu, M., Forbus, T.R. and LaPierre, R.B., *Am. Chem. Soc., Div. Pet. Chem., Prepr.*, 28: 279 (1983).
[75] Gallegos, E.J., *Chromatogr. Sci.*, 19: 177 (1981).
[76] Paul, P.R., *Trends Anal. Chem.*, 1: 237 (1982).
[77] Schucker, R.C. and Keweshan, C.F., *Am. Chem. Soc., Div. Fuel Chem., Prepr.*, 25: 155 (1980).
[78] Speight, J.G., *Am. Chem. Soc., Div. Pet. Chem., Prepr.*, 32(2): 413 (1987).
[79] Ignasiak, T., Kemp-Jones, A.V. and Strausz, O.P., *J. Org. Chem.*, 42: 312 (1977).
[80] Holy, N.L., *Chem. Rev.*, 74: 243 (1974).
[81] Speight, J.G. and Moschopedis, S.E., *Fuel*, 59: 440 (1980).
[82] Yen, T.F., Erdman, J.G. and Pollack, S.S., *Anal. Chem.*, 33: 1587 (1961).
[83] Speight, J.G., *Proc. Natl. Sci. Found. Symp., Fund. Org. Chem., Coal*, Knoxville, Tenn., p. 125 (1975).
[84] Speight, J.G. and Long. R.B., in: R.H. Filby (Editor), *Atomic and Nuclear Methods in Fossil Energy Research*. Plenum Press, New York, N.Y., 295 pp. (1982).
[85] Tissot, B.P. (Editor), *Characterization of Heavy Crude Oils and Petroleum Residues*. Editions Technip, Paris, 524 pp. (1984).
[86] Bjorseth, A., *Handbook of Polycyclic Aromatic Hydrocarbons*. Marcel Dekker, New York, N.Y., 727 pp. (1983).
[87] Lee, M.L., Novotny, M.S. and Bartle, K.D., *Analytical Chemistry of Polycyclic Aromatic Compounds*. Academic Press, New York, N.Y., 462 pp. (1981).
[88] Ball, J.S., Latham, D.R. and Helm, R.V., *J. Chem. Eng. Data*, 4: 167 (1959).
[89] Boduszynski, M., *Liq. Fuels Technol.*, 2: 211 (1984).
[90] Clerc, R.J. and O'Neal, M.J., *Anal. Chem.*, 33: 380 (1961).
[91] Helm, R.V., Latham, D.R., Ferrin, C.R. and Ball, J.S., *Chem. Eng. Data, Ser.*, 2: 95 (1957).
[92] Jacobson, J.M. and Gray, M.R., *Fuel*, 66: 749 (1987).
[93] Moschopedis, S.E. and Speight, J.G., *Am. Chem. Soc., Div. Pet. Chem., Prepr.*, 24(4): 1007 (1979).
[94] Moschopedis, S.E., Hawkins, R.W. and Speight, J.G., *Fuel*, 60: 397 (1981).
[95] Nicksic, S.W. and Jeffries-Harris, M.J., *J. Inst. Pet., London*, 54: 107 (1968).
[96] Schmitter, J.M., Ignatiadis, I. and Arpino, P.J., *Geochim. Cosmochim. Acta*, 47: 1975 (1983).
[97] Sinninghe Damste, J.S., Eglinton, T.I., and de Leeuw, J.W., *Am. Chem. Soc., Div. Fuel Chem., Prepr.*, 36(2): 710 (1991).
[98] Guiochon, G., in: G.C. Crump (Editor), *Petroanalysis '81*. John Wiley and Sons, Chichester (1982).
[99] Schmitter, J.M., Garrigues, P., Ignatiadis, I., De Vazelhes, R., Perin, F., Ewald, M. and Arpino, P., *Org. Geochem.*, 6: 579 (1984).
[100] Moschopedis, S.E. and Speight, J.G., *Fuel*, 55: 187 (1976).
[101] Moschopedis, S.E. and Speight, J.G., *Fuel*, 55: 334 (1976).
[102] Petersen, J.C., Barbour, F.A. and Dorrence, S.M., *Proc. Assoc. Asphalt Paving Technol.*, 43: 162 (1974).
[103] Speight, J.G. and Moschopedis, S.E., *Am. Chem. Soc., Div. Pet. Chem., Prepr.*, 26(4): 907 (1981).
[104] Rose, K.D. and Francisco, M.A., *J. Am. Chem. Soc.*, 110: 637 (1988).
[105] Sinninghe Damste, J.S., Eglinton, T.I., de Leeuw, J.W., and Schenck, P.A., *Geochim. Cosmochim. Acta*, 53: 873 (1989).
[106] Sinninghe Damste, J.S., Rijpstra, W.I.C., Kock-van Dalen, A.C., de Leeuw, J.W., and Schenck, P.A., *Geochim. Cosmochim. Acta*, 53: 1343 (1989).
[107] George, G.N., Gorbaty, M.L., and Keleman, S.R., in: W.L. Orr and Curt M. White (Editors), *Geochemistry of Sulfur in Fossil Fuels*. American Chemical Society, Washington, D.C., p. 220 (1990).
[108] Strausz, O.P., Lown, E.M., and Payzant, J.D., in: W.L. Orr and C.M. White (Editors), *Geochemistry of Sulfur in Fossil Fuels*. American Chemical Society, Washington, D.C., p. 366 (1990).
[109] Hausler, D.W., *Spectrochim. Acta*, 40B: 389 (1985).
[110] Baker, E.W., in: G. Eglinton and M.T.J. Murphy (Editors), *Organic Geochemistry*. Springer-Verlag, New York, N.Y., p. 464 (1969).

[111] Speight, J.G., Wernick, D.L., Gould, K.A., Overfield, R.E., Rao, B.M.L. and Savage, D.W., *Rev. Inst. Fr. Pét.*, 40: 51 (1985).
[112] Speight, J.G. and Moschopedis, S.E., *Fuel*, 56: 344 (1977).
[113] Moschopedis, S.E., Fryer, J.F. and Speight, J.G., *Fuel*, 55: 227 (1976).
[114] Winniford, R.S., *J. Inst. Pet., London*, 9: 215 (1963).
[115] Acevedo, S., Mendez, B., Rojas, A., Larisse, I. and Rivas, H., *Fuel*, 64: 1741 (1985).
[116] Moschopedis, S.E. and Speight, J.G., *Proc. Assoc. Asphalt Paving Technol.*, 45: 78 (1976).
[117] Penzes, S. and Speight, J.G. *Fuel*, 53: 192 (1974).
[118] Speight, J.G. and Penzes, S., *Chem. Ind.*, p. 729 (1978).
[119] Lehninger, A.L., *Biochemistry*. Worth, New York, N.Y., 833 pp. (1970).
[120] Ali, M.F. and Saleem, M., *Fuel Sci. Technol. Int.*, 6: 541 (1988).
[121] Storm, D.A., DeCanio, S.J., DeTar, M.M. and Nero, V.P., *Fuel*, 69: 735 (1990).
[122] Tissot, B.P. and Welte, D.H., *Petroleum Formation and Occurrence*. Springer-Verlag, New York, N.Y., 538 pp. (1978).
[123] Dalton, D.R., *The Alkaloids*. Marcel Dekker, New York, N.Y., 789 pp. (1979).
[124] Tyman, J.H.P., *Chem. Soc. Rev.*, 8: 499 (1979).
[125] Weiss, V. and Edwards, J.M., *The Biosynthesis of Aromatic Compounds*. John Wiley and Sons, New York, N.Y., 728 pp. (1980).
[126] Cantor, C.R. and Schimmel, P.R., *Biophysical Chemistry. Parts I, II, and III*. W.H. Freeman and Co., San Francisco, Calif., 1371 pp. (1980).
[127] Stryer, L., *Biochemistry*. W.H. Freeman and Co., New York, N.Y., 949 pp. (1981).
[128] Fieser, L.F. and Fieser, M., *Natural Products Related to Phenanthrene*. Reinhold, New York, N.Y., 704 pp. (1949).
[129] Hobson, G.D. and Pohl, W., *Modern Petroleum Technology*. Applied Science Publishers, London, 996 pp. (1973).
[130] Orr, W.L., *Am. Chem. Soc., Div. Fuel Chem., Prepr.*, 22(3): 86 (1977).
[131] Orr, W.L. and Sinnighe Damste, J.S., in: W.L. Orr and C.M. White (Editors),*Geochemistry of Sulfur in Fossil Fuels. Symposium Series No. 429*. American Chemical Society, Washington, D.C., p. 2 (1977); *Am. Chem. Soc., Div. Fuel Chem., Prepr.*, 22(3): 86 (1990).
[132] Dussel, H.J., Recca, A., Kolb, J., Hummerl, D.O. and Stille, J.K., *J. Anal. Appl. Pyr.*, 3: 307 (1982).
[133] Fitzer, E., Meuller, K. and Schaefer, W., *Chem. Phys. Carbon*, 7: 237 (1971).
[134] Hurd, C.D., *The Pyrolysis of Carbon Compounds*. Monograph Series, American Chemical Society, Washington, D.C., 278 pp. (1929).
[135] Lewis, I.C., *Carbon*, 18: 191 (1980).
[136] Lewis, I.C. and Singer. L.S., *Chemistry and Physics of Carbon*, 17: 1 (1981).
[137] Mochida, I., Tamaru, K., Korai, Y., Fujitsu, H. and Takeshita, K., *Carbon*, 20: 231 (1982).
[138] Singer, L.S. and Lewis, I.C., *Carbon*, 2: 115 (1964).
[139] Singer, L.S. and Lewis, I.C., *Carbon*, 5: 373 (1967).
[140] Swarc, M., *Chem. Rev.*, 47: 75 (1950).
[141] Siskin, M., Brons, G. and Payack, J.F., *Am. Chem. Soc., Div. Pet. Chem., Prepr.*, 32(1): 75 (1987).
[142] Siskin, M., Brons, G. and Payack, J.F., *Energy Fuels*, 1: 100 (1987).
[143] Pfeiffer, J.P. and Saal, R.N., *Phys. Chem.*, 44: 139 (1940).
[144] Swanson, J.M., *J. Phys. Chem.*, 46: 141 (1942).
[145] Moschopedis, S.E. and Speight, J.G., in: T.F. Yen (Editor), *Shale Oil, Tar Sands, and Related Fuel Sources. Advances in Chemistry Series 151*. American Chemical Society, Washington, D.C., p. 144 (1976).
[146] Speight, J.G., *Neftekhimiya*, 23(2): 147 (1984).
[147] Speight, J.G., *Am. Chem. Soc., Div. Pet., Soc., Prepr.*, 15(1): 57 (1971).
[148] LePage, J.F. and Davidson, M., *Rev. Inst. Fr. Pét.*, 41: 131 (1986).
[149] Speight, J.G., *The Desulfurization of Heavy Oils and Residua*. Marcel Dekker, New York, N.Y., 213 pp. (1981).
[150] Ternan, M., *Can. J. Chem. Eng.*, 61: 689 (1983).
[151] Hisadomi, M., Nakai, S. and Kono, H., *J. Jpn. Pet. Inst.*, 21: 237 (1978).
[152] Magaril, R.Z. and Aksenova, E.I., *Int. Chem. Eng.*, 8: 727 (1968).

[153] Magaril, R.Z. and Ramazaeva, L.F., *Izv. Vyssh. Ucheb. Zaved., Neft Gaz*, 12(1): 61 (1969).
[154] Magaril, R.Z., Ramazaeva, L.F. and Aksenova, E.I., *Khim. Tekhol. Topl. Masel*, 15(3): 15 (1970).
[155] Shiroto, Y., Nakata, S., Fukul, Y. and Takeuchi, C., *Ind. Eng. Chem., Process Des. Dev.*, 22: 248 (1983).
[156] Vercier, P., in: J.W. Bunger and N. Li (Editors), *The Chemistry of Asphaltenes. Advances in Chemistry Series 195*. American Chemical Society, Washington, D.C., p. 203 (1981).
[157] Speight, J.G., *Am. Chem. Soc., Div. Pet. Chem., Prepr.*, 34(2): 326 (1989).
[158] Furimsky, E., *Ind. Eng. Chem. Prod. Res. Dev.*, 17: 329 (1978).
[159] Yen, T.F., in: R.F. Meyer, J.C. Wynn and J.C. Olson (Editors), *The Future of Heavy Crude Oil and Tar Sands*. McGraw-Hill, New York, N.Y., p. 412 (1984).
[160] Dias, J.R., *Handbook of Polycyclic Hydrocarbons. Part A. Benzenoid Hydrocarbons*. Elsevier, New York, N.Y., 388 pp. (1987).
[161] Dias, J.R., *Handbook of Polycyclic Hydrocarbons. Part B. Polycyclic Isomers and Analogs of Benzenoid Hydrocarbons*. Elsevier, New York, N.Y., 404 pp. (1988).

This page intentionally left blank

Asphaltenes and Asphalts, 1. Developments in Petroleum Science, 40
edited by T.F. Yen and G.V. Chilingarian

Chapter 3

CHEMICAL CONSTITUTION OF ASPHALTENES

M.A. BESTOUGEFF and R.J. BYRAMJEE

DEFINITION OF ASPHALTENES AS A CHEMICAL GROUP OF HETEROATOMIC COMPOUNDS

A vast group of substances commonly termed "asphaltenes" has not yet found its place in the official organic chemistry system despite many studies on their chemistry and structure, which have been published recently. This situation may be explained by the fact that it has not yet been possible to isolate the individual compounds belonging to this group and consequently their exact chemical formulae have not been established. These bodies are often considered by "pure" chemistry experts as some kind of "materials" belonging to the technical sphere.

The crude asphaltenes are in fact quite complex mixtures of substances with high and variable molecular masses belonging to different types of chemical structures. Moreover, the common definition of petroleum asphaltenes is based on their solution properties in various solvents, but unfortunately this concept has been extended lately to products derived from other carbonaceous sources such as coal, shale oil, cracking residues, etc.

The present tendency, however, is to define the material precipitated from different sources and separated in several fractions in terms of chemical structure and chemical functions.

In this respect, the endeavor to separate the resins and asphaltenes into homologous series is a very difficult task, and hopes of attaining this highly desirable goal appeared on the horizon only very recently.

According to their elementary composition, asphaltenes belong to a class of heteroatomic compounds, i.e. organic substances which contain, in addition to carbon and hydrogen, atoms such as oxygen, sulfur and nitrogen. The set of available data on structure and properties of asphaltenes show that asphaltenes can be considered as a system of polycondensed molecules and must have their place in organic chemistry classification between micro- and macro-molecular compounds.

The main structural characteristic of asphaltenes is the "hydrocarbon skeleton" of their molecules which is made of three structural elements: (1) aromatic nuclei, (2) naphthenic nuclei (hydroaromatic), and (3) side and bridged chains. The presence of these three structural elements in an asphaltene molecule is the basis for its chemical definition.

As to heteroatoms of which asphaltenic molecules contain a relatively small number as compared to their carbon number, they do not substantially alter the skeletal structure of these bodies but do increase the variety of their structural details.

TABLE 3-1

Chemical composition of the asphaltene extracts obtained by boiling *n*-heptane extraction [a]

Asphaltene extract origin	Fraction No.	Weight [a] (%)	Melting point (°C)	n_d^{20}	Elemental composition (%)					C/H (wt%)
					C	H	S	N	O	
Hassi-Messaoud (Cambrian)	1	9.5	–	1.4970	86.32	13.18	0.15	0.03	0.32	6.55
% of asphaltene extract: 33.6 wt% [b]	2	15.0	80	–	90.12	9.02	0.90	0.03	–	9.99
	3	6.1	135	dark	90.22	7.60	0.92	0.49	0.73	11.87
	4	3.0	116	dark	86.08	8.57	1.25	0.64	3.46	10.04
Laghouat, Algeria (Triassic)	1	13.0	viscosity	1.540	–	–	–	–	–	–
% of asphaltene extract: 21.6 wt% [b]	2	7.4	120	dark	88.61	8.32	0.40	0.05	2.62	10.65
	3	1.2	112	dark	85.90	8.70	1.60	0.75	3.05	9.87
Iraq (Eocene)	1	3.7	viscosity	1.4810	–	–	–	–	–	–
% of asphaltene extract: 19.2 wt%	2	2.5	viscosity	1.5860	–	–	–	–	–	–
	3	10.1	75	1.6720	80.40	8.07	8.21	0.34	2.98	9.96
	4	1.9	75	dark	79.99	7.26	5.46	0.71	6.58	11.02
	5	1.0	115	dark	78.37	8.83	6.71	0.34	5.75	8.88
Boscan (Eocene)	1	0.5	viscosity	1.4938	85.10	12.7	0.80	0.10	1.30	6.70
% of asphaltene extract: 17.6 wt% [b]	2	8.5	60	1.6310	–	–	–	–	–	–
	3	3.4	100	dark	–	–	–	–	–	–
	4	3.3	120	dark	–	–	–	–	–	–
	5	1.7	60	dark	–	–	–	–	–	–
Scheibengard, France (Oligocene)	1	1.4	86	1.4880	–	–	–	–	–	–
% of asphaltene extract: 14.7 wt% [b]	2	8.6	70	1.6400	87.60	8.62	0.72	0.06	3.00	10.1
	3	2.4	135	dark	88.02	8.30	0.50	0.08	3.10	10.6
	4	2.3	160	dark	–	–	–	–	–	–

[a] Chromatography of asphaltene extract on Davidson-70 silica gel.
[b] % of crude asphaltene.

CHEMICAL COMPOSITION OF CRUDE ASPHALTENES

In spite of several standard methods for the separation of crude asphaltenes used in different countries, mostly for technical purposes, there is no universal method that can be used for research and comparison of results obtained by different authors.

The precipitate of the asphaltenes obtained by various methods contains a complex mixture of semi-solid to solid organic substances which are soluble in benzene and polar solvents. This precipitate, depending on the precipitation conditions, contains variable proportions of compounds, the nature of which does not correspond to the chemical definition of asphaltenes and which can be considered as *impurities*. These impurities are of different compositions and natures. For example, Long [1] points out that "asphalt chemists have known for a long time that some crude precipitated high melting waxes in their asphaltenes".

N-paraffin constituents [melting point (MP) = 83.5°C, molecular mass (MM) = 750] and crystalline wax constituents (MP = 40–55°C, MM = 720–890) corresponding to bicyclic naphthenic hydrocarbons and bicyclic sulfur compounds having the general formula $C_nH_{2n-12}S$, were separated by Bestougeff and Bargman [2] from a high melting wax of one Middle Eastern crude.

Knotnerus and Krom [3] have studied the isolation of wax from a variety of bitumens of various origin and more specifically the composition of this crystalline matter. They found, using X-ray method and molecular distillation followed by absorption chromatography, that:

(1) All the waxes contain sulfur, oxygen and nitrogen components.

(2) These components predominately consist of long paraffinic chains which are often bonded to saturated or aromatic rings or to a ring system containing heteroatoms.

The identification of individual wax components has not been possible, but occurrence of benzothiophenes derivatives with long substituents has been established (molecular mass of about 750).

McKay et al. [4] performed a complete analysis according to "the separation of compound types" of crude asphaltenes precipitated from a Wilmington, California crude oil by n-pentane. They detected in this crude material 3% of saturated hydrocarbons and 2% of aromatic and sulfur constituents.

The properties of saturate and aromatic hydrocarbons and, likewise, sulfur constituents isolated by McKay et al., are quite similar to the corresponding fractions of high melting point waxes studied by Bestougeff and Bargman, and Knotnerus and Krom.

In order to get more homogenous precipitates of crude asphaltenes, one can suggest the use of warm *n*-heptane as a solvent following extraction at an elevated temperature of the precipitate obtained with the same solvent.

This treatment permits the elimination of high melting point waxes and low solubility substances in cold *n*-paraffin solvents from the precipitate.

The data presented in Table 3-1 show that crude asphaltenes can contain an appreciable proportion of non-asphaltene constituent impurities, particularly in the precipitates obtained by methods using *n*-pentane.

In conclusion, one should emphasize that not only the asphaltenes in a given crude oil contain different groups of substances but that the corresponding asphaltene fractions separated from different petroleums may also vary considerably. Therefore the need to fractionate crude asphaltenes before proceeding to their chemical and physicochemical examination is obvious.

Indeed, an examination of narrow asphaltene fractions can provide a more precise answer to the structure of this complex mixture than the studies of "the average asphaltene molecule" carried out by many authors in past times.

MOLECULES, PARTICULES AND MICELLES OF ASPHALTENES

The great inconsistencies in the molecular mass (molecular weight) determination of asphaltenes by different methods emphasized to a greater extent the asphaltenes intermolecular association phenomena. It is generally recognized that intermolecular association gives a very high average value of the molecular masses of asphaltenes.

It has been suggested on the basis of mostly physical investigations that the asphaltene molecules in solution are associated in "particules" (several molecules), and these particules in their turn can form greater aggregates called "micelles" [5]. The pattern of intermolecular association can be either the electron attractions of peri-condensed polynuclear aromatic systems in asphaltene molecules or the coordination through heteroatoms. Yen [5] believes that the conventional meaning of molecular weight does not apply in the case of asphaltenes; however, he introduced a notion of single unit sheet in complex asphaltene particules, whose weight is around 1000. This single unit sheet is built by an aromatic condensed cycles system in the center surrounded by some aliphatic naphthene radicals. The asphaltene particule consists of several parallel unit sheets held together by physicochemical forces.

In terms of the difference in magnitude of molecular distances corresponding to the number of single unit sheets, he suggested two types of structures: microstructure (fine structure), 0.5–40 Å, and the macrostructure (bulk structure), 40–2000 Å. The unit sheet of the asphaltic particules can be dissociated by a number of methods, particularly shearing, interacting by dilute and polar solvents, elevated temperature, etc. The association–dissociation energy is 14 cal.

Furthermore, the chemical treatment can also cause the dissociation of asphaltene particules. For instance, Ignasiak et al. [6] obtained the drastic reduction of roughly half the molecular weight of silylated Athabasca Cold Lake and Peace River asphaltenes.

To date, many attempts have been made to establish a true molecular weight of asphaltene molecules. Bunger [7], studying asphaltenes from tar sand bitumen by different methods, found that the asphaltenes are monomeric in nature and possess average molecular weights in the range of 500–800, broadly distributed with respect to aromaticity and heteroatom content. Other studies such as Speight and Moschopedis [8], Witherspoon and Winniford [9], Sergienko et al. [10], apparently

accept that the molecular weight is higher than 1000 but that monomeric units in asphaltene polymer molecules are quite small (400–500) and connected through carbon–carbon or sulfide linkages [11,61]. There is a wide distribution of molecular weight which overlaps appreciably with the non-asphaltenes (resins). As to the average molecular weights of the coal-derived asphaltenes, after recent reported results, they vary from lows of about 200–300 to highs of about 800 [12].

It appears that significant disagreements remain now, not only for the true value of asphaltene molecular weight, but also for the interpretation of basic notions of "molecular weight" concerning molecules, particules and micelles.

The strength and prevalence of the intermolecular (and intramolecular) associations is very poorly defined, and the possible effects of these interactions on the physicochemical behavior of asphaltenes is not well understood. Further studies of the true molecular weight (mass) of asphaltenes are absolutely necessary with the clearly defined molecules with different building blocks bounded by valence links.

MOLECULAR STRUCTURE OF PETROLEUM ASPHALTENES

This section principally deals with the native crude oil asphaltenes which have been the most thoroughly investigated.

In studying the asphaltene fractions obtained by liquid absorption chromatography from different crude asphaltenes, Bestougeff [13] came to the conclusion that asphaltene molecules can be considered as polycondensed systems (Fig. 3-1). The structure of these systems may be interpreted by analogy with the formation of polymers in macromolecular chemistry, owing to the broadened concept of structural "monomers" or "pseudo-monomers".

Just as certain polymers can be obtained by polymerizing several different types of monomers, asphaltenes may be considered to be polymolecular aggregates produced by the polycondensation of a certain number of pseudo-monomers that can be distinguished in two ways:

(1) by their structural elements (carbon skeleton, location of heteroatoms or functions), and

(2) by the nature of heteroatoms and functions present in the pseudo-monomer. The multiplicity of possible combinations between these different pseudo-monomers explains the complexity of macromolecules obtained.

The structure obtained may be schematized as follows:

A–A–A′–A″–
A–B–B–C–
A–B–B′–C″–

etc., in which A, B, C are pseudo-monomer patterns corresponding to different carbonaceous structures, and A, A′, A″, etc. are pseudo-monomer patterns of the same carbonaceous structure, but having different functions or heteroatoms.

Yen [5] also believes that asphaltene molecules (or particules) from a multipolymer system contain a greater variety of building blocks, but he pointed out that the

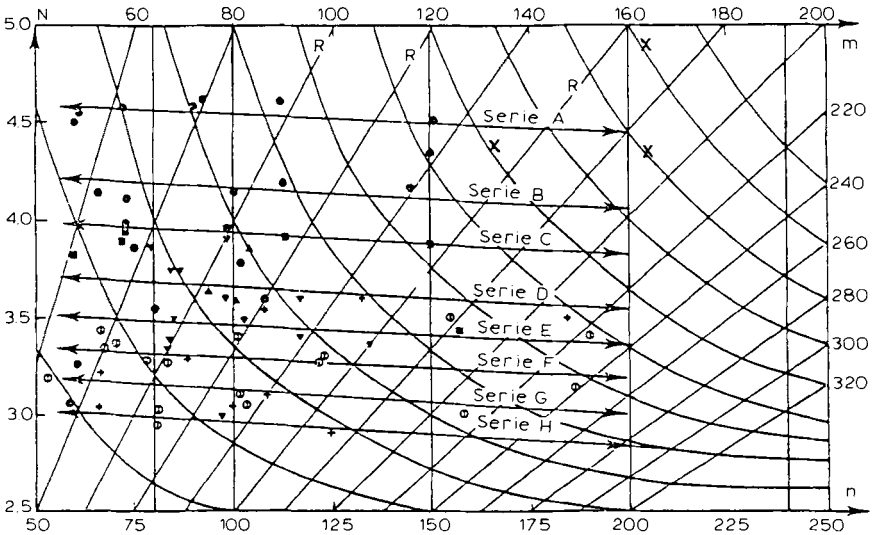

Fig. 3-1. Distribution of the chromatographic fractions of asphaltenes on the Jurkiewicz graph of the regular system of hydrocarbons. × = curves corresponding to the hydrocarbon homologous series, C_nH2_{n-x}; R = line corresponding to the number of aromatic cycles per molecule, where $R = (n - m + 2)/2$. The symbols used in this graph are: solid circle = Hassi-Messaoud; solid square = Laghouat; inverse solid triangle = Iraq; circle with line = Boscan; plus = Libya; solid triangle = Lagunillas.

conventional meaning of molecule (molecular weight) does not apply in the case of asphaltenes.

According to Jewell et al. [14], the resins and asphaltenes consist of a wide range of molecular sizes that can be viewed as "pseudo-polymers", as their chemical properties are essentially constant (independent of molecular weight) and similar to those of low-molecular-weight moieties.

Some experimental attempts aimed at producing the monomer block from Athabasca asphaltenes have been made using a variety of mild reduction degradation in order to maintain the integrity of the basic structural blocks of the polymer [15,16]. The experimental results show that 65% of Athabasca asphaltenes are a sulfur polymer in which the average carbon moieties, each consisting of an alicyclic-aromatic structure with some alkyl substituents, are held together by sulfide linkages (C_{25}–$H_{30}S$) × 8 (Fig. 3-3a). By the application of the naphthalene anion reduction method to the Cold Lake, Peace River and Lloydminster asphaltenes, it was also shown that the corresponding figures for the sulfide polymer in those products are much smaller: 22, 14, and 13%, respectively. Speight and Moschopedis [8] have doubts about a sulfur-polymeric nature of Athabasca asphaltenes. They pointed out that reaction to cleavage of the –C–S bonds used by Ignasiak et al. is not specific and that taking an asphaltene for a sulfur polymer is perhaps too presumptuous. The evidence is more favorable to some intermolecular carbon–carbon bonds of the type found in diphenylmethane or in diphenylethane with the asphaltene molecule being

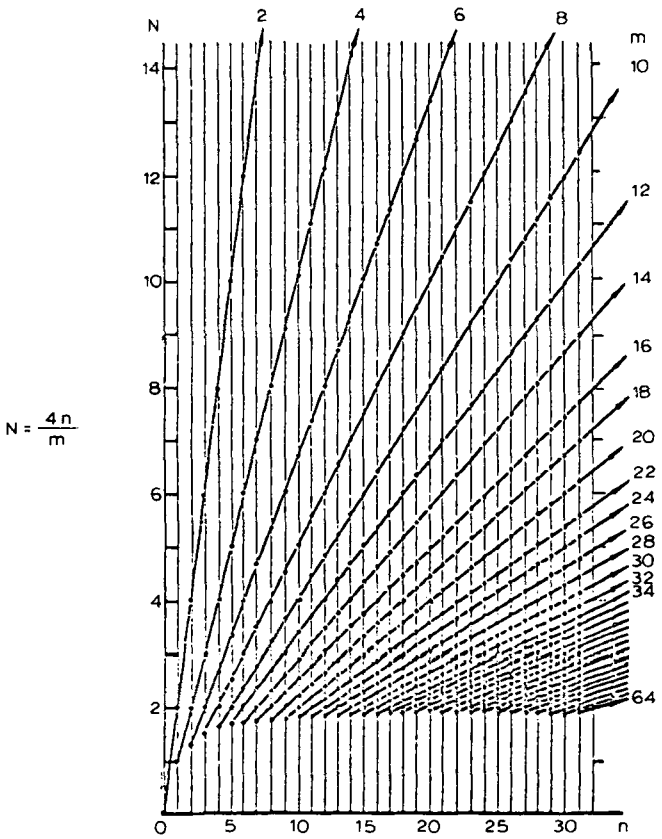

Fig. 3-2. Regular system of hydrocarbons. n = number of carbon atoms; m = number of hydrogen atoms.

much smaller than current physical or chemical investigations seem to indicate. As further evidence for the polymeric (polycondensed) nature of asphaltene molecules, data resulting from other investigations may be cited.

Ferris et al. [17] established quite early that the heteroatom and aromatic content increased rapidly with molecular weight in the resin fractions but very slowly in the asphaltenes. A sharp break occurs in the curve which marks the division between resin and asphaltene types of molecules. On the other hand, the low variation of index N on the Jurkiewicz graph (Fig. 3-2) in relation to molecular weight for the same series of asphaltenic constituents enables these series to be considered as polycondensed systems (it may be recalled that for a true polymer index N remains constant).

More recent investigations by Ignasiak et al. [18] on thermal degradation of different Alberta oil sand asphaltenes seem to favor the polymeric concept of the asphaltene molecule.

Finally, the assumption made by most authors that petroleum asphaltenes are

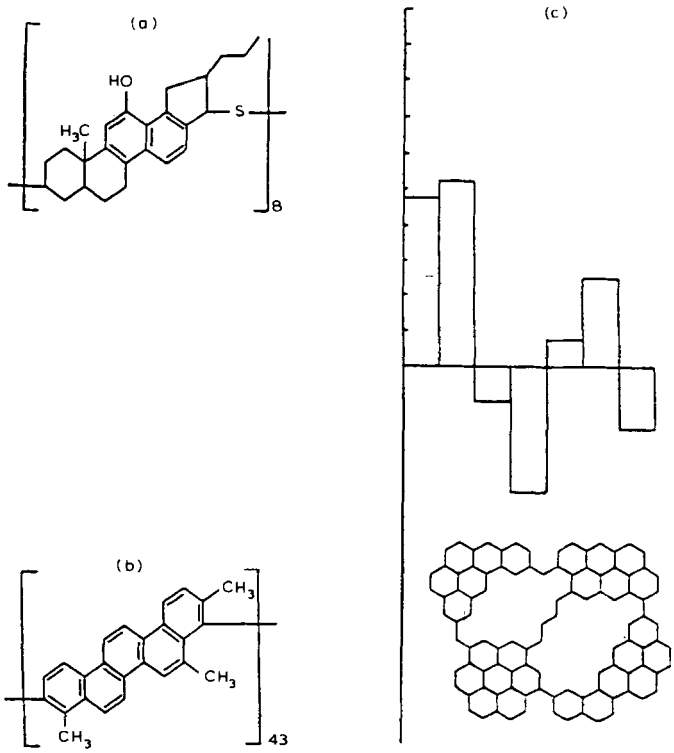

Fig. 3-3. (a) Hypothetical monomeric unit of Athabasca asphaltene [11]. (b) One type of monomeric unit of asphaltene. (c) Histograms and hypothetical units for decane-insoluble asphaltene from Alberta crude oils.

formed by addition of several smaller resin. molecules implies the recognition of the polycondensed (polymeric) structure of asphaltene molecules, at least for those derived from crude oils and natural asphalts (Fig. 3-3).

It is possible, however, to suggest the existence of a type of asphaltene molecule having a rather low molecular weight whose structure is not a polymeric (polycondensed) feature. In this particular case, the asphaltene molecules would originate by degradation of macromolecular substances, for instance kerogen, etc. Some of the fragments generated by this degradation having the asphaltene behavior (solubility) can be assimilated to monomeric asphaltene molecules, and are considered "primary" asphaltenes, in contrast to the "secondary" asphaltenes resulting from the condensation or polymerization of smaller moieties.

CARBON SKELETON OF THE ASPHALTENE MOLECULES

Ignasiak et al. [15] indicated that in general, petroleum asphaltene is characterized by its high heteroatom content, which in the case of the Athabasca asphaltene

is in the range of 8–9% sulfur, 2–3% oxygen and 1% nitrogen. However, it would be more correct to take in consideration the atomic ratio of elements. In this case, for every fifty carbon atoms there are only 1.5–2 sulfur atom, 1.0–1.2 oxygen atoms and 0.3–0.5 nitrogen atoms. Also, the number of heteroatoms in asphaltene molecules compared to carbon atoms is fairly limited so that carbon atoms actually determine the "hydrocarbon skeleton" of the asphaltenic molecule.

Given the importance of the carbon skeleton of the asphaltenic molecule, it is necessary to determine its place in the regular hydrocarbon system of Jurkiewicz and Rosinski [19], based on the carbon–hydrogen molecular ratio (C/H). This ratio, which can be presented as the function of

$$N = 4n/m$$

in which n = number of carbon atoms and m = number of hydrogen atoms, covers in the case of asphaltenes a definite area ranging from $N = 2.8$ to $N = 4.7$ (Fig. 3-1). This area borders those for coal constituents (index N above 4–4.5) and petroleum constituents (resins) with values for N below 3–3.2.

Therefore, heteroatoms, which are as mentioned above relatively few compared to carbon atoms, do not substantially alter the skeletal structure of asphaltenes but do increase the variety of their structural details.

DEVELOPED FORMULA OF ASPHALTENE MOLECULES

Many attempts have been made to establish a developed formula of the asphaltene molecule. Those attempts met a number of different obstacles. First, there is insufficient knowledge of the precise molecular weight, as well as the heterogeneity of samples of which the major part belongs to crude asphaltene precipitates and not to narrow and homogeneous fractions.

In these conditions, the previous research purpose was the determination of an "average molecular structure" which has a limiting value for asphaltene constituent structural chemistry. The writers feel it is much more justified to search for a "possible molecular structure field" before trying to do anything else.

The basic structural elements could be established with some precision, particularly with the use of the structural parameter calculation method and computer techniques.

This method appears to be a powerful tool in reconstructing complex asphaltene molecules. It requires analytical data obtained from elemental analysis, nuclear magnetic resonance (NMR), infrared spectrometry, X-ray diffraction, and molecular weight and density determinations.

Ten basic structural elements (parameters) are listed below, but the total relevant parameters can exceed several dozen:

(1) Total number of cycles.
(2) Number of aromatic cycles.
(3) Number of naphthenic cycles.
(4) Ring compactness factor.

(5) Number of internal carbon each bonded to the other aromatic carbon atoms.

(6) Number of aromatic peripheral carbon, each bonded to two other aromatic carbon atoms and one aliphatic or naphthenic carbon atom.

(7) Number and average chain length.

(8) Number of carbon atoms in the form of methyl and methylene groups.

(9) Nature and probable location of functional groups.

(10) CH, CH_2, and CH_3 groups attached to an aromatic ring.

In 1968, Bestougeff and Pierre [20] developed a mathematical method based on the graph theory to bring up the experimental data to the *linear programming* approach. These authors postulated that the establishment of a developed formula is equivalent to the construction of one graph corresponding to some constraints imposed by molecular structure type and analytical data. Any method of developed formula calculation will not escape explicit or implicit application of the graph theory. Another mathematical method for the determination of average structural parameters was proposed by Hirsch and Altgelt [21], who gave more reliable information, especially on the heteroatoms and amount and structure of naphthene carbon than had been available before. A key to this method is the introduction of four "floating parameters". These were selected in such a way that they vary within narrow limits and can be estimated fairly accurately. The heteroatom distribution into functional groups is approximated from infrared spectrometry results. The adjustments are made quite arbitrarily, but the authors estimate that the error in assignments has little effect on the results because the atom fraction of heteroatoms is generally quite small. This method is easily carried out on digital computers.

A new step in structure parameter analysis was achieved by Haley [22], Dickinson [23] and Klet et al. [24,25]. The equations which they proposed are simpler and easier to apply than those of Hirsch and Altgelt.

The application of these latter calculation methods to gel permeation chromatographic fractions [60], including the asphaltenes provided by various asphalts, have led to the following conclusions:

(1) All asphalt fractions (MM from 740 to 2950) are made of aromatic and naphthenic cycles, those with low molecular masses having few aliphatic chains attached to the cycles.

(2) The naphthenic rings are attached to other naphthenic rings forming a condensed system.

(3) The aliphatic chains attached to the naphthenic cycles are longer than those attached to the aromatic rings. In the latter case, the chains are often terminated by methyl groups.

Recently, Rosental et al. [26] gave a detailed description of "integral structure analysis" for petroleum heavy end fractions. The model asphaltene molecule presented by these authors is quite similar to that found by Hirsch and Altgelt. In each case, the aromatic cycles are distributed between 4–5 fused ring systems having from 5 to a maximum of 10 cycles and forming the great molecule (Fig. 3-4a, b).

As opposed to this picture, the asphaltene molecule (particule) suggested by Yen and other authors have greatly developed *aromatic fused ring systems* containing almost all aromatic rings.

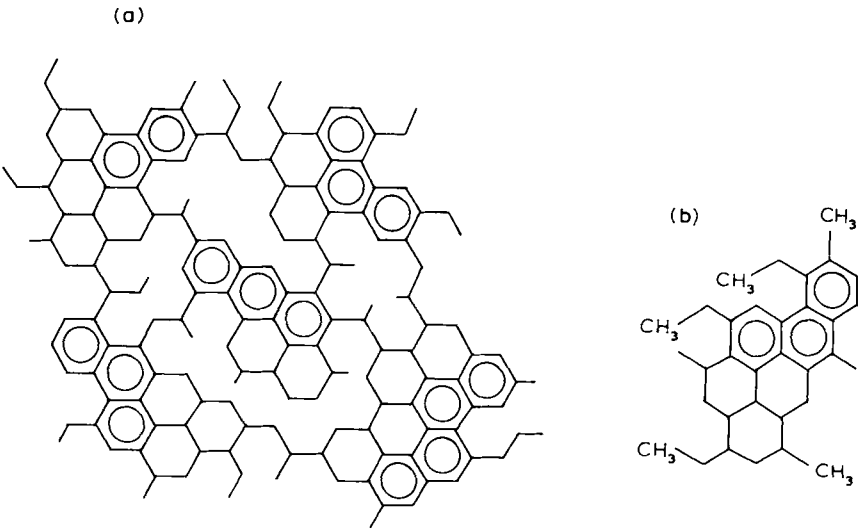

Fig. 3-4. (a) Model molecule of asphaltene [26]. (b) Average fragment of model molecule.

Bestougeff and Collet [27], using the calculation method of Bestougeff and Pierre, investigated a large field of "possible asphaltene molecules" with various molecular weights from C_{50} to C_{150} and particularly the molecular structure of C_{50} (MM = 640–680), which can be considered as a monomeric unit.

The results of these calculations are given in Table 3-2. Inspection of the figures in Table 3-2 (the last six columns) shows that the calculated values for a system of asphaltene molecule skeletons correlate with those found for various asphaltene samples derived from crude oils and other sources. So for a monomeric unit C_{50}, the

TABLE 3-2

Structural parameters of asphaltene molecule skeleton

	x (C_nH_{2-x})	Molecular mass	H/C (mol)	f_a [a]	Number of cycles in molecule					
					total		aromatic		naphthenic	
					min.	max.	min.	max.	min.	max.
$C_{50}H_{40}$	60	640	0.8	68.72	10	12	9	10	0	3
$C_{50}H_{50}$	50	650	1.0	56.60	9	13	6	8	1	7
$C_{50}H_{60}$	40	660	1.2	28.52	8	14	3	6	2	11
$C_{50}H_{70}$	30	670	1.4	10.40	5	15	0	5	0	15
$C_{50}H_{80}$	20	680	1.6	5.25	4	10	0	3	1	10
$C_{100}H_{120}$	80	1320	1.2	20.45	14	30	5	13	1	25
$C_{100}H_{160}$	40	1361	1.6	5.25	8	20	6	6	2	14
$C_{100}H_{180}$	120	1981	1.2	20.45	20	46	7	20	0	39

[a] Observed values of aromaticity factor.

total number of cycles and the number of aromatic rings cannot exceed 15 and 10, respectively. For most petroleum asphaltenes the aromatic cycle number varies on the average from 3 to 7 units. If one admits that the monomeric unit is greater than $C_{100}H_{120}$, the total number of cycles increases to a maximum of 30 and the number of aromatic cycles to 13.

These results show clearly that the structure of any narrow asphaltene fraction and moreover, of crude asphaltenes, cannot be established without the recognition of two basic principles: (1) the polymeric (polycondensed) nature of asphaltene molecules, and (2) the determination of the *molecular masses of monomeric and polymeric units* (molecules) of asphaltenes.

The various formulae suggested by a number of authors can be classified into two groups according to these two principles. On the one hand, the greater part of aromatic cycles are joined together forming an "aromatic sheet system" with a great number of cycles of 20–25 and more (Fig. 3-5). On the other hand, the cycles are distributed among several relatively small units (monomers) with a limited number of aromatic cycles by unit (Fig. 3-4). In this case, the sole aromatic condensed ring system cannot exist in molecules.

Lately, one intermediate structure was suggested with the "collection of sample" units lined head-to-tail in a completed cyclic system (Fig. 3-4) [8]. This system

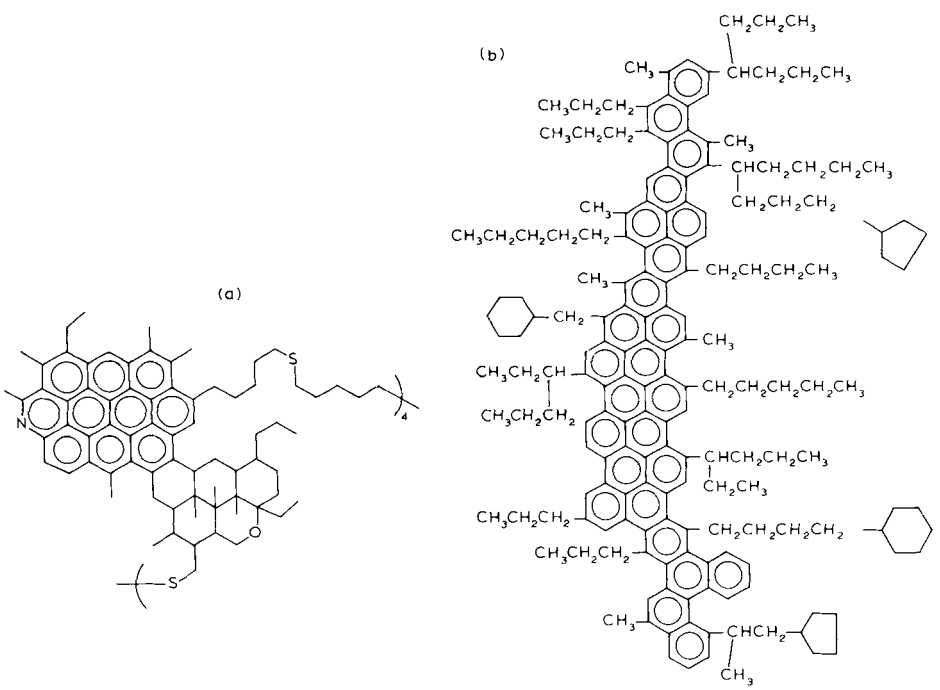

Fig. 3-5. (a) Hypothetical structures for asphaltenes, Lagunillas crude oil [5]. (b) Hypothetical structures for crude oil asphaltenes, Iraq [8].

supports a "hole structure" of asphaltene molecules, but it can be accommodated with Yen's idea of sheet unit structure by presenting a sheet as "carbon hole lamellae structure". Speight noted that the X-ray model is not unique and many variations on this subject are possible. Indeed, the structure of cyclic and particularly aromatic ring systems of asphaltene molecules vary very much according to its aromaticity index.

As indicated in Table 3-2, only high aromatic asphaltene constituents with a f_a-index of 0.6–0.7 can have a condensed aromatic ring system. All other asphaltene constituents with lower aromaticity, especially with a f_a-index below 0.25, cannot have this system. Inasmuch as asphaltene constituents derived from the same sample have quite different aromaticities, their molecular structures must also be different. From the study of asphaltene formation and evolution, it is possible to correlate the asphaltene constituent structures following general phenomena, like increasing H/C ratio, aromaticity and ring system condensation, which take place in nature during diagenetic and catagenetic processes (see section below on "Occurrence, formation, evolution"). It is important to point out that the asphaltenes derived from bitumens and recovered by means of sedimentary rock extraction have, in general, lower molecular masses and aromaticities and higher H/C ratios than petroleum asphaltenes. The asphaltenes recovered from the degradation products, under mild conditions of sporopollenin pyrolysis have a very low molecular mass and do not show a characteristic X-ray band (002) of aromatic condensed systems. However, this band can be observed after thermal treatment of sporopollenin asphaltenes at high temperature [28].

On the other hand, it is known that the aromaticity, degree of condensation of an aromatic ring system and other parameters of bitumen and petroleum asphaltenes increase with increasing age and depth of burial of the material, i.e., with the increasing degree of maturation process. Under these conditions, the aromatic ring systems undergo permanent transformation, directed towards aromatic unit sheet formation.

At the present time, the systematic analytical data on the constitution of asphaltene narrow fractions for selected asphaltene samples are insufficient to support and illustrate this picture. Several recent mass spectroscopic studies of asphaltene fragments can furnish some additional information of the carbon skeleton of asphaltenes. Some asphaltene fragments identified by Poljakova et al. [29] are given in Fig. 3-6.

In conclusion, it is evident that a reasonable model structure for the average asphaltene molecule has a limited significance for understanding the chemical nature of a given asphaltenic species. The molecules of asphaltenes from various sources and even from the same genetic material are composed of several structural types. The characterization of each type of chemical structure is necessary in order to have a better picture of asphaltene molecules for each particular asphaltene.

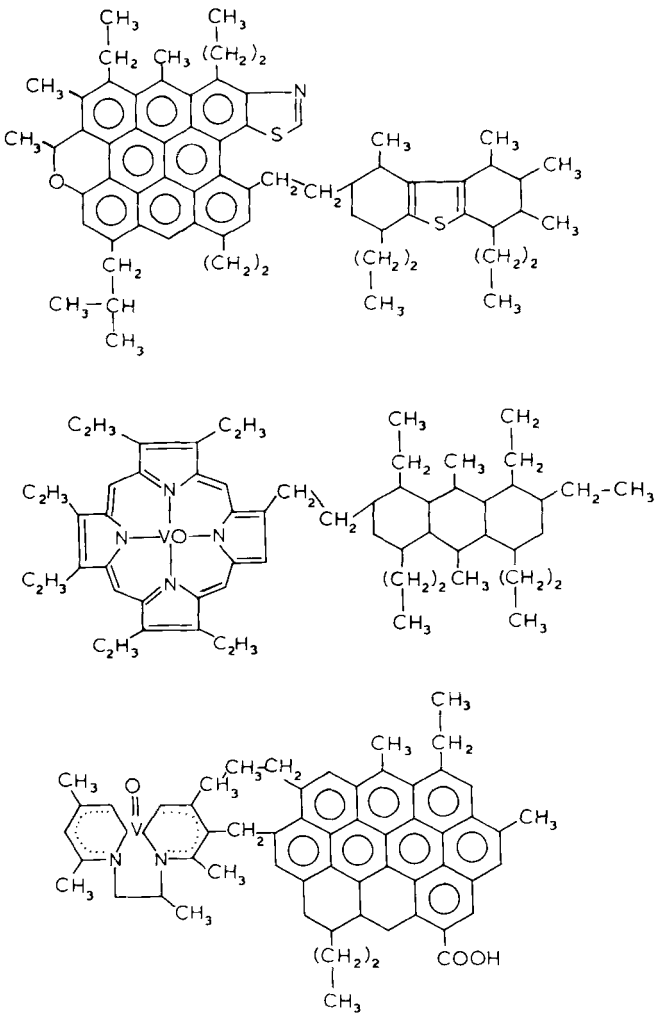

Fig. 3-6. Fragments of asphaltene molecules, from Romashkino crude oil, determined by mass spectrography [29].

LOCATION OF HETEROATOMS IN ASPHALTENE MOLECULES

The investigations on the location and functional behavior of S, O, and N atoms have been favored mostly by mass and NMR spectrometry development.

The analysis of crude asphaltenes usually indicates the presence of all three heteroatom types in the same asphaltene molecule. However, the data for asphaltene fractions obtained by various separation methods suggested that asphaltene constituents with two and one heteroatoms per molecule can exist, the isolation of which may be accomplished by means of more selective analytical techniques.

Sulfur. The sulfur atom in the asphaltene molecule may be either a part of heterocycles like benzothiophene, dibenzothiophene, naphtothiophene, etc., or reside in sulfide groups. The potentiometric determination of thiophenic (heterocyclic) and nonthiophenic (sulfide) sulfur type distribution in several resin and asphaltene fractions show that thiophenic sulfur content in asphaltenes is lower than in resin fractions of the same crude oil [30]. It is necessary to point out that generally the thiophenic sulfur content grows with the increase of the molecular weight of petroleum fractions. The sulfide sulfur content in asphaltenes of different origins can vary considerably, for instance, by a factor of four. Alberta crude oil asphaltenes contain from 13 to 65% sulfide sulfur (Table 3-3).

On the other hand, polarographic determinations indicate that often the sulfur atoms are situated in heterocyclic systems, benzothiophene, etc., type [5]. After Eliceev et al. [31], the asphaltene separated from Tadjikistan Kichik-bel crude oil contains tri- and tetracyclic thiocyclanes. These authors suggested also the presence of thiol groups in asphaltenes of several crude oils.

Oxygen. Oxygen may be present in various functional groups such as *hydroxyl* in phenols, alcohols and carboxylic acids, *carbonyl* in esters, ketones, and amides, and finally in the form of ethers and heterocycles. The determination of these functional

TABLE 3-3

Distribution of sulfide and thiophenic sulfur in asphaltenes and other constituents

Material and origin	Some properties	Nitrogen (%)		Sulfur content(%)		
		basic	total	sulfide	thiophenic	total
Hassi-Messaoud						
Heavy oil	MM[a] = 380 b.p.[b] = 350	0.07	0.11	8.7	91.3	1.84
Maltenes	MM = 570	0.1	0.13	12.0	88.0	1.25
Asphaltenes	Precipit. by	0.1	0.25	17.6	82.4	1.65
	n-heptane	–	0.18	19.1	80.9	1.80
Boscan						
Heavy oil	MM = 420 b.p. = 400	0.0	0.2	12.3	87.7	8.20
Maltenes	MM = 540	–	–	–	–	–
Asphaltenes	Precipit. by	0.83	1.4	24.4	75.6	6.22
	n-heptane	1.18	2.2	22.4	77.6	7.75
Iraq						
Heavy oil	MM = 430 b.p. = 400	–	–	25.0	75.0	5.60
Maltenes	MM = 600	–	–	15.67	84.3	5.90
Asphaltenes	Precipit. by	0.35	0.6	17.8	82.2	8.10
	n-heptane[c]	0.56	0.8	14.2	85.8	8.81

[a] Molecular mass.
[b] Boiling point.
[c] Fraction of asphaltene insoluble in sulfuric ether.

groups can be achieved by various analytical methods, namely, the infrared spectrometry, potentiometric titration, acetylation, silylation (for the hydroxyl group) and reduction-acetylation (for the carbonyl group).

Although some carbonyl oxygen is detected by infrared spectroscopy, it is scarce and there is absolutely no quinone or semiquinone type of oxygen in asphaltenes [5]. The data obtained from the chemical determinations of oxygen functional groups in Athabasca asphaltene showed that approximately 75% of the oxygen present is in the form of hydroxyl function. The infrared studies combined with acetylation, methylation and silylation indicated that the hydrogen bonding association of these groups is nearly complete and appears to be partly intermolecular. The infrared spectra also showed the presence of ketone and quinoid groups in Athabasca asphaltene [6]. Speight and Pokonova [32] admit that an OH-phenol group can be present in the same aromatic cycles or in neighboring cycles having hydroxyl or carbonyl groups.

Nitrogen. Like other heteroatoms, nitrogen may be present in various functional groups, but the identification of these groups in asphaltene molecules advances slowly [62]. Most studies were addressed to porphyrin compounds identified and separated from high molecular weight fractions of crude oils. But in asphaltenes, relatively small portions of nitrogen are present in porphyrin complex. According to the results of nitrogen compounds studies in resin fractions, one can suggest that asphaltenes have the same functional groups as these resins. The quantitative measurements of "basic nitrogen" by potentiometric titration achieved on different asphaltene fractions show the presence of NH, pyridine, and quinoline type nitrogen groups [30]. This compound type was already identified in petroleum fractions. In high-molecular-weight fraction (Emeraude crude oil) monoazoarenes with as many as eight aromatic cycles appear as major nitrogen constituents characterized by fused aromatic structures with C_2 or C_3-alkyl substitution [33].

SEPARATION OF ASPHALTENES ACCORDING TO THEIR CHEMICAL FUNCTIONS

As early as 1931, Marcusson et al. [34] separated acidic constituents ("asphaltogenic acids") from native asphalts. He used a classical chemical method-treatment of asphalt with a KOH alcohol solution.

Further advances in the asphaltene heteroatomic chemistry became possible with anion and cation resin chromatography. The total separation of acidic, basic, neutral and amphoteric asphaltene constituents was accomplished by different authors: (1) Schweighardt et al. [35] first separated the acid and basic asphaltene fractions by this method; (2) Kiselew [36], using anionic resin Amberlyst A27 and cationic resin Amberlyst 15, obtained from "Arabian" crude oil asphaltene, a series of acid, basic, and neutral fractions presented in Table 3-4. The results obtained by this chromatography indicate that not only the separation of acids and bases was possible but also that the concentration of oxygen and nitrogen constituents was determined.

A rapid method for separation and determination of acid constituents in asphaltenes was suggested by Ramljak et al. [37], using a chromatographic column of

TABLE 3-4

Separation of acid and basic asphaltene constituents

	Elemental analysis						Functional groups
	wt%	C	H	S	N	O[a]	
Asphaltene	100.0	82.98	7.11	6.26	1.25	2.40	$CHON_3$
1-Acid fraction	1.7	70.73	6.81	3.38	1.50	17.58	CHO_3
2-Acid fraction	14.3	81.75	7.11	6.04	2.21	2.89	CHO_3N
Total acid fraction	16.0	–	–	–	–	–	–
1-Basic fraction	19.0	82.01	7.17	5.87	1.36	3.59	CHN_3
2-Basic fraction	11.0	67.71	7.13	4.57	2.50	18.09	CHN
Total basic fraction	30.0	–	–	–	–	–	–
Neutral fraction	54.0	82.84	7.26	6.85	0.87	2.18	CHO/CHO_2

[a] By difference.

silica gel treated by a saturated solution of potassium hydroxide in isopropanol. The asphaltene derived from Iraq blown residuum was investigated by this method; 4% of acid material was recovered by elution with a solution of 20% phosphoric acid in chloroform. Zumer et al. [38,64] studied an asphaltene derived from Safania blown residuum by the acid–base separation. They found the presence of an important fraction of amphoteric compounds with double behavior (acid and basic) in this material, in addition to acid and basic constituents.

These authors carried out two series of asphaltene percolation successively: first, on silica gel treated by potassium hydroxide and then on alumina treated by phosphoric acid, secondly, by percolation on alumina before percolation on silica gel. The results obtained in these experiments are shown below:

	SiO_2-KOH	Percolation	Al_2O_3–H_3PO_4	Percolation
1	Acids (%)	Non-retained fraction (%)	Bases (%)	Neutral (%)
	24.5	75.5	53.0	22.5
	HP_2O_3–H_3PO_4	Percolation	SiO_2–KOH	Percolation
2	Bases (%)	Non-retained fraction (%)	Acids (%)	Neutral (%)
	70.9	29.2	7.1	22.0

The final results can be presented as follows:

Acid constituents: 7%
Basic constituents: 55%
Amphoteric constituents: 16%
Neutral constituents: 22%

It should be noted that the amphoteric constituents were found also in asphaltenes derived from coal [39], in which the infrared spectrum shows the presence of phenolic groups in basic constituents.

Separation of acid–basic constituents of straight, reduced and blown asphalts derived from Romashkino crude oil using chromatography on anion and cation exchange resins was also performed by Boduszynski [40] and Boduszynski et al. [58,41].

In addition to acid and base fractions, the neutral Lewis bases were separated by means of percolation on a column packed with attapulgus clay coated with ferric chloride. The purpose of these studies was to investigate the chemical composition of petroleum asphalts. As to the chemical structure of asphaltenes, these authors arrived at a rather erroneous interpretation of results.

In conclusion, it can be said that the progress accomplished in the determination of the chemical functions of asphaltenes is not sufficient for the determination of real locations of different functional groups on the asphaltene skeleton. More detailed studies using intercomplementary methods of fractionation on the basis of physical and chemical treatments of narrow fractions are needed.

OCCURRENCE, FORMATION AND GEOCHEMICAL EVOLUTION OF PETROLEUM ASPHALTENES

Occurrence

Asphaltenes are widely distributed throughout nature, being constituents of malts, natural asphalts, crude oils, bitumen, tar mats in oil fields, and dispersed organic matter in sediments. They can also be formed from chemical transformation of organic materials not containing asphaltenes. One can also mention the products industrially processed from heavy petroleum fractions, oil shales, coal, etc. During the natural transformation of kerogen, the asphaltenes are suggested to be the "transitional" step in the conversion of fossil organic material to oil.

Formation of asphaltenes

The formation process of asphaltenes in nature is not well understood, but the laboratory experiments with model components are helpful in demonstrating the interaction possibilities of the organic matter, active agents such as S, H_2S, O, and heating treatments [42,28]. From the chemical point of view, only two ways are possible for the formation of asphaltene molecules:

(1) Degradation processes imply conversion of high-molecular-weight molecules, for instance, a kerogen macromolecule into smaller asphaltene-size molecules. In fact, during the first kerogen thermal degradation step, Bestougeff et al. [28] observed the formation of asphaltene in great quantities. These asphaltenes are characterized by their high oxygen content (5–12%), high polarity, low aromaticity, and often moderate molecular mass.

(2) Condensation (or polymerization) of two or more rather small (middle-size) molecules such as resin molecules. This route of asphaltene formation is usually

presented by the following scheme: oil → resin → asphaltene. The condensation reactions are strongly activated by the action of H_2S, sulfur and oxygen, which can be present in the source or reservoir rocks (sediments). The functional groups OH–, SH, –CO–, NH–contained in some resin constituents also favor the formation of asphaltenes.

Geochemical evolution of petroleum asphaltenes

Most of the earlier studies reported in the literature on asphaltenes do not pay sufficient attention to the geochemical evolution aspect, whereby the chemical structure of asphaltenes changes continuously and, perhaps, more rapidly than that of other petroleum constituents. The asphaltenes are the most reactive petroleum constituents, and for this reason they undergo substantial transformation, after their formation, during diagenesis, catagenesis, and migration. The most important reactions are aromatization, oxidation, and sulfurization. Also, the reactions of desalkylation and partial cracking can take place under suitable temperature conditions. All these reactions can occur at the same time or successively one after another depending on geological and geochemical changing conditions.

Numerous analysis of asphaltenes separated from crude oils of various degrees of maturation clearly show this evolution. Thus, the asphaltenes of old formations, for instance, precipitated from Hassi-Messaoud crude oil (which resides in Cambrian rocks), have a highly condensed aromatic ring system (aromaticity factor f_a = 0.51). They contain less metals and sulfur than asphaltenes separated from younger oils [43]. Furthermore, the properties of sulfur-rich asphaltenes differ considerably from those which are poor in this component. These facts lead one to assume that asphaltenes, as well as other oil constituents, have been subjected to substantial transformations during petroleum evolution (maturation).

It should be kept in mind that the evolution of asphaltenes began before the accumulation of the oil-pools at the stage of initial presence of bitumens in source rocks (see the example of asphaltene separated from Toarcian shales, Paris Basin in Table 3-5). In this case, two factors can contribute to changes in physical properties and chemical structures of asphaltenes: (1) maturation of asphaltene already formed, and (2) maturation of the initial material, i.e., kerogen itself, with increasing depth of burial.

PRIMARY AND SECONDARY PETROLEUM ASPHALTENES

From the genetic point of view, petroleum asphaltenes are of considerable interest and can be divided in two groups according to their formation process: primary and secondary asphaltenes.

Primary asphaltenes: Primary asphaltenes originate from kerogen and other natural macromolecular materials, as was mentioned before, resulting from the decomposition reaction (cracking) of these materials.

TABLE 3-5

Composition of asphaltenes derived from sedimentary rock bitumens and crude oils

Sources	Shale bitumen, Colorado	Lake sediment	Sporopollen in degradation	Sedimentary rock bitumen (extract)						Crude oils			
					Volga-Ural		Fecocourt	Der	Essises	Ultra-Bulak	Arlanskoe	Krasnoborsk	Volga-Ural
Method*:	1	2	3	4	4	4	5	5	5	2	2	2	4
Geologic formation	Green River	Shallow	380°	Early Carbonif.	Devonian	Eiffel	Toarcian	Toarcian	Toarcian	Late Jura	Early Carbonif.	Middle Cambrian	Tertiary
Facies	–	mud	–	siltstone	limestone sand	limestone		shale "carton"		– –	– –	– –	– –
Depth (m)	<1000	0.6	–	>2000	>2000	>2000	600	1285	2540	2100	1300	1900	–
C (wt%)	74.35	72.47	83.50	79.05	76.38	74.87	77.36	80.17	85.45	87.10	83.70	87.93	87.17
H (wt%)	8.86	9.16	7.72	6.49	7.33	6.79	8.53	8.80	7.59	8.05	9.70	7.85	8.30
S (wt%)	1.80	0.31	–	1.45	3.42	2.76	4.83	4.96	1.15	4.80	4.36	0.45	1.68
N (wt%)	2.71	18.07	8.71	13.01	2.78	1.37	0.86	1.63	1.71	0.4	2.24	3.37	1.10
O (wt%)	10.32				10.09	14.21	8.43	4.45	4.10				1.75
Molecular mass**	1100[a]	1900[d]		1134[d]	1772[d]	2914[d]	6.36[e]	626[e]	664[e]	2100[d]	2285[d]	2129[d]	1928[d]
f_a aromaticity	0.24	–	–	–	–	–	0.32	0.34	0.53	–	–	–	–
H/C (atom)	1.42	1.50	1.10	0.98	1.11	1.10	1.31	1.31	1.06	1.10	1.38	1.06	1.13
O/C (atom)	0.104	0.166	0.078	0.109	0.099	0.142	0.081	0.042	0.036	0.003	0.01	0.022	0.02
ESR Xp. (10^{17}/g)	–	1.28	–	–	–	–	–	–	–	175.7	83.4	152.4	–
References	[44]	[45]	[46]	[47]	[47]	[47]	[48]	[48]	[48]	[45]	[45]	[45]	[47]

* *Asphaltene separation methods:* (1) "petroleum ether", b.p. = 30–60°C + extraction with petroleum ether, b.p. = 70–100°C and alcohol for precipitation [45]; (2) "petroleum ether", b.p. = 68–73°C + extraction with the same solvent for precipitation [47]; (3) *N*-pentane (20-fold volume) + extraction with the same solvent for precipitation [44,50,51]; (4) *N*-hexane + extraction with the same solvent for precipitation [48]; (5) *N*-heptane + extraction with the same solvent for precipitation [13,46,54].

** *Molecular mass determination methods:* [a] by VPO in THF (tetrahydorfuran); [b] by VPO in benzene; [c] by CRYOSCOPY nitrobenzene; [d] not indicated; [e] calculated from proton and ^{13}C-NMR data; [f] by viscosimetry; [g] by gel permeation chromatography.

Secondary asphaltenes: It is very likely that most components of asphaltenes in old and heavy crude oils are secondary products derived from the condensation and/or polymerization of the heavy organic debris during diagenesis and catagenesis. The variety and complexity of the asphaltene structures are rather extensive, taking into account those substances of different nature such as resins; polycyclic, aromatic, and naphthenoaromatic hydrocarbons; porphyrins; asphaltogenic acids; etc., which may contribute to their formation.

CHEMICAL COMPOSITION OF ASPHALTENES FROM SEDIMENTARY ROCKS

The comparative examination of the chemical composition of petroleum and sedimentary rock-derived asphaltenes is of considerable interest for understanding the origin and geochemical evolution of these compounds. As noted previously, the asphaltenes separated from dispersed organic matter and bitumens have in general a much higher oxygen content than petroleum asphaltenes.

The compositions of asphaltenes separated from various sources are presented in Table 3-5. The figures in this table show that (1) asphaltenes separated from dispersed organic matter, (2) sedimentary rock extracts, and (3) shale bitumens have rather different chemical compositions and especially differ from those of petroleum asphaltenes. The latter have not only a low oxygen content but are also distinguished by more aromatic and condensed structures.

The study of sedimentary rock-extracted asphaltenes by carbon- and proton-nuclear magnetic resonance spectroscopy reflects the differences and changes in composition of asphaltenes from Toarcian shales, Paris Basin, with increasing depth of burial. The evolution of structural parameters with the burial depth of shale indicates that the asphaltenes lose more and more H and O atoms and become more aromatic [48].

The differences and changes in the electron spin resonance (ESR) signal of one asphaltene derived from shallow sediments and several petroleum asphaltenes were determined by Chernova and Chutkerashvili [45]. They found a very great difference between the value of this signal for "shallow" and petroleum asphaltenes.

This signal can increase very much with the maturation of the original petroleum. Furthermore, in asphaltene fractions obtained from the same sample, by means of selective solvent fractionation, the ESR signal is higher for fractions separated by more polar solvent as indicated below:

Source of asphaltenes (field)	Geological age	ESR signal Xp. 10^{17}/g (density)				
		crude asphaltene	asphaltene fraction extracted[a]			
			A-1	A-2	B-1	B-2
Sivinskoe	Late Precambrian	158.4	163.8	221.1	267.7	297.0
Yarega	Devonian	83.2	–	78.2	95.7	102.1
Arlanskoe	Early Carboniferous	83.4	–	–	97.1	121.0

[a] A-1, A-2: isooctane + benzene (5 : 1); B-1, B-2: benzene.

TABLE 3-6

Composition of asphaltenes derived from various sources

Starting material	Sedimentary rock bitumen	Crude oils			Petroleum products			Shale	Bituminous coal			
		Scheiben-hard	Hassi-Messaoud	Boscan	Tuimazy		Bachaquero	Green River shale	Kentucky (volatile coal)		Liddell (medium-volatile bitum. coal)	
Geologic formation	Devonian	Oligocene	Cambrian	Eocene	Devonian	Devonian	Miocene	–	–	–	Permian	Permian
Product	bitumen	chromatogr. fraction	–	–	vacuum residuum	vacuum residuum	residuum	–	synthoil	synthoil GPC fraction	synthoil	synthoil
Treatment	extract	–	–	–	blowing	blowing	cracked	retorted + coked	hydrog.	hydrog.	hydrog.	hydrog.
Temp. condition	–	–	–	–	at 250°C	at 250°C			415°C	415°C	at 500°C	at 500°C
C (wt%)	77.80	87.88	88.20	81.10	83.00	83.10	85.00	81.25	85.91	85.30	85.80	85.70
H (wt%)	7.50	7.71	6.50	7.80	7.60	8.30	5.80	8.24	6.85	6.44	7.10	6.50
S (wt%)	5.67	0.70	0.80	6.70	5.30	4.80	4.60	0.81	1.46	0.67	<0.30	<0.30
N (wt%)	1.47	0.20	0.50	0.20	4.10	3.80	1.40	4.31	1.67	1.75	1.52	1.74
O (wt%)	7.56	3.51	4.00	4.20			1.50	3.04	4.11	5.85	5.40	6.00
Molecular mass *	1605 [d]	1210 [f]	1400 [f]	1200 [f]	2140 [d]	1475 [d]	3370 [f]	630 [a]	686 [b]	956 [a,b]	600 [g]	630 [g]
f_a (aromaticity)	0.28	0.39	0.48	0.24	–	–	0.63	0.43	0.70	0.66	0.71	0.72
H/C (atom)	1.15	1.04	0.88	1.14	1.09	1.19	0.81	1.22	0.900	0.90	0.99	0.90
S/C (atom)	0.028	0.003	0.003	0.031	0.024	0.022	0.02	0.004	0.006	0.003	–	–
N/C (atom)	0.016	0.02	0.021	0.009	–	–	1.14	0.046	0.017	0.025	0.015	0.017
O/C (atom)	0.073	0.030	0.034	0.039	0.035	0.033	0.013	0.028	0.036	0.052	0.047	0.053
References	[47]	[13]	[13]	[13]	[49]	[49]	[13]	[50]	[51]	[53]	[54]	[54]

* *Molecular mass determination methods:* [a] by VPO in THF (tetrahydorfuran); [b] by VPO in benzene; [c] by CRYOSCOPY nitrobenzene; [d] not indicated; [e] calculated from proton and ^{13}C-NMR data; [f] by viscosimetry; [g] by gel permeation chromatography.

The composition of asphaltene (Table 3-5) obtained in laboratory by thermal degradation of sporopollenin (kerogen Type II) is quite different from those separated from sedimentary rock bitumen and crude oils which were derived from immature formations. The sporopollenin asphaltene has a lower H/C ratio than that of sedimentary rock bitumen and higher O-content than that of petroleum asphaltenes. The composition of the sporopollenin asphaltene reflects its origin from oxygen-rich kerogen Type II and its thermal history, i.e., decrease of H/C ratio with maturation. The high nitrogen content of Green River Shale asphaltene reflects the nature of the source material.

Rodionova et al. [47] observed that the asphaltene samples separated from various Devonian rock extracts after saponification lost an important part of sulfur in the non-saponifiable portion. The content of saponifiable constituents in asphaltenes, originating from carbonate sediments, is lower (3.5% on average) than that of asphaltenes from terrigenous sediments (10–12.8%). The saponifiable constituents are composed chiefly of aromatic and naphtheno-aromatic acids.

In general, from NMR and other data, one can state that the shale oil asphaltenes, and also to some extent the sedimentary rock asphaltenes, consist of molecules with a heavily substituted, linked, or kata-condensed ring system [48,52]. Inasmuch as the crude oil asphaltenes have undergone maturation, i.e., chemical transformation and eventually sulfurization, their composition and structure reflect their geochemical history. In comparison with bitumen-derived asphaltenes, the petroleum asphaltenes have widely varying structural parameters and composition: (1) aromaticities vary from 0.24 to 0.4, (2) oxygen and nitrogen contents are lower, and (3) the variation of the sulfur content is very large and can be as low as 0.3% or higher than 9%. Upon maturation, the carbon ring system of asphaltene becomes more and more aromatic and peri-condensed.

CHARACTERIZATION OF CHEMICAL COMPOSITIONS OF ASPHALTENES DERIVED FROM DIFFERENT SOURCES

According to the definition, all compounds insoluble in *n*-pentane–*n*-heptane, regardless of their origin, are considered as asphaltenes. The comparison of so-called asphaltenes derived from very different sources, characteristics of which are presented below, shows that the definition of asphaltenes based only on solubility is very confusing and questionable. One can suggest that the asphaltene definition must also consider the chemical composition and origin of these compounds. Some analysis of typical asphaltene samples from various sources is given in Table 3-6. The data in the table illustrate significant and characteristic differences between the composition of asphaltenes derived from seven different sources: (1) solvent extract from Green River shale, (2) solvent extract from sedimentary rocks, (3) crude oils with low and high sulfur content, (4) blown refinery residue, (5) cracked refinery residue, (6) retorted shale oil, and (7) coal-derived synthoil.

ASPHALTENE CHARACTERIZATION

The asphaltenes derived from the first two sources are natural products and are characterized by the high hydrogen and oxygen content but relatively low sulfur content. Their aromaticity and the degree of condensation of their ring systems are quite small.

The *composition of "blown asphaltene"* (Table 3-6), which is a constituent of "blown asphalt", presents a particular case in comparison with all other asphaltenes due to the manner of its formation. During the blowing process, i.e., air oxidation at about 250°C, the main chemical reaction is chiefly dehydrogenation and polycondensation of resin and asphaltene molecules present in the initial material (petroleum residue). The greatest part of oxygen involved in the reaction (80–90%) is recovered as water. The other part of the reacting oxygen is bounded in the residue with small quantities of carbon dioxide and other oxidation compounds being formed. With increased blowing time, the contribution of other reactions, such as degradation, becomes more and more important, implying the formation of very physically and chemically complex heterogeneous mixtures, containing compounds with very different structures. The molecular mass of asphaltene increases at the beginning of blowing, after which it decreases. The chemical composition and properties of "blown asphaltene" vary widely with the nature of the initial residue and the severity of the blowing process. The composition and properties of a medium asphaltene sample derived from blown residue of heavy, high-sulfur crude oils are presented in Table 3-6.

The *aromaticity, polarity and reactivity of coal-derived asphaltenes* (f_a = 0.6–0.7) are higher than those of petroleum asphaltenes (f_a = 0.2–0.5).

The aromatic ring system of coal-derived asphaltenes is sparingly substituted (35–45%) with short chains, mostly methyl groups, whereas that of petroleum asphaltenes is extensively substituted (70–80%) with longer chains. The molecules of coal asphaltenes are less associated and quite small (MM about 300–1200) when compared to petroleum asphaltenes. High polarity and reactivity of coal-derived asphaltenes are due to the presence of phenolic and pyridine nitrogen functional groups.

The proton NMR study of coal asphaltene fractions shows that aliphatic-to-aromatic hydrogen ratios decrease with increasing molecular mass, implying that the ring system becomes more and more aromatic and condensed.

The coal asphaltenes consist of organic compounds of a rather wide range and different character as indicated by elemental analysis. The higher-molecular-mass fractions, insoluble in benzene but soluble in more polar solvents such as pyridine or tetrahydrofuran (THF), and called "preasphaltenes", have the lowest H/C ratio and condensed aromatic ring system, whereas the lower-molecular-mass GPC fractions, which are basically hydrocarbons, have on the average only four heteroatoms in every ten molecules [55].

CONCLUSION

(1) The present knowledge of the nature, chemical structure and physicochemical behavior of asphaltenes justify their recognition as a distinct and specific group of organic substances.

(2) This group must have its own definite place in the organic chemistry system between micro- and macro-molecular organic substances.

(3) Systematic study of these intermediate molecules will open a new chapter in organic chemistry, covering not only the specific field of asphaltenes, but generally speaking, that of the rules of organization of organic molecules according to their size.

(4) New progress in the knowledge of the chemical structure of asphaltenes cannot be made without achieving the following:

(a) Separation of crude asphaltene into narrow homogenous fractions [56,57,59].
(b) Improvement of analytical methods for separation of asphaltenes according to their chemical functions.
(c) Characterization and better identification of asphaltenes according to their origin.
(d) Setting up a classification and nomenclature of asphaltenes from different sources (mandatory to avoid all sorts of confusion).

STATUS AND PROGNOSIS

(1) A single standardized method of precipitation and purification of asphaltenes is absolutely mandatory to coordinate scientific studies carried out on these materials by different researchers from different countries.

(2) True molecular mass of asphaltenes and their monomers should be determined.

(3) The chemical composition of asphaltenic and non-asphaltenic constituents of precipitates (crude asphaltenes) should be studied, in particular for non-heteroatomic compounds (i.e., pure aromatic hydrocarbons, the existence of which remains to be proven).

(4) Pursuit of experimentation on the synthesis of model molecules of asphaltenes is a very promising and desirable approach.

(5) A systematic investigation of the geochemical transformation of asphaltenes in the laboratory and in nature should be carried out on a broader scale.

(6) Such a study (5) should be coordinated with some research on the generation of asphaltenes in natural geochemical conditions.

(7) Similar studies should be carried out on the formation of asphaltenes from other sources in nonnatural (artificial) conditions.

REFERENCES

[1] Long, P.B., The concept of asphaltenes. *Am. Chem. Soc. Meet., Div. Pet. Chem.*, Washington, September 9–14 (1979).

[2] Bestougeff, M.A. and Bargman, D., Nouvelles techniques de fractionnement des produits lourds des pétroles. *C.R. 5° Congr. Mondial Pétrole*, Rome, p. 213 (1955).
[3] Knotnerus, J. and Krom, C.J., The constitution of wax isolated from bitumen. *Asphalt Symp., Am. Chem. Soc. Meet.*, April 5–10 (1964).
[4] McKay, J.F., Amend, P. J., Cogswell, T.E. and Harnsberger, P.M., Petroleum asphaltenes — Chemistry and composition. *Am. Chem. Soc. Meet., Div. Pet.*, New Orleans, March 20–25 (1977).
[5] Yen, T.F., Structure of petroleum asphaltene and its significance. *Energy Sources*, 1(4): 447–463 (1974).
[6] Ignasiak, T., Kemp-Jones, A.V. and Strausz, O.P., Properties of asphaltenes from various Alberta crude oils. *Am. Chem. Soc., Div. Fuel Chem., Prepr.*, 22: 126 (1977).
[7] Bunger, J.W., Chemistry of asphaltenes — Summary of symposium. *Am. Chem. Soc. Meet., Div. Pet. Chem.*, Washington, September 9–14, pp. 1028–1031 (1979).
[8] Speight, J.G. and Moschopedis, S.E., On the polymeric nature of petroleum asphaltenes. *Fuel*, 59 (June): 440 (1980).
[9] Witherspoon, P.A. and Winniford, R.S., The asphaltic components of petroleum. In: B. Nagy and U. Colombo (Editors), *Fundamental Aspects of Petroleum Geochemistry*. Elsevier, Amsterdam, pp. 261–298 (1967).
[10] Sergienko, S.R., Taimova, B.A. and Talalaev, E.I., *Constituants Hétéroatomiques du Pétrole à Poids Moleculaire Elevé (Resines et Asphaltènes)*. Nauka, Moscow, pp. 132–146 (1979).
[11] Strausz, O.P., *Some Recent Advances in the Chemistry of Oil Sand Bitumen*. Unitar I, Rep. 28 (1979).
[12] Bunger, J.W. and Cogswell, D.E., Characteristics of tar sand bitumen asphaltenes and the effect of asphaltenes on conversion of bitumen by hydropyrolysis. *Am. Chem. Soc. Meet., Div. Pet. Chem.*, Washington, September 9–14, pp. 1017–1027 (1979).
[13] Bestougeff, M.A., Composition chimique et structure des asphaltènes et leur place parmi les substances organiques naturelles. *Bull. Soc. Chim. Fr.*, 12: 4773 (1967).
[14] Jewell, D.M., Ruberto, R.G., Albaugh, E.W. and Query, Distribution and structural aspects of sulfur compounds in residuals. *Am. Chem. Soc. Meet., Pet. Div.*, Chicago, August 24–29, p. 743 (1975).
[15] Ignasiak, T., Strausz, O. and Montgomery, D.S., Oxygen distribution and hydrogen bonding in Athabasca asphaltene. *Fuel*, 56: 359–365 (1977).
[16] Ignasiak, T., Ruo, T.C.S. and Strausz, O.P., Investigation of Alberta oils sand asphaltenes using thermal degradation reactions. *Am. Chem. Soc. Meet., Fuel Chem. Div.*, Washington, September 9–14, 24: 178–183 (1979).
[17] Ferris, S.W., Black, E.P. and Clelland, J.B., Aromatic structure in asphalt fraction. *Am. Chem. Soc. Meet.*, Pittsburgh, March 23–26, pp. B-130–139 (1966).
[18] Ignasiak, T., Bimer, J., Samman, N., Montgomery, D.S. and Strausz, O.P., Study of degradation of Athabasca asphaltlenes. *Am. Chem. Soc. Meet., Pet. Div.*, Washington, September 9–14, pp. 1001–1006 (1979).
[19] Jurkiewicz, J. and Rosinski, S., Coal tar compounds. *Koks, Smola, Gaz*, 1(4): 143–152 (1956); translated from Polish and published by National Science Foundation and Department of the Interior in 1962.
[20] Bestougeff, M.A. and Pierre, M., Recherche de formules développées d'hydrocarbures de poids moleculaire élevé. *Ann. Chim.*, 3: 481–490 (1968).
[21] Hirsch, E. and Altgelt, K.H., Integrated structural analysis. A method for the determination of average structural parameters of petroleum heavy ends. *Anal. Chem.*, 42: 1330 (1970).
[22] Haley, G.A., Unit sheet weights of asphalt fractions determined by structural analysis. *Anal. Chem.*, 44: 580 (1972).
[23] Dickinson, E.J., *Proc., Assoc. Asphalt Paving Technol.*, 43: 132 (1974).
[24] Klet, H.H., Blanchard, L.P. and Malhotra, S.L., *Science*, 12 (September): 607 (1977).
[25] Klet, H.H., Malhotra, S. and Blanchard, P., Structure parameter analyses of asphalt fractions by a modified mathematical approach. *Anal. Chem.*, 55: 1212 (1978).
[26] Rosental, D.A., Posadov, J.A., Popov, D.G. and Paukku, A.N., *Determination and Calculation Methods of the Structure Parameters of Heavy Ends of Crude Oil Fractions*. Technological Institute, Leningrad (1981).

[27] Bestougeff, M.A. and Collet, L., *Calculation of Structural Parameters of the High Molecular Mass Hydrocarbons*. TOTAL–Compagnie Française des Pétroles, Proprietary Report (1983).
[28] Bestougeff, M.A., Byramjee, R.J. and Pesneau, B., On the chemical mechanism of kerogen thermal transformation. Study of the transformation of sporopollenin. *Org. Geochem.*, 8(6): 389–398 (1985).
[29] Poljakova, A.A. et al., *IIeme Symp. Int. Chimie des Composes Organiques du Soufre*, Riga, June (1980).
[30] Lamathe, J., Dosage potentiométrique des fonctions soufrées non thiopheniques. Application aux produits d'origine pétrolière. *C.R. Acad. Sci. Paris, Sér. C*, 2633: 862–874 (1966).
[31] Eliceev, V.S., Kam'yanov, M.F. and Numanov, I.U., Structure of native asphaltenes of South Tadjikistan crude oil. *Neft Khim.*, 20: 277 (1980).
[32] Speight, J.G. and Pokonova J.V., Some observations on the structure and chemical transformation of petroleum asphaltenes. *Neftekhimiya*, 22(1): 33 (1982).
[33] Schmitter, J.M., Vajta, A. and Arpino, P.J., Investigation of nitrogen bases from petroleum (1980).
[34] Marcusson, J., Burchatrz, H. and Wilke P., *Die Naturlichen und Kunstlichen Asphalte*. Englemann, Leipzig, 2nd ed., 254 pp. (1931).
[35] Schweighardt, F.K., Retcofsky, H.L. and Raymond, R., Asphaltenes from coal liquefaction. *Am. Chem. Soc., Meet., Fuel Chem.*, August 29, 21: 27 (1976).
[36] Kiselew, V., Acid and basic components of native asphaltenes of petroleum and coal. *Neftekhimiya*, 19: 714 (1979).
[37] Ramljak, Z., Solc, A., Arpino, P., Schmitter, J.M. and Guichon, G., Separation of acids from asphalts. *Anal. Chem.*, 49: 1222 (1977).
[38] Zumer, M., Such, C. and Brûlé, B., Extraction et caractérisation des fractions acide et basique d'un bitume routier. *Analysis*, 9(7): 348–352 (1981).
[39] Schwager, I. and Yen, T.F., Determination of nitrogen and oxygen functional groups in coal-derived asphaltenes. *Anal. Chem.*, 51: 569 (1979).
[40] Boduszynski, M.M., Asphaltenes in petroleum asphalts — composition and formation. *Am. Chem. Soc. Meet., Div. Pet. Chem.*, Washington, September 9–14 (1979).
[41] Boduszynski, M.M., McKay, J.F. and Latham, D.R., Asphaltenes, where are you? *Asphalt. Paving Technol.*, 49: 123–143 (1980).
[42] Bestougeff, M.A. and Combaz, A., Action d'H_2S et de S sur quelques substances organiques actuelles et fossiles. *Actes, 6eme Congr. Int. Géochim. Org.*, Rueil-Malmaison, p. 747 (1973).
[43] Bestougeff, M.A., Guiochon, G. and Jacque, L., Etude thermogravimétrique des asphaltènes. *C.R. Acad. Sci. Paris*, 254: 266–268 (1962).
[44] Shue, F.F. and Yen, T.F., A comparison of asphaltenes from naturally occurring shale bitumen and retorted shale oils: The influence of temperature on asphaltene structure. In: H.C. Stanffer (Editor), *Oil Shale, Tar Sands and Related Materials. ACS Symposium Series 163* (1981).
[45] Chernova, T.G. and Chutkerashvili, E.E., Study of the structure of different nature asphaltenes by ESR method. *Chem. Technol. Fuels Lubr. Oils*, p. 57 (1976).
[46] Pesneau, B., *Etude de la Sporopollenine par Dégradation Partielle*. Thèse, Université de Paris VII (1979).
[47] Rodionova, K.F., Shishena, E.P. and Korolev, J.M., Composition study of asphaltenes derived from dispersed organic matter. *Geol., Pet. Gas*, 8: 15 (1963).
[48] Dereppe, J.M., Moreaux, C. and Castex H., Analysis of asphaltenes by carbon and proton nuclear magnetic resonance spectroscopy. *Fuel*, 57: 435 (1978).
[49] Chelton, H.M. and Traxler, R.N., *Proc. 5th World Petroleum Congress*, Section V, p. 247 (1959).
[50] Yen, T.F., Wen, C.S., Kwan, J.T. and Chow, E. The nature of shale-oil derived asphaltenes, In: O.P. Strasz, E.M. Lown (Editors), *Oil Sand and Oil Shale Chemistry*, Verlag Chemie Int., New York, NY (1978).
[51] Sternberg, F.K., Raymond, R. and Schweighardt, F., Acid–base structure of coal-derived asphaltenes. *Science*, 188: 49 (1975).
[52] Yen, T.F., The nature of vanadium complexes in the refining of heavy oil, *Energy Sources*, 4(3): 339–357 (1978).

[53] Jones, D.G., Rottendorf, H., Wilson, M.A. and Collin, P., Hydrogenation of Liddell coal. Yields and mean chemical structures of the products. *Fuel*, 59: 19 (1980).
[54] Gun, R.B., Composition of blown asphalts in terms of the main chemical groups. *Chem. Technol. Fuels Lubr. Oils*, 7: 51 (1959).
[55] Addington, D., *Absorption of Coal Derived Asphaltenes*. Ph.D. Thesis, University Microfilms Intern. Ann Arbor, Mich. (1978).
[56] Altgelt, K.H., Gel Permeations Chromatographie in der Structuranalyse von Bitumen. *Bitumen, Teere, Asphalte, Peche*, November, p. 475 (1970).
[57] Bestougeff, M.A., Fractionnement des asphaltènes par chromatographie. *C.R. Acad. Sci. Paris*, 262: 577 (1966).
[58] Boduszynski, M.M., Baldev, Raj, Chadha and Szkuta-Pochopien, T., Fractionation of Romashkino asphaltenes using ion-exchange chromatography. *Fuel*, 56: 3432 (1977).
[59] Brûlé, B., Contribution de la chromatographie sur gel perméable (G.P.C.) à la caractérisation qualitative et quantitative des bitumes. *Lab. Central des Ponts et Chaussées, Rapp. Rech.*, LCP 76 (1978).
[60] Brûlé, B., Application de la chromatographie sur gel perméable (G.P.C.) à la caractérisation de fractions d'asphaltènes. *Bull. Liaison Ponts et Chaussées*, 85: 97 (1976).
[61] Ignasiak, T., Kemp-Jones, A.V. and Strausz, O.P., The molecular structure of Athabasca asphaltlene. Cleavage of the carbon–sulfur bonds by radical ion electron transfer reactions. *J. Org. Chem.*, 42: 312–320 (1976).
[62] Moschopedis, S.E. and Speight, J.G., Investigation of nitrogen types in Athabasca bitumen. *Am. Chem. Soc. Meet., Div. Pet. Chem.*, Washington, September 9–14 (1979).
[63] Schwager, I. and Yen, T.F., A chromatographic separation and characterization of coal-derived asphaltenes. *Fuel*, 58: 219–227 (1979).
[64] Zumer, M., Such, C. and Brûlé, B., Caractérisation d'un bitume (et de ses fractions) par chromatographie en phase liquide à polarité de phases inversées. *Analysis*, 9(4): 145–148 (1981).

Asphaltenes and Asphalts, 1. Developments in Petroleum Science, 40
edited by T.F. Yen and G.V. Chilingarian

Chapter 4

FUEL OIL CHEMISTRY AND ASPHALTENES

E.V. WHITEHEAD

INTRODUCTION

The primary process in crude oil refining is distillation at atmospheric pressure or under vacuum, through fractionating towers fitted with a series of perhaps fifty condensation plates of bubble cap trays, arranged in such a way that the vapor from the lower tray rises and passes through the condensed liquid in the tray above as shown diagrammatically in Fig. 4-1.

The process is so regulated that each overlaying tray in the tower condenses molecules which become progressively smaller. It follows that the very complex mixture of crude oil hydrocarbons and heterocyclic compounds becomes segregated in its passage through the tower, into commercial products of decreasing boiling point, density, viscosity and carbon number. Finally, at the very top of the tower, one might expect to find the light gases like methane, ethane, propane and butane.

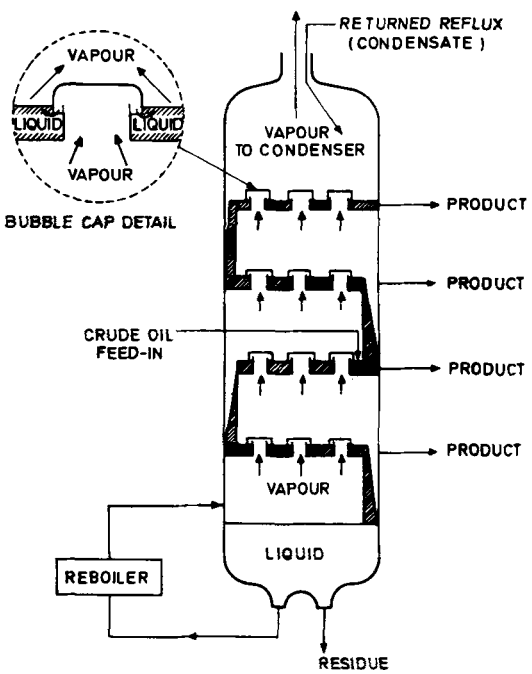

Fig. 4-1. Fractionation tower (diagrammatic).

It also follows that the commercial products which emerge from trays in the tower below the point of entry of heated crude oil, will contain the larger, slower-moving molecules. These will have a higher boiling point, density, viscosity and carbon number than the lighter products condensing as side streams above the point of entry.

These heavy involatile products leaving the bottom of the column contain a complex mixture of high-molecular-weight compounds known as residua form the principal components of fuel oils, which are discussed here.

DISCUSSION

A simplified but typical refinery flow diagram for atmospheric residue is highlighted in Fig. 4-2 and pinpoints many of the side streams and by-products that find their way into commercial fuel oils.

The information contained in Fig. 4-2 has inevitably introduced a plethora of petroleum products and refinery designations coined in the early 1900's. At that time, product names from allied industries were indiscriminately applied to petroleum processing and its products. All of these products, particularly the heavy high-molecular-weight ones, are very complex mixtures of petroleum hydrocarbons and heterocyclic compounds.

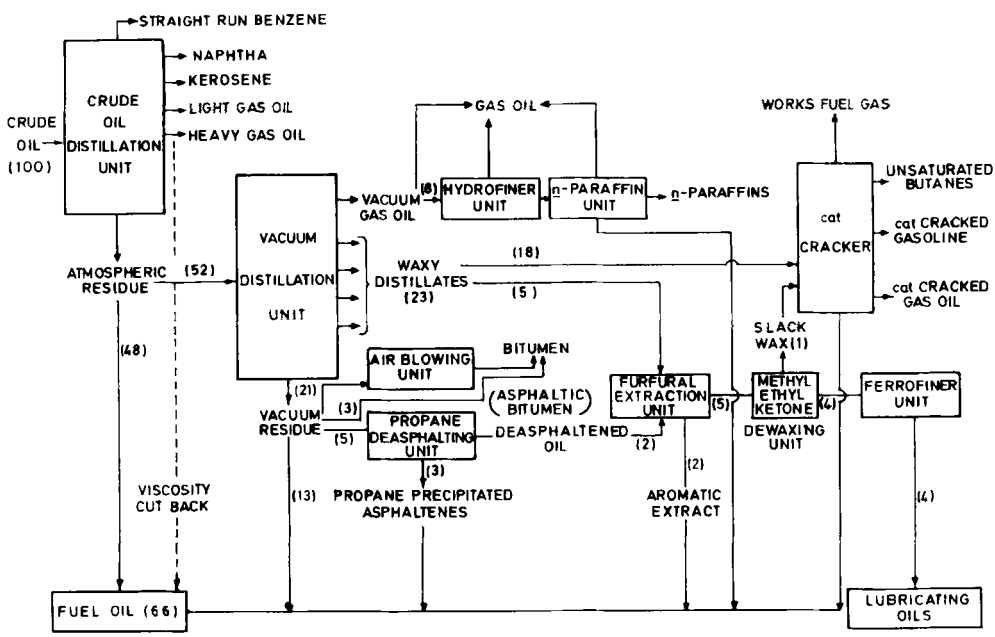

Fig. 4-2. Typical refinery flow diagram showing nominal yields.

TABLE 4-1

Heavy petroleum product terminology

Asphalt: Natural or commercial mixtures of bitumen and inert mineral matter. Natural asphalt, like lake asphalt, occurs as surface or near surface deposits as a petroleum colloidal system. In America, the term asphalt is usually synonymous with material known in England as asphaltic bitumen or bitumen.

Asphaltenes are obtained by solvent fractionation of residues. This process segregates soluble oily molecules from less soluble asphaltenes. The Institute of Petroleum method defined in the IP test method IP 143/77 uses *n*-heptane and defines asphaltenes as dark brown to amorphous solids insoluble in *n*-heptane but soluble in toluene or benzene.

Atmospheric residue is a refinery residue usually boiling above 350°C, which is left after the commercial distillates have been removed from crude oil. The material may sometimes be referred to as bitumen.

Bitumen or *asphaltic bitumen* is a black to dark brown semi-solid organic material, which gradually liquefies when heated. It is usually obtained as a residue from the distillation of petroleum through atmospheric or vacuum distillation units.

Blown bitumen is obtained when petroleum bitumen is treated with oxygen (air blown). It is a semi-solid or solid oxidized product from bubbling air through hot liquid bitumen. The process increases the melting point and viscosity of the product.

Carboids are very high molecular weight carbonaceous materials which may remain after asphaltenes have separated from: *deasphaltened oil.* Carboids are insoluble in both *n*-pentane and benzene or toluene.

Crude oils: No precise definition is possible, since the composition of each crude oil is unique. Most crude oils contain similar components, but their ratios and distributions are different in each crude oil.

Deasphalted oil (DAO) is the clear yellow to red oil remaining when a bitumen is deasphaltened commercially with propane or alternative solvents, or as in IP 143/77, with *n*-heptane. It is often the commercial material from which lubricating oils are manufactured.

Distillates are usually refinery distillates, like straight run benzene (SRB), naphtha, kerosene, light and heavy gas oils, diesel oils and waxy distillates obtained as side streams from either atmospheric or vacuum fractionating units in a refinery.

Fuel oil is a general term applied to an oil used in the production of power or heat. Any petroleum product or mixture of products that is burnt under boilers or in industrial furnaces. These oils are normally residues, but blends of distillates and residues are also used. An alternative term *liquid fuel* is sometimes used. They are thick, viscous, black oils.

Maltenes or *petrolenes:* A viscous liquid that can be divided into *resins* and oil by chromatography or solvent fractionation. Soluble in *n*-heptane.

Resins are light or dark colored, thick, viscous to amorphous solids which can be segregated by additional solvent fractionation or chromatography, from deasphaltened oils.

Vacuum residue is a refinery residue from a vacuum distillation unit (VDU) usually boiling above 500°C. It may sometimes be referred to as a bitumen but is often deasphaltened with propane to give deasphalted oil and a propane asphalt or true bitumen.

In Table 4-1, the principal technical terms, applied to heavy petroleum substances, are evaluated.

As the composition of each crude oil is unique, it is not possible to define the exact composition of any one. Certainly, similar families of hydrocarbons such as alicyclics, cyclics and aromatics are present in each, together with organic compounds

TABLE 4-2

Crude oil types

Origin of crude oil and products	Carbon number range	Intermediate		Heavy
		North Sea	Middle East	South American
Crude oil				
Sulfur (wt%)		0.3	2.5	5.5
Light gasoline	C_4–C_{10}			
Distills at 0–70°C yield		5.8	4.7	0.1
Sulfur (wt%)		0.001	0.020	0.100
Naphtha				
Distills at 70–140°C		11.0	7.9	1.1
Sulfur (wt%)		0.001	0.020	0.450
Kerosene	C_{11}–C_{12}			
Distills at 140–250°C		18.6	16.4	4.4
Sulfur (wt%)		0.02	0.02	2.80
Diesel fuel	C_{13}–C_{20}			
Distills at 250–350°C yield		19.1	15.3	9.6
Sulfur (wt%)		0.18	1.40	4.40
Residue	$>C_{40}$			
Distills above 350°C yield		43.5	54.4	84.8
Sulfur (wt%)		0.6	4.1	6.0
Metals: V, Ni (ppm)		12	63	1592

of sulfur, oxygen, nitrogen and traces of those containing nickel, vanadium, iron, molybdenum, chlorine, fluorine and other elements. Naturally then, the product composition will vary widely depending upon the crude oil fed to the crude oil distillation unit, and the variations illustrated in Table 4-2 are commonplace. Thus, refinery flexibility must be sufficient to adapt to changes in crude oil feed as well as to the market pattern of demand during winter, spring, summer and autumn.

This type of compositional information can be usefully assembled pictorially and is presented in Fig. 4-3 as a guide to the relationship between the boiling point of a refinery distillate and the carbon number of the molecules that it may contain [1]. Having described the methods of production and designated the principal components of fuel oil, it is possible with minimum confusion to summarize what is known of the chemical composition of the principal components.

The major hydrocarbon, sulfur, oxygen and nitrogen compounds that go to make up the bulk of the deasphaltened oil have been described in detail before [2], and they are catalogued for convenience in Figs. 4-4 to 4-9.

At this stage of our consideration of the chemistry of fuel oils, we have been able with reasonable certainty to outline and circumscribe the principal molecular components of deasphalted oils and petroleum distillates, accepting at the same time that the concentration of particular components will show very wide variation in practice.

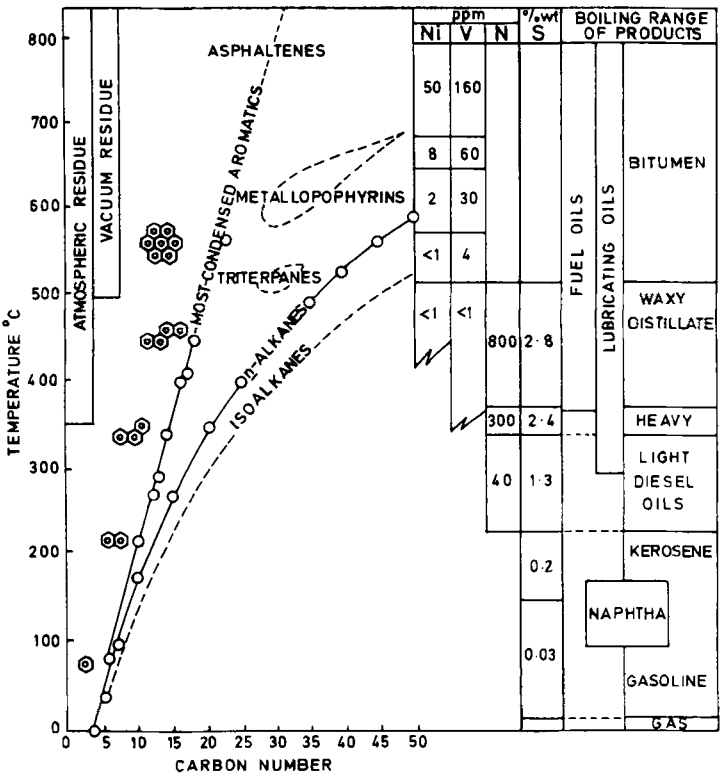

Fig. 4-3. Hydrocarbon boiling point versus carbon number with petroleum products. All hydrocarbons will be contained within the area enclosed by the lines plotted for isoalkanes and most-condensed aromatics petroleum products with approximate boiling ranges.

This leaves for consideration the much more complex and higher-molecular-weight, residual components of petroleum known subjectively as the asphaltic bitumens, which, of course, together with a variety of other petroleum oils and residues, turn up in fuel oils.

In 1967, Witherspoon and Winniford [3] summarized the state of our understanding of the asphaltic/bitumen components of petroleum and reviewed the literature up to 1964. Certainly, during the last few decades much more has become known about the physical chemical behavior of petroleum asphaltenes and their colloidal character. Their peptizing maltenes (petrolenes), (and the oil and resin components of these maltenes), together with petroleum bitumens, are still regarded as a complex colloidal system in chemical equilibrium.

Traditionally, the bitumen components have been separated by selective solubility in different solvents. From a physical-chemical point of view, this can be an inefficient system if individual components are sought for characterization in terms of chemical structure. Witherspoon and Winniford noted that asphaltenes segregated by *n*-heptane were inhomogeneous, and this view still holds today [47]. Elemental

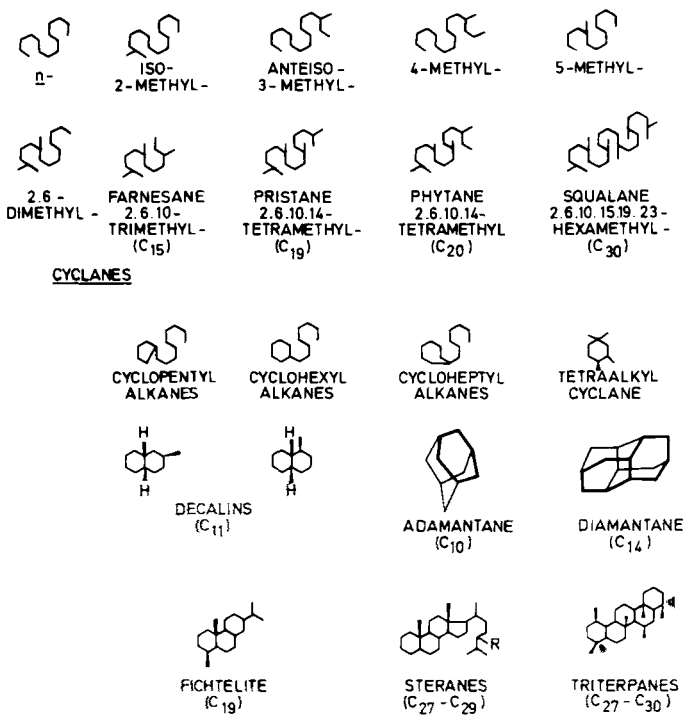

Fig. 4-4. Alkanes and naphthenes (cyclic hydrocarbons) found in deasphalted oils.

analysis of high molecular weight aromatic mixtures like coal [5] and asphaltenes can be notoriously difficult. Sometimes the sulfur and nitrogen contents, and often the oxygen contents, are determined by difference, for unknown structures which are difficult to burn. It is thus perhaps not surprising that the chemical structures of coal and asphaltenes remain a scientific enigma.

The asphaltic bitumen components of petroleum are traditionally separated (IP 143/77) by a paraffinic solvent, *n*-heptane, into: (a) a soluble maltene portion (which will contain high molecular weight waxes C_{30}–C_{90} washed out of precipitated asphaltene with hot *n*-heptane); and (b) a precipitated asphaltene which is insoluble in *n*-C_7 but soluble in benzene or toluene, and is defined in this way as a heptane asphaltene. The structure, and indeed separated asphaltene, will vary widely depending upon the crude source and the precipitating solvent [6,7]. The more recent work has highlighted the colloidal nature of petroleum bitumens, and as a consequence, the asphaltene-maltene-resin interactions are now better understood because this work has defined much more clearly the strong hydrogen bonding interactions between many of the components. The work has also established the presence of phenols, carboxylic acids, esters, ketones and basic nitrogen compounds [8–21] in these components, all good potential hydrogen bonding subunits.

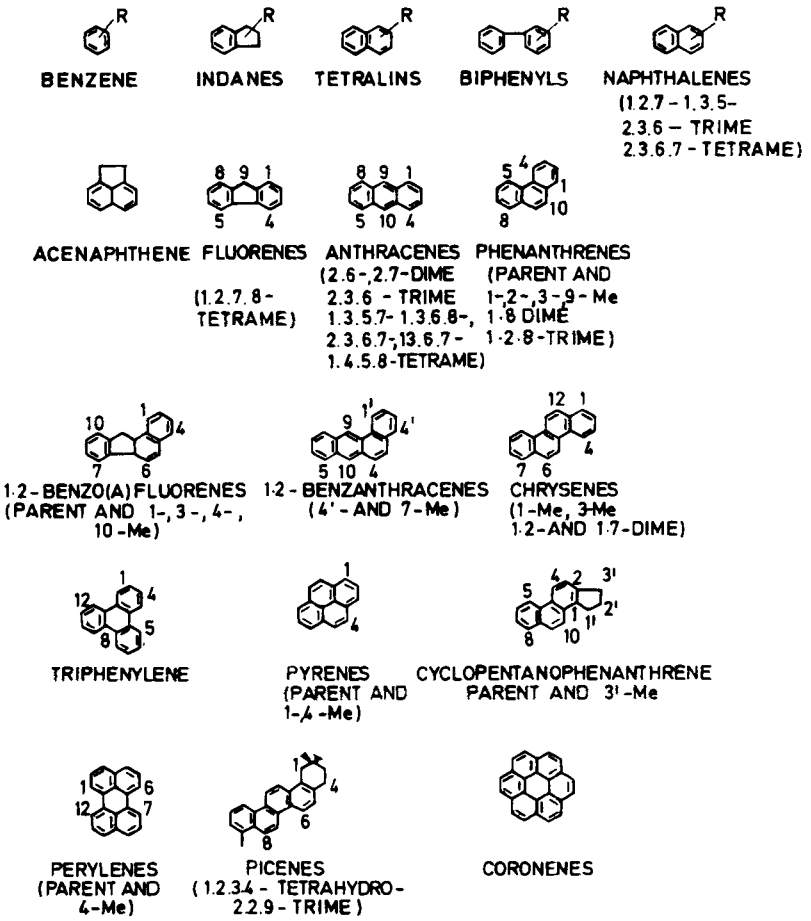

Fig. 4-5. Aromatic hydrocarbons of petroleum.

Thus, within this proposed colloid system, the aromatic high-molecular-weight asphaltenes are peptized by the maltenes (and the resins contained in the maltenes). The measured carboxyl and ester functionality is highest in the resin portion. During peptization, strong hydrogen bonds form between these acids and the abundant phenolic hydroxyls found in the asphaltenes. Hydrogen studies [22–24] support these ideas.

In these studies, asphaltenes were hydrogenated in decalin over a CoMo/alumina catalyst. Hydrogenation was slow even at 330–450°C due to the colloidal nature of the substrate. The micellular structure was destroyed in time by hydrogenolysis of C–O, C–S and C–N bonds, reducing hydrogen bonding as a consequence. Above 400°C, carbon-to-carbon bonds rupture, and saturated hydrocarbons dehydrocyclise or crack. The molecular weight of the products drop from the $1–2 \times 10^3$ range

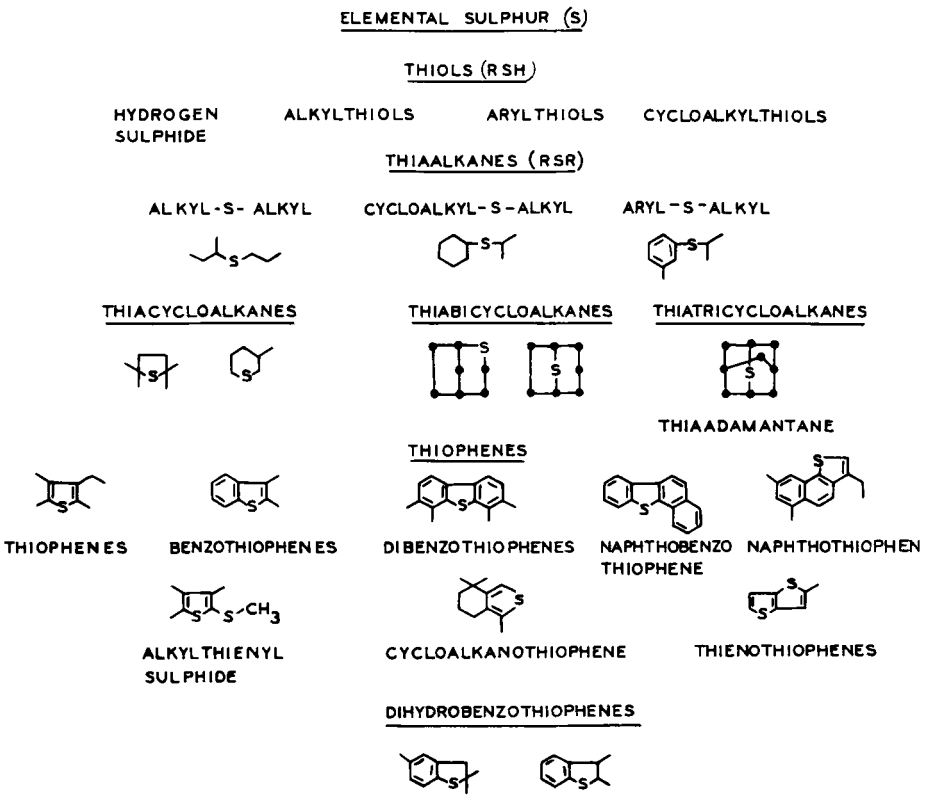

Fig. 4-6. Sulfur compound types found in deasphalted oil.

for asphaltenes to the 200–400 range for oils, which by NMR analysis appear as polyaromatic ring systems with minimal alkylations.

It is thus no surprise to find in the literature a very wide range of molecular weight values for asphaltenes in various states of aggregation and dissociation, in relation to the polar strength of the solvents used and the temperature of determination. After performing gel permeation chromatography separation of petroleum bitumens, Altgelt [25] reports values of 7000–30,000 for asphaltenes, 550–1200 for maltenes and 500–2500 for petroleum resins. Light scattering, X-ray and osmometric techniques suggest a range of 2–16 $\times$ 10^3 for different asphaltenes, whereas Moschopedis et al. [16] report a still lower range of 1–2 $\times$ 10^3 for Alberta crude oil asphaltenes dissociated in nitrobenzene.

Separation schemes [26] have been devised which permit the fractionation of bitumens chromatographically over ion-exchange resins and silica/alumina. In this way, benzothiophenes and napthobenzothiophenes, which are known in deasphalted oils [2], are also reported in petroleum maltenes. A second study on maltenes [11] showed that maltenes from a Romashkino bitumen (molecular weight 1000)

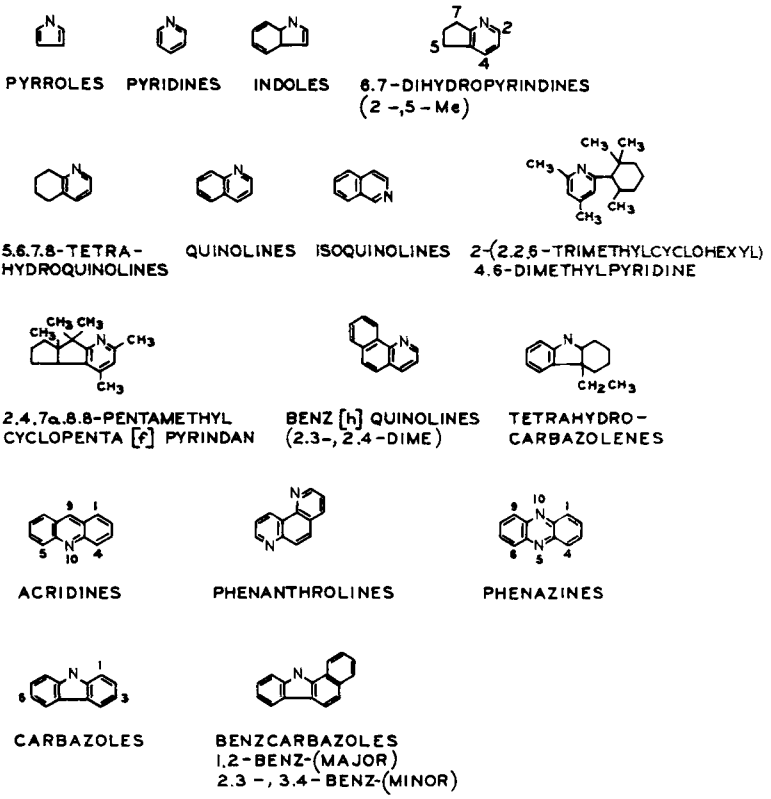

Fig. 4-7. Nitrogen compound types found in deasphalted oil.

contained 7.5 wt% of acidic polyaromatic components containing 1.2–1.9 nitrogen atoms and 1.3–1.4 sulfur atoms per molecule.

A basic component, 12.3 wt% at molecular weight 900–1000, was also aromatic, and contained 0.7–1.2 atoms of nitrogen and 2.1–2.4 atoms of sulfur per molecule. The nitrogen content increased in step with base strengths and oxygen in step with the acid strengths. The aromatic and sulfur compound types in an Athabasca bitumen have been described [31]; they mirror those known in deasphalted oil.

Hydrogenation studies have shown that asphaltenes can be dissociated from their colloidal state and reduced by heteroatom elimination to lower-molecular-weight oils. The complement of this step, oxidation, will be expected to shift the dynamic equilibrium (referred to earlier) in the opposite direction. Thus, asphaltenes can be formed from maltenes, resins and aromatics by air blowing (oxidation) [6,32,33]. Indeed, heating with sulfur, by a process of dehydrogenation, increases the asphaltene content at the expense of aromatics, resins and maltenes [34,35]. So-called synthetic asphaltenes are formed when maltenes, dimethylnaphthalenes or cholesterol are heated with sulfur. It is known that heavier asphaltenes, with

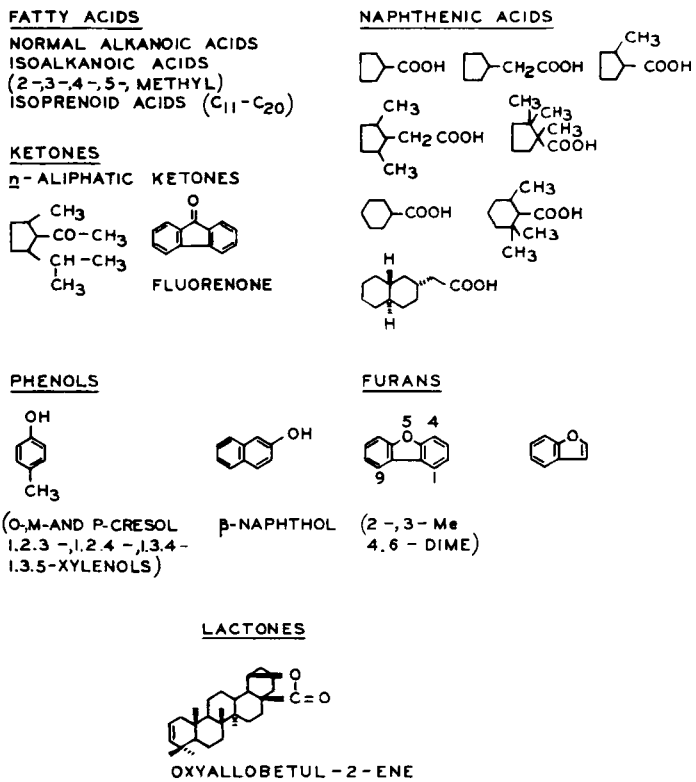

Fig. 4-8. Oxygen compound found in deasphalted oil.

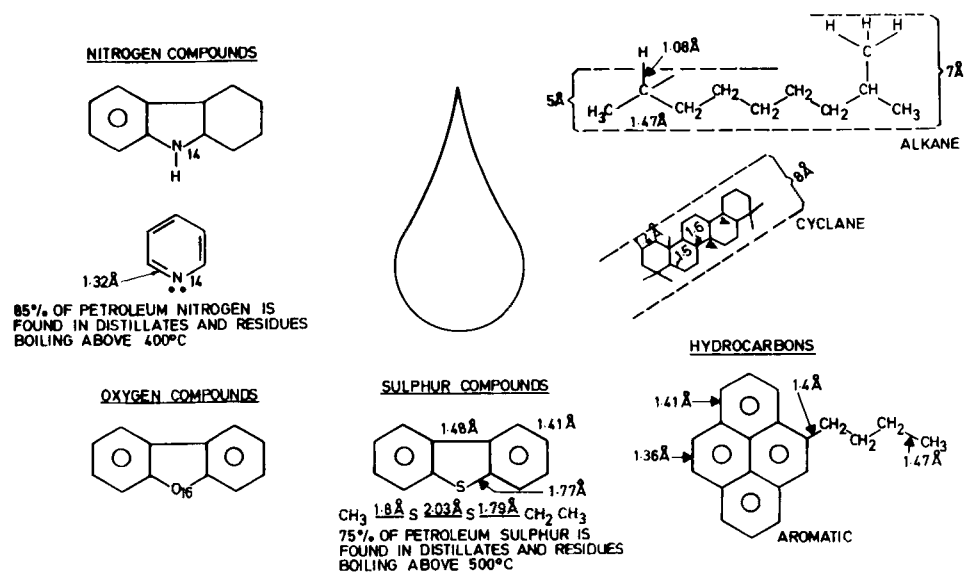

Fig. 4-9. Components of deasphalted oily drop.

enhanced aromaticity and a higher nitrogen content, are obtained when asphaltene complexes are precipitated with Lewis acids [36]. Thus, the injection of strong acids into oil-bearing formations could reduce permeability as a result of precipitation of asphaltenes. Such asphaltenes could appear as molecular clusters, coated with resins and high-molecular-weight (C_{30}–C_{90}) *n*-alkanes, which are known to be deposited in pipelines, tank bottoms, and well stems.

Pore size studies on asphaltenes have shown that like coal, asphaltenes contain pores which fall into two groups, the macropores (>200 nm) and pores that are less than 1.5 nm wide.

Of particular interest in this book may be the degradative pyrolysis studies on asphaltenes. Such studies [38–46] have revealed something of the comparative stabilities of resins, maltenes and asphaltenes, their progression to coke when heated, and have highlighted the order in which gas and light hydrocarbons evolve in the cracking sequence. The work has also confirmed the presence of long lipophilic paraffin chains, linked to the asphaltene aromatic core. This evidence is also supported by infra-red studies on native asphaltenes [47]. The aromatic nature of the asphaltene core is endorsed by oxidation studies in aqueous alkali [48] which demonstrate that 50–60% of petroleum asphaltene can be oxidized to mixtures of water-soluble aliphatic dicarboxylic acids and benzene carboxylic acids. With nitric acid, asphaltenes are converted in high yield to nitrohumates of undefined structure [49].

With this general information in hand, it becomes easier to understand the behavior of asphaltenes in petroleum, coal and shale products. They are obvious candidates for the very high viscosities noted in heavy residues [21,50,51], which fit the theory of molecular association and aggregation and are known to show rapid increases in viscosity.

Research work at the BP Research Center, Sunbury, has confirmed the inhomogeneity of asphaltenes. Thin-layer chromatography using the Iatroscan technique has shown [52] that IP 1343/77 asphaltenes are all readily divided by TC into mobilized component "A", loosely defined as "Resin A", and a higher molecular weight component that is not moved by chloroform/methanol from the spotted origin, referred to as "Resin B". The wide range of proportions of "Resins A and B", in both the deasphaltened oils and IP 143/77 asphaltenes (Fig. 4-10) demonstrates: (1) the inhomogeneity of IP 143/77 hard asphaltenes, (2) the inefficiency of the IP 143/77 solvent separation method, and (3) the large composition differences between different atmospheric residues from five different crude oils.

This survey reveals the continuing inadequacy of the understanding of the organic structure of petroleum maltenes, resins, asphaltenes, carbenes and carboids. Molecular spectroscopy using IR, UV, NMR, X-ray diffraction, all in their present states of development, provide only an indistinct outline of the statistical average molecule in any of the apparently inhomogeneous bitumen components. Electron microscopy [53] and pore size studies [36] demonstrate the porous nature of asphaltene components, whereas ESR studies [54–56] have confirmed the presence of strong stable free-radicals in asphaltenes.

The best available statistical average representation of the asphaltene micelle, in the author's opinion, is still that pioneered by Erdman [57] and Yen [58]. The

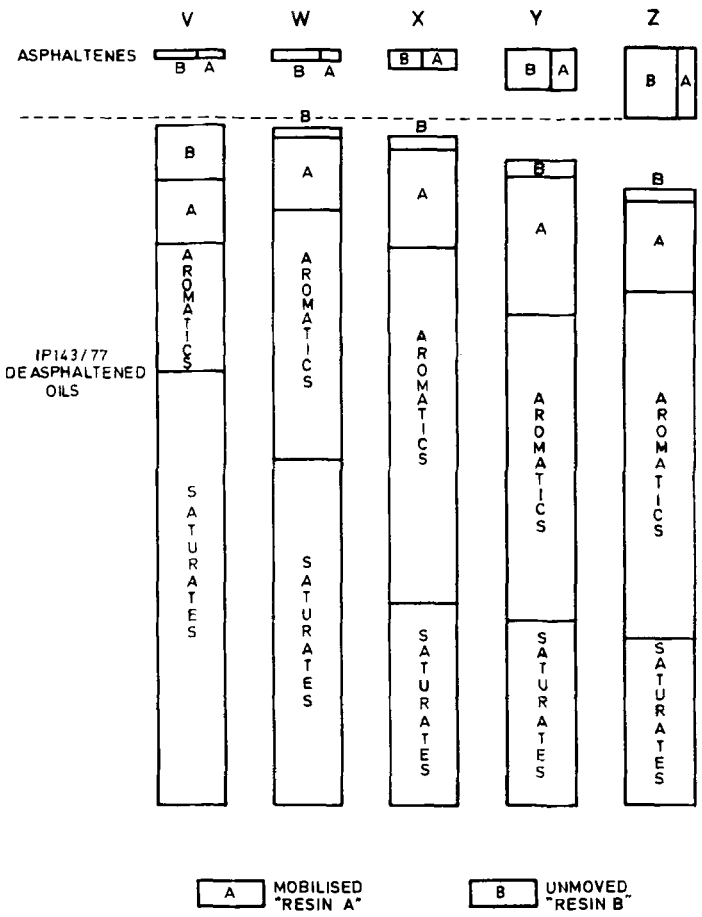

Fig. 4-10. Iatroscan TLC analyses of atmospheric residues from crude oils v–z.

data suggest molecular weights of 1–5 × 10^3 [3], possibly a molecular formula approximating to $(C_{79}H_{92}N_2S_20)_3$ and a molecular shape like the depicted in Fig. 4-11. The statistically average molecule might carry a core of stacked, flat sheets of condensed aromatic rings. Such aromatic sheets, perhaps five in number, each with 8–16 condensed rings, could be stacked without particular order, one above the other, at repeat distances of some 3.5–3.7 Å. Such a configuration would show and overall stack height of 16–20 Å. The stacked aromatic sheets may be interconnected by systems of sulfide, ether, aliphatic chain and/or naphthene ring linkages, which can slightly alter the stack height, tilt a plate, or displace it with respect to the remaining stack members. The condensed sheets will probably contain oxygen, sulfur and nitrogen atoms most likely associated with free radical sites. These sites are the expected anchor points for bound metals like non-porphyrin nickel, vanadium, molybdenum and iron. None of the subsequent structural investigations [55–66]

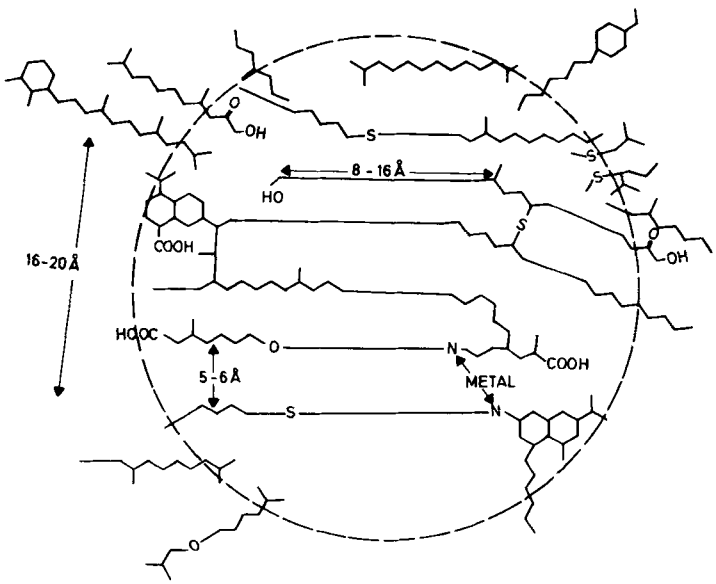

Fig. 4-11. Pictorial representation of petroleum asphaltene chemical structure within one micellular unit.

appear to offer a more attractive alternative to the original proposition for a likely chemical representation of asphaltene structure. Indeed, many research workers still attempt, perhaps in vain, to assign a specific molecular structure or configuration to individual asphaltic components, which may well be inhomogeneous. Does the industry still require a better definition of the supposed configuration based on the statistical average molecule data on a still complex mixture? Would it be advantageous to use analytical separatory methods to provide more homogeneous complex oils and "non-carbons", which might each be better understood in relation to what is known today of carbon structure or the high molecular weight of oily components of petroleum?

SUMMARY

The nomenclature and principal components of heavy petroleum products are discussed. A review in 1967 has been taken as a starting point from which to update the work reported during recent decades. The information emphasizes the inhomogeneity of asphaltic bitumen and questions the usefulness of the many statistical average molecule representations of supposed chemical structure.

Future advances are likely to come from a better appreciation of the colloidal nature and hydrogen bonding between oxygenated and nitrogenous components of petroleum and coal "heavy ends". Improved chromatography may reveal the real

nature of high carbon content components and perhaps explain the conversion of bitumen constituents to "asphaltene".

Meanwhile, the conventional picture of the asphaltene micelle due to Yen and others must still provide the best interpretation to refiners and combustion engineers of the constitution of the ultimate heavy ends of fossil fuel oils.

ACKNOWLEDGEMENTS

Permission to publish this chapter has been given by The British Petroleum Company Limited. It was presented at the Institute of Energy (South Coast Section) symposium "The Heavy End of the Barrel: Future Trends in Oil Firing Symposium" Portsmouth Polytechnic. The organizers agree to its publication.

REFERENCES

[1] Dean, R.A. and Whitehead, E.V., *6th World Petroleum Congress*, Frankfort-am-Main, 9: 261–279 (1963).
[2] Speers, G.C. and Whitehead, E.V., Crude petroleum, In: G. Eglinton and H.T.J. Murphy (Editors), *Organic Geochemistry Methods and Results*. Springer-Verlag, Berlin, pp. 638–675 (May 1970).
[3] Witherspoon, P.A. and Winniford, R.S., The asphaltic components of petroleum, In: B. Nagy and U. Colombo (Editors), *Fundamental Aspects of Petroleum Geochemistry*. Elsevier, Amsterdam, pp. 261–297 (1967).
[4] Kim, H.G. and Long, R.B., Characterization of heavy residuum by a small-angle X-ray scattering technique. *Ind. Eng. Chem. Fund.*, 18: 60–63 (1979).
[5] Kiss, L.T. and King, T.N., Expression of results of coal analysis: the case for brown coals. *Fuel*, 56: 340–341 (1977).
[6] Girdler, R.B., Paper presented at the Technical Session of the Association of Asphalt Paving Technologists, Philadelphia, Pa., February 15–17 (1965).
[7] Corbett, L.W. and Petrossi, U., Differences in distillation and solvent-separated asphalt residua. *Ind. Eng. Chem. Prod. Res. Dev.*, 17: 342–346 (1978).
[8] Moschopedis, S.E. and Speight, J.G., Investigation of hydrogen bonding by oxygen functions in Athabasca bitumen. *Fuel*, 55: 187–192 (1976).
[9] Koots, J.A. and Speight, J.G., Relation of petroleum resins to asphaltenes. *Fuel*, 54: 179–184 (1975).
[10] Brûlé, B., Characterization of bituminous compounds by Gel Permeation Chromatography (GPC). *J. Liq. Chromatogr.* 2: 165–192 (1979).
[11] Boduszynski, M., Chadha, B.R. and Pineles, H., Investigations on Romashkino asphaltic bitumen, 1: Use of ion-exchange and adsorption chromatography for the separation of maltenes. *Fuel*, 56: 145–148 (1977).
[12] Neuman, H.J., Parwini, B.A., Rahimian, I. and Kashab, M.A., *Gemeinschaftstagung OGEW DGMK*, Salzburg, October 4–6, pp. 978–985 (1976).
[13] Moschopedis, S.E., Fryer, J.F. and Speight, J.G., Investigation of the carbonyl functions in a resin fraction from Athabasca bitumen. *Fuel*, 55: 184–186 (1976).
[14] Bunger, J.W., Thomas, K.P. and Dorrence, S.M., Compound types and properties of Utah and Athabasca tar sand bitumens. *Fuel*, 58: 183–195 (1979).
[15] Speight, J.G. and Moschopedis, S.E., Influence of metal salts on bitumen oxidation. *Fuel*, 58: 235 (1979).
[16] Moschopedis, S.E., Fryer, J.R. and Speight, J.G., Investigation of asphaltene molecular weights. *Fuel*, 55: 227–232 (1976).

[17] Dwiggins, C.W., A small-angle X-ray scattering study of the colloidal nature of petroleum. *J. Phys. Chem.*, 69: 3500–3506 (1965).
[18] McKay, J.F., Amend, P.J., Cogswell, T.E., Harnsberger, R.M., Erickson, R.B. and Latham, D.R., Analytical chemistry of liquid fuel sources, tar sands, oil shale, coal, and petroleum. In: P.C. Uden, S. Siggia and H.B. Jensen (Editors), *ACS Advances in Chemistry Series 170*. American Chemical Society, Washington D.C., pp. 128–142 (1978).
[19] Gould, K.A., Effect of silylation on the molecular weights of petroleum and coal-derived asphaltenes. *Fuel*, 58: 550–552 (1979).
[20] Ramljak, Z., Šolc, A., Arpino, P., Schmitter, J.M. and Guiochon, G., Separation of acids from asphalts. *Anal. Chem.*, 49: 1222–1224 (1977).
[21] Nakajima, T., Chemical constituent changes during asphalt blowing. *J. Jpn. Pet. Inst.*, 18: 1068–1075 (1975).
[22] Šebor, G., Reynoso, S., Hajek, M., Weisser, O. and Mostecky, J., Study of hydrogenation of petroleum asphaltenes. *Coll. Czech. Chem. Commun.*, 46: 409–418 (1981).
[23] Kurokawa, K. and Kondo, T., Reaction of asphaltene under mild hydrotreatment conditions. *J. Jpn. Pet. Inst.*, 22: 59–63 (1979).
[24] Ignasiak, T.M. and Strausz, O.P., Reaction of Athabasca asphaltene with tetralin. *Fuel*, 57: 617–621 (1978).
[25] Altgelt, K.H., Asphaltene molecular weights by vapor pressure osmometry. *Bitumen, Teere, Asphalte, Peche*, 21: 475–486 (1970).
[26] Masek, V., *Erdöl Kohle*, 29: 364 (1976).
[27] Huc, A.H. and Roucache, J.G., Quantitative thin-layer chromatography of sedimentary organic matter. *Anal. Chem.*, 53: 914–916 (1981).
[28] Costantinides, G., Lomi, C. and Schromek, M., Electron microscopic examination of asphalt and of reconstituted mixtures. *Riv. Combust.*, 29: 405–408 (1975).
[29] Al-Kasheb, M. and Neuman, H.J., Separation and characterization of bitumen from the crude oil from the Kirkuk field. *Erdöl Kohle*, 30: 181 (1977).
[30] Nuzzi, M. and Casalini, A., Condensed thiophenic structures in the resudue of a Kuwaiti crude oil having asphaltenes removed by *n*-pentane. *Riv. Combust.*, 32: 295–298 (1978).
[31] Selucky, M.L., Chu, Y., Ruo, T.C.S. and Strausz, O.P., Chemical composition of Cold Lake bitumen. *Fuel*, 57: 9–16 (1978).
[32] Nakajima, T., *J. Jpn. Petrol. Inst.*, 18: 58–62 (1975).
[33] Haley, G.A., Changes in chemical composition of a Kuwait short residue under air-blowing. *Anal. Chem.*, 47: 2432–2437 (1975).
[34] Al-Farkh, Y.A., Rayyes, N.R.E. and Al-Zaid, K.A., Studies on Kuwait crudes. 1. Composition analysis of some asphalts and their sulfurized products. *Ind. Eng. Chem. Prod. Res. Dev.*, 17: 165–169 (1978).
[35] Costantinides, G., Lumi, C. and Schromek, N., Treatment of bitumens with sulfur: considerations on possible reactions. *Riv. Combust.*, 33: 1–13 (1979).
[36] Khokhlova, G.P., Plyusnin, A.N. and Kryazhev, Yu.G., Complexing of petroleum asphaltenes with Lewis acids. *Pet. Chem. USSR*, 18: 102–107 (1979).
[37] Parkash, S., Moschopedis, S. and Speight, J.G., Physical properties and surface characteristics of asphaltenes. *Fuel*, 58: 877–881 (1979).
[38] Strausz, O.P., Jha, K.N. and Montgomery, D.S., Chemical composition of gases in Athabasca bitumen and in low-temperature thermolysis of oil sand, asphaltene, and maltene. *Fuel*, 56: 114–120 (1977).
[39] Brodskii, E.S., Lukashenko, I.M. and Lebedevskaya, U.G., Analysis of sulfur-containing compounds of petroleum using mass spectrometry. *Ind. Chem. Eng.*, 18: 106–108 (1978).
[40] Yamaguchi, T., Preparation of activated carbon and light oil from petroleum asphaltenes. An attempt for the utilization of heavy oils. *Fuel*, 59: 444–445 (1980).
[41] Speight, J.G., Thermal cracking of Athabasca bitumen, Athabasca asphaltenes, and Athabasca deasphalted heavy oil. *Fuel*, 49: 134–145 (1970).
[42] Rubenstein, I. and Strausz, O.P., Thermal treatment of the Athabasca oil sand bitumen and its component part. *Geochim. Cosmochim. Acta*, 43: 1887–1893 (1979).

[43] Rubenstein, I., Spyckerelle, C. and Strausz, O.P., Pyrolysis of asphaltene: a source of geochemical information. *Geochim. Cosmochim. Acta*, 43: 1–6 (1979).
[44] Ritchie, R.G.S., Roche, R.S. and Steedman, W., Pyrolysis of Athabasca tar sands: analysis of the condensible products from asphaltene. *Fuel*, 58: 523–530 (1979).
[45] Ritchie, R.G.S., Roche, R.S. and Steedman, W., Pyrolytic formation of *n*-alkanes from Athabasca asphaltene. *Chem. Ind. (London)*, January 6, pp. 25–26 (1979).
[46] Ritchie, R.G.S., Roche, R.S. and Steedman, W., A pyrolysis-gas chromatographic analysis of Athabasca bitumen. *Ind. Eng. Chem. Prod. Res. Dev.*, 17: 370–372 (1978).
[47] Yen, T.F., Long chain alkyl substitutes in native asphaltic molecules. *Nature*, 233: 36–37 (1971).
[48] Antonishin, V.I., Gumenetskii, V.V. and Grinenko, B.B., Oxidation of petroleum asphaltenes into aliphatic dicarboxylic and benzenecarboxylic acids. *Pet. Chem. USSR*, 17: 244–256 (1978).
[49] Miki, T., Yoshida, H., Yamada, Y. and Arita, S., Preparation of nitrohumic acid-like substances from petroleum asphalt by nitric acid oxidation. *J. Jpn. Pet. Inst.*, 22: 13–20 (1979).
[50] Reerink, H., Size and shape of asphaltene particles in relationship to high-temperature viscosity. *Ind. Eng. Chem. Prod. Res. Dev.*, 12: 82–88 (1978).
[51] Corbett, L.W., Dumbbell mix for better asphalt. *Hydrocarbon Process.*, April, pp. 173–177 (1979).
[52] Ray, J.E., Oliver, K.M. and Wainwright, J.C., *Proc., Inst. Pet. (London) Symp. Petroanalysis 1981*, London, October 27–29 (1981).
[53] Dickie, J.P. and Yen, T.F., ACS Electron microscopic studies in petroleum asphaltics. *Am. Chem. Soc., Div. Pet. Chem. Prepr.*, 11(3): 39–47 (1966).
[54] Elofson, R.M., Schulz, K.F. and Hitchon, B., Geochemical significance of chemical composition and ESR properties of asphaltenes in crude oils from Alberta, Canada. *Geochim. Cosmochim. Acta*, 41: 567–580 (1977).
[55] Ferris, S.W., Black, E.P. and Clelland, J.B., Aromatic structure in asphalt fractions. *Ind. Eng. Chem. Prod. Res. Dev.*, 6: 127–132 (1967).
[56] Niizuma, S., Steele, C.T., Gunning, H.E. and Strausz, O.P., Electron spin resonance study of free radicals in Athabasca asphaltene. *Fuel*, 56: 249–256 (1977).
[57] Erdman, J.G., The molecular complex comprising heavy petroleum fractions. *ASTM Spec. Tech. Publ.*, 389: 259–300 (1965).
[58] Yen, T.F., Structures of petroleum asphaltene and its significance. *Energy Sources*, 1: 447–463 (1974).
[59] Ignasiak, I., Kemp-Jones, A.V. and Strausz, O.P., The molecular structure of Athabasca asphaltene. Cleavage of the carbon-sulfur bonds by radical ion electron transfer reactions. *J. Org. Chem.*, 42: 312–320 (1977).
[60] Magaril, R.Z., Chemical structure of petroleum asphaltenes. *Chem. Abstr.*, 84: 7341 (1976).
[61] Dereppe, J.M., Moreaux, C. and Castex, H., Analysis of asphaltenes by carbon and protein nuclear magnetic resonance spectroscopy. *Fuel*, 57: 435–440 (1978).
[62] Kiet, H.H., Blanchard, L.P. and Malhotra, S.L., The gel permeation chromatography of asphalt and the characterization of its fractions in terms of molecular and unit sheet weights. *Separation Sci.*, 12: 607–634 (1977).
[63] Speight, J.G. and Moschopedis, S.E., On the "polymeric nature" of petroleum asphaltenes. *Fuel*, 59: 440–441 (1980).
[64] Speight, J.G., Structural analysis of Athabasca asphaltene by proton magnetic resonance spectroscop. *Fuel*, 50: 102–112 (1971).
[65] Speight, J.G., *Fuel*, 49: 76–90 (1970).
[66] Haley, G.A., Molecular and unit sheet weights of asphalt fractions separated by gel permeation chromatography. *Anal. Chem.*, 43: 371–374 (1971).

Asphaltenes and Asphalts, 1. Developments in Petroleum Science, 40
edited by T.F. Yen and G.V. Chilingarian

Chapter 5

MULTIPLE STRUCTURAL ORDERS OF ASPHALTENES

TEH FU YEN

INTRODUCTION

Petroleum asphaltene belongs to a class of extremely complex organic macromolecules. During the last 35 years, various investigators have made significant contributions to its study, including this author. Its detailed structure, however, is still unknown.

For very complex molecules, a glimpse of the skeleton of the three-dimensional network by radiation and the resulting most frequently observed vectors or distances have become valuable. Simple macromolecules such as homopolymers (polyethylene, for example) only exhibit a repeating interchain distance of 4.5 Å; poly α-butane exhibits repeating distances of both 4.5 Å and 6.9 Å due to the side-chain appearance [1]. Asphaltenes are known as multipolymers [2], which are referred to as polycondensates with a great variety of repeating blocks, which number in the hundreds. They can be compared to copolymers (containing 2 blocks), terpolymers (containing 3 blocks) and so on, until the number of blocks increases indefinitely. A close example will be the corpuscular proteins which contain various amino acid residues of 20 or more. The X-ray diffraction of petroleum asphaltene revealed the 4.8 Å of γ-band (representing saturate structures of the carbon skeleton) and a 3.5 Å of (002)-band in conjunction with 2.1 Å of (10)-band and 1.1 Å of (11)-band (representing aromatics in carbon skeleton) [3]. Based on earlier X-ray diffraction work, a cross-sectional view of asphaltene model was suggested by Yen et al. [4]. In this model, sheet-like material (aromatics) is linked with zig-zag chain-like material (saturates). A ratio of aromatic carbons to saturated carbons can be approximated from the relative intensities of the 3.5 Å (002)-band, the interplanar distance, and the 4.8 Å γ-band, the interchain distance. Based on this ratio, an approximate value of aromaticity of asphaltene can be obtained. At present time, the use of ^{13}C NMR has become routine for aromaticity measurement; whereas in the past, the only tool available was X-ray diffraction. Based on γ- and (002)-bands, aromaticities have been quantified for different ranks of coals [5]. Although the validity of the measurements is supported by a number of model compounds and aromatic polymers (Table 5-1, Figs. 5-1 and 5-2), this approach has been criticized in recent years by Ebert [6]. Also, when f_a vs. treatment temperature plots for various fossil fuels are examined (e.g., coal liquid asphaltene, shale bitumen asphaltene, and petroleum asphaltene), the respective slopes are very similar. If the X-ray aromaticity contains errors, correlations are not possible [7]. Anyway, the aromaticity values of asphaltene have been verified by solution ^{13}C NMR and other techniques.

TABLE 5-1

Composition and properties of aromatic polymers synthesized for the modeling of X-ray diffraction studies of asphaltenes

Sample No.	Aromatic compounds	Elementary analysis (%)				Molecular weight		Color	Softening points (°C)
		found		calculated		VPO	repeating units		
		C	H	C	H				
1	benzene	92.7	6.8	93.3	6.7	3470	38	drab	185–220
2	naphthalene	93.6	6.0	94.2	5.8	970	7	white	175–220
3	anthracene	94.5	5.8	94.7	5.3	1760	9	bistre	
4	phenanthrene	94.1	6.0	94.7	5.3	828	4		200–215
5	biphenyl	93.6	6.7	93.9	6.1	926	6	dirty white	184
6	toluene	90.1	7.3	92.3	7.7	3500	34	light buff	170
7	*p*-cymene	90.2	7.3	90.3	9.7	1270	9	olive-brown	290
8	octahydro-phenanthrene	89.9	9.0	90.8	9.2	1340	7	bronze-green	
9	*p*-dicyclohexyl-benzene	89.0	9.8	89.7	10.3	2570	10	tan	255
10	*as*-hexahydro-pyrene	90.8	7.0	92.7	7.3	1525	7		>300
11	phenoxanthin	72.5	4.2	73.6	3.8	1270	6	yellow	180

THE UNIT SHEET

A sheet of aromatic-saturated carbon network is the basic unit of asphaltene structure. The sheet could contain one unit of each of the aromatic and saturated carbon systems (monomer), two units of each system (dimer), and so on. In most asphaltenes, however, this repeating sequence is limited, e.g., the oligomer only reaches 5. As a whole, the bulk of the asphaltene may contain only one or two types of arrangement.

Owing to strong aromatic π–π association, a single sheet is difficult to isolate. An easy way to do this is to subject the aromatic-saturated system to electron bombardment at 70 eV. Mass spectrometer studies indicate that for these systems, cleavage of the aliphatic substitution occurs at the β-position next to the aromatic ring. In this manner, distribution of the mass peaks directly corresponds to the aromatic nuclei well stripped of aliphatic substitution. In actual cases, both the singly- and doubly-charged masses are observed. These are termed disk weights [8], which can be directly converted into length diameters similar to layer diameter L_a in Å by using the following formulas:

$$L_a = (2.62\,C_A)^{1/2} \quad \text{for peri-condensation} \tag{5-1}$$

or

$$L_a = 0.615\,C_A - 1.23 \quad \text{for kata-condensation} \tag{5-2}$$

where C_A = number of aromatic carbons.

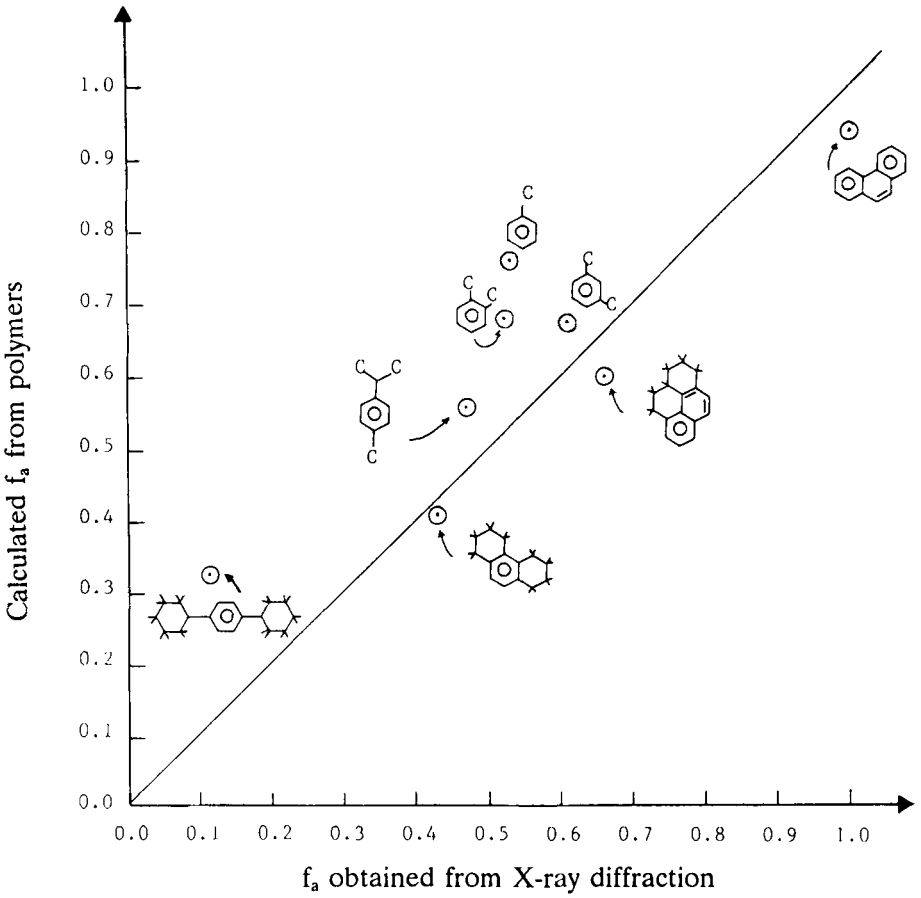

Fig. 5-1. Carbon aromaticity values (f_a) from a number of aromatic model polymers. Their properties are listed in Table 5-1. Each polymer is synthesized from the arene systems listed and formaldehyde.

The use of field ionization mass spectrometry and electron impact mass spectrometry in recent years has been improved; yet, the values obtained are still too low for the entire sheet.

A more useful quantity in the direct measurement of L_a, made by X-ray diffraction, is the (11)-band by the Diamond method. The determination of L_a from (10)-band encounters interference and should be avoided.

A chemical method has been developed to determine the weight of a single sheet, by allowing asphaltene to form an iodine complex with iodine molecules [9]. Normally, the stoichiometric complex exhibits transitional behavior, e.g., minimum resistivity and lowest energy gap. Most asphaltenes form a stable complex with iodine (3 : 2 iodine/asphaltene ratio). It is possible to determine the unit sheet weight from the mass iodine/asphaltene ratio. The unit weight (UW) can be obtained as follows:

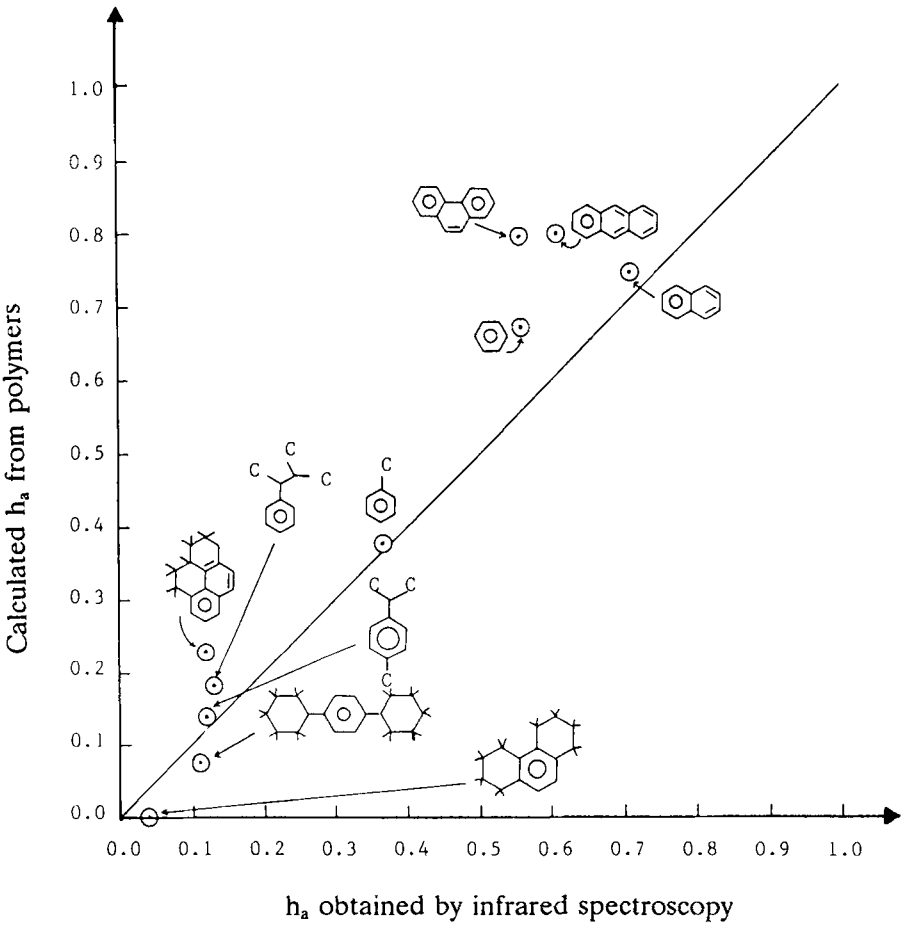

Fig. 5-2. Hydrogen aromaticity values (h_a) from a number of aromatic model polymers. Their properties are listed in Table 5-1. Each polymer is synthesized from the arene systems listed and formaldehyde.

$$UW = 254\,t^{-1}R(100 - t) \tag{5-3}$$

where R is the ratio of iodine to asphaltene, and t is the percentage of iodine corresponding to the transition in resistivity and gap energy.

Sheet weight is very difficult to measure by means of vapor-phase osmometry (VPO), owing to the fact that sheets engage in π–π association even at extremely low concentrations. Usually, the measurement of solvent with a high dielectric constant under high temperature is meaningful. If a large aromatic system is used as a solvent, there is a chance that a unit sheet weight may be obtained; for example, the molecular weight can be obtained by cryoscopic methods using naphthalene and phenanthrene.

It is rather easy to convert the disk weight or the aromatic disk weight into unit

sheet weight by the use of aromaticity:

$$\text{Unit sheet weight} = (\text{disk weight})/f_a \tag{5-4}$$

Inasmuch as the aromatic moiety of asphaltene is quite rigid, the layer diameter is a good indicator of the distance in the aromatic system. Because the saturated moiety is quite flexible, however, the paraffinic portion can be folded back if the methylene portion is larger than 4, and the naphthenic portion can have many different conformations. In order to circumvent this difficulty, one cannot use the extended trans-configuration or zig-zag syndiotectic configuration to denote the length (l) of long-chain paraffins in Å, namely,

$$l = (C - 1)(\sin\theta/2) \times 1.54 \tag{5-5}$$

where C is the number of carbon atoms and θ is the bond angle. Instead, one has to adopt the end-to-end distance calculation for macromolecules in solution state:

$$l = (C-1)^{1/2}\left[\frac{1-\cos\phi}{1+\cos\phi}\right]^{1/2}\left[\frac{1+\langle\cos\phi\rangle}{1-\langle\cos\phi\rangle}\right]^{1/2} \times 1.54 \tag{5-6}$$

where ϕ is the rotational angle indicating the degree of freedom when being hindered by bulky groups. The value of $\langle\cos\phi\rangle$ is an average over the molecules for free rotation; thus, $\cos\pi/2 = 0$ and the ϕ product can be dropped off. If the tetrahedral angle is assumed for θ, then the θ product will be the square root of 2. The C_7 chain length according to Eq. 5-5 is 7.57 Å, and according to Eq. 5-6, for free rotation, it is 5.33 Å. Probably, the correct end-to-end distance is the one for which both products can be dropped off:

$$l = (C - 1)^{1/2} \times 1.54 \tag{5-7}$$

Using Eq. 5-7, the C_7 chain length is equal to only 3.77 Å. In many approximations for mesomorphic states, the writer has adopted Eq. 5-7 for such a calculation, where C is halved due to the occurrence of more than 50% of short chains such as methyl or ethyl groups attached to the aromatic nuclei.

One of the techniques used is the measurement of the radii of charged asphaltene particles by mobility measurements [12]. Table 5-2 is a summary of all the measurements leading to the dimension of unit sheets. The values indicate that the length vector ranges from 1.2 to 3.0 nm. This is the first order of arrangement basic to the asphaltenes.

PARTICLE ASSOCIATION

All aromatic π-systems are known to associate owing to the overlapping of π-orbitals. Typical of the system are carbon and graphite, in which the layers of association are large. Even in polar solutions, porphyrins are known to stack up due to the fact that they belong to the diaza [16]–annulene system. The association and

TABLE 5-2

Average length of unit sheet

Tool	Reference	Parameter	Sample No.	Disk weight	Unit weight	L_a	Unit sheet length (nm)
MS (70 eV)	[8]	m/e	8	*653*	1301 [a]	1.19	2.31
XRD	[8]	L_a	9		1695 [a,b]	*1.27*	2.11 [c]
XRD	[4]	L_a	8			*1.31*	2.38 [d]
Iodine-complex	[9]	MW	2	1238	*2750*	1.65	1.96
Cryoscopic	[10,11]	MW	2		*2100*	1.51 [a]	1.79
Charge mobility	[12]	$r+$	3				1.98
		$r-$	(in 2 solvents)				1.20
VPO (ϕNO_2, 130°C)	[13]	MW	14		*1797*		1.70
MS (field ionization)	[14]	M_N, M_W	1		*902–1042*		1.39
MS (20 eV)	[15]	upper bound	2		*814–1270*		1.46

[a] Assuming $f_a = 0.5$.
[b] Based on individual f_a determined.
[c] C_A approximation is half for peri; the other half is for kata.
[d] Due to the height content of C_S, calculation of l is using 1/3 of the C from Eq. 5-7. C_S = number of saturated carbon atoms.

disassociation energies have been measured by a vanadyl probe method [17,18] and are on the order of 12–16 kcal/mol.

If care is not taken, these particle-like stacks can further agglomerate into large sizes. Direct measurements can be made from the spray of a dilute solution of asphaltene into a substrate: during the passage of solvent carrying the particle, the solvent evaporates without further possibility of particle–particle association. The electron microscope data obtained in this manner can be meaningful [19]. Owing to the carbon density distribution, however, the edge group may not be seen and, consequently, the diameter reported is on the low side.

The gel permeation chromatography (GPC) or size exclusive chromatography (SEC) is a good tool with which to study the association and agglomeration. Through the years, Speight and co-workers [13,20] have determined a great number of VPO molecular weights in different solvents. In the case of values determined at high temperature in nitrobenzene, they correspond to a unit sheet molecular weight [16]. All the remaining molecular weights determined in benzene at room temperature indicate association with the sheet. The effective layer of stacking, M_e, is about 4 to 6.

The vertical aromatic size parameter, L_c, can be an indicator, but the paraffinic and naphthenic contents have not been added to it. After correction, this quantity may reach 3 nm, which amounts to 5 layers.

The diameter (d) can be calculated from the known molecular weight (MW) as follows:

$$d = \left(\frac{6\,\mathrm{MW}^{1/3}}{\pi \rho N}\right) = (2.75\,\mathrm{MW})^{1/3} \tag{5-8}$$

TABLE 5-3

Diameters due to association

Tool	Sample No.	Parameter	Reference	Molecular weight	L_c	d (nm)
TEM	9	arithmetic mean		[a]		*2.76*
		geometric mean				*2.68*
XRD	7	L_c	[19]		*1.90*	2.97[a]
VPO	9	MW	[8]			
		ϕH		*5248*		2.43
		THF		*6015*		2.55
GPC	9		[8]			
		M_N		*3420*		2.11
		M_W		*6386*		2.60
Cryoscopic method		MW (in ϕH)	[21]	*5500*		2.47
XRD		L_c	[3]		*1.83*	2.90[a]
VPO	14	MW (nonpolar solvents)	[13]	*5047*		2.40
VPO	30	MW (crude oil)	[20]	*4995*		2.39
	24	MW (heavy residue)		*6022*		2.55

[a] Assuming unit sheet weight of 1200, f_a = 0.5 and C_S is only the summation from the top and bottom layers.

where d is expressed in Å, N is Avogadro's number, and ρ is assumed to be 1.15 g/cm^3. The data collected in Table 5-3 shows that the change in d is small even when the change in MW is large.

AGGLOMERATION

Lemerle et al. [22] presented the experimental evidence of multiple integers of the unit sheet weight. In their ultracentrifuge studies they correlated the molecular weight variations with polarities of 10-, 15-, 30- and 40-fold of the unit sheet weight of 2500. Most ultracentrifuge work confirmed the diameter of 5 nm.

The observation of a 50 Å band from the low-angle X-ray work also supported the ultra-centrifuge studies. Many GPC fractions contain higher molecular weight components, examples resulting from studies conducted by Gourlaouen and Petroff [23]. They also used laser light scattering or dynamic light scattering (DLS) for the measurement of solutions.

Often, the presence of high amounts of transition metals is the cause of agglomeration; such is the case of Boscan asphaltene. There is much evidence for the presence of asphaltenes containing high amounts of metals; e.g., Gourlaouen and Petroff [23] observed the Boscan > Safaniya > Minas sequence by GPC due to the metal contents. In general, the order of this spacing is around 5 nm (see summary in Table 5-4).

TABLE 5-4

Agglomeration distance

Tool	Reference	Sample No.	Molecular weight	*d* (nm)
Ultracentrifuge	[8]	1	34,000	4.54
Ultracentrifuge	[24]	1		*3.18–4.94*
Ultracentrifuge	[22]	1	22,500	3.94
			35,000	4.58
			73,000	5.85
			103,000	6.57
EM	[25]	1		*<6.5*
Osmotic pressure	[26]		20,000–80,000	3.8–6.4
XRD	[27]	3		*5.0*
GPC	[28]	1	40,000	4.79
GPC	[23]	3	18,000	3.67
			40,400	4.81
			36,000	4.66
			54,600	5.32
			63,500	5.59
DLS	[23]	3	22,000	3.93
			48,000	5.09
			45,000	4.98
			70,000	5.77
			100,000	6.50

ASSEMBLAGE

Assemblage is encountered primarily in various scattering studies, including the small-angle X-ray scattering (SAXS) and small-angle neutron scattering (SANS). Most studies give values of the radius of gyration, r, by Guinier's approach. The r values can be easily converted to a morphological diameter (d) as follows:

$$d = 2(5/3)^{1/2}r = 2.58\,r \tag{5-9}$$

Usually, parameter d is not influenced by solvent composition. Regardless of whether asphaltene is in petroleum, asphalt, or any polar or nonpolar solvent, the d-value remains constant.

Furthermore, the r-value obtained via SANS is slightly higher than that obtained by using SAXS. Ravey et al. [32] used a thin-shell (disk) model having two different diameters, a thickness e, and a diameter, d. The e is very small, usually about 0.4 nm. The d-values, as listed in Table 5-5, are comparable to d-values obtained by other methods. Overfield et al. [33] carried out SANS studies over a temperature range

TABLE 5-5

Morphological diameter for assemblages of asphaltenes

Total	Number of samples	Reference	r	d (nm)
SAXS	6	[29]	3.1 - 6.9	8.0 -14.0
SAXS	2	[27]	3.4 - 4.0	8.8 -10.3
SAXS	2	[30]	2.9 - 3.1	7.5 - 8.0
SAXS	4	[31]	2.5 - 3.5	6.5 - 9.0
SANS	5	[32]	-	12 -14
SANS	5[a]	[33]	5.1 -11.6	13.2 -29.9
SAXS	5	[5]	3.9 - 4.1	10.1 -10.6
SANS	2	[34]	7 - 8	18 -20
SAXS	7	[35]	2.9 - 5.6	7.5 -14
NOE	4[b]	[36]	-	14.9 -16.3
NOE	7[b]	[37]	-	3.27- 8.29
SANS	17[b]	[38]	3.01- 3.24	7.77- 8.36
SANS	17[b]	[39]	3.5	9.03

[a] Different terperatures.
[b] Different solvents.

of 25 to 250°C. The smallest r-value is 5.3 nm, which is measured at the highest temperature of 250°C. Sheu et al. [38] used a spherical model for SANS data and found that the r-values do not change with varying concentrations and polarities of the sample's environment.

It is important to note that the nuclear Overhouser effect (NOE) and dynamic nuclear polarization (DNP) studies for both asphalt and asphaltene yield a colloid particle size also deduced from the rotational correlation time. Poindexter [37] has obtained particle volumes in different solvent systems. Gulsun [36] also obtained the radius of these types of particles. These values are in close accord with those obtained on using the scattering data (see Table 5-5).

LARGE CLUSTERS

When assemblages or associated species grow, the usual consequence is a directional dependence, i.e., the cluster formed can be anisotropic and have planar and perpendicular dimensions. Reerink [40] explained his sedimentation data in this manner. Possibly, one of the axes is conditioned by the potential of the nearest surfaces. Recently, Lin et al. [41] found the differences between the two axes in their metal-shadowing electron microscopy work. It is interesting to note that the shorter axis also forms n multiplier of the basic unit cell dimension. The larger axis grows longer with increasing metal content, whereas the length of the shorter axis increases only with degree of oxidation.

Work by freeze-fracture electron microscopy also found the clusters with aromatic disks being squeezed at the center with the other moieties spreading out [42].

TABLE 5-6

Cluster sizes of planar and perpendicular distances

Tool	Reference	$d_{\perp}$ (nm)	$d_{\parallel}$ (nm)
Metal shadowing	[41]	7	241
Metal shadowing	[41]	9	215
Metal shadowing	[41]	35	107
Metal shadowing	[41]	28	93
Freezing fracture	[42]	400	1000
Freezing fracture	[42]	150	300
Holey carbon	[43]		1000
Porod SAS	[27]		
l_c			41.3– 42.9
l			59.4– 102
SAXS	[30]		620 –1520

These formations can be considered as precursors for mesophase or flocs.

An important observation made by Dwiggins [30] is that the largest cluster size (r) that can be observed by SAXS in alcohol solution was 590 nm. Afterwards, phase separation was initiated and the asphaltene precipitated. Two structural parameters mentioned in Table 5-6, i.e., the coherence length, l_c, a measure of the size of cluster and the inhomogeneity length, l, a measure of the average particles or voids in solid phase, are measured by Porod method.

SPHERULES AND FLOCS

When asphaltene is heated with rate control, the carbonaceous mesophase is formed [44,45], and when the temperature reaches 500°C, mesophase is the only solid in existence. During the heating between 400 and 500°C, Brooks–Taylor spherules are formed. These spheres are free-flowing in the pyrolyzed, viscous, anisotropic liquid medium. The normal size range of these liquid crystalline spherules is 10–60 μm, having clear domains that are observed by a light microscope. The quality of these spherules can be graded by optical texture index (OTI) from 0 to 30, with isotropic mesophase having the lowest and flow domain anisotropy the highest. Both fine isotropic spheres and the coarse mesophase spherules are precursors leading to carbon and graphite formation.

Large distance distribution functions have been made available by using the Bonse–Hart instrument [47]. These can be used for the study of flocculation occurring during asphaltene precipitation. Commonly observed values of these largest distances can be found in Table 5-7.

TABLE 5-7

Sizes of flocs and mosophase spherules (morphological diameter expressed in micrometers)

	d (μm)	Reference
Heavy petroleum	3	[34]
Asphaltene from coal liquid	1	[46]
Aged Red Wash crude oil	7.4	[47]
Isotropic mesophase sphere	2 – 5	[48]
Coarse mesophase spherules	8 –20	[49]
Solid Boscan asphaltene	6.5	[47]

CONCLUSION

The organization of the structure of asphaltene is in fairly good order. Asphaltene has a basic unit, in the order of 1.7–1.9 nm, which corresponds to a molecular weight of 2000–2500. Other higher structural units are made of a multiple number of this unit. The study of the structure of asphaltene is made using a combination of analytical, instrumental and physical methods. It is dangerous to reach any useful conclusions based on studies using a single tool; thus, a combination of several methods is strongly recommended. Asphaltene apparently contain a minimum of six structural orders, which are summarized in Table 5-8.

A great variety of instruments and analytical methods carried out by different investigators on asphaltene have yielded valuable information. The organization of asphaltene structure consistently contains fixed lengths and sizes. The macrostructure of asphaltene is ordered, beginning with a monomeric unit size of 2 nm, or a unit molecular weight corresponding to 2000–2500. Asphaltene can increase progressively in size with n integer multipliers, reaching a giant size, owing to the aggregation of spherules or flocs. There are six orders of regular arrangement of the basic unit, each order being denoted by a length vector. This model will be useful for future investigation of asphaltene properties. All structural orders used in this macromolecular model are based on experimental results, and none of the orders is based on hypothetical imagination or conception. Consequently, there

TABLE 5-8

Structural orders of asphaltene

	Vectors (nm)
Unit sheets	1.2–2.0
Association of stacks	3.0
Aggregation	5.0
Assemblage	10 –15
Cluster	200 –2000
Flocs, spherules	1000 –20,000

should be no place for the proposed swiss cheese model, spaghetti and sauce model, spider model, continuous matrix model, amphoteric model, etc., when discussing asphaltene in asphalt.

REFERENCES

[1] Sadeghi, M.-A., Chilingarian, G.V. and Yen, T.F., X-ray diffraction of asphaltenes. *Energy Sources*, 8: 99–123 (1986).
[2] Yen, T.F., Structural differences between asphaltenes isolated from petroleum and from coal liquids. *Adv. Chem. Ser.*, 195: 39–51 (1981).
[3] Yen, T.F. and Erdman, J.G., Aspahltene (petroleum) and related substances, X-ray diffraction, In: G.L. Clark, (Editor), *Encyclopedia of X-Rays and Gamma Rays*. Reinhold, New York, N.Y., pp. 65–68 (1963).
[4] Yen, T.F., Erdman, J.G. and Pollack, S.S., Investigation of the structure of petroleum asphaltenes by X-ray diffraction. *Anal. Chem.*, 33: 1587–1594 (1961).
[5] Yen, T.F., unpublished results (1992).
[6] Ebert, L.B., Comment on the study of asphaltenes by X-ray diffraction. *Fuel Sci. Tech. Int.*, 8(5): 563–569 (1990).
[7] Unsworth, J.F., Barratt, D.J. and Roberts, P.T., *Coal Quality and Combustion Performance*. Elsevier, Amsterdam, p. 97 (1991).
[8] Dickie, J.P. and Yen, T.F., Microstructures of the asphaltic fractions by various instrumental methods. *Anal. Chem.*, 39: 1847–1852 (1967).
[9] Sill, U.A. and Yen, T.F., Semiconduction of iodine complexes of asphaltenes. *Fuel*, 48: 61–74 (1969).
[10] Hilman, E.S. and Barnett, B., The composition of cracked and uncracked asphalts. *Proc. Am. Soc. Testing Materials*, 37: 558 (1937).
[11] Boyd, M.L. and Montgomery, D.S., Structural-group analysis of the asphaltene and resin components of Athabasca bitumen. *Fuel*, 41: 335–350 (1962).
[12] Reerink, H. and Lijzenga, The influence of electrolytic dissociation in the collodial properties of bitumens. *Electroanal. Chem. Interface Electro-Chem.*, 37: 213–225 (1972).
[13] Moschopedis, S.E., Fryer, J.F. and Speight, J.G., Investigation of asphaltene molecular weights. *Fuel*, 55: 228 (1976).
[14] Kyriacou, K.C., Baltus, R.E. and Rahimi, P., Characterization of oil residual fractions using intrinsic viscosity measurements. *Fuel*, 67(1): 109–113 (1988).
[15] Storm, D.A., DaCanio, S.J. and DeTar, M.M., Upper bound on number average molecular weight of asphaltene. *Fuel*, 69: 735–738 (1990).
[16] Speight, J.G., Wernick, D.L., Gould, K.A., Overfield, R.E., Rao B.M.C.R. and Savage D.W., Molecular weight and association of asphaltene, a critical review. *Rev. Inst. Fr. Pét.*, 40: 51–62 (1985).
[17] Tynan, E.C. and Yen, T.F., Association of vanadium chelates in petroleum asphaltenes as studied by ESR. *Fuel*, 43: 191–208 (1969).
[18] Shibata, K., Kakiyama, H., Sanada, J. and Sohma, J., ESR study of the aggregated state in petroleum residue at high temperature. *Fuel*, 57: 651–653 (1978).
[19] Dickie, J.P., Haller, M.N. and Yen, T.F., Electron microscopic investigation on the nature of petroleum asphaltics. *J. Colloid Interface Sci.*, 29: 475–484 (1969).
[20] Speight, J.G., *The Chemistry and Technology of Petroleum*. Marcel Dekker, New York, N.Y., 2nd ed., pp. 408, 411 (1991).
[21] Katz, M., Alberta bitumen. *Can. J. Res.*, 10: 435–451 (1934).
[22] Lemerle, J., Maquet, J., Basselier, J.J., Lambert, D., Desbene, P.L. and Boulet, R., Polarity and molecular weight of an asphaltene. *Proc., Lyon Int. Symp.*, pp. 379–383 (1984).
[23] Gourlaouen, C. and Petroff, N., Fractionation of asphaltenes by GPC and the characterization of the fraction. *Proc., Lyon Int. Symp.*, pp. 279–284 (1984).

[24] Ray, B.R., Witherspoon, P.A. and Grim, R.E., A study of the colloidal characteristics of petroleum using the ultracentrifuge. *J. Phys. Chem.*, 61: 1296 (1957).
[25] Katz, D.L. and Beu, K.E., Nature of asphaltic substances. *Ind. Eng. Chem.*, 37: 195–200 (1945).
[26] Labout, J.W.A. and Pfeiffer, J.P.H., *Properties of Asphaltic Bitumen*. Elsevier, Amsterdam, p. 36 (1950).
[27] Pollack, S.S. and Yen, T.F., Structural studies of asphaltics by X-ray small angle scattering. *Anal. Chem.*, 42: 623–629 (1970).
[28] Altgelt, K.H., Fractionation of asphaltenes by gel permeation chromatography. *Am. Chem. Soc., Div. Pet. Chem., Prepr.*, 10(3): 29–33 (1965).
[29] Dwiggins, C.W., Jr., A small angle X-ray scattering study of the colloidal nature of petroleum. *J. Phys. Chem.*, 69: 3500–3506 (1965).
[30] Dwiggins, C.W., Jr., Study of the colloidal nature of petroleum with an automated Bonse-Hart X-ray small angle scattering unit. *J. Appl. Crystallogr.*, 11: 615–619 (1978).
[31] Kim, H.G. and Long R.B., Characterization of heavy residuum by a small angle X-ray scattering technique. *Ind. Eng. Chem. Fundam.*, 18: 60–63 (1979).
[32] Ravey, J.C., Ducouret, G. and Espinat, D., Asphaltene macrostructure by small angle neutron scattering. *Fuel*, 67: 1560–1567 (1988).
[33] Overfield, R.E., Sheu, E.Y., Sinha, S.K. and Liang, K.S., SANS study of asphaltene aggregation. *Fuel Sci. Tech. Int.*, 7(5–6): 611–624 (1989).
[34] El Mohamed, S., Hardouin, F. and Gasparoux, H., Flocculation of heavy petroleum products. *J. Chim. Phys.*, 85: 135–144 (1988).
[35] Espinat, D., Tchoubar, D., Boulet, R. and Freund, E., Studies of heavy petroleum products by small angle X-ray scattering. *Proc., Lyon Int. Symp.*, pp. 146–152 (1984).
[36] Gulsun, Z., Dipolar relaxation and nuclear Overhauser effect in asphalt suspensions. *Proc., Lyon Int. Symp.*, pp. 335–339 (1984).
[37] Poindexter, E.H., Dynamic nuclear polarization and molecular aggregation in asphaltene suspensions. *J. Colloid Interface Sci.*, 38(2): 412–423 (1972).
[38] Sheu, E.Y., Storm, D.A. and DeTar, M.M., Asphaltenes in polar solvents. *J. Non-Cryst. Solids*, 131–133: 341–347 (1991).
[39] Senglet, N., Williams, C., Faure, D., Des Courieres, T. and Guilard, R., Microheterogeneity study of heavy crude petroleum by u.v.-visible spectroscopy and small angle X-ray scattering. *Fuel*, 69: 72–77 (1990).
[40] Reerink, H., Size and shape of asphaltene particles in relationship to high-temperature viscosity. *Ind. Eng. Chem. Prod. Res. Dev.*, 12: 82–88 (1973).
[41] Lin, J.R., Lian, H.J., Chen, J. and Yen, T.F., Morpohological size of asphaltene micelles in asphalt and heavy residue. In: M.K. Sharma (Editor), *Particle Technology and Surface Phenomena in Minerals and Petroleum*. Plenum, New York, N.Y., pp. 23–30 (1991).
[42] Glita, S. and Duval, P., Electron microsopy observation of clusters of asphaltenes in bitumens. *C.R. Acad. Sci. Paris*, 306(11): 1–3 (1988).
[43] Yen, T.F., A microstructure of petroleum asphalt. *Am. Chem. Soc., Div. Pet. Chem., Prepr.*, 35(3): 314–319 (1990).
[44] Weinberg, V.A., White, J.L. and Yen, T.F., Solvent fractionation of petroleum pitch for mesophase formation. *Fuel*, 62: 1503–1509 (1983).
[45] Wong, E. and Yen, T.F., Formation of the carbonaceous mesophase from a petroleum derived paving asphalt. *Energy Sources*, 10: 201–208 (1988).
[46] Ho, B. and Briggs, D.E., Small angle X-ray scattering from coal-derived liquids. *Colloids Surf.*, 4: 285–303 (1982).
[47] Dwiggins, C.W., Jr., Application of the indirect transform method to obtaining distance distribution functions of extremely large colloids and emulsion using small angle X-ray scattering data. *J. Appl. Crystallogr.*, 13: 572–576 (1980).
[48] Singer, L.S., Lewis, I.C. and Greinke, R.A., Thermal conversion of polynuclear aromatics to carbon. *Mol. Cryst. Liq. Cryst.*, 132: 65 (1986).
[49] White, J.L., Mesophase mechanisms in the formation of the microstructure of petroleum coke. *Am. Chem. Soc. Symp. Ser.*, 21: 282 (1976).

This page intentionally left blank

Asphaltenes and Asphalts, 1. Developments in Petroleum Science, 40
edited by T.F. Yen and G.V. Chilingarian

Chapter 6

COLLOIDAL NATURE OF PETROLEUM ASPHALTENES

D.A. STORM and E.Y. SHEU

INTRODUCTION

Asphaltenes are molecules that can be precipitated from carbonaceous liquids by certain non-polar solvents [1–3]. Traditionally, they were those molecules in petroleum residue that were soluble in benzene and insoluble in pentane. Over the years, however, molecules precipitated by other solvents, usually heptane [2], and molecules precipitated from other materials, such as coal and oil shale liquids, have been called asphaltenes [3]. As such, there can be many kinds of asphaltenes, each a mixture of a number of molecules. In this chapter, the authors discuss petroleum asphaltenes and, in particular, the heptane insolubles of crude oil and residuum.

It is surprising that it is useful to consider asphaltenes a "species", considering their rather arbitrary definition. Apparently, there is something special about molecules insoluble in heptane, but soluble in benzene, or toluene. It has been recognized that petroleum asphaltenes form colloidal particles in solvents, such as toluene, benzene, tetrahydofuran, 1-methylnaphthalene, or chloroform [4–15]. Colloidal particles have been also observed in crude oil using small-angle X-ray scattering techniques [16,17], in atmospheric residue by Klm and Long [18], in vacuum residue by Storm et al. [19], and in asphalt by Pollack and Yen [20]. The implication of this body of work is that the asphaltenes are the colloidal particles in crude oil. Support for this supposition is provided by the studies by Storm et al. [19,21] with synthetic and natural vacuum residues.

If asphaltenes are colloidal particles, this would explain why they appear to be a "species". Colloidal particles are macroscopic compared to the other molecules in a liquid, and so their presence influences the chemistry of the mixture. The molecular reasons responsible for their colloidal behavior are not presently known. Models describing two extreme situations can be imagined. It was suggested some time ago that asphaltenes are macromolecules [22]. In this model, crude oil and residuum would be similar to a polymeric solution in which very large molecules interact mainly with the surrounding smaller molecules. At the other extreme one could imagine several associated asphaltenic molecules forming a particle [23]. In this model, crude oil and residuum would be analogous to a micellar solution. Micellar solutions are colloidal liquids in which amphiphilic molecules self-assemble to form molecularly ordered particles suspended in water. The particles are typically small. The diameter of the micelle is approximately twice the length of the amphiphilic molecules. The colloidal particles in crude oil [16,17], in atmospheric and vacuum residue [18,19], and in asphalt [20] are in the size range of micelles, but it

would seem that the nature of the particles must be different, because hydrophilic interactions do not appear to play a role.

Thus in the simplest of models, asphaltenes are either macromolecules approximately 50–100 Å in linear dimension, or smaller molecules that have associated to form particles of this dimension. One might think that one could distinguish between these two alternatives by comparing the number average molecular weights of the asphaltenes and the non-asphaltenic fractions; unfortunately the number average molecular weight of asphaltenes is uncertain because asphaltenes are believed to associate in the various solvents that have been used to make the measurements [24]. The accepted range for average molecular weights is 1200–2700 [24]. Recent work indicates, however, that the number average molecular weights of asphaltenes from Ratawi and Alaska North Slope crude oils are smaller than the currently accepted low value [25]. Also, recent work by Sheu et al. [4] show that asphaltenes self-associate in nitrobenzene and pyridine at very low concentrations (<0.05 wt%). This suggests that measured average molecular weights are too large even when using these two solvents. The work of Storm et al. [25] implies that asphaltenic molecules are about the same size as non-asphaltenic molecules, and the observed colloidal behavior, therefore, suggests intermolecular associations as proposed by Dickie and Yen [23]. Recent work on the molecular weight of asphaltenes by DeCanio et al. [26] and Storm et al. [25], and on the self-association of asphaltenic molecules in pyridine and nitrobenzene by Sheu et al. [4] is reviewed in the next section.

Questions pertaining to the microstructure of asphaltenes are also reviewed in the next section. The molecular properties of asphaltenes have been the subject of numerous studies [2,3,27] and the references contained in these reviews. There are two problems inherent in the attempt to determine the molecular structure of the asphaltenic molecules. First, asphaltenes are a mixture of a great number of molecules, and because one cannot identify each molecule in the mixture, one must represent molecular information in a statistical manner [28,29]. Second, intermolecular associations prevent one from obtaining even a true number average molecular property [25,28,29]. Consequently, it appears that the best approach is to develop a molecular representation for the mixture that is consistent with the available analytical data [3].

In the subsequent section, the authors review the models for the macrostructure of asphaltenes based on the rheological measurements of Sheu et al. [5,6], Storm et al. [19,21], Kyriacou et al. [11], Rao and Serrano [12], Altgelt and Harle [14] and Reerink [30]. Earlier results were interpreted as supporting the macromolecular model, but the recent work of Sheu et al. [5,6] and Storm et al. [19,21] suggests asphaltenes behave as solvated spherical particles formed by the association of several molecules.

In the last section, the authors review the small-angle X-ray scattering results of Storm et al. [19], Herzog et al. [9], Klm and Long [18], and Dwiggins [16,17], and the small-angle neutron scattering results of Sheu et al. [4,7], Overfield et al. [8] and Ravey et al. [10]. Published models for the macrostructure based on these scattering studies are contradictory at present. Overfield et al. [8] proposed rod-like particles; Ravey et al. [10] and Herzog et al. [9] proposed disc-like macromolecules; and Sheu

et al. [4,7] and Storm et al. [19] proposed spherical particles with a distribution of sizes. The theory for small-angle X-ray scattering (SAXS) and small-angle neutron scattering (SANS) is described in this section to the extent needed to illustrate why different models can be obtained by using the standard methods of analyses for SAXS and SANS.

MICROSTRUCTURE OF ASPHALTENES

The work of Boduszynski [28,29] illustrates the immense molecular complexity of crude oil. Boduszynski [28,29] has pointed out that it is impossible to identify all the molecules in even the non-asphaltenic fraction of crude oil with current analytical methods. The asphaltenes appear equally complex [26]. There is the added complication that only a fraction of the asphaltenes can be analyzed as a mixture of independent molecules due to strong intermolecular forces [25,26]. Consequently, molecular properties must be represented in a statistical manner, and such representations must have a built-in error due to the influence of the intermolecular forces on measured analytical properties [3].

Representation theory is abstract, but provides the language needed to describe the microstructure of asphaltenes. For example, the elemental compositional data, or the H- and ^{13}C-NMR data of DeCanio et al. [26] presented in Table 6-1 provide

TABLE 6-1

Fractionation and compositional analysis of Ratawi vacuum residue

Analysis	Oil	Resin	Asph-1	Asph-2
Fractionation				
Residue (%)	71.6	7.6	18.3	2.6
C_5-I (%)	26.6	64.3	9.1	
Ultimate analysis				
C (%)	83.0	82.6	82.7	83.0
H (%)	11.0	10.5	8.4	7.9
S (%)	5.1	6.2	7.7	8.6
O (%)	0.6	0.2	1.2	0.4
Ni (ppm)	12	43	145	–
V (ppm)	24	89	308	–
NMR (% of spectra)				
H (ar)	7.3	10.6	13.5	18.3
H_a	14.0	12.5	20.0	22.9
H_b	59.6	53.3	50.9	45.4
H_c	19.0	23.6	15.6	13.5
C_{ar}	27.8	41.3	58.2	66.7
C_{al}	72.2	58.7	41.8	33.3
$C_{ar\text{-}H}$	10.2	16.2	16.5	20.9
$C_{ar\text{-}b3}$	(1.5)	0.4	9.8	9.9
$C_{ar\text{-}alk}$	9.9	11.7	14.1	17.8

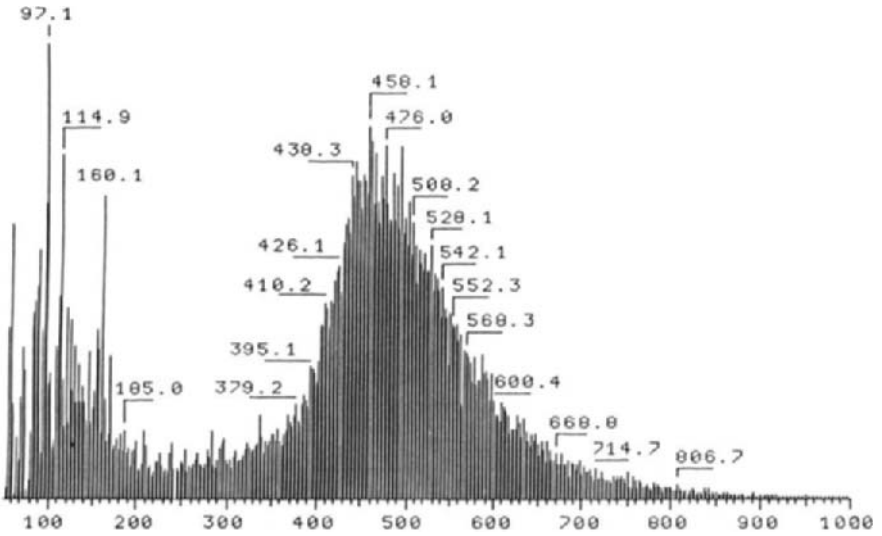

Fig. 6-1. Mass spectrum of Ratawi asphaltenes by electron impact mass spectroscopy. Ionization beam energy is 20 eV; the sample heating rate is 50°C/min; and the maximum sublimation temperature is 300°C.

representations of the microstructure of the Ratawi asphaltenes. Similarly, the mass spectrum of DeCanio et al. [26] shown in Fig. 6-1 provides another representation. In general, representations may or may not be faithful, i.e., they may not contain all the information about the set of objects. In fact, it is obvious that the above representations are not faithful, because they do not contain information about all the chemical functionalities in the mixture.

With respect to Table 6-1, Ratawi is a crude oil from the Neutral Zone in the Middle East, and Ratawi vacuum residue is the fraction of this crude oil that has a nominal boiling point above 1000°F. The oil and resin fractions are defined according to DeCanio et al. [26] as molecules soluble in pentane (oil), and molecules insoluble in pentane but soluble in heptane (resins), respectively. The asphaltenes (heptane insolubles) have been split into two groups. Asph-1 are the molecules insoluble in heptane, but soluble in cyclohexane, whereas Asph-2 are the molecules insoluble in cyclohexane, but soluble in toluene.

The data presented in Table 6-1 illustrate three chemical differences between asphaltenes and non-asphaltenes. First, asphaltenes have a lower H/C atomic ratio. Speight and Moschopedis [2] have pointed out that all petroleum asphaltenes (heptane insolubles) appear to have a characteristic H/C ratio of 1.15 ± 0.05. Second, asphaltenes contain most of the heteroatoms. Third, asphaltenes have a large amount of polynuclear aromaticity, as shown by the $C_{ar\text{-}b3}$ parameter in Table 6-1. The $C_{ar\text{-}b3}$ NMR parameter indicates the amount of carbon located inside a polynuclear aromatic structure.

The data presented in tables are not easily visualized. Consequently, the available analytical data have been often used to deduce an "average molecular structure"

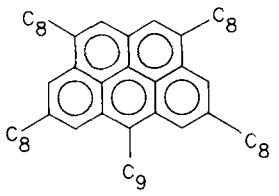

H = 72 S = 1.8 Ni = 0.002

N = 0.5 V = 0.005

Fig. 6-2. Representation of Ratawi asphaltenes. Concentrations of hydrogen, sulfur, nitrogen, nickel and vanadium are in units of atoms per "molecule".

[2,3,27]. These average structures are actually particular representations of the available analytical data. The chemical significance of such a representation is controversial [29,31]. Within the context of representation theory, however, their existence is well defined. A representation is shown in Fig. 6-2 for the Ratawi asphaltenes. The structure, or graph, can be viewed as follows: a non-linear mathematical function has been found to fit the NMR data of Table 6-1, and the graph of this functions looks like a molecule. It is not a molecule of course, but a particular representation of the analytical data. The function is also not unique; for example, several functions that differ only in the arrangement of the R-groups on the polynuclear aromatic structure would work equally as well. Such a representation may, or may not be useful in describing the chemistry of asphaltenes, depending on the chemical question asked. The representation of Fig. 6-2 was found to be useful in correlating vistar stability in visbreaking experiments, and in correlating fouling rates in the hydroconversion of vacuum residue by the H-Oil® process. In any case, the representation in Fig. 6-2 illustrates three distinguishing features about asphaltenic molecules: the C/H ratio, the heteroatom content, and the polynuclear aromaticity. It is important to note that the hydrogen atoms and heteroatoms were not included in the graph; to do so would create a representation containing more information than is corroborated by the analytical data obtained by the authors.

Average molecular weight

Average molecular weights for petroleum asphaltenes have been reported in the range of 900 to 500,000 depending on the analytical method used in the measurement [23,24]. Dickie and Yen [23] pointed out that it is very likely that the average weights of particles in various states of aggregation have been measured due to intermolecular and interparticle forces. Vapor pressure osmometry (VPO) is presently considered to be the most accurate method when a good solvent such as nitrobenzene is used to dissolve the asphaltenes [32]. Based on this technique, the accepted range for the average molecular weight of petroleum asphaltenes is

1200–2700 [24]. It has also been estimated that the asphaltenes contain molecules with molecular weights in the range of 1000 to 10,000 [24]. If these molecular weights are correct, then one cannot distinguish between the macromolecular and the association models. As a point of reference, the average molecular weight of the non-asphaltenic fraction of Ratawi vacuum residue(pentane solubles) is 615, and the biggest molecule in the mixture is in the range of 800–900 [26]. If there were molecules in the asphaltenes with molecular weights of 10,000, then several non-asphaltenic molecules could fit around these molecules in the manner of the macromolecular model. The work of Storm et al. [25], however, shows that the number average molecular weight of the Ratawi asphaltenes is actually less than 814; less than 30% larger than that for the non-asphaltenes. Also the largest molecule in the distribution is estimated to have a molecular weight of 1400 [25]. This work suggests that non-asphaltenic and asphaltenic molecules are about the same size.

The argument of Storm et al. [25] is mathematical, and it is based on the mass spectrum shown in Fig. 6-1. Figure 6-3 shows the mass spectrum for the Ratawi oil fraction (pentane solubles) according to DeCanio et al. [26] for reference. In these mass spectroscopy experiments, approximately 20 μg of the sample was dissolved in methylene chloride and inserted into a small glass sample holder. The sample was then sublimed in the spectrometer by heating the glass sample holder electrically from room temperature to 300°C at a rate of 50°C/min. Very little thermal fragmentation would be expected at 300°C considering the short time during which the sample was exposed to this temperature [33]. Sublimed molecules were ionized with 20 eV electrons in order to minimize fragmentation. The glass sample holder was weighed before and after the experiment in order to calculate the fraction of the sample that had actually sublimed.

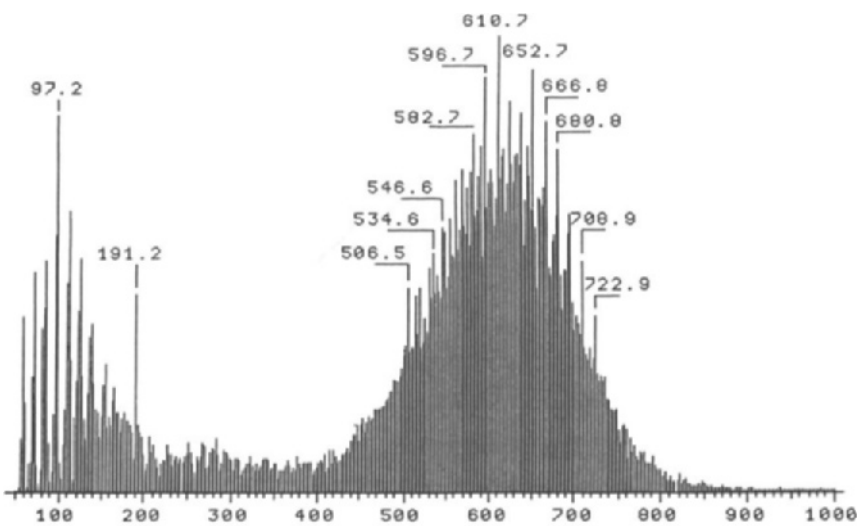

Fig. 6-3. Mass spectrum of Ratawi oil by electron impact mass spectrometry. Ionization beam energy is 20 eV; the sample heating rate is 50°C/min; and the maximum sublimation temperature is 300°C.

The spectra shown in Figs. 6-1 and 6-3 are mass distribution functions; they show the number (intensity) of molecules with a particular molecular mass. These distribution functions are inaccurate for two reasons. First, some of the molecules have fragmented in the electron beam, as is evident from the intensity at low mass. Second, only a fraction of the asphaltenes actually sublimed. One suspects that the larger molecules are missing from the mass distribution in Fig. 6-1. The error in the distribution however, is not arbitrary. The area under the missing part of the distribution curve is proportional to the mass left behind on the sample holder. One can calculate the effect of this error. One can also calculate the error due to molecular fragmentation [25]. When these two errors are taken into account, it can be shown that the true number average molecular weight is bounded from above by the right hand side of Eq. 6-1:

$$M \leq M_c \{1 + [(1 - f)W + F]/[fW - F]\} \tag{6-1}$$

where M is the true number average molecular weight for the mixture, M_c is the value calculated neglecting peaks below a certain mass due to fragmentation, f is the fraction of the sample with weight W that sublimed, and F is the mass loss due to sample fragmentation.

Table 6-2, taken from Storm et al. [25], shows the average molecular weights for fractions of Ratawi and Alaska North Slope vacuum residues. Average molecular weights were also measured for these fractions by VPO at 50°C using toluene as the solvent. The average molecular weights for the "oil" fractions by both mass spectroscopy (MS) and VPO agree with the upper bound calculated according to Eq. 6-1. The average molecular weights by mass spectroscopy and VPO diverge for the resin and asphaltene fractions because of the incomplete sample sublimation in mass spectroscopy, and the intermolecular associations in VPO. The upperbound shows that the VPO results for the resins and asphaltenes are at least twice as large as they should be. Also, as mentioned above, the average molecular weight for the Ratawi asphaltenes is at most 30% larger than that

TABLE 6-2

Number average molecular weight of subfractions of Ratawi and ANS vacuum residues

	Vacuum residue (wt%)	f	Molecular weight		
			MS	VPO	upper bound
Ratawi					
Oil	71.0	1.0	615	631	640
Resins	7.5	0.8	485	1420	647
Asphaltenes	21.5	0.58	450	2360	814
Alaska North Slope					
Oil	85.6	0.95	640	597	735
Resins	3.2	0.6	555	2100	970
Asphaltenes	11.2	0.4	470	3248	1270

for the non-asphaltenic fraction. This is an indication that asphaltenes are not macromolecules with respect to non-asphaltenic molecules. One can also conjecture the "biggest" molecule in the sample. The argument is not rigorous because one has to assume that the distribution is not bimodal [25]. Making conservative assumptions about the width of the distribution, Storm et al. [25] found the biggest molecule to have a molecular weight of 1400. Again this suggests that the asphaltenic molecules are not macromolecules with respect to those in the non-asphaltenic fractions.

Association of asphaltenic molecules

As discussed above, it is currently accepted that a reasonably accurate average molecular weight can be measured by VPO if nitrobenzene is used as the solvent [32]. The molecular weights of asphaltenes from heavy Alberta crude oils were approximately 1800 in nitrobenzene and 2700 in pyridine [32]. The measured molecular weight by VPO usually depends on the concentration, and so one makes measurements for a series of samples with concentrations in the range of 1–10%, and then extrapolates the molecular-weight-concentration curve to zero concentration. If the asphaltenic molecules have associated at a concentration below 1%, however, one will obtain the average particle weight by this procedure. It is important to determine, therefore, whether or not asphaltenes self-associate in nitrobenzene and pyridine at concentrations below 1 wt%.

The self-association of surfactant molecules in micellar chemistry is often observed by surface tension studies. At low surfactant concentrations, the surfactant molecules adsorb at the water–air interface, and reduce the surface tension. The surface tension usually decreases rapidly with surfactant concentration, because the amount adsorbed increases with surfactant concentration. At the critical micelle concentration (CMC), however, the surfactant molecules adsorb to a lesser extent, because the competing micellization process now reduces the concentration of free surfactant in solution. There is an abrupt change in slope of the surface tension vs. surfactant concentration curve at the CMC. For concentrations greater than the CMC, both micelles and free surfactant molecules are present in the solution.

Exactly this same phenomenon has been observed by Sheu et al. [4] for asphaltenic solutions. Figures 6-4 and 6-5 show the surface tension vs. asphaltene concentration curves for Ratawi asphaltenes in pyridine and nitrobenzene, respectively. The Ratawi asphaltenes obviously associate in these solvents at very low concentrations: 0.02 wt% in pyridine and 0.05 wt% in nitrobenzene. The work of Sheu et al. [4] provides direct evidence for the self-association of asphaltenic molecules.

In summary, recent results reviewed in this section indicate that the average molecular weight of Ratawi asphaltenic molecules is lower than currently accepted. The upper bound calculated by Storm et al. [25] suggests that asphaltenic molecules are about the same size as non-asphaltenic molecules. The surface tension results of Sheu et al. [4] indicate that asphaltenic molecules self-associate in pyridine and nitrobenzene at concentrations below those used in the VPO measurements. The

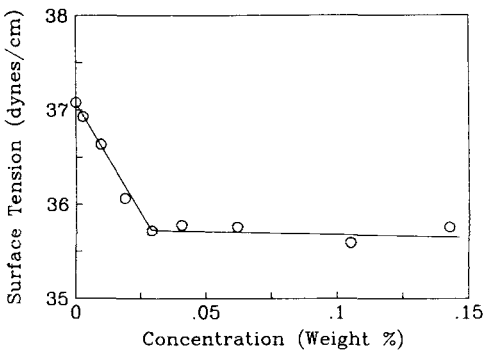

Fig. 6-4. Surface tension of Ratawi asphaltenes/pyridine solutions at 25°C.

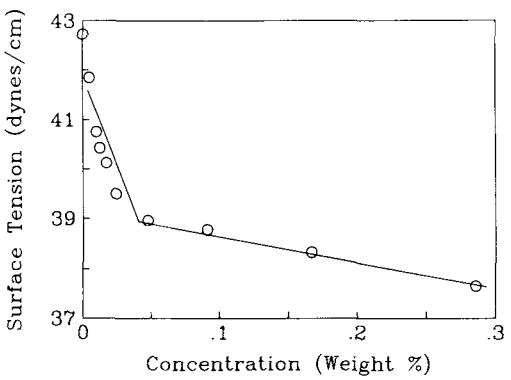

Fig. 6-5. Surface tension of Ratawi asphaltenes/nitrobenzene solutions at 25°C.

surface tension results show that asphaltenic molecules form colloidal particles in these two solvents by self-association, as suggested by Dickie and Yen [23].

RHEOLOGY OF ASPHALTENES IN SOLVENTS AND IN VACUUM RESIDUE

If asphaltenes self-associate and form solid particles suspended in crude oil, residuum, and solvents, these liquids would be expected to display a well-known response when subject to shear stresses. Rheology for such suspensions follows directly from the principles of hydrodynamics. According to Einstein [34]:

$$\eta_r = \eta/\eta_0 = 1 + [\eta]\phi \tag{6-2}$$

where η is the viscosity of the suspension, η_0 is the viscosity of the suspending liquid, η_r is the relative viscosity, $[\eta]$ is the intrinsic viscosity, and ϕ is the fraction of fluid volume occupied by the particles. The intrinsic viscosity contains information about the shape of the particle. It is 2.5 for spheres and larger for cylindrical or prolate ellipsoidal particles [35]. The suspension must be Newtonian, and Eq. 6-2 only holds

when each particle is free to move in the fluid as if the other particles were not present (dilute limit). There are higher-order terms in ϕ for more concentrated suspensions:

$$\eta_r = 1 + [\eta]\phi + k_1\phi^2 + k_2\phi^3 + \ldots \tag{6-3}$$

Many types of interactions contribute to these higher-order terms [36,37]. Direct interparticle interactions, hydrodynamic interactions and Brownian interactions all contribute to the second-order term [36,38]. If the direct interparticle interactions are short-range, then hydrodynamic interactions dominate at the higher shear rates [36]. In principle Eqs. 6-2 and 6-3 also hold for solutions of macromolecules, but it would be expected that the second-order term behaves differently for macromolecular solutions, because intramolecular interactions are important and depend on both solvent quality and concentration. The rheological data for Ratawi asphaltenes in toluene, toluene/pyridine mixtures and vacuum residue were analyzed by Sheu et al. [5,6] and by Storm et al. [19,21] using equations which describe suspensions of solid particles. The equations take into account the types of interaction expected for solid particles, and the excellent description of the rheology provided by these equations suggests that Ratawi asphaltenes behave as solid particles in these liquids.

As pointed out by Storm et al. [19,21], there is a problem in applying Eqs. 6-2 or 6-3 to the asphaltene case, because one does not know the hydrodynamic volume occupied by the asphaltenic particles in the fluid. This important point is often ignored in many rheological studies. Re-writing Eq. 6-2 in terms of a fraction that is well-defined:

$$\eta_r = 1 + [\eta]\rho/\rho_A(\text{sol})W_A = 1 + [\eta]_w W_A \tag{6-4}$$

where $\rho_A(\text{sol})$ is the density of the solvated particles in the fluid and $[\eta]_w$ is a new intrinsic viscosity that contains effects due to both the shape and solvation:

$$[\eta]_w = \rho/\rho_A(\text{sol})[\eta]$$

Equation 6-5 provides an operational definition of the volume fraction if one can determine $\rho/\rho_A(\text{sol})$ in some manner:

$$\phi = \rho/\rho_A(\text{sol})W_A \tag{6-5}$$

Figure 6-6 [5,6] and Fig. 6-7 [19] illustrate the application of Eqs. 6-2 and 6-3 for Ratawi asphaltenes in toluene and vacuum residue, respectively. The data in Fig. 6-7 were measured by dispersing vacuum residue in the non-asphaltenic fraction of the vacuum residue [19,21]. The volume fraction in Fig. 6-6 is on a dry basis [5], and differs from the weight fraction in Eq. 6-4 by the factor 1.013. Figures 6-6 and 6-7 show that Eq. 6-4 holds for concentrations less than 8 wt%. The intrinsic viscosities for the Ratawi asphaltenes extracted from the linear parts of the curves shown in Figs. 6-6 and 6-7 are 7.9 and 7.3, respectively. They are also shown in Tables 6-3 and 6-4 with other rheological parameters. If solvation effects are ignored, these values for the intrinsic viscosity indicate elongated particles.

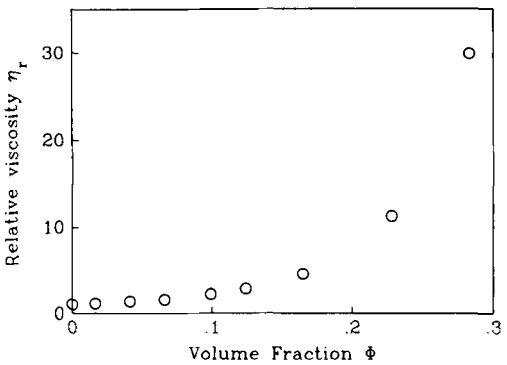

Fig. 6-6. Relative viscosity of Ratawi asphaltenes in toluene at 25°C. Volume fraction is on a dry basis (1.013 times the weight fraction).

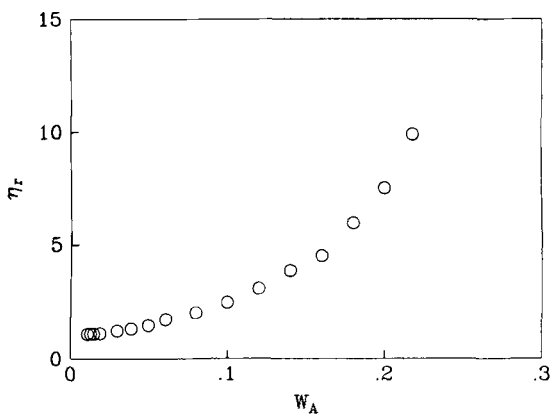

Fig. 6-7. Relative viscosity of Ratawi asphaltenes in vacuum residue at 93°C.

TABLE 6-3

Rheological parameters for Ratawi asphaltenes in toluene at 25°C

	Shape	$[\eta]$	$[\eta]_w$	K	ρ/ρ_A
Einstein	spheres	2.5	6.8		2.7
Pal–Rhodes	spheres			2.7	
Eilers	spheres	2.5	6.9	1.7	2.8
Campbell–Forgacs	spheres				~2.7
Grimson–Barker	spheres			2.2	

The viscosity of asphaltenic solutions or solutions of the "high-molecular-weight component" of crude oil and residuum have been studied in toluene, tetrahydofuran, 1-methylnaphthalene and benzene by Sheu et al. [5], Kyriacou et al. [11], Rao and Serrano [12], Altgelt and Harle [14], Reerink [30] and Mack [15]. The reported

TABLE 6-4

Rheological parameters for Ratawi asphaltenes at 93°C

	Shape	$[\eta]$	$[\eta]_w$	K	ρ/ρ_A
Einstein	spheres	2.5	7.3		2.9
Pal–Rhodes	spheres			2.9	
Eilers	spheres	2.5	6.9	2.5	2.8
Campbell–Forgacs	spheres				2.7
Grimson–Barker	spheres	2.5		2.2	

intrinsic viscosities were in the range of 5–10. Kyriacou et al. [11] interpreted their results as indicating planer macromolecules. Altgelt and Harle [14] suggested that their results indicate rod-like macromolecules, whereas Reerink [30] suggested prolate ellipsoidal macromolecules. Rao and Serrano [12] also interpreted effects due the higher-order terms in Eq. 6-3 as indicating intermolecular associations to form agglomerates. Solvation effects were not taken into account in this work.

Figures 6-6 and 6-7 illustrate the importance of the second and higher order terms for concentrations above 8%. As discussed above, there are many types of interactions that could contribute to these higher order terms. There is a particular hydrodynamic interaction that arises because of polydispersity [39]. Roscoe [39] assumed that the Einstein equation holds for each group of hard spheres with the same size, and that each group experiences the mean hydrodynamic field caused by all the other spheres in the fluid undergoing shear stresses, and derived the following equation for the relative viscosity:

$$\eta_r = (1 - \phi)^{-2.5} \tag{6-6}$$

By expanding Eq. 6-6 in powers of ϕ, it can be seen that Eq. 6-6 is a special case of Eq. 6-3 in which the higher-order terms arise because of a particular type of hydrodynamic interaction.

Again the problem arises that the volume occupied by the asphaltenic particles in the fluids is not known. If one assumes that the solvated volume is directly proportional to the dry volume, then:

$$\phi = K_0 V_A(\text{dry})/V = K_0 \rho/\rho_A(\text{dry}) W_A = K W_A \tag{6-7}$$

where the solvation constant K defines another volume fraction. This definition need not be consistent with that provided by Eq. 6-5, because the assumption leading to Eq. 6-7 is independent of the definition of $\rho_A(\text{sol})$ in Eq. 6-5. Making use of Eq. 6-7 in Eq. 6-6, the relative viscosity for free solvated spheres with different sizes is given by:

$$\eta_r = (1 - K W_A)^{-2.5} \tag{6-8}$$

Equation 6-8 is a basic equation in the rheological studies of Sheu et al. [5,6] and Storm et al. [19]. A form of this equation was recently given by Pal and

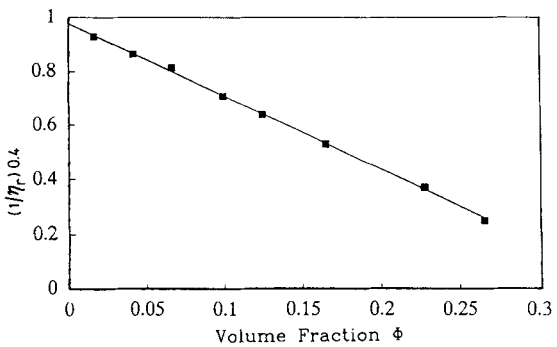

Fig. 6-8. Fit of Pal–Rhodes equation (Eq. 6-8) to the relative viscosity for Ratawi asphaltenes in toluene at 25°C. Volume fraction is on a dry basis (1.013 times the weight fraction).

Rhodes [40] to describe the viscosity of spherical flocs in microemulsions, and so this equation is referred to as the Pal–Rhodes equation. It is clear from the above derivation, however, that Eq. 6-8 applies to other kinds of particles than flocs. It is perhaps worth re-emphasizing the parameters contained in Eq. 6-8. The exponent 2.5 arises because the particles are spherical. The solvation constant arises because the particles occupy a larger volume in the fluid than would be expected based on their dry volume, and the functional form of Eq. 6-8 arises because the particles are free soft spheres with a distribution of sizes. As shown in Fig. 6-8, the rheology of Ratawi asphaltenes in toluene is described very well by this equation [5,6]. The rheology of Ratawi asphaltenes in natural and synthetic vacuum residue is also described well by the Pal–Rhodes equation (Fig. 6-9). These excellent fits suggest Ratawi asphaltenic particles can be modeled as solvated spheres with a distribution of sizes in both toluene and vacuum residue. Since this model is in conflict with

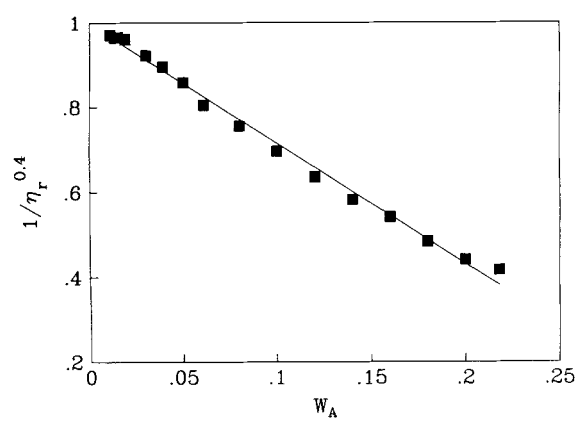

Fig. 6-9. Fit of Pal–Rhodes equation (Eq. 6-8) to the relative viscosity for Ratawi asphaltenes in vacuum residue at 93°C.

earlier published results, other independent methods have been used to analyze the data discussed here.

First, Eilers [41] proposed the following empirical equation for the viscosity of bitumen-water emulsions:

$$(\sqrt{\eta_r} - 1)/\phi = [\eta]/2 + (\sqrt{\eta_r} - 1)/\phi_m \tag{6-9}$$

where ϕ_m is an apparent maximum packing fraction for the spheres. If the packing is face-centered cubic, one would expect ϕ_m to be 0.74. Converting Eq. 6-9 from volume fraction to weight fraction using Eq. 6-5, one obtains:

$$(\sqrt{\eta_r} - 1)/W_A = [\eta]_w/2 + (\sqrt{\eta_r} - 1)/W_m \tag{6-10}$$

Figure 6-10 shows the data of Sheu et al. [5,6] for Ratawi asphaltenes in toluene plotted according to Eq. 6-10, using the volume fraction on a dry basis as discussed above, and Fig. 6-11 shows the data for Ratawi asphaltenes in vacuum residue also plotted according to Eq. 6-10. The agreement is quite good in both cases. One can extract a solvation parameter from the slope of the lines in Figs. 6-10 and 6-11 ($1/W_m$) that is independent of the Pal–Rhodes solvation parameter. The argument is as follow: If the asphaltenic particles were hard spheres, then the maximum packing fraction should be 0.74. Inasmuch as the spheres are solvated, the apparent packing fraction obtained from Figs. 6-10 and 6-11 is less. The ratio of the solvated volume to unsolvated volume is a solvation constant, and so by using Eq. 6-7 one obtains:

$$K_E = 0.74/W_m \tag{6-11}$$

Also, if the model of solvated spheres is correct, one would expect Eq. 6-10 to be consistent with Eq. 6-4, giving the same $[\eta]_w$ and the same solvation parameter. Tables 6-3 and 6-4 show that reasonably consistent parameters are obtained from

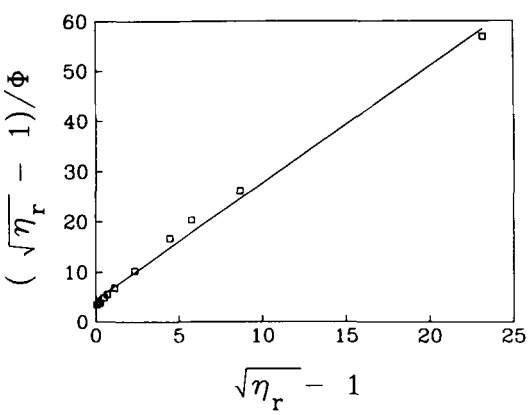

Fig. 6-10. Fit of Eilers equation (Eq. 6-10) to the relative viscosity for Ratawi asphaltenes in toluene at 25°C. Volume fraction is on a dry basis (1.013 times the weight fraction).

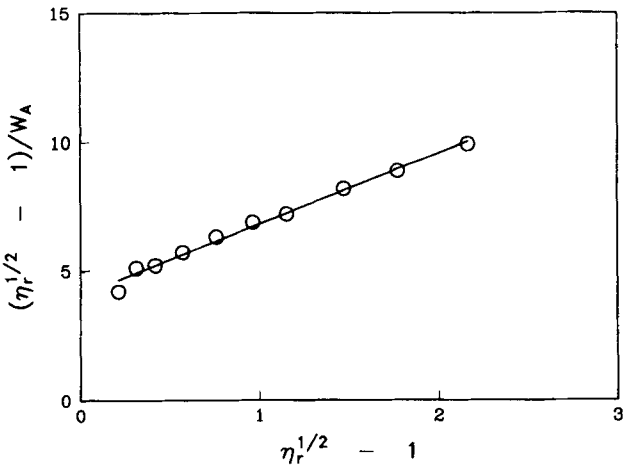

Fig. 6-11. Fit of Eilers equation (Eq. 6-10) to the relative viscosity for Ratawi asphaltenes in vacuum residue at 93°C.

these two equations for both Ratawi asphaltenes in toluene and in vacuum residue. An additional check is provided by Eq. 6-5. If the particles are spheres, then by dividing $[\eta]_w$ by 2.5 yields $\rho/\rho_A(\text{sol})$, which gives the same solvation parameters obtained from the slopes of the Pal–Rhodes and Eilers graphs. These parameters are given in Tables 6-3 and 6-4.

Another way to check the model of solvated spheres is by using the equation recently given by Campbell and Forgacs [42] based on percolation theory. Below a certain concentration called the percolation threshold ($\phi_c = 0.16$) the fluid consists of particles and clusters of particles free to move through the fluid. At the percolation threshold, a macroscopic cluster forms and the particles can only move into holes in the infinite cluster. Campbell and Forgacs [42] argued that the viscosity of the fluid is now determined by the number of holes available for the hard spheres to enter. Calculating the number of holes of various sizes at a given concentration, Campbell and Forgacs [42] derived the following equation for the relative viscosity:

$$\eta_r = e^{1/q} - 1 \tag{6-12}$$

where $q = (\phi_m - \phi)/(\phi_m - \phi_c)$.

Equation 6-12 only holds for hard spheres above the percolation threshold, but it should be approximately valid for solvated spheres(soft spheres) that are essentially free. Figure 6-12 shows the data of Sheu et al. [6,7] for Ratawi asphaltenes in toluene plotted according to Eq. 6-12 using the maximum packing fraction obtained from the Eilers analysis. Figure 6-13 shows the data for Ratawi asphaltenes in vacuum residue. The fits are good for both cases showing consistency with the Eilers equation. One can estimate a solvation constant $\rho/\rho_A(\text{sol})$ from the Campbell–Forgacs analysis. One could argue that the Campbell–Forgacs analysis should only be valid above the percolation threshold, which according to Fig. 6-12 and 6-13 is

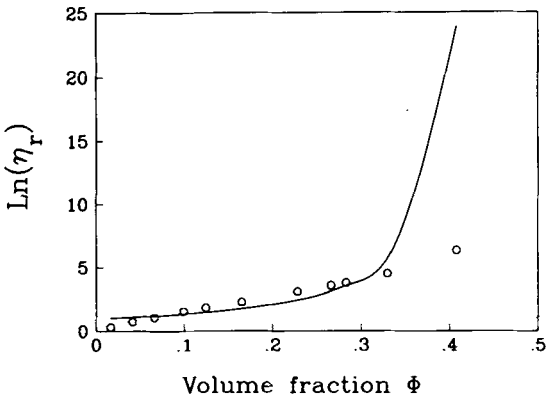

Fig. 6-12. Fit of the Campbell–Forgacs equation (Eq. 6-12) to the relative viscosity for Ratawi asphaltenes in toluene at 25°C. Volume fraction is on a dry basis (1.013 times the weight fraction).

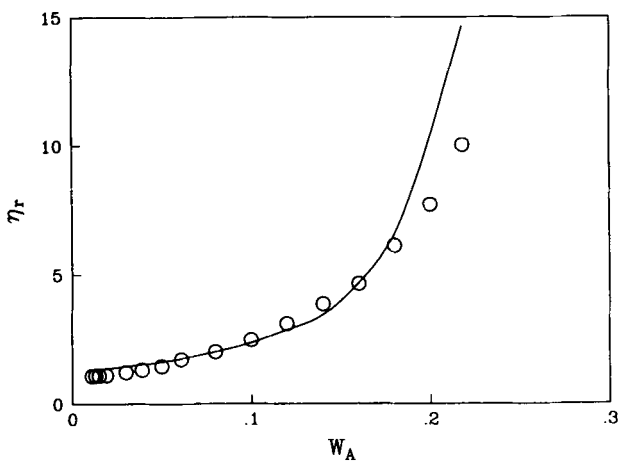

Fig. 6-13. Fit of the Campbell–Forgacs equation (Eq. 6-12) to the relative viscosity for Ratawi asphaltenes in vacuum residue at 93°C.

approximately 0.06. Using Eq. 6-5 to obtain the value of $\rho/\rho_A(\text{sol})$, the approximate Einstein solvation constant is found to be 2.7, which is consistent with the values obtained from the Pal–Rhodes and Eilers analyses.

Finally another independent check of the model of solvated spheres is provided by an equation developed by Grimson and Barker [43]. Grimson and Barker [43] considered a system of soft spheres with a hard inner core surrounded by a soft shell. The soft spheres interact with each other according to the following potential:

$$V(r) = \Lambda[\sigma/(r - \sigma)]^n$$

where Λ is the coupling constant in units of energy, σ is the radius of the hard inner core, r is the distance from the center of the core, and n is an exponent that

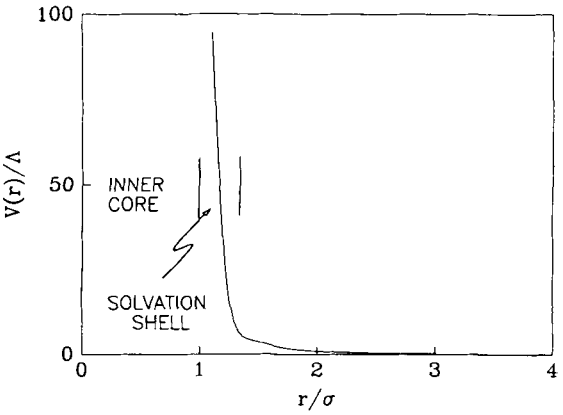

Fig. 6-14. Plot of Grimson–Barker soft-sphere potential. σ represents the hard sphere radius, r is the distance from the origin of the hard sphere, and Λ is the coupling constant in units of energy.

measures the "softness" of the interaction (when n is large, the soft shell is small). In this model, the soft spheres are essentially free; i.e., they interact infrequently by the above soft sphere interaction. Figure 6-14 shows this interaction potential for $n = 2$. Grimson and Barker [43] used this direct interparticle interaction to calculate a contribution to the second-order term in Eq. 6-3, and proposed that this contribution could be added to the contribution due to the hydrodynamic interactions. Majolino et al. [44] took the hydrodynamic interactions given by the Einstein equation and by adding the contribution due to the interparticle interaction according to Grimson and Barker [43], obtained the following equation:

$$\eta_r = (1 + 2.5\phi) + \Lambda[\phi/\phi_m]/\left[1 - (\phi/\phi_m)^{1/3}\right]^n \tag{6-13}$$

The application of Eq. 6-13 is somewhat subtle. One could argue that the first term in Eq. 6-13 accounts for hydrodynamic interactions between free spheres according to this approximation, so the volume fraction should be the dry volume fraction. The second term accounts for solvation effects through the interparticle potential. Figure 6-15 shows the data of Sheu et al. [5,6] for the Ratawi asphaltenes in toluene plotted according to Eq. 6-13, and Fig. 6-16 shows the data for Ratawi asphaltenes in vacuum residue. The maximum packing fractions were taken from the Eilers analyses as discussed above. The fits are very good for $n = 2$ and $\Lambda = 0.6$. A plot of the potential function for $n = 2$ is shown in Fig. 6-14. One can also obtain a qualitative estimate of a solvation constant from the Grimson–Barker analysis. As shown in Fig. 6-14, the soft part of the interaction potential extends out from the hard core about 1.3 times the hard sphere radius. As the solvation constant is basically the ratio of the solvated volume to the hard sphere volume, Fig. 6-14 yields an estimate of 2.2 for the solvation parameter.

In summary, Ratawi asphaltenes behave as solvated spheres in both toluene and vacuum residue at temperatures for which the particles are essentially free. This model is confirmed by five independent methods of analysis. The particles appear

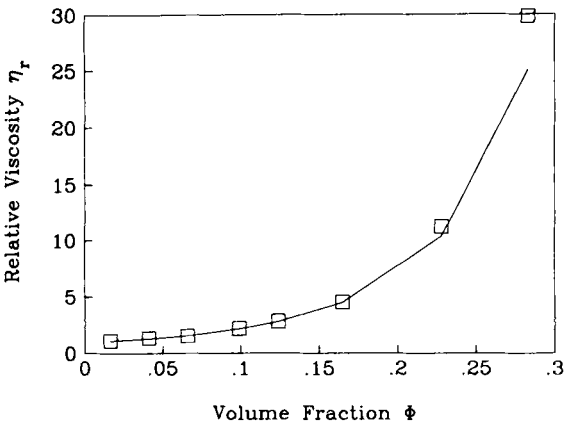

Fig. 6-15. Fit of the Grimson–Barker equation (Eq. 6-13) to the relative viscosity for Ratawi asphaltenes in toluene at 25°C. Volume fraction is on a dry basis (1.013 times the weight fraction).

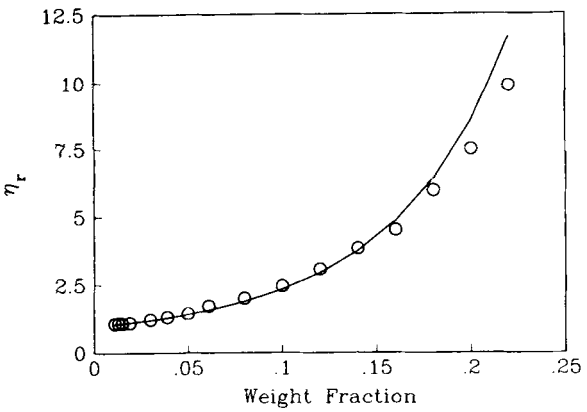

Fig. 6-16. Fit of the Grimson–Barker equation to the relative viscosity for Ratawi asphaltenes in vacuum residue at 93°C.

to have a hard inner core surrounded by a solvation shell forming a diffuse particle-solvent boundary. The Pal–Rhodes analysis suggests polydispersity. It is interesting that the rheological parameters are essentially the same for Ratawi asphaltenes in toluene as they are in their natural environment at the two temperatures chosen in this work. This is coincidental because the solvation parameters depend on temperature [19]. Nevertheless, the rheological properties of Ratawi asphaltenes in vacuum residue in the temperature range of 93–300°C are very similar to those in toluene at 25°C. This suggests that the dominant forces determining the structure of these fluids at these temperatures are between asphaltenic molecules and not between asphaltenic molecules and the non-asphaltenic molecules. Interparticle forces become much stronger in vacuum residue at lower temperatures, and the

simple description of the rheology provided by essentially free solvated spheres begins to break down [19].

SMALL ANGLE X-RAY AND NEUTRON SCATTERING

Small-angle X-ray scattering (SAXS) and small-angle neutron scattering (SANS) are often used to detect particles in colloidal liquids. The scattering centers in SAXS are localized fluctuations in electron density. Asphaltenes have a higher electronic density than their surroundings due to their polynuclear aromaticity, and so SAXS is useful for studying asphaltenes in their natural environment. The scattering centers in SANS are all the nuclei, and so this technique has not been used to study asphaltenes in their natural state. This technique, however, is very useful for the study of asphaltenes in solvents. One can increase the contrast between the asphaltenes and the surrounding fluids by using perdeuterated solvents. Protons and deuterons have significantly different scattering lengths. One then measures the localized fluctuations in deuteron density caused by the presence of the asphaltenic particles in the perdeuterated solvent.

The first application of SAXS to the problem of asphaltene macrostructure was made by Dwiggins [16], who identified scattering centers in crude oil. Scattering centers were also identified in asphalts by Pollack and Yen [20], in atmospheric residue by Klm and Long [1], and in vacuum residue by Storm et al. [19]. Particle radii are generally in the range of 30–70 Å. Particles are also reported for asphaltenes in various solvents by Herzog et al. [9], Klm and Long [1] and Pollack and Yen [20]. Herzog et al. [9] attempted to obtain more information about the macrostructure of these particles by comparing the scattering intensities for various particle shapes with the observed intensity. The agreement was best for a distribution of thin discs, 3.4 Å thick and with radii in the range of 13–800 Å. In contrast Storm et al. [19], following a procedure suggested by Sheu et al. [45], obtained a good fit of their data for a distribution of spherical particles with radii in the range of 20–50 Å.

The results from SANS analyses are equally conflicting at present. Overfield et al. [8] reported that an initial analysis of their data indicates elongated particles. Ravey et al. [10] argued that the shape of the scattering curve indicates scattering by flat particles, and they obtained excellent fits to their data for monodispersed discs. On the other hand, Sheu et al. [4,6,7] report excellent fits to their data for a distribution of spheres. Both Overfield et al. [8] and Sheu et al. [4] caution that there are complications. For example, a Guinier plot does not yield a straight line for data of Overfield et al. [8]. Also a well-defined ratio of surface area to volume according to a Porod analysis does not exist for the data of Sheu et al. [4,7], as shown in Fig. 6-17. Consequently, an analysis by standard techniques might be expected to lead to vastly different models for the macrostructure, because the scattering equations used in such analyses strictly hold only for monodispersed particles with sharp boundaries. In the next few paragraphs, the authors briefly describe the theory to the extent that is necessary to illustrate why such anomalies can occur, and why conflicting models can be obtained for the macrostructure.

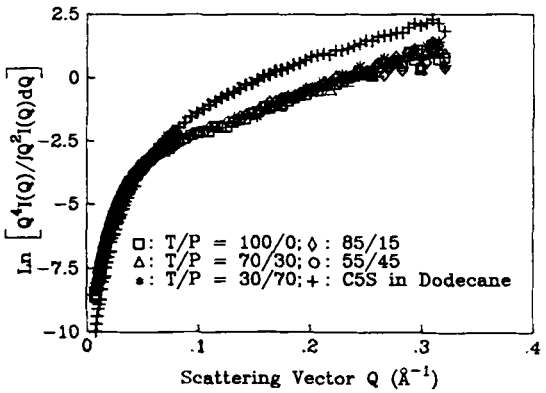

Fig. 6-17. Small-angle neutron scattering data for Ratawi asphaltenes in toluene/pyridine solutions plotted according to Porod's Equation (Eq. 6-23). *T* represents toluene, *P* represents pyridine and *C5S* represents the pentane-soluble fraction of Ratawi vacuum residue.

Theory

The scattering equations are the same for X-rays and neutron (see Feigin and Svergun [46] for a general reference for this section). As X-rays or neutrons hit the sample, they scatter due to collisions with the particles in the liquid. The intensity of this scattered radiation is measured as a function of the scattering angle, 2θ, defined with respect to the direction of the incident beam. The basic equation used to analyze the scattering intensity $I(Q)$ is:

$$I(Q) = N_p(\Delta\rho)^2 V_p^2 F_0^2(Q) \tag{6-14}$$

where Q is the scattering wave vector:

$$Q = 4\pi \sin\theta/\lambda;$$

λ is the wave length of the X-rays or neutrons; N_p is the number density of the particles; $\Delta\rho$ is the contrast between the particles and their surroundings; V_p is the volume of the particle; and $F_0(Q)$ is the normalized form factor for a particle with a particular shape, averaged over all orientations of the particle with respect to the direction defined by the incident radiation. Equation 6-14 strictly holds only for a mixture of isolated and identical particles. The rest of this subsection will be concerned with how Eg. 6-14 should be modified if the sample is polydispersed and there are interparticle interactions.

Scattering is unambiguous when the scattering center is a point. The incident X-rays or neutrons are represented by a plane wave, and the scattered X-rays or neutrons are represented by a radial wave that emanates from the scattering center. From the amplitude of the scattered wave one can extract a parameter characteristic of the scattering center, called the scattering length. The first complication arises when one replaces the point by a finite particle. Now, there are interference effects between waves scattering from different parts of the particle. If the particle is not

very dense (few scattering centers) and if the cross-sections for scattering by the centers are small, then the first-order approximation to the scattering amplitude is:

$$f(Q) = \frac{1}{4\pi} \int d^3 r \phi(r) \, e^{iQr} \tag{6-15}$$

where $f(Q)$ is the scattering amplitude, r is the distance from an arbitrary origin in the particle, and $\phi(r)$ is the scattering density distribution of the particle: it contains all the information about the structure of the particle. As Eq. 6-15 has the form of a Fourier transform, one can in principle obtain information about the structure of the particle by taking the inverse Fourier transform of the scattering amplitude as follows:

$$\phi(r) = \frac{1}{2\pi} \int d^3 Q f(Q) \, e^{-iQr}$$

In fact, however, one measures the scattering intensity:

$$I(Q) = |f(Q)|^2$$

The inverse Fourier transform of the scattering intensity gives the well known Patterson function:

$$P(r) = \int d^3 Q I(Q) \, e^{-2\pi i Qr} \tag{6-16}$$

If the scattering is weak in the sense described above, the Patterson function is the self-convolution of the scattering density, and hence it is directly related to the structure of the particle. It is important to remember that the Fourier transform in Eq. 6-16 always exists, but it can be interpreted in terms of the particle structure unambiguously, only when the point scattering centers in the particle are weak scatterers. This is the first example of how structural information can be lost due to the inability to account for interference effects properly.

The next simplest case is a fluid composed of particles of the same size and shape. The observed scattering intensity is obtained by averaging the scattering intensity for a single particle over all orientations of the particle. The intensity $I(Q)$ is:

$$I(Q) = N_p F^2(Q) \left\{ 1 - \frac{N_p}{V} \int [1 - g(r)] \frac{\sin(Qr)}{Qr} 4\pi r^2 \, dr \right\} \tag{6-17}$$

where N_p is the number of particles per unit volume; $F(Q)$ is the form factor, representing the scattering intensity from the particle due to the difference in contrast between particle and solvent; V is the volume of fluid; and $g(r)$ is the pair correlation function. The interference term in Eq. 6-17, which arises due to closeness of one particle to another, is called the structure factor:

$$S(Q) = \left\{ 1 - \frac{N_p}{V} \int_0^\infty [1 - g(r)] \frac{\sin(Qr)}{QR} 4\pi r^2 \, dr \right\} \tag{6-18}$$

and it becomes significant for wave vectors smaller than $2\pi/r_c$, where r_c is the most probable interparticle separation, because $\sin(Qr)$ begins to oscillate for $Q > 2\pi/r_c$. Therefore, for concentrated solutions when $r_c < \infty$, there will be interference effects for some values of Q.

It is customary to re-write the average scattering intensity $F(Q)$ in terms of a normalized form factor for a particular particle shape $F_0(Q)$ by factoring out the volume of the particle and the difference in contrast between the particle and solvent:

$$F(Q) = V_p(\Delta\rho)F_0(Q) \tag{6-19}$$

Substituting Eq. 6-19 into Eq. 6-17 and neglecting the interparticle interactions, one obtains Eq. 6-14. It is the basic equation of many SAXS and SANS analyses as mentioned above.

Normalized form factors have been derived for particles with simple shapes, such as spheres, rods and discs. One can compare the normalized form factor for a particular particle shape to the observed scattering intensity, and deduce the shape of the particles according to Eq. 6-14. This is the procedure followed by Ravey et al. [10]. If the sample is polydispersed, however, the Debye equation must be averaged over all particle sizes and shapes to obtain Eq. 6-20 below:

$$\langle I(Q)\rangle = \sum_{ij} \int D_j(R_j)N_p(R_j)F^2(Q, R_j)S(Q, R_j, R_i)R_j^2\,\mathrm{d}R_j \tag{6-20}$$

where $S(Q, R_i, R_j)$ is a complicated interference term analogous to the one in Eq. 6-18, and the sum in Eq. 6-20 is formally over all particles. The quantity $D_j(R_j)$ is the probability for having particles of shape j and characteristics dimensions R_j in the volume element defined by R_j and $R_j + \mathrm{d}R_j$. Equation 6-20 is a complicated average. If one assumes all the particles have the same shape, and interparticle interactions are negligible, then one obtains a simpler equation:

$$\langle I(Q)\rangle = \int D(R)V_p^2(R)\Delta\rho^2(R)F_0^2(Q, R)R^2\,\mathrm{d}R$$

At this point it can be seen that the observed scattering intensity need not have the same Q-dependence as the normalized form factor. Particles with dimension $R \sim 2\pi/Q$ contribute most to the scattering intensity, and so a different part of the distribution is highlighted for each value of Q when calculating the above integral. If the distribution function is not sharply peaked about a particular size, the product of the volume, contrast, form factor, and interference effects can be different for different size ranges, and the Q-dependence of the observed intensity (integral) need not be the same as that of the normalized form factor.

An equation with the form of Eq. 6-14 is obtained for a polydispersed system by replacing the average of the product of normalized form factor, particle volume and contrast by a product of averages:

$$\langle I(Q)\rangle = \langle N_p\rangle\langle V_p\rangle^2\langle\Delta\rho\rangle^2 F_0(Q)^2 \tag{6-21}$$

The asymptotic form of Eq. 6-21 as Q becomes large is the same as that of the normalized form factor, but information has been lost in obtaining Eq. 6-21 from Eq. 6-20. This loss of information is why fits to the data are not unique. Operationally there are shape parameters in F_0 and distribution parameters in the averages that one can independently adjust to obtain a good fit.

Sheu et al. [7] have suggested that it is possible to remove some ambiguity in Eq. 6-21 by applying a constraint to the fit, which follows naturally from the expectation that the average contrast should be independent of parameters in the assumed distribution function. That is, the basic scattering equation is:

$$\langle I \rangle = A F_0^2$$

where for a given form factor one would expect the normalization constant A to be:

$$A = \langle N_p \rangle \langle V_p \rangle^2 \langle \Delta\rho \rangle^2$$

By assuming that the particle size distribution function remains the same as concentration varies, then one requires that:

$$\alpha = \frac{A}{\langle N_p \rangle^2 \langle V_p \rangle^2} \tag{6-22}$$

remains constant. This procedure was used by Sheu et al. [4,7] and Storm et al. [19] to analyze SANS and SAXS data.

Returning now to Eq. 6-16 for the Patterson function, as mentioned above, the Patterson function is the self-convolution of the scattering density, if the scattering centers in the particles are weak scatters. In this case one can show:

$$I(Q) = \int d^3r\, P(r) \cos(Qr)$$

Averaging the scattering intensity over the solid angle in wave number space, one obtains:

$$I(Q) = 4\pi \int_0^\infty \gamma(r) \frac{\sin(Qr)}{Qr} r^2\, dr$$

where:

$$\gamma(r) = \frac{1}{4\pi} \int_0^{4\pi} P(r)\, d\Omega$$

is called the correlation function. If one assumes that the particles are isolated, identical, and compact in the sense that they have a well-defined smooth boundary, then it can be shown that for large wave numbers:

$$I(Q) \sim -8 \frac{\pi}{Q^4} \gamma'(0) \quad \text{as } Q \to \infty$$

For homogeneous particles, ρ is constant and one can calculate the Patterson function and $\gamma(r)$; then by evaluating the derivative, one obtains the Porod law:

$$I(Q) \sim 2\frac{\pi}{Q^4}\rho^2 S \quad \text{as } Q \to \infty$$

where S is the surface area of the particle. Porod also derived the invariant:

$$T = \int_0^\infty Q^2 I(Q)\,\mathrm{d}Q$$

which for homogeneous particles is:

$$T = 2\pi\rho^2 V$$

Thus, in the case of homogenous monodispersed particles, which are compact and have smooth boundaries, one would expect:

$$\lim Q^4 I(Q) \Big/ \int_0^\infty Q^2 I(Q)\,\mathrm{d}Q = \frac{S}{V} \quad \text{as } Q \to \infty \tag{6-23}$$

As mentioned above, the data of Sheu et al. [4,7] (Fig. 6-17) show that this analysis fails for Ratawi asphaltenes dispersed in toluene. This suggests that problems might be encountered when analyzing data using techniques based on isolated monodispersed particles.

Another equation that is commonly used to analyze scattering data is the Guinier equation. The Guinier equation follows quite generally from the form factors for various particle shapes, and states that in the small angle region ($QR_g < 1$):

$$I(Q) = I(0)\,\mathrm{e}^{-Q^2 R_g^2/3} \tag{6-24}$$

where R_g is the radius of gyration of the particle, and:

$$I(0) = 4\pi \int_0^D \gamma(r) r^2\,\mathrm{d}r \tag{6-25}$$

where D is the largest dimension of the particle. Normally, one plots $\ln I(Q)$ vs. Q^2 and obtains the radius of gyration from the slope. Klm and Long [18] and Dwiggins [16,17] used this method to analyze their data.

Inasmuch as Q must be small for Eq. 6-24 to be valid:

$$\frac{I(0)}{I(Q)} = 1 + \tfrac{1}{3}Q^2 R_g^2$$

and using the fact that the correlation function $\gamma(r)$ in Eq. 6-25 is the self convolution of the scattering density, one would expect:

$$I(0) = kMC$$

where M is the mass of the particle, C is the concentration and k is an instrument constant determined experimentally by making measurements with solutions of various concentrations of particles with known M; then:

$$\frac{kC}{I(0)} = \frac{1}{M}\left[1 + \tfrac{1}{3}Q^2R_g^2\right] \tag{6-26}$$

This was the equation used by Overfield et al. [8] to determine both the apparent molecular weights and radii of gyration from their SANS data.

SAXS

Dwiggins [16] showed that SAXS could be used to observe colloidal particles in crude oil. Colloidal particles had been separated from crude oil by ultracentrifugation [47,48], but one could argue that the particles were formed in the gravitational fields generated in the experiments. Thus Dwiggins' work [16] shows the presence of colloidal particles in crude oil directly. Using a Guinier analysis (Eq. 6-24), Dwiggins [16] calculated radii of gyration of particles in several crude oils in the range of 30–40 Å. An exception was Rhodes crude oil from Kansas, which had a non-linear Guinier plot, and appeared to have much larger particles. The radii of gyration for particles in Lagunillas crude oil from Venezuela did not change significantly with temperature in the range of 27–73°C, but the radii of gyration did appear to become larger when mineral oil was added to the crude oil, suggesting that the particles were beginning to aggregate. Dwiggins [16] noted that the scattering intensity could be fitted by assuming either monodispersed ellipsoidal particles, or polydispersed spherical particles. Inasmuch as the ultracentrifugation work of Ray et al. [47] suggests polydispersed spherical particles, Dwiggins favored the spherical model for the macrostructure of asphaltenes.

In 1978, Dwiggins [16] reported measurements with an instrument capable of higher precision at lower wave numbers. He obtained good Guinier plots for the Tia Juana and Santa Maria crude oils from California, but obtained non-linear behavior at small scattering angles for the Rhodes crude oil, and for the Tia Juana asphaltenes when propane or decane was added. The more intense scattering at low wave numbers causing the non-linearity in the Guinier plots could be eliminated by removing large particles from these liquids by ultracentrifugation. This result illustrates that non-linear Guinier plots can be caused by polydispersity.

Klm and Long [18] used SAXS to study atmospheric residues from Jobo and Tia Juana crude oils from California. The Guinier plots were reasonably linear and indicated radii of gyration of 25–30 Å. The radii of gyration were the same in benzene, toluene, tetrahydrofuran (THF), pyridine, decane, and when more of the non-asphaltenic fraction was added. Klm and Long [18] interpreted these results as indicating that the asphaltene particles were non-associated macromolecules.

Herzog et al. [9] studied samples of atmospheric residue from Grenada and Pematang crude oils, and a vacuum residue from Safaniya crude oil using synchrotron X-rays from the storage ring at the L.U.R.E. facility of the Université d'Orsay in Paris, France. The accessible wave vector range was 0.0075–0.15 $Å^{-1}$. They fit the

scattering intensity $I(Q)$ with the function $1/Q^{\alpha}$, and found α to be 1.69 for Pematang and Safaniya and 1.59 for Grenada crude oil. Inasmuch as the scattering intensity for thin discs falls as $(1/Q)^2$, they fit the observed scattering intensities using a power law distribution of discs 3.4 Å-thick and with radii distributed in the range of 13–800 Å. The authors also calculated the correlation function $\gamma(r)$ and its companion $r^2\gamma(r)$, and compared them to those predicted by their model. The model correlation functions have the right shape, but not the correct magnitude indicating some problem with the fit. Herzog et al. [9] also noted that the data could be fit with a fractal-type model in which the particles resemble the unit sheets of Yen [27].

Storm et al. [19] reported SAXS results for several vacuum residues and samples of synthetic vacuum residue prepared by dispersing a particular vacuum residue in its corresponding non-asphaltenic fraction. Inasmuch as all this work, including the rheology discussed above, indicates that the asphaltenes are polydispersed, the measured scattering intensities were analyzed according to Sheu et al. [45]. The best fit was obtained with a Schultz distribution of spherical particles, shown in Fig. 6-18 for the case of Ratawi vacuum residue. The Schultz distribution has the form:

$$D(R) = [(z+1)/R_a]^{z+1} R^z \, e^{-(z+1)R/R_a} / \Gamma(z+1) \tag{6-27}$$

where R_a is the average radius, $\Gamma(z+1)$ is a gamma function, and z is a width parameter related to the polydispersity as follows:

$$\text{Polydispersity} = \sqrt{\langle R^2 \rangle - \langle R_a^2 \rangle}/R_a = 1/\sqrt{z+1}$$

This distribution function is shown in Fig. 6-19 for the case of Ratawi vacuum residue. The observed scattering intensities could be fit with other models, monodispersed cylinders for example, but the factor α in Eq. 6-22 depended on asphaltene

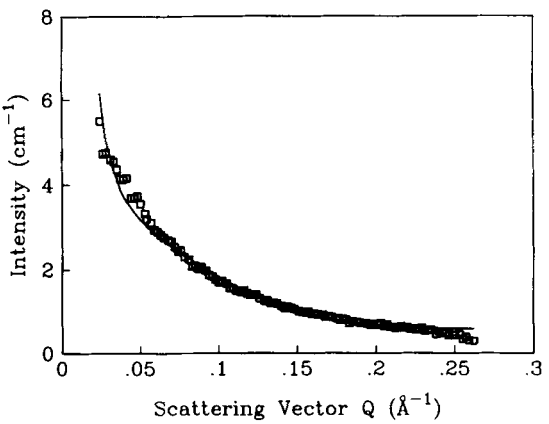

Fig. 6-18. Small-angle X-ray scattering data for Ratawi asphaltenes in vacuum residue at 93°C. The square symbols indicate experimental data and the solid curve is a fit for a system of polydispersed spheres.

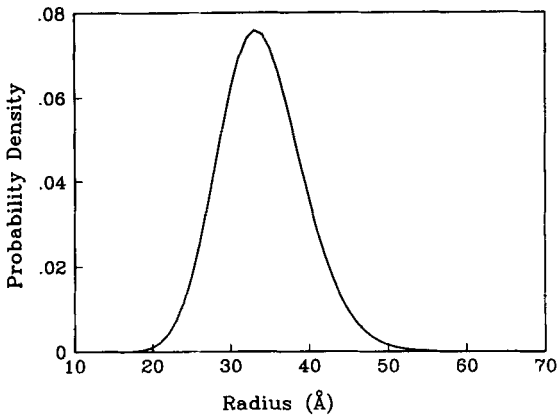

Fig. 6-19. Small-angle X-ray scattering data for Ratawi asphaltenes in vacuum residue at 93°C. Radii of spherical colloidal particles are distributed according to the Schultz distribution (Eq. 6-27).

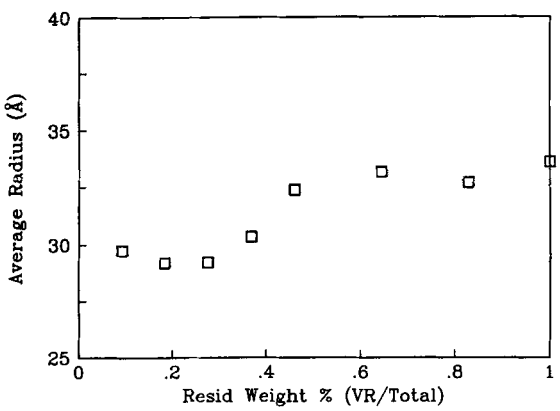

Fig. 6-20. The average radii of Ratawi colloidal particles at 93°C according to small-angle X-ray scattering data. The concentration of asphaltenes in Ratawi vacuum residue is 21.6 wt%.

concentration in these cases. The average radii for Ratawi asphaltenes in these samples are shown in Fig. 6-20. The scale for the ordinate is the fraction of vacuum residue in the mixture. The asphaltene concentration (w/w) can be obtained by multiplying by 0.21. On the whole, the average radius does not change much with concentration. There does seem to be a small decrease in radius for the more dilute samples. The distribution functions shown in Fig. 6-21 suggest that this occurs because the larger particles in the vacuum residue have dissolved, or de-aggregated at low concentrations. The average radii for asphaltenic particles in other vacuum residues are shown in Fig. 6-22. These values agree very well with the radii of gyration reported by Dwiggins [16,17] and Klm and Long [18]. One might worry about the neglected interparticle interactions in the analysis due to Sheu et al. [45]. As discussed above, these interference effects decrease the intensity for the smallest wave

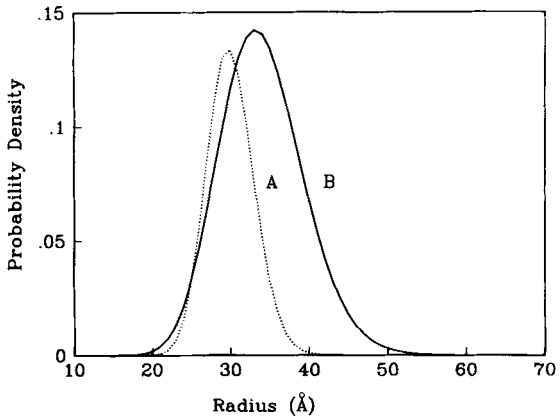

Fig. 6-21. Distribution of radii of Ratawi asphaltenes at 93°C according to small-angle X-ray scattering data. Curve *A* is for a sample containing 2.2 wt% asphaltenes, curve *B* is for Ratawi vacuum residue.

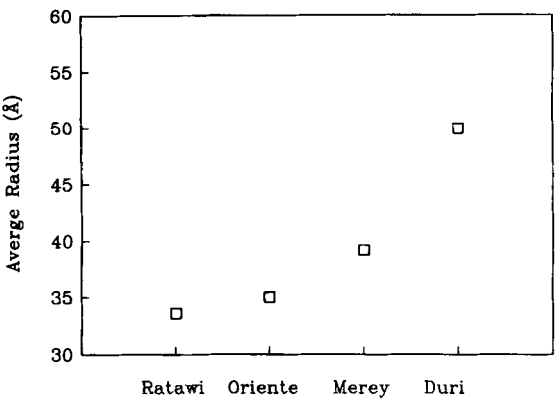

Fig. 6-22. The average radii for asphaltenic colloidal particles in various vacuum residues at 93°C.

vectors (see Fig. 6-18), but this portion of the curve is not critical in determining the parameters of the fit.

SANS

Ravey et al. [10] studied asphaltenes from Safanya crude oil in THF, benzene and pyridine by SANS using the Pace spectrometer at the Leon Brilloin Laboratory in Saclay, France. Wave vectors were in the range of 0.005–0.5 $Å^{-1}$. In order to minimize the effects due to polydispersity, solutions of the asphaltenes were fractionated by GPC before analysis. Ravey et al. [10] noted that the measured scattering intensities decreased as $1/Q^2$. The authors pointed out that this Q-dependence is characteristic of scattering by discs, and, therefore, fit the measured intensities by monodispersed discs with diameters in the range of 130–850 Å for

the various asphaltenic fractions. The discs are approximately 3.4 Å thick, and this dimension appears constant for all the fractions in all the solvents. These authors also noted that the scattering intensity could be fit by flattened spheroids. The large dimension in this case was in the range of 80–190 Å, depending on the fraction, and the minor dimension was again constant in all the studies. The large dimension of either discs or spheroids becomes larger in more concentrated THF solutions; and for a given concentration, this dimension is larger in benzene than in pyridine. These results suggest association or aggregation, but it is curious that the small dimension is apparently the same in all these samples.

Ravey et al.'s [10] arguments are persuasive. As discussed above, one would expect the asymptotic dependence of the scattering intensity according to Eq. 6-14 or Eq. 6-21 to be that of the normalized form factor. As discussed above, however, this correspondence is not unique. The Q-dependence of the observed intensity need not be that of the normalized form factor if the distribution function is not sharp and if the particles are not homogeneous. Although Ravey et al. [10] fractionated the asphaltenes according to GPC, the GPC curves for the fractionated samples were almost as broad as the one for the non-fractionated sample; thus, it is possible that the effects due to polydispersity were not completely eliminated in this work.

Overfield et al. [10] studied asphaltenes in toluene over the temperature range of 25–250°C using a cell fabricated in a manner that allowed the asphaltene/toluene mixture to be at the vapor pressure corresponding to the temperature. The experiments were preformed at the National Bureau of Standards using neutrons with a wave length of 7 Å. The scattered neutrons were captured by a two-dimensional array detector for wave vectors in the range of 0.005–0.15 $Å^{-1}$. The authors declined to propose a definite model for the macrostructure due to complications associated with polydispersity, interparticle interference effects, possible particle orientation effects, and a possible multi-phase mixture. The Guinier plots were not linear. As discussed above this may be due to polydispersity. Using Eq. 6-25 they extrapolated $1/I(Q)$ to $Q = 0$, and obtained both the average molecular weight and radius of gyration. By comparing the molecular weight/radius of gyration relationships for model spheres, rods, and random coils of polystyrene, according to Eq. 6-25, the authors concluded that the particles had an elongated shape. Additional support for this conclusion was provided by a Porod plot indicating rod-like particles. As the temperature was increased from 25° to 250°C, the radius of gyration and the apparent molecular weight decreased significantly, indicating a disaggregation of the particles. The molecular weight at 250°C was 6000 and the radius of gyration was 53 Å.

Sheu et al. [4,7] reported SANS results for the Ratawi asphaltenes in toluene and toluene/pyridine mixtures using the Intense Pulsed Neutron Source at Argonne National Laboratory. Wave vectors were in the range of 0.007–0.35 $Å^{-1}$. The effect of polydispersity was taken into account as discussed above, and again good fits were obtained for a Schultz distribution of spheres. The average radii for the Ratawi asphaltenes in the various mixtures are given in Table 6-5. The average radii are independent of concentration, and do not depend on the amount of pyridine in the

TABLE 6-5

Average radius and percent polydispersity for Ratawi asphaltenes according to SANS analysis

Concentration (wt%)	Toluene/pyridine	Radius (Å)	Polydispersity (%)
8	100/0	32.4	17.6
8	85/15	31.3	19.2
8	70/30	30.4	20.4
8	55/45	30.8	20.5
8	30/70	30.1	21.7
4	80/20	30.8	18.6
4	60/40	31.6	19.7
4	40/60	31.1	20.4
4	20/80	30.7	21.3
2	80/20	31.6	19.0
2	60/40	31.8	19.4
2	40/60	31.3	19.6
2	20/80	30.8	20.2
1	80/20	31.6	19.7
1	60/40	31.5	19.0
1	40/60	32.0	19.7
1	20/80	31.0	19.0

toluene/pyridine mixtures. It is interesting that the average radius for these particles is about the same in vacuum residue according to SAXS. Also the average radius agrees with the radii of gyration reported by Dwiggins [16,17] and Klm and Long [18]. Sheu et al. [4] also reported a plot of

$$\lim Q^4 I(Q) \Big/ \int_0^\infty Q^2 I(Q)\, \mathrm{d}Q \quad \text{as } Q \sim \infty$$

which according to Eq. 6-23 should be the ratio of the particle's surface area to volume. As shown in Fig. 6-17, the ratio in Eq. 6-23 does not have a limit in this range of Q-values. This suggests that the particle boundary is diffuse, as it would be if solvation effects were significant.

In summary, both SAXS and SANS measurements indicate the presence of particles, in the colloidal size range, in crude oil, residuum, and asphaltenes in various solvents. These liquids are complex and it appears that the shape of these particles cannot be determined unambiguously by common techniques of analysis. The particles could be flat discs or spheres. Both models make chemical sense based on current understanding of the microstructure of asphaltenes. The fitting procedure suggested by Sheu et al. [45] provides a constraint on the fit that follows in a natural manner from the scattering equations. By following this procedure, Ratawi asphaltenes are found to be spheres with a distribution of sizes in both toluene and vacuum residue. This result is consistent with the rheological results of Sheu et al. [5,6] and Storm et al. [19,21]. Also, the average radii obtained by

this procedure are consistent with the radii of gyration reported earlier by Dwiggins [16,17] and Klm and Long [18]. It appears in several studies that asphaltenes aggregate in some solvents such mineral oil, propane, decane, benzene, toluene, and possibly THF. This aggregation increases polydispersity. Guinier plots appear to become non-linear when this occurs.

ACKNOWLEDGEMENTS

The authors would like to thank Intense Pulsed Neutron Source (IPNS) of Argonne National Laboratory for granting small-angle neutron beam time. In particular, they would like to thank D.P. Thiyagarajan and Mr. D. Wozniak for helpful assistance. IPNS is operated under the auspices of the U.S. Department of Energy, BES–Materials Sciences, under contract number W-31-109-ENG-38, to whom thanks are extended for the use of their facilities. The authors would also like to thank the Solid State Division of Oak Ridge National Laboratory for granting small-angle X-ray beam time, and Dr. J.S. Lin for assistance during the measurements. The SAXS experiments performed at Oak Ridge National Laboratory are partially supported by the Division of Materials Sciences, U.S. Department of Energy under contract number DE-AC05-84OR21400, with Martin Marietta Energy Systems, Incorporated.

REFERENCES

[1] Long, R.B., The concept of asphaltenes. In: J.W. Bunger and C. Norman (Editors), *Chemistry of Asphaltenes. Adv. Chem. Ser.*, 195: 17–27 (1981).
[2] Speight, J.G. and Moschopedis, S.E., On the molecular nature of petroleum asphaltenes. In: J.W. Bunger and N.C. Li (Editors), *Chemistry of Asphaltenes. Adv. Chem. Ser.*, 195: 1–15 (1981).
[3] Yen, T.F., Structural differences between asphaltenes isolated from petroleum and from coal liquid. In: J.W. Bunger and N.C. Li (Editors), *Chemistry of Asphaltenes. Adv. Chem. Ser.*, 195: 39–51 (1981).
[4] Sheu, E.Y., Storm, D.A. and DeTar, M.M., Asphaltenes in polar solvents. *J. Non-Cryst. Solids*, 131–133: 341–347 (1991).
[5] Sheu, E.Y., DeTar, M.M. and Storm, D.A., Rheological properties of vacuum residue fractions in organic solvents. *Fuel*, 70: 1151–1156 (1991).
[6] Sheu, E.Y., DeTar, M.M. and Storm, D.A., Structure, interaction and phase transition of vacuum residue in apolar solvents. *Fuel Sci. Tech. Int.*, 10: 607–647 (1992).
[7] Sheu, E.Y., DeTar, M.M. and Storm, D.A., Solution properties of colloids formed by petroleum vacuum residue. *Macromol. Rep.*, A28: 159–175 (1991).
[8] Overfield, R.E., Sheu, E.Y., Simha, S.K. and Liang, K.S., SANS study of asphaltene aggregation. *Fuel Sci. Tech. Int.*, 7: 611–624 (1989).
[9] Herzog, P., Tchoubar, D. and Espinat, D., Macrostructure of asphaltene dispersions by small-angle X-ray scattering. *Fuel*, 67: 245–250 (1988).
[10] Ravey, J.C., Ducouret, G. and Espinat, D., Asphaltene macrostructure by small-angle neutron scattering. *Fuel*, 67: 1560–1567 (1988).
[11] Kyriacou, K.C., Baltus, R.E. and Rahimi, P., Characterization of oil residual fractions using intrinsic viscosity measurements. *Fuel*, 67: 109–113 (1988).
[12] Rao, B.M.L. and Serrano, J.E., Viscometric study of aggregation interactions in heavy oil. *Fuel Sci. Tech. Int.*, 4: 483–500 (1986).

[13] Sakai, M., Sasaki, K. and Inagaki, M., Hydrodynamic studies of dilute pitch solutions: The shape and size of pitch molecules. *Carbon*, 21: 593–596 (1983).
[14] Altgelt, K.H. and Harle, O.L., The effect of asphaltenes on asphalt viscosity. *Ind. Eng. Chem. Prod. Res. Dev.*, 14: 240–246 (1975).
[15] Mack, C., Colloid chemistry of asphalts. *J. Phys. Chem.*, 36: 2901–2914 (1932).
[16] Dwiggins, C.W., Jr., Study of the colloidal nature of petroleum with an automated Bonse–Hart X-ray small-angle scattering unit. *J. Appl. Crystallogr.*, 11: 615–619 (1978).
[17] Dwiggins C.W., Jr., A small angle X-ray scattering study of the colloidal nature of petroleum. *J. Phys. Chem.*, 69: 3500–3506 (1965).
[18] Klm, Hyo-gun and Long, R.B., Characterization of heavy residuum by small-angle X-ray scattering technique. *Ind. Eng. Chem. Fundam.*, 18: 60–63 (1977).
[19] Storm, D.A., Sheu, E.Y., Barresi, R.J. and DeTar, M.M., Colloidal properties of asphaltenes in vacuum residue. In: *International Symposium on the Chemistry of Bitumens, June 5–8, 1991, Rome*, Vol. II, pp. 813–841.
[20] Pollack, S.S. and Yen, T.F., Structural studies of asphaltics by X-Ray small-angle scattering. *Anal. Chem.*, 42: 623–629 (1970).
[21] Storm, D.A., Barresi, R.J. and DeCanio, S.J., Colloidal nature of vacuum residue. *Fuel*, 70: 779–782 (1991).
[22] Pfeiffer, J.Ph. and Saal, R.N.J., Asphaltic bitumen as colloid system. *J. Phys. Colloid Chem.*, 44: 139–148 (1940).
[23] Dickie, J.P. and Yen, T.F., Macrostructures of the asphaltic fractions by various instrumental methods. *Anal. Chem.*, 39: 1847–1852 (1967).
[24] Speight, J.G., Wernick, D.L., Gould, K.A., Overfield, R.E., Rao B.M.L. and Savage, D.W., Molecular weight and association of asphaltenes: A critical review. *Rev. Inst. Fr. Pét.*, 40: 51–62 (1985).
[25] Storm, D.A., DeCanio, S.J. and DeTar, M.M., Upper bound on number average molecular weight of asphaltenes. *Fuel*, 69: 735–738 (1990).
[26] DeCanio, S.J., Nero, V.P., DeTar, M.M. and Storm, D.A., Determination of the molecular weights of Ratawi vacuum residue fractions — A comparison of mass spectrometric and vapor phase osmometry techniques. *Fuel*, 69: 1233–1236 (1990).
[27] Yen, T.F., Erdman, J.G. and Pollack, S.S., Investigation of the structure of petroleum asphaltene by X-ray diffraction. *Anal. Chem.*, 33: 1587–1594 (1961).
[28] Boduszynski, M.M., Composition of heavy petroleums, 1. Molecular weight, hydrogen deficiency, and heteroatom concentration as a function of atmospheric equivalent boiling point up to 1400°F. *Energy Fuels*, 1: 2–11 (1987).
[29] Boduszynski, M.M., Composition of heavy petroleums, 2. Molecular characterization. *Energy Fuels*, 2: 597–613 (1988).
[30] Reerink, H., Size and shape of asphaltene particles in relationship to high-temperature viscosity. *Ind. Eng. Chem. Prod. Res. Dev.*, 12: 82–88 (1973).
[31] Boduszynski, M.M., Limitations of average structure determination for heavy ends in fossil fuels. *Liq. Fuels Technol.*, 2: 211–232 (1984).
[32] Moschopedis, S.E., Fryer, J.F. and Speight, J.G., Investigation of asphaltene molecular weights. *Fuel*, 55: 227–232 (1976).
[33] Steedman, W., Holder, K. and Mackenzie, J., Low temperature thermolysis of heavy oil and residues. In: *International Symposium on the Chemistry of Bitumens, June 5–8, 1991, Rome*, Vol. I, pp. 408–417.
[34] Einstein, A., Berichtigung Zu Meiner Arbeit: Eine Neue Bestimmung Der Molekul-Dimensionen. *Ann. Phys.*, 34: 591–592 (1906).
[35] Frisch, H.L. and Simha, R., The viscosity of colloidal suspensions and macromolecular solutions. In: F.R. Eirich (Editor), *Rheology, Vol. 1.* Academic Press, New York, N.Y., pp. 525–613 (1956).
[36] Russel, W.B. and Gast, A.P., Nonequilbrium statistical mechanics of concentrated colloidal dispersions: Hard spheres in weak flows. *J. Chem. Phys.*, 84 (1986).
[37] Russel, W.B. The rheology of suspensions of charged rigid spheres. *J. Fluid Mech.*, 85: 209–232 (1978).

[38] Batchelor, G.K., The effect of brownian motion on the bulk stress in a suspension of spherical particles. *J. Fluid Mech.*, 83: 97–117 (1977).
[39] Roscoe, R., The viscosity of suspensions of rigid spheres. *Br. J. App. Phys.*, 3: 267–269 (1952).
[40] Pal, R. and Rhodes, E., Viscosity/concentration relationships for emulsions. J. *Rheol.*, 33: 1021–1045 (1989).
[41] Eilers, H., Die Viskositat von Emulsionen Hochviskoser Stoffe als Funktion der Konzentration. *Kolloid-Zeitschrift*, 97: 313–321 (1941).
[42] Campbell, G.A. and Forgacs, G., Viscosity of concentrated suspensions: An approach based on percolation theory. *Phys. Rev. A*, 41: 4570–4573 (1990).
[43] Grimson, M.J. and Barker, G.C., Interaction corrections to the viscosity of concentrated colloidal dispersions. *Europhys. Lett.*, 3: 511–517 (1987).
[44] Majolino, D., Mallamace, F. and Micali, N., Viscosity measurements in dense microemulsions, evidence of aggregation process. *Solid State Commun.*, 74: 465–468 (1990).
[45] Sheu, E.Y., Liang, K.S., Sishal, S.K. and Overfield, R.E., Particle size distribution of a non-interacting dispersed system studied by small-angle scattering. *J. Colloid Interface Sci.*, 153: 399–410 (1992).
[46] Feigin, L.A. and Svergun, D.I., *Structure Analysis by Small- Angle X-Ray and Neutron Scattering*. Plenum Press, New York, N.Y., 335 pp. (1987).
[47] Ray, B.R., Witherspoon, P.A. and Grim, R.E., A study of the colloidal characteristics of petroleum using the ultracentrifuge. *J. Phys. Chem.*, 61: 1296–1302 (1957).
[48] Lorentz, P.B., Bolen, R.J. and Dunning, H.N., Ultracentrifugation and viscosities of crude oils. *J. Colloid Sci.*, 16: 493–496 (1961).

This page intentionally left blank

Asphaltenes and Asphalts, 1. Developments in Petroleum Science, 40
edited by T.F. Yen and G.V. Chilingarian

Chapter 7

STRUCTURAL PARAMETERS FROM ASPHALTENES AND THEIR GEOCHEMICAL SIGNIFICANCE

TEH FU YEN and GEORGE V. CHILINGARIAN

INTRODUCTORY REMARKS

Using physicochemical analytical techniques to define the chemical structures of native asphaltenes and porphyrins from a small but diverse group of petroleums, Yen and co-workers [1–6] showed marked differences in structural characteristics. Further examination of the observed differences suggest that these parameters may reflect the effects of geologic time on the composition of these complex petroleum constituents and thereby indicate how such components change throughout the natural lifetime of a petroleum in situ.

Petroleum asphaltenes and porphyrins are not produced by biological systems [7]; and are assumed to have formed as a result of natural transformations. Evidence of changes in asphaltene composition during geologic time was cited by Bestougeff [8] and a mechanism of asphaltene formation, which is a by-product of petroleum evolution, has been proposed [9].

Because complete production data (such as individual well identification, precise production depth, and specific horizons or sections of formation contributing to production) was not available for many of the samples analyzed, the following interpretations on the influence of time and burial depth on chemical structures are not as conclusive. Instead, the available data show only a general trend of changes. The crude oils represented in this chapter do not constitute an adequate sampling of the wide range of depths and geologic ages that petroleum reservoirs are known to cover. One of the greatest shortcomings of this study is the near absence of data for oil samples. In spite of these limitations, the observed relations exhibit significant trends, which should encourage a more elaborate future program of analyses of a more representative suite of samples.

Details of the preparation procedures for isolating the asphaltene and porphyrin fractions are described elsewhere [10,11]. A list of the petroleums included in this study, together with available geologic data, are presented in Table 7-1.

An attempt was made to correlate several structural parameters of native asphaltenes and their associated porphyrins to the age of enclosing sediments. The geochemical significance of geologic age is based on the recognition that petroleum composition undergoes gradual but continuous change with time [12]. Such transformations are dependent on the relative stabilities of chemical components of petroleum, with transformation rates being generally related positively to temperature. Geologic age is, therefore, an indication of the length of time during which

TABLE 7-1

Geologic ages and depths of burial of petroleum-producing horizons

Crude	Formation	Age	Average producing depth (ft)
Agha Jari	Asmari	Lower Miocene	7500
Athabasca	McMurray	Lower Cretaceous	100
Bachaquero	–	Miocene–Eocene	–
Baxterville	L. Tuscaloosa	Middle Cretaceous	8740
N. Belridge	Tulare and Etchegoin	Pleistocene–Pliocene	730
Boscan	Boscan and B. Icotea	Eocene–Lower Oligocene	7300
Burgan	Burgan Sands	Middle Cretaceous	4100
Gilsonite	Green River	Lower Eocene	–
Lagunillas	Lagunillas	Oligocene–Miocene	–
Mara	Capacho and Apon	Middle Cretaceous	2500
Melones	Oficina	Upper Oligocene	–
Ragusa	Taormina	Upper Triassic	6000
Raudhatain	Mauddud	Middle Cretaceous	3250
Rozel Point	–	Recent	–
Santiago	Leutholtz	Upper Miocene	2570
Wafra A-1	Ratawi	Lower Cretaceous	–
Wafra 17	First Sand (Burgan)	Middle Cretaceous	–
West Texas (South Ward)	Yates and Seven River	Silurian	2325
Wilmington	–	Miocene	4225

transformations can occur. In as much as older sediments generally occur at greater depths and temperature gradients of the earth's crust are universally positive, older sediments are typically exposed to higher temperatures than are younger sediments. Because sedimentation rates were not uniform everywhere, burial depths may, in some instances, exercise a greater influence than the time factor on transformation rates. Thus, wherever possible, relations of structural parameter to burial depths are considered in this study.

TRANSFORMATION OF PORPHYRINS WITH TIME

Chlorophyll and hemin pigments are considered to be the precursors of the vanadyl and nickel chelates of porphyrins found in a variety of sediments. The predominant precursor in sediments is chlorophyll, i.e., chlorophyll *a*, *b* or *Chlorobium* chlorophyll and bacteriochlorophyll. All chlorophylls belong to the reduced form of porphyrins, the chlorophyll *a*, *b* or *Chlorobium* chlorophyll being chlorin type (dihydroporphyrin) and the bacteriochlorophyll being tetrahydroporphyrin type. As shown in Fig. 7-1a, usually in the case of chlorophyll (I) demetallation will result in pheophytin (II), with subsequent hydrolysis of the ester to form pheophorbide (III). The pheophorbide subsequently undergoes oxidation of the chlorin hydrogens and saturation of vinyl hydrogens to form the pheoporphyrin (IV). The pheoporphyrin is then decarboxylated at the cyclopentane ring to result in phylloerythrin

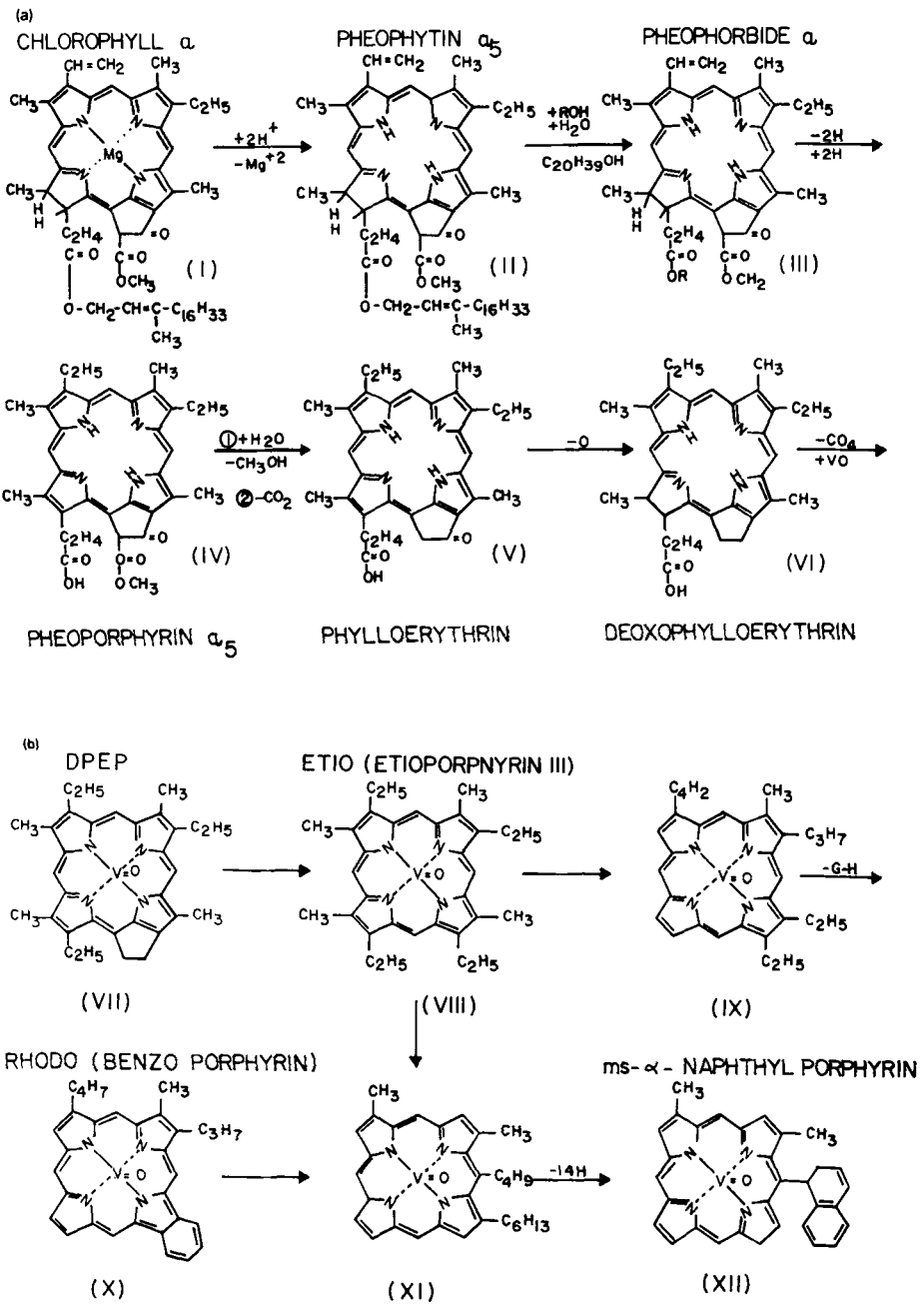

Fig. 7-1. Proposed geochemical transformation of chlorophyll to vanadyl DPEP and other stable vanadyl chelates. (a) Chlorophyll to dexophylloerythrin. (b) DPEP to ms-α-naphthyl porphyrin.

(V). The phylloerythrin is reduced upon removal of the carbonyl function at the cyclopentane to form deoxyphylloerythrine (VI). Finally, the latter is decarboxylated to deoxyphylloerythroetioporphyrin (DPEP) (VII) (Fig. 7-1b).

The above mechanism had been suggested by Treibs [13] and is borne out by the present results. It was found that in the recent sediments the major pigments are the chlorins, together with a number of the DPEP intermediates which bear the oxygen functional groups.

Conversion of the phylloporphyrins DPEP (VII) into the etioporphyrins (VIII) must involve a diagenetic process during which the strain of the fused cyclopentane ring has been released. The broadening of the bandwidth of porphyrin homologs is an indication of the scrambling owing to transalkylation (IX or XI). It is not too unusual for old petroleum to contain long-chain alkyl groups at the aromatic nuclei [14].

Highly aromatic porphyrins, such as benzoporphyrin (X) or meso-α-naphthylporphyrin (XII), which exist in the ancient sediments are probably due to thermodynamic processes. The binding and stabilization caused by the π-system of the host sites are known [15]. Vanadyl porphyrins are found to be highly associated with other π-systems in the organic portion of the minerals [16,17]. The studies of vanadium by ESR indicate that the charge-transfer is an essential feature. Nitrogen superhyperfine structures are quite normal for vanadium complexes in their native state [18].

It can be safely stated that the major portion of the vanadium exists as porphyrin types of chelates during the transformation of molecules in sediments. Other types of vanadium complexes do exist in certain sediments, especially at the early stages of diagenesis. The square planar tetradentates of mixed donor atoms [19–21] still represent a deviation from the 4-nitrogen ligand of porphyrin, because in the former case the nitrogen atoms are displaced by either sulfur or oxygen atoms [21].

The mechanism as outlined in Fig. 7-1a and b essentially offers a plausible explanation why vanadium often associates with the heavy end fraction of petroleum. Chlorin form (I, II, III) is only a partially-aromatized system; the phylloporphyrin form (IV, V, VI, VII) is an extended conjugated system; the etioporphyrin form (VII, IX, XI) is a fully 18 π-electron diazoannulene system; and the aromatic porphyrin (X, XII) is an excessive π–π system. The force exhibited by the π–π association explains the affinity of the porphyrins (π-system) to heavy residues (π-system). Increasing association is anticipated with the increment of time.

Vanadyl porphyrins are stable molecules which survive during geologic time. This is the reason why porphyrins can be used as a geochemical biomarker in geochemistry. Thus, the statement that vanadyl porphyrins are likely to be found in meteorites or other extraterrestrial sources is plausible [22].

Biochemically, vanadium plays an important role in lipid and choline metabolism [23,24]. A possible link between vanadium and cholesterol in the inhibition bioprocess may involve the binding between the oxygen donor atoms in mevalonic acid and vanadium. Other metabolic processes such as choline deficiency may involve the chelation of the sulfur and nitrogen donor atoms in methionine and vanadium. In as much as lipid is the precursor of petroleum [9], vanadium present in these minerals definitely can find use as a geochemical indicator.

Σ DPEP/Σ etio SERIES RATIO

The Σ DPEP/Σ etio ratio is the ratio of the total intensity of all the peaks in the mass spectrum of the deoxophylloerythroetioporphyrin series (DPEP) to the total intensity of all the mass peaks in the alkylporphyrin (etio) series [10]. The major portion of the petroporphyrins in asphaltene fractions consists of two homologous series of porphyrins as observed by using low-voltage (12 eV, 260° direct solid probe insertion) mass spectrometry. The DPEP series corresponds to a molecular weight of $308 + 14n$ or in a more general form $[(401 + 14n) - 65]$; whereas the etio series corresponds to a molecular weight of $310 + 14n$ or $[(375 + 14n) - 65]$ where n, an integer from 0 to n, represents the total number of saturated carbons. The values 375 and 401 are the molecular weights of the parent skeletons of etio and DPEP, respectively, and the value 65 corresponds to the elimination of VO and addition of 2H to the structure. The petroporphyrin can be examined either as a free-base demetallized product or by direct analysis of the total fraction with a high-resolution, high-mass spectrometer:

$$\frac{\sum \text{DPEP}}{\sum \text{etio}} = \frac{\sum_{x}^{x+14n} I_{\text{DPEP}}}{\sum_{x}^{x+14n} I_{\text{etio}}}$$

where x = molecular weight of nucleus, and I = intensity.

Relations of Σ DPEP/Σ etio ratio to age and to depth of burial are shown in Figs. 7-2 and 7-3, respectively. In these graphs, the series ratio (plotted on a logarithmic scale) decreases with age or burial depth. This trend supports the concept that DPEP is a precursor of the etio molecule. As discussed before, chlorophyll *a* and the related natural homologues (DPEP structures) are generally considered to be the source of petroporphyrins (etio structures). The concept of chemical stability enters here also: the cycloalkane ring on the porphin nucleus of DPEP imposes a strain on the molecule. Thus DPEP is less stable than the etio molecule.

Since the earlier investigation of Yen et al. [25,26] in 1968 and 1969 concerning the DPEP and etio series, many investigators subsequently have used the relative proportions of DPEP and etio series in either oil or sediments as thermal maturity indicators. To cite a few examples, the application in petroleum generation correlation in organic geochemistry is overwhelming [27–34]. Even the porphyrin maturity parameter (PMP), defined as:

$$\text{PMP} = C_{28}\,\text{etio}/(C_{28}\,\text{etio} + C_{32}\,\text{DPEP})$$

is based on this principle by Sundararaman [35]. Kinetically speaking, regardless of whether the relative abundances of DPEP and etio are the result of consecutive or parallel reaction, the apparent empirical correlation is real [36].

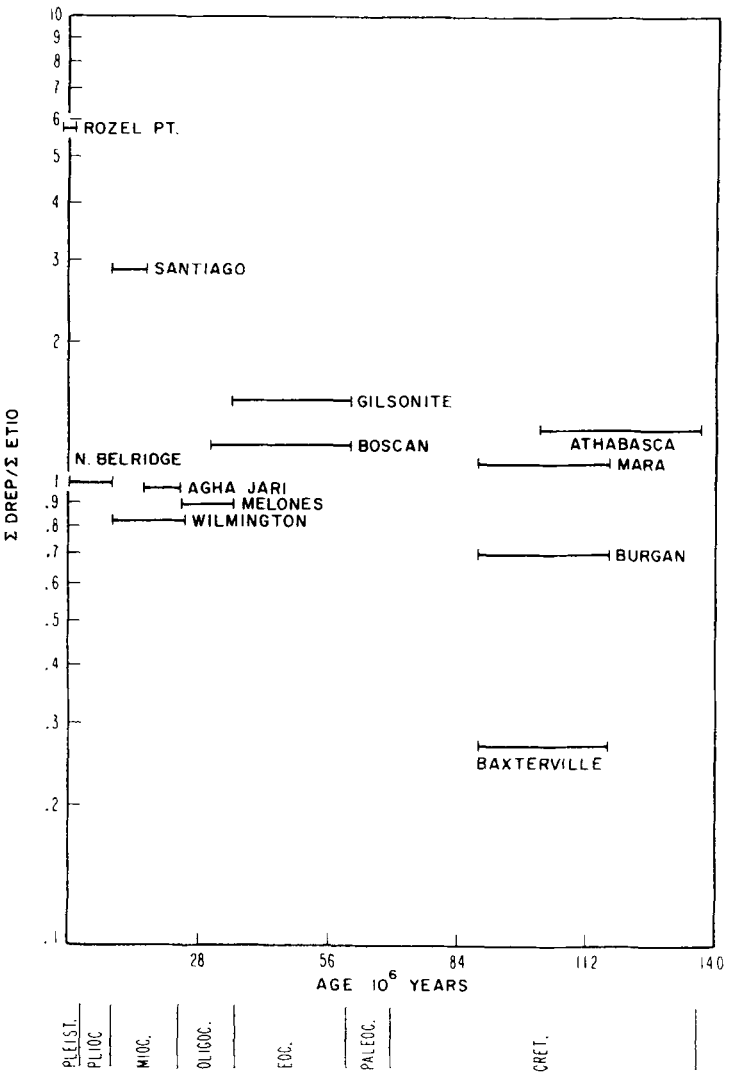

Fig. 7-2. Σ DPEP/Σ etio ratio vs. age.

BAND WIDTH OF PETROPORPHYRINS (σ)

Like the Σ DPEP/Σ etio series ratio, the band width parameter also can be obtained from mass spectrometric data for the asphaltene fraction. This parameter is given as the standard deviation (σ) in mass units, computed by the formula:

$$\sigma = \left[\left(\sum_{x}^{x+14n} IM^2 \Big/ \sum_{x}^{x+14n} I \right) - \left(\sum_{x}^{x+14n} IM \Big/ \sum_{x}^{x+14n} I \right)^2 \right]^{1/2}$$

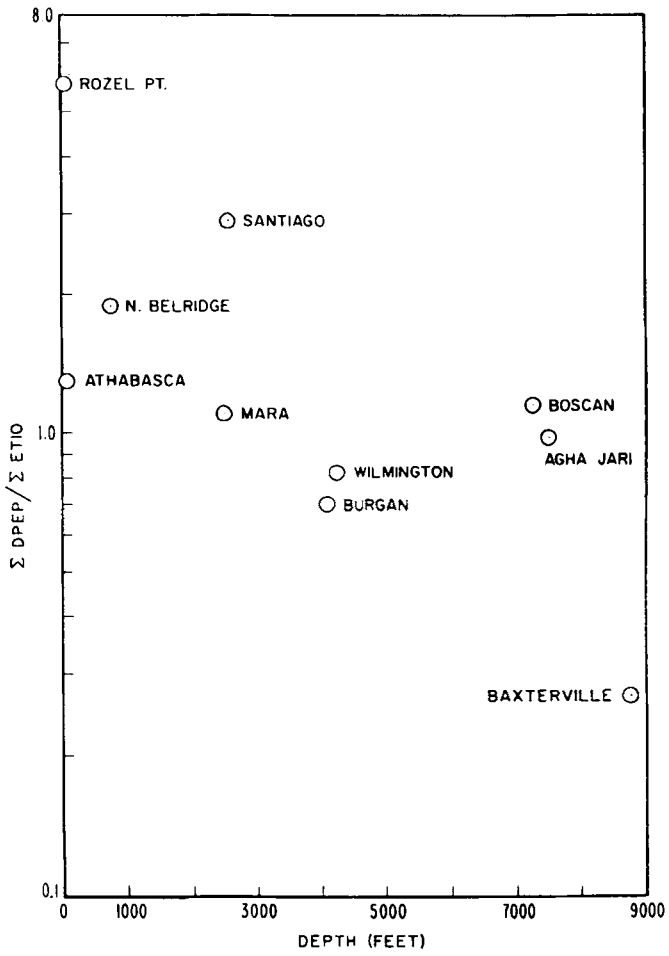

Fig. 7-3. Σ DPEP/Σ etio ratio vs. depth.

where I is the intensity, M is the mass, and x is the molecular weight of the nucleus. Statistically, 2σ is the mass range below and above the mean mass encompassing ca. 95% of all the isomeric porphyrins. Hence, for each distribution there is a σ, i.e., σ_{etio} and σ_{DPEP} [10]. Examples of etio and DPEP bands are illustrated in Fig. 7-4.

The σ parameter denotes the number of saturated substituents on the porphin nucleus — the greater the bandwidth, the greater the number of substituents and vice-versa. It may be regarded as a measure of porphyrin transformation because both DPEP and etioporphyrin molecules have substituents on more than 50% of the possible substitution sites of the porphin nucleus. Maturation reactions should produce a larger variety of homologous products containing both more and less substituents than the pre-transformation molecule. This tendency for diversification is indicated by laboratory studies [26] in which thermal treatment induces rearrange-

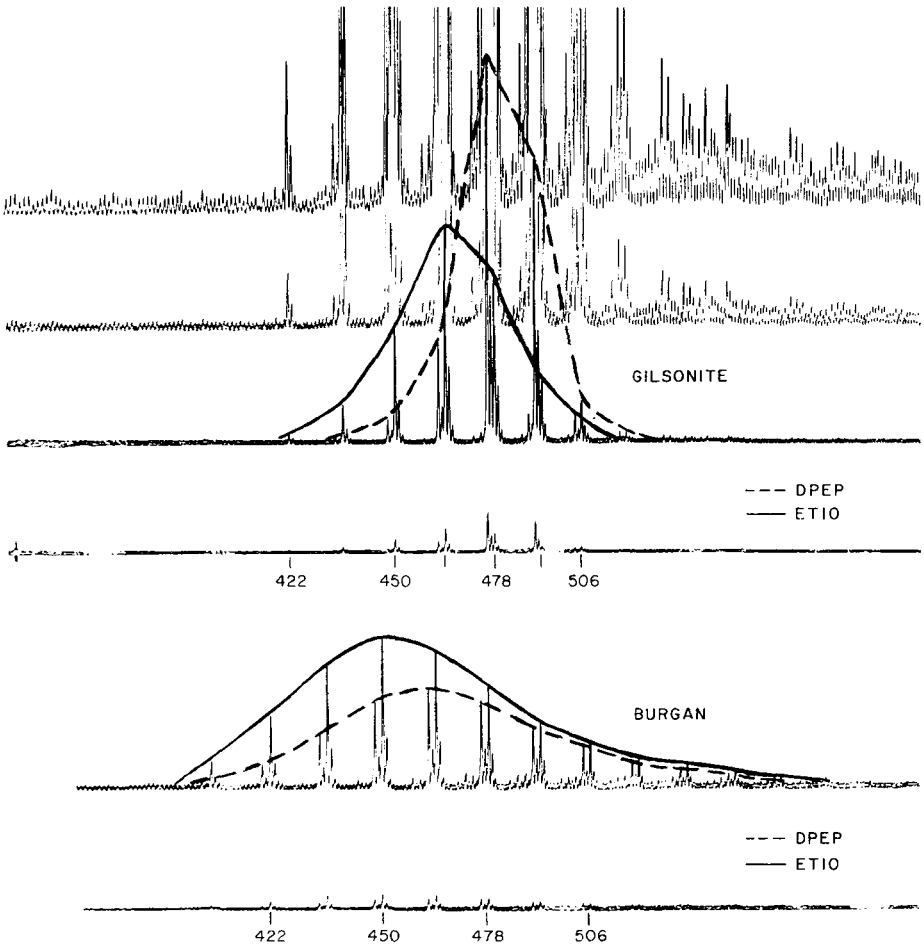

Fig. 7-4. Portion of mass spectra illustrating different band widths (σ_{DPEP} and σ_{etio}) of gilsonite and Burgan crude asphaltenes.

ments (probably by transalkylation) resulting in a broader distribution of substituted configurations. A trend of increasing σ values with increasing age is shown in Figs. 7-5 and 7-6, for the DPEP and etio bands, respectively. Both σ's (DPEP and etio) also show a distinct tendency to increase with increasing burial depth (Fig. 7-7).

AROMATICITY OF ASPHALTENE

Major structural parameters concerning the aromatic portion are the aromaticity, f_a, extent of condensation, H_I/C_A or H_{aru}/C_{ar} ratio, and degree of fusion, F/C_a. Relationship of aromaticity to geologic time and thermal maturation is discussed

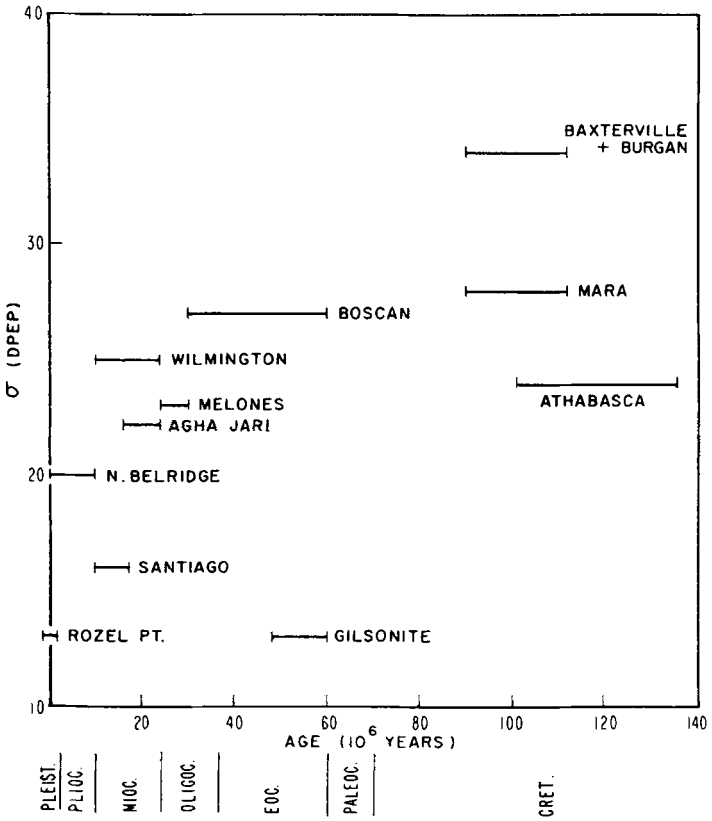

Fig. 7-5. Band width σ_{DPEP} vs. age.

thoroughly in Chapter 12 of this book. Aromaticity is always a linear function of the heat-treatment temperature. The writers have used the oil-shale asphaltene in the past as a model, with their samples being treated at various temperatures [37]. Later, various coal-liquid derived asphaltenes were studied at even higher temperatures, e.g., up to the 450°C required for mesophase formation [38]. Recently, Lian and Yen [39] studied refinery asphaltenes from paving asphalt. In all cases studied, the slopes of aromaticity, when plotted versus the heat treatment temperature, are approximately the same [36]. This indicates that the chemical change in the aromatic system under thermal stress is similar even if the asphaltene is from a different source.

Differences in the extent of ring condensation could also result from thermal maturation or bacterial degradation. Both of these processes make the oil more aromatic. Thermal transformations have been studied by Rogers et al. [40] and Milner et al. [41]. Cracking of large hydrocarbons is achieved by H_2 removal of the aromatization from the cyclic structures. These hydrocracking and disproportionation reactions proceed simultaneously, yielding light hydrocarbons and asphaltene-like

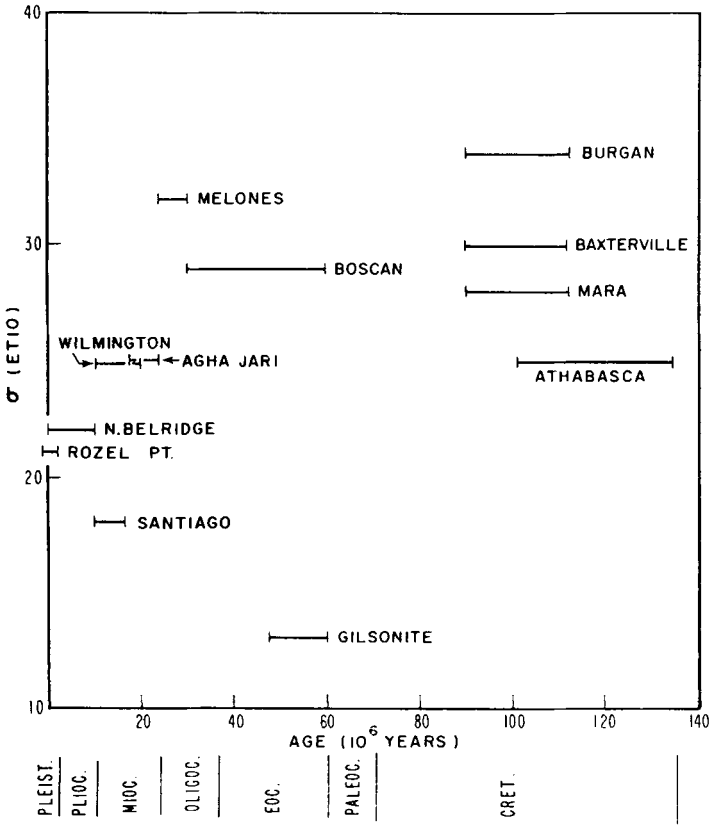

Fig. 7-6. Band width σ_{etio} vs. age.

structures. There have been detailed kinetic studies on such reaction pathways. To avoid significant maturation effects from clouding the migration effects, however, care must be taken to study source rock–oil pairs that have the same geologic environments and life-spans.

The extent of ring condensation can differentiate kata, peri, or linked aromatic systems, but cannot yield more information on ring fusion. This can be achieved by employing the F/C_A ratio, the degree of fusion parameter [42]. Some asphaltenes in the crude oil can retain a high degree of fusion, i.e., when the ratio of the internal quaternary carbons to the edge carbons is large, the duration of exposure must be longer for that petroleum in a specific thermal environment. In this manner, additional information may be procured. A perfect tool is the solid-state ^{13}C NMR technique, e.g., the dipolar dephasing ^{13}C NMR spectroscopy [43,44].

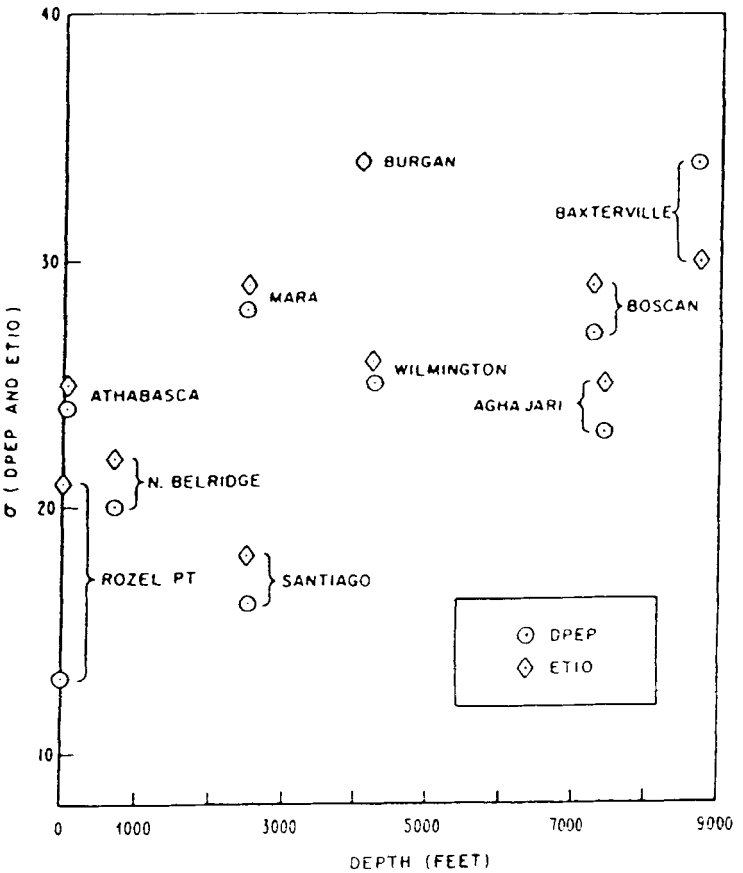

Fig. 7-7. Band width σ_{DPEP} and σ_{etio} vs. depth of burial.

MOLECULAR WEIGHT OF ASPHALTENES

The molecular weight parameter (particle weight) is obtained by vapor pressure osmometry in benzene (using benzil as standard) or in tetrahydrofuran (THF) (using tristearin as standard). This number–average particle weight is a measure of the ease of dissociation of various asphaltenes in a given solvent. Some particles retain their unit cell structures essentially intact, whereas others separate into smaller units with loss of one or more unit sheets [50]. Some even approach the dimensions of the unit sheet as determined from X-ray or mass spectrometric analysis [45].

According to proposed petroleum maturation mechanisms [8,9], the molecular weight average of asphaltenes should increase with age. Figures 7-8 and 7-9 show relations of molecular weights to age determined in benzene (ϕH) and in tetrahydrofuran (THF) solutions, respectively. Despite some scatter, the molecular weight versus burial depth curves (Fig. 7-10) show an overall trend with a positive relation.

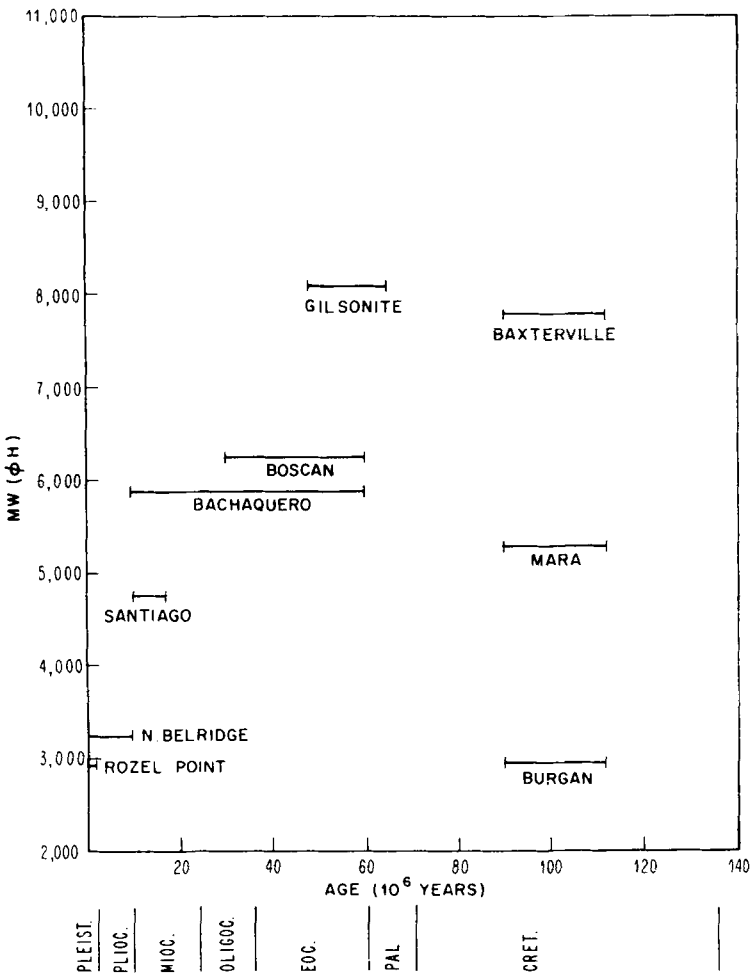

Fig. 7-8. Molecular weight of asphaltenes in benzene solution vs. age.

AVERAGE LENGTH OF SUBSTITUENTS ON ASPHALTENES, (C_S/C_{SU}) and (C_{MP}/C_{SU}) + 1

The C_S/C_{SU} parameter denotes the average number of carbon atoms attached to positions on the edge of an aromatic nucleus. Alternately, it can be defined as the number of saturated carbon atoms per substituent attachment site. The data are based on NMR spectra of the asphaltene fraction and calculated from the relation:

$$C_S/C_{SU} = (h_s - H_{sme}/3H)(H_\alpha/H)$$

h_s can be obtained from the relation:

$$h_s = 1 - H_A/H$$

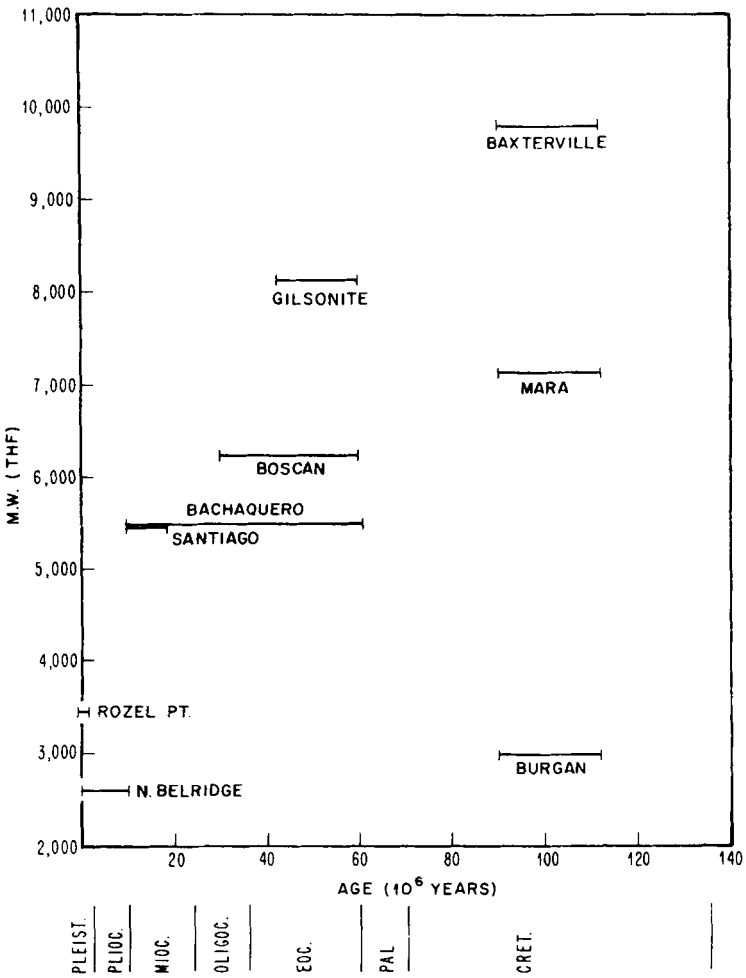

Fig. 7-9. Molecular weight of asphaltenes in tetrahydrofuran (THF) solution vs. age.

where H_A, H_{sme}, and H_α are numbers of aromatic protons, saturated methyl protons, and α-substituted protons, respectively [46]; H is the total number of protons.

The $[C_{MP}/C_{SU}) + 1]$ parameter is a measure of the average chain length of the straight chain paraffinic portion of the asphaltenes. It is obtained from the absorptivity of the infrared 720 cm^{-1} methylene rocking vibrations (E_R) using the following calibration curve (see Table 7-2):

$$C_{MP}/C_{SU} = kE_R$$

where constant $k = 1.92$. This parameter involves only those lengths of carbon chain which do not contain alicyclic (naphthenic) or branched paraffins [47,48] and does not include the terminal methyl group on the chain. The addition of one unit to this

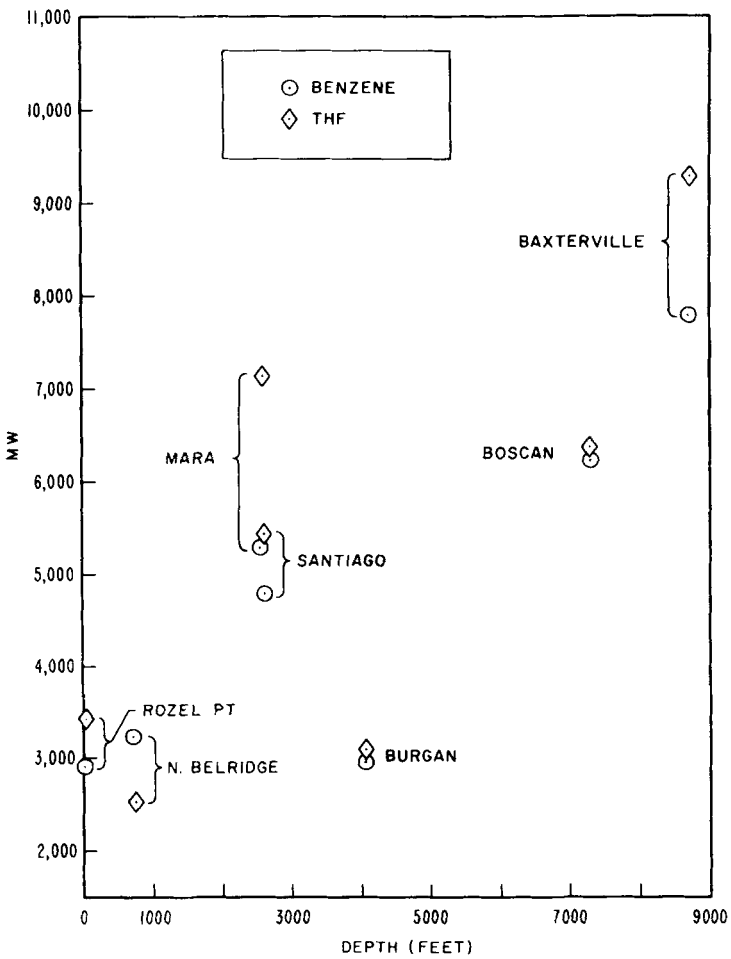

Fig. 7-10. Molecular weight vs. depth of burial.

parameter, resulting in the value $[C_{MP}/C_{SU}) + 1]$, takes the terminal methyl group into account, thereby indicating the total number of carbon atoms in the paraffin chain.

Plots of C_S/C_{SU} versus age (Fig. 7-11) and of $[(C_{MP}/C_{SU}) + 1]$ versus age and depth (Figs. 7-12 and 7-13) indicate that substitute lengths on the asphaltene molecule tend to increase with increasing age and depth. The significance of these relations may not be as readily apparent as some of the other compositional trends, but they may serve to point out the existence of certain interrelations among petroleum components.

The petroleum maturation mechanisms suggested by carbon isotope studies [9] imply that asphaltenes and other complex polycyclic constituents are formed simultaneously with low-molecular-weight hydrocarbons in the course of petroleum

TABLE 7-2

Principal infrared methylene bending vibrations and the magnitude of methylene chains of a number of asphaltenes, resins, and related substances

No.	Sample	Geological age	Rock [a]		Scissor	Wag	C_S/C_{SU} [b]	C_{MP}/C_{SU} [c]
			ν_R	E_R	ν	ν		
Petroleum asphaltenes								
1	Baxterville	Upper Cretaceous	727	0.98	1319	1465	3.0	1.9
2	Lagunillas (Kuwait)	OligoMiocene	725	0.87	1312	1467	2.2	1.7
3	Burgan (Kuwait)	Middle Cretaceous	729	1.2	1304	1463	2.6	2.3
4	Wafra No. A-1	Lower Cretaceous	728	1.4	1319	1465	3.1	2.7
5	Mara	Lower Cretaceous	729	1.1	1322	1463	4.6	2.1
6	Wafra	Middle Cretaceous	730	1.3	1319	1468	2.3	2.5
7	Raudhatain	Middle Cretaceous	730	1.3	1308	1461	2.7	2.5
8	Ragusa	Upper Triassic	724	1.5	1314	1467	3.8	2.9
9	Lybia (Zs)	–	720	2.5	1318	1466	–	4.8
10	Rozelpoint	Recent	723	1.7	1310	1464	–	3.3
11	West Texas	Silurian	729	1.1	1320	1468	–	2.1
12	Belridge	Pliocene	722	0.72	1318	1463	–	1.4
13	San Tiago	Pliocene	725	0.57	1318	1464	–	1.1
14	Libya (WV)	–	721	3.0	1310	1468	–	5.8
Petroleum resins								
15	Baxterville narrow cut	Upper Cretaceous	725	1.8	1308	1468	2.4	3.5
Gilsonite asphaltene								
16	Tabor vein	–	722	0.70	1310	1465	3.3	1.3
Refinery asphaltene								
17	Kuwait visbreaker tar	–	731	0.77	1321	1462	1.6	1.5

[a] Average values of at least two determinations, ν_{max} expressed in cm^{-1} and E at ν_{max} expressed as ml g^{-1} mm^{-1}.
[b] C_S/C_{SU} Derived from NMR data solely, this quantity minus one will yield the none-methyl value.
[c] Calculation based on $1.92E_R$ from empirical relation.

formation and evolution, and concentrations of both varieties of components should increase with age. Yet, it is recognized [12] that asphaltic components are more abundant in geologically youthful oils than in older oils. This discrepancy can be explained by recognizing that simultaneous generation of light paraffins and asphaltenes creates a condition of instability, because these components cannot coexist in solution. Thus, as concentrations of light and heavy maturation products continue to increase, a condition will be reached in which asphaltenes will precipitate and separate from the liquid oil phase. This explains why petroleums derived from older sediments are low in asphaltene content and can account for the observed increase in substituent lengths on the asphaltene molecule with increasing age, because only

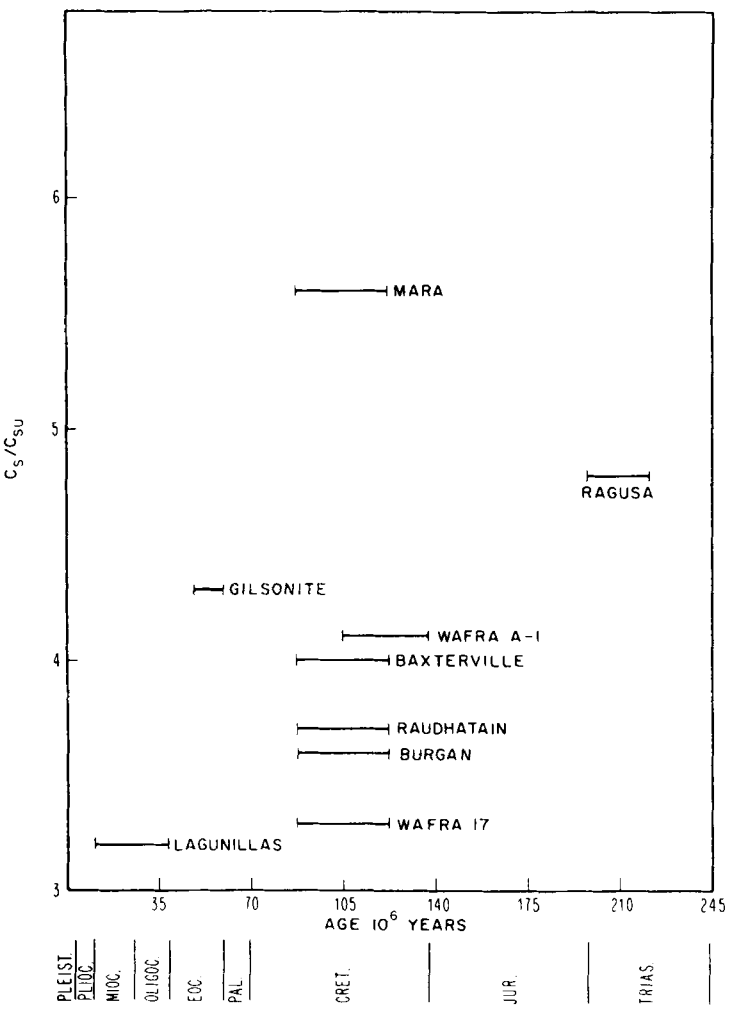

Fig. 7-11. C_S/C_{SU} ratio vs. age.

such substituted asphaltenes will be sufficiently soluble in liquid petroleum to persist as a petroleum constituent. As in the case of porphyrin maturation products, asphaltenes of highly diverse complexities can be formed in the course of transformation processes, and it is conceivable that only those asphaltenes with longest substituent chains will be sufficiently soluble to persist in the liquid petroleum phase.

CONCLUDING REMARKS

The results of this study indicate that several compositional parameters of the complex molecules of asphaltene and porphyrin of petroleums are related to age

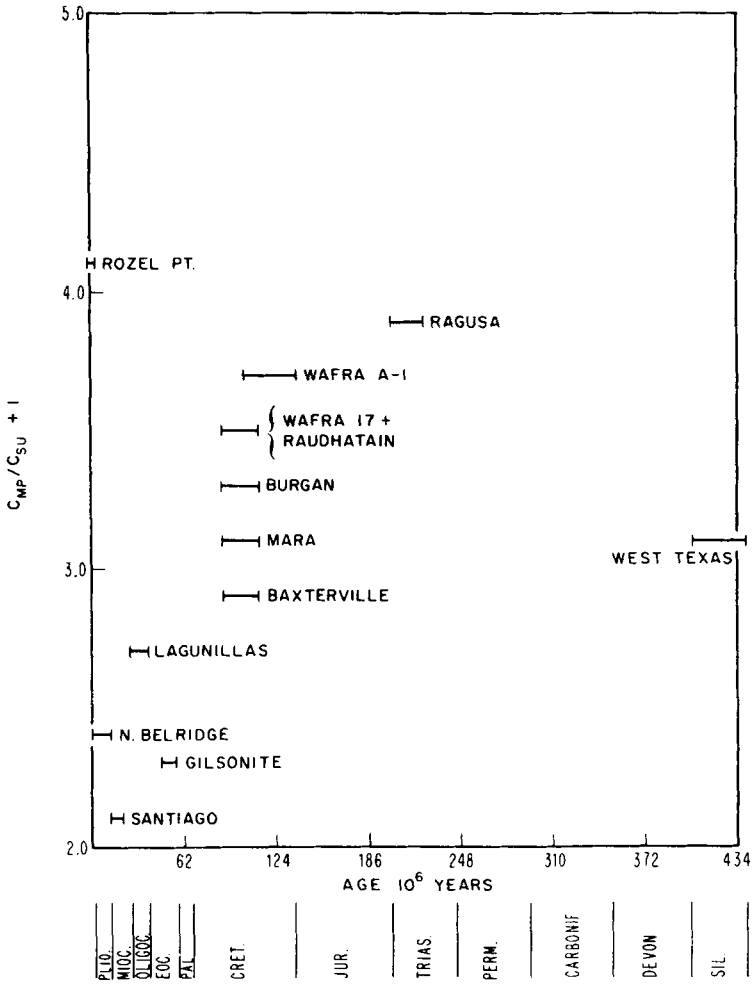

Fig. 7-12. $[(C_{MP}/C_{SU}) + 1]$ vs. age.

or depth of burial. Proportions of etioporphyrin type structures relative to deoxophylloerythroporphyrin structures increases with age, and this direction of change is compatible with the concept that stable components persist at the expense of the unstable ones. Diversity of DPEP and etioporphyrin homologues increases with age and this change is also a reasonable consequence of proposed transformation processes. With increasing age, asphaltenes increase in molecular weight and also in size of substituent nonaromatic groups. The former is a direct consequence of petroleum maturation processes and the latter points out possible types of interactions that involve petroleum constituents in the course of petroleum transformations. Other parameters, intimately related to those discussed above, such as sizes of aromatic centers within asphaltene molecules and asphaltene aromaticity, also show tenden-

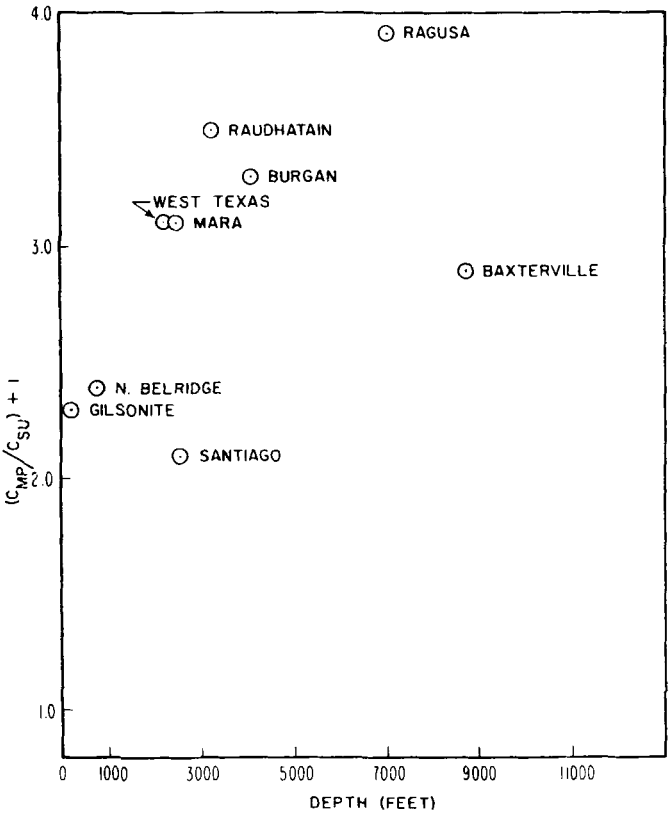

Fig. 7-13. $[(C_{MP}/C_{SU}) + 1]$ vs. depth.

cies to increase with age as would be expected from other evidences of petroleum transformation. Aromaticity is discussed in Chapter 12. These implications, offered by the results of a survey of a limited and not especially representative group of petroleums, suggest that, in the future, a more thorough program of analyses on a more representative variety of samples should further the knowledge of petroleum formation and alteration. (Also see [50].)

REFERENCES

[1] Yen, T.F., Structure of petroleum asphaltene and its significance. *Energy Sources*, 1: 447–463 (1974).
[2] Yen, T.F., *The Role of Trace Metals in Petroleum*. Ann Arbor Science Publishers, Ann Arbor, Mich., 221 pp. (1975).
[3] Yen, T.F., The role of asphaltene in heavy crude and tar sands. In: R.F. Meyer and C.T. Steele (Editors), *The Future of Heavy Crude and Tar Sands*. McGraw Hill Inc., New York, N.Y., pp. 174–179 (1980).
[4] Yen, T.F., The nature of asphaltenes in heavy oil. In: *Proc., 1st Pan Pacific Synfuel Conference, Vol. II*. The Japan Petroleum Institute, Tokyo, pp. 547–557 (1982).

[5] Yen, T.F., Characterization of heavy oil. In: *Second International Conference of Heavy Crude and Tar Sands, Caracas, Venezuela.* McGraw-Hill, New York, N.Y., pp. 412–423 (1984).
[6] Yen, T.F., Asphaltic materials. In: H.S. Mark, N.M. Bikales, C.G. Overberger and G. Menges (Editors), *Enclyopedia of Polymer Science and Engineering, Supplementary Vol.*, John Wiley and Sons, New York, N.Y., 2nd ed., pp. 1–10 (1989).
[7] Hodgson, G.W., Baker, B.L. and Peake, E., Geochemistry of porphyrins. In: B. Nagy and U. Colombo (Editors), *Fundamental Aspects of Petroleum Geochemistry.* Elsevier, Amsterdam, pp. 177–260 (1967).
[8] Bestougeff, M.A., Petroleum hydrocabons. In: B. Nagy and U. Colombo (Editors), *Fundamental Aspects of Petroleum Geochemistry.* Elsevier, Amsterdam, p. 103 (1967).
[9] Silverman, S.R., Carbon isotopic evidence for the role of lipids in petroleum formation. *J. Am. Oil Chem. Soc.*, 44: 691 (1967).
[10] Baker, E.W., Yen, T.F., Dickie, J.P., Rhodes, R.E. and Clark, L.F., Mass spectrometry of porpyrins II. Charaterization of petroporphyrins. *J. Am. Chem. Soc.* 89: 3631–3639 (1967).
[11] Yen, T.F., Erdman, J.G. and Pollack, S.S., Investigation of the structure of petroleum asphaltenes by X-ray diffraction. *Anal. Chem.*, 33: 1587–1594 (1961).
[12] Andreev, P.F., Bogomolov, A.I., Dobryanskii, A.F. and Kartsev, A.A., *Transformation of Petroleum in Nature.* Pergamon Press, Oxford, 449 pp. (1968).
[13] Treibs, A., Chlorophyll und Heminderivate in organischen Mineralstoffen. *Angew. Chem.*, 49: 682 (1936).
[14] Yen, T.F., Evidence concerning the presence of long-chain alkyl substituents in native asphaltic molecules. *Nature Phys. Sci.*, 233: 36 (1971).
[15] Yen, T.F., Terrestrial and extraterestrial stable organic molecules. In: R.F. Landel and A. Rembaum (Editors), *Chemistry in Space Research.* Elsevier, New York, N.Y., pp. 105–153 (1972).
[16] Tynan, E.C. and Yen, T.F., Association of vanadium chelates in petroleum asphaltenes as studied by ESR. *Fuel (London)*, 43: 191 (1969).
[17] Yen, T.F., Tynan, E.C., Vaughan, G.B. and Boucher, L.J., ESR studies of petroleum asphaltics. In: R.A. Friedel (Editor), *Spectrometry of Fuels.* Plenum Publishing Corp., New York, N.Y., pp. 187–201 (1970).
[18] Yen, T.F., Nitrogen superhyperfine splittings of vanadyl porphyrins in native asphaltenes. *Naturwissenschaften*, 58: 267 (1971).
[19] Boucher, L.J. and Yen, T.F., Spectral properties of oxovanadium(IV) complexes, II. Bistrifluoroacetyl-acetoneethylenediimine. *Inorg. Chem.*, 7: 2665 (1968).
[20] Boucher, L.J. and Yen, T.F., Spectral properties of oxovanadium(IV) complexes, III. Salicylamidines. *Inorg. Chem.*, 8: 689 (1969).
[21] Boucher, L.J., Tynan, E.C. and Yen, T.F., Spectral properties of oxovanadium(IV) complexes, I. β-ketimines. *Inorg. Chem.*, 7: 731 (1968).
[22] Hodgson, G.W. and Baker, B.L., Porphyrin in meterorites; metal complexes in Orquil, Murray, Cold Bokkeveld and Mokoia carbonaceous chondrites. *Geochim. Cosmochim. Acta*, 33: 943 (1969).
[23] Azarnoff, D.C., Brock, F.E. and Curran, G.L., A specific site of vanadium inhibition of cholesterol biosynthesis. *Biochim. Biophys. Acta*, 51: 397 (1961).
[24] Mountain, J.T., Delker, L.L. and Stokinger, H.E., Studies in vanadium toxicology. *A.M.A. Arch. Ind. Hyg. Occup. Med.*, 8: 406 (1953).
[25] Yen, T.F., Boucher, L.J., Dickie, J.P., Tynan, E.C. and Vaughan, G.B., The nature of vanadium complexes and porphyrins in asphaltenes. *Pet. Chem. Prepr.*, 13(1): 59–75 (1968).
[26] Yen, T.F., Boucher, L.J., Dickie, J.P., Tunan, E.C. and Vaughan, G.B., Vanadium complexes and porphyrins in asphaltenes. *J. Inst. Pet. (London)*, 55: 87–99 (1969).
[27] Barwise, A.J.F. and Park, P.J.D., Petroporphyrin fingerprinting as a geochemical marker. In: M. Bjoroey, C. Albrecht, C. Cornford, K. de Groot, G. Eglinton, E. Galimov, D. Leythaeuser, R. Pelet, J. Rullkoetter and G. Speers (Editors), *Advances in Organic Geochemistry 1983.* Wiley, Chichester, pp. 668–674 (1983).
[28] Louda, J.W. and Baker, E.W., Geochemistry of tetrapyrrole, carotenoid and perylene pigments in sediments from the San Miguel Gap (Site 467) and Baja California borderland (Site 471), Deep Sea Drilling Project, Leg 63. *Init. Rept. DSDP*, 63: 785–818 (1981).

[29] Mackenzie, A.S., Quirke J.M.E. and Maxwell, J.R., Molecular parameters of maturation in the Toarcian shales, Paris Basin, France, II. Evolution of metalloporphyrins. In: P.A. Schenck, J.W. de Leeuw and G.W.M. Lijmbach (Editors), *Advances in Organic Geochemistry 1979*. Pergamon Press, Oxford, pp. 107–116 (1980).

[30] Barwise, A.J.G. and Roberts, I., Diagenetic and catagenetic pathways for porphyrins in sediments. In: A.G. Douglas and J.R. Maxwell (Editors), *Advances in Organic Geochemistry 1983*. Pergamon Press, Oxford, pp. 167–176 (1984).

[31] Shi, J., Petroporphyrins in oils and sediments from Zhanhua depression. *Sci. Sinica, Ser. B* (Engl. ed.), 26(8): 865–875 (1983).

[32] Mackenzie, A.S., Quirke, J.M.E. and Maxwell, J.R., Molecular parameters of maturation in the Toarcian shales., Paris Basin, France, II. Evolution of metalloporphyrins. *Phys. Chem. Earth*, 12: 239–248 (1980).

[33] Didyk, B.M., Alturki, Y.I.A., Pillinger, C.T. and Eglinton, G., Petroporphyrins as indicators of geothermal maturation. *Nature (London)*: 256, 563–565 (1975).

[34] Liao, Z., Huang, D. and Shi, J., Discovery of special predominance of vanadyl porphyrin and high abundance of Di-DPEP in nonmarine strata. *Sci. Sinica, Ser. B.*, 33(5): 631–640 (1990).

[35] Sundararaman, P., Biggs, W.R., Reynolds, J.G. and Fetzer, J.C., Vanadylporphyrins, indicators of kerogen breakdown and generation of petroleum. *Geochim. Cosmochim. Acta*, 52: 2337–2341 (1988).

[36] Yen, T.F., unpublished work (1992).

[37] Shue, F.F. and Yen, T.F., A comparison of asphaltenes for naturally occurring shale bitumen and retorted shale oils; The influence of temperature on asphaltene structure. *Am. Chem. Soc. Symp. Ser.*, 163: 129–138 (1981).

[38] Weinberg, V.L., Yen, T.F., Gerstein, B.C. and Murphy, P.D., Characterization of pyrolyzed asphaltene by diffuse reflectance-Fourier transform infrared and dipolar dephasing-solid state ^{13}C Wader magnetic resonance spectroscopy. *Am. Chem. Soc., Div. Pet. Chem., Prepr.*, 26(4): 810–824 (1981).

[39] Lian, H.J. and Yen, T.F., Classification of asphalt by NMR asphaltene aromaticity approach. *Int. Symp. on Asphaltene Particles*, Las Vegas (1992).

[40] Roger, M.A., McAlery, J.D. and Bailey, N.J.L., Significance of reservoir bitumens to thermal maturation studies, Western Canada Basin. *Bull., Am. Assoc. Pet. Geol.*, 58: 1806 (1974).

[41] Milner, C.W.D., Rogers, M.A. and Evans, C.R., Petroleum transformations in reservoirs. *J. Geochem. Explor.*, 7: 101 (1977).

[42] Yen, T.F. and Dickie, J.P., The compactness of the aromatic systems in petroleum asphaltenes. *J. Inst. Pet. (London)*, 54: 50–53 (1968).

[43] Weinberg, V.L., Yen, T.F, Murphy, P.D. and Gerstein, B.C., Hypothetical average structures of two coal liquid asphaltenes from solid-state 13-C nuclear magnetic resonance and 1-H nuclear magnetic resonance data. *Carbon*, 21(2): 149–156 (1983).

[44] Murphy, P.P., Gerstein, B.C., Weinberg, V.L. and Yen, T.F., Determination of chemical function in asphaltene by high solution solid state carbon-13 nuclear magnetic resonance. *Anal. Chem.*, 54: 522–525 (1982).

[45] Dickie, J.P. and Yen, T.F., Macrostructures of asphaltic fractions by various instrumental methods. *Anal. Chem.*, 39: 1847–1852 (1967).

[46] Yen, T.F., Wu., W.H. and Chilingarian, G.V., A study of the structure of petroleum asphaltene by proton nuclear magnetic resonance. *Energy Sources*, 7(3): 273–302 (1983).

[47] Yen, T.F., Wu, W.H. and Chilingarian, G.V., A study of the structure of petroleum asphaltenes and related substances by infrared spectroscopy. *Energy Sources*, 7(3): 203–234 (1983).

[48] Yen, T.F. and Erdman, J.G., Infrared studies in the bending regions of petroleum asphaltenes: nature of alkyl groups. *Am. Chem. Soc., Div. Anal. Chem., Abstr.*, pp. 29B–30B (1965).

[49] Boucher, L.J., Tynan, E.C. and Yen, T.F., Correlation of ESR spectra with ligand type for oxovanadium(IV) complexes. In: *Electron Spin Resonance of Metal Complexes*. Plenum, New York, N.Y., pp. 111–130 (1969).

[50] Pollack, S.S. and Yen, T.F., Structural studies of asphaltenes by X-ray small angle scattering. *Anal. Chem.*, 42(6): 623–629 (1970).

Asphaltenes and Asphalts, 1. Developments in Petroleum Science, 40
edited by T.F. Yen and G.V. Chilingarian

Chapter 8

ASPHALTENE AND OTHER HEAVY ORGANIC DEPOSITIONS

SANG JIN PARK, JOEL ESCOBEDO and G. ALI MANSOORI

INTRODUCTION

Asphaltene and other heavy organic depositions during production and processing of crude oil present a very serious problem in many areas throughout the world. The economic implications of such a problem are tremendous considering that a well workover cost could get as high as a quarter of a million dollars. For example, in a petroleum production field, formation of asphaltic sludges after temporarily shutting in a well and/or after stimulation treatment by acid has resulted in partial or complete plugging of the well [1].

Miscible flooding of petroleum reservoirs by carbon dioxide, natural gas, and other injection fluids has become an economically viable technique for petroleum production [2–4]. The most common problem in petroleum recovery is poor reservoir volumetric sweep efficiency, which is due to channeling and viscous fingering, because of the large difference between the mobilities of displacing and displaced fluids. Introduction of a miscible fluid in petroleum reservoirs, will, in general, produce a number of alterations in the flow behavior, phase equilibrium properties, and reservoir rock characteristics. One such alteration is the heavy organic deposition (asphaltene and paraffin/wax), which is expected to affect productivity of a reservoir in the course of oil recovery [3–9]. In most of the observed instances, heavy organic deposition may result in plugging or wettability reversal in the reservoir [10]. Effects of heavy organic deposition could be positive or negative, depending on whether it can be controlled or predicted.

The parameters that govern precipitation of heavy organic from petroleum fluids appear to be the *composition* of crude and injection fluid, *pressure* and *temperature* of the reservoir. With alterations in these parameters, the nature of the heavy organic substances which precipitate will vary [11]. Also, it is a proven fact that the precipitation of asphaltene is in general followed by polymerization (flocculation) of the resulting precipitate. This process produces an insoluble material in the original reservoir fluid [12–17]. Because of the complex nature of heavy organic substances, the phenomena of organic deposition are not well understood. Also, in view of the complexity of the petroleum reservoirs, study and understanding of the in-situ precipitation of organic substances seems to be a challenging and timely task. Such an understanding will help design a more profitable route for miscible gas flooding projects.

Over the last five decades a number of investigators have conducted research on the nature of heavy organics and the mechanisms of heavy organic deposi-

tion. One important conclusion arrived at through experimental work is that heavy organic compounds (asphaltene), which are deposited, possess a wide range of polarities and molecular weights. This suggests that such compounds may be partly dissolved and partly in the colloidal state, dispersed and stabilized primarily by resin molecules adsorbed on the macromolecular surface. The concept that heavy organic (asphaltenes) compounds are present as colloidal particles is credited to Nellensteyn [18]. He proposed that asphaltic compounds were made of micelles, protected by adsorbed resins and hydrocarbon materials, all dispersed in a hydrocarbon medium. He also found that peptizing or precipitating properties of different common solvents with respect to asphaltic compounds are closely related to the surface tension. Swanson [19] and Witherspoon and Munir [20] proposed that the resins were required for asphaltenes to dissolve in the distillate portion of a crude oil. According to Dickie and Yen [21] petroleum resins provide a transition between the polar (asphaltene) and the relatively non-polar (oil) fractions in petroleum, thus preventing the assembly of polar aggregates that would be non-dispersible in the oil. Koots and Speight [22] considered that asphaltene clusters associated with resin molecules could the dominant species allowing the asphaltenes to exist in the colloidal state in a crude oil. Leontaritis and Mansoori [23] proposed a thermodynamic–colloidal model which is capable of predicting the onset of asphaltene flocculation. According to their model, asphaltenes exist in oil as solid particles in colloidal suspension, stabilized primarily by resin molecules adsorbed on their surface.

The present chapter is designed with the purpose in mind of applying modern theoretical and experimental techniques of statistical mechanics and thermodynamics to develop the methods that will predict organic deposition during production and processing of crude oil. First, a continuous thermodynamic (CT) model is presented in which the theory of heterogeneous polymer solutions is utilized for the predictions of the onset point and amount of organic deposits from petroleum crude. Then, a steric colloidal (SC) model which is capable of predicting the onset of organic deposition is described. A combination of the two models results in a fractal aggregation (FA) model. Chromatographic methods for the characterization of crude oils and organic deposits from petroleum fluids are discussed. Model predictions of the onsets and amounts of heavy organic deposits are presented along with the experimental results. Finally, an overview of the organic deposition problem is presented in this chapter.

MODELS OF ORGANIC DEPOSITION

One question of major interest in the oil industry is "when" and "how much" heavy organics will flocculate out of solution under certain conditions. Because the crude consists generally of a mixture of oil, aromatics, resins, and asphaltenes it has become possible to consider each of the constituents of this system as a continuous or discrete mixture interacting with each other. The available laboratory and field data prove that the heavy organic substances which exist in oil consist of very many particles having molecular weights ranging from one thousand to

several hundred thousands. As a result, distribution-function curves are used to report their molecular weight distribution. Two different models have been proposed [2,23,25,26,34] which are based on the statistical mechanics of particles (monomers and polymers) dissolved or suspended in oil. A combination of the two models is generally enough to predict the asphaltene–oil interaction problems (phase behavior and/or flocculation) wherever it may occur during oil production and processing. The principles of thermodynamics of multicomponent mixtures and phase equilibria, the theory of continuous mixtures, the statistical mechanical theory of monomer/polymer solutions, the theory of fractal aggregation kinetics are utilized here to analyze and predict the onset and amount of organic deposition from petroleum crudes.

Continuous thermodynamic (CT) model [2,25,26]

The degree of dispersion of heavy organics in petroleum oils depends upon the chemical composition of the petroleum [27–29]. Deposition of such compounds can be explained by an upset in the balance of oil composition. The ratio of polar to non-polar molecules and the ratio of high- to low-molecular-weight molecules in a complex mixture such as petroleum are the two factors primarily responsible for maintaining mutual solubility. The addition of miscible solvents will alter these ratios. Then the heavy and/or polar molecules separate from the mixture either in the form of another liquid phase, or as a solid precipitate. Hydrogen bonding and the sulfur- and/or nitrogen-containing segments of the separated molecules could start to aggregate (or polymerize) and, as a result, produce the irreversible heavy organic deposits which are insoluble in the liquid phase (oil).

Inasmuch as heavy organics have a wide range of size, or molecular weight distribution, one may consider such compounds as heterogeneous polydisperse polymers. Then, in order to predict the phase behavior of heavy organics one can assume that the properties of heavy organic fractions depend on their molecular weights. To perform phase equilibrium calculations, the necessary condition for chemical equilibrium must be satisfied. That is, the chemical potential of every heavy organic fraction in the liquid phase, μ_i^{L}, has to be equal to its chemical potential in the solid phase, μ_i^{S};

$$\mu_i^{\mathrm{S}} = \mu_i^{\mathrm{L}}; \quad i = 1, 2, 3, \ldots \tag{8-1}$$

In this model, the Scott and Magatt theory of heterogeneous polydisperse polymer solutions [30,31] is employed for calculation of the chemical potentials of heavy organic fractions. Because organic substances such as asphaltenes consist of mixtures of molecules with virtually continuous molecular weight distributions, one can utilize the continuous mixture theory [32,33], joined with the thermodynamic theory of heterogeneous polymer solutions. Introduction of the continuous mixture theory results in a model that contributes to better characterization of heavy organics and prediction of the onset of deposition and phase behavior under the influence of a miscible solvent. Figure 8-1 shows the comparison of molecular weight of asphaltenes from petroleum crude oil before and after flocculation, as predicted by

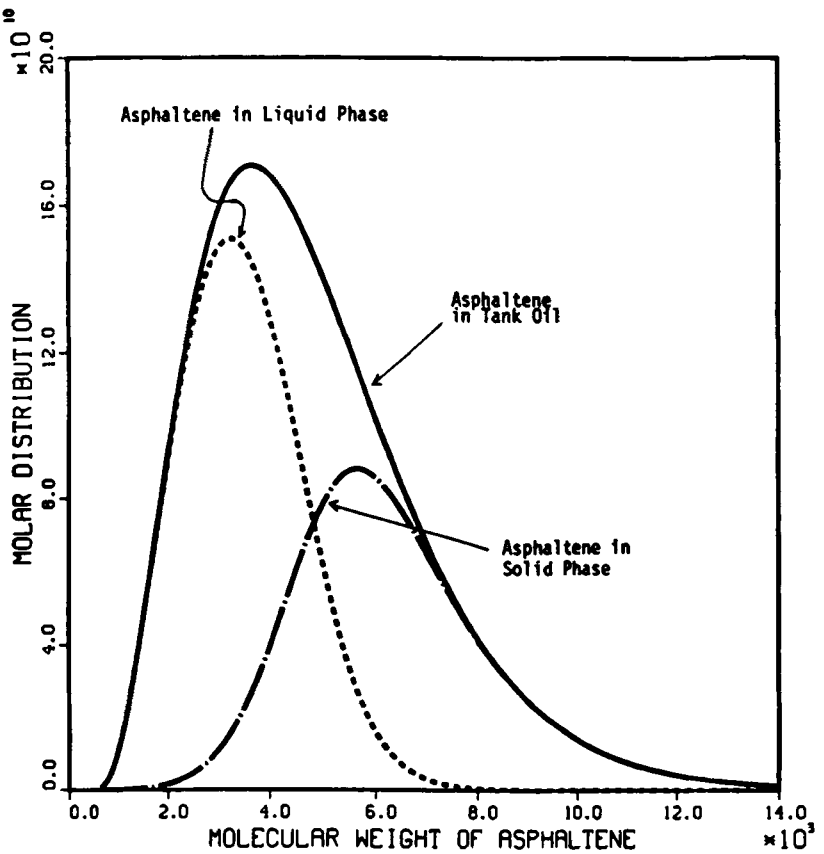

Fig. 8-1. Relations between molar concentration distributions of asphaltene in different phases in equilibrium resulting from the addition of a given amount of miscible solvent (20.00 cm^3 *n*-heptane) to one gram of the tank oil.

the model. According to this figure, the fractions of asphaltene with high molecular weights tend to deposit earlier that the fractions of asphaltene with lower molecular weight.

Steric colloidal (SC) model [23,34]

This model is based upon the assumption that heavy organics (asphaltenes) exist in oil as suspended particles. Their suspension is assumed to be caused by resins (heavy and mostly aromatic molecules), which are adsorbed to the surface of heavy organic particles and keep them afloat because of the repulsive forces between resin molecules in the solution and the adsorbed resins on the macromolecular (asphaltene) surface (see Fig. 8-2). Stability of such a suspension is considered to be a function of the concentration of resins in the solution, the fraction of asphaltene surface sites occupied by resin molecules, and the equilibrium conditions between

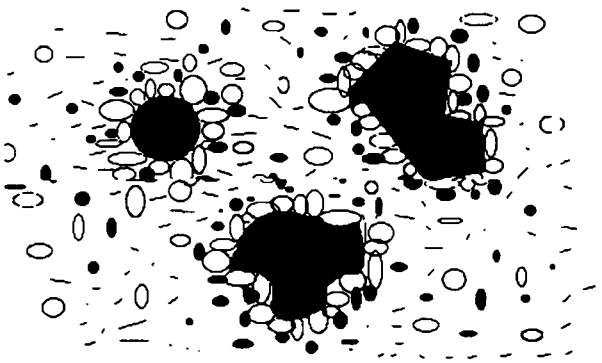

NOTES

1 0 ○ represents resin molecules

2 0 ● represents aromatic molecules

3 0 — represents oil molecules of different size and paraffinic nature

4 0 represents asphaltene particles of different sizes and shapes

Fig. 8-2. Asphaltene particle peptization.

the resins in solution and on the asphaltene surface. According to thermodynamics, a necessary condition for chemical equilibrium between two phases is that the chemical potential of each component in one phase is equal to its chemical potential in the other phase. Writing this condition for the resins in the asphaltene and oil phase one will obtain:

$$\mu_{\text{resin}}^{\text{asphaltene phase}} = \mu_{\text{resin}}^{\text{oil}} \tag{8-2}$$

The significance of the SC model is that the asphaltene particles will remain completely covered regardless of how the nature of the liquid mixture (i.e., add or remove miscible solvent) is changed. So long as the calculated chemical potential remains equal to (or above) the critical chemical potential. Calculation of the chemical potential of the resins in the solid phase would require utilizing small-system thermodynamic techniques. This model, however, requires only one calculation of the chemical potential of the macroscopic asphaltene-free oil phase, and as a result, macroscopic chemical potential calculations are adequate.

Utilization of the SC model requires the following:

(1) Resin chemical potential calculation based on the statistical mechanical theory of polymer solutions.

(2) Studies regarding resin adsorption on asphaltene particle surface and measurement of the related Langmuir constants.

(3) Calculation of the streaming potentials generated during flow of charged asphaltene particles.

(4) Development and use of asphaltene colloidal and aggregation models for estimating the amount of asphalt which may be irreversibly aggregated and flocculated out of solution.

The amount of resins adsorbed is primarily a function of their concentration in the liquid state (the oil). So, for a given system (i.e., fixed type and amount of oil and asphaltenes) changing the concentration of resins in the oil will cause the amount of resins adsorbed on the surface to change accordingly. This means that one may drop the concentration of resins in the oil to a point at which the amount of resins adsorbed is not high enough to cover the entire surface of asphaltenes. This may then permit the asphaltene particles to come together (irreversible aggregation), grow in size, and flocculate.

Fractal aggregation (FA) model [11,34]

The FA is a realistic model for the interaction of heavy and light components of crude oils and accounts for both the solubility and colloidal effects. It is constructed by joining the concepts of continuous thermodynamic theory of solid–liquid phase transition, Fractal aggregation theory of colloidal growth, and steric colloidal collapse and deposition models. This model is capable of predicting the onsets and amounts of asphaltene deposition from petroleum crudes under the influence of miscible solvents. This model is based on the fact that resins play a key role in the solubilization of asphaltenes because they reduce asphaltene aggregation. Therefore, the degree of solubility of asphaltenes in the oil depends on the peptizing effect of resins with respect to asphaltenes, as well as on the resin concentration in the solution (i.e., the change of resin concentration in the oil due to the addition of a miscible solvent).

In the petroleum reservoir, asphaltene particles have been considered as colloidal particles, or micelles, being comprised of clusters of heavy particles associated principally via $\pi-\pi$ interactions [21]. These particles are sterically stabilized by resin molecules adsorbed on their surface; thus, they remain suspended in the oil mixture. It may be assumed that the repulsive forces between resin molecules and the adsorbed resins on the macromolecular (asphaltene) surfaces keep clusters of asphaltene particles from aggregating. Introduction of a miscible solvent into the oil mixture will cause the resin concentration to vary accordingly. A decrease in resin concentration may be followed by desorption of the resin molecules from the asphaltene-particle surface, and, therefore, allow the clusters of asphaltene particles to be subject to mutual interactions. This may result in a situation in which clusters of asphaltene particles contact each other on resin-uncovered sites, aggregate (irreversible aggregation), and flocculate out of solution [35,36]. During the flocculation process, the clusters of heavy particles are assumed to remain suspended in the solution randomly and independent of one another as Brownian particles due to the molecularly induced thermal motion. Van der Waals' attractive forces and electrical (electrostatic or electrokinetic) repulsive (or attractive) forces

would be the factors causing the aggregation and flocculation of heavy organic particles.

The peptizing properties of the resin molecules in the solution are closely related to surface characteristics of asphaltene particles. Because of the surface characteristics of asphaltene particles, an attempt to increase the surface area will require energy to be spent. The energy to increase the surface area is called surface free energy. Because the surface of asphaltene particles is in a higher free energy state than the bulk solution (oil), a spontaneous tendency exists for the surface area of asphaltene particles to achieve a minimum value. Therefore, all colloidal systems have a built-in tendency to spontaneously flocculate and precipitate unless prevented by other stabilizing factors. The flocculation process, affected by the collision between particles, is assisted by thermal motions of molecules of the dispersion medium. In order to account properly for the phenomenon of asphaltene deposition a model must incorporate the following:

(1) The role of resin concentration in such a deposition mechanism and its effect on the colloidal aggregation process of heavy-organic particles under the influence of miscible solvents.

(2) The growing size distribution of clusters of heavy-organic particles by introducing the irreversible kinetics of aggregation.

(3) Determination of the onset of heavy organic deposition, solubility of heavy organics in the solution, the size distributions of heavy organic deposits in the precipitated phase and of heavy organics remaining soluble upon changes in pressure, temperature and composition.

In order to formulate the necessary model for the prediction of the phase behavior of heavy organic deposition, there is a need to study the mechanism of kinetic aggregation of clusters of heavy particles. There have been numerous attempts to understand the mechanism and kinetics of aggregation of clusters of heavy particles. Up to now, most of the studies on the cluster–cluster aggregation were concerned with the geometrical aspects of the aggregates, which include the Euclidian dimension (d), the fractal dimension of clusters (D), and the average radius of clusters (R). It has been noted that in addition to the geometrical aspects another important characteristic of the colloidal aggregation model is the existence of a given function for the size distribution of the clusters of heavy particles [37]. By utilizing the kinetic theory of fractal aggregation along with the theory of heterogeneous polymer solutions, the FA model is able to describe properly the growing mechanism of asphaltene clusters, the growing size distributions of asphaltene, and the geometrical aspect of asphaltene aggregation in the oil due to several factors. In addition to the characteristics of oil and asphaltene, temperature, pressure, and concentrations of resin and miscible solvent in the oil are governing factors in the FA model. The FA model is also used for predictions of the phase behavior and deposition region of asphaltene in mixtures consisting of crude oil and miscible gases (carbon dioxide and propane) at high pressures and different temperatures.

One may consider a system consisting of N_C clusters of N_0 asphaltene particles (identical particles of radius R_0 and unit mass m) which are suspended randomly

in an oil and stabilized by resin molecules adsorbed on the surfaces of asphaltene particles. The clusters of asphaltene particles act as Brownian particles, which are suspended due to the thermal motions of molecules of the dispersion medium. Introduction of a miscible solvent into this system may result in a new condition in which the clusters of asphaltene particles would rigidly stick to each other. That is, a cluster of mass m_i colliding with a cluster of mass m_j would form a single new cluster of a mass m_{i+j}. This process is then repeated. The kinetics of such an aggregation are assumed to obey the following mechanism:

$$A_i + A_j \xrightarrow{K_{ij}} A_{i+j} \tag{8-3}$$

where A_j is the cluster of mass m_j, and K_{ij} is a concentration-independent kinetic (or collision) kernel which describes the aggregation mechanism.

This mechanism was originally proposed by Smoluchowski [38] for coagulation and by Flory [39] for branched polymerization. It is extensively studied in the theory of aggregation, as well as in the theory of colloidal suspension. The rate of aggregation, R_{ij}, at which an i-cluster of a given mass m_i and a j-cluster of a given mass m_j may come into contact with each other and form an $(i + j)$ cluster is given by $R_{ij} = K_{ij} C_i C_j$; $C_i = n_i / N_0$. Here, n_i is the number of clusters of mass m_i (containing i asphaltene particles of unit mass m) and N_0 is the total number of particles. Because the population of the resulting k-cluster ($k = i + j$) increases by all collisions between i-clusters and j-clusters and decreases when a k-cluster combines with another cluster, then $C_k(t)$ will satisfy:

$$\frac{\partial C_k(t)}{\partial t} = \frac{1}{2} \sum_{j=1}^{k-1} K_{k-j,j}\, C_{k-j}(t)\, C_j(t) - C_k(t) \sum_{j=1}^{\infty} K_{k,j}\, C_j(t) \tag{8-4}$$

This expression is known as Smoluchowski's coagulation equation. This irreversible growth mechanism of asphaltene particles implies that the tendency of asphaltene particles to aggregate depends on their mass and the concentration of resin in the solution. A major advantage of Smoluchowski's coagulation equation is that many analytic results can be obtained from it. For some forms of K_{ij} (i.e., $K_{ij} = 1, i + j$, or $i \times j$), analytic solutions to Smoluchowski's equation can be obtained. Different investigators have tried to improve this aggregation mechanism by considering the reactivity of a k-cluster to be proportional to its effective surface area, s_k [40–45]. A characteristic radius, R_k (for cluster of size k), will be proportional to the size of the cluster. The fractal dimension, D, of a given cluster is defined through the following expression

$$R_k \sim k^{1/D}; \quad D < d \tag{8-5}$$

it follows then that $s_k \sim k^w$; w is an exponent (positive or negative) characterizing the effective surface area. Thus, the kinetic (or collision) kernel adopts the forms:

$$K_{ij} \sim (i \times j)^w \quad \text{(product kernel)} \tag{8-6}$$

$$K_{ij} \sim (i^w + j^w) \quad \text{(sum kernel)} \tag{8-7}$$

In order to apply this aggregation mechanism of clusters to the phenomena of aggregation and deposition of asphaltene from petroleum crudes, one is interested in these two kinetic kernels which are proportional to the effective surface area of clusters. Therefore, one must account for the geometrical aspects of clusters in the expression of these kinetic kernels. Consider a system composed of a number of kinetically growing clusters, in which a cluster of size k, before sticking to another cluster, diffuses randomly in space of Euclidian dimension, d, along a trajectory of the dimension of diffusion walk d_w (where $d \geq d_w$). The volume, V_0, of a system can be defined as $V_0 = l_0^d$; l_0 is the length of the lattice. Let us also assume that the kinetically growing cluster of size k has a surface diffusion velocity given by: $v_k = l^{d_w}/t$; l is the "walk-length" (average distance between clusters); t is the walk time. It can also be assumed that this diffusion velocity is inversely proportional to the diffusing cluster size, $v_k \sim k^\alpha$; α is a negative exponent. If a cluster of size k is assumed to contain k identical particles of unit mass it follows that: $v_k \sim m^\alpha$. It is possible to show how the exponent w, characterizing the surface area in the expression of the kinetic kernel, can be expressed in terms of other characteristic constants of the system (d, d_w, α, and D) [42]. The time (t) necessary for a cluster of size k having a walk-length l is given by $t \sim l^{d_w} k^{-\alpha}$ or (in terms of the characteristic radius) $t \sim l^{d_w} R_k^{-D\alpha}$. Because Eq. 8-4 is invariant under a semi-group of similarity transformation a change of length scale in the whole system can be performed such that each length is rescaled by a factor of b:

$$\frac{l}{l'} = \frac{L_0}{l_0'} = \frac{R_k}{R_k'} = b \tag{8-8}$$

The corresponding rescaling of time (from t to t') will be $t \sim b^{d_w - D\alpha} t'$. Considering that Smoluchowski equation, Eq. (8-4), is scale-invariant, the K_{ij}, which has the dimension of a volume divided by time, must be rescaled as:

$$\frac{K_{ij}}{(K_{ij})'} = \frac{V_0}{t} \Big/ \frac{V_0'}{t'} = \frac{l_0^d t'}{l_0^{d\prime} t} = b^{d - d_w + D\alpha} \tag{8-9}$$

One may redefine (for convenience) a parameter $b = \lambda^{1/D}$. As a result, the general scaling relation of coagulation kernels, can be written as $K_{\lambda_i,\lambda_j} = \lambda^n K_{ij}$; K_{λ_i,λ_j} is the new notation for the transformed coagulation kernel K_{ij}' and $n = (d - d_w)/D + \alpha$. It can be concluded that when $n = 2w$ the product kernel is used and when $n = w$ the sum kernel is used [40,41]:

$$\begin{aligned} w &= \alpha + (d - d_w)/D \quad \text{for the sum kernel} \\ w &= \frac{\alpha + (d - d_w)/D}{2} \quad \text{for the product kernel} \end{aligned} \tag{8-10}$$

Because the nature of the growing clusters is fractal, their fractal dimension must be determined. The fractal dimension D, as defined by Eq. (8-5) for a kinetic clustering phenomenon can be obtained through numerical simulations [42,43,46,47]. In the numerical simulations it is considered that clusters are placed randomly on the

TABLE 8-1

Fractal dimension, D, of a growing cluster as a function of its Euclidian dimension d

d	D
2	1.38 ± 0.03
3	1.72 ± 0.11
4	2.02 ± 0.11
5	2.30 ± 0.15
6	2.60 ± 0.15

The fractal dimensions D are determined for $d_w = 2$ (random walk).

L^d lattice sites. By performing numerical simulation assuming cluster aggregation in the square ($d = 2$) or a hypercubic lattice model in d-dimensions ($d > 2$) and periodically bounded in all directions, Meakin [46] and Jullien et al. [43] predicted the fractal dimension, D, of the growing clusters in different Euclidean dimensions, d, as it is reported in Table 8-1.

Because resin molecules are responsible for asphaltene particle peptization, one must consider, also, the effect of resin concentration on the kinetics of growing asphaltene clusters. Thus, the exponent w, which characterizes the effective asphaltene-cluster-surface area that is available for interaction with other clusters in aggregation and growth process, should depend on the concentration of resin, C_R, in a mixture of stock tank oil and a miscible solvent as in the functional form $w = w(C_R)$. This functionality of w will be utilized in the expressions of the growing average mass of clusters of asphaltene particles and the analytical expression of a "reduced" size distribution of clusters of asphaltene particles. Because the asphaltene cluster of size k can be assumed to contain k identical particles of unit mass, one can see that $t \sim l^{d_w} m^{-a}$. From this expression, the dynamical behavior with respect to time for the asphaltene cluster of mass m can be written in the power law form $m(t) \sim t^{\gamma}$. The dynamical behavior of average mass of clusters of asphaltene particles with respect to time can be expressed in terms of the fractal dimension D as follows [42]:

$$\langle m(t) \rangle \sim t^{\gamma}; \quad \gamma = \frac{1}{1 - [\alpha + (d - d_w)/D]} \tag{8-11}$$

It can be shown that $\gamma = \gamma(w; C_R)$; thus, the kinetic theory of fractal aggregation process can be utilized in order to describe properly the growing size distribution of clusters of asphaltene particles due to the influence of miscible solvents. For the mechanism of irreversible kinetic aggregation of diffusive clusters, Botet and Jullien [42] have derived the size distribution of clusters which gives us the analytical expression of a "reduced" size distribution of clusters at a given step of the growing aggregation mechanism. The analytic equation for the "reduced" size distribution of clusters of asphaltene molecules can be shown as follows:

$$F(y; C_R) = \frac{(1 - 2w)^{1-2w} \gamma^{-2w} \exp[-(1 - 2w)\gamma]}{\Gamma(1 - 2w)} \tag{8-12}$$

where $y = m/\langle m\rangle$ and $w = w(C_R)$.

Eq. (8-12) has the following characteristics:

(1) For $w < 0$, the size distribution exhibits a maximum.

(2) For $0 < w < 1/2$, the size distribution is always decreasing.

(3) For $w > 1/2$, the shape of the size distribution function inverts at a finite time, which is known as the signature of the gelation phenomenon [42].

Utilization of the kinetic aggregation of diffusive clusters has enabled the derivation of the relationship between the concentration of resin in a mixture of stock tank oil and a miscible solvent and the growing size distribution of clusters of asphaltene particles. By using the above equations and the principle of phase equilibria, one can derive the expressions for predicting the phase behavior of asphaltene particles under the influence of miscible solvents.

In a heterogeneous polymer mixture, one can specify different fractions of polymers based on their molecular weight. Assuming that a heavy organic behaves as a heterogeneous polymer, one can equate chemical potentials in the oil phase, μ_y^L, and the precipitated phase, μ_y^S. This corresponds to the heavy organics remaining soluble in an oil phase in equilibrium with the heavy organic content of a precipitate:

$$\mu_y^S = \mu_y^L; \quad y = m/\langle m\rangle, \quad 0 < y < \infty \tag{8-13}$$

The Scott and Magat statistical mechanical theory of heterogeneous polymer solutions permits calculation of chemical potentials of asphaltene fractions through the equation:

$$\frac{\Delta\mu_y}{RT} = \ln\phi_y + 1 - (m_y/\langle m_y\rangle)(1-\phi_B) - m_y\phi_B + f m_y\phi_B^2 \tag{8-14}$$

Subscripts y and B refer to the yth fraction of asphaltene and solvent, respectively. The volume fraction, f, is defined by the volume, V, of a component divided by the total volume, V_{mix}, of a mixture. Therefore,

$$\phi_y = \frac{V_y}{V_{mix}}, \quad \phi_B = \frac{V_B}{V_{mix}}, \quad \text{and} \quad \left(\sum\phi_y\right) + \phi_B = 1 \tag{8-15}$$

The segment number of the yth fraction of asphaltene, m_y, is defined by the ratio of molar volume, v_y, of the yth fraction of asphaltene over the molar volume, v_B, of a solvent, $m_y = v_y/v_B = M_y/(\langle\rho_A^{mass}\rangle v_B)$; $\langle\rho_A^{mass}\rangle$ is the average mass density of the yth fraction. The segment number of the solvent is unity. The average segment number, $\langle m_y\rangle$, of asphaltene may be defined by $\langle m_y\rangle = \sum x_y m_y$; where x_y is the mole fraction of the yth fraction of asphaltene with respect to the total asphaltene (i.e., $\sum x_{yi} = 1$). The parameter f in Eq. (8-14) is defined as:

$$f = \frac{1}{r} + \frac{v_B[(\delta_A - \delta_B)^2 + 2K_{AB}\delta_A\delta_B]}{RT} \tag{8-16}$$

where r is the coordination number between two successive segments in asphaltene molecules (r has a value between 3 and 4 [30,31]), K_{AB} is the interaction parameter between asphaltene and asphaltene-free oil, given by $K_{AB} = a + b\langle M_B\rangle$ (it is

assumed to be linearly proportional to the average molecular weight of asphaltene-free oil, $\langle M_B \rangle$); δ_A is the average solubility parameter of asphaltene, and δ_B is the solubility parameter of asphaltene-free oil. Solubility parameter δ is defined by the square root of the molar internal energy change of vaporization, Δu^{vap}, over the molar volume:

$$\delta = \left(\frac{\Delta u^{vap}}{v} \right)^{1/2} \tag{8-17}$$

By utilizing Eqs. 8-13 and 8-14, after simple mathematical manipulations, the following equation can be obtained:

$$\frac{\phi_y^L}{\phi_y^S} = \exp\left\{ m_y \left[\left(\frac{1}{\langle m_y^L \rangle} - \frac{1}{\langle m_y^S \rangle} \right) + \left(1 - \frac{1}{\langle m_y^L \rangle} \right) \phi_B^L - f^L (\phi_B^L)^2 \right] \right\} \tag{8-18}$$

The "reduced" growing size distribution, Eq. 8-12, of clusters of asphaltene molecules must be joined with Eq. 8-18 for calculation of the total volume fraction of asphaltene remaining soluble in a mixture in equilibrium with a precipitated asphaltene phase. Thus this model can predict the solubility of heavy organic in the solution, the size distributions of heavy organics in the precipitated phase and heavy organics remaining soluble in an oil mixture upon changes in pressure, temperature, and composition under the influence of miscible solvents. This may contribute significantly toward better prediction of the phase behavior of the heavy organic deposition mechanism under the influence of miscible solvents.

CHARACTERIZATION OF ORGANIC COMPOUNDS [48]

Experimental data suggest that asphaltic compounds (asphaltenes and resins) are very important components of crude oil because they play a crucial role in the asphaltene deposition problem. Yet, not enough is known about their physical and chemical properties. Conventional methods for characterizing asphaltenes and resins (i.e., finding their physical, chemical, and thermodynamic properties) consist primarily of physically separating these compounds from the original oil and then subjecting them to different analyses using the available techniques. The separation step is apparently the most difficult and error-prone in these methods. In the technique used in our laboratory the separation of asphaltenes and resins is accomplished by gel permeation chromatography (GPC) and high performance liquid chromatography (HPLC). Two asphaltic crude oils were used in these studies, the heavier 27.13°API gravity Brookhaven oil and the lighter 30.21°API gravity DK-107 oil. The detailed experimental methods used in our laboratory are reported in previous publications [48].

The key oil fraction here of major interest is the "polar" fraction. Another name given to this fraction in the literature is "heteroatoms" [49,50]. By the description of each method it is evident that the words "resins", "polars", and "heteroatoms" refer to very similar but not necessarily identical compounds. As a result, the

TABLE 8-2

Hydrocarbon group separation by HPLC method

Component	Brookhaven oil	DK-107 oil
Asphaltenes (wt%)	1.25 ± 0.03 [a,b]	0.53 ± 0.03 [b]
Saturates (wt%)	70.57 ± 0.42	47.00 ± 0.28
Aromatics (wt%)	22.94 ± 0.33	43.22 ± 0.17
Polars (wt%)	5.24 ± 0.06	9.25 ± 0.08

[a] A minimum of three measurements for each data point were made to determine the precision, which was taken as the average distance from the mean.
[b] These are n-C_6 asphaltenes.

relatively simple high performance liquid chromatography (HPLC) method, with some modifications, can be used for determining the percent of resins in the crude oil and physically separating them for further analysis, i.e., determination of critical properties, molecular weight, gravity, etc.

Table 8-2 presents a summary of the hydrocarbon group separation analysis data for both Brookhaven oil and DK-107 oil using the HPLC method. The results of the modified HPLC methods for determining resin content are compared with those of the adsorption method in Table 8-3. Table 8-3 indicates that, taking into account the experimental error involved in determining the resin content of a crude by conventional adsorption method, and the error involved in determining the polars content of a crude by the HPLC method, the fraction called "resins" becomes nearly equal to the fraction called "polars" if the difference between the amount of n-pentane and n-hexane asphaltenes is deducted from the amount of polars.

Samples of n-pentane, n-hexane, and n-heptane flocculated asphaltenes from both crude oils were prepared and run through a waters GPC (gel permeation chromatograph). The obtained particle size distribution of Brookhaven oil samples were normalized in order to compare them with the predicted particle size distribution by the proposed CT model. Figure 8-3 shows a comparison between the experi-

TABLE 8-3

Comparison of crude oil resin content by adsorption and HPLC methods

Crude oil	Resin content by adsorption (wt%)	Polars content by HPLC (wt%)	Resin content [a] by HPLC (wt%)
Brookhaven	4.59 ± 0.12 [b]	5.24 ± 0.06	4.84 ± 0.23
DK-107	8.30 ± 0.27	9.25 ± 0.08	8.73 ± 0.14

[a] The resin content by HPLC is obtained by deducting the difference of the n-C_5 and n-C_6 asphaltenes from the polars content by HPLC. The n-C_5 asphaltenes are 1.65 ± 0.05 wt% and 1.05 ± 0.03 wt%, respectively, for Brookhaven and DK-107 oils. The n-C_6 asphaltenes are given in Table 8-2.
[b] A minimum of three measurements for each data point were made to determine the precision, which was taken as the average distance from the mean.

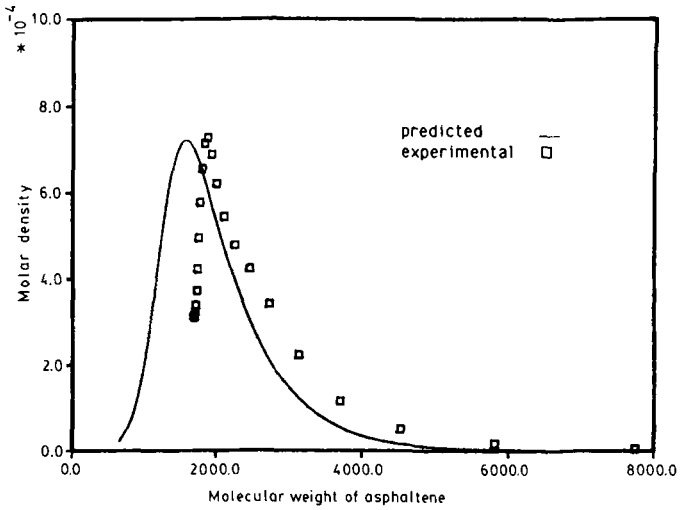

Fig. 8-3. Comparison of experimental and predicted asphaltene molecular weight distributions. The asphaltenes were flocculated from Brookhaven oil with *n*-pentane using the standard method ASTM D-3279-83.

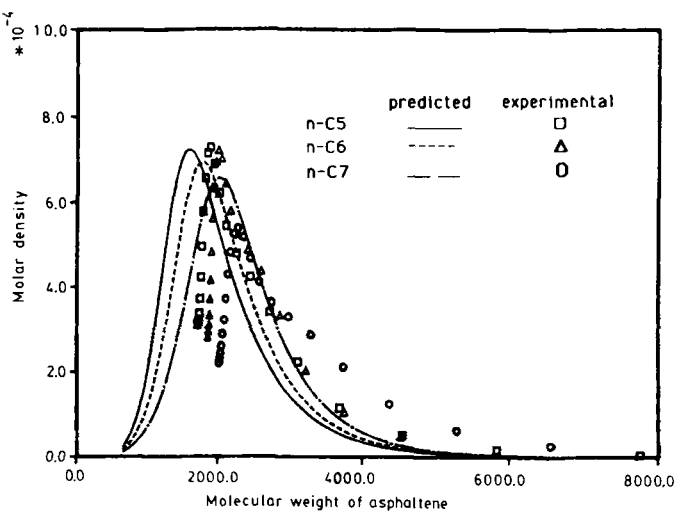

Fig. 8-4. Comparison of experimental and predicted asphaltene molecular weight distributions. The asphaltenes were flocculated from Brookhaven oil with different *n*-paraffins using the standard method ASTM D-3279-83.

mental and predicted molecular weight distributions of *n*-pentane asphaltene. The molecular size distributions for the different flocculant carbon number are plotted in Fig. 8-4. Inasmuch as the experimental molecular size distributions were determined relative to narrow dispersity polystyrene standards, the comparisons should focus on the trend of molar density with respect to molecular weight and functional

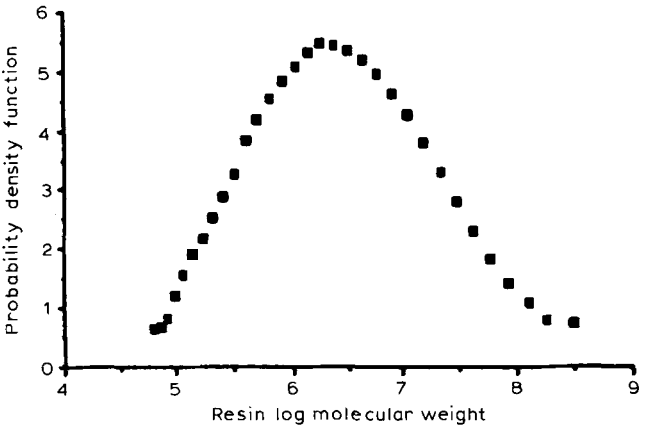

Fig. 8-5. Resin molecular weight distribution of Brookhaven oil as determined by gel permeation chromatography (GPC).

relationship of the flocculant carbon number. The Brookhaven oil resins were run through the GPC and their molecular weight size distribution was obtained; these data are shown in Fig. 8-5. This is a standard normal distribution and, as a result, it indicates that, with respect to size, resins distribute evenly around their mean in the crude oil.

Effective separation of asphaltenes and especially resins from crude oil for further analysis is a major stumbling block in the characterization process. Katz and Beu [51] and Swanson [19] demonstrated that once the desorption equilibrium of the resins between the solid and liquid phases is disturbed, i.e., by adding paraffin solvent, the asphaltene particles flocculate irreversibly. This means that in order for them to flocculate they grow in size and, as a result, their apparent molecular weight changes. If the flocculated asphaltenes are redissolved in a good solvent, i.e., benzene or toluene, after some time passes they begin to grow in size again. However, if the asphaltenes are redissolved in benzene (or other appropriate solvent) that contains enough resins for complete peptization, then the particles remain permanently peptized and do not grow in size. This suggests that any experimental work that is destined for characterizing asphaltenes as they exist in the original oil should be performed while the asphaltene particles are still peptized as Fig. 8-4 depicts, if the data are to correspond to the original asphaltene particles.

The resin behavior is different because the resin molecules are in true solution in the original oil and so the problem of aggregation does not exist. Thus, the resins can be separated from the original oil and subjected to reasonably severe experimental analysis without any alteration to their molecular size and structure. This is a bonus from nature, because, in certain situations, accurate resin thermodynamic properties are needed for predicting asphaltene flocculation by the SC model.

THE ONSET AND AMOUNTS OF ORGANIC DEPOSITION

Using the proposed CT, SC, and FA models described, one is able to predict the onset and amount of organic (asphaltene) deposition from petroleum crudes. Table 8-4 contains experimental and predicted data (by the SC model) regarding the onset of asphaltene deposition due to different precipitating solvents. The experimental data are for an oil sample reported in Hirschberg et al. [49]. Table 8-4 shows the results of the three computer runs based on the SC model, assuming that the entire asphaltene content is in colloidal state. In each computer run one set of experimental data is used to fit the model and rest is predicted. It should be pointed out that the *n*-heptane-fitted runs make the worst predictions, whereas the *n*-hexadecane and *n*-dodecane runs make rather good predictions. Using the CT model, the amounts of asphaltene deposition are predicted and they are compared with the same experimental data in Table 8-5. According to this table, all the onsets and amounts of asphaltene deposition (except for *n*-heptane case) are in close agreement with the experimental data. In Table 8-6, the CT-model-predicted amounts of asphaltene deposition for different normal paraffin solvents are listed along with experimental titration data for Brookhaven oil which is generated in the authors' laboratory. By comparing the predicted values of amount of asphaltene deposition with the experimental data, one notices that the CT model provides a fairly good prediction. Results shown in Tables 8-4, 8-5, 8-6 can be explained by our proposed CT and SC models. According to Tables 8-4 and 8-5, the required amount of the miscible flocculant to arrive at the onset decreases as the molecular

TABLE 8-4

Experimental [40] and predicted onset data

Solvent	Predicted onsets		Experimental onsets	
	(mol)	(cm^3/g oil)	(mol)	(cm^3/g oil)
Hexadecane experimental onset used for fitting the model (amount of hexadecane added at the onset is 75.3 mol)				
Pentane	309	1.6	–	>1.3
Heptane	169	1.1	210	1.4
Decane	158	1.4	158	1.4
Dodecane	124	1.3	125.8	1.3
Dodecane experimental onset used for fitting the model (amount of dodecane added at the onset is 125.8 mol)				
Hexadecane	76.3	1.0	75.3	1.0
Pentane	316	1.6	–	>1.3
Heptane	172	1.2	210	1.4
Decane	160	1.4	125.8	1.4
Heptane experimental onset used for fitting the model (amount of heptane added at the onset is 210 mol)				
Decane	194	1.72	158	1.4
Dodecane	150	1.55	125.8	1.3
Hexadecane	92.3	1.23	75.3	1.0
Pentane	349	1.83	–	>1.3

TABLE 8-5

The experimental vs. prediction for the onset and amount of asphaltene deposition from the tank oil [a]

Dilution ratio (cm^3 diluent/g tank oil)	n-C_5		n-C_6		n-C_{10}	
	exp.	cal.	exp.	cal.	exp.	cal.
1.35	–	–	–	–	–	OF
1.40	–	–	–	OF	OF	–
1.90	NT	OF	–	–	–	–
2.22	–	–	OF	–	–	–
5	–	3.31	1.53	1.52	1.34	1.30
10	3.61	3.67	1.82	2.28	1.45	1.53
20	3.79	3.75	1.89	2.43	1.50	1.45
50	3.87	3.73	1.87	2.29	–	1.13

[a] The experimental titration data (wt% tank oil) are taken from Botet and Jullien [40].
Exp.: experimental values; cal.: calculated values; OF: onset of flocculation; NT: onset of asphaltene deposition is not determined.

TABLE 8-6

The amount of asphaltene flocculated by titration of Brookhaven oil with n-paraffins [a]

Flocculant	Asphaltene (wt%)	
	exp.	cal.
n-Pentane	1.65	1.41
n-Hexane	1.25	1.23
n-Heptane	0.95	0.99
n-Decane	0.72	0.69
n-Dodecane	0.60	0.63
n-Hexadecane	0.52	0.49

[a] The experimental data are taken from Leyvraz and Tschudi [39].
Exp.: experimental values; cal.: calculated values.

weight of the miscible solvent increases. This trend can be explained by the views of the SC model. In hydrocarbon mixtures (as in most cases), size difference between the components is a major factor affecting their solubility. In this case, resins are expected to be more soluble in heavier than in lighter paraffins. As a result, the required amount of flocculant for arriving at the onset will be inversely proportional to the flocculant molecular weight, provided that the amount of resins that needs to be desorbed from the asphaltenes in order to arrive at the onset is constant regardless of the flocculant used.

According to Tables 8-5 and 8-6, the tendency toward amounts of asphaltene deposition decreases as the molecular weight of the miscible flocculant increases. However, this tendency can be explained by views of the CT model. Inasmuch as the high-molecular-weight molecules are less soluble in lower-molecular-weight solvents, the amount of asphaltene deposition by the lower-molecular-weight solvent

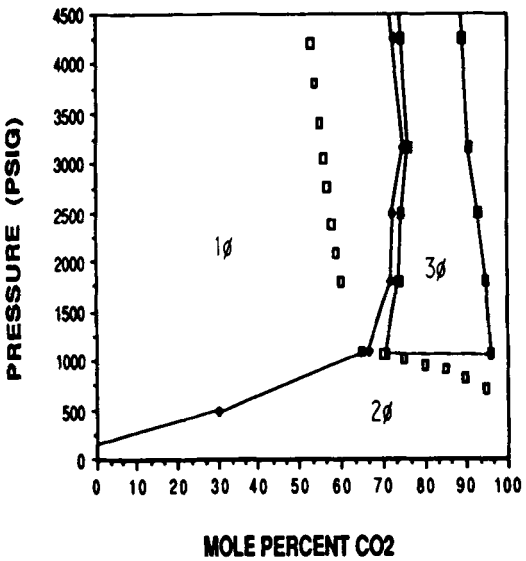

Fig. 8-6. Phase diagram for mixtures of Brookhaven stock-tank oil and carbon dioxide at 317 K. Region 1ϕ is the homogeneous liquid phase area, 2ϕ is the vapor–liquid phase equilibrium area, 3ϕ is the liquid–solid–vapor phase area. The region to the right of the vertical hollow square tick marks and to the top of the horizontal hollow square tick marks is the predicted 3ϕ region. Experimental data are taken from Leyvraz [45].

is higher, because the average molecular weight of an oil is lowered upon mixing with this low-molecular-weight paraffin. This can also be expected because the lower-molecular-weight paraffins are more lyophobic with reference to asphaltenes, and, therefore, separate them more completely. The proposed CT and SC models can also be applied to the prediction of the pressure/composition region of asphaltene deposition at high pressure under the influence of a miscible gas. Figure 8-6 shows the predicted (by CT model) pressure/composition region of asphaltene deposition from Brookhaven oil. The experimental data are taken from Monger and Fu [52]. There is a good agreement between the experimental and predicted 3ϕ (vapor–liquid–solid phase) envelopes. Similar comparisons between experimental and predicted data were made using the FA model. Figure 8-7 shows a comparison between the size distributions of asphaltene clusters for different phases: (a) is for the precipitated asphaltene phase and (b) is for the liquid phase. This has been done for the stock tank oil reported by Monger and Fu [52]. Figure 8-8 shows the effect of carbon number of miscible solvent on the amount of asphaltene deposition from Brookhaven oil. One can notice a fairly good agreement between predicted and experimental data. Figure 8-9 shows the effect of the solubility parameter of solvent on the amount of asphaltene deposition. Again a satisfactory agreement between experimental and predicted data is observed. The FA model can also be applied to the prediction of the pressure/composition region of asphaltene deposition at high pressures under the influence of a miscible gas. Figure 8-10 shows these

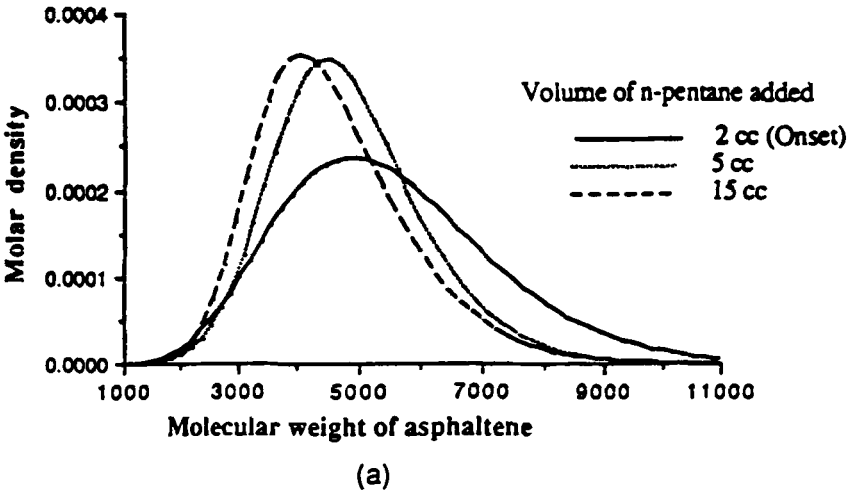

(a)

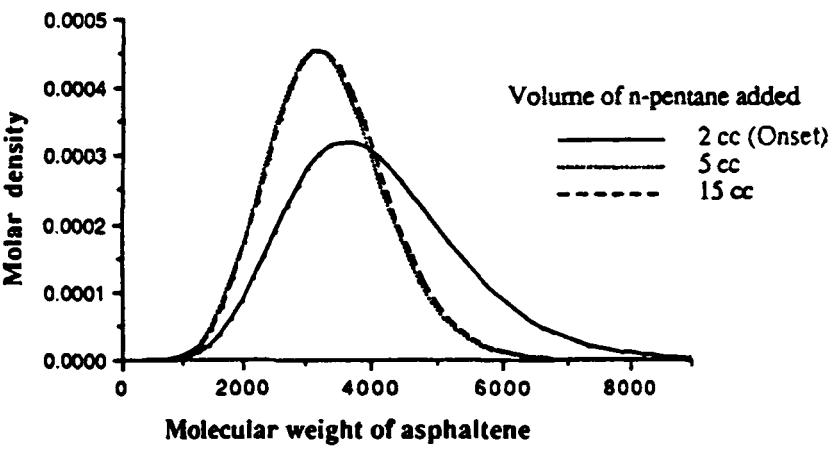

(b)

Fig. 8-7. Comparison of the size distributions of asphaltene clusters for different phases: (a) is for the precipitated asphaltene phase and (b) is for the liquid phase.

predicted data along with the experimental data reported by Monger and Fu [52] for Brookhaven crude oil. From this figure one can see a good agreement between predicted and experimental data.

Overall, the proposed models (CT, SC and FA) are general enough to be used successfully to predict the phase behavior of heavy organic deposition from the petroleum crudes under the influence of miscible solvents.

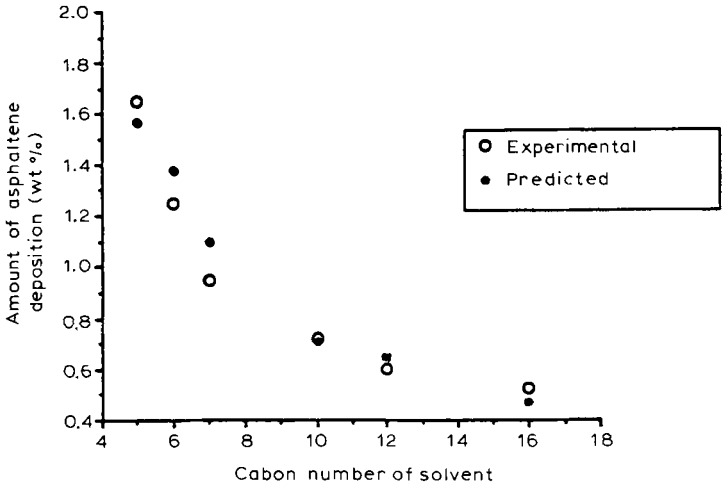

Fig. 8-8. Effect of the carbon number of miscible solvent on the amount of asphaltene deposition from Brookhaven oil.

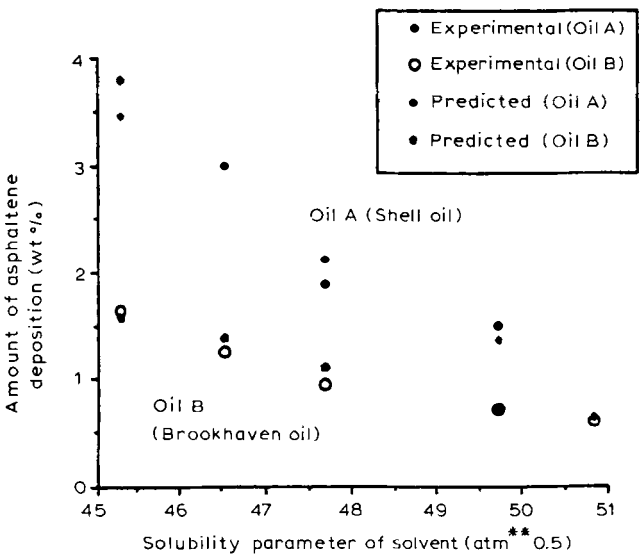

Fig. 8-9. Effect of solubility parameter of solvent on the amount of asphaltene deposition.

HEAVY ORGANIC DEPOSITION IN PRODUCING WELLS AND TRANSPORT PIPELINES [53]

The models described above are general enough to predict the onset and amounts of deposition of heavy organics from petroleum fluids under the influence of a miscible solvent. However, when crude oils are being produced, precipitation may occur in the production tubing-string. In this case, the onset and amounts of heavy organic

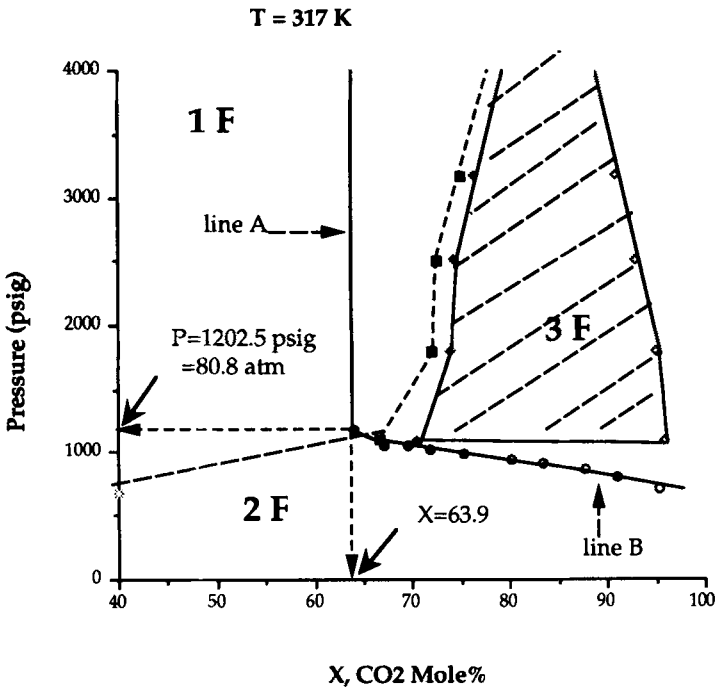

Fig. 8-10. Phase diagram for mixtures of Brookhaven stock-tank oil and carbon dioxide at 317 K. Region *1F* is the homogeneous liquid phase area, *2F* is the vapor–liquid phase area, and *3F* is the liquid–vapor–solid phase area. The region to the right of the line *A* and to the top of line *B* is the predicted *3F* region by the FA model. The shaded area is the experimental *3F* region. The experimental data are taken from Monger and Fu [52].

deposition do not depend solely on the composition of the miscible solvent injected into the reservoir. Deposition of heavy organics in the production tubing-string will be the result of a combined multi-phenomena effect. This multi-phenomena effect makes the deposition mechanism of heavy organics inside the well more complex than the mechanism described in the previous models. Also, heavy organic deposition may occur in the transport pipelines which may not be induced solely by addition of a miscible solvent but rather by a combination of different phenomena (i.e., streaming potential, flow regime, temperature drops, diffusion effects, etc). Therefore, a different approach in the modeling of heavy organic deposition in oil-producing wells and oil-transport pipelines is required in order to account for the different effects leading to this undesirable problem. Prediction of any potential deposition inside the wells and transport pipelines is crucial considering the fact that, from the economical standpoint, there is a need for a continuous supply of petroleum fluids to the refineries. Therefore, one may think of oil-producing wells and oil-transport pipelines as the arteries of the fossil fuel industry through which the revenues of a given company are controlled. However, the proper performance of these arteries is hindered by a number of problems arising according to the

quality of the fluids flowing through them. Among these problems, the one of major concern is indeed the heavy organic (asphaltene–paraffin/wax) deposition, which in extreme cases may render in a disastrous complete plugging of these flow channels.

In some wells and pipelines, the primary heavy organic deposition is mainly comprised of paraffin/wax. There exists an abundance of information reported in the literature regarding this type of deposition and its treatment. However, in most cases the heavy organic deposition will be much more complex than a classical solid-liquid phase transition such as that followed by paraffin/wax during their segregation from the liquid phase. In this case, there is a need for more detailed analyses of the heavy organic deposits and petroleum fluids to determine their nature and phase behavior in order to provide and/or devise preventive techniques. Thus, a primary aspect one must focus on is the determination of the causes leading to heavy organic deposition.

Asphaltene particles are electrically charged, and thus they can be precipitated by application of an electrical potential. This suggests that application of a counter-potential may prevent the precipitation of asphaltenes. It has been observed that the electrical interactions with the conduit walls can disturb the stabilizing electrical forces around the asphaltene micelles causing aggregation of the asphaltene particles. When crude oil is being produced or transported, a streaming potential is generated due to the charged character of this colloidal particles which has been found to assist their flocculation by neutralizing the weak asphaltene charges [54]. It has also been found that the generated streaming potential is a function of the flow regime, pipe-wall conductivity, physical properties of the suspending media, and of size, shape and electrical properties of the asphaltene particles [23]. Lichaa and Herrera [1] found that the amount of asphaltene deposition due to electrical effects is a function of temperature as well. The streaming potential has a direct effect on the diffusivity of asphaltene particles to the walls, which combined with Brownian and Eddie (if turbulent flow) diffusivity effects can render in a disastrous heavy organic deposition. Roughness of pipe-wall surface plays, also, an important role in the heavy organic deposition. A very rough surface may be sufficient to initiate the deposition process and trigger simultaneously the effect of other phenomena. Another important phenomenon is the appearance of paraffin/wax crystals at the cloud point of a petroleum fluid. Large and soft paraffin/wax crystals appear to serve as nuclei about which asphaltene particles deposit.

Interesting observations were made after an analysis of the experimental and field data collected from oil wells prone to heavy organic deposition in the Tecoaminoacan and Jujo fields (Mexico). In this Mexican oil-producing area, the heavy organic deposition problem was severe affecting the production of light crude oil; in extreme cases it resulted in complete plugging of some of the wells [55,56]. This fields are produced by primary mechanisms (i.e., no fluids are injected into the reservoir) and, therefore, deposition is not induced by the addition of miscible solvents. Experimental data collected for a crude oil and a heavy-organic deposit from the same crude are presented in Table 8-7. A thorough analysis of these data allowed to conclude that the streaming potential generated during production of this crude oil was high enough to cause flocculation of the asphaltene particles. This generated streaming

TABLE 8-7

Characterization of crude and deposit from well T-127 of Tecoaminoacan field [56]

Elemental analysis	Crude AT-127	Organic deposit DT-127
Carbon (wt%)	86.1	84.5
Hydrogen (wt%)	12.5	8.6
Nitrogen (wt%)	0.4	0.4
Iron (ppm)	<1	267.0
Copper (ppm)	<1	3.0
Nickel (ppm)	<1	20.0
Vanadium (ppm)	1	171.0
Zinc (ppm)	<1	6.0
Specific gravity (20/4°C)		0.837
API gravity (°)	36.7	
Viscosity sus., at 60°F	45.2	
at 70°F	42.2	
at 77°F	41.0	
Pour point (°C)	−30	
Sulfur (wt%)	0.9	2.9
n-C_5 asphaltenes	1.5	42.0
Solubles (wt%)	89.7	48.0
saturated (wt%)	52.3	42.1
aromatics (wt%)	37.4	5.1
resins or polars (wt%)	8.8	10.0

TABLE 8-8

Estimated values for the generated streaming potential

Production rate (m^3/day)	U_{avg} (m/s)	Potential E (V)
200	0.51	13.1
443 (field data)	1.132	52.7864
600	1.532	88.6889
800	2.044	146.883
1000	2.555	216.847

potential was estimated as shown in Table 8-8. In these calculations it was assumed a asphaltene-particle diameter of 2700 Å (i.e., precipitated asphaltenes), and a normal pipe wall conductivity. Therefore, the actual values of this streaming potential are expected to be at least two to three orders of magnitude higher. An interesting observation was made after having analysed the field data collected for thirteen wells in which the heavy organic deposition was severe. These data are presented in Fig. 8-11. These data suggest a linear relationship between the bubble point pressure depth and depth at which the organic deposits are found. For the majority

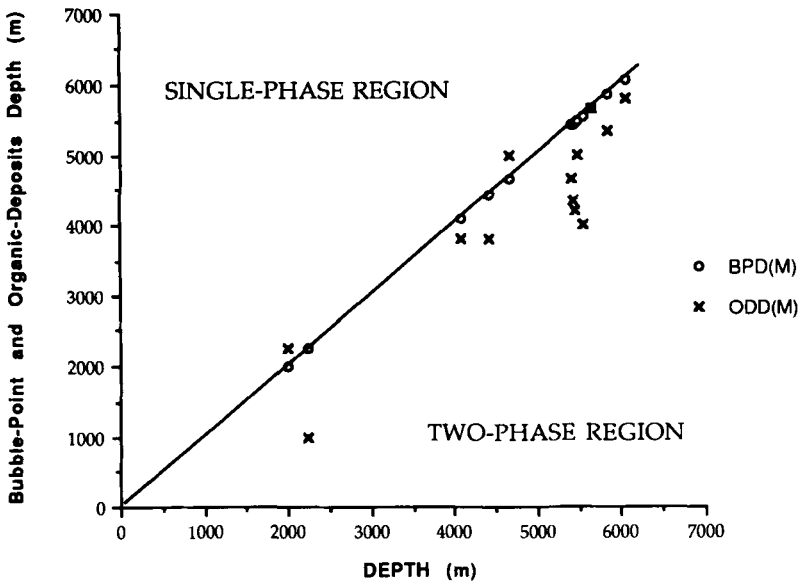

Fig. 8-11. Comparison between depth at which the bubble point (BPD) occurs and depth at which the organic deposits (ODD) are found.

of these wells, the organic deposits are found after the bubble point pressure has been reached (i.e., two-phase region). This suggests that the appearance of a gas phase somehow enhances the deposition process and its effect becomes critical at a certain distance after the bubble point in the two-phase region. After a thorough analysis of the data collected, it was concluded that a good model for the heavy organic deposition in oil-producing wells must incorporate the combined effects of the generated streaming potential, fluid dynamics (i.e., compressible character of crude oil), and temperature and pressure drops on the asphaltene aggregation rate and on asphaltene particle diffusivity towards the wall. This way one will be able to predict the location and amount of heavy organic deposition inside the well and/or transfer pipeline.

CONCLUSIONS

The proposed models for heavy organic deposition from petroleum crudes are based on two different facts. In the CT model, the heavy organics are considered to be dissolved in an oil which may or may not form a solid phase depending on the thermodynamic conditions of temperature, pressure, and composition. In the SC model, heavy organics are considered as solid particles of different sizes suspended colloidally in the oil and stabilized by large polymeric molecules (i.e., resins) adsorbed on their surface. In the FA model, incorporation of the CT and SC models is made and the fractal aggregation theory of colloidal growth is employed.

This model considers the asphaltenes to be partly dissolved and partly in the colloidal state; thus it accounts for both the solubility and colloidal effect of heavy organics in light components. The proposed CT, SC and FA models can provide the tool for making satisfactory prediction of the phase behavior of heavy organic deposition.

Because the asphaltene deposition problem is so elusive, it seems that before one can formulate a comprehensive model describing the problem, the true asphaltene deposition mechanism must be clearly understood and backed by field and experimental data; then an accurate and representative model can be formulated. The objective here is to develop a comprehensive model which can describe properly the mechanism of heavy organic deposition inside the oil reservoir, production wells, transport pipelines, etc. Utilization of kinetic theory of fractal aggregation has enabled the development of the FA model. This model allows to describe properly several situations, such as phase behavior of heavy organic deposition, growing mechanism of the heavy organics, the geometrical aspects of aggregates, the size distributions of precipitated deposits, and the solubility of heavy organics in the solution under the influence of a miscible solvent. In general, the proposed models are applicable to the prediction of heavy organic deposition (asphaltene, paraffin/wax, resin) from petroleum crudes due to changes in pressure, temperature and composition. Further modeling must involve the prediction of the location and amount of heavy organic deposition inside the producing wells and oil-transport pipelines.

ACKNOWLEDGEMENTS

The authors would like to thank the financial support from IMP (Mexican Petroleum Institute), ARCO, UNDP and Nova-Husky.

REFERENCES

[1] Lichaa, P.M. and Herrera, L., Electrical and other effects related to the formation and prevention of asphaltene deposition. *Proc., Int. Symp. on Oilfield Chemistry*, Dallas, Tex., January (1975)

[2] Mansoori, G.A. and Jiang, T.S., Asphaltene deposition and its role on enhanced oil recovery. *Proc., 3rd European Conf. on Enhanced Oil Recovery*, Rome (1985).

[3] Stalkup, F.I., *Miscible Displacement. SPE Monograph*. Society of Petroleum Engineers, Richardson, Tex., pp. 137–151 (1983).

[4] Leontaritis, K.J. and Mansoori, G.A., Asphaltene deposition: a survey of field experiences and research approaches. *J. Pet. Sci. Eng.*, 1: 229–239 (1988).

[5] David, A., Asphaltenes flocculation during solvent simulation of heavy oils. *Am. Inst. Chem. Eng., Symp. Ser.*, 68(127): 56, 58 (1973).

[6] Monger, T.G. and Khakoo, A., The phase behavior of CO_2-Appalachian oil systems. *SPE 10269, Soc. Pet. Eng.* (1981).

[7] Orr, F.M., Yu, A.D. and Lien, C.L., The phase behavior of CO_2 and crude oil in Low Temperature Reservoirs. *SPE 8813, SPE/DOE 1st Joint Symp. on EOR*, Tulsa, Okla., April 20–23 (1980).

[8] Preckshot, G.W., Delisle, N.G., Cottrell, C.E. and Katz, D.L., Asphaltic substances in crude oils. *Inst. Min. Metall. Pet. Eng.*, 151: 188–194 (1943).

[9] Shelton, D.A. and Yarborough, L., Multiple phase behavior in porous media during CO_2 or rich gas flooding. *J. Pet. Technol.*, 29: 1171 (1977).

[10] Kim, S.T., Boudh-Hir, M.E. and Mansoori, G.A., The role of asphaltene in wettability reversal. *SPE 20700, Proc., 1990 Annu. Conv. Soc. Pet. Eng.* (1990).
[11] Park, S.J. and Mansoori, G.A., Organic deposition from heavy petroleum crudes (a fractal aggregation theory approach). *Proc., UNITAR/UNDP 4th Int. Conf. on Heavy Crudes and Tar Sands*, Edmonton, Alta., August (1988).
[12] Cole, R.J. and Jessen, F.W., Paraffin deposition. *Oil Gas J.*, 58: 87 (1960).
[13] Hirschberg, A., The role of asphaltenes in compositional grading of a reservoir's fluid column. *SPE 13171, Soc. Pet. Eng.* (1984).
[14] Hunt, Jr., E.B., Laboratory study of paraffin Deposition. *J. Pet. Technol.*, 225: 1259 (1962).
[15] Lhioreau, C., Briant, J. and Tindy, R., Influence de la pression sur la flocculation des asphaltenes. *Rev. Inst. Fr. Pét.*, 22: 797 (1967).
[16] Shock, D.A., Sadbury, J.D. and Crockett, J.S., Studies of the mechanism of paraffin deposition and its control. *J. Pet. Technol.*, 7(9): 23 (1955).
[17] Speight, J.G., Long, R.G. and Trawbridge, T.D., Factors influencing the separation of asphaltenes from heavy petroleum feedstocks. *Fuel*, 63(5): 616 (1984).
[18] Nellensteyn, F.I., The colloidal structure of bitumens. In: A.E. Dunston. (Editor), *The Science of Petroleum, Vol. 4.* Oxford University Press, London, pp. 2760–2764 (1938).
[19] Swanson, J., A contribution to the physical chemistry of the asphalts. *J. Phys. Chem.*, 46: 141–150 (1942).
[20] Witherspoon, P.A. and Munir, Z.A., Size and shape of asphaltic particles in petroleum. *Prod. Mon.*, 24: 20–31 (August, 1960).
[21] Dickie, J.P. and Yen, T.F., Macrostructures of asphaltic fractions by various instrumental methods. *Anal. Chem.*, 39: 1847 (1967).
[22] Koots, J.A. and Speight, J.C., Relation of petroleum resins to asphaltenes. *Fuel*, 54: 179 (1975).
[23] Leontaritis, K.J. and Mansoori, G.A., Asphaltene flocculation during oil recovery and processing: A thermodynamic–colloidal model. *SPE 16258, Proc. 1987 Soc. Pet. Eng. Symp. on Oil Field Chemistry*, Richardson, Tex. (1987).
[24] Leontaritis, K.J., Mansoori, G.A. and Jiang, T.S., Asphaltene deposition in oil recovery: A survey of field experiences and field approaches. *Proc. Int. Conf. on Advanced Technology*, De Kalb, Ill., April (1986).
[25] Kawanaka, S., Park, S.J. and Mansoori, G.A., The role of asphaltene deposition in EOR gas flooding: A predictive technique. *SPE/DOE 17376, Proc. 1988 SPE/DOE Enhanced Oil Recovery Symp.*, Tulsa, Okla., April 17–20, p. 617 (1988).
[26] Mansoori, G.A., Jiang, T.S., Kawanaka, S., Asphaltene deposition and its role in petroleum production and processing. *Arab. J. Sci. Eng.*, 13: 17 (1988).
[27] Chorn, L.G. and Mansoori, G.A. (Editors), C_7 + *Fraction Characterization. Advances in Thermodynamics, Vol. I.* Taylor and Francis, New York, N.Y., pp. 57–78 (1988).
[28] Benmekki, E.H. and Mansoori, G.A., Pseudoization technique and heavy fraction characterization with equation of state models. *Adv. Thermodyn.*, 1: 57–78 (1989).
[29] Mansoori, G.A. and Chorn, L.G., Multicomponent fraction characterization. *Adv. Thermodyn.*, 1: 1–11 (1989).
[30] Scott, R.L. and Magat, M., Thermodynamics of high polymer solutions. *J. Chem. Phys.*, 13: 172 (1945).
[31] Scott, R.L., Thermodynamics of high-polymer solutions: II. The solubility and fraction of a polymer of heterogeneous distribution. *J. Chem. Phys.*, 13: 178 (1945).
[32] Du, P.C. and Mansoori, G.A., A continuous mixture computational algorithm for reservoir fluids phase behavior. *SPE 15082, Proc. 1986 Calif. Reg. Meet. Soc. Pet. Eng.*, Richardson, Tex. (1986).
[33] Mansoori, G.A., Du, P.C. and Antoniades, E., Equilibrium in multiphase polydisperse fluids. *Int. J. Thermophys.*, 10(6): 1181–1204 (1989).
[34] Park, S.J. and Mansoori, G.A., Aggregation and deposition of heavy organics in petroleum crudes. *Int. J. Energy Sources*, 10(6): 109–125 (1988).
[35] Leontaritis, K.J., Kawanaka, S. and Mansoori, G.A., Descriptive accounts of thermodynamic and colloidal models of asphaltene flocculation. In: *Proc. Symp. on Advances in Oil Field Chemistry*, 33(1): 196–204 (1988).

[36] Kawanaka, S., Leontaritis, K.J., Park, S.J. and Mansoori, G.A., Thermodynamic and colloidal models of asphaltene flocculation. In: J.K. Borchardt and T.F. Yen, *Oil Field Chemistry. ACS Symposium Series 396*. American Chemical Society, Washington, D.C., pp. 443–459 (1989).

[37] Botet, R., Jullien, R. and Kolb, M., Hierarchical model for irreversible kinetic cluster formation. *J. Phys. A: Math. Nucl. Gen.*, 17: L75 (1984).

[38] Smoluchowski, V.M., Dreo Vortraege ueber Diffusion, Brownsche Molekular bewegung und Koagulation von Kolloidteilchen. *Phys. Z.*, 17: 593 (1916).

[39] Flory, P.J., *Principles of Polymer Chemistry*. Cornell University Press, New York, N.Y. (1953).

[40] Leyvraz, F. and Tschudi, H.R., Singularities in the kinetics of coagulation process. *J. Phys. A: Math. Nucl. Gen.*, 14: 3389 (1981);

[41] Leyvraz, F. and Tschudi, H.R., Singularities in the kinetics of coagulation process. *J. Phys. A: Math. Nucl. Gen.*, 15: 1951 (1982).

[42] Botet, R. and Jullien, R., Size distribution of clusters in irreversible kinetic aggregation. *J. Phys. A: Math. Nucl. Gen.*, 17: 2517 (1984).

[43] Jullien, R., Kolb, M. and Botet, R., Scaling properties of growth by kinetic clustering. In: F. Family and D.P. Landau (Editors), *Kinetics of Aggregation and Gelation*. North-Holland, Amsterdam, p. 101 (1984).

[44] Ernst, M.H. and Hendriks, E.M., Smoluchowski's equation with surface interaction and exponents in the cluster size distribution. In: F. Family and D.P. Landau (Editors), *Kinetics of Aggregation and Gelation*. North-Holland, Amsterdam, pp. 225–228 (1984).

[45] Leyvraz, F., Critical exponents in Smoluchowski's equations of coagulation. In: F. Family and D.P. Landau (Editors), *Kinetics of Aggregation and Gelation*. North-Holland, Amsterdam, pp. 201–204 (1984).

[46] Meakin, P., Formation of fractal clusters and networks by irreversible diffusion-limited aggregation. *Phys. Rev. Lett.*, 51(13): 1119–1122 (1983).

[47] Kolb, M., Botet, R. and Jullien, R., Scaling of kinetically growing clusters. *Phys. Rev. Lett.*, 51(13): 1123–1126 (1983).

[48] Leontaritis, K.J. and Mansoori, G.A., Fast crude oil heavy-component characterization using combination of ASTM, HPLC, and GPC methods. *J. Pet. Sci. Eng.*, 2: 1–12 (1989).

[49] Hirschberg, A., de Jong, L.N.J., Schiper, B.A., and Meijers, J.G., *Influence of Temperature and Pressure on Asphaltene Flocculation*. Koninklijke/Shell Exploratie en Productie Laboratorium, Rijswijk, Publ. No. 61 (1983).

[50] Sachanen, A.N., *The Chemical Constituents of Petroleum*. Reinhold, New York, N.Y., pp. 385–427 (1945).

[51] Katz, D.L. and Beu, K.E., Nature of asphaltic substances. *Ind. Eng. Chem.*, 37: 195 (1945).

[52] Monger, T.G. and Fu, J.C., The nature of CO_2-induced organic deposition. *SPE 16713, Proc. 62nd Annu. Tech. Conf. Exhib. Soc. Pet. Eng.*, Dallas, Tex., September 27–30 (1987).

[53] Escobedo, J. and Mansoori, G.A., Heavy organic deposition and plugging of wells (analysis of Mexico's experience). *SPE 23696, Proc. II LAPEC, Soc. Pet. Eng.*, Richardson, Tex., March (1992).

[54] Dykstra, H., Beu, K. and Katz, D.L., Precipitation of asphalt from crude oil by flow through silica. *Oil Gas J.*, 43: 79 (1944).

[55] Garcia, F.H., Silva, P.L. and Lopez, N.A., Causas que originan la depositacion de material asfaltico en pozos del area Cretacica Chiapas–Tabasco., *Ing. Pet.*, September, p. 17 (1989).

[56] Garcia, F.H., Estudio sobre el control de la depositacion organica en pozos del area Cretacica Chiapas–Tabasco (Metodo correctivo). *Ing. Pet.*, July, p. 39 (1989).

This page intentionally left blank

Asphaltenes and Asphalts, 1. Developments in Petroleum Science, 40
edited by T.F. Yen and G.V. Chilingarian

Chapter 9

THE ADSORPTION OF ASPHALTENES AND RESINS ON VARIOUS MINERALS

GASPAR GONZÁLEZ and MARIA BÁRBARA C. MOREIRA

INTRODUCTION

Asphaltenes and resins are the polar fractions of crude oil and bitumen that can be precipitated by the addition of low-molecular-weight alkanes. The fractions are formed by molecules containing paraffinic, naphthenic or aromatic hydrocarbons and functional groups containing oxygen, nitrogen or sulphur. Owing to this amphiphilic structure, these compounds possess the ability to aggregate and adsorb to the interfaces. Asphaltenes and resins adsorb onto minerals primarily by interactions between their functional groups and the polar groups present on the mineral surface. The adsorption may be very important for oil production as it may induce changes in wettability that are detrimental for residual oil recovery by the injection of water or aqueous fluids into the reservoir [1]. On the other hand, it is well established that fine particles showing partial wettability by water and oil collect at the oil–water interface stabilizing water-in-oil or oil-in-water emulsions depending on the contact angle at the solid-water-oil contact region [2]. Particles produced or removed and transported from the reservoir wells during oil production, therefore, may contribute to the stabilization of the water-in-crude oil emulsions normally formed in this process.

In this study, the authors used asphaltenes and resins isolated from shale oil. The Petrosix process [3] for shale oil production, in one of its earlier stages, produced a stream of mixed oil containing nearly 12 wt% of finely divided mineral particles dispersed in the oil. This particulate material is separated using centrifuges and press filters to produce the clean "filtered oil". The filter cake still contained an important amount of oil (nearly 16 wt%) that remained strongly attached to the solid particles. This material is called the "shale oil sludge" and its separation and purification is important in improving the oil recovery and safely disposing of the exhausted particles in the environment. The oil remaining in the shale oil sludge may be extracted using organic solvents, like toluene, to produce an oil fraction, which in this case the authors have called "recovered shale oil". In previous articles [4], the authors have referred to this fraction as "extracted shale oil". The name "recovered shale oil", however, seems less misleading. This oil fraction is primarily formed by all the components that remain attached to the particles after the various stages of the Petrosix shale oil production process are executed.

This study is part of a research project the objective of which is to recover the oil remaining in the shale oil sludge. In this chapter the authors analyze the adsorption

of shale oil polar fractions separated from filtered and/or recovered shale oil, onto different minerals, and how this process influences the accumulation of fines in the oil phases.

EXPERIMENTAL DETAILS

Filtered and extracted shale oil samples

The two samples of oil were extracted from bituminous shale from the Irati Formation oil shale of the São Mateus do Sul deposit, in Paraná, South of Brazil. The filtered oil was the final oil produced by the Petrosix process. The recovered oil was not the oil recovered by this process but that retained by the particles in the filter cake. To separate this oil, the sludge was Soxhlet extracted with toluene followed by evaporation of the solvent. A schematic representation of the stages producing both types of shale oil are shown in Fig. 9-1.

Isolation of asphaltenes and resins

Asphaltenes and resins were isolated from the two samples of shale as described above. The experimental method used was the ASTM 2007 standard procedure. The asphaltene fraction was dissolved in toluene and filtered through a Millipore filter to eliminate insoluble material before use.

Reagents

The organic solvents (*n*-pentane and toluene) and all the chemicals were Analar grade products. The surfactants, which were supplied by Henkel do Brazil Indústrias Químicas, presented more than 98% purity, and were used without further purification. The pH of the aqueous solutions was modified using HCl and NaOH. Distilled water obtained from a Millipore Milli-Q water purifier was used in all cases.

Preparation of the mineral samples

The samples of the various minerals were prepared by the following procedure: big lumps of pure mineral were cut into pieces using a diamond saw and subsequently ground in an agate poulverisette (Fritach), at 1000 rpm for a period of four hours. The powder was divided into three fractions using a set of sieves of 200, 270, 325 and 400 mesh. The fraction +270 to +325 mesh was washed once with an aqueous solution having a pH of 2.8 and twice with distilled water to remove fine particles which might remain deposited on the surface of the larger particles. The sample was finally dried at 105°C in an electric oven (Fanem Ltda, São Paulo, Brazil). This fraction was used for the adsorption tests. Table 9-1 presents the surface area for each mineral sample. The +400 mesh fraction was used for the determination of the electrophoretic mobility. The +325 to +400 mesh fraction was used for the immersion tests.

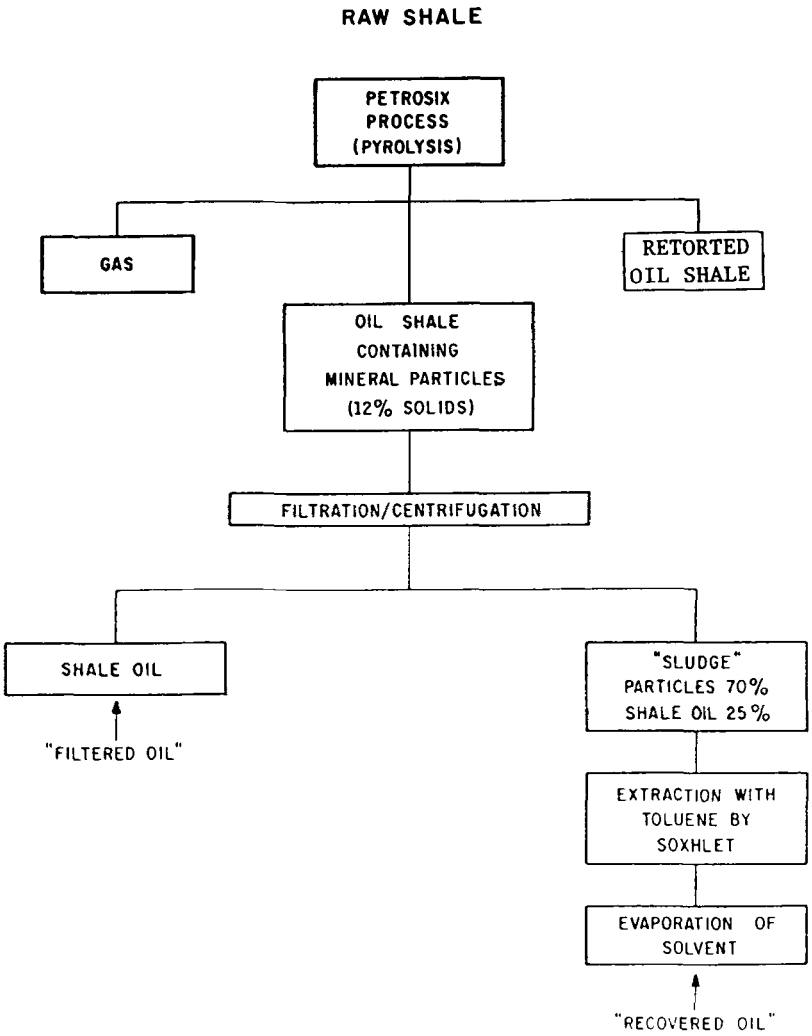

Fig. 9-1. Separation of filtered shale oil and recovered shale oil.

The solid mineral surfaces for contact angle measurements were prepared according to the following procedure: calcite and magnesite were carefully cleaved across their cleavage planes. Quartz and fluorite were cut to an appropriate size using a diamond saw. One face of these square mineral pieces was polished on a rotating plate using a polishing cloth impregnated with cerium oxide polishing powder (particle size: 1–3 μm). The samples were then carefully rinsed with warm distilled (twice) water and treated for five minutes with a solution containing 30% H_2O_2 and 0.1% ammonium hydroxide to remove organic contaminants that may render the surface hydrophobic. Subsequently, the samples were rinsed again with

TABLE 9-1

Surface area and adsorption of extracted shale oil on various minerals

Mineral	Area	Adsorption	
	(m^2/g)	(mg/g)	(mg/m^2)
Kaolin	16.0	25.0	1.56
Smectite	42.0	12.0	0.29
Feldspar	3.20	3.00	0.94
Quartz	1.00	1.00	1.00
Calcite	1.00	2.00	2.00
Hematite	1.20	–	–
Fluorite	1.00	2.00	2.00

double-distilled water and kept immersed in toluene or aqueous solutions, depending on which solvent will be used as the continuous phase for the contact angle measurements. The mica surface was prepared simply by peeling a layer of mineral from the mica surface and leaving the solid specimen immersed in the liquid phase before the contact angle measurement.

EXPERIMENTAL TECHNIQUES

Adsorption

The adsorption of asphaltenes or resins by the mineral samples was determined by measuring the reduction in concentration of the toluene solution of these compounds after a contact period of 4 hours with the minerals. The concentrations were measured at 400 nm using a double beam Shimadzu 240 spectrophotometer. At this wavelength, asphaltenes and resins show a relatively high adsorption although a small shoulder rather than a well defined adsorption peak is observed. This method has been used successfully to determine the adsorption of this type of compounds on solid substrates [5].

In order to assess the effect of surfactants on the asphaltene adsorption, two alternative procedures were followed. In the first case, 0.5 g of quartz was left in contact with 25 ml of a 80 mg/dm^3 asphaltene solution plus different amounts of the various amphiphiles. The final concentration was determined as previously described. In an alternative procedure, the adsorption test was initiated by the same method used to obtain an isotherm, using 10, 50, 100 and 150 mg/dm^3 as initial concentration of asphaltenes. After three hours of contact between the mineral particles and asphaltene solution, a small volume of a concentrated amphiphile solution was added to attain a final amphiphile concentration of 100 mg/dm^3. The final asphaltene concentration was determined following the previously described procedure after another period of three hours.

ELECTROPHORETIC MOBILITY

The electrophoretic mobilities of the mineral samples were measured using an electrophoresis apparatus (Rank Bros., UK) set up with a thin glass cylindrical cell. A stock suspension, containing 200 mg of mineral in 200 ml of 5×10^{-3} mol/dm^3 KNO_3 solution, was prepared using an ultrasonic bath. For each measurement, the pH of the suspension was modified and maintained at a particular value for five minutes, by the addition of HNO_3 or NaOH. The pH was measured again after another period of five minutes and this value was considered the equilibrium pH. Ten measurements of the velocity of the particles were taken for each pH and averaged to calculate the electrophoretic mobility. All measurements were made in a temperature-controlled room at 25°C.

The zeta potentials (ζ) were calculated by the Smoluchowski equation:

$$\zeta \text{ (mV)} = 12.85 \times \text{ mobility } (\mu\text{m s}^{-1})/(\text{V cm}^{-1}) \qquad (9\text{-}1)$$

Immersion tests

The immersion tests were carried out simply by carefully pouring 60 mg of 325–400 mesh mineral powder upon the surface of a liquid contained in a test tube and verifying whether the solid particles penetrated into the liquid phase. In a positive test, the particles sank within a few seconds whereas when immersion was not spontaneous the powder remained on the surface of the liquid almost indefinitely. The tests were made at 25 ± 1°C using aqueous solution with a pH of 5. Methanol, ethanol and mixtures of these solvents with water were used as a liquid phase of different surface tensions.

Contact angles

The contact angles at the mineral–water–oil interface were measured using a NRL Rame Hart Model 100–00 Goniometer by the sessile drop technique. In the experiments in which the effect of pH was studied, water was used as the continuous phase and a drop of toluene was deposited underneath a plate of mineral maintained immersed with its surface parallel to the aqueous surface. In all cases, the contact angle was measured over the aqueous phase, and the asphaltene concentrations were equivalent to the surface saturation values (for quartz and calcite: 200 mg/dm^3; for magnesite and mica: 100 mg/dm^3).

Interfacial tension

The interfacial tension was measured at 25°C using the de Nouy, semi-automatic, ring tensiometer (Kruss GmbH, Hamburg, FRG). In the case of low interfacial tensions (one point for alkaline pH in Fig. 9-9), the authors used a spinning drop apparatus constructed in their laboratory.

RESULTS

Adsorption

Figures 9-2 and 9-3 show the adsorption of asphaltenes and resins extracted from filtered and recovered shale oil onto various minerals. In the case of filtered oil, the curves do not present evidence of surface saturation and their shapes are characteristic of Freundlich adsorption isotherms [6]. The results of Menon and Wasan [7] for asphaltenes extracted from shale oil of Rundle, Australia, show a similar adsorption isotherm. For the extracted oil, the adsorption follows a Langmuir-type isotherm for all the minerals except hematite, leveling off for an equilibrium concentration of the order of 100 mg/dm^3. The surface saturation for the adsorption of asphaltenes are presented in Table 9-1.

The clay minerals kaolin and smectite show a fairly high adsorption per gram; however, when the values are expressed as mg/m^2, these adsorption values may be considered comparable or slightly lower than the values obtained for single minerals such as quartz and calcite, or even feldspar, another aluminosilicate. These values exhibit good agreement with results reported by Marlow et al. [8] for illite, but are lower than the values obtained for well or poorly crystallized kaolin [9]. The highest adsorption for the asphaltenes extracted from shale oil, from Rundle, were also of about 2 mg/m^2 [7,10]. Hematite presented a different behavior. For filtered shale oil, the adsorption reached values between 15 and 20 mg/m^2, which is very high compared with the adsorption observed for other minerals. In the case of extracted oil, the isotherm for hematite differed from the Langmuir-type shape. It showed moderate adsorption for low asphaltene concentrations, followed by a sudden increase and an ill-defined adsorption plateau, higher than those observed for the other minerals and occurring at higher equilibrium concentrations.

Adsorption studies were also carried out for magnesite and fluorite. The results were similar to those obtained for calcite, the maximum adsorption density being between 2.0 and 2.5 mg/m^2.

Effect of non-ionic surfactants on the adsorption process

Figure 9-4 presents the effect of nonyl phenols with different degrees of ethoxylation on the adsorption of asphaltenes on quartz. In the absence of additives, the asphaltenes concentration used for these tests (80 mg/dm^3) is slightly higher than half of the concentration corresponding to the maximum adsorption density. The results indicate that these compounds inhibit the adsorption of asphaltenes and that the degree of ethoxylation is important.

When the surfactant is added after part of the adsorption process has occurred, the products show only a moderate efficiency. As shown in Fig. 9-5, when the concentration of asphaltenes is very low, the non-ionic surfactant dislocate the asphaltene molecules from the solid surface and the final (after six hours) adsorption is lower than the adsorption after three hours. For higher concentration, the final adsorption is always larger or at least equal to that observed in the absence of

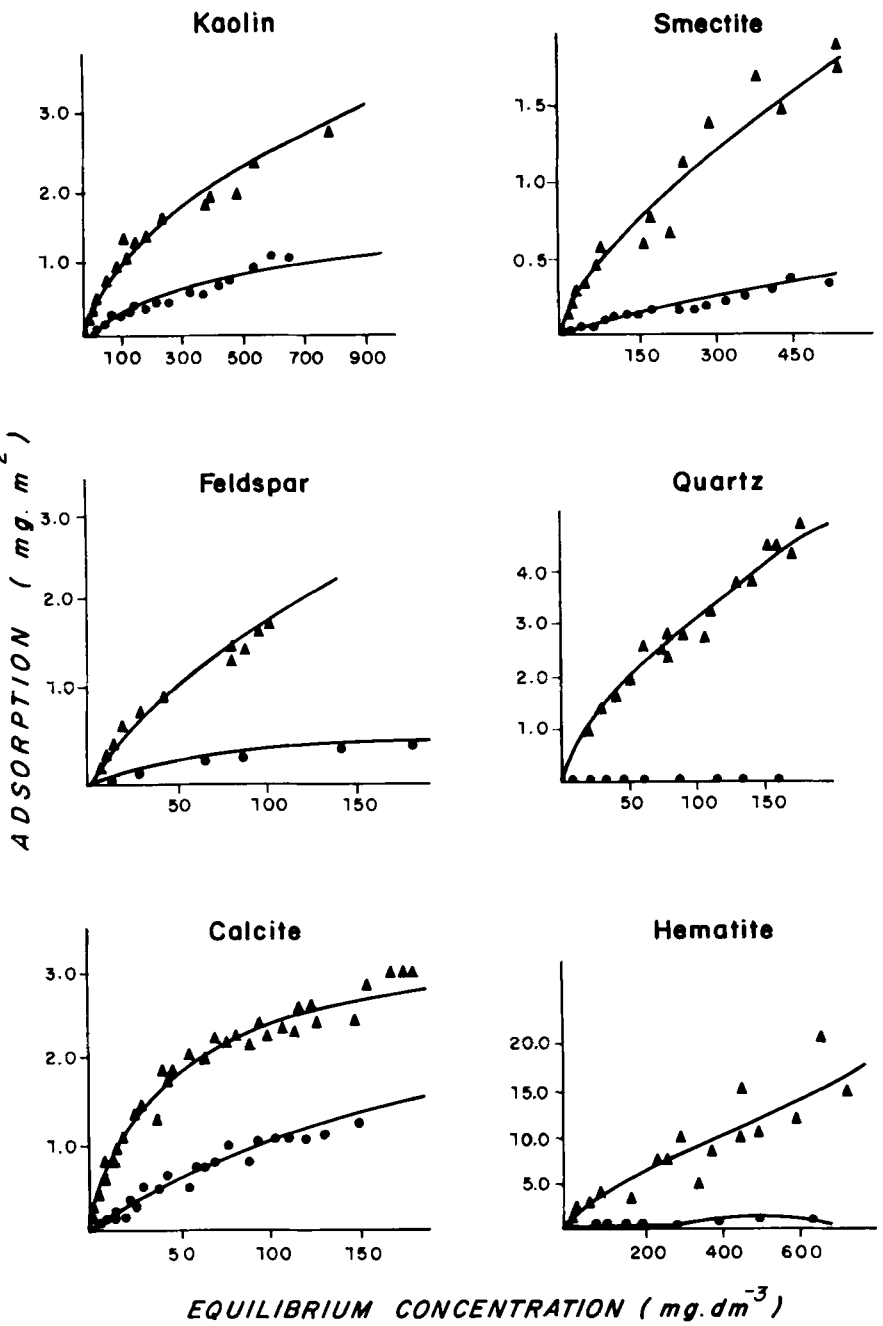

Fig. 9-2. Adsorption of asphaltenes and resins isolated from filtered shale oil on various minerals.

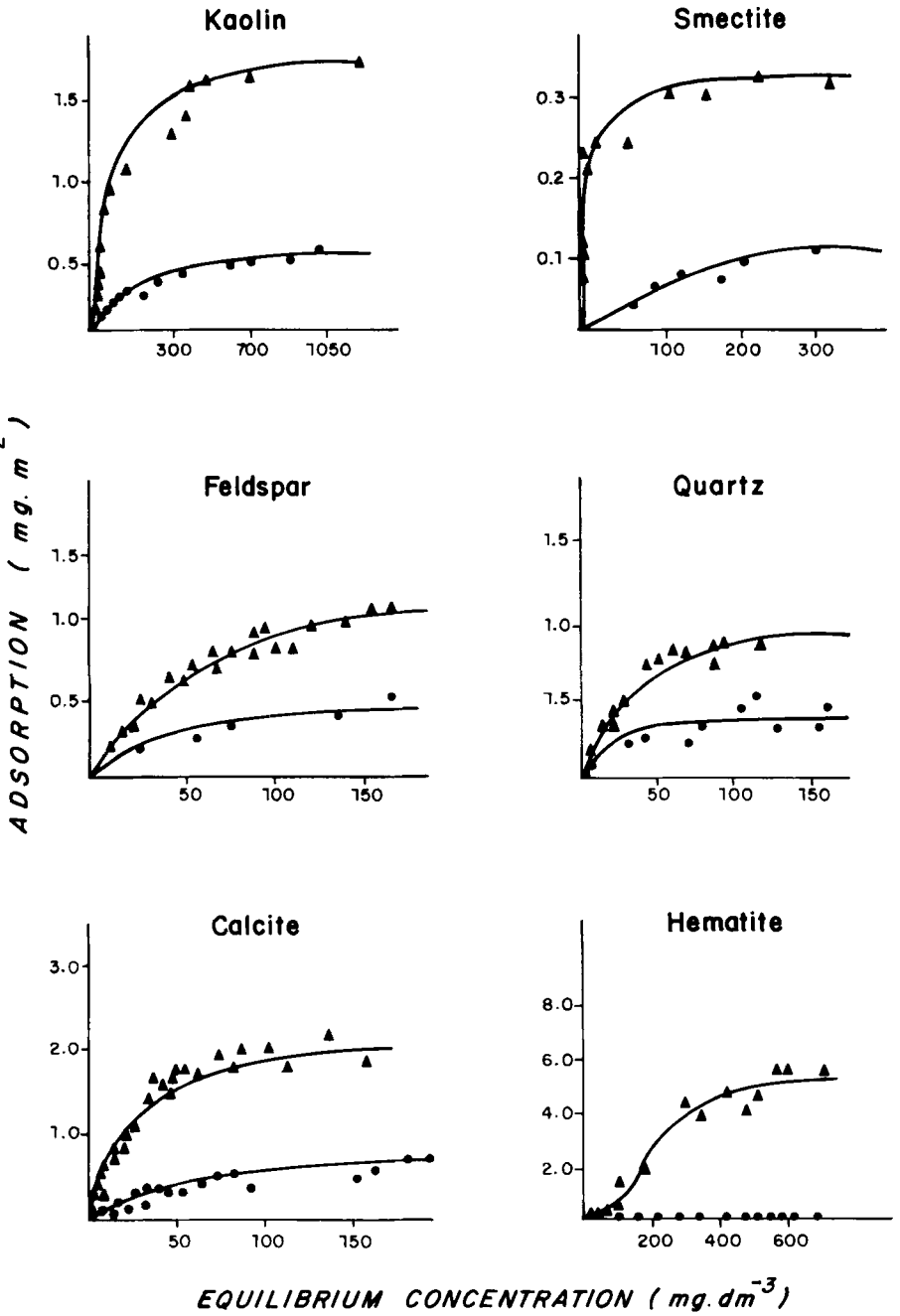

Fig. 9-3. Adsorption of asphaltenes and resins isolated from recovered shale oil on various minerals.

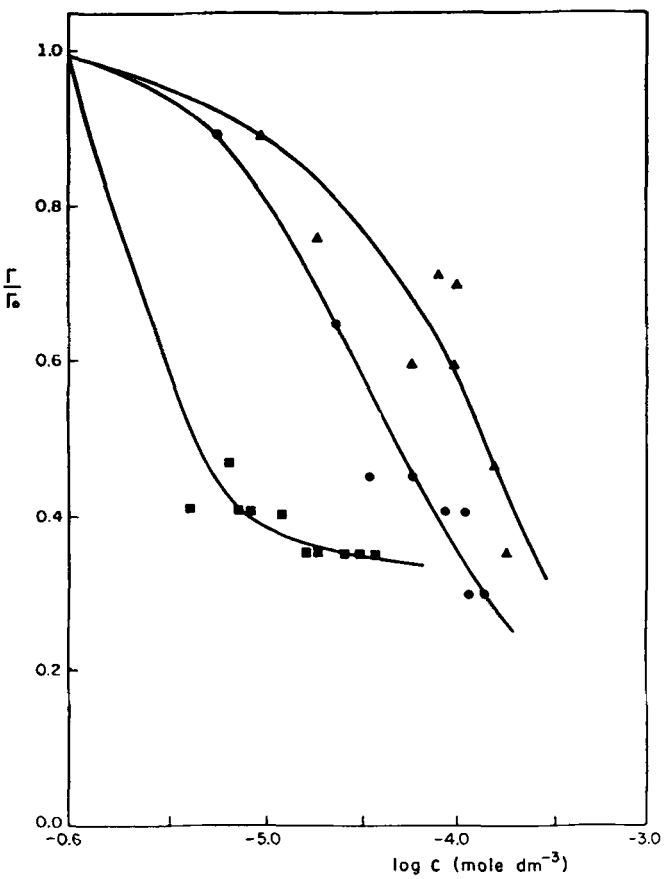

Fig. 9-4. Effect of surfactants on the adsorption of asphaltenes on quartz. ■ = NP10E; ● = NP23E; ▲ = NP100E. Asphaltenes and surfactants added at the same time. Asphaltene concentration was 80 mg/dm^3.

the surfactant, i.e., after three hours. This means that for these high asphaltene concentrations the adsorption process continues independently of the presence of the surfactant in the solution.

ELECTROPHORETIC MOBILITY

The electrophoretic mobility studies were carried out using samples of quartz, calcite and fluorite. The authors selected these minerals because in the case of quartz the groups present at the mineral solution interface are the weakly acidic SiOH or SiO^-, whereas in the case of calcite and fluorite the weakly basic CaOH and Ca^+ groups should predominate at the surface of the particles. Moreover, the isoelectric point of the calcite and fluorite samples were less than 6 and 9,

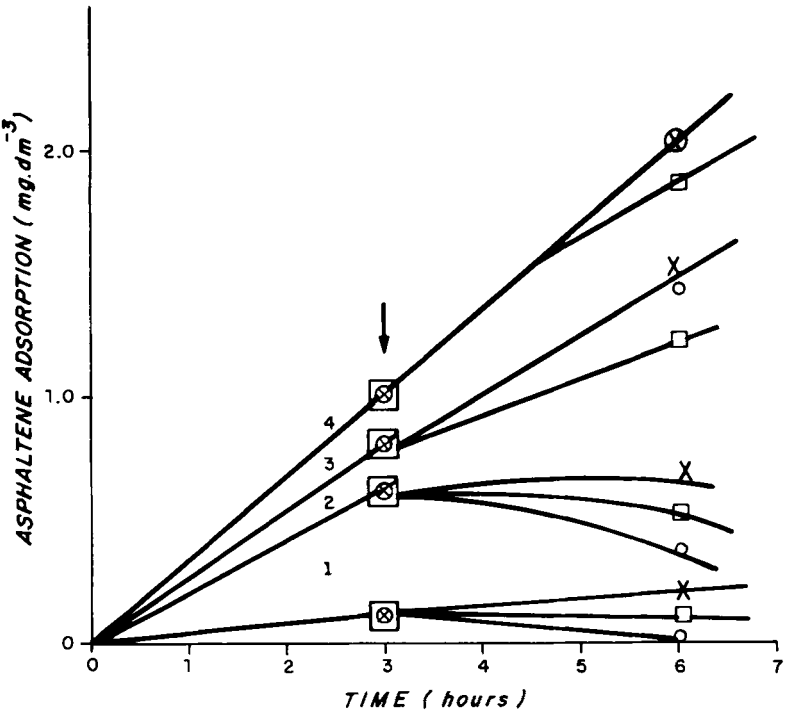

Fig. 9-5. Effect of surfactants on the adsorption of asphaltenes on quartz. × = NP23E; ○ = NP30E; □ = NP100E. Surfactant concentration: 100 mg/dm^3. Asphaltene initial concentration: curve 1: 10 mg/dm^3; curve 2: 50 mg/dm^3; curve 3: 100 mg/dm^3; curve 4: 150 mg/dm^3.

respectively; therefore, the two minerals have opposite charges in the intermediate pH region.

Figure 9-6 presents the results for quartz. The electrophoretic mobility of the sample containing adsorbed asphaltenes is slightly smaller than that corresponding to the bare mineral particles. This difference seems to be more significant at low pH; however, the changes are detected more for being systematic rather than for their magnitude. For calcite, the differences are clearly more important for alkaline pH, as shown in Table 9-2, where the zeta-potentials of calcite particles with or without adsorbed asphaltenes are presented for pH = 8 and 11. For the latter pH value, the zeta-potentials of the particles containing asphaltenes are slightly higher. Similar results have been reported for other samples of asphaltenes adsorbed on feldspar [11].

As shown in Fig. 9-7, for the case of fluorite the differences are much more important. The electrophoretic mobility is reduced in the pH region in which the mineral has a positive charge and increase in the region in which the charge is negative or neutral. Furthermore the isoelectric point is shifted from pH 9 to pH 6.5. These changes are typical of the specific adsorption of negatively charged amphoteric molecules on the mineral surface [12]. Other studies also indicate that

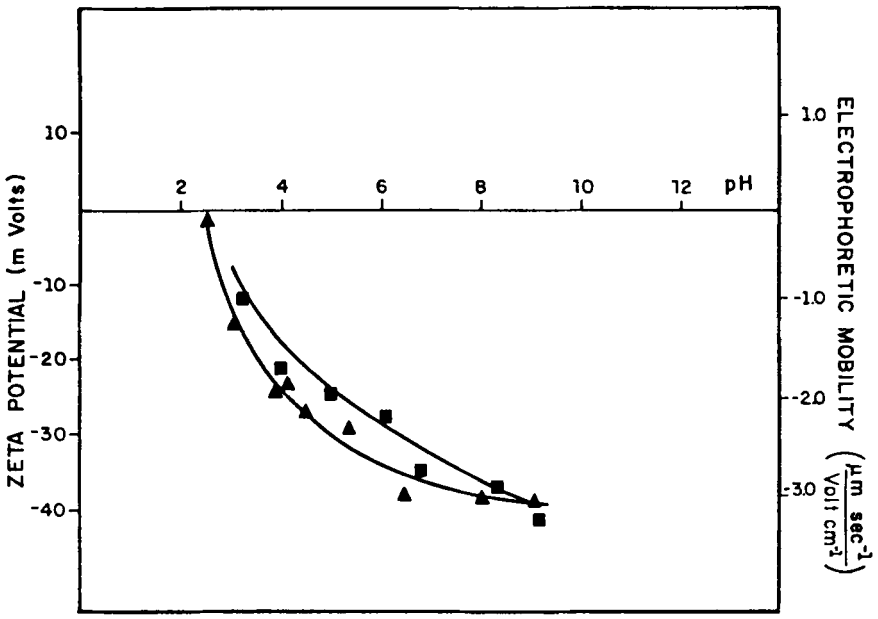

Fig. 9-6. Electrophoretic mobility and zeta potential of quartz (▲) and quartz with adsorbed asphaltenes extracted from recovered shale oil (■).

TABLE 9-2

Zeta potential of calcite in the presence of different asphaltic fractions

	Zeta potential (mV)	
	pH = 8	pH = 11
Pure calcite	−16.45 ± 0.51	−26.06 ± 1.16
Fraction adsorbed on calcite:		
extracted shale oil	−16.06 ± 0.26	−31.38 ± 1.54
filtered shale oil	−14.42 ± 0.88	−29.68 ± 1.29

asphaltic material dispersed in aqueous media exhibits negative surface potential [13].

Wetting and contact angle

The immersion tests carried out in aqueous solutions permit the observation of the differences between the solid samples and the polar fractions. As expected, in aqueous electrolyte solutions all minerals exhibited spontaneous immersion, indicating that they are naturally hydrophilic. The adsorption of asphaltenes promoted a hydrophilic–hydrophobic transition in the minerals. The particles with adsorbed lay-

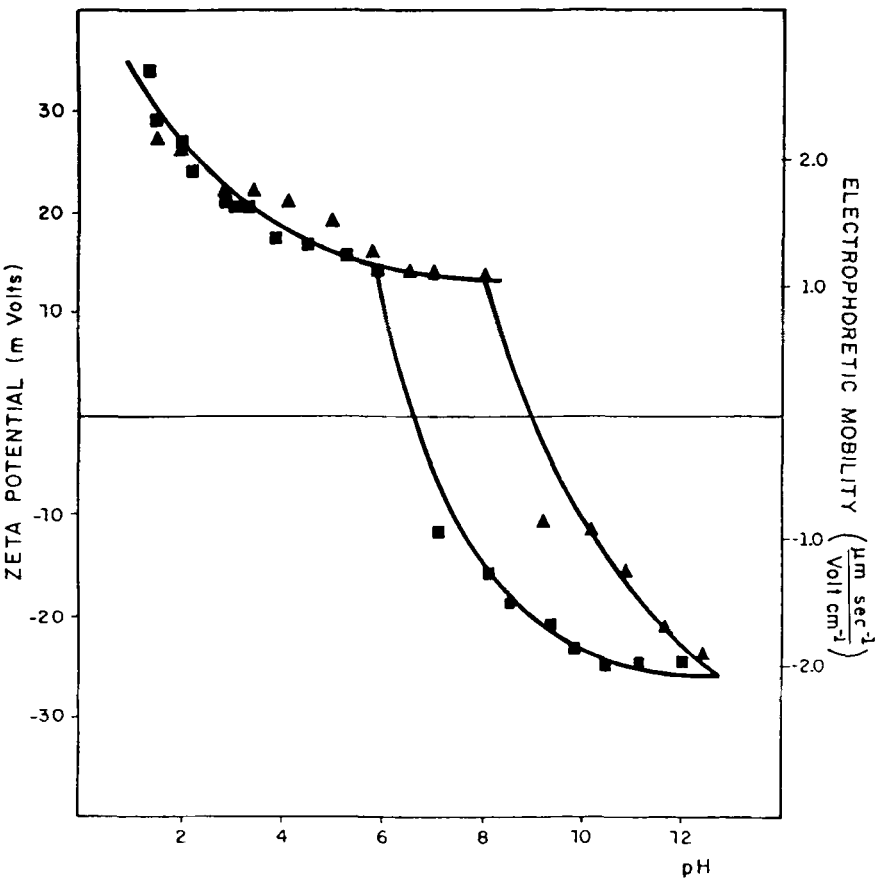

Fig. 9-7. Electrophoretic mobility and zeta potential for fluorite (▲) and fluorite with adsorbed asphaltenes (■) extracted from recovered shale oil.

ers of asphaltenes did not immerse spontaneously in aqueous solutions, remaining on the liquid surface for a period greater than 72 hours.

As the immersion process is closely related to the wetting behavior of the solids, it is possible to use the immersion experiments to evaluate the hydrophobicity of solid surfaces by measuring the surface tension for which immersion becomes spontaneous in mixtures of solvents [14]. This value of γ is sometimes called "critical surface tension" (γ_{crit}) for the immersion process [15]. Table 9-3 presents the composition and corresponding surface tension in which immersion of an asphaltene-covered mineral occurred for the mixtures methanol–water and ethanol–water. The experiments were carried out for the asphaltene fractions separated from two types of oil and only small difference was observed between these two oil samples. The values of γ_{crit} for the mineral samples covered by asphaltenes separated from filtered shale oil were slightly lower than values corresponding to the recovered shale oil. It

TABLE 9-3

Critical surface tension for the immersion of different minerals containing adsorbed asphaltenes (all mineral immerse in the absence of asphaltenes)

Mineral	Ethanol conc. (%v/v)	Surface tension (mN/m)	Methanol conc. (%v/v)	Surface tension (mN/m)
Extracted shale oil				
Kaolin	13	44.0	21	51.0
Smectite	17	40.5	31	44.8
Feldspar	19	38.2	32	44.0
Quartz	21	38.5	31	44.8
Calcite	3	61.0	5	63.0
Hematite	15	42.0	24	47.6
Magnesite	4	52.8	18	57.0
Filtered shale oil				
Kaolin	11	46.0	19	51.5
Smectite	14	43.0	27	46.4
Feldspar	16	41.5	28	45.5
Quartz	16	41.5	19	51.5
Calcite	0	72.0	0	72.0
Hematite	16	41.5	24	47.6
Magnesite	2	52.6	12	57.0

TABLE 9-4

Equilibrium contact angle at the mineral–water–toluene solution interface for pure minerals and minerals with adsorbed oil fractions

	Contact angle (°)			
	quartz	calcite	magnesite	mica
1. Pure mineral	34.8 ± 2.6	30.2 ± 1.6	34.5 ± 0.6	34.5 ± 1.2
2. Asphaltenes:				
extracted shale oil	102	89	72	110
filtered shale oil	114	95	97	114
3. Resins:				
extracted shale oil	72	68	58	43
filtered shale oil	94	85	62	77

is also clear that calcite and magnesite become less hydrophobic than other minerals by the adsorption of asphaltenes, independently of the origin of asphaltenes.

Table 9-4 presents the results of equilibrium contact angle measured at the mineral–water–toluene solution interface, using the sessile (water) drop technique. The minerals selected for these studies were quartz, calcite, magnesite and mica to avoid roughness effects. For quartz it was possible to obtain a very smooth surface by polishing, using cerium oxide particles. Calcite and magnesite also were polished after careful cleavage along their cleavage planes. For mica, it is possible to obtain

molecularly smooth surfaces simply by peeling the surface layer of the mineral under controlled conditions. For the pure minerals, contact angles between 30° and 34.50° were obtained for all the samples. As in previous studies [4], the angles measured for particles covered with asphaltenes were higher than those measured for resins; and the asphaltenes separated from filtered shale oil gave rise to higher contact angles. Calcite showed the lowest contact angle of all the cases. These results confirm the qualitative observations formulated in the previous paragraph, when commenting on the critical surface tension for the immersion of asphaltene-covered mineral particles.

Figure 9-8 shows the contact angle at the mica–water–toluene solution interface for different asphaltene concentrations. The values reported on the abscissa of Fig. 9-8 are initial concentrations; however, as the surface area of the solid specimen is very small, these values should not differ too much from the equilibrium concentration. The highest value for the contact angle is obtained at asphaltene concentrations between 10 and 20 mg/dm^3. The results of Table 9-5 illustrate the reversibility of the hydrophobization process. For surfaces obtained at low asphaltene concentrations, i.e., small surface coverage, the contact angle may be reduced by

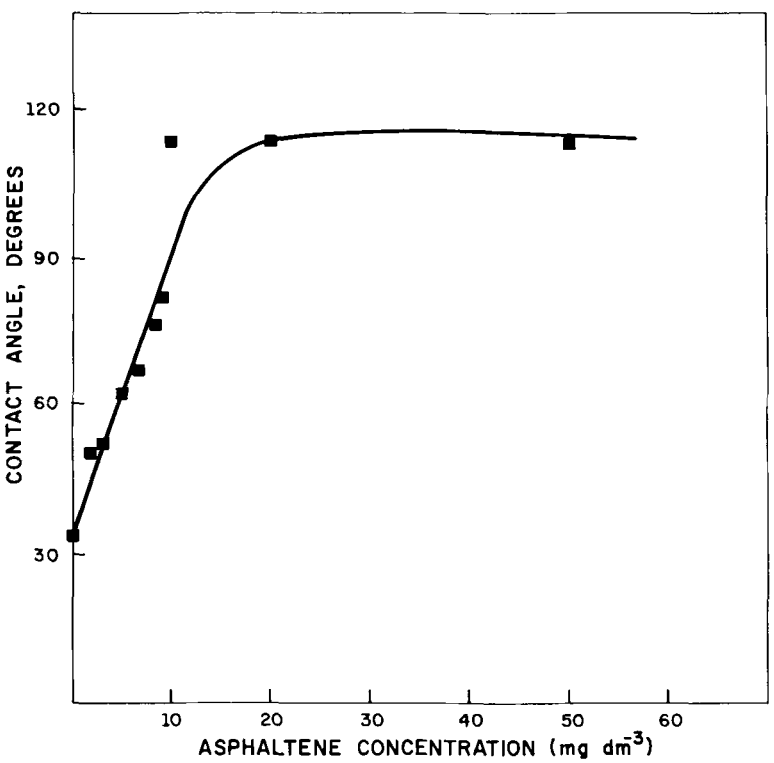

Fig. 9-8. Contact angle at the mica/water + toluene solution interface for various concentrations of asphaltenes isolated from recovered shale oil.

TABLE 9-5

Changes in the contact angle at the interface mica–water–toluene after exposure of the mineral with adsorbed asphaltenes to toluene

Asphaltene concentration (mg/dm^3)	Contact angle (°)	
	initial	final
3	52	34
5	62	40
7	67	58
8	77	62
9	82	67
10	113	113
50	113	113

exposure of the solid to the pure solvent. This reduction, however, was not possible when the concentration of asphaltene was high, i.e., when the surface coverage was close to or at saturation.

Figure 9-9 shows the effect of pH of the aqueous phase on contact angle. For these measurements, the continuous phase was water and a drop of toluene was

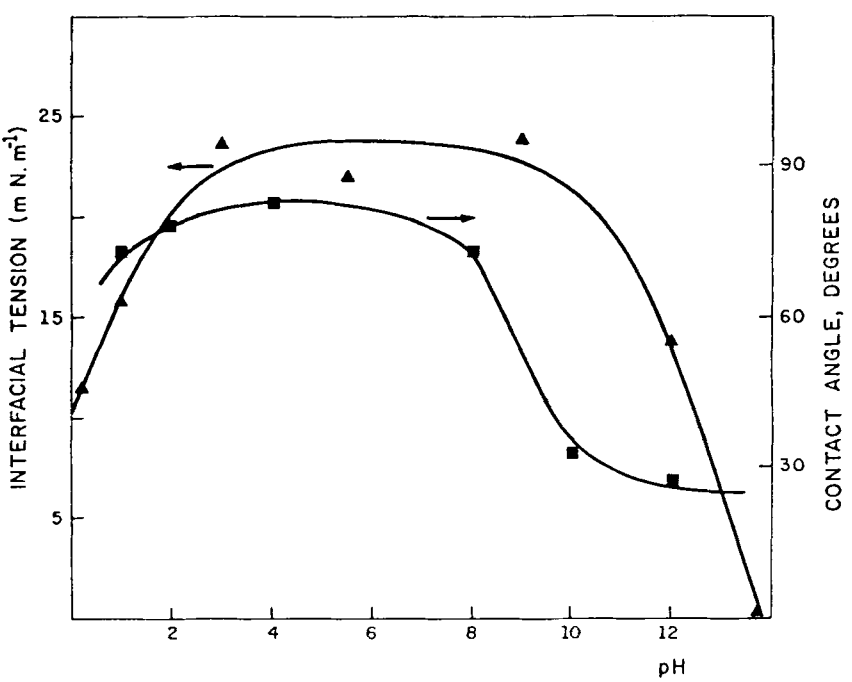

Fig. 9-9. Contact angle at the mica/water + toluene solution interface (■) and interfacial tension (▲) as a function of pH. Asphaltene concentrations: (1) for contact angle: 50 mg/dm^3, (2) for interfacial tension: 150 mg/dm^3.

deposited on the solid surface as described in the section on experimental methods. The aqueous meniscus, therefore, recedes to attain the equilibrium contact angle. In the previous experiments, the water phase advanced to attain the equilibrium value. For this reason, the contact angles in the neutral pH, shown in Fig. 9-9, are somewhat smaller than those reported in Table 9-4 and Fig. 9-8. The interfacial tensions for solution toluene and water containing 50 mg/dm^3 asphaltene as a function of pH are also presented in Fig. 9-9. The contact angle and interfacial tension show a similar dependence on pH. In both cases, lower values are observed at extreme pH values and the effect is more important in the alkaline region. The changes in contact angle may be ascribed to the presence of weak amphoteric groups on an overall hydrophobic surface, the ionization of which at extreme pH values reduces the contact angle. Similarly, this ionization process increases the surface activity of the asphaltenes dissolved in the organic phase and reduces the interfacial tension.

DISCUSSION

The results presented in Figs. 9-2 and 9-3 indicate that there are differences in the adsorption behavior of the asphaltene fractions extracted from filtered and recovered shale oil. These differences result in different shapes of the adsorption isotherm. In the case of the asphaltenes extracted from filtered oil, the adsorption follows a Freundlich-type isotherm, in which the adsorption, expressed as Γ (for instance, in milligrams adsorbed per gram of adsorbent) is given by Eq. 9-2 [16]:

$$\Gamma = kc^{1/n} \tag{9-2}$$

where k is a constant, usually called solid surface adsorption capacity, c is the concentration in mg/dm^3 and $1/n$ is another constant associated with the "intensity of the adsorption". Although Eq. 9-2 represents an empirical description of the adsorption process, it has been derived [17] assuming a heterogeneous surface with different sites, each one conforming to a Langmuir-type adsorption isotherm. In the present case, the solid sample has a homogeneous surface, containing only one type of polar surface sites or at the most two types in the case of clays and feldspar. The asphaltene fraction, however, is formed by a number of chemically different components that present a similar solubility behavior. In this context, for instance, Yen [18] has suggested that this fraction may be identified as the oil components having Hildebrand solubility parameter [19] of 9.5, that corresponds to the solvent in which asphaltenes exhibit the highest solubility. It may, therefore, be assumed that different energy values may be associated to the interaction of the surface sites with each of these chemically different components. These differences would result in a Freundlich-type isotherm.

For the asphaltenes extracted from the recovered oil, the situation is different. Inasmuch as the oil was recovered from the sludge containing a large percentage of mineral particles, the polar components of this fraction should be those showing the higher affinity for the solid particles because the molecules remain attached to them

during the separation process. This behavior may result in a narrower distribution of the interaction energies between the surface sites and the components of the asphaltenes extracted from the recovered oil. This situation may result in Langmuir-type adsorption isotherms, such as those presented in Fig. 9-3. In this case, the adsorption is given by Eq. 9-3 [16]:

$$N_2^S = \frac{N^S K a_2}{1 + K a_2} \tag{9-3}$$

where a_2 represents the activity of the solute, N^S is the number of active sites for the adsorption on the solid, N_2^S is the number of molecules adsorbed on the solid surface, and K is the apparent equilibrium constant for the adsorption process, represented by the pseudo-equilibrium:

$$\text{adsorbed solvent} + \text{solute in solution} \overset{K}{\rightleftharpoons} \text{adsorbed solute} + \text{solvent in solution}$$

Equation 9-3 may be transformed to:

$$\frac{1}{\Gamma} = \frac{1}{n^S M_2} + \frac{1000\rho}{n^S K M_1 C_2} \tag{9-4}$$

where Γ is the "surface concentration" in mg/g of adsorbent; C_2 is the solution concentration in mg/dm^3; M_2 and M_1 are the solute and solvent molecular weights, n^S is the number of active sites per gram of adsorbent and ρ is the density of the solution. Figure 9-10 shows the results for asphaltenes plotted in this way for some minerals. The curves of Fig. 9-2 and 9-3 were drawn by adjusting the experimental points ($1/\Gamma$ against $1/C_2$) by a least-squares fit to Eq. 9-4. From the slope and the intercept, that represents the maximum adsorption, it was then possible to obtain the parameters for Eq. 9-4.

Equation 9-4 has three unknown quantities: M_2, n^S and K. The authors determined the weight average molecular weights of the asphaltenes and resins by means of gel permeation chromatography and obtained a value of 1250 and approximately 800, respectively. The calculations, however, were based on rather broad curves and using polystyrene as a standard for the calibration curves. The average molecular weights were identical for the resins and asphaltenes extracted from both oil samples. Using these figures for the results shown in Fig. 9-10, it was possible to calculate the apparent equilibrium constant and the free energy of adsorption using Eq. 9-5 (the results are presented in Table 9-6):

$$-\Delta G = 2.3RT \log K \tag{9-5}$$

The apparent equilibrium constant may be considered an empirical measure of the affinity of the solute for the solid surface, although the assumptions underlying Langmuir isotherm can not hold for this system, in which solute and solvent have very different types of molecules.

Asphaltenes and resins are chemically related fractions being formed by paraffinic and naphthenic chains as well as condensed aromatic hydrocarbons. The functional

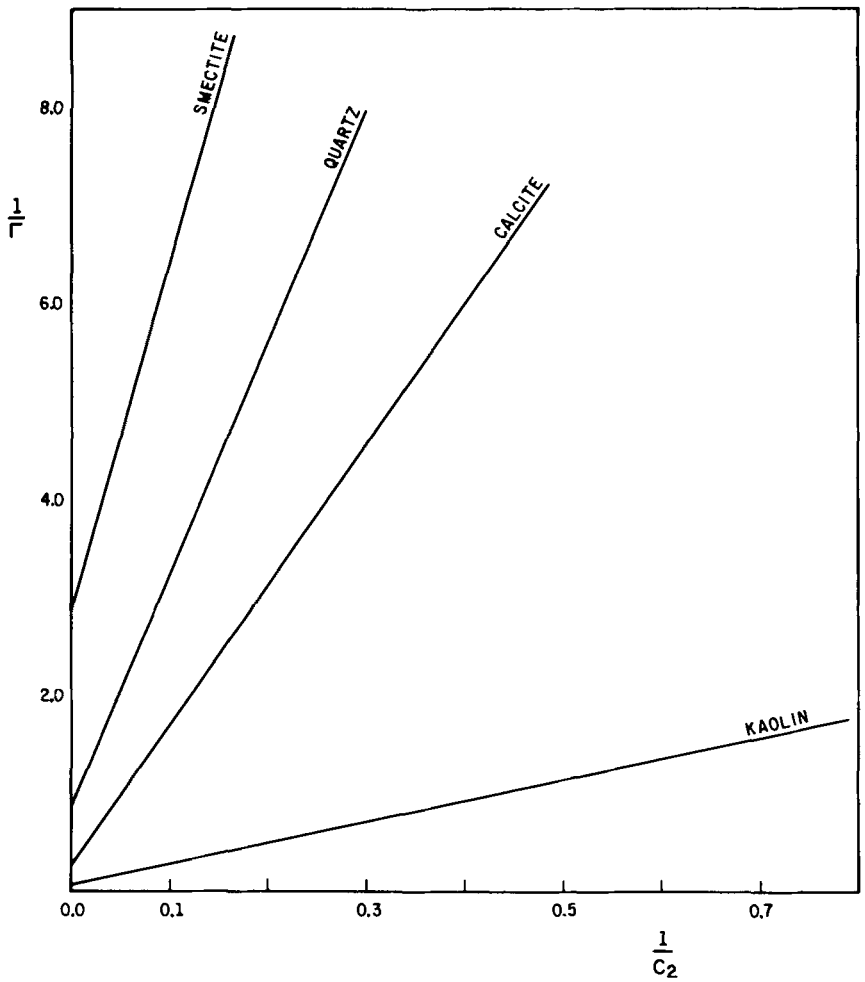

Fig. 9-10. Langmuir-type reciprocal plot for the adsorption of asphaltenes isolated from recovered shale oil on various minerals. Γ = adsorption; C_2 = concentration in mg/dm^3.

groups present in these molecules contain oxygen, nitrogen and sulphur, elements also being present as heteroatoms [20]. These groups are responsible for aggregation of molecules of asphaltic material and for their tendency to adsorb onto the solid–solution interface. The groups on the surface of calcite are, at least in part, positively charged (or neutral), weakly basic groups. Quartz and clays instead contain mainly negatively charged or neutral, weakly acid silanol groups. The interaction between calcite particles and asphaltic material, therefore, should occur preferentially through these groups and acid groups, such as carboxylates, phenols, alcohols, etc., forming the molecular structure of the asphaltic material. For quartz and clays, the driving mechanism for the adsorption process should be the interactions between

TABLE 9-6

Apparent equilibrium constant (K) and free energy (ΔG) for the recovery shale oil

Mineral	Γ_{max} (mg/m^2)	K	$-\Delta G$ (kJ/mol)
Asphaltene			
Kaolin	2.1	2.10×10^2	13.40
Smectite	0.3	1.16×10^3	17.68
Quartz	1.1	4.46×10^2	15.29
Calcite	3.3	5.19×10^2	15.17
Resins			
Kaolin	0.55	5.30×10	9.95
Smectite	0.12	2.03×10	7.55
Quartz	0.48	1.92×10^2	12.18
Calcite	0.94	1.31×10^2	12.21

the surface groups and the weakly basic groups present in the asphaltic material. The results in Figs. 9-2 and 9-3 reveal that resins (lower curves) show lower affinity for the mineral surface, indicating that the interaction between this fraction and the polar groups of the minerals are weaker in this case. Most likely, this is owing to the smaller size of the resin molecules, which may result in a better solvation compared to asphaltenes [21].

The results of Table 9-6 seem to indicate that the mineral–asphaltic material interactions, which determine the adsorption process, are rather non-specific. The pseudo-equilibrium constant and the adsorption free energies are relatively low compared, for instance, to the figures reported for the adsorption of pyrene onto graphon and polar or organophilic graphite [22]. This suggests a low affinity of the surface sites for the asphaltene molecules. From this point of view, the process parallels the adsorption of synthetic polymer or macromolecules in which the interactions are of low energy, but enough in number to account for the irreversibility of the adsorption process [23].

The maximum adsorption density values obtained by the extrapolation of the curves of Fig. 9-10 to abscissa equal to zero (Γ_{max}) are similar, although slightly higher than the values obtained at the plateau of the curves in Fig. 9-3 as shown in Table 9-1. The k parameter in Freundlich's equation applied to the results of Fig. 9-2 follows a similar sequence for the various minerals. The values in this case, however, correspond to an equilibrium concentration of 1 mg/dm^3 and, therefore, are very small. No further analysis was carried out on the adsorption of asphaltenes and resins isolated from the filtered oil due to the difficulties in understanding the parameters of Eq. 9-2 in this complex system.

The preventive effect on the adsorption exhibited by non-ionic surfactant may be due to the two alternative mechanisms. One possibility is that these surfactants may act as peptizing agents for the asphaltenes, thus reducing the tendency to adsorb. However, considering that aromatic solvents like benzene, xylene, toluene, etc., have always been considered good solvents for these compounds, this alternative does not

seem to be very likely. A much more realistic hypothesis would be to consider that the surfactants, having oxyethylene groups on their molecules, should also adsorb on quartz. Thus, they could occupy the active sites on the solid surface, preventing the adsorption of the resins or asphaltenes.

The adsorption process does not modify the electrophoretic mobility of the calcite or quartz particles significantly. The negative zeta potential is slightly higher for the asphaltene-covered calcite particles, but the increment never exceeds 20%.

For fluorite that exhibits a positive charge in the intermediate pH region, the effect becomes very important, providing evidence for the adsorption of negatively charged species. At a pH corresponding to the isoelectric point of the pure mineral, the asphaltene-covered particles show a zeta potential of −21 mV. The relationship between the surface charge density and the surface potential, obtained from the Gouy–Chapman theory of the electrical double layer, may be written in the simple form [24]:

$$-\sigma_0 = \sigma_d = 11.72\, C^{1/2} \sinh 0.016\, \Psi_\delta \tag{9-6}$$

where σ_0 and σ_d are the surface charge density and the charge in the diffuse double layer, respectively, expressed in μ coulombs/cm^2; C is the electrolyte concentration in mol/dm^3; and Ψ_δ is the electric potential in the Stern plane. Using Eq. 9-6, it is possible to show that a very small charge density (one charged site in about 20 nm^2) is enough to account for the change in zeta potential. This small change was not observed for negative particles like quartz, clays, calcite or feldspar, probably because the effect was shrouded by the high mobility that the particles exhibit (negative zeta potential) at neutral or alkaline pH. The presence of charged groups on the surface of mineral particles is important because they may be apparent even in a non-aqueous solvent [25]. In this case, the double layers are rather diffuse, resulting in an effective electrostatic repulsion between particles. Results reported for illite dispersions in toluene/hexane mixtures indicate that electrostatic repulsive forces as well as steric repulsion forces (caused by the overlap of hydrocarbon chains of adsorbed molecules) are important for the stabilization of asphaltene-covered illite particles in hydrocarbon media [8].

The free energy of immersion for a powder in a liquid, ΔG_i, per unit area is defined by Eq. 9-7:

$$\Delta G_i = -\gamma_{LV} \cos\theta \tag{9-7}$$

where γ_{LV} is the liquid surface tension and θ is the contact angle at the solid–liquid–vapor interface. This relation indicates that immersion is spontaneous for $\theta \leq 90°$. Above 90°, ΔG_i is positive and the particles will not immerse in the liquid. The results obtained show that both types of asphaltenes modify the wettability of most of the minerals to such an extent that θ becomes larger than 90°. As a consequence, these particles with adsorbed layers of asphaltenes may present a higher affinity for oil than for water. Calcite and magnesite are the only minerals that show a lower tendency to become hydrophobic by the adsorption of asphaltenes. In fact, a small reduction in the surface tension of the liquid phase is enough to obtain

TABLE 9-7

Interfacial tensions, free energy values for the oil-to-water transfer (ΔG_t) for quartz, calcite, magnesite and mica particles covered with adsorbed asphaltic fractions (γ_{H_2O} = 72 mN/m)

	γ_{ow} (mN/m)	Free energy, ΔG_t (mJ/m^2)			
		quartz	calcite	magnesite	mica
Asphaltenes					
Extracted shale oil	25	5.2	−1.6	−7.7	8.5
Filtered shale oil	20	7.9	1.7	2.4	8.1
Resins					
Extracted shale oil	27	−8.5	−10.3	−14.3	−19.7
Filtered shale oil	29	2.0	−2.5	−11.3	−6.5

wettability in the case of asphaltenes from recovered shale oil and the particles (with adsorbed asphaltenes from shale oil) immersed in water. The resins are less effective in changing the wettability of mineral particles and most of the minerals, containing adsorbed layers of the resin fraction, spontaneously immerse in pure water.

From the experimental results, it is possible to calculate the change in the free energy associated with the transference of mineral particles from the oil phase to an aqueous environment (ΔG_t). This change is given by:

$$\Delta G_t = -\gamma_{ow} \cos\theta_{swo} \tag{9-8}$$

where γ_{ow} is the interfacial water–oil tension and θ_{swo} is the equilibrium contact angle at the solid–water–oil interface. The data are presented in Table 9-7 together with the interfacial tensions for water in contact with the asphaltenic fraction dissolved in toluene. For neutral pH, asphaltenes and resins possess low surface activity, but for acidic or alkaline pH they reduce the interfacial tension to a very low value (Fig. 9-9). The hydrophilic–hydrophobic transition produced by the adsorption of shale oil polar fraction is less important for calcite and magnesite than for quartz and mica. For the latter two minerals, asphaltenes produce a surface which would prefer a non-polar environment and would not be wetted by an aqueous phase. In the oil industry this type of particles or surfaces are called "oil wet". On the other hand, for calcite and magnesite, only the particles covered with asphaltenes extracted from filtered shale oil become "oil wet", whereas all the others remain "water wet", i.e., they would separate preferentially into an aqueous phase. Results reported by Menon and Wasan [7,10] and by Papier et al. [26] confirm the results for mica and indicate that other clays also become "oil wet" by the adsorption of asphaltenes. These considerations explain why quartziferous materials and clays have been found to predominate in shale dusts extracted from filter cakes and in sludges separated from refinery water treatment plants.

The sudden reduction in the contact angle and in the interfacial tension between water and an asphaltenes solution in toluene shown in Fig. 9-9 at low and high pH is most likely caused by the ionization of weak acids and bases present in

the asphaltene fraction. These results corroborate the results of electrophoretic mobility measurements described in the previous paragraph for fluorite (Fig. 9-7). They also indicate that the ionizable groups, even being weak and small in number, are sufficient to increase the surface charge and alter the wettability of mineral particles as well as to increase the surface activity of this fraction. Based on different separation procedures and by quantification of each fraction, Thyrion [21] concluded that the acids and bases are present only in the resins and asphaltenes and discarded a zwitterionic structure for the molecules contained in these fractions. On the other hand, studies on extra heavy oil [27] seem to indicate that the surface activity displayed by crude oil from the Orinoco oil belt may be ascribed to asphaltenes for acidic pH and to resins for alkaline pH. The present results and previous studies with asphaltenic fractions extracted from crude oil from the Carmópolis field, Sergipe, Brazil [28] do not confirm this last contention. They indirectly confirm the presence of the ionizable groups, acids and bases, in the asphaltenes extracted from shale oil from Irati Formation and indicate that the acids predominate over bases in this particular case. The acid–base behavior of a crude oil or a bitumen is very important because it influences the formation of stable emulsions and the viscosity of oil. The contents of acid and bases, however, depend to a great extent on the origin of oil.

Table 9-5 shows the reversibility of the hydrophilic–hydrophobic transition caused on mica by the adsorption of asphaltenes. It is clear that reversion to a more "water-wet" surface is easier when the surface coverage is small, below an equilibrium concentration of 10 mg/dm^{-3}, which corresponds to the concentration where the surface saturation is reached (Fig. 9-8). Beyond this concentration, the maximum adsorption density is attained and reduction in contact angle by exposure to the solvent is no longer possible. This result resembles the effect of non-ionic surfactants on the adsorption of asphaltenes as shown in Fig. 9-5. In that case, the inhibition of the adsorption process was also not possible when there was a high concentration of asphaltenes already adsorbed on the solid surface. An explanation for these results is given in Fig. 9-11. For low or intermediate coverage (Fig. 9-11), the adsorbed asphaltene molecules are isolated on the solid surface. These molecules, therefore, may be individually desorbed and replaced either by other asphaltene molecules or by solvent or surfactant molecule as indicated in Fig. 9-11. For high coverage, the behavior of the asphaltenes at the interface change and the results in Fig. 9-5 and Table 9-5 seem to indicate that the desorption process is no longer possible. This modification may be ascribed to a reorganization of the molecules at the interface with lateral interaction between the adsorbed asphaltene molecules, as shown schematically in Fig. 9-11. In this new structure, the desorption process implies the simultaneous desorption of various molecules, which is a low-probability process, or the disruption of the lateral interactions by the desorption of one isolated molecule and its substitution by the solvent or the surfactant molecule. This second alternative is also very remote.

Earlier studies carried out by Pfeiffer [29], also seem to provide evidence for the existence of lateral interactions between the asphaltenes at the interfaces. He measured the molecular weight of asphaltenes of different origins using a

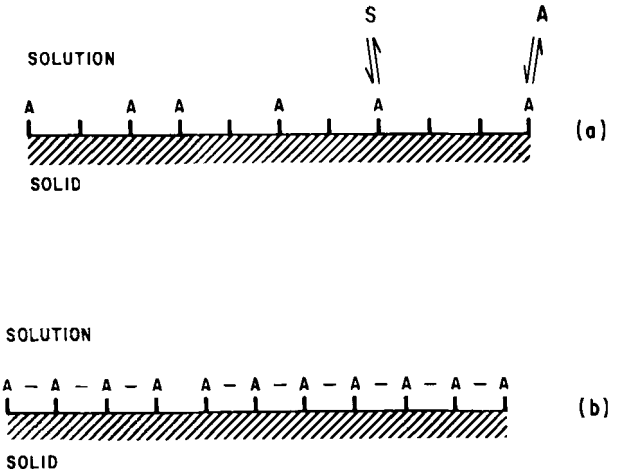

Fig. 9-11. Schematic representation of the adsorption/desorption process of asphaltenes (*A*) at the solid–solution interface. *S* represents a solute or surfactant molecule.

technique based on the colligative properties (cryoscopy in benzene) of asphaltene solution. The values obtained for three samples were 5000, 4000 and 2400. When the molecular weight was determined for the asphaltenes spread on the surface of water by using the Langmuir film balance [30], the values obtained were 150,000, 100,000 and 26,000, respectively.

The irreversibility of the adsorption process is well known to petroleum engineers and oil field chemists, when dealing with problems related to asphaltenes, such as desorption emulsification, wettability reversal, or precipitation of asphaltic sludge. It is always an easier and wiser practice to prevent the problems rather than attempt to resolve them once they occur.

CONCLUSIONS

The experimental work described in this chapter was carried out using samples of asphaltenes and resins extracted from shale oil. However, studies carried out with asphaltenes isolated from other types of oil or bitumen produce comparable results [4,10,11,28,31–33]. The present study is consequently applicable to the adsorption of asphaltenes onto minerals more or less as a general rule. The main conclusions can be summarized as follows:

(1) Asphaltenes adsorb on mineral particles up to a maximum adsorption density of 2–3 mg/m^2. The adsorption density of resins is lower and the effect in this case is less important than in the case of asphaltenes.

(2) The adsorption is a low-energy process that resembles the adsorption of polymers or macromolecules. The interactions are of low energy but enough in number to account for the irreversibility of the adsorption process.

(3) Non-ionic surfactants prevent the adsorption of asphaltenes on the mineral particles. This effect, which depends on the degree of ethoxylation of the surfactant, seems to result from the preferential adsorption of the surfactants on the mineral surfaces.

(4) Asphaltenes produce moderate changes in the electrical properties of the mineral–solution interface. These changes are not evident for minerals exhibiting a large negative zeta potential, but become apparent in the case of fluorite which exhibits a positively charged surface in the intermediate pH range.

(5) The adsorption process produces a hydrophilic–hydrophobic transition for the mineral particles. This effect is more pronounced for quartz and clays than for calcite and magnesite.

(6) Adsorption of asphaltenes seems to be reversible at low surface coverage, but irreversible when the adsorption density is close to saturation. This effect has been ascribed to lateral interactions between the adsorbed asphaltene molecules.

ACKNOWLEDGEMENTS

The authors acknowledge Miss Maria S. González for the help in the preparation of the manuscript and typing.

REFERENCES

[1] Anderson, W.G., Wettability literature survey, Part 6. The effects of wettability on waterflooding. *J. Pet. Technol.*, 39: 1605–1622 (1987).
[2] Schulman, J.H. and Leja, J., Control of contact angle at the oil–water–solid interfaces. Emulsions stabilized by solid particles ($BaSO_4$). *Trans. Faraday Soc.*, 50: 598–604 (1954).
[3] Batista, R., Ivo, O.C. and Piper, E.M., Commercialization of oil shale with the Petroxis process. *Easter Oil Shale Symp.*, Lexington, Ky., November 26–28 (1984).
[4] González, G. and Middea, A., The properties of the calcite–solution interface in the presence of adsorbed resins and asphaltenes. *Colloids Surf.*, 33: 217–229 (1988).
[5] Collins, S.H. and Melrose, J.C., Adsorption of asphaltenes and water on reservoir rock mineral. *SPE 11800, Soc. Pet. Eng.*, Dallas, Texas (1983).
[6] Adamson, A.W., *Physical Chemistry of Surfaces*. Interscience, New York, N.Y., 2nd ed., 625 pp. (1960).
[7] Menon, V.B. and Wasan, D.T., Particle–fluid interactions with application to solid-stabilized emulsions, Part I. The effect of asphaltenes adsorption. *Colloids Surf.*, 19(1): 89–105 (1986).
[8] Marlow, B.J., Sresty, G.C. Hughes, R.D. and Mahajan, O.P., Colloidal stabilization of clays by asphaltenes in hydrocarbon media. *Colloids Surf.*, 24: 283–297 (1987).
[9] Dean, K.R. and Mcatee, J.L. Jr., Asphaltene adsorption on clay. *Appl. Clay Sci.*, 1: 313–319 (1986).
[10] Menon, V.B. and Wasan, D.T., Particle–fluid interactions with application to solid-stabilized emulsions, Part II. The effect of water. *Colloids Surf.*, 19: 107–122 (1986).
[11] González, G. and Middea, A., Asphaltene adsorption by quartz and feldspar. *J. Dispersion Sci. Technol.*, 8: 525–548 (1987).
[12] Hunter, J., *Zeta Potential in Colloid Science*. Academic Press, London, 300 pp. (1981).
[13] Margansky, R.E. and Rowel, R.L., Electrophoretic mobility distribution in aqueous bituminous coal dispersions. *J. Dispersion Sci. Technol.*, 4(4): 415–424 (1983).
[14] Zisman, W.A., Relation of the equilibrium contact angle, wettability and adhesion. *Adv. Chem. Ser.*, 43: 1–51 (1964).

[15] Ellison, A.H., Fox, H.W. and Zisman, W.A., Wetting of fluorinated solids H-bonding liquids. *J. Phys. Chem.*, 57: 622–627 (1953).
[16] Himenz, P.C., *Principles of Colloids and Surface Chemistry*. M. Dekker, New York, N.Y., pp. 287–290 (1977).
[17] Hasley, G.D., The role of surface heterogeneity in adsorption. *Adv. Catal.*, 4: 259–269 (1952).
[18] Yen, T.F., Characterization of heavy oil. In: R.F. Meyer (Editor), *Unitar Second Conference on the Future of Heavy Oil*. McGraw-Hill, New York, N.Y., pp. 412–423 (1984).
[19] Hildebrand, J.H. and Scott, R.L., *The Solubility of Nonelectrolytes*. Reinhold, New York, N.Y., 435 pp. (1950).
[20] Tissot, B., Connaissances actuelles sur les products lourds du pétrole. *Rev. Inst. Fr. Pét.*, 36(4): 429–446 (1981).
[21] Thyrion, F.C., Les asphaltenes: composition et propriétés. *Bull. Soc. Chim. Fr.*, 9/10: 393–408 (1981).
[22] Grozek, A.J., Adsorption of polycyclic aromatic hydrocarbons onto graphite. *Discuss. Faraday Soc.*, 59-1A-4B (1975).
[23] Eirich, F.H., The conformational state of macromolecules adsorbed at solid–liquid interface. *J. Colloid Interface Sci.*, 58: 423–436 (1977).
[24] Lyklema, J., The electrical double layer on oxides. *Croatica Chem. Acta*, 43: 249–260 (1971).
[25] Labib, M.E., The origin of the surface charge on particles suspended in organic liquids. *Colloids Surf.*, 29: 293–304 (1988).
[26] Papier, E., Bourgeors, C., Siffert, B. and Bullard, H., Chemical nature and water/oil emulsifying properties of asphaltenes. *Fuel*, 61(8): 732–734 (1982).
[27] Layrisse, L. and Rivas, H., Isolation and characterization of natuaral surfactants present in extra heavy crude oils. *J. Dispersion Sci. Technol.*, 5(1): 1–18 (1984).
[28] González, G., Lobato, C.S.D.D., Bruning, I.M.R.A., Mainier, F.B., Teixer, Z.N., Lima, H.A. and Santana, J.S., *Studies on the Treatment and Chemical Demulsification of Carmópolis Crude Oil* (in Portuguese). Relatório Cenpes, Petrobrás, 589 pp. (1985).
[29] Pfeiffer, J.P., *The Properties of Asphaltic Bitumen*. Elsevier, New York, N.Y., pp. 35–37 (1950).
[30] Gaines, G.L., *Insoluble Monolayers at Liquid–Gas Interfaces*. Intercience, New York, N.Y., 51 pp. (1966).
[31] Berezin, V.M., Adsorption of asphaltenes by oil producing rocks (in Russian). *Neft. Delo*, 5: 25–27 (1979).
[32] Denekas, M.O., Mattax, C.C. and Davies, G.T., Effect of crude oil components on rock wettability. *Trans. AIME*, 216: 330–333 (1959).
[33] Menon, V.B. and Wasan, D.T., Particle–fluid interactions with applications to solid-stabilized emulsions, Part III. Asphaltene adsorption in the presence of quinaldine and 1,2-dimethylindole. *Colloids Surf.*, 23: 353–362 (1987).

This page intentionally left blank

Asphaltenes and Asphalts, 1. Developments in Petroleum Science, 40
edited by T.F. Yen and G.V. Chilingarian

Chapter 10

EFFECTS OF ASPHALTENE PRECIPITATION ON THE SIZE OF VANADIUM-, NICKEL-, AND SULFUR-CONTAINING COMPOUNDS IN HEAVY CRUDE OILS AND RESIDUA

JOHN G. REYNOLDS

INTRODUCTION

Asphaltenes have been utilized in fossil fuel characterization for several decades. Originating from the concept that crude oils are colloids [1], asphaltenes have been studied extensively in the analysis of liquid carbonaceous fuels such as heavy crude oils, tar-sand bitumen, shale oil, and coal liquids [2]. Asphaltenes have also been utilized as indicators of processability and extent of processing for crude oils and synthetic fuels [3].

By definition, asphaltenes are the alkane-insoluble portion formed by mixing the liquid fuel with an alkane (usually hot) for several minutes to hours. An insoluble, usually finely powdered solid precipitates. The chemical composition of this resulting solid depends upon many variables, including choice of alkane co-solvent, volumes, temperatures, and times of mixing [4–7], as well as the carbonaceous fuel source (coal and petroleum asphaltenes differ considerably (for example, Bunger and Li [2])). The most common conditions now employed are the use of hot pentane or heptane as the precipitation solvent, 40 : 1 or more by volumetric ratio to oil, and mixing for one hour or more.

Given the wide range of precipitation conditions found in the literature, however, asphaltenes derived from crude oils have similar elemental analyses. Table 10-1 [8] is a summary of selected properties of asphaltenes from many different sources. Although specific extreme variations exist, the major properties seem to be remarkably constant. These materials generally (1) contain most of the metals and nitrogen of the crude oil; (2) contain a large portion of the sulfur; (3) have a high coking tendency; and (4) are primarily non-distillable material. These properties are consistent with properties of polar and heteroatomic material separated from crude oils.

Asphaltenes, by definition, exist separated from the fuel source, but much research in the last several years indicates they may not exist in the source itself [9]. Molecular weight determinations by various techniques have shown values from 1000 daltons to over 100,000 daltons [10]. However, values for whole crude oils and residua measured by more contemporary techniques, like field desorption and field ionization mass spectrometry, show upper limits of 1000 to 2000 daltons [9,11]. In addition, separation studies, using molecular distillation methods (DISTACT), indicate very large agglomerated structures expected to give these very high molecular weights are not likely in high concentrations in the whole feed [9,12].

TABLE 10-1

Range of elemental composition and atomic ratios of petroleum asphaltenes (from Speight [8])

General composition	
Carbon	82.0 ± 3.0 wt%
Hydrogen	8.1 ± 0.7 wt%
Nitrogen	1.0 ± 0.5 wt%
Oxygen	1.0 ± 0.8 wt%
Sulfur	5.0 ± 3.0 wt%
Atomic ratios	
H/C	1.15 ± 0.05
N/C	0.10 ± 0.003
O/C	0.200 ± 0.005
S/C	0.030 ± 0.005

Regardless of the controversy about asphaltenes, models of the moiety have been formulated and are used in petroleum chemistry regularly. X-ray diffraction shows ordered carbon structures in asphaltenes [13], which have been used to develop (along with other properties) the miscellar-type asphaltene structure (Fig. 10-1a) [14]. This has been used in a variety of studies to interpret coking mechanisms [15], carbon fouling in hydroprocessing [16], surfactant behavior in bitumen extraction [17], and pyrolysis products from kerogen breakdown [18].

Several other asphaltene models have been proposed [20] based on other chemical analyses, e.g., elemental analyses, nuclear magnetic resonance and infrared spectroscopies. Examples of these models are linear polymeric-type polynuclear aromatic systems (Fig. 10-1b) [19], and small molecules bound by sulfur-type bridges (Fig. 10-1c) [21], and others [15].

The purpose of this chapter is not to argue the existence of the asphaltene moiety in petroleum-related materials, but is to discuss whether the concept of asphaltenes is appropriate to use when discussing certain aspects of petroleum-chemistry characterization, process monitoring and design — where size is an important factor. An important question to consider is whether the asphaltene concept helps or hinders understanding in these cases.

SIZE CHARACTERIZATION

As lighter crude oils are being depleted, refinery feed slates are incorporating heavy crude oils in higher concentrations. The properties of heavy crude oils differ significantly from the properties of light, conventional refining stocks. Heavy crude oils have high specific gravities, viscosities, heteroatom content (nitrogen, sulfur, oxygen, nickel, iron, vanadium), coking carbon precursors, and non-distillable materials ($650°F^+$ and $1000°F^+$).

The complex nature of these heavy feeds has rendered standard analytical methods inadequate as tools for understanding and predicting the impact of the refining

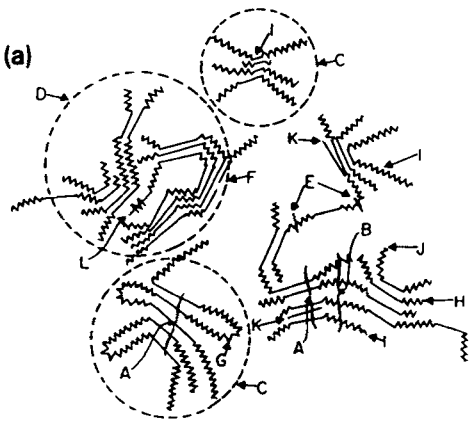

Macrostructure of Asphaltics

A. Crystallite	B. Chain Bundle
C. Particle	D. Micelle
E. Weak Link	F. Gap and Hole
G. Intracluster	H. Intercluster
I. Resin	J. Single Layer
K. Petroporphyrin	L. Metal (M)

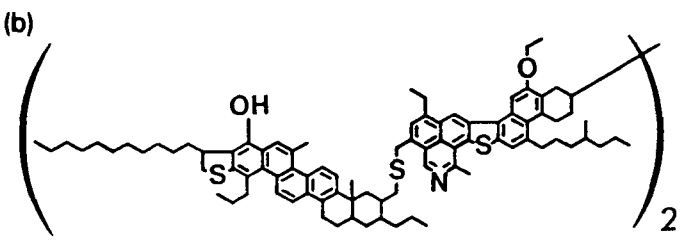

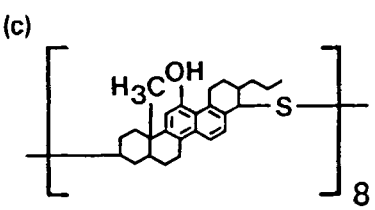

Fig. 10-1. Models of asphaltene structures: (a) macrostructure model (from Yen [14]); (b) polymer aromatic model (from Suzuki et al. [19]); and (c) sulfur-type bridge model. (After Ignasiak et al. [21].)

process. As a result, several new analytical techniques have been developed, such as high performance liquid chromatography coupled directly with specific-element detection [22–24]. This particular combination allows the separation of complex mixtures based on physical properties (size, polarity, aromaticity) with direct on-line detection of a variety of elements. Because of the extensive use of catalysts in the petroleum industry for upgrading [15], size-exclusion chromatography (SEC) is an attractive and pertinent method of separation. The catalyst pore–molecule size relationship is very important in understanding the chemical changes generated by catalysts. For detection, inductively-coupled plasma directly linked to atomic emission spectroscopy (ICP-AES) has been utilized. This method can be directly connected with SEC, and several studies on feed and process characterization have been conducted monitoring nickel, vanadium, sulfur, which are generally the elements of interest. Combined with other spectroscopic techniques, SEC-ICP-AES is a very powerful analytical tool for characterizing petroleum related materials.

Feed characterization: metals

The asphaltene precipitation is commonly used in the characterization of metal-containing compounds in feeds and processed products. This is principally due to the concentrating effects the precipitation has on the metals. Table 10-2 shows the concentrations of nickel and vanadium in the SARA (ASTM D 2007-80 with asphaltene precipitation) separated fractions for selected heavy crude oil residua [5,25,26]. The concentrations of the metals in the asphaltene fraction vary due to the concentrations of the metals in (and the classification of) the feed. In all

TABLE 10-2

Concentrations of nickel and vanadium in SARA-separated fractions of selected heavy crude oil residua (data from [5,25,26])

Residuum	Metals	Saturates	Aromatics	Resins	Asphaltenes
Maya 650°F$^+$	Ni	<3	9	44	286
	V	<3	<6	242	1602
Arabian Heavy 650°F$^+$	Ni	<3	11	30	170
	V	<3	11	81	594
Beta 650°F$^+$	Ni	9	<12	124	429
	V	9	<12	147	749
Kern River 650°F$^+$	Ni	<3	<12	149	492
	V	<3	<12	75	361
Boscan 1000°F$^+$	Ni	<3	19	160	375
	V	<3	<3	1595	4410
Hondo 850°F$^+$	Ni	<3	4	105	474
	V	<3	2	198	979
HMaya 650°F$^+$	Ni	6	3	21	202
	V	<1	<1	77	1140

cases in the table, the polar fractions of the feeds (resins and asphaltenes) contain 90 to 100% of the nickel and vanadium, and in most cases, the majority of the metals are separated into the asphaltene fraction. (In more paraffinic residua, more metals tend to be separated into the resin fraction.) Clearly, the concentrations are high in the asphaltenes, which allows for application of several different types of spectroscopy that can be concentration limited (electron paramagnetic resonance, ultra-violet-visible, extended X-ray absorption fine structure spectroscopies).

Although the asphaltene precipitation clearly benefits analysis by concentrating vanadium and nickel, it does appear to effect the size of metal-containing compounds. The asphaltene precipitation does, at least in part, separate the large-size compounds from the small-size compounds. Hall and Herron [27] showed by preparative gel permeation chromatography (GPC), the asphaltenes from several crude oils and residua have a much larger mean size than those of the maltenes, and that the asphaltenes were harder to process than other fractions. This increased difficulty in processing was probably due to the larger size of the asphaltenes.

The asphaltene precipitation not only appears to separate, on the average, the larger-size molecules from the smaller-size molecules, but also to produce metal-containing molecules which are larger than those found in the whole feed, in some cases. Figure 10-2 shows the SEC-ICP-AES vanadium profiles for Boscan 1000°F$^+$ residuum and the corresponding isooctane-derived asphaltenes and maltenes [28]. The profile is a plot of vanadium emission at 292.4 nm as a function of elution time. The large components elute first (on the left side of the profile), and the smallest components elute last. The residuum profile has the behavior which is very similar to that of SEC-ICP-AES vanadium profiles for most heavy crude oils, i.e., a bimodal distribution with maxima at approximate molecular weight of 800 and 9000 (polystyrene equivalent), which have been assigned to extractable petroporphyrins, and metallo-nonporphyrins respectively.

Figure 10-2 also shows the vanadium SEC-ICP-AES profile for the isooctane-derived asphaltenes from Boscan 1000°F$^+$ residuum [28]. The important feature of this profile is the formation of larger-size metal compounds not existent in the Boscan 1000°F$^+$ residuum profile. The asphaltene precipitation clearly changes the molecular size of the metal-containing compounds relative to those of the vacuum residuum. The size change is significant enough to place a large portion of these compounds near to or outside the practical resolution range of the column. This formation of larger material not present in the Boscan 1000°F$^+$ residuum indicates that the asphaltene precipitation has other effects in addition to just separating components. This same behavior is seen in the SEC-ICP-AES nickel profiles for Boscan 1000°F$^+$ residuum [28]. In addition, this behavior has been seen in size studies of Maya 650°F$^+$ (see below) [28].

This agglomeration behavior has been seen in other cases as well. Fish et al. [29] have also examined the size and molecular weight distribution of vanadium for Boscan, Cerro Negro, Wilmington, and Prudhoe Bay crude oils by SEC utilizing graphite furnace atomic absorption (GFAA) as the detection method. In these studies, polystyrene and vanadium model compounds were used for molecular weight calibration. Although polystyrene standards generally give exaggerated molecular

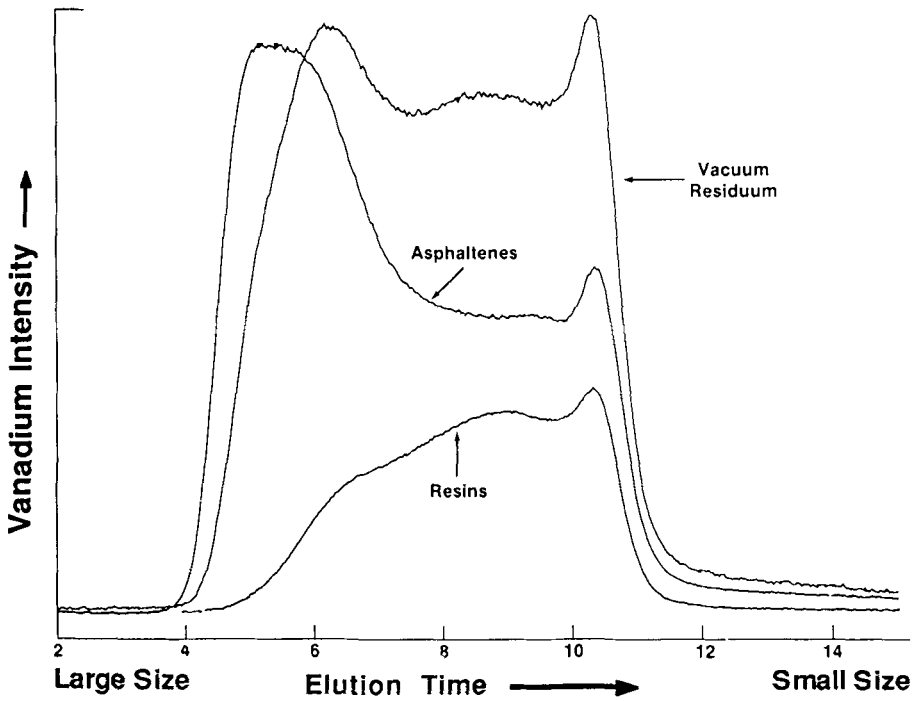

Fig. 10-2. SEC-ICP-AES vanadium profiles of Boscan 1000°F$^+$ residuum, and the asphaltenes and maltenes derived from the isooctane precipitation of Boscan 1000°F$^+$ residuum. (From Reynolds and Biggs [28].)

weight calibrations, they can be used as effective *relative* markers on the SEC column. Figure 10-3 shows the weight balanced distribution of vanadium (measured by SEC-GFAA) based on fractions collected in molecular weight ranges of (in daltons) >2000, <2000 to >900, <900 to >400, and <400 for Boscan, Cerro Negro, Wilmington, and Prudhoe Bay crude oils before and after the asphaltene precipitation. The sum is the weight-balanced molecular weight calculated from the individual components (maltenes and asphaltenes after separation). Clearly, the precipitation effects the molecular weight distribution of vanadium for all the crudes. For Boscan and Cerro Negro crude oils, the precipitation increases the overall distribution to higher molecular weight, indicating that the asphaltene precipitation is causing an artifactual increase in the molecular weight. For Wilmington and Prudhoe Bay crude oils, however, the effect is the opposite, indicating the asphaltene precipitation is causing an artificial decrease in molecular weight.

This difference in behavior of the two sets of crudes is probably linked to the amount of asphaltenes and the amount of metals in the asphaltenes. The latter two crudes have relatively low asphaltene contents (6.9 and 3.7 wt% of feed, respectively) compared to the Venezuelan crudes (23 and 20 wt% of feed, respectively). Also the Venezuelan crudes have the majority of their metals separated into the

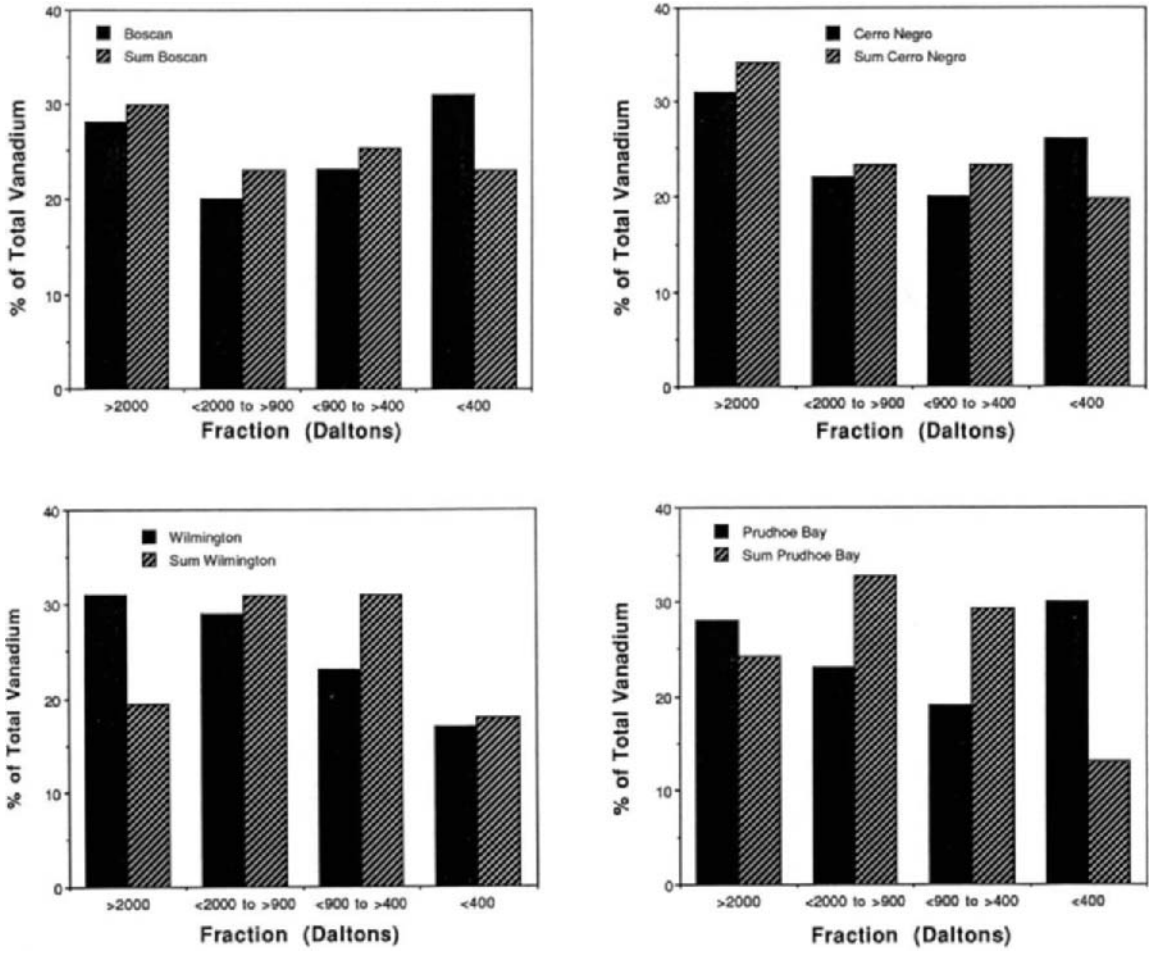

Fig. 10-3. Weight-balanced molecular weight distribution of vanadium for Boscan, Cerro Negro, Wilmington, and Prudhoe Bay crude oils determined by SEC-GFAA. (Data from Fish et al. [29].)

asphaltenes, whereas the latter two crudes do not. The behavior of these latter two crude oils is similar to that of Kern River 650°F$^+$ residuum shown in Table 10-2. Also, comparing histogramic outputs from these experiments clearly shows the agglomerating effect of the asphaltene precipitation for Boscan and Cerro Negro crude oils, but not for Wilmington and Prudhoe Bay crude oils.

Hausler [23] and Hausler and Carlson [30] have examined the effect the SARA separation has on the vanadium compounds in Hondo 650°F$^+$ residuum. The majority of the vanadium was separated into the heptane or pentane asphaltene fraction, with a smaller amount collected in the resin fraction. The SEC-ICP-AES analysis of the fractions showed that the vanadium compounds in the asphaltene fraction had the largest molecular size and some were larger than those detected in the whole residuum. Arabian Heavy 650°F$^+$ separated and examined under the same conditions, however, did not show the same SEC-ICP-AES behavior for vanadium. In this case, the whole residuum exhibited vanadium compounds which were slightly larger than those found in the asphaltenes. Because the profiles were not compared on the same chromatogram, this inconsistency of Arabian Heavy 650°F$^+$ residuum could be due to minor differences in flow conditions or to true differences in the behavior of the two feeds.

Some efforts have been made to chemically understand the origin of this agglomeration seen in the SEC-ICP-AES profiles. It has been suggested that this behavior of the metals during asphaltene precipitation could be due to an agglomeration of polar organic components [28,31–33]. Recent measurements on heavy crude oil residua and asphaltenes by light scattering have shown a dramatic increase in the bulk micellular subunit size upon precipitation of the asphaltene [34]. Infrared and nuclear magnetic resonance spectroscopic results indicate donor–acceptor interactions may be responsible for this agglomeration [31,35–37]. This hypothesis was tested further, where phenol was add to Boscan 1000°F$^+$ and Maya 650°F$^+$ residua, and the effect on the size distribution of the metal-containing compounds was examined by either SEC-ICP-AES or SEC-DCP-AES (DCP, direct current plasma). Infrared evidence showed definite interactions of the phenol with the residuum. SEC-DCP-AES vanadium profiles showed a definite decrease in size of Maya 650°F$^+$ residuum asphaltenes upon addition of phenol. Figure 10-4 shows the effect of this on the radius of gyration (as measured with polystyrene standards) [28]. The largest decrease was seen in the 508 to 162 Å size range, while the largest relative increase was observed in the 162 to 28 Å size range. These results, along with infrared spectroscopic [28,36] and chemical reaction [38] results indicate the agglomeration was due to intermolecular interactions.

Feed characterization: sulfur

Some studies have been conducted on the effect of the asphaltene precipitation on the sulfur-containing compounds, but not as many as for the metals. The size behavior of sulfur during the asphaltene precipitation, however, appears not to be the same as the behavior of the metal compounds. Kern River 650°F$^+$ and Boscan 650°F$^+$ residua were separated utilizing an isooctane precipitation. Unlike

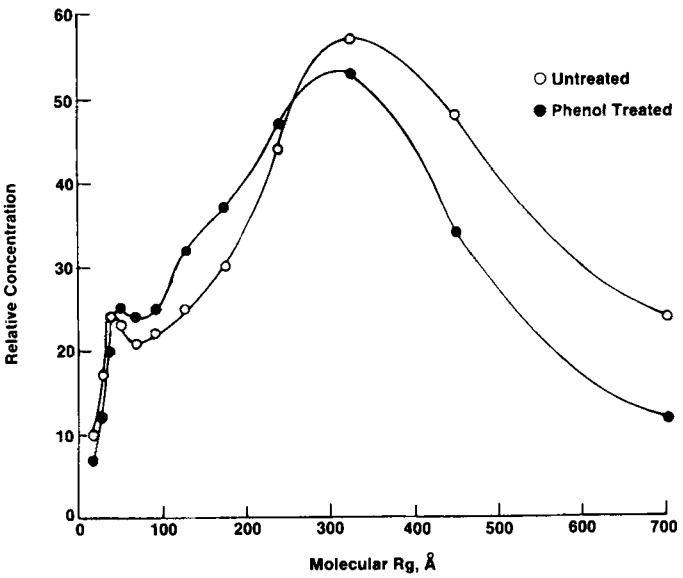

Fig. 10-4. Radius of gyration, R_g (in Å), for Maya 650°F$^+$ isooctane-derived asphaltenes with and without phenol added as measured by SEC-DCP-AES. (From Reynolds and Biggs [28].)

the vanadium behavior during this separation, the sulfur in the asphaltenes accounts for only 20 wt% of the total feed sulfur. The resulting fractions were examined by SEC-ICP-AES with sulfur-specific detection. The weight-balanced profiles are shown in Fig. 10-5 [39]. Several interesting features are observed in this figure: (1)

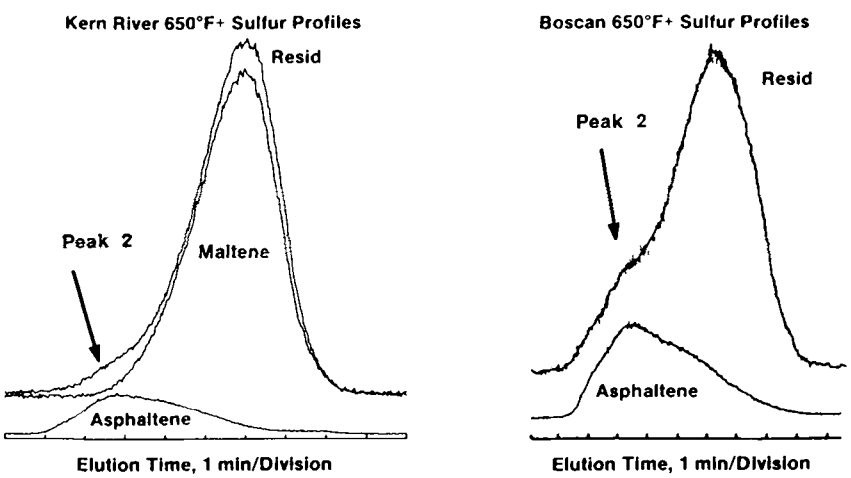

Fig. 10-5. SEC-ICP-AES sulfur profiles of Kern River and Boscan 650°F$^+$ residua and corresponding isooctane-insoluble asphaltenes. (From Reynolds and Biggs [39].)

the sulfur profiles of both feeds do not exhibit the agglomeration and increase in molecular size seen in the SEC-ICP-AES vanadium profiles for Boscan (Fig. 10-2); (2) the intensity maximum of the asphaltene profiles visually correlate with the shoulders (labeled peak 2) on the corresponding residuum profile; and (3) the areas of the asphaltene profiles roughly correlate with the areas of the shoulders. This visual identification suggests the asphaltenes are possibly a class of compounds in the whole residuum which are large, but not artificially agglomerated as in the case of vanadium compounds. This class of sulfur compounds is comprised of the largest sulfur-containing compounds in the whole residuum.

Empirical efforts to relate the shoulder in the SEC-ICP-AES residuum profile with other properties have met with limited success. SEC-ICP-AES sulfur profiles for Boscan, Kern River, Maya, Hondo, Beta, and Offshore California atmospheric residua indicate the integrated area of the shoulder found in the large molecular size range (peak 2 in Fig. 10-5) roughly correlates with the amount of alkane insolubles (asphaltenes). Figure 10-6 shows this relationship. For each feed, the isooctane-derived asphaltenes (open squares) correlate roughly linearly with the% of total sulfur determined by integration of the shoulder from the SEC-ICP-AES sulfur profile of the corresponding residuum, but are slightly higher than the 1 : 1 correlation (straight line). The heptane asphaltene values (solid circles) are much more scattered. The average values (solid squares) in the figure (average of the isooctane and heptane values) give the best correlation [40], although still not a very good correlation.

Table 10-3 shows an attempt to further correlate the integrated areas of the shoulders in the SEC-ICP-AES sulfur profiles with the weight-balanced distribution of the sulfur in the asphaltenes of the samples. The top four entries are data from

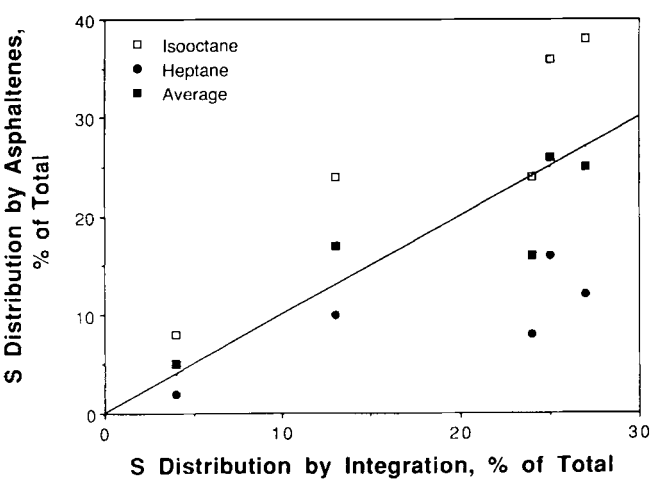

Fig. 10-6. Relationship between the sulfur distribution in asphaltenes determined by SEC-ICP-AES profile integration and the weight percent asphaltenes determined by isooctane insolubility. (Data from Reynolds and Biggs [39].)

TABLE 10-3

Comparison of sulfur-containing compounds in asphaltenes determined by SEC-ICP-AES profile integration to the sulfur distribution in asphaltenes determined by weight balance of elemental analysis of heptane- or isooctane-insolubles (data from [25,28,41])

Sample	Percentage by SARA separation (%)	Percentage by SEC-ICP-AES (%)
Arabian Heavy 980°F+ [a]	18.4	19.8
Product 1 980°F+ [a]	16.7	17.7
Product 2 980°F+ [a]	10.9	12.5
Product 3 980°F+ [a]	13.4	13.7
Maya 650°F+ [b]	36.3	25.0
Arabian Heavy 650°F+ [b]	24.3	24.0
Beta 650°F+ [b]	23.9	13.0
Kern River 650°F+ [b]	7.8	4.0

[a] Heptane asphaltenes (from Olbrich et al. [41]).
[b] Isooctane asphaltenes (from Reynolds [25] and Reynolds and Biggs [28]).

Olbrich et al. [41] who studied the effects of uni- and bimodal catalysts on the sulfur distribution upon catalytic upgrading of Arabian Heavy 980°F+ residuum. In this study, the residuum and the 980°F+ residuum cuts of the products were also characterized by a modified SARA separation using a hot heptane precipitation and the resulting fractions were analyzed for sulfur content. Table 10-3 shows the weight balanced distribution of the sulfur in the asphaltene fraction and compares it to the integrated intensity of the shoulder (peak 2 in Fig. 10-5) of the SEC-ICP-AES sulfur profiles for the same materials. Also included are the same types of data for selected 650°F+ residua separated into isooctane-derived asphaltenes [25,39].

The agreement of the two sets of values are good for the Arabian Heavy 980°F+ residuum and the 980°F+ cuts of the processed products. The correlation breaks down with Maya 650°F+ and Beta 650°F+. Both of these latter feeds correlate poorly with either isooctane- or heptane-derived asphaltenes, as shown in Fig. 10-6. The reasons for this are not clear, but possibly could be a result of the 980°F+ distillation allows for better characterization of the larger-size components.

The rough correlations in Table 10-3 and Fig. 10-6 do suggest some similarities (at least from the size perspective) between the shoulder at large molecular size in the SEC-ICP-AES profiles and sulfur content in the asphaltenes. Both certainly consist of at least some of the largest sulfur-containing compounds, and the asphaltene precipitation does not appear to affect the size distribution to any extent.

ANALYTICAL AND PROCESS IMPLICATIONS

Effects on metal-containing compounds

The apparent increase in size of the metal-containing compounds caused by the asphaltene precipitation, should have an effect on understanding metals behavior

during processing. Reynolds and Biggs [28,42] have demonstrated that the size of the vanadium-containing compounds are very important in the ease of removal, particularly for small-pore hydrodesulfurization (HDS) catalysts. In that study, the small-size compounds, which fit into the catalyst pores, appear to be quickly and easily removed, while the larger vanadium-containing compounds require more severe process conditions to be removed (probably due to mechanisms which do not utilize the catalyst pore in the first step). Larger-pore, demetalation catalysts were found to be much more effective in the relative removal of the larger vanadium-containing compounds. Sughrue et al. [43] examined the hydrodemetalation activity of several heavy crude oil residua, including Arabian Heavy, Maya, and Hondo, and found two different demetalation rate constants, which suggests two types of metals — easy-to-remove and hard-to-remove. SEC-ICP-AES vanadium profiles of the two types of metals roughly correlated with small- and large-size metal-containing compounds, respectively. De Waal et al. [44] have shown that in the hydroprocessing of Gach Saran and Kuwait atmospheric residua, increasing the size of the catalyst pore (as in demetalation catalysts), greatly improves the effective removal of vanadium-containing compounds in the large-size molecular range.

These studies show that the diffusional limitation of the larger-size metal-containing compounds greatly impacts the rate of removal. It is important, therefore, to consider that when characterizing a feed for studies of fixed-bed catalysts, the asphaltene precipitation can affect the analysis of the metals reactivity, because it can artificially increase the size metal complexes. This could be deleterious in determining the optimal size range and pore distributions of the catalysts, particularly when assessing the behavior of the whole feed through the behavior of the isolated asphaltenes.

In studying SDA (solvent deasphaltene) processing, however, this agglomeration of metal complexes due to asphaltene precipitation does not affect the analysis of the metals behavior. The SEC-ICP-AES vanadium profiles of the resin and asphaltene fractions of Boscan 1000°F$^+$ residuum (Fig. 10-2) suggest that the SDA process has some preference to separate the largest of the metal-containing compounds in the asphaltene fraction. The net result is the production of the DAO (deasphalted oil) fraction which has lower metals concentration than the feed and the metals complexes are, on the average, smaller than the average size found for the feed. Further processing of the DAO, therefore, should be easier to accomplish not only because of lower concentration of the metals, but also because the metals are smaller. More active, smaller-pored catalysts could then be used to prepare the DAO for downstream processing.

This agglomeration of the metal-containing complexes due to the precipitation seen in the asphaltenes can be reduced significantly by high-energy processing. Drushel [45] observed, by GPC, that the molecular weight distribution of the asphaltenes derived from an unspecified crude oil dramatically decreased upon severe thermal treatment or hydrotreating. Hall and Herron [27] showed, by preparative GPC, a similar decrease in size for both the metals and sulfur in the visbreaking or hydrotreating of asphaltenes derived from Arabian Light 1000°F$^+$ residuum. Savage et al. [46] observed, by SEC-ICP-AES, a decrease in size of the vanadium- and

sulfur-containing compounds during pyrolysis or hydropyrolysis of asphaltenes from an offshore California crude oil. Conditions were severe enough and the shifts to smaller size were significant enough to suggest that these decreases were not only due to destruction of the agglomeration interactions, but also due to the size reduction caused by cracking reactions. Thus, the larger molecules are reduced in size allowing the use of smaller-pore catalysts for further processing.

Effects on sulfur-containing compounds

Agglomeration does not seem to be as much of an issue for sulfur-containing compounds. As shown above, the agglomeration observed in the case of metals is not really significant for the sulfur components. In effect, the asphaltene precipitation could be used as a method of size separation. However, the true chemical significance of such a separation for sulfur-containing compounds is not clear. Results from the SARA separation of several heavy residua show that the sulfur concentration in the asphaltenes is highest of all the fractions [5,25,26]. The sulfur concentrations, however, are also high in the resin and aromatic fractions. For the aromatic fraction, this is generally considered to be thiophenic sulfur which is collected in this fraction due to similar polarity with aromatic hydrocarbons but not similar functionality [47]. The resin fraction, however, is more polar and exhibits elemental properties which are more similar to the asphaltenes. The type of sulfur-containing compounds in this fraction could be structurally similar to those in the asphaltenes. (Examination of unspecified heavy crude oil residua and corresponding asphaltenes by X-ray photoelectron spectroscopy and X-ray absorption near edge structure spectroscopy has shown the same types of sulfur-containing compounds (sulfidic and thiophenic) in both types of materials [48,49].) This could lead to analytical problems if the asphaltene is considered to be the only fraction representative of the polar-type sulfur-containing compounds.

CONCLUSIONS

Although asphaltene precipitation concentrates the metal compounds, it does tend to increase the average molecular size of the metal-containing compounds through agglomeration. This can cause analysis difficulties when size-related properties, for example, catalyst pore-metal-containing molecule interactions are being considered.

The effect on the sulfur-containing compounds appears to be different. Although the asphaltene precipitation does concentrate the sulfur-containing compounds to some extent, there is little evidence that the precipitation increases the average size of these compounds through agglomeration. The asphaltene precipitation, however, does separate some sulfur-containing compounds from the resin fraction. This could cause analytical difficulties if not accounted for, because these sulfur-containing compounds in the resin fraction can have similar structures to those of the asphaltenes.

ACKNOWLEDGMENTS

This work was performed under the auspices of the U.S. Department of Energy by the Lawrence Livermore National Laboratory under contract number W-7405-ENG-48.

REFERENCES

[1] Pfeiffer, J.P.H. and Saal, R.N.J., Asphaltic bitumen as colloid system. *J. Phys. Chem.*, 44: 139–149 (1940).
[2] Bunger, J.W. and Li, N.C., *Chemistry of Asphaltenes. Adv. Chem. Ser.*, 195 (1981) and references therein.
[3] Takeuchi, C., Fukul, Y., Nakamura, M. and Shiroto, Y., Asphaltene cracking in catalytic hydrotreating of heavy oils, 1. Processing of heavy oils by catalytic hydroprocessing and solvent deasphalting. *Ind. Eng. Chem. Process Des. Dev.*, 22: 236–242 (1983).
[4] Mitchell, D.L. and Speight, J.G., The solubility of asphaltenes in hydrocarbon solvents. *Fuel*, 52: 149–152 (1973).
[5] Reynolds, J.G., Characterization of heavy residua by application of a modified D 2007 and asphaltene separation: effect of solvents on physical and chemical properties of fractions derived from Hondo 850°F residuum. *Fuel Sci. Tech. Int.*, 5(5): 593–620 (1987).
[6] Speight, J.G., Long, R.B. and Trowbridge, T.D., On the definition of asphaltenes. *Am. Chem. Soc., Div. Pet. Chem., Prepr.*, 27(3): 268–275 (1982).
[7] Speight, J.G., Long, R.B. and Trowbridge, T.D., Factors influencing the separation of asphaltenes from heavy petroleum feedstocks. *Fuel*, 63: 616–620 (1984).
[8] Speight, J.G., Latest thoughts on the molecular nature of petroleum asphaltenes. *Am. Chem. Soc., Div. Pet. Chem., Prepr.*, 34(2): 321–328 (1989).
[9] Boduszynski, M.M., McKay, J.F. and Latham, D.R., Asphaltenes, where are you? *Assoc. Asphalt Paving Technol.*, 49: 123–143 (1980).
[10] Long, R.B., Concept of asphaltenes. *Adv. Chem. Ser.*, 195: 17–28 (1981).
[11] McKay, J.F., Latham, D.R. and Haines, W.E., Composition of petroleum heavy ends, 3. Comparison of the composition of high boiling petroleum distillates and petroleum >675°C residues. *Fuel*, 60: 27–34 (1981).
[12] Boduszynski, M.M., Composition of heavy petroleums. 1. Molecular weight, hydrogen deficiency, and heteroatom concentration as a function of atmospheric equivalent boiling point up to 1400°F (760°C). *Energy Fuels*, 1: 2–11 (1987).
[13] Dickie, J.P. and Yen, T.F., Macrostructures of the asphaltic fractions by various instrumental methods. *Anal. Chem.*, 39(14): 1487–1852 (1967).
[14] Yen, T.F., Structural differences between asphaltenes isolated from petroleum and from coal liquid. *Adv. Chem. Ser.*, 195: 39–51 (1981).
[15] Speight, J.G., *The Chemistry and Technology of Petroleum*. Marcel Dekker, New York, N.Y. (1980).
[16] Galiasso, R., Blanco, R., Gonzalez, C. and Quinteros, N., Deactivation of hydrodemetallization catalyst by pore plugging. *Fuel*, 62: 817–822 (1983).
[17] Sadeghi, K.M., Sadeghi, M-A. and Yen, T.F., Uses of generated surfactants from a new tar sand process for extracting hydrocarbons from natural and man-made materials. *Proc., 1989 Eastern Oil Shale Symp., IMMR89*, 209: 18–29 (1990).
[18] Bandurski, E., Structural similarities between oil-generating kerogens and petroleum asphaltenes. *Energy Sources*, 6(1/2): 47–66 (1982).
[19] Suzuki, T., Itoh, M., Takegani, Y. and Watanabe, Y., Chemical structure of tar-sand bitumens by ^{13}C and ^{1}H n.m.r. spectroscopic methods. *Fuel*, 61: 402–410 (1982).
[20] Speight, J.G. and Pancirov, R.J., Some aspects of the structure of petroleum asphaltenes. *Am. Chem. Soc., Div. Pet. Chem., Prepr.*, 28(5): 1319–1332 (1983).

[21] Ignasiak, T., Kemp-Jones, A.V. and Strausz, O.P., The molecular structure of Athabasca asphaltene. Cleavage of the carbon-sulfur bonds by radical ion electron transfer reactions. *J. Org. Chem.*, 42: 312–320 (1977).

[22] Biggs, W.R., Fetzer, J.C., Brown, R.J. and Reynolds, J.G., Characterization of vanadium compounds in selected crudes, I. Porphyrin and non-porphyrin separation. *Liq. Fuel Technol.*, 3(4): 397–421 (1985).

[23] Hausler, D.W., Molecular size distribution of specific elements in petroleum crudes and 650°F$^+$ residua by size exclusion chromatography with inductively coupled plasma spectrometry detection. *Spectrochim. Acta*, 40B(1/2): 389–396 (1985).

[24] Fish, R.H. and Komlenic, J.J., Molecular characterization and profile identifications of vanadyl compounds in heavy crude petroleums by chromatography/graphite furnace atomic absorption spectrometry. *Anal. Chem.*, 56: 510–517 (1984).

[25] Reynolds, J.G., Characterization of heavy residua by application of a modified D 2007 separation and electron paramagnetic resonance. *Liq. Fuel Technol.*, 3(1): 73–105 (1985).

[26] Reynolds, J.G., Can the D 2007-80 with asphaltene separation (SARA) separation, size exclusion chromatography with element specific detection, and hydrogen distribution by NMR help at all in predicting residuum processability? *Am. Chem. Soc., Div. Pet. Chem., Prepr.*, 34(2): 455–470 (1989).

[27] Hall, G. and Herron, S.P., Size characterization of petroleum asphaltenes and maltenes. *Adv. Chem. Ser.*, 195: 137–153 (1981).

[28] Reynolds, J.G. and Biggs, W.R., Effects of asphaltene precipitation and a modified D 2007 separation on the molecular size of vanadium- and nickel-containing compounds in heavy residua. *Fuel Sci. Tech. Int.*, 4(6): 749–777 (1986).

[29] Fish, R.H., Komlenic, J.J. and Wines, B.K., Characterization and comparison of vanadyl and nickel compounds in heavy crude petroleums and asphaltenes by reverse-phase and size-exclusion/graphite furnace atomic absorption spectroscopy. *Anal. Chem.*, 56: 2452–2460 (1984).

[30] Hausler, D.W. and Carlson, R.S., On-line SEC-ICP: a new element specific, molecular sizing tool for the petroleum industry. *Am. Chem. Soc., Div. Pet. Chem., Prepr.*, 30(1): 28–35 (1985).

[31] Ignasiak, T., Strausz, O.P. and Montgomery, D.S., Oxygen distribution and hydrogen bonding in Athabasca asphaltene. *Fuel*, 56: 359–365 (1977).

[32] Boduszynski, M.M., Asphaltenes in petroleum asphalts-composition and formation. *Am. Chem. Soc., Div. Pet. Chem., Prepr.*, 24(4): 935–948 (1979).

[33] McKay, J.F., Amend, P.J., Cogswell, T.E., Harnsberger, P.M., Erickson, R.B. and Latham, D.R., Petroleum asphaltenes: chemistry and composition. *Adv. Chem. Ser.*, 170: 128–142 (1978).

[34] Senglet, N., Williams, C., Faure, D., Des Courieres, T. and Guilard, R., Microheterogeneity study of heavy crude petroleum by u.v.-visible spectroscopy and small angle X-ray scattering. *Fuel*, 69: 72–77 (1990).

[35] Altgelt, K.H. and Harle, O.L., The effect of asphaltenes on asphalt viscosity. *Ind. Eng. Chem. Prod. Res. Dev.*, 14: 240–246 (1975).

[36] Moschopedis, S.E. and Speight, J.G., Investigations of hydrogen bonding by oxygen functions in Athabasca bitumen. *Fuel*, 55: 187–192 (1976).

[37] Monin, J.C. and Vignat, A., Mise en evidence d'associations par pont hydrogène dans les asphaltenes par chromatographie d'exclusion stérique. *Rev. Inst. Fr. Pét.*, 39(6): 821–827 (1984).

[38] Acevedo, S., Mendez, B., Rojas, A., Layrisse, I. and Rivas, H., Asphaltenes and resins from the Orinoco basin. *Fuel*, 64: 1741–1747 (1985).

[39] Reynolds, J.G. and Biggs, W.R., Analysis of residuum desulfurization by size exclusion chromatography with element specific detection, Part II. *Fuel Sci. Tech. Int.*, 6(3): 329–354 (1988).

[40] Herbrandson, H.F. and Neufeld, F.R., Organic reactions and the critical energy density of the solvent. the solubility parameter, δ, as a new solvent parameter. *J. Org. Chem.*, 31: 1140–1143 (1966).

[41] Olbrich, H.C., Hung, C-W. and Howell, R.L., Characterization of straight run and demetallized Arabian heavy atmospheric resid. *Am. Chem. Soc., Div. Pet. Chem., Prepr.*, 32(2): 450–456 (1987).

[42] Reynolds, J.G. and Biggs, W.R., Application of size exclusion chromatography coupled with element-specific detection to the study of heavy crude oil and residua processing. *Acc. Chem. Res.*, 21: 319–326 (1988).

[43] Sughrue, E.L., Hausler, D.W., Liao, P.C. and Strope, D.J., Application of size exclusion chromatography with inductively coupled plasma emission spectrometric detect to residual oil hydrodesulfurization (HDS) and hydrodemetalation (HDM) studies. *Ind. Eng. Chem. Res.*, 27: 397–401 (1988).

[44] De Waal, W.A.J., Kuiper, C.C.H.M., Maessen, F.J.M.J., Kraak, J.C., Wijnands, R. and Jonker, R.J., Selection of conditions for the molecular size speciation of vanadium and nickel complexes in oil by size exclusion chromatography coupled with inductively coupled plasma-atomic emission spectrometry. *J. Chromatogr.*, 462: 115–135 (1989).

[45] Drushel, H.V., Micro techniques for the characterization of high-boiling materials. *Am. Chem. Soc., Div. Pet. Chem., Prepr.*, 21(1): 146–164 (1976).

[46] Savage, P.E., Klein, M.T. and Kukes, S.G., Asphaltene reaction pathways. 3. Effect of reaction environment. *Energy Fuels*, 2: 619–628 (1988).

[47] Payzant, J.D., Hogg, A.M., Montgomery, D.S. and Strausz, O.P., A field ionization mass spectrometric study of the maltene fraction of Athabasca bitumen, Part II. The aromatics. *AOSTRA J. Res.*, 1(3): 183–206 (1985).

[48] Kelemen, S.R., George, G.N. and Gorbaty, M.L., Direct determination and quantification of sulfur forms in heavy petroleum and coals, 1. The X-ray photoelectron spectroscopy (XPS) approach. *Fuel*, 69: 939–944 (1990).

[49] Gorbaty, M.L., George, G.N. and Kelemen, S.R., Direct determination and quantification of sulfur forms in heavy petroleum and coals, 2. The sulfur K edge X-ray absorption spectroscopy approach. *Fuel*, 69: 945–989 (1990).

Asphaltenes and Asphalts, 1. Developments in Petroleum Science, 40
edited by T.F. Yen and G.V. Chilingarian

Chapter 11

ROLE OF ASPHALTENES ON OIL RECOVERY AND MATHEMATICAL MODELING OF ASPHALTENE PROPERTIES

M.R. ISLAM

INTRODUCTION

Asphaltenes are known to deposit in the vicinity of production wells during miscible floods, after acid stimulations, or during pressure changes in a mature field with an asphaltic crude. Many reservoirs produce without any asphaltene problems until the oil stability is perturbed during later stages of oil production. After the initial problems with asphaltenes, catalytic behaving stimulus, such as an acid job, may continue to exhibit problems long after operations return to normal. This problem may persist even for crude oils containing small amount of asphaltenes.

Asphaltenes are complex organic materials that are considered to be arranged in stacked, multi-ring structures. They contain nitrogen, oxygen, and sulfur atoms in addition to carbon and hydrogen atoms within the repeating unit [1–4]. Asphaltenes have a wide range of potential structures and also vary in physical properties from reservoir to reservoir. The actual structure of asphaltenes depends on the source of the oil as well as asphaltic materials. Asphaltenes are not truly soluble in most crude oils. They exist as 35–40 μm platelets and are maintained in suspension by materials called maltenes and resins. These smaller suspending molecules are soluble and act in what has been described as "micellar type" arrangements in order to keep the asphaltenes in suspension. When stabilizing factors are altered, the asphaltenes coalesce under certain pressure, temperature, or compositional conditions. This leads to the formation of larger groups, called flocs, that precipitate and have been reported to have a density of 1.2 g/ml [5]. Asphaltene content of crude oils may vary from 0 to 60% [6]. On the other hand, resin-to-asphaltene volume ratios vary from 1 : 1 to 20 : 1 in oils that are stable and to less than 1 : 1 in oils that are characterized by rapid precipitation of asphaltenes [7]. Even though it is generally understood that asphaltene content of a crude oil increases with decreasing API gravity, asphaltene precipitation has been reported in light oils as well.

Asphaltene precipitation

The mechanism of asphaltene precipitation is very complex and despite a wealth of research on the topic, controversy as to the nature of asphaltene solutions persists. There are two differing schools of thoughts as to the nature of asphaltenes in solutions. The first one considers asphaltenes to be dissolved in oil in a true liquid state. In this case, asphaltene precipitation is considered to depend on ther-

modynamic conditions of temperature, pressure and composition. This particular school of thought recognizes asphaltene precipitation as a thermodynamically reversible process [8,9]. The second school of thought considers asphaltenes to be solid particles which are suspended colloidally in the crude oil and are stabilized by large resin molecules. Consequently, the deposition process is considered to be irreversible. This particular approach uses methods used to describe colloids to describe the phenomena of asphaltene precipitation [10–12]. Asphaltene precipitation may occur when the equilibrium of the stabilizing forces has been perturbed. The most important compositional change occurs during miscible flooding. However, changes in pressure and temperature during production, even in primary mode, may cause asphaltene precipitation. Also, during acid stimulation or cyclic CO_2 injection, similar destabilization may occur. The major destabilizing forces which may cause asphaltene precipitation [13] are as follows:

(1) *CO_2 injection:* The role of CO_2 in destabilizing asphaltene–crude oil equilibria is well documented [1,14–18]. CO_2 causes the destabilization of asphaltene equilibria by lowering pH, by changing oil composition, and by creating turbulence. CO_2 is also responsible for formation of rigid emulsions in presence of an asphaltic crude [19]. Some degree of asphaltene precipitation has been observed in almost every CO_2 flood operation. Usually, asphaltene precipitation increases as the volume of CO_2 available to the crude oil increases during the later stages of CO_2 injection or stimulation. The most noticeable primary locations of asphaltene deposition are the wellbore and the pump regions.

(2) *Miscible flooding:* Flooding of a rich gas destabilizes the asphaltene–crude oil mixture by lowering the carbon-to-hydrogen ratio in the solution [17]. Usually stripping gas from the oil has been shown to improve the solubility of asphaltenes [20]. The straight-chain hydrocarbons have less affinity for the asphaltic ring structures than oils that have a higher carbon-to-hydrogen ratio. The negative effect of rich gas is at a maximum near the bubble point [14,20–22]. This effect is alleviated after the bubble point is reached [20]. This peculiar behavior near the bubble point is more pronounced for a rich gas than for carbon dioxide [14].

(3) *pH shift:* A shift in pH of the crude oil–asphaltene solution may be invoked by CO_2, mineral acid, or naturally occurring or bacterially produced organic acids. Several of these factors may become important during a particular period of the life of a producing well [11].

(4) *Mixing of crude streams:* The most likely causes for such asphaltene precipitation are a shift in pH by a natural organic acid in an incoming crude, CO_2 counter-current flow, and physical shear or other perturbations caused by cavitation in some pumps and mixing manifolds or chambers [20]. It may be caused also by local instabilities which may not occur under more complete mixing [20]. This type of precipitation may be prevented by more complete mixing of the crude streams under reduced shear.

(5) *Incomplete organic chemicals:* It is well known that isopropyl alcohol, methyl alcohol, acetone, and even some glycol, alcohol, or surfactant based solvents, that do not have an aromatic component, may selectively wet or attract the maltenes and resins and precipitate asphaltenes.

(6) *Well stimulation:* Severe asphaltene precipitation may be caused by well stimulations, such as acidizing, etc. [17,23,24]. Acidizing, for instance, involves a drastic shift in local chemical equilibria, pH and CO_2 gas liberation. It may also increase the concentration of some ions, such as iron [25], which may influence the formation of asphaltic sludges, flocs, etc. The most common asphaltic deposits found after acidizing are iron/asphaltene sludges and emulsions stabilized by asphaltene particles.

(7) *Shear:* The problem of instability due to shear has recently been identified in rod pumps and electrical submergible pumps (ESPs) [19,20,26]. Shear is closely associated with pressure drop in downhole operation and with mixing in surface equipment.

(8) *Pressure drop:* Pressure drop is one of the most important factors to influence solid deposits from asphaltic crudes. The effect of pressure is most intense when the crude oil is rich in light ends in an oil just above the bubble point. Depending on the location of pressure drops, asphaltene deposition may occur in different parts of the reservoir as well as in the wellbore and in the production stream [16,20,21]. A change of pressure is usually accompanied by a change in temperature. These changes cause physicochemical instability leading to asphaltene precipitation from the crude oil. Pressure change alone can also invoke similar asphaltene precipitation [22]. Also, turbulence has been known to accelerate asphaltene precipitation, whereas improved mixing of different crude streams leads to the prevention of asphaltene precipitation [20].

(9) *Streaming potential:* It has been reported that flow of crude oil through porous media can result in precipitation of asphaltic materials [5,27]. This has been generally attributed to the neutralization of the particles charged by the "streaming potential". Even though the streaming potential through porous media has been identified as a cause of asphaltene precipitation, very little information on this phenomenon is available in the literature. Also, this phenomenon has been associated with pressure drop or charge [1,3,21].

(10) *Temperature drop:* As pointed out earlier, pressure drops often are associated with temperature drops. Temperature is usually considered to have an indirect effect on asphaltene precipitation, which results from destabilization of related forces caused by temperature alterations. As pointed out by Monger and Fu [28], temperature may affect the solubility of maltenes and resins and a temperature drop may lead to the creation of paraffin precipitation, which traps some asphaltene during solidification. This temperature effect may be more readily invoked by expansion of CO_2 during a CO_2 injection operation (following gas breakthrough).

(11) *Charged, bare metal surfaces:* It has been noted that the colloidal material in crude oil is electrically charged [27,29]. Imposition of a potential across a small body of oil results in electrodeposition of asphaltene material at the positive electrode. This shows that the materials in the crude oil which were deposited had a negative charge. It also shows that the neutralization of this charge can result in precipitation of the material. This condition may be a combination of the problems of shear stress and pressure drop and is one of the least understood of the destabilizing forces [19,25,26].

ROLE OF ASPHALTENE DURING PRIMARY DEPLETION

Field conditions for precipitation

In 1965, Haskett and Tartera [30] used the argument that since the addition of low-molecular-weight paraffin hydrocarbons causes the precipitation of asphaltenes, associated resins, and naphthenes, it could be expected that the release of these components, when the pressure of the crude oil in the tubing falls below the bubble point, reduces the tendency for the asphaltenes to become depeptized. Consequently, the deposition of asphaltenes would occur generally in the single-phase crude oil. This single-phase crude oil, which undergoes no compositional change, is subject to changes in pressure and temperature, turbulence and possible electrical effects near the wellbore. As one of the first field examples of asphaltene deposition during primary depletion, Haskett and Tartera [30] presented results observed in the giant oil field of Hassi Messaoud, Algeria. This reservoir is situated at a depth of 3610 m and the initial reservoir pressure was 471 atm. The bubble point for this 42°API crude varied from 147 to 199 atm. The gas/oil ratio varied from 183 to 248 std m^3/m^3. It was observed that:

– The asphaltene deposit became less severe with increasing depth. This was true regardless of the depth at which the deposit was found. This indicated that the most favorable condition for deposition was just before the bubble point was reached. This corresponded to the lowest pressure, the lowest temperature and the longest flowing time for the given tubing diameter, flow rate, and surface pressure.

– The deposits of asphaltene were repeptized when the wellhead pressure was once again reduced. Otherwise, asphalt deposits were extended all the way to the surface. Locations of these extensions correlated to positions where the bubble points were reached in the tubing.

– An extension was found even when the only change invoked was closing the well for measuring the asphalt profile. This was attributed to the reabsorption of the liberated gas as the oil level rose in the tubing. This created an excess of hydrocarbons in the oil phase, which caused the immediate precipitation of asphaltenes and associated elements.

– One well, which produced at a wellhead pressure considerably above the bubble point, showed asphaltene deposition up to the surface, except on the downstream side of the choke where the pressure was below the bubble point.

From the above observations, it was recommended that the Hassi Messaoud wells be put on production at low wellhead pressure so that two-phase flow would occur sufficiently deep in the tubing to minimize asphaltene deposition. Placing mechanical choke deep into the tubing was tried in a few cases with success.

Asphaltene problems in some Venezuelan medium oil reservoirs were reported by Lichaa [11]. He presented asphaltene problems in the Mata-Acema field of Venezuela. This sandstone reservoir was located at a depth of 3773 m and at a temperature of 135°C. The crude contained 25% of light fractions, whereas the rest was C_{7+}. Even though this crude contained only 0.4–9.8% asphaltene, the wells showed considerable asphaltene deposition problems during natural depletion

or acid stimulation. Interestingly, no asphaltene precipitation was observed for a nearby Boscan heavy-oil reservoir, even though this crude contained an asphaltene concentration higher than 17.2%. This formation is at a depth of 2789 m and a temperature of 82°C. This Boscan crude was found to prevent electrodeposition of asphaltene from the Mata-Acema crude. Lichaa [11] also reported the use of Boscan crude as a stabilizing agent for emulsions injected as displacing fluids in enhanced oil recovery processes. Laboratory investigations on the crude of these fields revealed the following:

- The resins which serve as peptizing agents for the asphaltenes are easily oxidized. This process increases the crude viscosity and provides favorable conditions for precipitation of the depeptized asphaltenes.
- Asphaltenes are found to migrate and deposit at the cathode upon application of an electric field. Consequently, the particles migrate back and deposit at the other electrode, if the polarity of electrodes is reversed.
- Effective inhibition of asphaltene deposits in the formation appeared to be possible by injecting sufficient amounts of peptizing agents to the formation.
- Electrical effects play an important role in asphaltene deposition problems. Controlling the electrodeposition of asphaltene particles could lead to a preventative technique for asphaltene deposition.

One of Lichaa's important observations was that at times (the case of Boscan field, for instance) the asphaltene content in crude may play a lesser role than the amount of peptizing agent, such as resins, in the flocculation process. Consequently, a crude oil with high asphaltene concentration may not necessarily show deposition problems due to the lack of peptizing agents.

Von Albrecht et al. [31] reported asphaltene deposition problems in another Venezuelan oil field. It was reported that in the oil field of Lake Maracaibo, conventional completion techniques led to costly workover requirements. This partially dolomitized limestone reservoir was located at a depth of 4593–5249 m with initial reservoir pressure as high as 849 atm. Severe asphaltene problems were alleviated by modifying completion techniques similar to those practiced at the Hassi Messaoud field of Algeria.

In 1982, Adialalis [32] reported field results which showed field performance to be opposite to that reported by Hasket and Tartera [30]. Severe asphaltene deposition problems were encountered in the Prinos field of the North Aegean Sea. Production from wells, which occurred at a rate of 3000 barrels per day, fell to negligible amounts only after a few days of production. Workovers in this region were considered to be so expensive (over quarter million dollars each due to the presence of sour gas) that production from this reservoir appeared to be economically unattractive. The reservoir was a sandstone formation with shale barriers, which separated several producing layers. This reservoir is located at a depth of approximately 2800 m. The initial reservoir pressure was close to 400 atm, whereas the bubble point ranged from 76 to 86 atm depending on the location in the 6 km^2 reservoir. The gas/oil ratio ranged from 140 to 160 std m^3/m^3. The reservoir temperature was reported to be 128°C. For this particular reservoir, severe asphaltene problems were encountered throughout, and, unlike the Hassi Messaoud

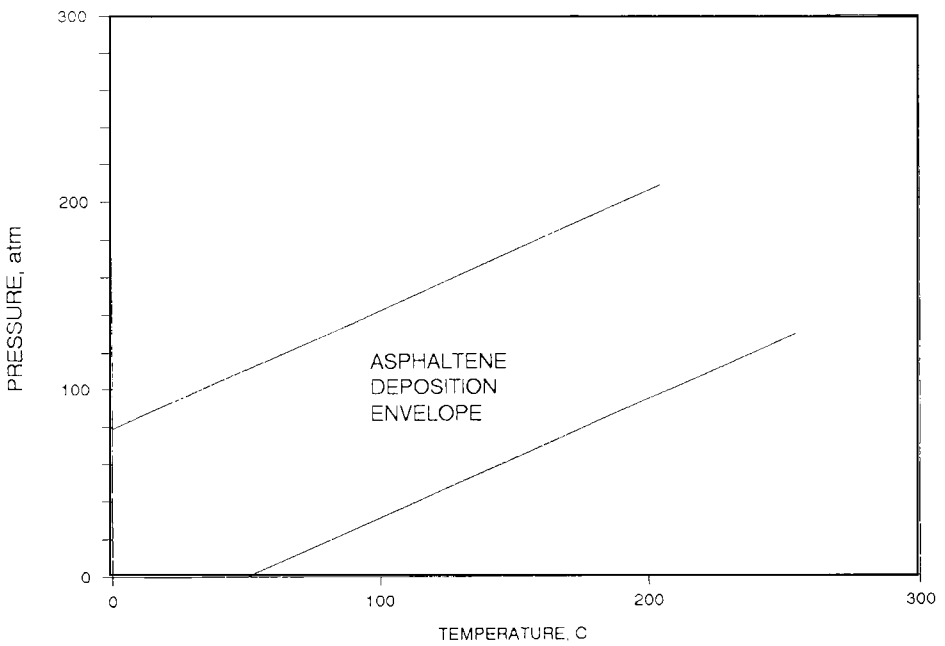

Fig. 11-1. Asphaltene deposition envelope for the Prinos field. (After Adialalis [32].)

field case, asphaltene precipitation was observed in the tubings, separators, pumps, and virtually all locations. A laboratory analysis of the reservoir crude gave rise to the asphaltene deposition envelope as shown in Fig. 11-1. Unlike the case of Hassi Messaoud, it was decided to produce this reservoir at a high wellhead pressure. Also, it was recommended to use dual completion for cleaning with solvents during production. Finally, more production was carried out from the top reservoir, which was separated from the bottom one by a shale barrier and exhibited fewer asphaltene problems. Initially, production was being carried out from all the layers simultaneously.

It is well known that highly undersaturated (with respect to gas) crude oil reservoirs may show asphaltene precipitation during the course of primary depletion. Strong undersaturation may also occur in fluids with a natural gas cap if the hydrocarbon column is of large vertical extent. If there is a producing gas/oil ratio gradient present in the reservoir, the wells in the lower horizon are expected to show more asphaltene precipitation problems than those in the upper horizon. This was observed in several field cases. For instance, at the Ventura field of California, heavy asphaltene precipitation was observed in the well tubing when the reservoir pressure was above the bubble point. After the bubble point pressure was reached, the wells showed no sign of asphaltene problems [19]. The reason for this observation can be explained by the Hirschberg [33] model which indicates that pressure decline in the reservoir would cause precipitation of the asphaltenes. Inasmuch as no production problems were encountered for production under the bubble point, however, it is

clear that asphaltene precipitation in the reservoir does not cause any major plugging of the formation. This indicates that, in such a reservoir, pressure reduction down to the bubble point by production from the upper part of the field could be used to reduce the risk of plugging the wells with asphalt deposits. This particular reservoir is located at a depth of 2789 m. The initial reservoir pressure was 586 atm, whereas the bubble point ranged from 241 to 310 atm.

Inasmuch as asphaltene stability is very sensitive to the dissolution of condensate in the reservoir crude, asphaltene precipitation may occur near the wellbore during retrograde condensation. Once again, such a problem may be reduced by constraining the producing gas/oil ratio.

In the above discussion of different field experiences, it is clear that asphaltene precipitation and its remedies thereof are dependent on particular cases. Asphaltene deposition could not be correlated with even known factors, such as pressure, temperature, and composition. Controversy on pressure dependence of asphaltene precipitation is particularly disturbing. For instance, it was recommended for the Hassi Messaoud oil field that wells be produced at a low wellhead pressure. This approach was found to be successful with Hassi Messaoud as well as Ventura or some Venezuelan oil fields. As pointed out by Leontaritis and Mansoori [21], this observation is in line with the refining propane deasphalting process where propane is mixed with the crude oil to reduce the asphalt solubility in the crude and flocculate it out. It is apparent that producing these fields with low wellhead pressures led to the extraction of a large portion of gas from the reservoir crude, which would alter the composition necessary for the peptization of asphaltenes. The experience at the Prinos field of the North Aegean sea, however, was totally opposite to those of other reservoirs cited above. It was reported that a high wellhead pressure (as high as 100 atm) alleviated asphaltene precipitation problems. Whereas this particular reservoir had a very high concentration of sour gases, the effects of these sour gases on such different asphaltene deposition problems was never discussed. In order to explain some of the controversy observed in different oil fields, Leontaritis and Mansoori [21] emphasized the importance of geological conditions which may favor the formation of an oil with a resin concentration less than critical. The critical resin concentration for a given crude is the concentration below which asphaltene particles flocculate and above which they cannot flocculate regardless of how much the oil mixture is agitated or refluxed. According to Leontaritis and Mansoori [21], geological conditions may be responsible for the transformations undergone by the hydrocarbon deposits. They recommended further research to identify these geological conditions for different cases of resin concentrations correlated with critical resin concentrations for oil reservoirs around the world. This might, in their view, lead to accurate predictive techniques for asphaltene deposition for reservoirs which have not yet produced. More recently, Novosad and Costain [34] conducted numerical simulations of field precipitation cases in the presence of CO_2. This study shed some light on the controversy of the pressure dependence of asphaltene precipitation. This aspect of their study will be discussed in a later section.

Effect of pressure

Inasmuch as pressure decline is the most dominating factor during primary depletion, it is appropriate to discuss the effect of pressure on asphaltene precipitation in this section.

One of the earliest observations of pressure effects on asphaltene flocculation was made by Bilheimer et al. [35]. They observed that the purified bitumen was precipitated from its solution or dispersed in tetralin by the addition of *n*-pentane and that the separation occurred at lower weight fractions of *n*-pentane at lower temperatures. The bitumen–tetralin solutions showed some colloidal characteristics at temperatures below 71.1°C at which the bitumen separates as a solid phase. At states remote from the phase boundaries and at temperatures above 71.1°C, these characteristics become less evident. Under these latter circumstances the mixtures tend to follow the behavior of true solutions, particularly in regard to the approach to heterogeneous equilibrium. Figure 11-2 shows the variation in asphaltene precipitation as a function of pressure and temperature as presented by Bilheimer et al. [35]. Note that there is a consistent decrease in asphaltene precipitation as the pressure is increased. This trend is more obvious for a high temperature (104.4°C). This observation was further validated by Lhioreau et al. [36]. They reported that pressure can increase asphaltene solubility. Figure 11-3 shows asphaltene precipitation as a function of pressure for a temperature of 20°C. As can be seen from this figure, pressure dependence of asphaltene precipitation is

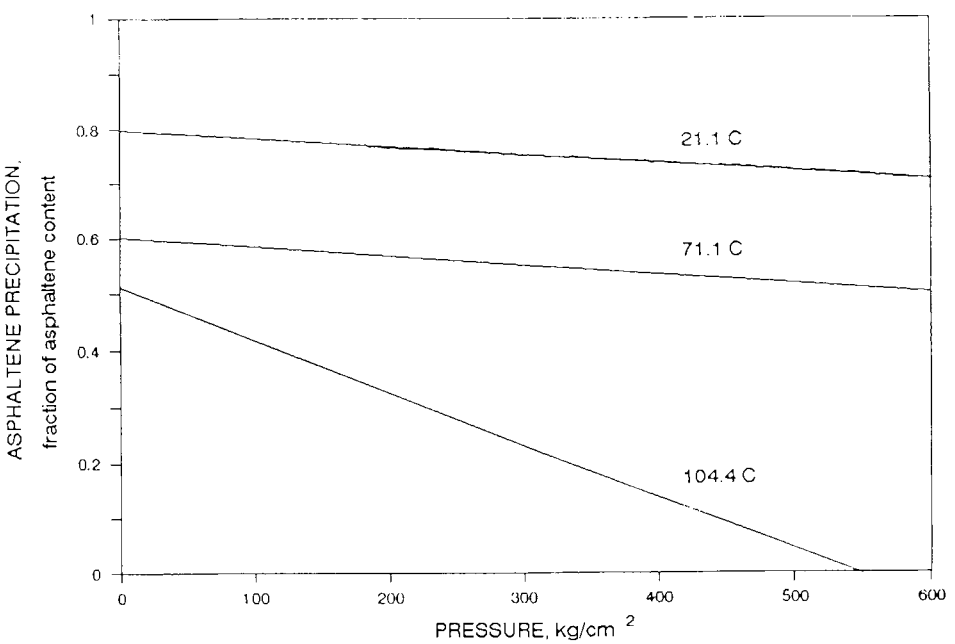

Fig. 11-2. Effect of pressure and temperature on asphaltene precipitation. (After Bilheimer et al. [35].)

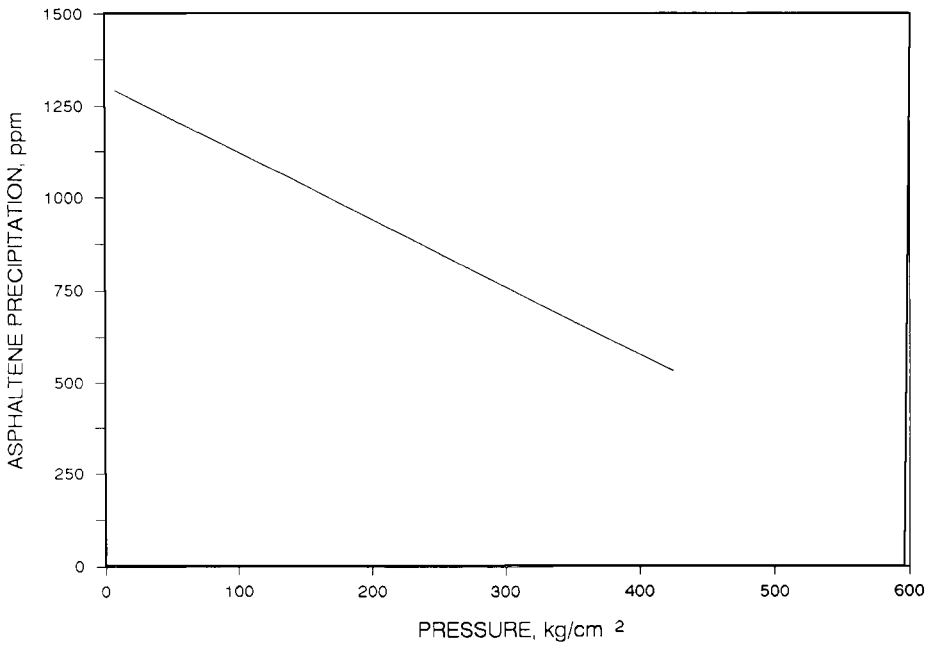

Fig. 11-3. Effect of pressure on asphaltene precipitation at 20°C. (After Lhioreau et al. [36].)

linear, similar to what Bilheimer et al. observed. Similar effect was also observed for experiments conducted at 80°C.

Hirschberg [33] studied the effect of pressure change on asphaltene precipitation in a crude–propane (weight ratio of 1:7) mixture. The mixture of crude and propane was placed in a windowed cell. The amount of precipitate was measured as a function of pressure at two different temperatures of 22° and 94°C. Before each measurement, the mixture was allowed to equilibrate for at least 24 hours. Results of these tests, for which both tank oil and downhole samples were used, are presented in Table 11-1. It was observed that at low temperature (22°C) and low pressure (20 bar) the precipitation was brownish-grey and expected to contain paraffin wax. At high temperatures (94°C, below 280 bar), the precipitation was a black liquid which contained mainly resins. At about 280 bar, the liquid vanished and black solid particles were formed, also showing a strong tendency to adhere to the windows. The amount of solid formed was roughly in agreement with the amount of *n*-heptane present in the crude oil. As the pressure was increased from 280 to 1000 bar, the propane-rich phase became darker, indicating that some asphaltenes were being dissolved. In this study, asphaltene precipitation appears to be reversible. This is particularly evident for the asphaltene particles formed on the windows above 300 bar. When the pressure was reduced, they began to grow, liquefy and drop out, leaving perfectly clean windows (160 bar).

TABLE 11-1

Effect of pressure and temperature on asphaltene precipitation for crude/propane (1:7 wt%) mixture (after Hirschberg et al. [8])

T (°C)	Pressure (bar)	Volume precipitate / Volume tank oil	Comments
1st Experiment (tank oil)			
22	20	2×10^{-2}	brownish grey flakes
22	100	8×10^{-3}	brownish grey flakes
22	200	8×10^{-3}	brownish grey flakes
22	300	4×10^{-3}	black deposit on windows
22	400	n.a.	windows obscured
2nd Experiment (tank oil)			
94	600	–	black particles on windows
94	350	–	black particles on windows
94	300	–	particles grow and become brownish
94	280	–	droplets on windows, begin to drop oil
94	160	1.2×10^{-2}	black liquid
94	1000	3×10^{-3}	black solid particles
94	280	3×10^{-3}	onset of liquid drop-out
94	75	4×10^{-2}	black liquids; windows perfectly clear
3rd Experiment (downhole sample)			
87	280	2×10^{-3}	black solid particles
87	130	6×10^{-3}	black liquid
87	70	4.4×10^{-2}	black liquid

Role of asphaltene in bubble flow in heavy-oil reservoirs

Although asphaltenes have been synonymous with production problems, at least one aspect of asphaltenes has been recognized as benefiting oil production. Recently, it has been recognized that asphaltenes act as a nucleation site for microbubbles in some heavy-oil reservoirs of Canada. These microbubbles help reduce the apparent viscosity of the oil without causing coalescence and eventual blockage.

It has been known for some time that the production of heavy oil from Canadian reservoirs has led to many anomalous results. Conventional prediction techniques do not account for an unusually high recovery efficiency during primary production from these reservoirs. Previously, such a high recovery was attributed to "high-permeability channels resulting from sand production". Elkins et al. [37] hypothesized the existence of "worm hole" porosity in the unconsolidated sands held together only by the viscous oil. This hypothesis has often been supported by sudden collapse in injection schemes or failure of drilling and workover operations in heavy-oil reservoirs in Canada. This concept has often been used to introduce negative skin factors in modeling heavy-oil reservoirs. Whereas this technique has given satisfactory results in several occasions, the technique has been criticized as being scientifically inaccurate. In fact, Islam and George [38] have demonstrated

through laboratory experimentation that sand redistribution or even sand/fines removal would actually decrease the near-wellbore permeability.

Smith [39] was the first researcher to relate production anomalies of the Canadian heavy-oil reservoirs to the rheology of microbubbles which, in turn, depends on the asphaltene content of the heavy oil. He suggested that solution gas drive in Canadian heavy-oil reservoirs involves the simultaneous flow of oil and many tiny gas bubbles. He proposed a new model for predicting the performance of heavy-oil reservoirs in Canada. He postulated that the complex fluid within the pore space in a heavy-oil reservoir is comprised of a true liquid, large molecular particles (asphaltenes as molecules of MW $\simeq$ 1000 or micelles of MW $\simeq$ 100,000) and gas bubbles of similar size. Conventional reservoir analysis considers bubbles of gas dispersed in the reservoir to be immobile until a critical gas saturation is reached. This analysis is based on the belief that gas bubbles are too large to move through pore throats and that a rapid reduction in oil permeability with small gas saturations is a result of pore throat blockage. This assumption of large bubble size results from the theory of thermodynamic stability, which indicates that bubbles of radius of more than 200 μm are likely to grow unstably. However, recently Ward et al. [40] concluded through experimental and theoretical studies that microbubbles can be in stable equilibrium under the constraint of a closed volume and for reasonable conditions of liquid temperature and pressure. Their analysis indicates that it is possible to generate micro-sized bubbles in a porous medium. Because these bubbles are much smaller than the average pore throat size, they can flow even when the gas phase is not continuous. This is contrary to the popular hypothesis of the conventional reservoir engineering approach. In this regard, the analysis of Ward and Levart [41] should be mentioned. Their analysis indicates that very small bubbles may be present in thermodynamically stable form in the presence of a rough surface. This surface may be either that of the boundary or that of particles suspended in the solution. Similar surface roughness maybe provided by asphaltene molecules, which are usually abundant in heavy oil. Microbubbles formed in this way are stable in such a way that only further reduction in pressure may make them grow, reducing the possibility of growth by coalescence. This analysis supports the surmise that the presence of asphaltene molecules in heavy oil would enhance the possibility of forming thermodynamically stable microbubbles. This aspect was experimentally investigated by Islam and Chakma [42]. They demonstrated that asphaltenes may play an important role in capturing microbubbles and that bubble size may depend on the concentration of nucleation sites provided by asphaltene molecules. The effect of asphaltene concentration on gas/liquid volume is depicted in Fig. 11-4. There appears to be a distinct impact of asphaltene concentration on the gas-bearing capability of the mixture. This translates into one of the major factors in determining the bubble size. That is, as the asphaltene concentration increases, the size of the microbubbles decreases. A decrease in bubble size leads to lower equivalent viscosity of the gas–oil mixture as envisaged by Smith [39]. Islam and Chakma [42] quantified the effect of microbubble size in the case of heavy-oil flow.

Figure 11-5 shows the effect of microbubble size on pressure drop across a capillary tube. A low pressure drop for this case indicates that the field recovery

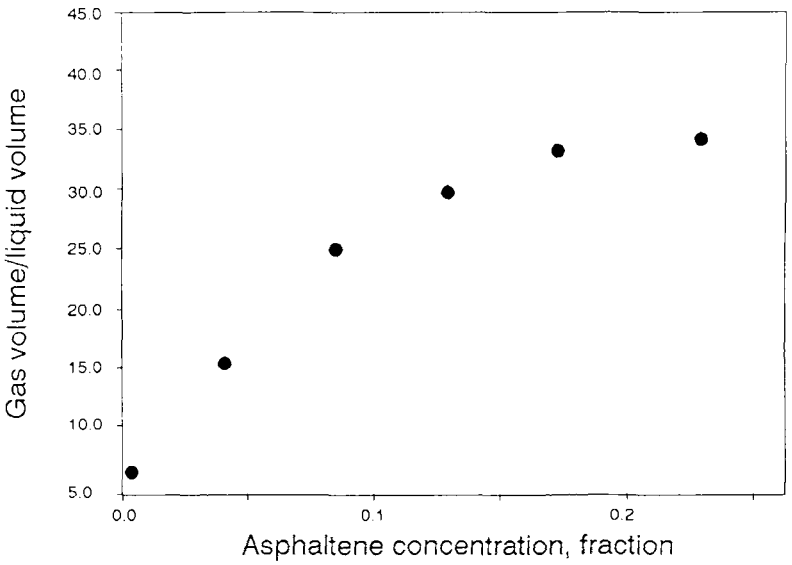

Fig. 11-4. Effect of asphaltene concentration on gas/liquid volume. (After Islam and Chakma [42].)

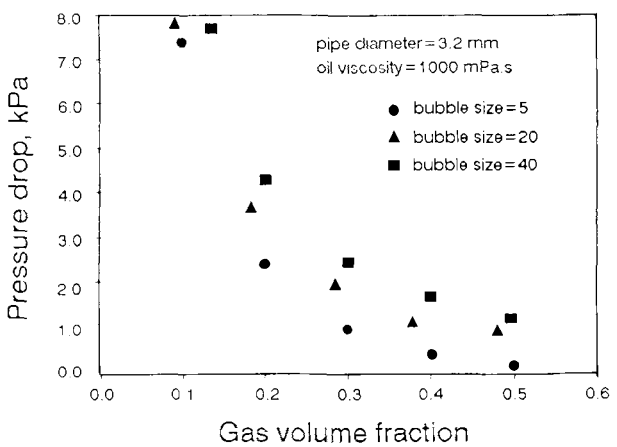

Fig. 11-5. Effect of bubble size on pressure decline. (After Islam and Chakma [42].)

would be higher for a given gas–oil mixture. Figure 11-5 indicates that, even though the shapes of the pressure drop vs. gas volume fraction curves are similar for all different bubble sizes, actual pressure drop values tend to increase as the bubble size increases. This indicates that the generation of tiny microbubbles in heavy-oil reservoirs will enhance fluid flow for a given pressure decline. The actual size of microbubbles in heavy-oil reservoirs is not known. Results in Fig. 11-5, however, indicate that a substantial increase in fluid flow may occur by mere decrease in gas bubble size. Islam and Chakma [42] further investigated the role of microbubbles.

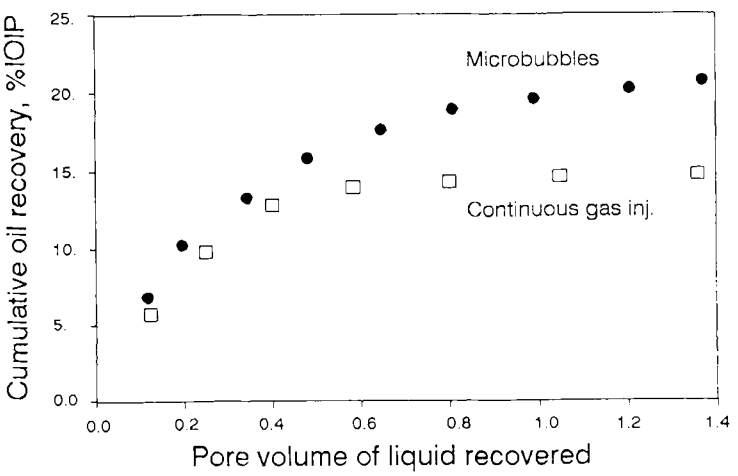

Fig. 11-6. Role of microbubbles as displacing agents. (After Islam and Chakma [42].)

Figure 11-6 shows that a substantial increase in heavy-oil recovery may take place if microbubbles are allowed to form. These microbubbles were attributed to the presence of asphaltene.

The presence of asphaltene is likely to increase the possibility of the formation of microbubbles in heavy oil which, in turn, would lead to a decrease in the equivalent viscosity of the oil–gas mixture. Consequently, oil recovery by primary depletion would be improved.

Effect of asphaltene adsorption on rock properties

The presence of asphaltene in a crude oil has been shown to affect rock properties. Most of these effects have been recognized to be the result of asphaltene adsorption on the rock surface. This has tremendous effect on rock wettability, enhanced oil recovery (EOR) fluid adsorption, etc.

Some of the first observations on the effects of adsorption of asphaltene particles on reservoir rock characteristics were made by Clementz [43]. Interactions of asphaltene particles with clay and sand minerals depend on the dipolar ion species in the asphaltenes and resins, and on the large condensed aromatic ring structure. It is believed that the ionic species are responsible for the initial attraction of the asphaltene and resins to mineral surfaces. Once in close approximation to these surfaces, the large condensed aromatic ring structure causes further strengthening of the adsorptive beds through electron interaction with surface oxygens. It has been reported that the adsorption of asphaltene to sand surfaces is reduced as the water saturation is increased. However, even for high water saturations, there is a competition for adsorption sites. As the water saturation decreases, the rate of adsorption increases. Clementz [43] concluded that the maximum adsorption may be achieved within a day for dry samples. Analysis of the equilibrium solution after

the adsorption process showed that the basic nitrogen content was reduced. This substantiated the importance of dipolar ion structures in the adsorption process. It was observed that the adsorption of asphaltene particles followed the Langmuir isotherm form. This led to the belief that asphaltene adsorption is essentially limited to a monolayer coverage of the rock surface. The adsorption was also found to be dependent upon the exchangeable cations on the clay surfaces. In general, divalent cations caused more asphaltene adsorption. However, all the common mono- and divalent ions adsorbed in the same order of magnitude.

Inasmuch asphaltenes are largely solvent-stabilized, the magnitude and sign of charge on the molecules is likely to be controlled by the solvent. Consequently, asphaltene adsorption depends upon the solvent environment as well. Solvents which can ionize the asphaltenes, such as nitrobenzene, cause much higher adsorption than those aromatic solvents similar in character to the asphaltenes. Consequently, the nature of the crude oil, which acts as a carrier solvent for the asphaltenes, is also important [43].

Asphaltene adsorption to the rock surface is likely to cause a shift toward the "oil-wet" nature of the rock. It was confirmed by Clementz [43] who conducted wettability tests on Berea sandstones. He observed that an untreated core, which was water wet, was rendered "neutral" in wettability after being treated with petroleum heavy ends. This indicated some dispersed coverage of the rock surface with asphaltene particles. This would have considerable impact on the end-point permeabilities and residual oil saturations following an enhanced oil recovery treatment. Because any surface active fluid injected during an EOR process would compete for the same adsorption sites, the presence of adsorbed asphaltene particles will undoubtedly affect the adsorption of the injected fluid. The extent and nature of this effect is not clearly understood. However, preliminary studies show that a core treated with asphaltene exhibits a reduction in adsorption to the injected surfactant solutions. Figure 11-7 shows the effect of heavy ends treatment on surfactant elution through the Nevada sand as reported by Clementz [43]. Although the amount adsorbed in the treated sample was initially higher than that in the untreated sample, the percent retained in the core upon dilution with distilled water was zero in the case of the treated sample, as compared to 22% in the untreated sample. Although initially more surfactant is attracted to the asphaltene-saturated surface, this is a relatively weak interaction. The dodecylobenzene sulfonate (DBS) is eluted easily with a distilled water flush. It is expected that better adsorption would take place in the presence of an asphaltene-treated rock surface. Experimental procedures, which determine surfactant adsorption for EOR applications, should consider this phenomenon for reservoirs with asphaltic crudes. It would be desirable to keep the surface films intact during an adsorption test with native cores. Figure 11-8 shows an illustration of the effect of adsorption on the amount of DBS adsorption on montmorillonite. This figure, redrawn from Clementz [43], shows that although there may be a tendency for the sulfonate to be attracted to the asphaltene-treated surface, the blockage of surface charge sites and restrictions of movement into the inter-micellar space of the clay minerals out-weigh by far any interaction of the sulfonate with the asphaltene structure.

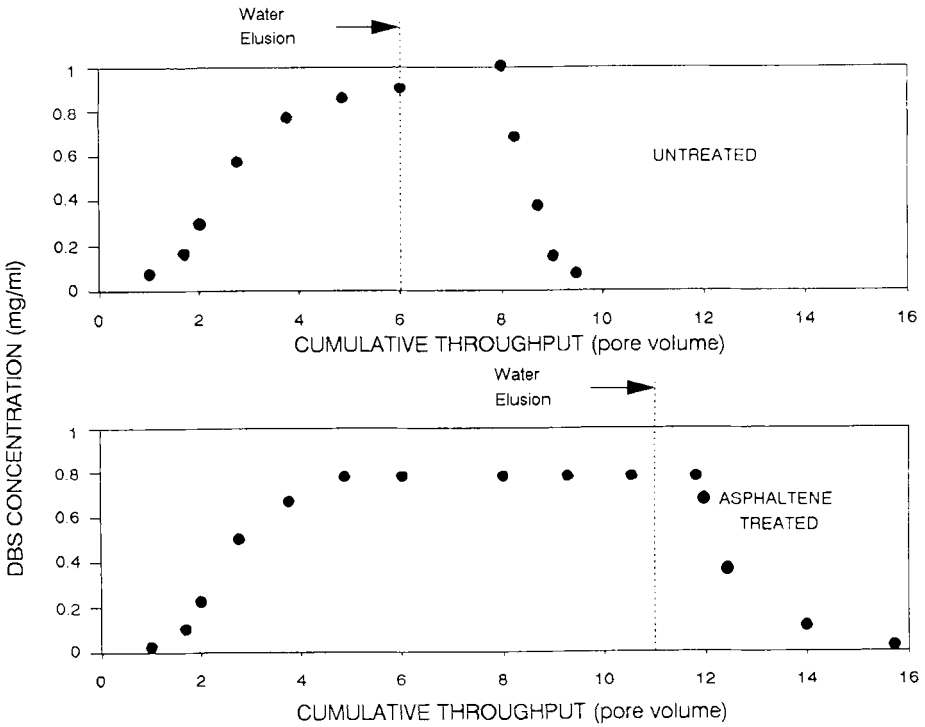

Fig. 11-7. Effect of heavy and adsorption on surfactant elusion. (After Clementz [43].)

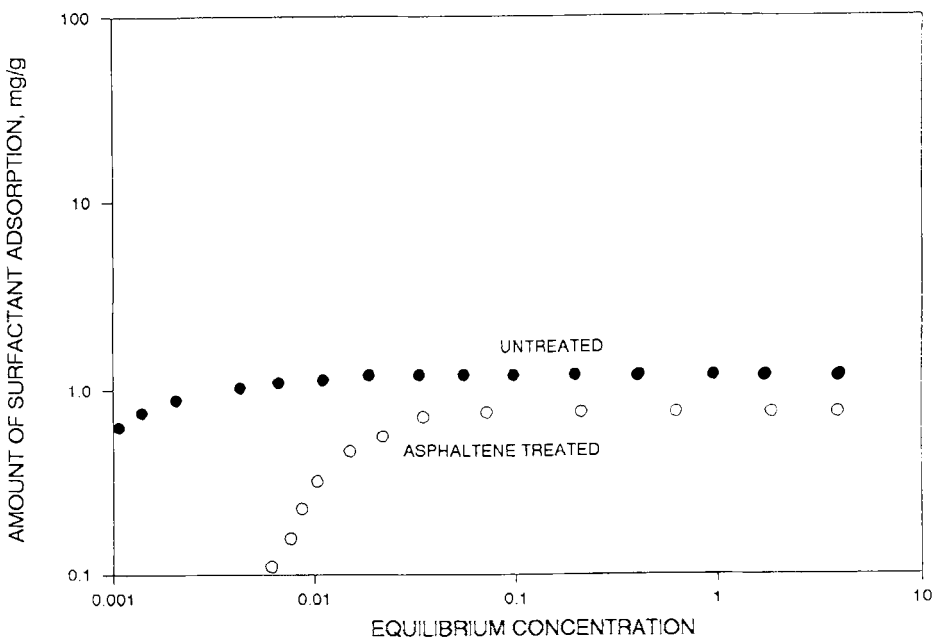

Fig. 11-8. Effect of asphaltene adsorption on DBS adsorption. (After Clementz [43].)

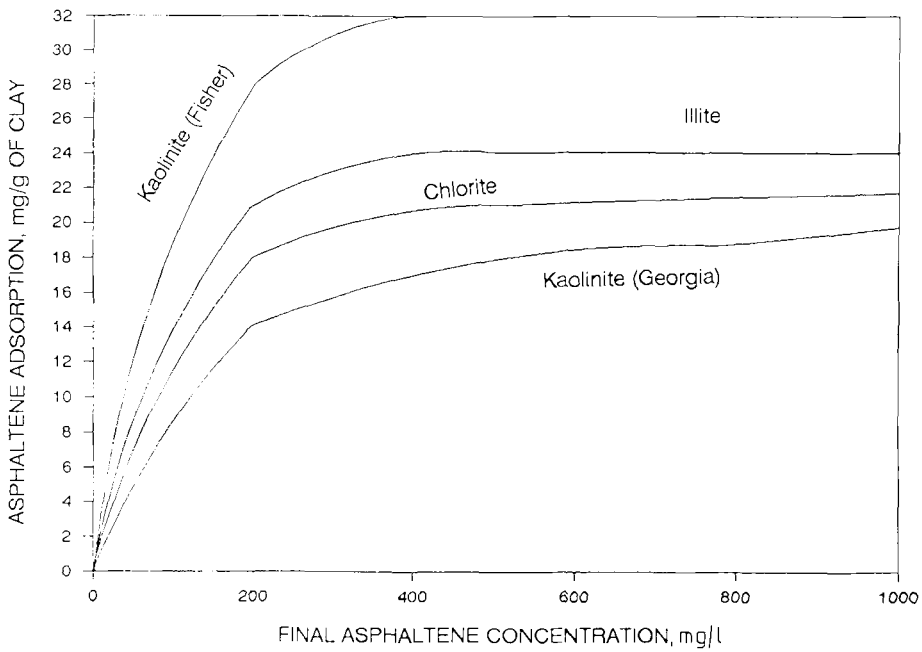

Fig. 11-9. Asphaltene adsorption on various dry clay samples. (After Collins and Melrose [44].)

Collins and Melrose [44] reported detailed studies on the effect of asphaltene adsorption and wettability alteration. They determined adsorption isotherms on dry samples of kaolinite, illite, chlorite, and Berea sandstone. Figure 11-9 shows adsorption curves for various clay samples. They reported that the plots of the ratio of asphaltene concentration to the amount of adsorbed asphaltene vs. asphaltene concentration indicated some deviation from Langmuir isotherm behavior. This deviation occurred especially near low concentrations. Table 11-2 shows maximum adsorption values for various dry clay and sandstone samples. They also studied the effect of water on asphaltene adsorption. Figure 11-10 compares various adsorption curves in the presence of varying amounts of water in the sample. They noted that the adsorption of asphaltenes on clay minerals may depend on the equilibrium time, especially in those cases where water was present. This change, however, did not take place after a month. They concluded that asphaltene adsorption on kaolinite, chlorite, and illite are similar to those on dry montmorillonites. If equivalent surface area is considered, Berea sandstones showed similar adsorption behavior as well. As can be seen from Fig. 11-10, the presence of water reduces asphaltene adsorption considerably. Asphaltene adsorption, however, is not completely eliminated. It was observed that, on the basis of surface area covered by asphaltenes, the thickness of the co-adsorbed water on kaolinite corresponds to about 30–50 monolayers, which indicated the formation of liquid bridges between clay particles. This observation was also supported through measurements of oil–water contact angles.

TABLE 11-2

Adsorption of asphaltene on various dry surfaces (from Collins and Melrose [44])

Sample	Surface area (m^2/g)	Maximum adsorption (mg/g)	Maximum adsorption (mg/m^3)
Kaolinite (Fisher)	19.3	30	1.55
Kaolinite (Ward National Science Establishment)	18	20	1.11
Illite	24	26	1.08
Chlorite	13	24	1.85
Berea Sandstone	1.26	1.8	1.43

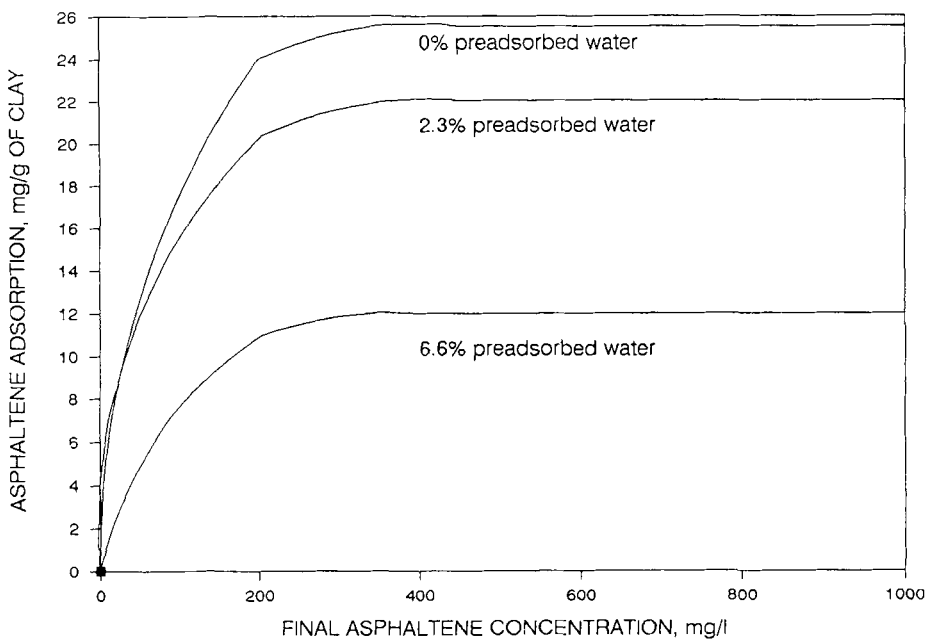

Fig. 11-10. Adsorption on kaolinite from water-saturated toluene. (After Collins and Melrose [44].)

In a different study, Melrose [45] explained the possibility of mixed wettability in asphaltic crude oil reservoirs. He explained this behavior through the existence of repulsive interaction in wetting films arising from osmotic forces associated with the diffusion electrical double layers at the boundaries between such films and the adjoining bulk phases. The dependence of the interaction force on electrolyte concentration follows from the experimentally observed dependence of zeta potential on concentration, for solid–brine and oil–brine systems. This phenomenon should be affected by the presence of asphaltenes.

Crocker and Marchin [46] observed wettability change toward the oil-wet state in Berea Sandstone. This effect was found to be concentration dependent. They

confirmed their observation for three different crude oils with polar fractions of 1, 5, and 10%. However, similar amounts of asphaltene and polar fractions were absorbed. Inasmuch as asphaltene has a much higher molecular weight than that of the polar fraction, similar amounts of absorption meant more molecules of polar fractions were adsorbed on the Berea sandstone pore surfaces.

Danesh et al. [1] conducted micromodel studies to observe the effect of asphaltene deposition on rock wettability. They used soda-lime glass surfaces as a model of an hydrophillic surface with zero contact angle for a water–air system. As the first step, the model was saturated with crude oil to irreducible water saturation. Due to water-wet nature of the micromodel, thin films of water were evident. This effect was manifested by relatively thick opaque grain boundary lines. When this oil-saturated model with connate water was allowed to age for a few hours, a gradual but minor alteration of the model wettability was observed in parts of the model, indicating the presence of intermediate or neutral wettability. This condition was confirmed by subsequent flooding of the model with water, which flowed through the bulk of the pore spaces and advanced the front menisci through the larger available pore throats. In spotted places where water-wet conditions prevailed, capillary forces assisted water imbibition. Wettability is believed to be changed mainly by the components adsorbed on the rock surface. Crude oil may contain polar compounds which are sufficiently water-soluble to pass through the water phase and be adsorbed on the solid surface to make them oil wet. This is mainly due to the presence of heavy ends in the crude. This was confirmed by repeating the experiment using normal hexadecane in place of crude oil. In this case no wettability alteration was observed. In case of profuse asphaltene precipitation in the presence of propane, the model surfaces were rendered completely oil-wet. This was observed when the model was initially saturated with crude–propane mixture and was flushed with crude oil to remove asphaltene precipitations. This was followed by a waterflood. In this case, it was observed that water advanced through the bulk of the pore spaces, leaving a thick film of oil on the throat walls. The nature of early breakthrough and consequent high water/oil ratio were indicative of an oil-wet nature of the model.

ASPHALTENE PRECIPITATION DURING MISCIBLE INJECTION

Asphaltenes are characterized by a larger carbon-to-hydrogen ratio than is typically found in a crude oil. The low-molecular-weight paraffin solvents are thought to cause precipitation of the asphaltenes by removing the maltenes (dissolution and desorption). Subsequently, the asphaltene micelles flocculate and precipitate from the liquid. The onset of asphaltene flocculation by the addition of solvents under static conditions has been studied experimentally by several authors [8,47].

Shelton and Yarborough [48] recognized that the mixing of oil with high-ethane-content hydrocarbon gases or CO_2 can produce multiple liquid phases and asphaltic precipitation in low-temperature reservoirs. They conducted core tests to show the formation of multiple phases leading to a residual hydrocarbon saturation during a displacement process. Even though other authors [49,50] before Shelton and

Yarborough observed multiple liquid-phase phenomena with some miscible gases and West Texas crude, they did not evaluate the effect on oil displacement. Shelton and Yarborough [48] concluded that the precipitation of solids is likely to occur when the reservoir oil is asphaltic. The solids and the oil-rich liquid phase are likely to be left as a residual saturation. They recommended core tests for determining the magnitude of the resulting saturations in a flow system. The residual saturation, even if small, may lead to three-phase flow effects and reduce the relative permeability to water during an alternate gas–water injection. For several mixtures, they observed a small pressure region (maximum of 8.3 atm) where four phases were present. These phases, from the top of the cell down, were a gas phase, a driving gas-rich phase, an oil-rich phase, and a solid gray precipitate (asphaltene) at the cell bottom. Figure 11-11 shows such occurrence of four phases.

Some of the initial reporting of asphaltene precipitation problems during miscible gas flooding projects were for the Little Creek CO_2-injection project in Mississippi. In this field, the asphaltene deposition problem was not reported during the primary or waterflooding phases. This problem was caused by the CO_2 in the produced crude oil, which acted in a manner similar to propane in causing deposition of the asphaltenes. In addition, CO_2 is known to cause rigid films at the oil/water interface because of its effect on pH [19]. These rigid films can also contribute to the deposits.

Lhioreau et al. [36] conducted a series of experiments to show the pressure dependence of asphaltene precipitation from an asphaltic crude with methane. Table 11-3 shows amounts of asphaltene precipitation with methane for pressure

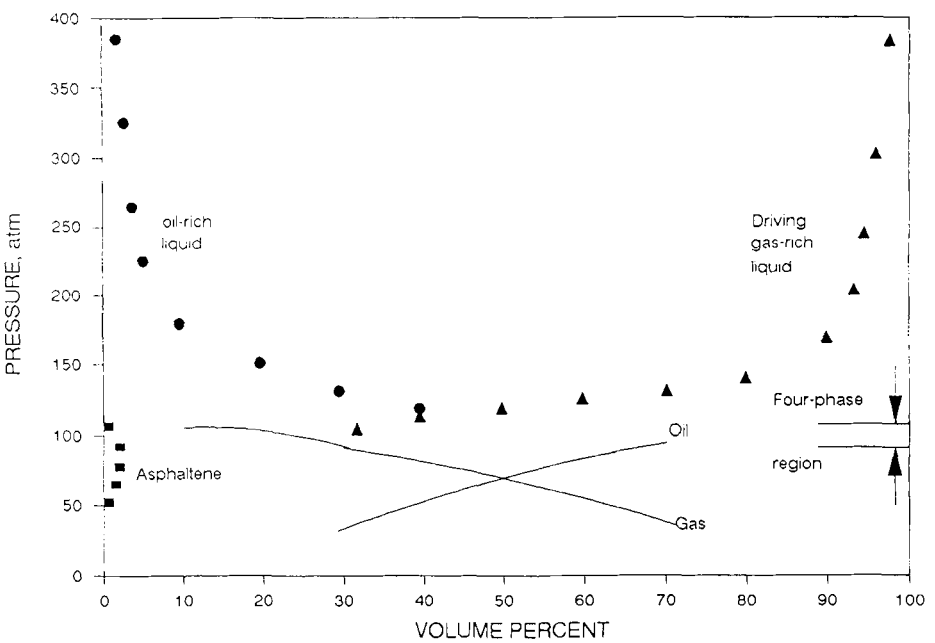

Fig. 11-11. Occurrence of four-phase region. (After Shelton and Yarborough [48].)

TABLE 11-3

Asphaltene precipitation (ppm) by methane (from Lhioreau et al. [36])

Pressure		at 450 kg/cm^2
60 kg/cm^2	104	300
	283	203
	45	33
120 kg/cm^2	200	216
	486	406
169 kg/cm^2	287	45

ranging from 60 to 350 kg/cm^2. As can be seen from this table, there is a wide range of variations for different sets of experiments. Lhioreau et al. [36] attributed this variation to the fact that the mixture was not formed spontaneously. During fill-up, the relatively high gas concentration should invoke precipitation of asphaltenes which may not be reproducible.

Harvey et al. [51] used ethane and heavier components in the injected rich gas for determining amounts of asphaltene precipitation during a miscible flood. In three of the reported four projects, productions took place with the water in alternate slugs as rich gas occurred at anticipated rates. In the fourth West Texas project, however, an unanticipated reduction in the water injection rates occurred after injection of the initial slugs of rich gas. Field results indicated that the problems existed in depth within the reservoir and it was not just a wellbore problem. This led to the study of Shelton and Yarborough [48] who presented pressure–volume–temperature (PVT) cell data that showed the occurrence of two liquid phases and an asphaltic precipitate when high-ethane-content rich gas and reservoir oil are mixed under reservoir conditions.

Hirschberg et al. [8] reported that a series of experiments was carried out in which recombined crude was contacted (at a pressure of 156 bar and temperature of 54.5°C) with separator (lean) and enriched gas. The amount of asphaltene precipitated was determined by extracting asphaltenes from the residue left in the cell after evacuation of the gas and crude. In the first experiment, separator crude (1.9 wt% asphaltene) was recombined with separator gas at a gas/oil ratio (303 std m^3/m^3) higher than the original gas/oil ratio of the reservoir crude (90 std m^3/m^3). On recombination, 0.6 wt% tank oil of asphaltenes dropped out (Table 11-4). In subsequent experiments, the recombined crude (0.3 wt% asphaltene) was contacted with 612 std m^3/m^3 of lean or 883 std m^3/m^3 of enriched gas. Table 11-4 compares the measured and predicted amounts of precipitate. The predicted values have been determined by using solubility values slightly higher than the values obtained from titration experiments. Results shown in Table 11-4 indicate that asphaltene precipitation may also be induced upon separator gas injection.

In a previous section, the findings of Hirschberg et al. [8] regarding the effect of pressure on asphaltene precipitation for a propane–crude mixture is discussed.

TABLE 11-4

Asphaltene precipitation with gas injection (after Hirschberg et al. [8])

Gas	Amount of gas added (scf/bbl)	Asphaltene content (wt% tank oil)	Precipitate measured (wt% tank oil)	Precipitate predicted (wt% tank oil)
Separator	1180	1.9	0.56	0.64
Lean	3400	1.3	0.2[a]	0.0
Enriched	4900	1.3	1.3	1.3

[a] Precipitation may be caused by slight over saturation of the recombined crude sample with respect to asphaltenes.

These results indicate that asphalt precipitation in a miscible drive project can be strongly induced by increasing the pressure. Although asphalt precipitation is reduced, precipitation of pure asphaltene may be induced. As a general rule of thumb, Hirschberg et al. [8] stated that asphalt precipitation precludes pure asphaltene flocculation because the asphaltenes are dissolved in the asphalt.

Danesh et al. [1] conducted a series of experiments for observing asphaltene deposition in oil reservoirs by miscible gas flooding. They used flow visualization experiments, which used high-pressure glass micromodels. The micromodels, at times packed with glass beads, allowed them to observe asphaltene precipitation during a miscible flood at a pore level. Miscible displacement of oil with propane was found to produce no significant asphaltene precipitation at the pore level. In a field situation, considerable mixing of the injection fluid and the reservoir oil occurs in the well tubing and reservoir fractures. It is likely that the resultant precipitates would enter the pores and plug the passages. This is a phenomenon which may occur even though insignificant precipitation occurred at the pore level. In order to observe the effect of bulk mixing, they mixed oil with propane and then injected the mixture into the micromodel. This was followed by flooding the model with oil and the pressure drop across the system was monitored. At this point asphaltic particles were observed flowing into the model and heavy deposition was initiated in the low-velocity domain of the flow. Consequently, most deposition occurred in the tighter pores perpendicular to the main direction of flow, leading ultimately to a severe blockage of the pore channels. It was observed that continuing injection of propane could not remove the asphaltene deposits, whereas a supply of fresh oil resulted in gradual disappearance of the deposits. Actual damage in permeability was monitored by knowing the pressure across the system. For this particular case, permeability damage was estimated to be 69% of the original permeability during asphaltene precipitation. This permeability damage was further increased by continuous injection of propane which led to over 90% reduction in original permeability. Permeability was restored during continuous injection of fresh crude oil. This led one to believe that asphaltene was dissolved by the fresh crude and the adhesion was weakened, and eventually asphaltene deposits were removed.

Jiang et al. [52] presented experimental data on the amount of asphalt and asphaltene precipitation due to addition of solvents to stock tank oil from the

West Sak reservoir of Alaska. Solvents used for this study were ethane, carbon dioxide, propane, *n*-butane, *n*-pentane, *n*-heptane, Prudhoe Bay natural gas, and natural gas liquids. One set of experiments was conducted to observe asphaltene precipitation due to the addition of CO_2 to recombined West Sak crude under reservoir conditions. They observed for all the solvents that there is an increase in the amount of asphaltene precipitated for increasing solvent/oil ratios for lower values of solvent/oil ratios. As the solvent/oil ratio was increased, the asphaltene precipitation leveled off. Figure 11-12 shows that for normal paraffinic solvents, the amount of asphalts precipitated (at maximum solvent/oil dilution ratio) increased with decrease in molecular weight of solvents, whereas the amount of asphaltenes precipitated remained relatively unchanged. The mutual solubility of resins in oil decreases with decreasing molecular weight of solvents. They also studied the effect of pressure on asphaltene precipitation for a CO_2 and live oil mixture. Details of these results are discussed in a later section. One of their major observations was that the asphaltene precipitation was the highest at the bubble point pressure and decreased with increasing pressure above the bubble point pressure and with decreasing pressure below the bubble point pressure.

Kokal et al. [53] used high-pressure micromodels to observe asphaltene precipitation from Canadian heavy oils with light hydrocarbon gases, such as, methane, propane, ethane/propane mixtures, and CO_2 under various pressure and temperature conditions. Figure 11-13 shows the maximum amounts of asphaltene precipitated as a function of carbon number for Suffield and Lindberg crude oils. They

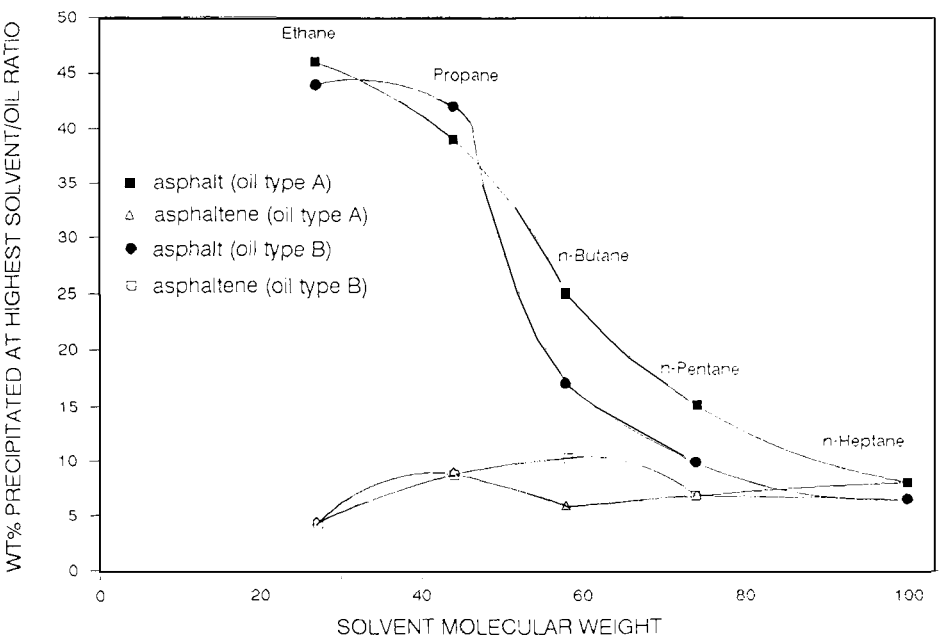

Fig. 11-12. Effect of solvent molecular weight on asphaltene precipitation. (After Jiang et al. [52].)

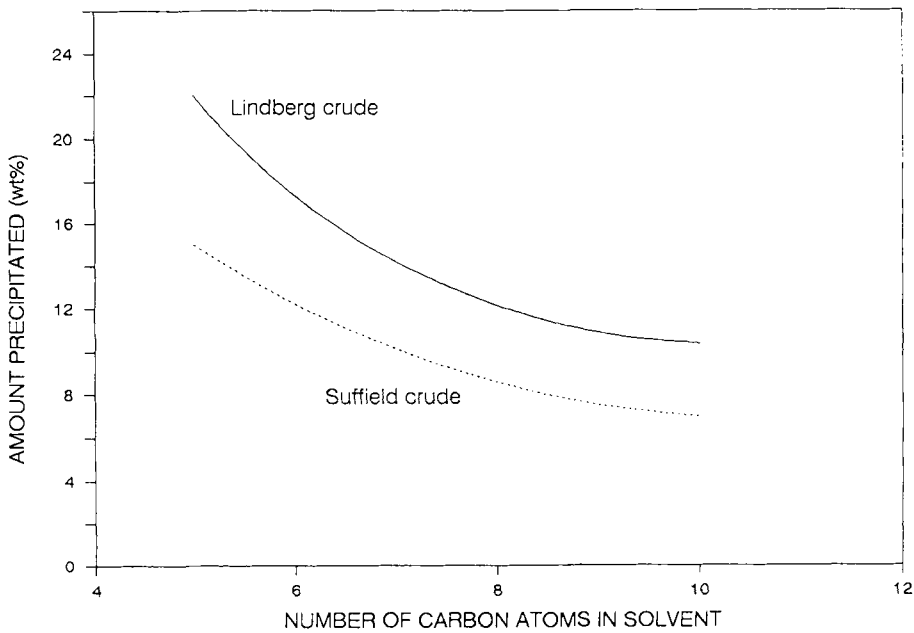

Fig. 11-13. Relation of amount precipitated to carbon number in solvent. (After Kokal et al. [53].)

noticed that the Lindberg precipitates were more crystalline even when precipitation was incomplete at lower solvent/oil ratios. The Lindberg crude had a higher asphaltene content than the Suffield crude. Figure 11-13 indicates that as the carbon number of the solvent increases, the maximum amount precipitated becomes less sensitive to the carbon numbers. One of the first of similar correlations was presented by Mitchell and Speight [54]. Figure 11-14 shows asphaltene precipitation from Athabasca bitumen as a function of the number of carbon atoms for different solvents. A series of experiments was carried out to determine the onset of asphaltene precipitation using various light gases under different pressure and temperature conditions. These results, based on visual observation, are shown in Figs. 11-15 and 11-16 for both crude oils. Note that they did not observe any precipitation with methane for a pressure of up to 20 MPa. They argued that such a behavior is expected because methane only acts as a strippant. This observation was in agreement with that of Hirschberg et al. [8] and Lhioreau et al. [36]. Kokal et al. [53] also observed that for a mixture of ethane and propane at a 1 : 1 volume ratio, asphaltene precipitation took place at a higher pressure than that of propane alone for all temperatures. This, in their view, occurred due to the competition between ethane and propane with ethane acting as a strippant and propane dissolving into the oil and causing precipitation.

Novosad and Costain [34] reported a series of experimental results along with numerical simulation on asphaltene precipitation during miscible CO_2 injection in the Midale reservoir of Canada. They investigated asphaltene phase behavior

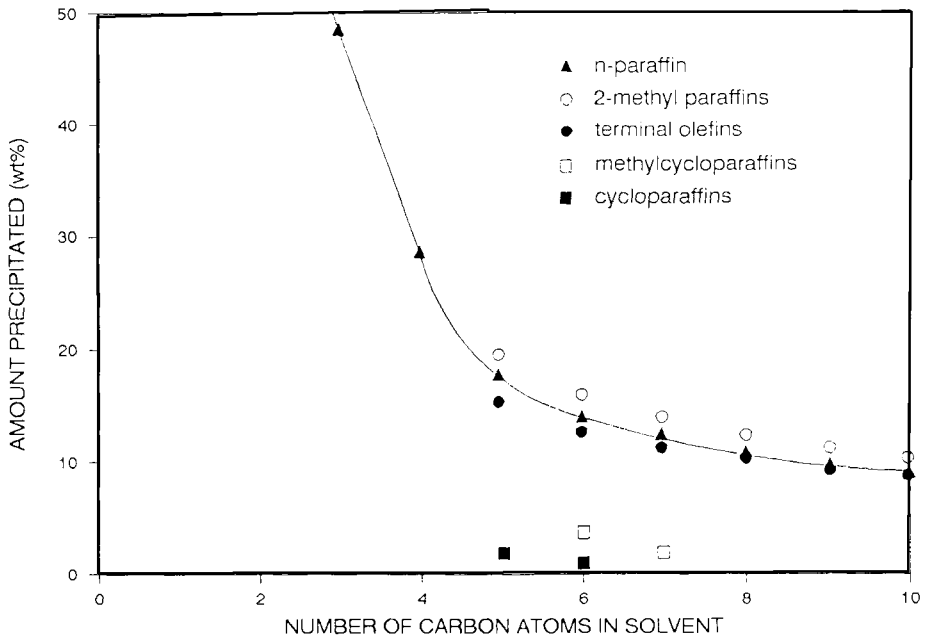

Fig. 11-14. Relation of amount precipitated to carbon atoms in non-aromatic solvents. (After Mitchell and Speight [54].)

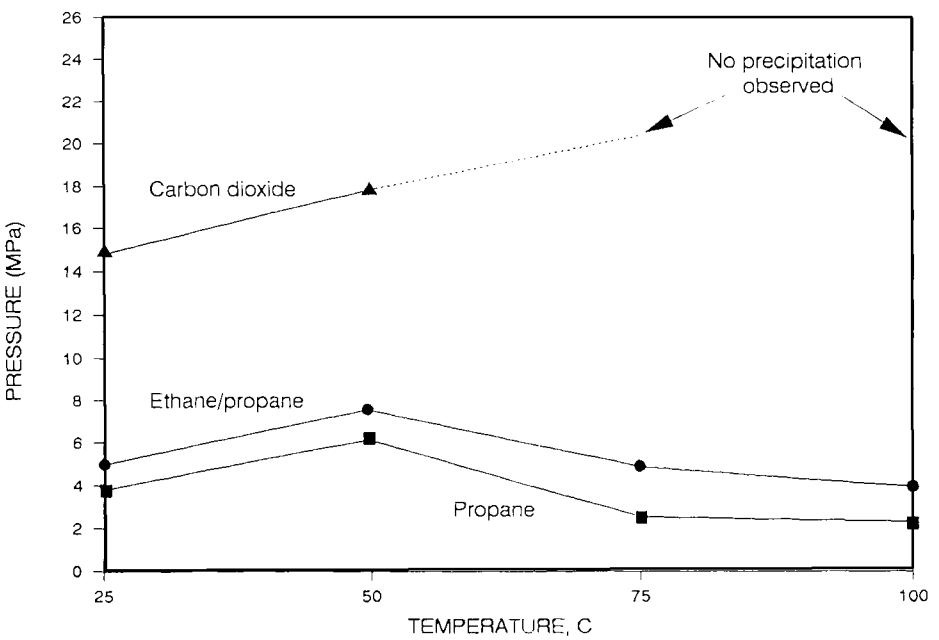

Fig. 11-15. Onset of asphaltene precipitation for Suffield crude. (After Kokal et al. [53].)

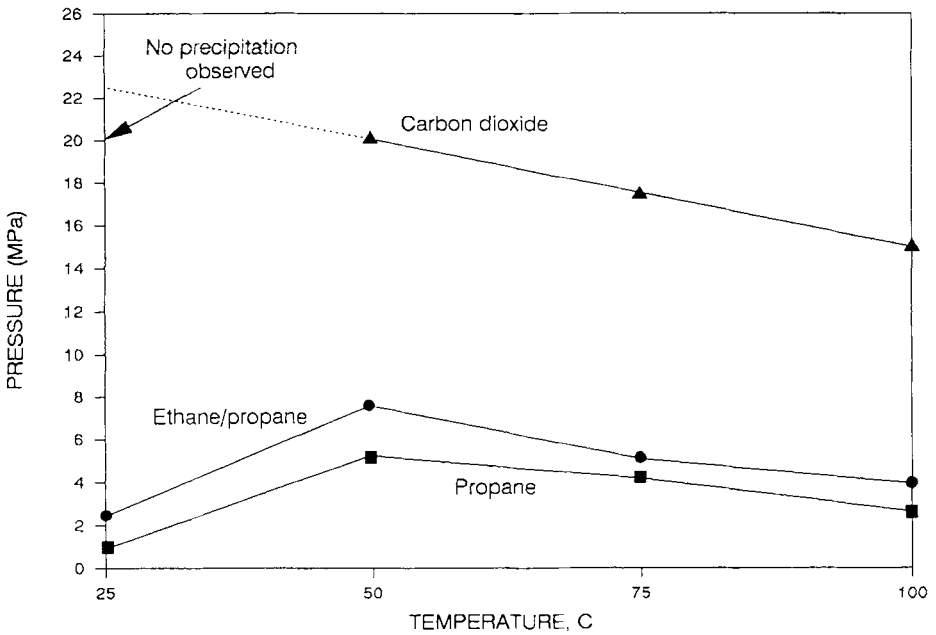

Fig. 11-16. Onset of asphaltene precipitation for Lindberg crude. (After Kokal et al. [53].)

and the extent of asphaltene precipitation in live oil for a range of pressures and temperatures in the presence of CO_2. They also used a modified version of the Hirschberg et al. [8] model. Further details of this work will be provided in a later section.

ASPHALTENE PRECIPITATION DURING WELL STIMULATIONS

Water, acid, and CO_2 can contribute to the precipitation of asphaltenes. The asphaltene concentrates at the water or acid interface and causes the formation of rigid films. Carbon dioxide appears to cause a reduction in solubility of asphaltenes (similar to propane) and, in addition, can cause the formation of rigid films because of its effects on the pH of any water present.

Well stimulation in fluids, such as HCl, can cause significant damage in wells that produce asphaltic crude oil. The acid can cause precipitation of asphaltenes and rigid films when it contacts the crude oil and, in turn, cause significant damage to the porous media near the wellbore. Attempts to remove the deposited asphaltenes and rigid films are often unsuccessful, requiring the redrilling of the well in severe cases. It is important to test for compatibility of stimulation fluids with reservoir crudes whenever the reservoir crude is known to be asphaltic.

Some of the earlier reports on the problem of sludge formation by crude oil on contact with acid have been in Californian wells [55]. Following acidizing, the

wells were very slow to clean up and often a great deal of asphalt-like material was returned with the treating fluids. In some cases, complete or partial plugging of wells resulted from the treatment. Analytical studies revealed that these wells formed solid precipitates upon contact with acids. These precipitates were mainly asphaltenes, resins, paraffin waxes, and other high-molecular-weight hydrocarbons. These materials were apparently precipitated from the crude oil by the reduction of pH as a result of acid contact. Moore et al. [55] also recognized that electrolysis of various oils produced asphaltic deposition on the positive electrode. They found that for an oil which contained negatively charged particles and was treated with 15% HCl for 24 hours and then electrolyzed, the majority of deposited asphaltic material occurred on the negative electrode. It seems possible that the simple neutralization or reversal of the polarity of the particle might be responsible for the precipitation of some asphaltic acid sludges.

Lichaa and Herrera [12] and Lichaa [11] presented detailed results of asphaltene precipitation in the presence of acid for Mata-Acema and Boscan reservoir crudes of Venezuela. Characteristics of these two reservoirs have been presented in a previous section. For the Mata-Acema crude, they observed that the asphaltene precipitation ranged from 35 to 87% for the 5% acid (HCl) and from 60 to 96% for 15% acid for different samples. When mixing time was increased to six hours, a minimum of 78% asphaltene precipitation for 15% acid and 75% precipitation for a 5% acid were observed. Interestingly, the Boscan crude, which had a much higher asphaltene concentration, did not suffer from any asphaltene deposition problems in the field. In the laboratory, no precipitate was observed for the Boscan crude even when a 15% HCl was used. Lichaa [11] reported the use of Boscan crude as a stabilizing agent for the Mata-Acema crude. It was found that even when only 10% Boscan crude was added to a mixture with the Mata-Acema crude, no precipitation was observed in the presence of acid as strong as 15%. He concluded that the Boscan crude acts as a protective agent and stabilizer for the asphaltene upon contact with acid.

Lichaa [11] conducted coreflood tests which showed that a severe permeability damage could take place during HCl injection (up to 96% reduction from the original permeability) for the Mata-Acema crude. In a previous study, Lichaa and Herrera [12] reported permeability damage even for an acid concentration of 5% or 10%. Even though reduction in permeability could occur due to spontaneous deposition of asphaltenes from these crudes and due to surface tension and relative permeability effects, it is believed that the acid plays a major role in depeptizing the asphaltenes. Whereas the use of commercial inhibitor reduced permeability damage considerably, the most reduction in permeability damage was caused by the use of the Boscan crude mixed with the Mata-Acema crude. A small portion of Boscan crude (up to 10%) reduced permeability damage by at least 50%.

It is obvious from the above discussion that a compatibility test should be performed on stimulation fluid and reservoir oil in order to prevent a possible asphaltene plugging problem. This is true even if the asphaltene content of the reservoir crude oil is low.

MODELING OF COMPOSITIONAL DEPENDENCE OF HEAVY OILS/BITUMENS

Physicochemical background

The chemical constitutive molecules are classified based on their solubility parameters and are usually divided into two distinct groups: maltenes (soluble in 40 volume of *n*-pentane) and asphaltenes (soluble in toluene but insoluble in *n*-pentane). A third group which usually occurs in small quantities in unprocessed bitumen, but usually increases in concentration upon thermal upgrading, is termed "coke", defined as the product which is insoluble in toluene.

The spatial organization of maltenes and asphaltenes leads to the macrostructural and microstructural properties, of which viscosity is of paramount importance for bitumen recovery, transportation, and processing considerations. Dickie and Yen [56] investigated macrostructure of asphaltene and found them to be composed of polynuclear aromatic molecules, with attached alkyl chains. These constitutive "asphaltene unit molecules" are grouped in layers having several unit molecules (typically 5 or 6) surrounded or immersed in maltene fluid. The latter is composed of free saturates, mono- and di-aromatics and resins which may be associated with the asphaltenes. This structural organization may be considered to be the microstructure of the system. The microstructural system described above forms aggregates due to thermodynamic reasons; several unit layers of asphaltenes arrange themselves together, surrounded or associated with maltenes, to form a micellar structure. These micellar structures formed as a result of association or aggregation of unit asphaltene layers are also known as macrostructures.

The macrostructural arrangement to large extent depends on the size of the unit asphaltene layers. Low-molecular-weight asphaltenes (MW up to about 1000) consist of single sheets of condensed aromatic and naphthenic rings to which relatively short alkyl chains are attached, while high-molecular-weight asphaltenes consist of several sheets of condensed ring systems connected to each other by short chains [56–58]. Altgelt and Harle [58] found that aggregates formed by low-molecular-weight asphaltenes (MW $<$ 10,000) result in only a slight increase in viscosity due to their relatively compact structures. They found that aggregates formed by high-molecular-weight asphaltenes increase viscosity substantially. This is due to the stacking of higher-molecular-weight asphaltene sheets which may result in a complex structure with extended shape that exhibits higher hydrodynamic resistance, as reflected in higher viscosity. The molecular weight of petroleum asphaltenes are very high and range from 1000 to 2,000,000. This wide variation in molecular weights of asphaltenes is partly due to the difference in measuring techniques used, but mostly due to the association of asphaltene units at the conditions of measurement. For example, highly associated asphaltenes will give higher molecular weight than the mildly associated ones. Among the various techniques available, vapor pressure osmometry is the most frequently used one. Ultracentrifuge- and electron-microscopy-based techniques give very high molecular weights. Molecular weight determination by vapor pressure osmometry may not always provide

consistent results, as the molecular weight is affected by the nature of the solvent and its dielectric constant.

In addition to molecular weight, the degree of asphaltene aggregation is also a strong function of the composition of the solvent, i.e., the maltene fluid. In the presence of aromatic compounds, asphaltenes are colloidally dispersed in the maltene fluid. In the presence of excess paraffinic hydrocarbons, asphaltene precipitation occurs. Algelt and Harle [58] used the Hildebrand solubility parameter, δ, as a measure of solvent power to dissolve asphaltenes. They observed that between δ-values of 8 and 11, solvent power to dissolve asphaltenes increases with increasing δ. As δ increases above 11, solvents tend to be polar and hydrogen bondings lose their power to dissolve asphaltenes. Algelt and Harle [58] measured concentration dependency of Boscan asphaltenes having a molecular weight of 20,000 with different solvents and found the viscosity to be a function of asphaltene concentration as well as the solvent type. The poorer the solvent, the lower is the solubility of the asphaltene in that solvent and, hence, the stronger is the aggregation.

Numerous studies on the effects of temperature on bitumen viscosity have been conducted by various researchers in recent years and a number of viscosity correlations have been proposed, among which the one-parameter correlation of Mehrotra and Svrcek [59] is worth mentioning. Owing to the complexities involved in determining the extent of aggregation and other related factors, however, not much attention has been paid towards the compositional variation of viscosity. The presently available viscosity correlations mostly deal with temperature effects only and are not capable of providing an adequate representation of viscosity under varying reservoir conditions. There is a need, therefore, to develop a new correlation with compositional effects incorporated in it.

From the above discussion, it is very clear that any attempt to quantify the effect of asphaltenes on viscosity of bitumen must include molecular weight and solvent characteristics along with asphaltene concentration in such quantification. Such a model was proposed by Islam and Chakma [60]. The following is a description of this model.

Modeling of asphaltene concentration dependency

Probably the first correlation relating viscosity of a solution to the viscosity of a solvent is the Arrhenius equation given as:

$$\frac{\mu}{\mu_o} = K^c \tag{11-1}$$

where μ is the viscosity of the solution, μ_o is the viscosity of the solvent, K is a constant, and c is the concentration. The Arrhenius equation, however, does not take into account the molecular weight of the dissolved solute. It was pointed out earlier that the molecular weight of the asphaltene affects the viscosity of bitumen/heavy oils, and consequently this simplistic equation cannot be directly used.

The classical Einstein's formula [61] relates the viscosity of an infinitely dilute suspension of solid spherical particles to the viscosity of the dispersion medium as

follows:

$$\frac{\mu}{\mu_o} = 1 + k_E\phi \tag{11-2}$$

where μ is the viscosity of the suspension, μ is the viscosity of the dispersion medium, ϕ is the volume fraction of the solids, and k_E is the so-called Einstein coefficient. Although this equation represents some improvement over the Arrhenius equation, molecular weight still is not considered as a separate variable. Staudinger rearranged Einstein's equation as follows [62]:

$$\frac{\mu}{\mu_o} - 1 = k_E\phi \tag{3}$$

and replaced the left-hand side of the equation by μ, which was defined as the "specific viscosity" and expressed the term k_E as $k_E = K_V \times MW$, where K_V is a constant to be determined from viscosity data and MW is the molecular weight of the solute. This allowed viscosity to be related to concentration as well as molecular weight of the solute.

The first attempt to correlate the effect of asphaltene concentration on viscosity of petroleum oils was made by Mack [62]. He noted, after analyzing the viscosity–concentration data of Kendall and Monroe [63] for solutions of naphthalene in benzene, that when logarithms of the relative viscosities are plotted against concentration, a straight line is obtained. Based on this, he proposed the following equation:

$$\log\left(\frac{\mu}{\mu_o}\right) = K_U \times MW \times \phi \tag{11-4}$$

where K_U is a universal constant. The validity of Eq. 11-4 was tested by determining molecular weight from viscosity data using Eq. 11-4 and checking the results with those obtained from cryoscopic method for sucrose in water and benzyl–benzonate in water systems; excellent agreement was found.

In the presence of association and/or solvation, a plot of relative viscosity versus concentration may not yield a straight line. Mack [62] introduced a solvation factor, f, to take into account the association and/or solvation:

$$\log\left(\frac{\mu}{\mu_o}\right) = f^2 K_M \times MW \times \phi \tag{11-5}$$

In recent years, efforts have been made to extend the applicability of Einstein's equation to higher concentrations. It has been shown that Einstein's equation, as was derived in his original paper, is incorrect for higher concentrations and the correct version is given by:

$$\frac{\mu}{\mu_o} = \frac{1 + \phi/2}{1 - \phi} \tag{11-6}$$

which reduces to Eq. 11-2 when ϕ approaches zero. Because, Einstein's equation does not take into account the particle interactions, Gillespie [64] suggested that ϕ

be replaced by ϕ_{eff} defined as:

$$\phi_{eff} = \alpha\phi + k\alpha^2\phi^2 \tag{11-7}$$

where α is a function of the number of particles in aggregate, aggregate shape and the packing factor of the particles in the aggregates, and k is the parameter which is equal to 0.9 for a suspension of unidisperse and unisize solid particles. It increases with an increase in the axial ratio of aggregates and decreases if the particles are of different sizes.

Other empirical methods for determining viscosity of mixtures are also available. For light hydrocarbons, the one-constant Lederer equation [65], which is given below, has been found to be satisfactory [66]:

$$\ln \mu = X \ln \mu_A + (1 - X) \ln \mu_B \tag{11-8}$$

where

$$X = \frac{\alpha V_A}{\alpha V_A + (1 - V_A)} \tag{11-9}$$

In the above formulation, μ is the viscosity of the mixture, μ_A is the viscosity of component A, μ_B is the viscosity of component B, V is the volume fraction of the component A, and α is a constant having an upper limit of unity.

Shu [66] related α to the Einstein constant k_E as follows:

$$\alpha = \frac{k}{\ln(\mu_A/\mu_B)} \tag{11-10}$$

The same author correlated k_E as functions of densities of "A" and "B" using heavy-oil solvent data from different sources and obtained the following equation for k_E:

$$k_E = 17.04\, \Delta\rho^{0.537} \rho_A^{3.2745} \rho_B^{1.6316} \tag{11-11}$$

$$\Delta\rho = \rho_A - \rho_B \tag{11-12}$$

Islam and Chakma [60] attempted to modify the Einstein equation in the following manner to model the influence of asphaltene on viscosity. Following Staudinger [67], the Einstein coefficient, k_E, was replaced by $C \times MW$, where C is a constant and MW is the molecular weight of the asphaltenes. The volume fraction, ϕ, was replaced by an effective volume fraction, ϕ_{eff}, given by the Eq. 11-7. Thus, the following equation was obtained:

$$\frac{\mu}{\mu_o} - 1 = C \times MW \times \alpha\phi(1 + k\alpha\phi) \tag{11-13}$$

The values of α, k, and C need to be determined by fitting experimental viscosity data. Islam and Chakma [60] used the data provided by Altgelt and Harle [58] to obtain a set of parameters. Figure 11-17 shows an excellent agreement between experimental and theoretical results (as generated by Eq. 11-13). The values of the

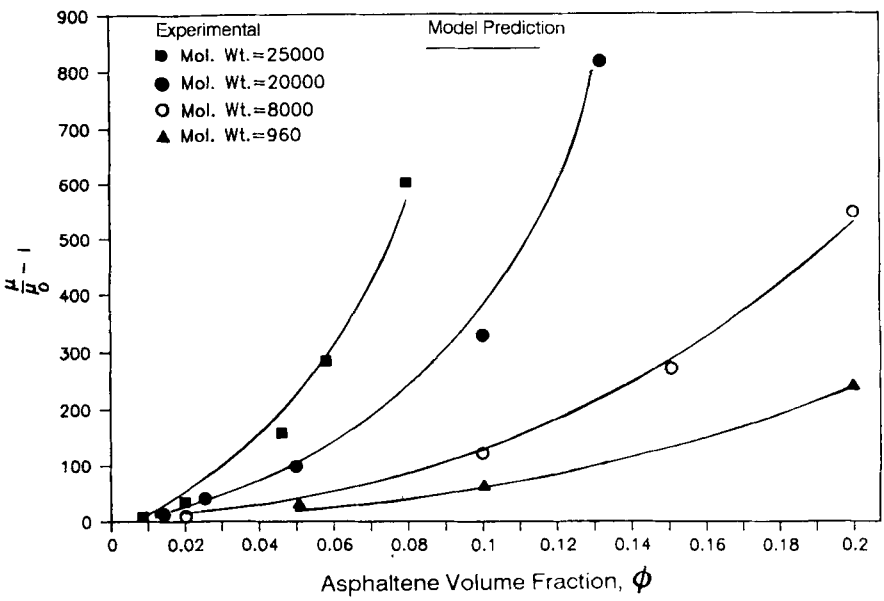

Fig. 11-17. Comparison of experimental results with model predictions. (After Islam and Chakma [60].)

TABLE 11-5

Coefficients C, α, and ϕ (mathematical model of Islam and Chakma [60])

Molecular weight	α	ϕ	C
960	10	89	0.0006968
8000	6.76	50	0.0006968
20,000	7.85	50	0.0006968
25,000	10	49.9	0.0006968

parameters are listed in Table 11-5. More recently, Storm et al. [68] used a modified form of the Einstein equation in order to describe the rheology of asphaltenes from various reservoir samples. They re-wrote the Einstein equation as:

$$\frac{\mu}{\mu_o} = (1 + [\eta]_w)\, W_A \tag{11-14}$$

where W_A is the weight fraction of the suspended material and $[\eta]_w$ is the intrinsic viscosity, which depends on solvation effects as well as on the particle shape. The above equation, when expressed in terms of specific viscosity ($\mu_{sp} = (\mu - \mu_o)/\mu_o$), gave excellent agreement with observed viscosities for the Alaskan North Slope samples as well as Oriente samples (mixture of asphaltene and deasphalted oil) for an asphaltene weight concentration of up to 8%. They also observed excellent agreement between experimental observation and the viscosity model, which allows size distribution of suspended particles, for Oriente vacuum residue samples. This

model is given by

$$\frac{\mu}{\mu_o} = (1 - \phi)^{-2.5} \tag{11-15}$$

Even though this representation provides excellent agreement with experimental results for limited concentration values, it does not incorporate the compositional effect or the effect of higher asphaltene concentrations.

Impact of compositional dependence of heavy-oil viscosity on thermal recovery

The viscosity of bitumens/heavy oils may be related to the tendency of the asphaltenes to form aggregates. In many petroleum reservoirs around the world, reservoir fluid composition has been found to vary with location and depth [69–73]. In almost all the cases, reservoir fluid density increases with depth of the reservoir [69]. Patel [74] found the viscosities of Athabasca, Peace River, Wabasca and Cold Lake bitumen to vary with the depths of the formations. In most of the cases, samples obtained from greater depth showed greater viscosity. Schulte [71] studied compositional variations within a hydrocarbon column due to gravity and found that gravitational forces are responsible for the variation in composition in thick reservoirs. He found the extent of this variation to be higher with larger aromatic fractions in the hydrocarbon fluid. Hirschberg [33], in his analysis of the role of asphaltenes in compositional variation of a reservoir fluid column concluded that the heavy polar components play a key role in this regard and in particular identified asphaltene segregation to have a dominant effect.

One of the principal effects of compositional variation is the variation of viscosity. For a reservoir oil sample from a North African Field, Hirschberg [33] found the viscosity to increase by a factor of 4 (from 9 to 36 mPa s) when asphalt content increased from 10 to 16%. Indeed the effect of asphaltene concentration on the viscosity of an oil has been known for a long time. Mack [62] presented viscosity data on asphalt and oil mixtures obtained from a Mexican asphalt which clearly showed an increase in viscosity of the mixture with increasing asphaltene concentration. Waxman et al. [75] as well as Kitzan and Parsons [76] found the viscosities of Peace River bitumen samples to vary with asphaltene concentration. Dealy [77] studied the effect of asphaltene concentration on the viscosity of Athabasca bitumen by adding 5 wt% of Athabasca bitumen sample, which originally contained 16 wt% of asphaltene. Bitumen viscosity was found to increase from about 300 Pa s to 1000 Pa s. When high shear stress was applied, the viscosity of the mixture was found to decrease to the original level. This indicated formation of asphaltene aggregates, which caused the rise in viscosity, and their eventual desaggregation with the application of high shear. Datta [78] presented viscosity data of various asphaltene blends of a California oil which also show an increase of viscosity with asphaltene concentration.

Altgelt and Harle [58] also studied the effect of asphaltenes on asphalt viscosity. They found asphaltenes to form aggregates in solution, the degree of which was found to depend on structure, molecular weight and concentration of the as-

phaltenes and solvent power. They concluded that the viscosity of asphaltene is primarily due to this aggregation, and, therefore, there is ample evidence available which clearly shows that viscosity of bitumens/heavy oils is a strong function of asphaltene concentration and its nature.

Compositional variability of heavy oils may also be caused by selective gradation of oil due to various processes. There has been evidence of oil seepage from a reservoir to the surface where the oil comes in contact with oxygen. This may lead to oxidation and biodegradation causing conversion of the oil into tar or asphaltic deposits. Similar phenomena may also occur when oil comes in contact with oxygenated near-surface meteoric water. Besides, light components may dissolve into water or may be lost to the gas cap. All these phenomena which may be responsible for alteration of oil composition are detailed by Ward and Clark [73].

Viscosity variation in heavy-oil/bitumen reservoirs due to variation in asphaltene content may have profound effect on recovery techniques. Mostly, these reservoirs are produced under thermal recovery schemes, such as steam injection, in situ combustion, etc. Even at steam temperature, it is likely that the displacement fluid will encounter reservoir fluids at higher viscosity with increasing depth. Hot oil at the top will be more mobile than the hot oil at the bottom of the reservoir. This phenomenon will enhance the natural tendency of steam to override the formation, leading to a poor vertical conformance and a steam breakthrough, earlier-than-expected, from production wells. However, the significance of natural variation in viscosity, as compared to those of other phenomena, such as reservoir heterogeneities, fracture orientation, etc., has yet to be assessed. Whereas numerical simulation has often been used to assess the effects of reservoir heterogeneities, etc. on thermal recovery processes, oil property is commonly assumed to be constant throughout the reservoir. Introduction of a depth vs. viscosity profile into a reservoir simulator would have great impact on predictions for thermal processes [79].

Under the elevated temperature conditions created in a reservoir undergoing steam recovery, the ability of an oil to solubilize asphaltenes can be affected [8,75]. Deposition of asphaltenes deep in a reservoir may actually improve performance, by reducing permeability in the steam-swept regions, and improving produced oil quality. On the other hand, deposition in the vicinity of producing wells can greatly reduce inflow and lead to poor well performance. Asphaltene precipitation in surface equipment is also a concern. No study to-date has been reported on the overall effect of asphaltene in reservoir and production problems during thermal recovery schemes.

Distillation studies have shown that higher-viscosity oils found at the bottom of the reservoir contain higher amount of resins and asphaltenes than those at the top part of the reservoir [79]. Consequently, during heating with a thermal recovery technique, these oils are more likely to lose asphaltenes as precipitates. Depending on the recovery mechanism involved, this phenomena may be harmful or beneficial to the recovery process. Also, the effects of this phenomena are likely to be more intense when oil from the bottom part of the reservoir is being produced by preference. Such is the case during mature stages of steam injection or during the steam-assisted gravity drainage process.

NUMERICAL MODELING OF ASPHALTENE PRECIPITATION

Asphaltene deposition during heavy-oil production under various enhanced oil recovery schemes is a well known phenomenon. Introduction of fluids which are miscible with the reservoir oil or which cause thermal and, therefore, compositional alterations of the in situ oil usually cause changes in flow behavior, phase equilibrium properties, and the reservoir rock characteristics. One such change is the deposition of asphaltenes. Such deposition is expected to affect productivity of the reservoir during heavy-oil recovery. Often this is considered to be one of the most worrisome problems in the design of miscible floods [18,29,80–92]. The effects of heavy organic deposition, such as asphaltene, could be positive or negative depending on whether it could be controlled and predicted before it occurs [83]. This need for predicting asphaltene behavior in crude oil has been recognized for the past 50 years. Despite extensive efforts to establish a reliable description of asphaltene structure and equilibria, considerable controversy among researchers still persists. Asphaltenes are described as molecular entities dissolved in oil, colloidal particles, or a combination of the two. In formulating asphaltene thermodynamic models, two distinct approaches have emerged. The first one, called the "molecular solubility" model was proposed by Hirschberg et al. [8]. The other approach was used to formulate the "colloid suspension model" and was proposed by Mansoori and co-workers [17,26].

Background

The concept that asphaltic compounds are present as a colloidal system is credited to Nellensteyn [84]. He postulated that asphaltic compounds were made of micelles protected by adsorbed resin and hydrocarbon materials, all dispersed in a hydrocarbon medium. He considered surface tension to be the governing factor in the peptizing or precipitating properties of different common solvents with respect to asphaltic compounds. Swanson [85] and Witherspoon and Munir [86] recognized that resins are required to dissolve asphaltene in the distillate portion of a crude oil. Dickie and Yen [56] concluded that petroleum resins provide a transition between the polar (asphaltene) and the relatively non-polar (oil) fractions in petroleum. This prevents the assembly of polar aggregates that would be non-dispersible in the oil. Koots and Speight [87] considered that asphaltene clusters in resin molecules are the dominant species, which allow the asphaltenes to exist in the colloidal state in a crude oil. One of the first thermodynamic models was developed by Hirschberg et al. [8]. This model considers the oil to be a binary mixture of two liquids (asphalt and solvent). In their model, asphalt (resin and asphaltene) precipitates as a single homogeneous compounds. In 1987, Leontaritis and Mansoori [26] proposed a thermodynamic–colloid model which is capable of predicting the onset of asphaltene flocculation. This model postulates that asphaltenes exist in the oil as solid particles in colloidal suspension, stabilized by resins absorbed on their surface. More recently, Kawanaka et al. [15] reported a continuous dynamic model in which the onset as well as the amount of asphaltene deposits can be predicted with the

molecular weight distributions of asphaltenes. They considered asphaltenes to be heterogeneous polydispersed polymers. Later, Park and Mansoori [83] combined the two theories, namely, continuous thermodynamic model [15] and steric colloidal model [26], and developed the so-called fractal aggregation model theory of heterogeneous polymer solutions for the prediction of the onset and amount of asphaltene precipitations.

Molecular solubility model

Hischberg et al. [8] developed this model in order to study the effect of temperature and pressure on asphaltene flocculation. Based on experimental information, the possibility of reversibility of asphaltene precipitation was postulated, leading to a thermodynamic model. A colloidal model was used for asphaltene–resin interactions, as the asphaltene aggregates were assumed to be kept in solution by a layer of resins.

A combination of vapor–liquid and a liquid–liquid model was used instead of a full three-phase model. This simplified the modeling process considerably. Using a detailed compositional simulator based on a Soave equation of state, liquid phase composition was calculated assuming no asphaltene precipitation. A Soave equation of state is given by

$$P = \frac{RT}{V - v} - \frac{a}{V(V + b)} \tag{11-16}$$

where $a = \sum\sum x_i y_j (1 - k_{ij})(a_i a_j)^{0.5}$.

It was assumed that the vapor–liquid equilibrium would remain unaltered during asphaltene precipitation. At this point, the Flory–Huggins polymer solution theory was used to estimate the asphaltene precipitation from the liquid phase. Typically, the volume fraction of dissolved asphaltene is equal to the maximum volume fraction soluble in the solvent. Two pseudocomponents, namely asphalt and solvent, were defined to describe the liquid as a quasibinary mixture. The deasphalted crude or crude/solvent was treated as single component. The composition of this component was calculated by using the vapor–liquid equilibrium model. Using the solubility parameter and molar volume of the liquid phase, the solubility parameter and molar volume of the deasphalted phase were calculated using Eq. 11-17 and 11-18:

$$\delta_s = \frac{\delta_L - \phi_A^L \delta_a - \phi_R^L \delta_r}{1 - \phi_A^L - \phi_R^L} \tag{11-17}$$

$$V_s = \frac{1 - \phi_A^L - \phi_R^L}{\dfrac{1}{V_L} - \dfrac{\phi_A^L}{V_A} - \dfrac{\phi_R^L}{V_L}} \tag{11-18}$$

where δ_s is the solubility parameter of the deasphalted liquid, and V_s is the volume fraction of asphaltenes soluble in the crude oil. The maximum volume fraction of asphaltenes soluble in the crude was given by

$$\phi_{A_{max}} = \exp\left\{\frac{V_A}{V_L}\left[1 - \frac{V_A}{V_L} - \frac{V_L}{RT}(\delta_A - \delta_L)^2\right]\right\} \quad (11\text{-}19)$$

The values of solubility parameters of asphaltenes were found to be fairly insensitive to the molar volume of asphaltenes. Consequently, the amounts of asphaltenes precipitated in a mixture of tank oil and *n*-heptane were fitted with a molar volume of asphaltenes of 4 m^3/kmol and solubility parameter of 19.59 $MPa^{0.5}$. Theoretical prediction results are compared with experimental ones in Table 11-4.

Effect of pressure

As pressure was reduced, a decrease in the solubility parameter of the oil was observed until the bubble point pressure was reached. This decrease resulted from the decrease in oil density with reduction in pressure. Below the bubble point, evolution of solution gas enriched the oil with heavier components. The precipitation, therefore, could be expected at the bubble point pressure. This was found to confirm the experimental data showing higher precipitation near the bubble point.

Effect of temperature

Temperature would affect the internal energy of vaporization and density of liquid. Consequently, reduction in the temperature of oil would result in increase in the solubility parameter of the oil. The closer the solubility parameters of the oil and the asphaltenes are, the less is the precipitation. The experimental results were found to confirm this.

Disadvantage of the model

The most serious drawback of the model is that it overestimates the solubility of asphaltene at high dilutions, when resins are separated from the asphaltenes. Recent studies show that resins play a key role in the solubilization of asphaltenes because they reduce asphaltene aggregation. Another shortcoming is that this model overestimates the solubility of asphaltenes at very high dilution ratios, which Hirschberg et al. [8] attributed to separation of resins from asphaltenes.

Steric colloidal model

This model was presented by Leontaritis and Mansoori [26]. In the model development, it was assumed that asphaltenes exist in the oil as small solid particles in colloid suspension. These asphaltene particles are assumed to be suspended because of resins (heavy and mostly aromatic molecules) which are adsorbed to the surfaces of heavy organic particles, keeping them afloat because of the repulsive forces between resin molecules and the adsorbed resins of the macromolecular (asphaltene) surface. The following factors were considered to contribute to the stability of suspension: (1) concentration of resins in the solution; (2) the fraction of asphaltene surface sites occupied by resin molecules; and (3) equilibrium conditions between the resins in solution and the asphaltene surface.

Thermodynamically, a necessary condition for chemical equilibrium between two phases is that the chemical potential of each component in one phase is equal to its chemical component in the other phase. That is, resins in the oil phase will have the same potential as the resins in the asphaltene phase. The steric colloidal model is based on the assumption that the asphaltene particles remain completely covered irrespective of how the nature of the liquid mixture is changed, as long as the calculated chemical potential remains equal to or above the critical chemical potential. The model requires calculation of the chemical potential of the macroscopic asphaltene-free oil phase. The following steps are followed in the utilization of the steric colloidal model:

- calculation of the resin chemical potential by the statistical mechanical theory of polymer solutions;
- study of resin adsorption on asphaltene particle surface and measurement of the related Langmuir constants;
- calculation of streaming potentials generated during flow of charged asphaltene particles; and
- development and use of asphaltene colloidal and aggregation models for estimating the amount of asphalt which may have irreversibly aggregated and flocculated out.

Inasmuch as the amount of resins adsorbed is a function of their concentration in the oil phase, a change in concentration of resins in the oil phase would lead to changes in the amount of resins adsorbed. Consequently, if the amount of resins in the oil is low enough, adsorbed amount of resins will no longer cover the entire surface of asphaltenes. This would lead to irreversible aggregation of asphaltene particles, which would eventually grow in size and flocculate.

Continuous thermodynamic model

This model was developed by Kawanaka et al. [15] and Mansoori and Jiang [17]. The model is based on the fact that the deposition of heavy organic compounds can be explained by an upset in the balance of oil composition. The sustaining of mutual solubility is attributed mainly to the ratio of polar and non-polar molecules and the ratio of high- to low-molecular-weight molecules in a petroleum mixture. These ratios are perturbed by the addition of a solvent. Consequently, the polar molecules separate from the mixture in the form of a solid precipitate or another liquid phase. At this point, polymerization could take place in separated molecules, which contain hydrogen bonding and the sulfur and/or the nitrogen. These molecules are likely to have a wide range of distributions in molecular weights and sizes. This calls for the prediction of phase behavior for each fraction depending on its molecular weight. This involves conducting phase equilibrium calculations by equating chemical potential of each heavy organic fraction in the liquid and solid phases. The theory of heterogeneous polydispersed polymer solutions by Scott and Magat [88] is used to calculate the chemical potential of each heavy organic fraction. Inasmuch as asphaltene contains a virtually continuous distribution of molecular weights, the continuous mixture theory [89] is used in conjunction with

the thermodynamic theory of heterogeneous polymer solutions. This model has been detailed by Mansoori in Chapter 8 [90]. This model allows the calculation of the distribution of asphaltenes in the solvent-rich liquid phase, in the solid phase, and in the original petroleum crude. The model successfully predicts the phase behavior and precipitation region of asphaltene in CO_2-crude oil mixtures at different pressure, temperatures, and compositions of the injected fluid.

Fractal aggregation model

The continuous thermodynamic model and the steric colloidal model were combined by Park and Mansoori [83] in order to develop the fractal aggregation model. It is considered that asphaltenes are principally associated via $\pi-\pi$ interactions [56]. These suspensions are fully peptized by resin molecules during their suspension. This prevents them from aggregating into clusters because of the repulsive forces between resin molecules and the absorbed resins on the macromolecular surfaces. As mentioned earlier, stability of such suspensions is considered to be a function of concentration of resins in the solution. When a solvent is introduced in the system, the concentration of resins changes leading to mutual interactions of asphaltene particles. This process may lead to contacts of asphaltene molecules to form clusters, to grow in size due to irreversible aggregation, or to flocculate. During the flocculation process, the clusters of asphaltene particles are assumed to remain in suspension randomly and independent of one another as Brownian particles due to the molecularly-induced thermal motions. At this point, Van der Waals attraction forces and electrical (electrostatic or electrokinetic) repulsive/attractive forces would be the major factors in causing aggregation and flocculation of asphaltenes. Therefore, the proposed model should account for the following:
- the role of resin concentration in the deposition mechanism and its effect on the colloidal aggregation process of asphaltenes under solvent injection;
- utilization of the irreversible aggregation kinetic to account properly for the size distributions of cluster of asphaltene particles;
- utilization of the statistical mechanical theory of heterogeneous polymer solutions; and
- applications of the principles of thermodynamics of multicomponent mixtures and phase equilibria.

Further detail of this model is given in Mansoori [90].

Application of theoretical models

More recently, Kamath et al. [91] worked on a thermodynamic model incorporating Flory–Huggins polymer solution theory to predict asphaltene precipitation during the injection of a solvent in miscible flooding. Figure 11-18 shows the flow diagram of steps involved in prediction of asphaltene precipitation. In step I, COATS compositional simulator was tuned incorporating Peng–Robinson equation of state and PVT data of the reservoir fluid in question (heavy-oil reservoir of West Sak, Alaska, in this case). Using 23 components of the oil, equation of state constants Ω_A

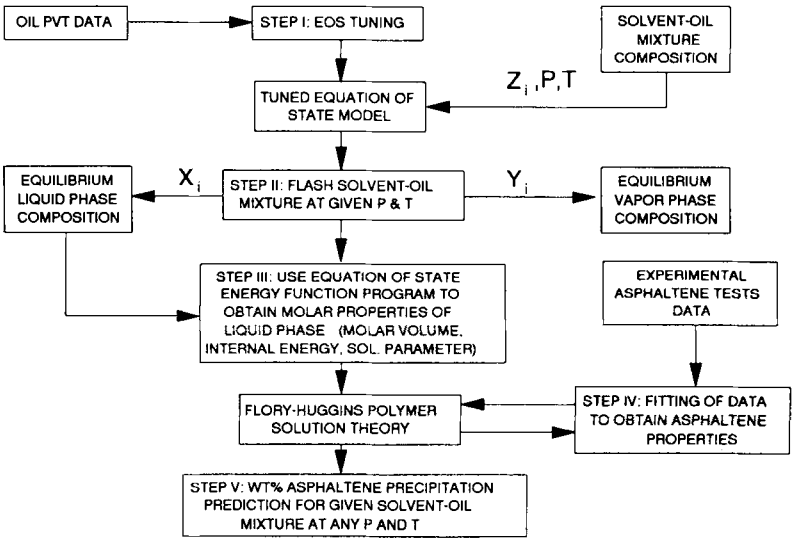

Fig. 11-18. Flow diagram of steps involved in prediction of asphaltene precipitation used by Kamath et al. [91].

and Ω_B were obtained for methane and C_{23+} fractions, respectively. Also the binary interaction parameter between methane and the C_{23+} fraction was established. This was based on the fact that it was found to be predominating the interaction amongst the various components of the oil. In step II, the tuned equation of state model was used to obtain equilibrium vapor phase and equilibrium liquid phase compositions of the flashed solvent oil mixture at the given pressure and temperature conditions. In step III, the equilibrium liquid phase composition was used to calculate liquid molar volume, internal energy of vaporization and solubility parameter as per the equations shown below:

$$\Delta u_L^v = \left(\frac{a_L}{2\sqrt{2}\,b_L} - \frac{T}{2\sqrt{2}\,b_L}\frac{da_L}{dT}\right)\ln\left(\frac{V_L + 2.414\,b_L}{V_L - 0.414\,b_L}\right) \tag{11-20}$$

$$\frac{da_L}{dT} = \sum_i \sum_j x_i x_j (1-\delta)(a_i a_j T_{c_i} T_{c_j})^{1/2} \left\{\left[1 + K_j(1-\sqrt{T_{r_j}})\right]\left[-\frac{K_i}{2}\sqrt{T_{r_i}}\right] + \left[1 + K_i(1-\sqrt{T_{r_i}})\right]\left[-\frac{K_j}{2}\sqrt{T_{r_j}}\right]\right\} \tag{11-21}$$

where V_L is given by:

$$V_L = \frac{Z_L RT}{P} \tag{11-22}$$

and δ_L is given by:

$$\delta_L = \left[\frac{\Delta u_L^v}{V_L}\right]^{0.5} \tag{11-23}$$

Jiang et al. [52] presented experimental data on asphaltene precipitation following the addition of solvents, such as ethane, carbon dioxide, propane, *n*-butane, *n*-pentane, *n*-heptane, Prudhoe Bay natural gas, and natural gas liquids, to crude oil from the West Sak reservoir of Alaska. These data were fitted to obtain molar volume, solubility parameter and molecular weight of asphaltenes. An optimization subroutine was used to minimize the objective function to obtain a good fit. For the eight solvents mentioned above, the data were fitted separately, because different ranges of molecular weights were expected to precipitate with different solvents. In step IV, the asphaltene properties as well as liquid phase molar properties were used to calculate volume fractions of asphaltenes soluble in the liquid phase using the following Flory–Huggins polymer solution equation:

$$\phi_A = \exp\left[\frac{V_A}{V_L} - 1 - \frac{V_A}{RT}(\delta_A - \delta_L)^2\right] \tag{11-24}$$

where $\delta_i = \left[\Delta u_i^v / V_i\right]^{0.5}$.

The weight fraction of asphaltenes that would precipitate at given conditions of temperature and pressure can then be calculated from the following equation:

$$W_A = \frac{(1-\phi_A)\dfrac{M_L}{V_L}}{(1-\phi_A)\dfrac{M_A}{V_A} + \phi_A \dfrac{M_L}{V_L}} \tag{11-25}$$

Table 11-6 compares experimental and predicted results for eight solvents at different solvent/oil ratios. The amounts of asphaltene precipitation were predicted with reasonable accuracy for these solvents as long as the solvent/oil ratio was not extreme. Table 11-7 gives various parameter values, which gave optimum match between experimental and predicted values.

Burke et al. [92] reported a thermodynamic model based on Flory–Huggins polymer solution theory. The basis for this selection was the similarity between bulky asphaltene molecules with polymer molecules, considering the remaining polymer molecules in the crude oil as solvent phase and hence the extension of the mechanism of thermodynamics of polymer solution theory, which is normally used in paint and polymer industry. First, the vapor–liquid equilibrium of the reservoir fluid was modeled and the fluid properties of the liquid phase obtained. In the liquid–liquid equilibrium, the model was considered to consist of two liquid phases, an oil-rich phase which acts as the solvent and an asphaltene-rich phase which behaves as the polymer. The simplified version of the Flory–Huggins polymer solution theory incorporated in this model to give volume fraction of asphaltenes soluble in the oil is:

$$\phi_A = \exp\left\{\frac{V_A}{V_L}\left[1 - \frac{V_L}{V_A} - \frac{V_L}{RT}(\delta_A - \delta_L)^2\right]\right\} \tag{11-26}$$

where the solubility parameter is defined as a measure of internal pressure exerted by the molecules within a solution and is given by:

TABLE 11-6

Experimental and predicted results of Jiang et al. [52]

Solvent used	Solvent/oil ratio (by weight)	Asphaltene (wt%)	
		experimental	predicted
CO_2	3.5	5.5	5.5
CO_2	13	5.8	6.0
Ethane	3	5.15	5.15
Ethane	13	5.25	5.25
Propane	4.8	8.7	8.4
Propane	7.8	8.6	9.2
Propane	16.5	9.25	9.28
n-Butane	2	6.2	6.2
n-Butane	8	6.4	6.45
n-Butane	13.5	6.5	6.5
n-Pentane	7	6.15	6.4
n-Pentane	12.5	6.3	5.5
n-Pentane	20.1	6.7	7.3
n-Heptane	7.3	5.34	5.41
n-Heptane	13.5	7.5	7.05
n-Heptane	20.1	7.32	7.67
NGL	7.3	5.35	5.45
NGL	13.5	7.45	7.05
NGL	20.1	7.2	7.67
Prudhoe	1.59	5.49	6.22
Bay Gas (PBG)			
PBG	1.70	7.40	6.24
PBG	5.85	8.15	7.54
PBG	10.42	8.08	8.48

$$\delta_i = \left(\frac{\Delta u_i^v}{V_i}\right)^{0.5} \tag{11-27}$$

When two liquids possessing significantly different molecules are mixed together, the internal pressure exerted by the liquid with a higher internal pressure will throw the molecules with the lower internal pressure out of the solution matrix, resulting in two immiscible phases. The solubility parameter is additive on volume fraction basis, i.e.,

$$\delta_M = \sum \phi_i \delta_i \tag{11-28}$$

When the solubility parameter of the solvent approaches that of the solute, the two substances become more miscible. Burke et al. [92] simulated reservoir conditions very closely by using live reservoir fluid during the laboratory tests. Experimental data were collected on solvent–oil systems using live reservoir fluids with stock tank gravities ranging from 40° to 18°API. The experiments performed consisted of PVT measurements, compositional analyses, measurements of physical properties, and static precipitation tests. The experimental data collected were

TABLE 11-7

Optimized values of asphaltene solubility parameters (from Kamath et al. [91])

Solvents	δ_A (psi$^{0.5}$)	V_A (ft^3/lb mol)	M_A (lb/lb mol)
Ethane	219.69	14.48	2491
Carbon dioxide	219.71	14.48	1531
Propane	220.57	14.48	3080
n-Butane	208.06	5.17	1100
n-Pentane	216.84	3.76	1605
n-Heptane	219.89	6.68	2483
NGL	217.00	4.21	1468
PBG	202.70	6.37	1738

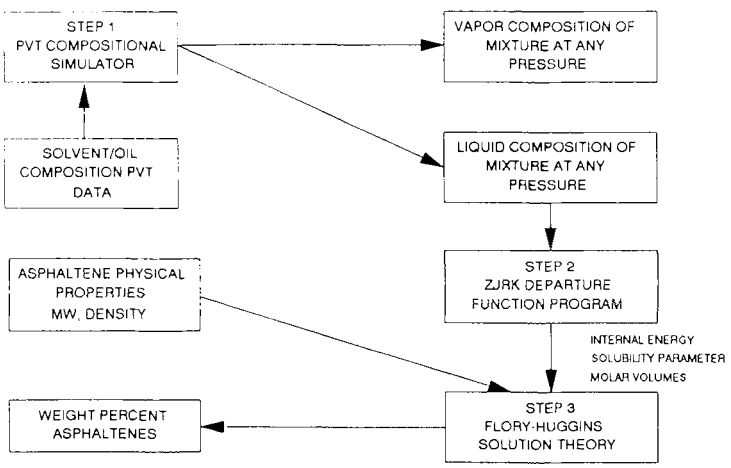

Fig. 11-19. Flow diagram of precipitation model used by Burke et al. [92].

then used to test the thermodynamic model developed based on the Flory–Huggins polymer solution theory. They used the Zudkevich–Joffe–Redlich–Kwong (ZJRK) equation of state and tuned a compositional simulator to match experimental results with theoretical predictions. Figure 11-19 shows steps involved in the modeling technique. The equation of state parameters were regressed until fluid properties calculated by the equation of state matched the experimentally measured properties. After proper tuning of the equation of state, it was used to predict the composition and fluid properties of the oil and/or solvent–oil mixture at other pressure and temperature conditions. In the second stage of the model development, predicted fluid properties, liquid phase compositions and the final equation of state tuning parameters were used to calculate internal energy of the liquid oil phase using thermodynamic departure function for multicomponent mixtures. The liquid densities generated by the equation of state were then used to calculate molar volumes. Using

internal energy of vaporization and liquid molar volume, the solubility parameter of oil was calculated using Eq. 11-27. In the last stage, the regressed data and liquid oil phase data were used to calculate soluble fraction of asphaltenes using Eq. 11-26. The tuning of the polymer solution theory model was done by varying the molecular weight, density and solubility parameter of the asphaltene and oil phase to match the experimental precipitation data. Table 11-8 shows a comparison between experimental and predicted values of asphaltene precipitation.

TABLE 11-8

Experimental and predicted results of Burke et al. [92]

Type of oil/solvent	Amount of solvent (mol%)	Asphaltene precipitation	
		experimental	predicted
Oil #3/naphtha	0	0.03	0.00
Oil #3/naphtha	20	0.04	0.00
Oil #3/naphtha	40	0.02	0.00
Oil #3/naphtha	60	0.02	0.00
Oil #3/naphtha	80	2.73	0.00
Oil #5/NGL	0	0.00	0.00
Oil #5/NGL	20	0.01	0.00
Oil #5/NGL	40	0.01	0.00
Oil #5/NGL	60	0.02	0.00
Oil #5/NGL	80	0.02	0.00
Oil #5/natural gasoline	0	0.00	0.00
Oil #5/natural gasoline	20	0.02	0.00
Oil #5/natural gasoline	40	0.01	0.00
Oil #5/natural gasoline	60	0.01	0.00
Oil #5/natural gasoline	80	0.01	0.00
Oil #5/naphtha	0	0.00	0.00
Oil #5/naphtha	20	0.01	0.00
Oil #5/naphtha	40	0.01	0.00
Oil #5/naphtha	60	0.00	0.00
Oil #5/naphtha	80	0.01	0.00
Oil #2/HCG #2 (high P)	0	0.14	0.00
Oil #2/HCG #2 (high P)	20	0.27	0.00
Oil #2/HCG #2 (high P)	50	1.46	6.80
Oil #2/HCG #2 (high P)	70	1.65	7.80
Oil #2/HCG #2 (high P)	78	3.21	7.18
Oil #2/HCG #2 (high P)	85	1.29	0.40
Oil #2/HCG #2 (high P)	90	1.10	0.00
Oil #2/HCG #2 (low P)	0	0.20	0.00
Oil #2/HCG #2 (low P)	24	0.12	0.00
Oil #2/HCG #2 (low P)	50	0.15	0.00
Oil #2/HCG #2 (low P)	70	0.10	0.00
Oil #2/HCG #2 (low P)	85	0.36	0.73

Novosad and Costain [34] conducted experimental and modeling studies of asphaltene equilibria for Midale Unit in southeastern Saskatchewan of Canada. This extensively fractured carbonate formation was discovered in 1952 and has been under waterflooding since 1962. CO_2 miscibility pressure is reported to be about 2250 psi. The authors adopted Hirschberg's molecular solubility model. They obtained relevant asphaltene precipitation data for the studied fluids and developed correlations using the above mentioned model. It was observed that CO_2 floods in reservoir cores at 13 to 16 MPa indicated no asphaltene precipitation or plugging. This was also confirmed by the pilot data. The contradiction observed between the static equilibrium tests outside the porous media and the dynamic tests in the porous media were attributed to low fluid velocities as the streaming potential generated during the low velocities might not have been large enough to cause flocculation of destabilized asphaltenes. The asphaltene precipitation data for the reservoir fluid of interest was successfully correlated using the model. However, it was recommended that asphaltenes be described as a continuous (polydispersed) phase (as proposed by Kawanaka et al. [15], which would improve accuracy of predictions. They also emphasized the need for more data on physical properties of asphaltenes and resins to predict asphaltene stability and the extent of their precipitation with higher level of confidence. They applied their numerical simulator for predicting asphaltene behavior under reservoir conditions. They carried out numerical simulation for three sets of bottom hole pressure over tubing head pressure ratios (BHP/THP) with a range of CO_2/crude volume ratios. It was observed that the predicted asphaltene stability occurs (corresponding to a minimum in predicted amount of precipitate) as the fluids move up the wellbore. This behavior was a result of combined effects of the changes of pressure, temperature, and composition. This

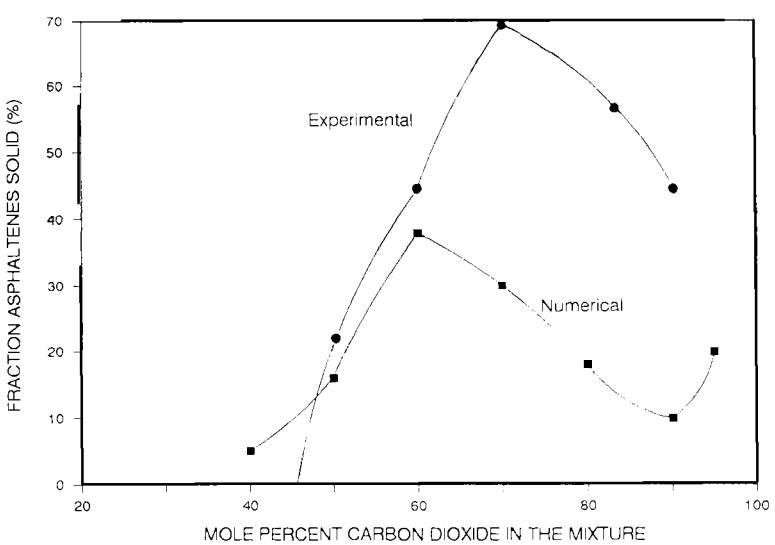

Fig. 11-20. Comparison of experimental and numerical results. (After Novosad and Costain [34].)

TABLE 11-9

Asphaltene properties (after Kokal et al. [53])

Property	Type of crude	
	Suffield	Lindberg
δ_a $(MPa)^{0.5}$	21.15	20.24
V_a, *n*-pentane/asphaltene (m^3/kg mol)	1.10	1.20
V_a, *n*-hexane/asphaltene (m^3/kg mol)	1.37	1.79
V_a, *n*-heptane/asphaltene (m^3/kg mol)	1.57	
V_a, *n*-octane/asphaltene (m^3/kg mol)	1.68	2.14
V_a, *n*-decane/asphaltene (m^3/kg mol)	1.85	2.36

asphaltene behavior partially explains the seemingly contradictory data reported on the role of wellhead pressure on asphaltene precipitation control. As indicated earlier, some field experiences indicate that asphaltene precipitation was minimized with low wellhead pressure, whereas in others the best result was obtained when the wellhead pressure was very high. Figure 11-20 compares experimental and model prediction results as obtained by Novosad and Costain [34].

Recently, Kokal et al. [53] conducted a series of high-pressure micromodel studies to determine the nature of asphaltene precipitation in the presence of two Canadian heavy crude oils and various solvents. In order to numerically model asphaltene precipitation, they used a combination of the Peng–Robinson equation of state (PRES) and the Flory–Huggins models similar to the procedure outlined by Hirschberg et al. [8]. The PRES was used in its translated form [93] to calculate the liquid phase composition assuming no asphaltene precipitation. This was followed by the use of Flory–Huggins model to calculate the amount of asphaltene precipitated from the liquid phase, assuming this precipitation does not affect the vapor–liquid equilibrium. For the purpose of liquid–liquid modeling, the system was considered to consist of three components, namely, deasphalted oil+solvent, resins, and asphaltenes. Solubility parameters that gave the best agreement of experimental results with numerical prediction values are given in Table 11-9. This table also gives the values of V_a (molar volume of asphaltene). These values were in close agreement with the data reported by Hirschberg et al. [8] and Burke et al. [92].

CONCLUSIONS

Asphaltene precipitation or the mere presence of asphaltenes may invoke many implications in recovering asphaltic crude oils. Asphaltene precipitation may occur under various thermally or non-thermally enhanced oil recovery schemes or even primary production conditions. Also, when in solution, asphaltenes have major effects on the rheology of crude oils. Some of these effects may be beneficial to oil production due to the formation of microbubbles with asphaltenes acting as nucleation sites. In most cases, however, asphaltene precipitation leads to the severe

problems of near-wellbore plugging or blocking of production tubing. Despite its large volume, today's literature on asphaltene properties is not able to provide one with a complete production strategy. Most efforts in the past have been in the areas of miscible flooding. Many questions of asphaltene properties under primary or thermal conditions remain unanswered. Due to the complex nature of asphaltenes, much more research is necessary to identify all governing factors influencing asphaltene precipitation. The process of accurately describing asphaltene behavior may begin at that stage. To-date, however, tremendous efforts have been made to describe known phenomena of asphaltene precipitation. Nevertheless, no model has been able to predict asphaltene precipitation with good accuracy. Also, most models, with different degrees of rigorousness, rely on experimentally determined parameters or adjustable coefficients. Due to the complexity and inexactness of asphaltene properties, such a problem is expected.

NOMENCLATURE

a	parameter in Soave equation of state, Pa m^{-6} $kmol^{-2}$
b	parameter in Soave equation of state, m^3 $kmol^{-1}$
c	concentration
C	constant in Eq. 11-13
f	solvation factor
k	parameter in Eq. 11-7
k_{ij}	interaction coefficient between ith and jth components
k_E	Einstein coefficient
K_M	coefficient introduced by Mack [62]
K_U	universal constant
MW	molecular weight
P	pressure, bar
R	ideal gas constant, J $kmol^{-1}$ K^{-1}
T	absolute temperature, K
T_{c_i}	critical temperature of a component i, K
Δu_i^v	internal energy of vaporization of component i, J $kmol^{-1}$
V	molar volume, m^3 $kmol^{-1}$
V_i	volume fraction of a component i
x_i	mole fraction of component i

Greek symbols

α	functional coefficient in Eq. 11-7
δ_i	Hildbrand's solubility parameter of component i, $MPa^{0.5}$
ϕ_i	volume fraction of component i
μ	viscosity of suspensions, mPa s
μ_o	viscosity of the dispersions, mPa s
μ_s	specific viscosity
ρ_i	density of the component i, g ml^{-1}

Subscripts

A	asphaltenes
R	resins
L	liquid oil phase
M	mixture

S solvent
i pertaining to component i
j pertaining to component j
max maximum

REFERENCES

[1] Danesh, A., Krinis, D., Henderson, G.D. and Peden, J.M., Asphaltene deposition in miscible gas flooding of oil reservoirs. *Chem. Eng. Res. Des.*, 66: 339–344 (1988).

[2] Yen, T.F., Present status of the structure of petroleum heavy ends and its significance to various technical applications. *Am. Chem. Soc., Div. Fuel Chem., Prepr.*, 17(4): 102–114 (1972).

[3] Leontaritis, K.J., Asphaltene deposition: a comprehensive description of problem manifestations and modeling approaches. *SPE 18892, Soc. Pet. Eng.* (1989).

[4] Dubey, S.T. and Waxman, M.H., Asphaltene adsorption and desorption from mineral surfaces. *SPE 18462, Soc. Pet. Eng.*, (1989).

[5] Witherspoon, P.A., Ray, B.R. and Grim, R.E., A study of the colloidal characterisitics of petroleum using an ultracentrifuge. *J. Phys. Chem.*, 61: 1296–1302 (1957).

[6] Bunger, J.W., Chemistry of asphaltenes — Summary of Symposium. Salt Lake City, pp. 1028–1031 (1979).

[7] Sachanen, A.N., *The Chemical Constituents of Petroleum*. Reinhold, New York, N.Y., 451 pp. (1945).

[8] Hirschberg, A., de Jong, L.N.J., Schipper, B.A. and Meijer, J.G., Influence of temperature and pressure on asphaltene floculation. *Soc. Pet. Eng. J.*, June, pp. 283–293 (1984).

[9] Mansoori, G.A., Jiang, T.S. and Kawanaka, S., Asphaltene deposition and its role in petroleum production and processing. *Arabian J. Sci. Eng.*, 13(1): 17–34 (1987).

[10] Leontaritis, K.J., *Asphaltene Deposition: A Thermodynamic-Colloidal Model*. Ph.D. Dissertation, University of Illinois, Chicago, Ill. (1988).

[11] Lichaa, P.M., Asphaltene deposition problem in Venezuela crudes — Usage of asphaltene in emulsion stability oil sands. *CIM, Spec. Vol.*, June, pp. 609–624 (1977).

[12] Lichaa, P.M. and Herrera, L., Electrical and other effects related to prevention asphaltene deposition. *SPE 5304, Soc. Pet. Eng.* (1975).

[13] Trbovich, M.G. and King, G.E., Asphaltene deposition removal: long lasting treatment with a co-solvent. *SPE 21038, Soc. Pet. Eng.* (1991).

[14] Monger, T.G. and Trujillo, D.E., Organic deposition during CO_2 and rich-gas flooding. *SPE 18063, Soc. Pet. Eng.* 18063 (1988).

[15] Kawanaka, S., Park, S.J. and Mansoori, G.A., The role of asphaltene deposition in EOR gas flooding: a predictive technique. *SPE/DOE 17376, Soc. Pet. Eng/DOE* (1988).

[16] Fuhr, B.J., Klein, L.L., Komishke, B.D., Reichert, C. and Ridley, R.K., Effects of diluents and carbon dioxide on asphaltene flocculation in heavy oil solutions. *Proc. 4th UNITAR/UNDP Conf. on Heavy Crude and Tar Sands*, 2: 637–648 (1989).

[17] Mansoori, G.A. and Jiang, T.S., Asphaltene deposition and its role in EOR miscible gas flooding. *Proc. 3rd European Conf.*, Rome (1985).

[18] Monger, T.G. and Khakoo, A. The phase behavior of CO_2-Appalachian oil systems. *SPE 10269, Soc. Pet. Eng.* 10269 (1981).

[19] Tuttle, R.N., High-pour-point and asphaltic crude oils and condensates. *J. Pet. Technol.*, 35(7): 1192–1196 (1983).

[20] Thaver, R., Nicoll, D.C. and Dick, G., Asphaltene deposition in production facilities. *SPE 18473, Soc. Pet. Eng.* (1989).

[21] Leontaritis, K.J. and Mansoori, G.A., Asphaltene deposition: a survey of field experiences and research approaches. *J. Pet. Eng. Sci.*, 1: 229–239 (1988).

[22] Akbar, S.H. and Saleh, A.A., A comprehensive approach to solve asphaltene deposition problem in some deep wells. *SPE 17965, Soc. Pet. Eng.* (1988).

[23] Addison, G.E., Identification and treating of downhole organic deposits. *SPE 18894, Soc. Pet. Eng.* (1989).
[24] Newberry, M.E. and Barker, K.M., Formation damage prevention through the control of paraffin and asphaltene deposition. *SPE 13796, Soc. Pet. Eng.* (1985).
[25] Claassen, E.J., Iron sulfide as water-deposited scale in sour gas wells. *Corrosion, Pap.*, 191, St. Louis, Mo. (1988).
[26] Leontaritis, K.J. and Mansoori, G.A., Asphalten flocculation during oil production and processing: a thermodynamic colloidal model. *SPE 16258, Soc. Pet. Eng.* (1987).
[27] Katz, D.L. and Beu, K.E., Nature of asphaltic substances. *Ind. Eng. Chem.*, 43: 1165 (1945).
[28] Monger, T.G. and Fu, J.C., The nature of CO_2-induced organice deposition. *SPE 16713, Soc. Pet. Eng.* (1987).
[29] Preckshot, G.W., Delisle, N.G., Cottrell, C.E. and Katz, D.L., Asphaltic substances in crude oils. *AIME Trans.*, 151: 188–194 (1943).
[30] Hasket, C.E. and Tartera, M., A practical solution to the problem of asphaltene deposits — Hassi Messaoud field, Algeria. *J. Pet. Technol.*, April, pp. 387–391. (1965).
[31] Von Albrecht, C., Salathiel, W.M. and Nierode, D.E., Stimulation of asphaltic deep wells and shallow wells in Lake Maracaibo. *CIM, Spec. Vol.*, June, pp. 55–62 (1977).
[32] Adialalis, S., *Investigation of Physical and Chemical Criteria as Related to the Prevention of Asphalt Deposition in Oil Well Tubings*. M.Sc. Thesis, Department of Petroleum Engineering, Imperial College, London, (1982).
[33] Hirschberg, A., The role of asphaltenes in compositional grading of a reservoir's fluid column. *J. Pet. Technol.*, January, pp. 89–94 (1988).
[34] Novosad, Z. and Costain, T.G., Experimental and modeling studies of asphaltene equilibria for a reservoir under CO_2 injection. *SPE 20530, Soc. Pet. Eng.* (1990).
[35] Bilheimer, J.S., Sage, B.H. and Lacey, W.N., Multi condensate phases in the *n*-pentane–tetialin–butane system. *Trans. AIME*, November, p. 283 (1949).
[36] Lhioreau, C., Briant, J. and Tindy, R., Influence de la flocculation des asphaltenes. *Rev. Inst. Fr. Pét.*, 22: 797–806 (1967).
[37] Elkins, L.F., Morton, D. and Blackwell, W.A., Experimental fireflood in a very viscous oil in unconsolidated sand reservoir south east Pauls Valley field, Oklahoma. *SPE 4086, Soc. Pet. Eng.* (1972).
[38] Islam, M.R. and George, A.E., Sand control in horizontal wells in heavy oil reservoirs. *J. Pet. Technol.*, July, pp. 844–853 (1991)
[39] Smith, G.E., Fluid flow and sand production in heavy-oil reservoirs under solution-gas drive. *Soc. Pet. Eng., Prod. Eng.*, May, pp. 169–179 (1988).
[40] Ward, C.A., Tikuisis, P. and Venter, R.D., Stability analysis in a closed volume of liquid–gas solution. *J. Appl. Phys.*, 53(9): 6076–6084 (1982).
[41] Ward, C.A. and Levart, E., Conditions for stability of bubble nuclei in solid surfaces containing a liquid–gas solution. *J. Appl. Phys.*, 56(2): 491–500 (1984).
[42] Islam, M.R. and Chakma, A., Mechanics of bubble flow in heavy oil reservoirs. *SPE 20070, Soc. Pet. Eng.* (1990).
[43] Clementz, D.M., Alteration of rock properties by adsorption of petroleum heavy ends: implications for enhanced oil recovery. *SPE/DOE 10683, Soc. Pet. Eng./DOE* (1982).
[44] Collins, S.H. and Melrose, J.C., Adsorption of asphaltenes and water on reservoir rock minerals. *SPE 11800, Soc. Pet. Eng.* (1983).
[45] Melrose, J.C., Interpretation of mixed wettability states in reservoir rocks. *SPE 10971, Soc. Pet. Eng.* (1982).
[46] Crocker, M.E. and Marchin, L.M., Wettability and adsorption characterisitcs of crude-oil asphaltene and polar fractions. *J. Pet. Technol.*, April, pp. 470–474 (1988).
[47] Sutherland, J.M., *A Proposed Model of Asphaltene Solution Behavior*. M.Sc. Thesis, Imperial College, London (1982).
[48] Shelton, D.A. and Yarborough, L.J., Multiple phase behavior in porous media during CO_2 or rich gas flooding. *J. Pet. Technol.*, 29(11): 1171–1180 (1977).

[49] Rutherford, W.M., Miscibility relationship in the displacement of oil by light hydrocarbons. *Soc. Pet. Eng. J.*, December, pp. 340–346 (1962).
[50] Huang, E.T.S. and Tracht, J.H., The displacement of residual oil by carbon dioxide. *SPE 4735, Soc. Pet. Eng.* (1974).
[51] Harvey, M.T., Jr., Shelton, L.J. and Kelm, C.H., Fluid injectivity experiences with miscible recovery projects using alternate rich gas and water injection. *J. Pet. Technol.*, September, pp. 1051–1055 (1977).
[52] Jiang, J.C., Patil, S.L. and Kamath, V.A., Study of asphalt/asphaltene precipitation during additional solvents to West Sak crude. *Paper presented at the Am. Chem. Soc. Meet.*, Washington, D.C, August (1990).
[53] Kokal, S.L., Najman, J., Sayegh, S.G. and George, A.E., Asphaltene precipitation of heavy oils by gas injection. *CIM/AOSTRA, Pap.*, 91-10 (1991).
[54] Mitchell, D.L. and Speight, J.G., The solubility of asphaltenes in hydrocarbon solvents. *Fuel*, 52: 49–152 (1973).
[55] Moore, E.W., Crowe, C.W. and Hendrickson, A.R., Formation effect in prevention of asphaltene sludges during stimulation treatments. *J. Pet. Technol.*, September, pp. 1023–1028 (1965).
[56] Dickie, J.P. and Yen, T.F., Macrostructures of the asphaltic fractions by various instrumental methods. *Anal. Chem.*, 39: 1847. (1967).
[57] Ferris, S.W., Black, E.P. and Clelland, J.B., Aromatic structures in asphalt fractions. *Ind. Eng. Chem. Prod. Res. Dev.*, 6: 127 (1967).
[58] Altgelt, K.H. and Harle, O.L., The effect of asphaltenes on asphalt viscosity. *Ind. Eng. Chem. Prod. Res. Dev.*, 14: 240–246. (1975).
[59] Mehrotra, A.K. and Svrcek, W.Y., One parameter correlation for bitumen viscosity. *Chem. Eng. Res. Des.*, 66(4): 323–327 (1988).
[60] Islam, M.R. and Chakma, A., Compositional dependence of viscosity of bitumens/heavy oils. *CIM, Pap.*, 89-40: (1989).
[61] Einstein, A., Eine neue Bestimmung der Molekül-dimensionen. *Ann. Phys. Leipzig*, 19: 289–306 (1906).
[62] Mack, C., Colloid chemistry of asphalts. *J. Phys. Chem.*, 36: 2901 (1932).
[63] Kendall, J. and Monroe, K.P., *J. Am. Chem. Soc.*, 39: 1802 (1917).
[64] Gillespie, T., The effect of aggregation and particle size distribution on the viscosity of Newtonian suspensions. *J. Colloid Interface Sci.*, 94(1) (1983).
[65] Lederer, E.L., A test of adsorption equations on the basis of adsorption measurements on a highly active charcoal. *Proc. World Pet. Congr.*, London, 2: 526 (1933).
[66] Shu, W.R., A viscosity correlation for mixtures of heavy oil, bitumen and petroleum fractions. *SPE 11280, Soc. Pet. Eng.* (1982).
[67] *Ber.*, 63, 222, 1930; quoted by Mack [62].
[68] Storm, D.A., Sheu, E.Y., Barresi, R.J. and DeTar, M.M., Structure and phase transitions of asphaltenes in solutions. *Proc. Bitumen Chemistry*, Rome (1991).
[69] Sage, B.H. and Lacey, W.N., Gravitational concentration gradients in static columns of hydrocarbon fluids. *Trans. AIME*, 132: 12–131 (1939).
[70] Hunt, M., *Petroleum Geochemistry and Geology*. W.H. Freeman and Co., San Francisco, pp. 381–391 (1979).
[71] Schulte, A.M., Compositional variations within a hydrocarbon column due to gravity. *SPE 9235, Soc. Pet. Eng.* (1980).
[72] Hetherington, G. and Horan, A.J., Variations with elevation of Kuwait reservoir fluids. *J. Inst. Pet. Technol.*, 46: 109 (1960).
[73] Ward, S.H. and Clark, K.A., Determination of the viscosities and specific gravities of Athabasca bituminous sand. *Alberta Res. Counc., Rep.*, 57, March (1950).
[74] Patel, M.S., Determination of viscosities of oils from Mannville Formation oil sand. *Alberta Res. Counc., Rep.*, October (1973).
[75] Waxman, M.H., Closmann, P.J. and Deeds, C.T., Thermal alteration of asphaltenes in Peace River tars. *SPE 9510, Soc. Pet. Eng.* (1980).

[76] Kitzan, P. and Parsons, L.J., *The Thermodynamic and Transport Properties of Bitumens and Heavy Oils*. AOSTRA (1984).
[77] Dealy, J.M., Rheological properties of oil sands bitumens. *Can. J. Chem. Eng.*, 57: 677–683 (1979).
[78] Datta, P., *Rheological Studies on Asphaltic Crude Oils of California*. M.Sc. Thesis, University of California, Los Angeles, Calif. (1962).
[79] Erno, B.P., Chriest, J.R. and Wilson, R.C., Depth related oil viscosity variation in Canadian heavy oil reservoirs. *CIM, Pap.*, 89-40-70 (1989).
[80] David, A., Asphaltene flocculation during solvent stimulation of heavy oils. *AIChE Symp. Ser.*, 69(127): 56 (1973).
[81] Orr, F.M., Yu, A.D. and Lien, C.L., Phase behavior of CO_2 and crude oil in low temperature reservoirs. *SPE 8813, Soc. Pet. Eng.* (1980).
[82] Stalkup, F.I., *Miscible Displacement. SPE Monograph.* Society of Petroleum Engineers, June (1983).
[83] Park, S.J. and Mansoori, G.A., Organic deposition from heavy petroleum crudes — A fractal aggregation theory approach. *Proc. 4th Int. Conf. Heavy Crude and Tar Sands, 2, Pap.*, 225: 471. (1989).
[84] Nellensteyn, F.J., Constitution of asphalt. *J. Inst. Pet. Technol.*, 10: 311 (1924).
[85] Swanson, J., Physical chemistry of asphalts. *J. Chem. Phys.*, 46: 141 (1942).
[86] Witherspoon, P.A. and Munir, Z.A., Size and shape of asphaltic particles in petroleum. *Prod. Mon.*, 25: 20–31 (1960).
[87] Koots, J.A. and Speight, J.G. Relation of petroleum resins to asphaltenes. *Fuel*, 54: 179 (1975).
[88] Scott, R.L. and Magat, M., Thermodynamics of high polymer solutions. *J. Chem. Phys.*, 13: 172 (1945).
[89] Du, P.C. and Mansoori, G.A., A continuous mixture computational algorithm for reservoir fluids phase behavior. *SPE 15082, Soc. Pet. Eng.* (1986).
[90] Mansoori, G.A., Asphaltene deposition. In: T.F. Yen and G.V. Chilingarian (Editors), *Asphaltenes and Asphalts, 1*. Elsevier, Amsterdam, pp. 125–158 (this volume).
[91] Kamath, V.A., Islam, M.R., Patil, S.A., Jiang, J.C. and Kakade, M.G., The role of asphaltene aggregation in viscosity variation of reservoir hydrocarbons and in miscible processes. In: M.K. Sharma and G.D. Sharma (Editors), *Particle Technology and Surface Phenomena in Minerals and Petroleum*. Plenum Press, New York, N.Y., pp. 1–21 (1991).
[92] Burke, N.E., Hobbs, R.D. and Kashou, S.F., Measurement and modeling of asphaltene precipitation from live reservoir systems. *SPE 18273, Soc. Pet. Eng.* (1988).
[93] Kokal, S.L. and Sayegh, S.G., Gas saturated bitumen in situ predictions using volume-translated Peng–Robinson equation of state. *J. Can. Pet. Technol.*, 29(5): 77–82 (1990).

Asphaltenes and Asphalts, 1. Developments in Petroleum Science, 40
edited by T.F. Yen and G.V. Chilingarian

Chapter 12

THE USE OF BITUMEN ASPHALTENES AS THERMAL MATURATION INDICATORS

M.M. SHARMA, G.V. CHILINGARIAN and T.F. YEN

THERMAL MATURATION INDICATORS — INTRODUCTION

Geochemical analyses are now an essential part of any oil and gas prospecting program. A great deal has been learned about the various factors that control the oil-generating capacity of a sedimentary deposit. It is now possible to make semiquantitative estimates of the oil and gas that have been produced or will be produced from a source rock, if the type, quality, quantity and thermal maturity of kerogens are determined. The evaluation of oil-source capacity depends on four conditions, which must be simultaneously met in order to yield petroleum [1]:

$$\text{Oil expelled from source rock} = Q_1 \cdot Q_2 \cdot M \cdot E$$

where Q_1 and Q_2 are the scaled factors for quantity and quality of the kerogen, M is the generating ion factor corresponding to the thermal maturity of the kerogen, and E is the expulsion or migration efficiency of the source sequence. Even in the cases where the "total oil" and the "oil already generated" are calculable on the basis of Q_1, Q_2 and M, the migration efficiencies are so highly variable that no predictions of the reservoired petroleum are possible. This chapter focuses on the possibility of using the structural characteristics of the asphaltene fractions in reservoired crude oils as possible indicators of thermal maturity.

A wide variety of thermal maturation indicators are available today. Such geochemical parameters are available for the rock, the kerogen or the bitumen. These parameters include the elemental compositions, H/C ratio, the ratio of residual carbon to total carbon, and the carbon preference index (CPI) or the odd–even preference (OEP) for the kerogen. Bitumen thermal maturation indicators are also similar and include the ratio of the aromatics to saturated hydrocarbons in the organic extract, and the CPI. The H/C atomic ratio and the percent solubility in carbon disulfide were shown to be indicators of thermal maturity [2]. The H/C ratio of less than 0.53 indicates a thermally metamorphosed dry gas area. When this ratio lies between 0.53 and 0.58, it indicates a wet gas area, and a mature oil area when greater than 0.58. Rogers et al. [2] also distinguished between (a) thermal alteration of the oil to dry gas and solid bitumen, and (b) the deasphalting of the oil as large amount of gas enters solution. This distinction is made on basis of carbon isotopic ratios. Reservoir bitumens formed by deasphalting have isotopic ratios like the original oil, whereas those formed by thermal maturation have significantly heavier ratios relative to Chicago Belemnite standard [3].

The ratio of the organic extract to the total organic carbon (OE/TOC) increases with increasing thermal maturity of the sediment, until the gasification stage is reached, when it again begins to decrease. The amount of aromatics and saturates in the organic extract, however, tend to increase with thermal maturity.

Bray and Evans [4] developed the CPI as an indicator of thermal maturity. A CPI (defined as the ratio of the sum of concentrations of odd normal paraffins to the sum of the even normal paraffins, taken over a certain range of carbon numbers) value higher than 1.0 indicates an immature bitumen. As catagenesis proceeds, the CPI value approaches 1.0. Porphyrins have been suggested as indicators of thermal maturity [5]. The molecular weight of the normal paraffins increases as sediment matures and disproportionation reactions yield gas and heavier more aromatic components. This could be used as a maturation indicator.

Tissot et al. [6] have shown that polycyclic hydrocarbons undergo some predictable changes during catagenesis. The concentration of polycyclic hydrocarbons decreases, whereas those of saturated and aromatic hydrocarbons increase. The relative abundance of each species is shown in his study, and the trends are quite evident. The approach requires a detailed analysis that is too time consuming for routine analysis. Alexander et al. [7] have proposed that the aromaticity of the bitumens be regarded as a thermal maturity indicator.

The single most important disadvantage of using any of the above approaches is that the value of the parameters depend on numerous extraneous factors in addition to thermal maturity. For example, the OE/TOC ratio or the CPI value of a bitumen depends more on the precursor organic material than on the diagenetic and catagenetic transformations. Many instances are now documented [8,9] in which CPI values of less than 1.0 have been reported for immature sediments. Such anomalies and many others lead one to believe that although the general trends stated above may be true under ideal conditions, it is not unlikely that other geologic factors such as the nature of the starting organic material, the geologic environment, bacterial degradation, migration processes, and other low-temperature diagenetic processes may reverse the trend. It is for this reason that geochemical maturation parameters often prove to be unreliable and difficult to interpret.

The above discussion suggests that an ideal thermal maturation indicator is the one that is highly sensitive to thermal maturation, or catagenetic processes, but relatively insensitive to the nature of the starting biomaterial, and low-temperature diagenetic processes. It is with this objective in mind that aromatic structures in bitumen asphaltenes are suggested as thermal maturity indicators. It is shown in the following sections that although structural parameters of asphaltenes may seem to be good indicators of thermal maturity, care must be taken in using them as such.

STRUCTURAL CHARACTERIZATION OF BITUMEN ASPHALTENES

Bitumen is defined as the organic solvent-soluble part of the petroleum or oil shale. The insoluble part is termed kerogen. The fraction of the bitumen that is insoluble in excess pentane and is soluble in benzene at ambient temperatures is

termed asphaltene. The resin fraction is the propane-insoluble and pentane-soluble component of the bitumen. Together, the resins and asphaltenes comprise the asphaltic fraction. The asphaltic fraction contains almost all of the non-hydrocarbons in the bitumen, with varying amounts of nitrogen, oxygen, sulfur, and metals, particularly nickel and vanadium.

A great deal of work has been done at Yen's laboratory [10–17] to develop an average hypothetical structure for asphaltene. The difficulty encountered in such attempts stems from the fact that asphaltene structures vary considerably in size, shape and composition from one sample to another. Structurally, asphaltene may best be described as a multipolymer. It is composed of a wide variety of building blocks, which are associated with each other by weak covalent or hydrogen bonds. At high concentrations, these structural subunits tend to associate and form micelles. The petroleum then behaves as a colloidal system in which the dispersed phase consists of asphaltenes complexed with high-molecular-weight components of the aromatics and resins. The asphaltenes remain peptized to varying degrees, depending on the aromatics and resin content of the maltene phase. Although the asphaltene micelle may itself not bear a significant net charge [18], it is associated and complexed with polar molecules, which act as peptizing agents [19].

The average structure of the molecules that constitute the asphaltic fraction of bitumens has been studied by the authors using a variety of methods [20,21]. Petroleum asphaltenes and oil shale asphaltenes were studied by these techniques. Densimetric and ring compactness analysis [12,14] and a combination of NMR and X-ray analysis [22] show that the aromatic nuclei of petroleum asphaltenes are peri-condensed. These π-systems are linked by a number of short-chain alkanes and kata-condensed naphthenics. X-ray diffraction studies indicate that aromaticities range from 0.25 to 0.5. The diameters of the aromatic sheets range from 9.5 to 15 Å, whereas the intersheet distances vary from 3.55 to 3.7 Å [13]. About 50–70% of these sheets are substituted by other alkyls and naphthenics. Polarography and oxidation studies indicate that the heteroatoms N, S and O occur in chemically stable configurations, probably rings such as benzothiophene structures.

Electron spin resonance (ESR), in conjunction with metalization studies, have shown that the sites for the unpaired electrons as well as for metal coordination are probably "imperfections" or "holes" in the aromatic sheets, caused by the loss or replacement of internal carbons with heteroatoms such as nitrogen [15].

In addition to the microstructure just outlined, the π-systems associate with each other to form layered structures. In the case of petroleum asphaltenes, these stacks are about 5 layers thick as determined from X-ray diffraction studies. These layered structures may in turn form aggregates of substantial size so that they behave as colloidal particles [23]. The molecular weight of such micelles can be determined from ultracentrifugation and film spreading experiments, etc. [24–26].

SAMPLE AQUISITION AND SUPPORTING INSTRUMENTAL METHODS

The data reported in Tables 12-1, 12-2, 12-4, and 12-5 were obtained for asphaltenes recovered from widely different locations. Most of the petroleum samples were collected at the wellhead in the field. Other bitumens were obtained from tar sand, seeps, and oil shale. Inasmuch as there is no clear-cut line for differentiating between the various kinds of bitumens, no such gradations were attempted. The Athabasca bitumen sample, for example, could be called either an asphalt or a heavy oil. The Rozel Point sample originates from a tar seep owing its origin to a fault. It has an exceptionally high sulfur content, but no hydrogen sulfide. All the remaining samples were native crudes. The oil shale sample, which was obtained from the

TABLE 12-1

List of samples with locations, age, abbreviations used in this text, aromaticity and percentage of asphaltene in the bitumen

Sample	Age	Geographic location	Notation	f_a	Asphaltene content (%)
Kermit Ellenburger	Ordovician	Texas	Abal		0.25
Athabasca A[a]	Lower Cretaceous	Canada	AA	0.31	15.0
Athabasca B[a]	Lower Cretaceous	Canada	AB	0.38	22.0
Bachequero	Middle/Lower Miocene	Venezuela	Bach	0.41	12.5
Baxterville A[b]	Upper Cretaceous	Mississippi	BxA	0.51	14.5
Baxterville B[b]	Upper Cretaceous	Mississippi	BxB	0.53	
Belridge	Pliocene	California	Bel	0.30	3.8
Boscan A[c]	Cretaceous	Venezuela	Bos A	0.35	21.8
Boscan B[c]	Cretaceous	Venezuela	Bos B	0.35	20.0
Burgan	Middle Cretaceous	Kuwait	Bur	0.38	
Hiseville	Devonian	Kentucky	His		0.18
Keystone	Permian	New Mexico	Key		0.25
Lagunillas	Middle/Lower Miocene	Venezuela	Lag		13.4
Amal	Ordovician	Libya	Lib		0.25
Mara	Lower Cretaceous	Venezuela	Mara	0.35	4.1
Melones	Cretaceous	Venezuela	Mel	0.38	13.9
Raudhautain	Middle Cretaceous	Kuwait	Rau	0.32	
Rozel Point	Recent	Utah	R.P.	0.18	23.0
Ragusa	Upper Triassic	Sicily	Rag	0.26	0.25
Sand Hill	Ordovician	New Mexico	Sad		0.5
Santiago	Pliocene	California	Sant	0.31	5.6
South Ward	Silurian	Texas	Siw		0.9
North Ward Estates	Permian	Texas	NW		0.4
Wafra Estates A1	Lower Cretaceous	Neutral Zone	WA#1	0.37	
Wafra A17	Middle Cretaceous	Neutral Zone	WA#17	0.35	
Yorba Linda	Pleistocene	California	YL	0.38	

[a] A and B represent two different samples obtained at different locations, all from Mildred Lake Quarry, Northeast of McMurray.

[b] All from C.V. Coops No. 1 well, lower Tuscaloose; sample A obtained in 1955; sample B obtained in 1945.

[c] All from Zulia, Venezuela; from different depths.

Green River Formation at Anvil Point, Colorado, had a low bitumen content, i.e., only 2.1% bitumen by weight after crushing and solvent (10% methanol in benzene) extraction for 72 hours. Table 12-1 provides some basic geographic and geologic information pertaining to the samples.

Asphaltenes were isolated from the bitumen by precipitation with a 20-fold volume of *n*-pentane. The oil/resin fraction was separated from the precipitate by filtration through a thimble followed by Soxhlet extraction with *n*-pentane. The asphaltene fraction was obtained by Soxhlet extraction of the residue with toluene in a conventional manner.

Proton and ^{13}C NMR spectra were obtained on a Varian XL-100 spectrometer operating at 100.1 MHz for proton or 25.2 MHz for carbon. Proton NMR was measured in CD_2Cl_2 (central peak at 77.1 ppm). Usually a sample of asphaltene (0.5 g) was dissolved in 2.5 ml of $CDCl_3$ with 35 mg of $Cr(acac)_3$ added to it. To obtain reliable quantitative results, a delay time of 4 s after each 35° pulse and 0.68 s acquisition time was used in the gated decoupling sequence. All chemical shifts were reported in ppm downfield from TMS (tetramethyl silane) [27].

ESR spectra were taken from a Varian V4502 X-band spectrometer equipped with a 12-inch Varian V4013A magnet and V-FR-2100 "Fieldal". Some spectra were taken from a Varian E-4 E.P.R. system. A freshly prepared *p*-benzosemiquinone radical exhibiting a 5-line pattern was used as reference of the measurement of *g*-values. The splitting of hyperfine lines of 2.368 G and the center at $g = 2.00468$ of this benzosemiquinone radical were employed for calculation. The frequency differences between sample and reference were cancelled by using a dual cavity. Spin concentrations were determined at three power levels between 0.5 and 0.05 mW. The spin number of the sample was calculated from that of the reference by using the following equation:

$$N_S = N_r \left(\frac{K_S}{K_r}\right) \left[\frac{(\Delta H_S)^2}{(\Delta H_r)^2}\right] \left(\frac{I_S}{I_r}\right) \tag{12-1}$$

where ΔH is the field spacing between the field at resonance for the sample (S) and the reference (r), I is the intensity, and K is the rate constant. More details of the experimental procedures were published previously [11,15,16,22,27].

SIMULATED THERMAL MATURATION EXPERIMENTS WITH GREEN RIVER OIL SHALE ASPHALTENE

The generation of oil and gas during catagenesis takes place at high temperatures. The high temperature provides the required activation energy for the breakdown of the complex kerogen structure into simpler subunits. Temperature is not a crucial factor during diagenesis which occurs at lower temperatures and shallow depths. As a result, high temperature retorting does not simulate the processes during diagenesis. Lopatin [28] put together these ideas into a factor, which he called the time–temperature index (TTI) of maturity. Lopatin's basis for developing the TTI

was the assumption that the rate of decomposition of kerogen could be represented by an Arrhenius type of temperature dependence:

$$K(T) = A\,e^{-E_A/RT} \tag{12-2}$$

where $K(T)$ is the temperature dependent rate constant, A is the Arrhenius constant for the reaction, and E_A is the pseudo-activation energy for the reaction. He estimated that in the range of activation energies commonly encountered in kerogen decomposition (≈1600 cal/mol), the rate of reaction would double for every 10°C rise in temperature. In accordance with these principles, high temperatures and relatively short times were used to simulate thermal maturation in the laboratory.

The sample of Green River oil shale from Anvil Points, Colorado, was crushed to 8–20 mesh size and then Soxhlet-extracted exhaustively with 10% methanol in benzene for 72 hours. The bitumen yield was 2.1% by weight. The retorting was done in a cylindrical quartz column 47 mm in diameter and 300 mm in length. Heat was provided by two sets of heating wires wrapped around the quartz cell. The temperature was raised rapidly to the desired level and maintained there for three hours. Asphaltenes were isolated by the procedure outlined earlier. The three asphaltene samples obtained were A (without retorting), A_{425} (after retorting at 425°C), and A_{500} (after retorting at 500°C) [29].

ESTIMATION OF STRUCTURAL PARAMETERS

Owing to the complexity of the asphaltene structure, the so called "average structural parameters" [30] approach was used to characterize the gross structural features. Average structural parameters include aromaticity (f_a), degree of substitution of the aromatic sheet (σ or C_S/C_{SU}), the ratio of peripheral carbons per aromatic sheet to total aromatic carbons (H_I/C_A or H_{aru}/C_{ar}) and the aliphatic H/C ratio. The parameters were calculated from ^{13}C NMR spectra of the samples and from elemental analysis according to the following equations:

$$f_a = \frac{\mathrm{C/H} - (H_\alpha/X + H_\beta/Y + H_\gamma/3)}{\mathrm{C/H}} \tag{12-3}$$

$$\sigma = \frac{H_\alpha/X}{H_A + H_\alpha/X} \tag{12-4}$$

$$n = (H_\alpha/X + H_\beta/Y + H_\gamma/3)(H_\alpha/X) \tag{12-5}$$

$$H_{aru}/C_{ar} = \frac{H_A + H_\alpha/X}{\mathrm{C/H} - (H_\alpha/X + H_\beta/Y + H_\gamma/3)} \tag{12-6}$$

$$H_S/C_S = (\mathrm{H/C})\,[(1 - H_A)/(1 - f_a)] \tag{12-7}$$

For the ESR data, the number of spins per gram (N_g) is proportional to the intensity I, multiplied by the square of the line width, if the amplitude modulation is small:

$$N_g \propto I(\Delta H)^2 \tag{12-8}$$

The simplified g-tensor can be expressed as:

$$|g - g_e| \sim 2 \sum \rho_k \xi_k / \Delta E_k \tag{12-9}$$

where g_e is the Lande g-value for an unpaired electron exhibiting "spin only" paramagnetism equalling 2.0023, ρ_k is the electron spin density of the given atom, ξ_k is the spin orbital coupling constant for atoms having p electrons, and ΔE_k is the energy separation between the given atom's electronic ground state and first excited state.

CORRELATION OF THE THERMAL INDICATOR

The structural parameters obtained from the NMR and X-ray diffraction studies for the asphaltenes derived from native crudes are listed in Table 12-2. These parameters include the aromaticity (f_a), the degree of substitution of the aromatic sheet (σ), number of carbon atoms per alkyl substituent (n), the ratio of peripheral carbon per aromatic sheet to total aromatic carbons (H_{aru}/C_{ar}), and the aliphatic H/C ratio. The same parameters are also tabulated for the artificially matured sample of Green River Shale oil asphaltene (Table 12-3). The elemental analysis of the samples is provided in Table 12-4.

Plots of these parameters as a function of age and as a function of retorting temperature for the native petroleum and shale samples, respectively, are shown in Figs. 12-1 to 12-7. The aromaticity increases with age for the artificially matured samples, with no apparent clear trend (Fig. 12-1). The H/C ratio shown in Fig. 12-2 is consistent with the aromaticity variation (H/C increases as f_a decreases). The opposite trends are, therefore, observed in Fig. 12-3. The number of carbon atoms per substituent decreases with the retorting temperature, but increases with increasing maturation. The artificially matured samples also show very clear trends

TABLE 12-2

Structural parameters of some asphaltene samples

Sample [a]	f_a	σ (C_{SU}/H_I)	n	H_{aru}/C_{ar} (H_I/C_A)
Baxterville	0.53	0.62	4.0	0.34
Lagunillas	0.41	0.71	3.2	0.43
Burgan	0.38	0.51	3.6	0.52
Wafra No. A-1	0.37	0.61	4.1	0.42
Mara	0.35	0.48	5.6	0.38
Wafra No. A-17	0.35	0.60	3.4	0.53
Raudhautain	0.32	0.57	3.7	0.48
Ragusa	0.26	0.70	4.8	0.40

[a] Refer to Table 12-1 for locations and ages.

TABLE 12-3

Average structural parameter of Green River asphaltene at various stages of heat treatment

Structural parameter	Bitumen	A_{425} [a]	A_{500} [a]
f_a	0.24	0.51	0.60
σ (C_{SU}/H_I)	0.73	0.53	0.51
n (C_S/C_{SU})	4.16	2.42	1.98
H_{aru}/C_{ar} (H_I/C_S)	0.99	0.75	0.66
H_S/C_S	1.80	2.18	2.22

[a] Samples subjected to heat treatment at 425°C and 500°C, respectively.

TABLE 12-4

Elemental analysis of some asphaltene samples

Sample [a]	C (%)	H (%)	N (%)	O (%)	S (%)	Atomic ratios		Σ NSO
						H/C	O/C	
Athabasca A	80.5	8.1	1.1	1.9	7.4	1.207	0.0177	10.4
Athabasca B	81.3	8.2	1.2	1.9	3.4	1.210	0.0175	6.5
Bachequero	85.5	7.7	2.0	3.0	2.4	1.081	0.0263	7.4
Baxterville A	84.5	7.2	1.4	<0.5	3.5	1.022	0.0036	5.4
Belridge	83.8	8.3	2.6	2.2	0.5	1.188	0.0197	5.3
Boscan A	80.5	7.7	1.9	2.8	6.2	1.148	0.0261	10.9
Boscan B	80.8	7.8	2.2	2.4	7.5	1.158	0.0223	12.1
Libya	85.2	8.9	0.7	0.67	0.5	1.254	0.0059	1.87
Melones	83.4	8.2	2.0	0.8	6.1	1.180	0.0072	8.9
Rozel Point	71.8	8.4	1.4	3.4	15.3	1.404	0.0355	10.1
Santiago	84.4	8.6	2.0	2.2	1.8	1.223	0.0195	6.0
Yorba Linda	82.2	8.3	1.4	2.3	2.0	1.211	0.021	5.7

[a] See Table 12-1 for locations and ages.

in the plots of σ and H_{aru}/C_{ar} versus age (Figs. 12-4 and 12-5). No clear trends, however, are obvious for the naturally matured samples.

Results from the ESR spectra are provided in Table 12-5. As shown in Fig. 12-7, there seems to be a correlation between the number of spins per gram (N_g) and the age of the sample. Rozel Point sample is not suitable for this plot, because it is a surface seep with a large amount of sulfur and oxygen being present. It, therefore, does not follow the general trend. The g tensor shows that there is a trend towards higher g values as maturation increases (Fig. 12-6).

Rubenstein et al. [31], in working with highly biodegraded oils such as the Alberta oil sands, have observed that the asphaltene fraction of the oil remains unaltered during biochemical degradation. This is significant because it provides a way to obtain geochemical information about the precursor biomass before it was biochemically degraded. The differences in the hydrocarbons obtained from asphaltene pyrolysis experiments and those contained in the biodegraded crude oil provide useful information on the origin of oil prior to asphaltene formation.

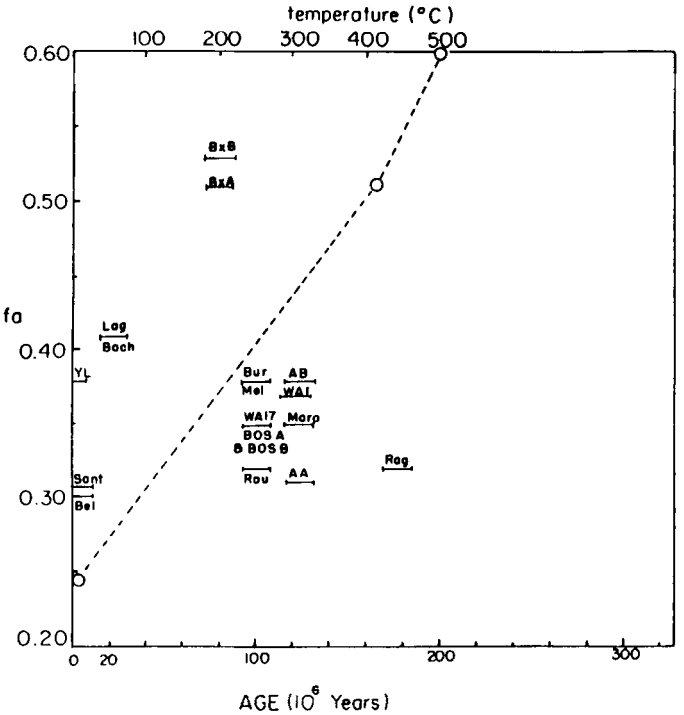

Fig. 12-1. Aromaticity (f_a) vs. geologic age and temperature.

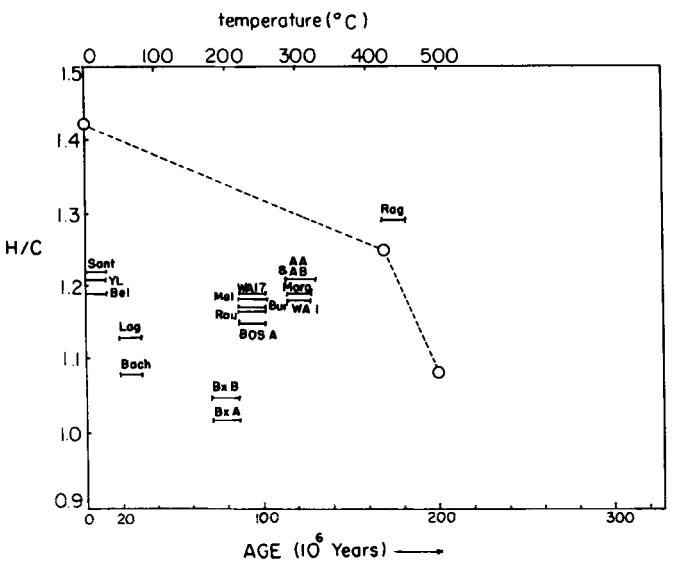

Fig. 12-2. H/C ratio vs. geologic age and temperature.

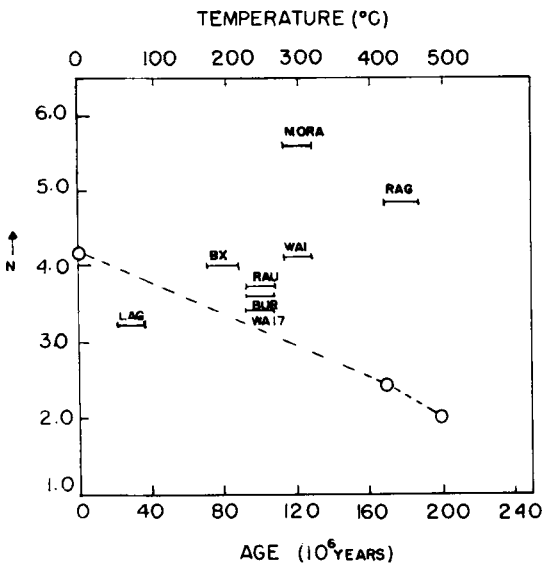

Fig. 12-3. Number of carbon atoms per alkyl substituent (n) vs. age and temperature.

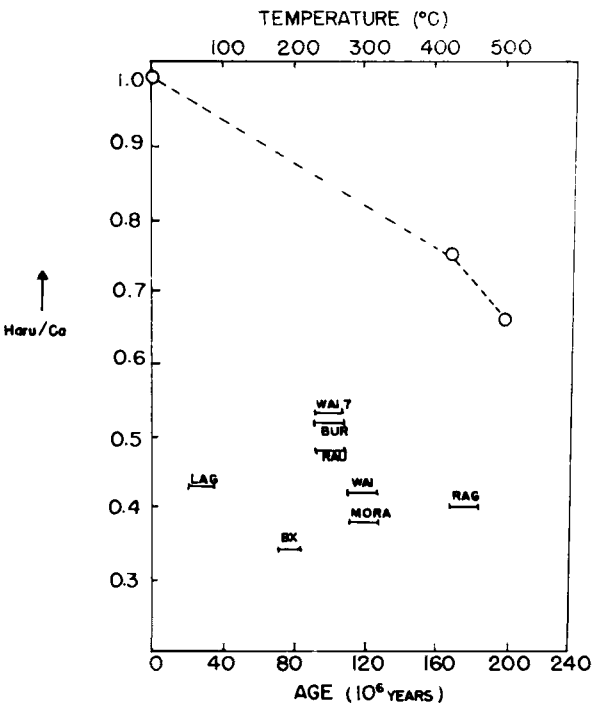

Fig. 12-4. Ratio of peripheral carbon to aromatic carbon atom (H_{aru}/C_{ar}) vs. age and temperature.

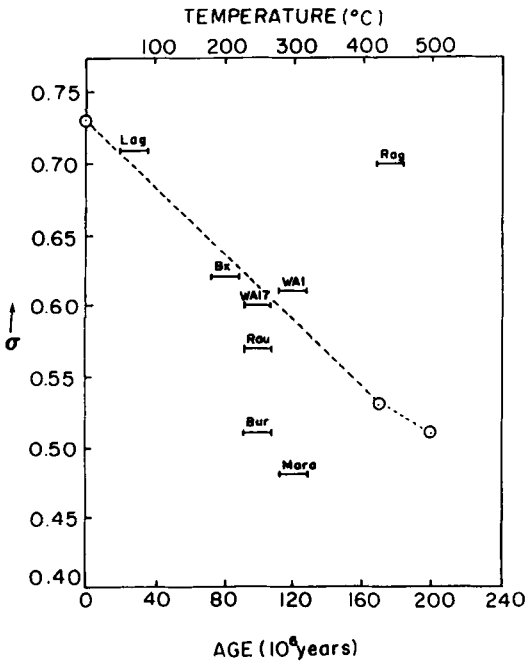

Fig. 12-5. Degree of substitution (σ) vs. age and temperature.

TABLE 12-5

ESR parameters of some native asphaltenes

Sample[a]	N_g ($\times 10^{-18}$)	$(g-2) \times 10^4$
Athabasca A	5.6	33
Athabasca B	5.5	32
Bachequero	4.4	31
Baxterville A	6.4	29
Belridge	10.4	28
Boscan A	1.8	34
Boscan B	1.7	35
Libya	8.0	26
Melones	4.0	32
Rozel Point	1.7	40
Santiago	11.0	28
Yorba Linda	8.5	28
Mara	1.7	30
Ragusa	2.1	27
Wafra A-1	1.9	36
Baxterville B	4.4	30

[a] See Table 12-1 for locations and ages.

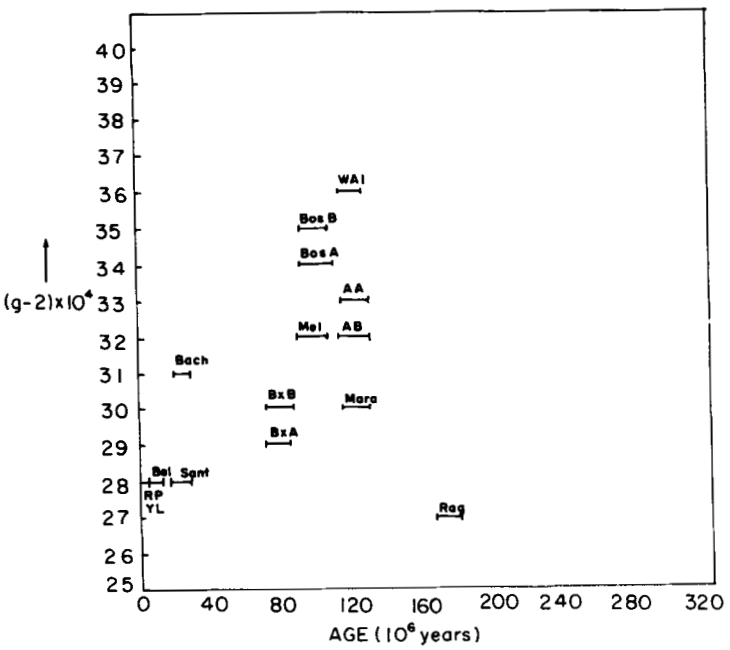

Fig. 12-6. g tensor vs. age and temperature.

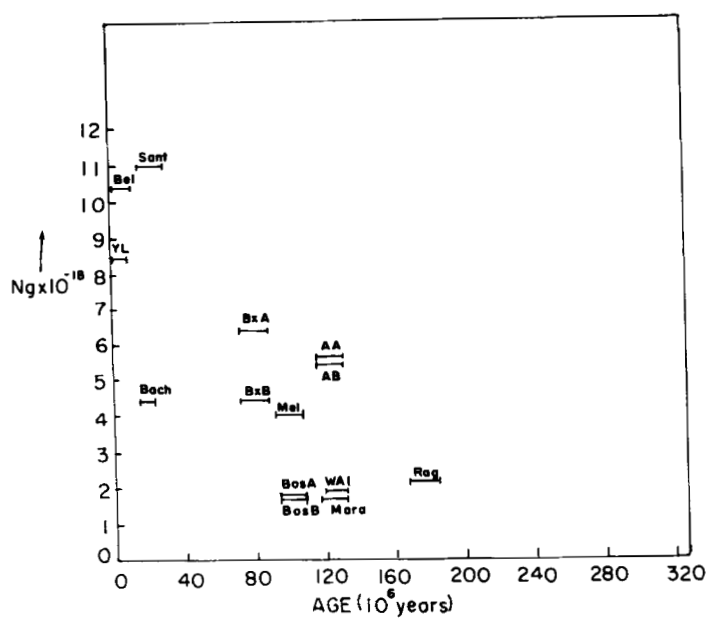

Fig. 12-7. Number of spins per gram (N_g) vs. age and temperature.

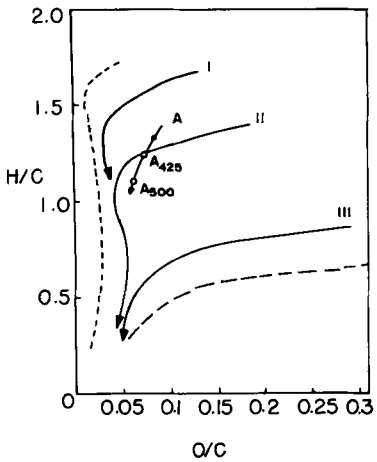

Fig. 12-8. Relationship between H/C and ratios for heat-treated samples of Green River oil shale asphaltene, shown on a Tissot et al. [6] diagram.

Various studies on the thermal maturation or pyrolysis of asphaltene have shown that they follow essentially the same reaction pathways as kerogen. The H/C, O/C and S/C ratios decrease with increasing maturity or pyrolysis temperature in accordance with Tissot et al.'s [6] diagram (Fig. 12-8) as is observed in the study. Disproportionation reactions cause the asphaltenes to yield hydrocarbons and highly graphitic carbonaceous residues [32]. As pointed out by Tissot [33], the striking similarity between the hydrocarbon pyrolysis products of asphaltene and those occurring naturally in the crude oil leads one to the conclusion that asphaltenes are an important intermediate product of catagenesis.

Asphaltenes stored unaltered over long periods of biodegradation constitute an important source of geochemical information [31]. Biomarkers, such as the steranes and hopanes, present in the asphaltene can be used regardless of the occurrence of precipitation of asphaltene. The results of this study show, however, that structural correlations for maturation based on the structural parameters of asphaltene must account for precipitation and peptization of asphaltene micelles.

MATURATION AND ASPHALTENE PRECIPITATION

From Figs. 12-1 and 12-7, one can see that there seem to be opposing trends in the structural changes that occur during catagenesis. It is generally believed that the formation of oil and gas from the precursor kerogen follows the following scheme:

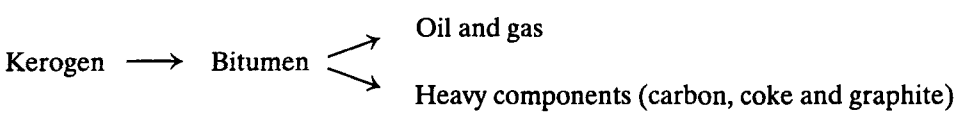

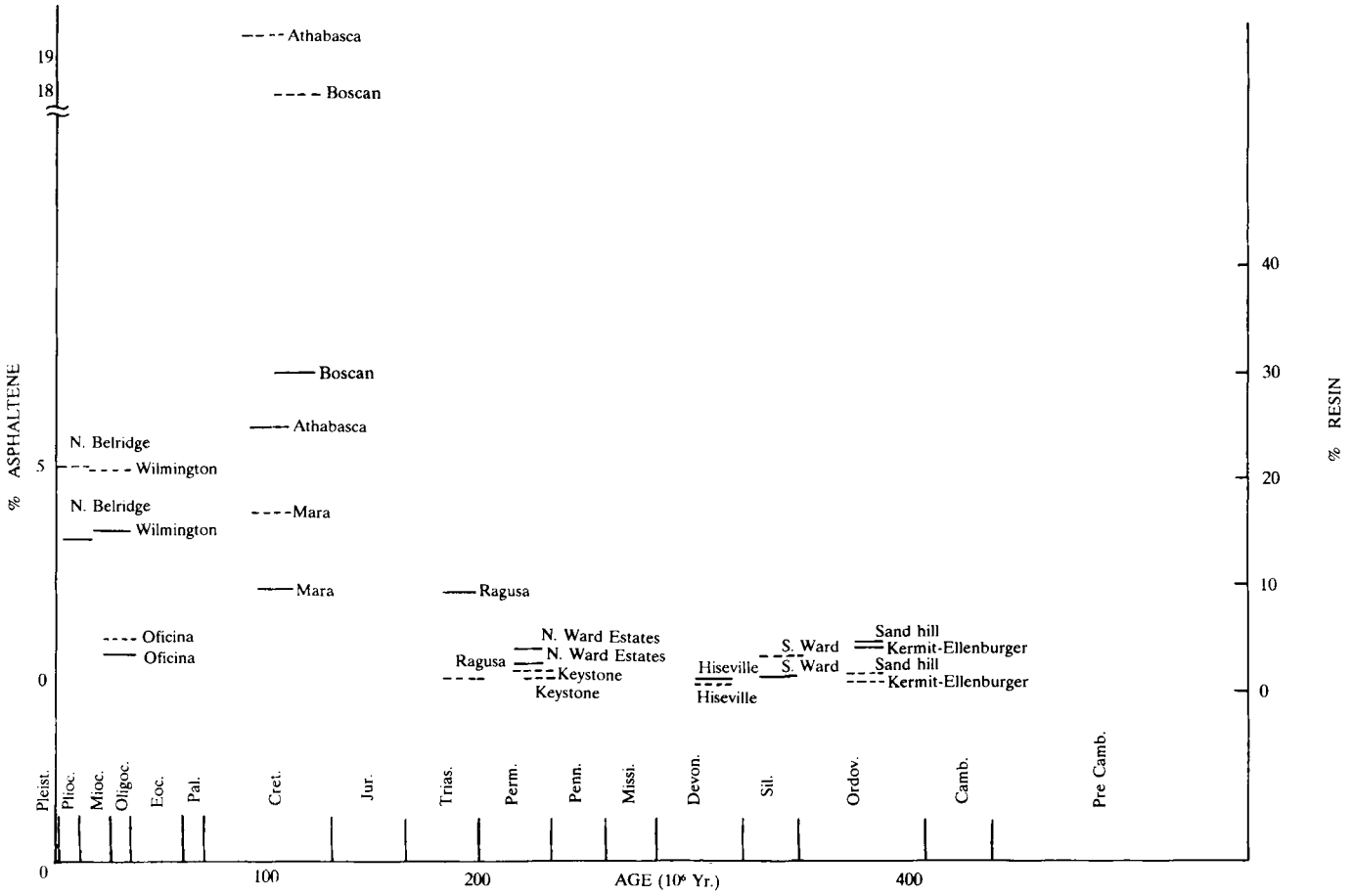

Fig. 12-9. Relationship between the asphaltene or resin content (%) in the bitumen and geologic age of the sample (dotted line: asphaltene content; solid line: resin content).

On the basis of this scheme, one would expect that the amount of asphaltenes in a sediment would increase with maturation. It is well known, however, that this is not the case. Older, more mature deposits of petroleum have very little asphaltene as compared to the younger ones (Fig. 12-9). This discrepancy can be explained by postulating that asphaltenes are being continuously lost from the petroleum as catagenesis proceeds, owing to precipitation on the reservoir rocks. The maltene phase, which keeps the asphaltenes in suspension, becomes progressively lighter and the asphaltenes become progressively heavier as disproportionation reactions occur. Both of these processes cause the asphaltene to become more coagulated and less soluble, causing it to precipitate out. A more accurate description of the processes involved is, thus, as follows:

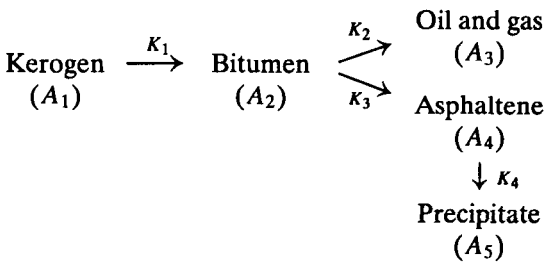

From simple kinetic considerations and assuming that each of the rate steps is first order, one obtains the following expressions for the variation of the concentrations of various species with time:

$$A_1 = A_{10} \exp[-K_1 t] \tag{12-10}$$

$$A_2 = K\{\exp[-K_1 t] - \exp[-(K_2 + K_3)t]\} \tag{12-11}$$

$$A = \frac{K}{K_4 - K_1} \exp[-K_1 t] - \frac{K \exp[-(K_2 + K_3)t]}{K_4 - K_2 - K_3} + c \exp[-K_4 t] \tag{12-12}$$

where

$$K = \frac{K_1 K_3 A_{10}}{-K_1 + K_2 + K_3}$$

$$c = \frac{K}{K_4 - K_2 - K_3} - \frac{K}{K_4 - K_1}$$

It is clear from Eq. 12-12 that if the rate of precipitation of the asphaltene is greater than the rate of kerogen conversion, then the amount of asphaltene in the bitumen will actually decrease with maturation as is usually observed. The kinetic scheme adopted here is obviously an oversimplification of the actual processes. For example, the rate of precipitation will depend not only on the concentration of the asphaltenes in the bitumen as is assumed here, but also on the structure of the asphaltene and resin and gas–oil phases, which are constantly changing with time. One would, therefore, expect K to increase with time, because the solubility of asphaltene in the bitumen decreases as catagenesis proceeds.

If the system attains a pseudo-steady state:

$dA_4/dt = K_3A_2 - K_4A_4 = 0$

and $A_4 = (K_3/K_4)\,A_2$.

This essentially means that the proportion of asphaltene in the bitumen will be governed by the ratio of rate constants. If, in accordance with the previous discussion, K_4 increases with time, then one can conclude that the fraction of asphaltene in the bitumen will decrease with maturation.

The preceding analysis, although oversimplified, serves to illustrate the importance of asphaltene precipitation in determining the composition of the bitumen. Using this analysis, one can partly resolve the apparent contradictions that are shown in Figs. 12-1 through 12-5. Thermal maturation tends to increase the aromaticity and decrease the H/C ratio of the asphaltene fraction, as seen from the simulated maturation experiments (Figs. 12-1 and 12-2). The naturally matured samples, however, follow a reverse trend. This is because the more aromatic systems are less soluble in the maltene phase and precipitate out. With increasing age, the maltene phase will peptize molecules of lower aromaticities. As a net effect, aromaticities will decrease with time, whereas the H/C ratio will increase (see Table 12-6).

A similar argument may be applied to the parameters n, σ and H_{aru}/C_{ar}. As the number of carbons in the substituents (n) increases, the solubility in hydrocarbons increases for approximately the same molecular weight species. It should, therefore, be expected that the asphaltenes left in the bitumen will have longer substituents if they are to remain in suspension [34]. This is the trend seen in the naturally matured samples. Thermal maturation, on the other hand, tends to shorten these substituents, presumably due to cracking of the long chains to yield more aromatic structures. This trend is seen in the artificially matured samples.

The degree of condensation of the aromatic sheets (H_{aru}/C_{ar}) and the degree of substitution of the aromatic sheets (σ) exhibit no clear trends in the native petroleum asphaltene samples. The artificially matured samples, however, show marked trends with both H_{aru}/C_{ar} and σ, decreasing with maturation. In the native asphaltenes, these trends are erased by the opposing influence of precipitation which tends to increase both H_{aru}/C_{ar} and σ.

The ESR data plotted on Figs. 12-6 and 12-7 show some maturation trends, too. The number of spins per gram (N_g) decreases with maturation, whereas the g tensor increases. As noted earlier [16], the g-value increases almost linearly with the heteroatom content of the petroleum asphaltene. Thus, it seems that the heteroatom content of the asphaltenes increases with maturation. The simulated maturation results seem to indicate that the heteroatom content of the asphaltenes decreases slightly with age. It is, however, quite possible that the heteroatoms being polar sites are more easily peptized than the aromatic systems and are consequently enriched as precipitation occurs. The present data seem to suggest such a process.

Unlike some of the biomarkers that are often used as thermal maturation indicators, asphaltenes are produced as an intermediate product in the maturation

TABLE 12-6

Variation of various structural parameters of bitumen asphaltene due to thermal maturation and precipitation of insoluble fractions on resevoir rocks

Structural parameter	Thermal maturation	Precipitation
f_a	↑	↓
σ	↓	↑
n	↓	↑
H_{aru}/C_{ar}	↓	↑
H/C	↓	↑
Heteroatom content	↓	↑

process. It has been found that both the composition and structure of the asphaltenes are relatively insensitive to the composition of the precursor biomass. As Rubenstein et al. [31] have pointed out, in addition to this, the asphaltene fraction in the oil remains unaltered by the later maturation processes such as biochemical degradation. These facts would suggest that asphaltenes could be excellent indicators of thermal maturation and burial history. As has been discussed in the preceding sections, however, this approach should be used with caution. Although asphaltene provides advantages as a thermal maturation indicator, owing to its stability and relative structural independence from the precursor biomass, it introduces an added complication because of being present both in the oil and in a separate solid phase.

ACKNOWLEDGEMENTS

Partial support of the work through the grant ACS-PRF No. 16319-AC5, 2 is appreciated.

REFERENCES

[1] Waples, D., *Organic Geochemistry for Exploration Geologists*. Burgess, Minneapolis, Minn. (1981).
[2] Rogers, M.A., McAlary, J.D. and Bailey, N.J.L., Significance of reservoir bitumens to thermal-maturation studies, Western Canada Basin. *Am. Assoc. Pet. Geol., Bull.*, 58: 1806–1824 (1974).
[3] Craig, H., Isotopic standards for carbon and oxygen and correction factors for mass spectrometric analysis of carbon dioxide. *Geochim. Cosmochim. Acta.*, 12: 133–149 (1957).
[4] Bray, E.E. and Evans, E.D., Hydrocarbons in non-reservoir rock source beds. *Am. Assoc. Pet. Geol., Bull.*, 49: 248–257 (1965).
[5] Casagrande, D.J. and Hodgson, G.W., Generation of homologous porphyrins under simulated geochemical conditions. *Geochim. Cosmochim. Acta*, 38: 1745–1758 (1974).
[6] Tissot, B., Califet-Debyser, Y., Deroo, G. and Oudin, J.L., Origin and evolution of hydrocarbons in early Toarcian shales. *Am. Assoc. Pet. Geol., Bull.*, 55: 2177–2193 (1971).
[7] Alexander, R., Kagi, R.I. and Woodhouse, G.W., A new method for measuring maturity of petroleum in source rocks. *J. Aust. Pet. Explor. Assoc.*, 19: 90–93 (1979).
[8] Welte, D.H. and Waples, D.W., Even *n*-alkane predominance in sedimentary rock extracts. *Naturwissenschaften*, 60: 516–517 (1973).

[9] Dembicki, H., Meinschein, W.G. and Hattin, D.E., Possible ecological and environmental significance of the predominance of even-carbon number $C_{20}C_{30}$ *n*-alkanes. *Geochim. Cosmochim. Acta*, 40: 203–208 (1976).

[10] Yen, T.F. and Erdman, J.G., Investigation of the structure of petroleum asphaltenes and related substances by infrared analysis. *Am. Chem. Soc., Div. Pet. Chem., Prepr.*, 7(3): 5–18 (1962).

[11] Yen, T.F. and Erdman, J.G., Investigation of the structure of petroleum asphaltenes and related substances by proton NMR. *Am. Chem. Soc., Div. Pet. Chem., Prepr.*, 7(3): 99–111 (1962).

[12] Yen, T.F., Erdman, J.G. and Hanson, W.E., Reinvestigation of densimetric methods of rings analysis. *J. Chem. Eng. Data*, 6: 443–448 (1961).

[13] Yen, T.F., Erdman, J.G. and Pollack, S.S., Investigation of the structure of petroleum asphaltenes by X-ray diffraction. *Anal. Chem.*, 33: 1587–1594 (1961).

[14] Yen, T.F. and Dickie, J.P., The compactness of aromatic systems in petroleum asphaltics. *J. Inst. Pet.*, 54: 50–53 (1968).

[15] Yen, T.F., Erdman, J.G. and Saraceno, A.J., Investigation of structure of petroleum asphaltenes and related substances by electron spin resonance. *Anal. Chem.*, 34: 694–700 (1962).

[16] Yen, T.F. and Sprang, S.R., Contribution of E.S.R. analysis toward diagenic mechanisms in bituminous deposits. *Geochim. Cosmochim. Acta*, 41, 1007–1018 (1977).

[17] Vaughan, G.B., Tynan, E.C. and Yen, T.F., Vanadium complexes and porphyrins in asphaltenes, II. The nature of highly aromatic substituted porphyrins and their vanadyl chelates. *Chem. Geol.*, 6: 203–219 (1970).

[18] Wright, J.R. and Minesinger, R.R., Electrophoretic mobility of asphaltenes in nitromethane. *J. Colloid. Interface Sci.*, 18: 223–230 (1963).

[19] Lian, J.J., Lin, J.R. and Yen, T.F., Peptization studies of asphaltene in asphalt systems and correlation by solubility parameter spectra. In: M.K. Sharma (Editor), *Particle Technology and Surface Phenomena in Minerals and Petroleum*. Plenum Press, New York, N.Y., pp. 39–48 (1991).

[20] Yen, T.F., Structure of petroleum asphaltene and its significance. *Energy Sources*, 1: 447–463 (1974).

[21] Yen, T.F., Structural differences between asphaltenes isolated from petroleum and from coal liquid. *Adv. Chem. Ser.*, 195: 39–51 (1981).

[22] Yen, T.F., Wu, W.H. and Chilingar, G.V., A study of the structure of petroleum asphaltenes and related substances by proton nuclear magnetic resonance. *Energy Sources*, 7(3): 273–302 (1983).

[23] Yen, T.F., Asphaltic materials. In: J.I.Kroschwitiz (Editor), *Encyclopedia of Polymer Science and Engineering, Supplementary Volume*. John Wiley and Sons, New York, N.Y., 2nd ed., pp. 1–10 (1989).

[24] Wales, M. and Van der Waarden, M., Molecular weights of asphaltenes by ultracentrifugation. *Am. Chem. Soc., Div. Pet. Chem., Prepr.*, 9(2): B21–B24 (1964).

[25] Pfeiffer, J., *The Properties of Asphaltic Bitumen*. Elsevier, New York, N.Y., 285 pp. (1950).

[26] Yen, T.F., Experimental evidence leading to various structural orders of asphaltenes. In: C. Giovarini and J.G. Speight (Editors), *Int. Symp. on the Chemistry of Bitumens, Rome, Vol. 1.* University of Wyoming Research Corp., Laramie, Wyo., pp. 382–407 (1991).

[27] Yen, T.F., Wu, W.H. and Chilingar, G.V., A study of structure of petroleum asphaltenes and related substances by infrared spectroscopy. *Energy Sources*, 7(3): 203–234 (1984).

[28] Lopatin, N.V., Temperature and geologic time as factors in coalification. *Izv. Akad. Nauk SSSR, Ser. Geol.*, 3: 95–106 (1971).

[29] Shue, F.F. and Yen, T.F., Comparison of asphaltenes from naturally occurring shale bitumen and retorted shale oils. Influence of temperature on asphaltene structure. *Am. Chem. Soc., Symp. Ser.*, 163: 129–138 (1981).

[30] Brown, J.K. and Ladner, W.R., Hydrogen distribution in coal-like material by high resolution NMR spectroscopy, II. A comparison with infrared measurement and the conversion to carbon structure. *Fuel*, 39: 87–96 (1960).

[31] Rubenstein, I., Spyckerelle, C. and Strauz, O.P., Pyrolysis of asphaltenes: A source of geochemical information. *Geochim. Cosmochim. Acta*, 43: 1–6 (1979).

[32] Moschopedis, S.E., Prakash, S. and Speight, J.G., Thermal decomposition of asphaltenes. *Fuel*, 57: 431–434 (1978).

[33] Tissot, B.P., Recent advances in petroleum geochemistry applied to hydrocarbon exploration. *Am. Assoc. Pet. Geol., Bull.*, 68: 545–563 (1984).

[34] Yen, T.F., Evidence concerning the presence of long chain alkyl substituents in native asphaltic molecules. *Nature, Phys. Sci.*, 223: 9–13 (1971).

[35] Yen, T.F., Chemical aspects of metals in native petroleum. In: T.F. Yen (Editor), *The Role of Trace Metals in Petroleum*. Ann Arbor Science Publishers, Ann Arbor, Mich., pp. 1–30 (1975).

[36] Yen, T.F., Tynan, E.C. and Vaughan, G.B., Electron spin resonance studies of petroleum asphaltics. In: R.A. Friedel (Editor), *Spectrometry of Fuels*. Plenum Press, New York, N.Y., pp. 187–201 (1970).

This page intentionally left blank

Asphaltenes and Asphalts, 1. Developments in Petroleum Science, 40
edited by T.F. Yen and G.V. Chilingarian

Chapter 13

MATHEMATICAL MODELS OF INFLUENCE OF ASPHALT AND RESIN CONTENTS ON PHYSICAL PROPERTIES OF OILS FROM THE APSHERON OIL- AND GAS-BEARING REGION

R.D. DJEVANSHIR, L.A. BURYAKOVSKY and G.V. CHILINGAR

INTRODUCTION

Oil is a complex system consisting of materials of different classes with a considerable predominance of different hydrocarbon groups. Data on hydrocarbon group composition of oils, as a whole and in various fractions, are of great importance for understanding the process of the transformation of petroleum and constructing a genetic classification of oils. Knowledge of group composition is necessary to evaluate oil as an industrial raw material, because such evaluation is defined strongly by the content of some components in oil fractions.

As it is known, oil is not only a complex, but also a regular system, some elements of which are closely related with each other.

Establishment of regularities in changes of oil properties, depending on different natural factors and oil composition, assists one in clarifying the processes of formation of oil deposits, predicting their properties, and in technological calculations used in developing oil deposits. A detailed study of properties of oils is also necessary to evaluate petroleum as an industrial product.

MODELS OF HYDROCARBON GROUP COMPOSITION AND MAIN PROPERTIES OF OILS

The most clear representation of hydrocarbon group composition of oils, which consist of paraffins, naphthenes, and aromatics, may be obtained on a mixture triangle or Gibbs triangle [1,2]. Based on the data of over 100 samples of oils from deposits in the Apsheron Archipelago, a group composition of light oil products (gasoline and ligroin *) is shown in Fig. 13-1a. An analogous graph is built according to the experimental data [3] from the study of oils from 14 deposits of the Apsheron Peninsula, divided into fractions by boiling from 65° to 350°C (Fig. 13-1b).

As shown in Fig. 13-1b, there is a continuous sequence of fractions boiling at increasingly higher temperatures, which differ both in a hydrocarbon group composition and physical properties. Table 13-1 gives generalized data on 56 suites from 14 deposits in the Apsheron Peninsula. With increasing boiling temperature, density and molecular weight of residual increase regularly. It should be noted

* Petroleum distillate.

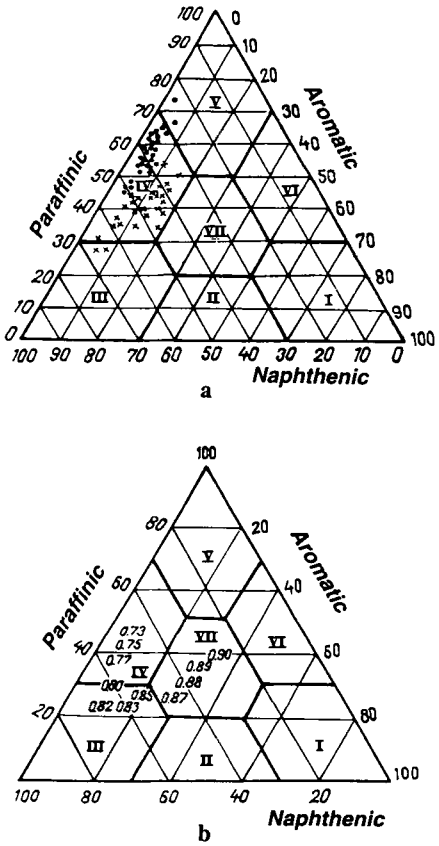

Fig. 13-1. (a) Group composition of light oil products from Neftyanyé Kamni (Oil Rocks) deposit. o = gasolines, + = ligroins. (b) Average hydrocarbon group composition of oils from Apsheron Peninsula. Distillate density is 0.88 g/cm^3.

that these relationships are not linear (Fig. 13-2), which results in a non-linear relationship between density and molecular weight of a residual.

As shown in Fig. 13-1b, with increasing temperature transition occurs from paraffinic–naphthenic fractions to naphthenic–paraffinic ones, and then to paraffinic–naphthenic–aromatic fractions, with a regular increase of density from 0.73 to 0.90 g/cm^3.

Due to division of oil into fractions, the entropy changes which is a measure of heterogeneity of the oil composition [4]. The relative entropy of oil as a heterogeneous system of light-boiling fractions (from 65° to 150°C) is 0.6–0.7, which increases up to 0.8 with appearance of fractions with boiling ranges of 150° to 225°C. For high-boiling fractions (225° to 350°C) relative entropy reaches the limiting value of 1 (Fig. 13-3).

Entropy evaluation used as a measure of complexity of an oil composition has a certain advantage over the usual nomenclature classification of oils, because it

TABLE 13-1

Properties of oils in the Apsheron Peninsula

Boiling ranges of fractions (°C)	Fractions boiling over (wt% of oil)	Density (g/cm^3)	Molecular weight	Hydrocarbon group composition (%)		
				aromatic	naphthenic	paraffinic
Averages from 14 deposits						
to 65	0.5	–	89	–	–	–
65– 95	1.5	0.725	97	4.9	43.5	51.6
95–122	2.4	0.749	108	5.6	50.7	43.7
122–150	3.4	0.773	122	7.7	55.8	36.5
150–175	3.8	0.796	135	11.6	60.0	28.4
175–200	4.2	0.816	150	15.1	64.5	20.4
200–225	5.1	0.835	166	18.6	61.1	20.3
225–250	5.8	0.852	185	23.8	54.8	21.4
250–275	5.9	0.867	203	30.0	50.6	19.4
275–300	6.4	0.880	225	29.9	40.9	29.2
300–325	6.0	0.892	247	30.1	35.4	34.5
325–350	5.8	0.902	272	34.1	31.7	34.2
Averages from 56 suites						
to 65	0.4	0.687	88	–	–	–
65– 95	1.5	0.726	96	4.0	48.5	47.5
95–122	2.6	0.749	108	5.1	53.3	41.6
122–150	3.7	0.773	121	7.5	57.1	35.4
150–175	4.1	0.796	135	10.8	59.2	30.0
175–200	4.4	0.816	150	15.6	61.1	23.3
200–225	5.3	0.834	166	18.2	59.2	22.6
225–250	6.2	0.850	184	22.8	51.6	25.6
250–275	6.1	0.866	204	28.6	49.3	22.1
275–300	6.3	0.876	225	28.5	40.4	31.1
300–325	6.0	0.888	247	28.3	33.8	37.9
325–350	5.8	0.900	272	31.8	31.1	37.1

allows a numerical evaluation of the degree of oil heterogeneity. Expressed as relative entropy, this evaluation is in the range of 0 to 1, with 0 characterizing the vertices of the triangle of the mixtures and 1 characterizing the center of the triangle.

Inasmuch as the technique of entropy calculation and use of an isentropic triangle of a mixture are not discussed here, readers interested in this subject may refer to the work of Buryakovskiy [4], where the same method of study was used in the investigation of rocks as a heterogeneous system.

One more widely used model of a group oil composition seems to be of interest. It represents a dependence of content of various groups of hydrocarbons on boiling temperature of a fraction. According to the experimental data of Ashumov [3], Fig. 13-4 shows this model for oils of the Apsheron Peninsula. The results obtained by Dobryanskiy [1] and Kartsev [5] for "world" oils are given for a comparison. Analogous studies were carried out for offshore deposits of the Apsheron Archipelago

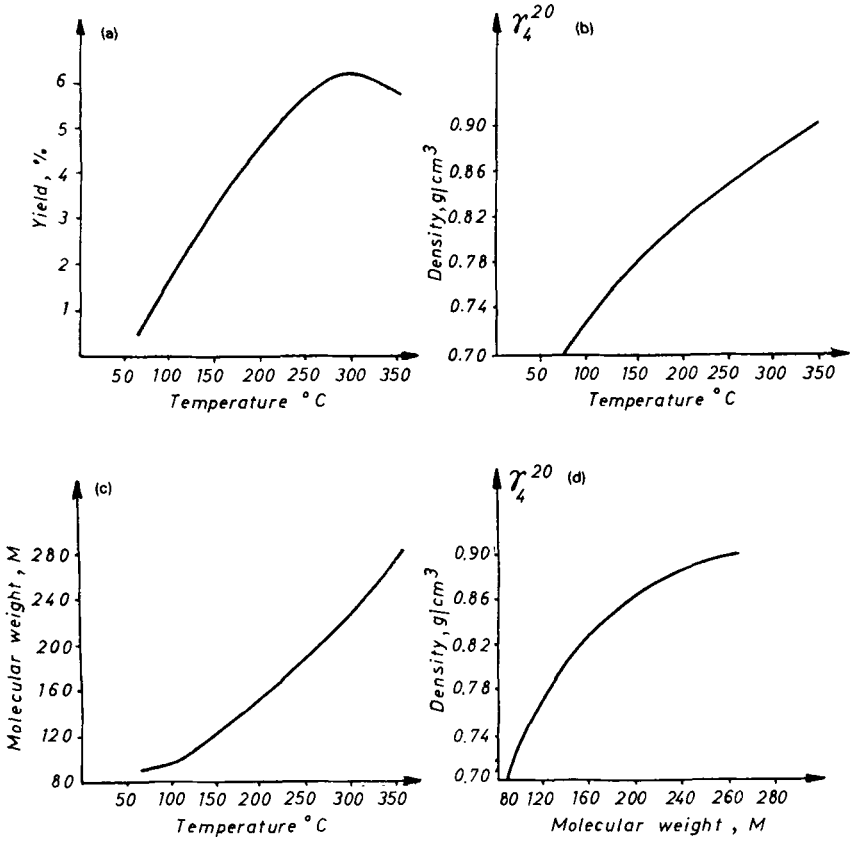

Fig. 13-2. Dependence of (a) yield, (b) density (γ), and (c) molecular weight (M) on temperature. (d) Relation between density and molecular weight of oil residuals.

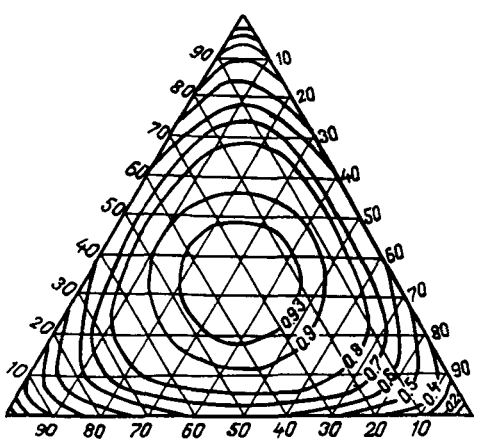

Fig. 13-3. Isentropic triangle of a mixture.

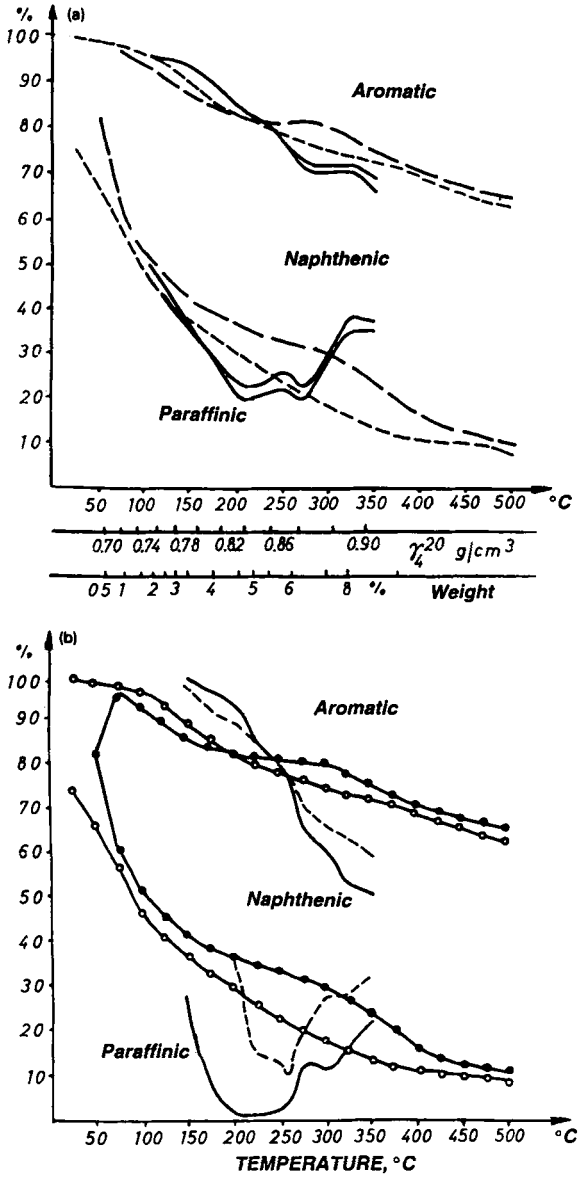

Fig. 13-4. Models of hydrocarbon group composition of oils from: (a) Apsheron Peninsula (continuous lines) as compared with "world" oils (dashed lines); (b) Neftyanyé Kamni (Oil Rocks) deposit (dashed lines) and Mud Volcano (continuous lines) deposits as compared with "world" oils.

(Fig. 13-4b). With increasing boiling temperature, content of aromatic hydrocarbons in fractions increases, as a rule, and content of paraffins decreases.

Physical properties of oils of the Apsheron Peninsula and adjacent areas of the Caspian Sea are based on the data of numerous analyses. Figure 13-5 gives the data

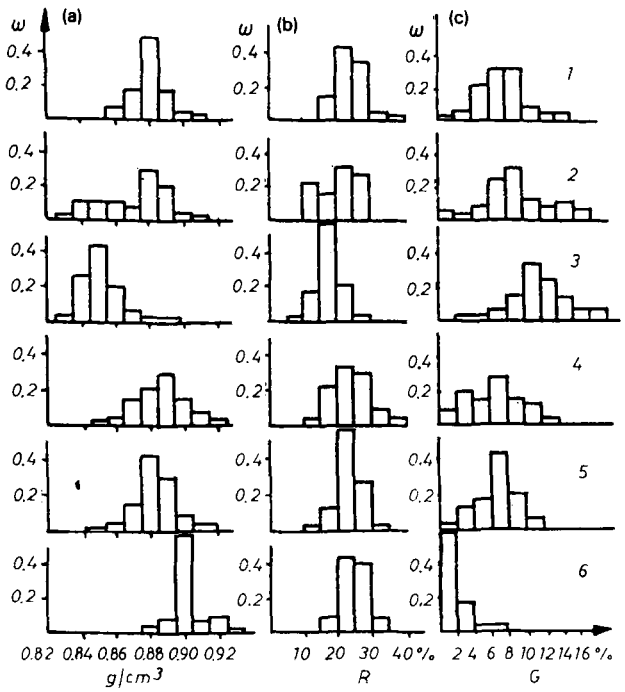

Fig. 13-5. Histograms of distributions of (a) oil density, (b) content of resins (R), and (c) content of gasoline (G) in oils from Neftyanyé deposit in suites Balakhany (*1*), "Pereryv" (*2*), NKP (*3*), KS (*4*), PK (*5*), and KaS (*6*).

on oil density and content of asphalt–resin materials, gasoline, and ligroin from the deposit of Neftyanyé Kamni (Oil Rocks) in the Apsheron Archipelago [6] as histograms.

On the whole, over the northwestern part of the archipelago (Darwin Bank, Artyom Island, and Gyurgyany Sea), average values of parameters of oil properties with evaluation of their variation within 2σ limits (95% confidence), based on 1642 analyses, can be written as follows:

$\gamma = 0.9137 \pm 0.0240$ g/cm^3; $\gamma = 0.9137 \pm 0.0006$ g/cm^3;
$R = 37.2 \pm 15.1\%$; $R = 37.2 \pm 0.37\%$;
$G = 1.54 \pm 1.20\%$; $G = 1.54 \pm 0.03\%$;
$L = 7.4 \pm 1.3\%$; $L = 7.4 \pm 0.03\%$;

where γ is density, R is content of asphalt–resin materials, G is content of gasoline, and L is content of ligroin.

Over the southeastern part of the archipelago [Zhiloy Island, Gryazevaya Sopka (Mud Volcano), and Neftyanyé Kamni (Oil Rocks)], based on 820 analyses, these properties can be written as:

$\gamma = 0.8800 \pm 0.0380$ g/cm^3;	$\gamma = 0.8800 \pm 0.0013$ g/cm^3;
$R = 22.7 \pm 11.8\%$;	$R = 22.7 \pm 0.41\%$;
$G = 7.4 \pm 7.5\%$;	$G = 7.4 \pm 0.26\%$;
$L = 9.6 \pm 8.0\%$;	$L = 9.6 \pm 0.28\%$;

Inasmuch as the oils from the northwest part of the archipelago contain more asphalt–resin materials and less light-boiling fractions, their density is higher than that of the oils from the southeast part of the archipelago.

Using both numerical characteristics, histograms, or frequency polygons (related frequencies), one can solve different geologic and geochemical problems. For example, Fig. 13-5 shows the distribution of oil densities and contents of asphalt–resin materials and gasoline in different suites of the Oil Rocks deposit. With depth of burial, density of oils and resin content increase, whereas gasoline content decreases. Nevertheless, these regularities disappear in the upper part of the productive strata. The increase of density in the upper part of the productive strata is caused by the oxidation of oils with surfactants, that results in the increase of the role of asphalt–resin components and decrease in the gasoline content.

RELATIONSHIP BETWEEN COMPOSITION AND PROPERTIES OF OILS

One can observe correlation between oil properties and its composition, relationship between the components, regularities among the contents of microelements in oils, and other interrelationships. They can all be studied by correlation and regressive analyses. The correlation analysis establishes the presence, strength, and sign of connection between the correlated values, whereas the regression analysis enables one to establish a connection, i.e., to construct an individual or general model of the studied object or phenomenon. For example, correlation matrices for oils from offshore deposits of the Apsheron Archipelago were obtained by the correlation analysis. Several variants of correlation matrices with a different number of oil analyses and, therefore, with a different reliable value of the correlation coefficient were calculated. Table 13-2 gives a generalized matrix of correlation coefficients over the deposits of the Apsheron Archipelago. Instead of numerical values of correlation coefficients, the authors give only signs of these coefficients in Table 13-2, where all the values are reliable.

Due to different interrelations, determination of some parameters of the given oil may be sufficient to get an idea about the values of other parameters. The simplest and, at the same time, one of the main properties of oil is its density, which is closely dependent on a fractional composition and content of asphalt–resin materials in oil. Studying interrelationships among the major oil parameters is of great interest from the point of view of petroleum geochemistry, and equations from these interrelationships obtained by the method of regression analysis can serve as mathematical models of the oils studied. Oils from some deposits of the Apsheron oil- and gas-bearing region and adjacent offshore areas of the Caspian Sea were used as an object for the most thorough and detailed investigation. These oils are

TABLE 13-2

Matrix of pair correlations of parameters of properties of oils from deposits of the Apsheron Archipelago

	Properties				Microelements											
	coking ability	acidity	viscosity	content of resins and asphaltenes	V	Fe	Ni	Cr	Ti	Co	Pb	Mo	V/Ni	Be	Sr	Sn
Properties																
Density	+	+	+	+	+		+			+						
Coking ability		+	+	+	+		+			+		+	+			
Acidity			+	+	+							+	+			
Viscosity				+						+			+			
Content of resins and asphaltenes					+		+			+			+			
Microelements																
V						+	+	+		+		+				−
Fe							+						+			
Ni											−	+			+	
Cr																
Ti																+
Co														+		

referred to as high-quality oils of a naphthenic–paraffinic type. Their densities range from 0.81 to 0.93 g/cm^3 and depend on the relative amounts of various components, mainly heavy (resins and asphaltenes) and light (gasoline and ligroin).

The influence of the main components of oil on density can be studied by correlation of four variables: γ, R, G, and L, where γ is oil density in g/cm^3, R is content of resins and asphaltenes in %, G is content of gasoline in % (100°C — 40%), L is content of ligroin in % (150° — 12%). A correlation table (Table 13-3) based on 820 analyses is given as an example. The empirical equation of correlation between density and content of resins and asphaltenes in oils is as follows (in a form of regression R on γ):

$$\gamma = 0.826 + 0.00237\,R \tag{13-1}$$

or in a form of regression γ on R:

$$R = 212(\gamma - 0.778) \tag{13-2}$$

The coefficient of correlation is 0.710.

Inasmuch as the existence of two different regression equations (Eqs. 13-1 and 13-2) is not always convenient, it is desirable to have a single correlation equation. Thus, an equation of orthogonal regression was suggested [7].

In order to calculate the orthogonal regression it is necessary to give a probability of enclosing the empirical data into the ellipse of correlation, i.e., $Q(\chi)$, according to which one can calculate the ellipse parameter by the formula:

$$\chi = \sqrt{-2\ln[1 - Q(\chi)]} \tag{13-3}$$

Thus, when $Q(\chi) = 0.98$, the parameter of the correlation ellipse is $\chi = 2.8$. The higher the probability $Q(\chi)$, the greater the parameter χ is.

Having available data on the values of χ, $\bar{R}$, γ, σ_R, σ_γ, $r_{R\gamma}$ one can estimate parameters of the orthogonal regression equation which represents the main axis of the correlation ellipse, where coordinates of the ends in a normalized scale are calculated by the following formulae:

$$A_R = \chi\sqrt{(1 + r_{R\gamma})/2}\cdot\sigma_R\,; \quad A_\gamma = \chi\sqrt{(1 + r_{R\gamma})/2}\cdot\sigma_\gamma \tag{13-4}$$

where σ = standard of deviation and r = correlation coefficient. Hence, for $Q(\chi) = 0.98$ and $\chi = 2.8$, calculation using Eq. 13-4 gives:

$$A_R = 15.22 \quad \text{and} \quad A_\gamma = 0.0516$$

In a natural scale, corresponding coordinates can be written as follows:

$R_{1,2} = R \pm A_R$, i.e., $R_1 = 22.75 + 15.22 = 37.97\%$, $R_2 = 22.75 - 15.22 = 7.53\%$;

$\gamma_{1,2} = \gamma \pm A_\gamma$, i.e., $\gamma_1 = 0.9316$ g/cm^3, $\gamma_2 = 0.8284$ g/cm^3.

The equation of the main axis of the correlation ellipse at the given basic probability $Q(\chi)$, i.e., equation of orthogonal regression, may be obtained as an equation of a straight line passing through two points with coordinates (R_1, γ_1) and

TABLE 13-3

Dependence of oil density on content of asphaltenes and resins

Density, $\Delta\gamma$ (g/cm^3)	$\overline{\gamma}_i$ (g/cm^3)	Content of resins and asphaltenes (%)										M_γ
		ΔR:	5–10	10–15	15–20	20–25	25–30	30–35	35–40	40–45	45–50	50–55	
		$\overline{R}_i$:	7.5	12.5	17.5	22.5	27.5	32.5	37.5	42.5	47.5	52.5	
0.815–0.825	0.82		2										2
0.825–0.835	0.83		3	3	3								9
0.835–0.845	0.84		1	10	20	4							35
0.845–0.855	0.85		3	20	35	8							66
0.855–0.865	0.86			16	24	11	2						53
0.865–0.875	0.87			4	32	47	11						94
0.875–0.885	0.88			3	32	130	56	3	3				227
0.885–0.895	0.89			3	13	95	63	3					177
0.895–0.905	0.90				2	39	43	6	2				92
0.905–0.915	0.91				1	7	10	8	7	2	1		36
0.915–0.925	0.92						4	8	4	1	1		18
0.925–0.935	0.93						1	3	1		2	1	8
0.935–0.945	0.94						1	1	1				3
		M_R	9	59	162	341	191	32	18	3	4	1	820

(R_2, γ_2): (37.98, 0.9316) and (7.53, 0.8284). The equation of this straight line is:

$$R = 295(\gamma - 0.805) \quad \text{or} \quad \gamma = 0.0034\,R + 0.805 \tag{13-5}$$

Both of the above equations are equal. Conjugated equations of regressions (13-1) and (13-2) are conjugated diameters of the correlation ellipse.

According to Eq. 13-5, oils with density of 0.805 g/cm^3 do not contain resins and asphaltenes. It should be noted that the value 0.805 g/cm^3 corresponds approximately to the density of ligroin obtained by refining oils from deposits of the Apsheron oil- and gas-bearing region. At the content of resins and asphaltenes from 57 to 87%, the density reaches 1.0–1.1 g/cm^3, i.e., oil is transformed into asphalt.

Besides coefficients of correlation, the eccentricity of the ellipse of correlation, e, may be used as a measure of degree of correlation:

$$e = c/a \tag{13-6}$$

where c is half of the distance between the focuses and a is half of the length of the main axis of the ellipse.

To calculate the distance between the focuses, one should estimate the coordinates of the ellipse focuses according to the following formulae (in a normalized scale):

$$f_R = \chi\sqrt{r}\cdot\sigma_R\,; \quad f_\gamma\chi\sqrt{r}\cdot\sigma_\gamma \tag{13-7}$$

which under the corresponding substitutions gives: $f_R = 13.8$ and $f_\gamma = 0.0468$. In a normal scale $C_R = f_R$ and $C_\gamma = f_\gamma$, where: f = coordinates of ellipse focuses according to the normalized coordinate axes R or γ; C = coordinates of ellipse focuses in a normal scale. Therefore,

$$e = 13.8/15.22 = 0.905$$

The ellipse eccentricity does not depend on the major probability $Q(\chi)$. The value of this probability defines only the number of points entering the ellipse of correlation. One can count a number of points beyond the limits of the correlation ellipse according to the formula $N_{\text{beyond}} = N[1 - Q(\chi)]$. In the given case, $N_{\text{beyond}} = 16$ with $N = 820$.

Conjugated and orthogonal regression lines, the equations of which are given above, are plotted in Fig. 13-6a. Besides, lines of equal values of frequencies of the pairs γ and R are drawn in accordance with the correlation table (see Table 13-3). As shown, the shape and tightness of isolines extending along the average line may also show a sufficiently close correlation between density of oil and content of resins and asphaltenes. Coefficients of variation equal to $\upsilon_R = 26.0\%$ and $\upsilon_\gamma = 2.2\%$ show that content of resins and asphaltenes varies more as compared with density, stability of which is determined by the stability of the main composition of oil.

The oil density is also affected considerably by the content of its low-boiling components. With increasing content of gasoline and ligroin, density of oils decreases. On the basis of 792 analyses of oils given in the generalized correlation table, the

authors have calculated equations of regression to correlate oil density with gasoline content (G):

$$\gamma = 0.9063 - 0.00380\,G \tag{13-8}$$

$$G = 143.7 - 155\,\gamma \tag{13-9}$$

The equation of orthogonal regression (the main axis of the correlation ellipse) is:

$$\gamma = 0.915 - 0.00500\,G \quad \text{or} \quad G = 200(0.915 - \gamma) \tag{13-10}$$

The correlation coefficient of 0.760 shows a sufficiently close reverse linear relation between γ and G. With γ = 0.915 g/cm^3, oils do not contain gasoline fraction any more. The coefficient of variation for distribution of gasoline content is 51.4% and for density, as before, it is 2.2%. The variation in gasoline content is very large and does not specify the same variation in density.

Isofrequency lines form concentrically spaced ovals along the main axis, which is a geometric place for the points of the main axis of the ellipse of normal correlation (Fig. 13-6b). The eccentricity of the ellipse is 0.94.

Results of the calculation of all coefficients of paired correlation are given in Table 13-4. Having the available data on all paired relations, one can get an equation of multivariate relation of all the three main parameters between oil composition and density.

The equation of multivariate regression has a form of a linear function:

$$\gamma = \gamma_0 + aR + bG + cL \tag{13-11}$$

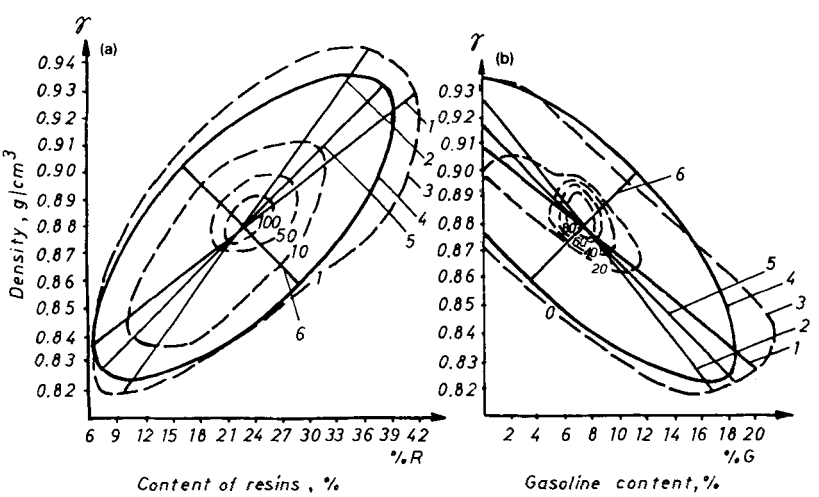

Fig. 13-6. Orthogonal and conjugated regression lines for relation between the oil density and content of (a) resins and (b) gasoline from Oil Rocks deposit. *1* = regression γ on R or G; *2* = regression R on G or γ; *3* = isofrequency curves; *4* = ellipse of correlation; *5* = main axis of the ellipse (orthogonal regression); and *6* = auxiliary axis of the ellipse.

TABLE 13-4

Correlation coefficients of paired and multivariate connections

Dependence between	Correlation coefficient
γ and R	+0.71
γ and G	−0.76
γ and L	−0.47
G and R	−0.60
L and R	−0.12
L and G	+0.64
γ and R, G, L	0.83

where a, b, and c are numerical coefficients defined according to the factual data and γ_0 is the density of oil when $R = G = L = 0$.

The equation of the sought correlation with numerical coefficients can be written as follows:

$$\gamma = 0.864 + 0.0021\,R - 0.0023\,G - 0.0014\,L \qquad (13\text{-}12)$$

Table 13-4 gives also a coefficient of multivariate correlation, which is higher than any paired coefficient of correlation. It shows that the equation of multivariate correlation (Eq. 13-1), considering the influence of all properties, describes empirical relations more reliably than paired equations of regression. In deriving the latter regressions, a part of parameters is fixed at an average level.

To speed up the calculations, a nomogram (Fig. 13-7) was constructed using Eq. 13-12. Figure 13-7 shows how to use it. For example, at given values of $R = 23\%$, $G = 7.2\%$, and $L = 7.0\%$, γ is equal to 0.882 g/cm^3.

Inasmuch as the dependence of density on variation in ligroin content in oil is characterized by small tightness (closeness), a member from the Eq. 13-12 of multivariate relation, which corresponds to the influence of ligroin on density, may be eliminated and replaced by a constant value. In this case, this equation can be

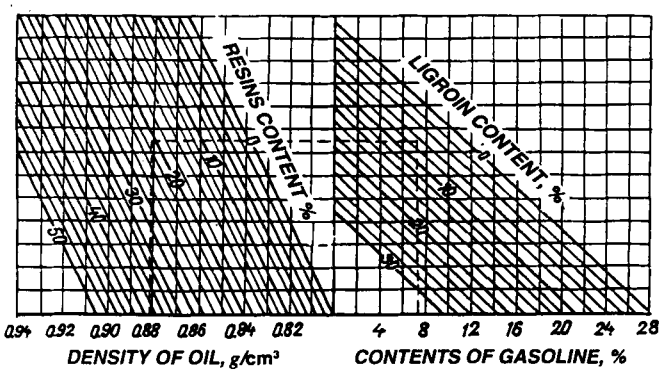

Fig. 13-7. Nomogram relating density of oils and contents of resins, gasoline, and ligroin.

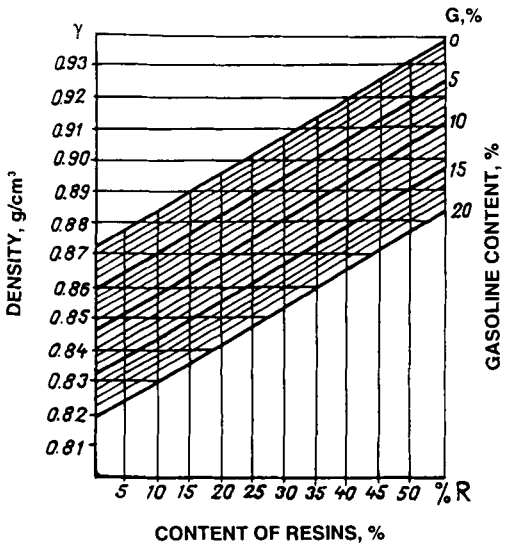

Fig. 13-8. Dependence of oil density on contents of resins and gasoline.

written as follows:

$$\gamma = 0.8707 + 0.0013\,R - 0.0027\,G \tag{13-13}$$

The coefficient of multivariate correlation is 0.830. Graphically this relation is given in Fig. 13-8. As it is seen, the dependence of oil density on the contents of resins, asphaltenes, and gasoline (excluding ligroin influence) only is expressed graphically more vividly and can be used for calculations as well.

It is known [1,2,6,8,9] that content of paraffins in oils increases parallel to the decrease in density. High-paraffin oils contain many light fractions boiling up to 150°C and few asphalt–resin materials. Correspondingly, content of paraffins in oils, which are close in consistency to asphalts, is practically equal to zero.

Experimental data on the content of resins and paraffins for the oils of the

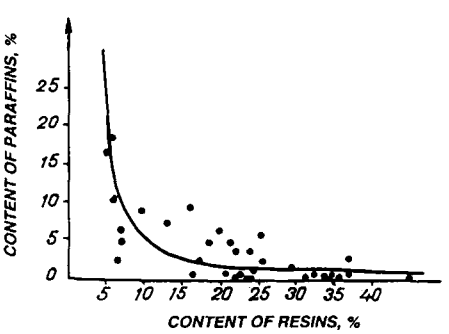

Fig. 13-9. Relationship between the contents of resins and paraffins.

TABLE 13-5

Correlation between contents of paraffins and asphalt-resin materials in oils (according to data from Gadzhi-Kasumov [9] and data from the authors)

Deposit	Suite, horizon	Content (%)	
		resins	paraffins
Binagady	NKP	35.0	0.20
Balakhany–Sabunchi–Ramany	PK	32.0	0.15
Surakhany	Sabunchinskaya	6.5	2.48
–	PK	25.6	2.07
–	KaS	24.0	3.71
Karachukhur	Balakhany	7.0	6.0
–	NKG	7.0	4.95
–	PK	18.6	4.95
–	KaS	21.4	4.95
Peschanyy-Moré (sea)	VIII	5.8	18.6
–	IX	5.2	16.5
Kala	KaS	36.8	2.92
Gousany	KaS	19.8	6.33
Lokbatan	NKP	22.5	3.7
Karadag	VII	16.0	9.3
–	VIII	13.0	7.5
Sangachaly Sea–Duvanny-Moré (sea)	VII	25.3	5.8
Darwin Bank	PK	45.0	0.03
Artyom Island	PK	34.0	0.13
Zhiloy Island	KaS	36.0	0.12
Mud Volcano	KaS	37.0	0.66
Oil Rocks (Neftyanyé Kamni)	Sabunchinskaya	29.3	1.72
–	Balakhany	24.6	1.08
–	"Pereryv"	21.6	0.79
–	NKP	17.7	2.50
–	KC-1	28.2	0.41
–	KC-2	22.6	0.69
–	PK-1	22.4	0.58
–	PK-2	23.8	0.56
–	PK-3	23.6	0.89
–	KaS-1	24.7	0.64
–	KaS-2	16.5	0.49
–	KaS-3	24.7	0.38

Apsheron oil- and gas-bearing region and adjacent offshore areas of the Caspian Sea is presented in Table 13-5. The data given in Table 13-5 and Fig. 13-9 confirm the above-mentioned discussion about the interrelation between the content of paraffins (P) and resins (R) in oils. An empirical equation of this relation can be written as follows:

$$P = 30/(R - 4) \tag{13-14}$$

Consequently, one can obtain relationship between contents of paraffins and low-boiling fractions in oils.

MATHEMATICAL MODEL OF OIL VISCOSITY

Now let us consider an interrelationship between viscosity and density of oils changing simultaneously under the influence of temperature. Oils from the same deposits of Azerbaijan discussed above have been investigated. Depths of burial of productive reservoirs change within large limits from 500 to 3500 m. Reservoir temperatures at these depths range from 30° to 90°C. Due to the influence of different factors, density of oils varies within the limits of 0.83 and 0.93 g/cm^3. Such an important parameter as viscosity or internal friction is dependent on oil density and temperature.

Relationship between the dynamic viscosity or coefficient of internal friction, η, and kinematic viscosity, ν, is as follows:

$$\nu = \eta/\gamma \tag{13-15}$$

where γ is the density of a liquid (oil in this case).

Table 13-6 shows dependence of oil viscosity on density at five different temperatures: 10, 20, 30, 40, and 50°C. 580 analyses were made for developing an empirical correlation equation.

Variational curves of kinematic viscosity constructed for the five temperatures show a clear dependence of viscosity on temperature (Fig. 13-10). A logarithmic scale was used for viscosity transforming asymmetric empirical distributions into symmetric ones, close to the normal distributions. It shows that viscosity and temperature are related by logarithmic or degree laws.

A graph of dependence of oil viscosity on density and temperature is constructed for approximation of the empirical relation (Fig. 13-11).

TABLE 13-6

Dependence of kinematic viscosity (centistokes) on oil density and temperature

Average density (g/cm^3)	Temperature (°C)				
	10	20	30	40	50
0.82	5.6	4.2	2.8	2.8	1.4
0.83	5.6	5.6	4.5	3.9	2.5
0.84	11.2	9.9	5.6	5.4	4.3
0.85	14.0	12.9	7.9	5.8	5.2
0.86	20.5	13.7	9.4	6.5	5.6
0.87	22.4	20.3	12.4	10.5	7.6
0.88	39.2	23.2	18.3	11.7	10.3
0.89	53.0	32.6	21.9	14.4	11.0
0.90	86.4	50.3	30.9	22.7	15.1
0.91	118.5	94.5	50.5	30.2	24.1
0.92	–	133.5	89.2	53.7	33.6
0.93	–	356.0	178.0	111.0	55.8
0.94	–		178.0	178.0	89.2

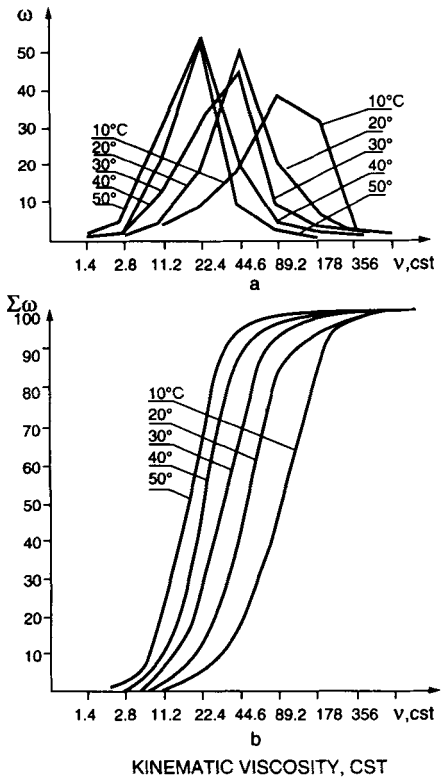

Fig. 13-10. Curves of distribution of oil viscosity at five different temperatures: (a) differential, (b) cumulative. cst = centistokes; ω = frequency; $\Sigma\omega$ = cumulative frequency.

The analysis of the graphical dependence of kinematic viscosity on density and temperature shows that it is described best by an exponential function:

$$\nu = \nu_0 e^{-bT} \tag{13-16}$$

where e is the base for natural logarithms, T is the oil temperature in °C, ν_0 is the oil viscosity at $T = 0$°C, depending only on viscosity according to the exponential law:

$$\nu_0 = a e^{c\gamma} \tag{13-17}$$

where γ is the oil density in g/cm^3; a and c are numerical coefficients determined from the factual experimental data, a being the oil viscosity when $T = 0$ and $\gamma = 0$; b is the numerical coefficient depending on oil density by the following equation:

$$b = m\gamma - n \tag{13-18}$$

where m and n are numerical coefficients calculated using the experimental data.

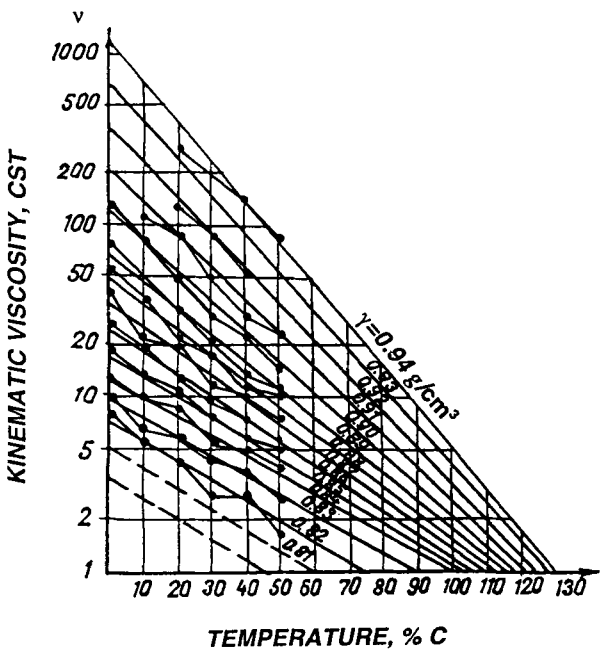

Fig. 13-11. Dependence of kinematic viscosity on oil density and temperature.

Substituting Eqs. 13-17 and 13-18 into Eqs. 13-16 one obtains:

$$\gamma = a\, e^{c\gamma - m\gamma T + nT} \tag{13-19}$$

or, after taking logarithms, the equation in a form more convenient for practical calculations is obtained:

$$\lg \nu = a_o + a_1\gamma - a_2\gamma T + a_3 T \tag{13-20}$$

Coefficients a_i of the last equation are calculated from the correlation data of Tables and Figs. 13-10 and 13-11.

Substituting numerical values of coefficients a_i into Eq. 13-20, one obtains:

$$\lg \nu = 16.6\,\gamma - 0.100\,\gamma T + 0.072\,T - 12.8 \tag{13-21}$$

In SI units, the equation becomes:

$$\lg \nu = 0.0166\,\gamma - 0.0001\,\gamma T + 0.072\,T - 12.8 \tag{13-22}$$

where γ is expressed in kg/m^3, T is in °C, and ν is in m^2/s.

Dynamic viscosity can be obtained from the following equation:

$$\eta = a\gamma\, e^{c\gamma - m\gamma T + nT} \tag{13-23}$$

Substituting Eq. 13-5 into Eq. 13-13, oil viscosity can be related to the content of asphalts–resins as follows:

$$\nu = a' e^{c'R - mRT + n'T} \tag{13-24}$$

where a', c', m' and n' are empirical coefficients. Or in a form analogous to the Eq. 13-21, one obtains the following equation:

$$\lg \nu = 0.6 + 0.0565\, R - 0.0034\, RT - 0.083\, T \tag{13-25}$$

RESULTS AND CONCLUSIONS

Empirical equations of interrelationships among compositions and properties of oils, and conditions of their burial (i.e., temperature) were developed based on the experimental data. These equations are not only of practical, but also of theoretical interest [1,6,8]. As far as we know, analytical expressions such as Eqs. 21 or 25 have not been obtained up to now. Equations 13-21 and 13-25 give theoretical correlations between the parameters studied and may be used in calculations where temperature, density, and contents of asphalt–resin materials and low-boiling fractions are variables.

From the practical point of view, extrapolation of graphical or analytical dependencies in the areas beyond the limits of the factual experimental material is of great interest. Thus, extrapolation of graphs in Fig. 13-11 based on Eq. 13-21 to temperatures above 50°C enables one to predict viscosity of oils of different density up to 100–120°C, i.e., to depths of 5500–6000 m. Such depths correspond to deposits located in more bathypelagic parts of the Apsheron–Pribalkhany threshold. These deposits are most likely to be gas-condensate due to the low viscosity of the fluid at reservoir temperatures. For additional information, consult references [10], [11], and [12].

Extrapolation to the near-surface conditions with an average annual temperature of +14.5°C, confirms the fact that under such conditions, due to hypergene factors, oil is transformed into a non-flowing mass like asphalt with a density of 1.0–1.1 g/cm^3. Similar deposits of bituminous sands are known to occur at outcrops of oil reservoirs in different parts of the world.

REFERENCES

[1] Dobryanskiy, A.F., *Geochemistry of Petroleum*. Gostoptekhizdat, Moscow (1948).
[2] Mansoori, G.A., Jiang, T.S. and Kawanaka, S., Asphaltene deposition and its role in petroleum production and processing. *Arab. J. Sci. Eng.*, 13(1): 17–34 (1988).
[3] Ashumov, G.G., Azerbaijan oils. *Izd. Akad. Nauk Azerb. SSR* (1961).
[4] Buryakovskiy, L.A., Entropy as a measure of heterogeneity of rocks. *Sov. Geol.*, 3: 135–138 (1968).
[5] Kartsev, A.A., The geochemistry of petroleum. *Neft. Khoz.*, 9: 20–22 (1950).
[6] Bagir-zade, F.M., Buryakovskiy, L.A. and Babaev, F.R., *Geochemistry of Petroleum and Natural Gases of the Apsheronsk–Pribalkhany Threshold*. Nedra, Moscow (1974).
[7] Buryakovskiy, L.A., Listengarten, B.M. and Bairamalibeily, N.I., Correlation of conjugated parameters of physico-geological properties of oil and gas deposits. *Izv. Akad. Nauk Azerb. SSR, Ser. Nauk Zémlé*, (5): 80–88 (1974).

[8] Leontaritis, K.J. and Mansoori, G.A., Asphaltene deposition: a survey of field experience and research approaches. *J. Pet. Sci. Eng.*, 1(1): 229–239 (1988).
[9] Gadzhi-Kasumov, A.S., *Reasons for Variety of Properties of Oils in the Apsheron Region.* Azerneshr, Baku (1971).
[10] Buryakovskiy, L.A., Distribution patterns of oil and gas deposits within Apsheron Archipelago. *Int. Geol. Rev.*, 16(7): 749–758 (1974).
[11] Buryakovskiy, L.A. and Babaev, F.R., About laws of distribution of parameters of physical and chemical oil properties. *Azerb. Khim. Zh.*, (4): 98–103 (1976).
[12] Samedov, F.I. and Buryakovskiy, L.A., Characteristics of oils of the productive strata in the southeastern part of Apsheron Archipelago. *Azerb. Neft. Khoz.*, (8): 6–10 (1958).

Asphaltenes and Asphalts, 1. Developments in Petroleum Science, 40
edited by T.F. Yen and G.V. Chilingarian

Chapter 14

ROLE OF ASPHALTENES IN PETROLEUM CRACKING AND REFINING

RENJUN ZOU and LUJIA LIU

INTRODUCTION

It is widely known that asphaltenes, which are concentrated in heavy crude oils, are the most troublesome fractions for efficient processing. Owing to the increasing demand for fuel and light distillates, however, the need for processing the heavier fractions containing higher contents of asphaltenes increases. Consequently, many attempts have been made to upgrade the technology for refining heavy oils containing asphaltenes and to understand the changes in asphaltenes during processing.

CHARACTERISTICS OF HEAVY OILS, STRUCTURE OF ASPHALTENES, AND THE PROCESSING DIFFICULTIES CAUSED BY ASPHALTENES

Petroleum heavy oils include atmospheric residues (AR) and vacuum residues (VR) by distillation, topped crude oils, coal oil extracts, crude oils extracted from tar sands, etc. They have a high specific gravity, a low hydrogen-to-carbon ratio, and a high carbon residue. In addition, they contain large amounts of asphaltenes, sulfur and nitrogen, and heavy metals such as vanadium and nickel. Table 14-1 shows the general properties of Khafjji vacuum residue produced in the Middle East, Athabasca bitumen produced in Canada, and, finally, Boscan crude oil from Venezuela, an ultraheavy oil having a specific gravity of more than one, a hydrogen-to-carbon ratio not exceeding 1.5, a sulfur content of about 5 wt%, and an asphaltene content of 8–10 wt%. The characteristic difference of the above heavy oils lies in the content of heavy metals, such as vanadium.

Asphaltenes are huge polyaromatic compounds, with molecular weight ranging from 1000 to about 20,000 and generally possess a boiling point above 1000°F. A well-known macrostructural model of petroleum asphaltenes, as presented by Dickie and Yen [1], has been confirmed by many researchers. It is understood that the unit structure of asphaltenes is a polyaromatic ring sheet, each consisting of a polyaromatic nucleus and oxygen-, nitrogen-, and sulfur-containing heterocyclic compounds, with a molecular weight of about 1000. The polyaromatic ring sheets and resin collapse about each other, associate with alkyl side chains on the edges of aromatic compounds, and compose a particle which has a diameter of about 20 Å and a molecular weight of about 6000. More than two of the particles link with organometallic porphyrin compounds. The latter is termed a micelle, which has a molecular weight of up to ten thousands.

TABLE 14-1

Properties of some heavy oils (after Nakamura et al. [2])

	Khafji VR	Athabasca bitumen	Boscan crude
Yield of crude (vol%)	30.5	100	100
Specific gravity, d^{15}	1.023	1.003	1.004
Viscosity at 100°C (cP)	1162	125	216
Asphaltenes (heptane-insolubles, wt%)	11.4	7.7	11.9
Ash content (wt%)	0.04	0.45	0.21
Elements (dry and ash free, wt%)			
C	84.18	83.26	82.43
H	10.28	10.43	10.52
S	4.96	4.61	5.22
N	0.40	0.44	0.69
Metals (ppm)			
V	130	150	1190
Ni	41	78	112

The differences in the chemical structures of the asphaltenes produced from different sources exist in the size of each structural unit and the number of units in each molecule.

Asphaltenes pose many difficulties in heavy oil processing such as hydrocracking and hydrorefining (hydrodesulfurization and hydrodemetallization). Asphaltenes are readily adsorbed onto the surface of catalysts. The heavy metals, such as vanadium and nickel, which are primarily associated with asphaltenes, are also deposited on the catalyst particles, thus blocking the catalyst pores and preventing other molecules from coming into contact with the active sites. Furthermore, at high temperatures, asphaltenes polymerize and cause plugging of the catalyst bed and the downstream lines and equipments. Consequently, how these asphaltenes are treated will influence the processing technology of heavy oils.

THERMAL DECOMPOSITION OF ASPHALTENES

Considerable portions of asphaltenes could be converted to hydrocarbon-soluble materials only by thermal treatment. For example, about 30% of the original Khafjji asphaltenes had been converted into heptane-soluble materials at the temperature of 400°C [3] and 50% of the original Athabasca asphaltenes into pentane-soluble materials upon thermal treatment at 390°C, with a hydrogen-donating solvent such as tetralin [4].

Asphaltenes begin to dissociate slightly at moderate temperatures of 190–200°C. The gases (CH_4, C_2H_6, CO, and CO_2) are released upon the facile decomposition of the carboxylic function and thermally labile alkyl moieties on the periphery of the asphaltene molecules. More severe decomposition of the asphaltene structure, however, does not occur until reaching elevated temperatures (>350°C) [5]. Table

TABLE 14-2

Gas distribution from Athabasca asphaltene pyrolysis (after Moschopedis [5])

	Temperature (°C)							
	200	250	300	350	400	450	500	600
Fraction of asphaltenes appearing as gases (wt%)	1.7	2.5	4.3	8.5	18.5	40.4	49.5	54.3
Volume of gases per 100 g asphaltenes (cm^3)	750	1450	2750	5000	6000	8000	10,000	12,000
Gas analysis (mol/100 g) of asphaltenes								
H_2	0	0	0	3.0	12.5	36.5	41.5	67.5
CO_2	16.0	20.0	21.5	24.0	26.0	28.0	34.5	37.5
CO	0	7.5	14.5	17.5	18.5	24.0	24.0	27.3
H_2S	0	0	5.0	9.5	24.5	36.5	48.0	56.2
CH_4	8.9	21.5	48.9	133.0	142.0	180.5	230.0	260.3
C_2H_6	8.5	15.5	33.0	34.5	36.0	38.5	55.0	61.6
$C_3H_8 + C_4H_{10}$	0	0	0	1.5	7.5	11.5	17.0	22.5
$C_2H_4 + C_3H_6$	0	0	0	0.5	1.0	1.5	2.0	2.7

14-2 shows that the distributions of gas products from Athabasca asphaltene pyrolysis are markedly different at temperatures above 350°C. The presence of H_2S and much higher amounts of the hydrocarbon gases indicate the breaking of C–S bonds and the elimination of alkyl side chains. Table 14-3 is the analytical data on gaseous

TABLE 14-3

Analytical data on gaseous products from Khafji asphaltene pyrolysis (after Nakajima et al. [3])

Run No.	1	2	3	4	5	6
Reaction temperature (°C)	350	400	400	450	500	500
Reaction time (min)	60	60	60	60	60	60
Initial pressure (kg/cm^2)	1	1	10	1	1	10
Maximum pressure during coking reaction (kg/cm^2)	9	23	42	43	69	88
Final pressure after cooling to room temperature (kg/cm^2)	4	10	19	17	29	38
Total gas volume (l)	0.35	1.27	1.30	2.88	5.02	4.89
Gas analysis (%)						
CH_4	21.0	36.0	49.7	50.8	51.5	64.3
C_2H_6	10.8	17.1	19.7	17.8	21.8	21.3
C_2H_4	0.2	0.3	–	0.2	–	–
C_3H_8	5.3	7.7	8.2	6.5	8.3	7.5
C_3H_6	0.1	0.2	0.1	0.1	0.1	0.1
nC_4H_{10}	0.3	0.3	0.3	0.2	0.3	0.2
iC_4H_{10}	0.1	0.1	0.1	0.1	0.1	0.1
Others	62.2	38.3	21.9	24.3	17.9	6.5

products of Khafjji asphaltene pyrolysis, which exhibit similar results to those for the Athabasca asphaltenes.

Composition, infrared spectra, and X-ray diffraction analysis of the Khafjji asphaltene pyrolysis residue are shown in Figs. 14-1 to 14-3. With increasing reaction temperature, the total residue decreases with increasing volume of gaseous products. The coke and the asphaltene contents considerably increase or decrease, respectively, up to 400°C and remain relatively constant at temperatures above 400°C. The maltene content has a maximum value at temperatures near 400°C. A large quantity of asphaltenes is obtained at 350°C with a composition similar to that of the original asphaltenes; however, at temperatures above 400°C, only a very small amount of brown to black powder is obtained. These results suggest that the side chains of the original asphaltenes almost split off at a temperature near 400°C and then pass into coke, and that most of the gases produced at temperatures above 400°C result from the decomposition of maltenes. The maltenes are mainly composed of normal paraffins from C_5 to C_8. Ignasiak and Strausz [4] reported the presence of paraffins of up to C_{34} from Athabasca asphaltenes. This provides

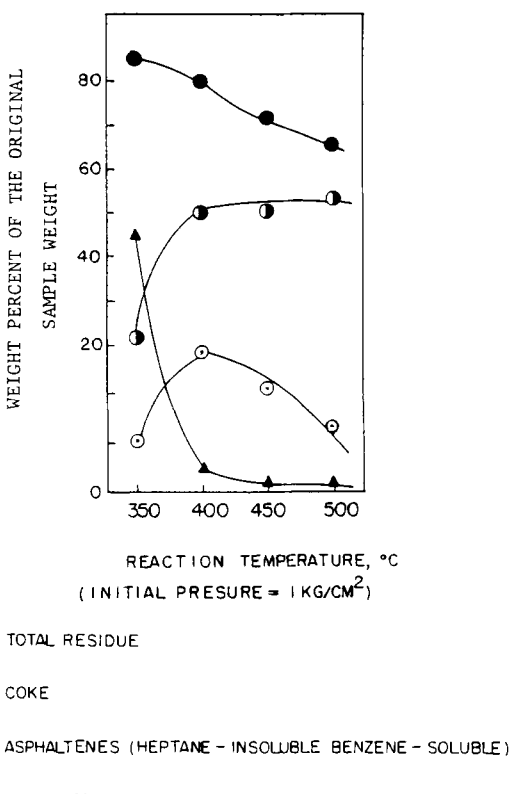

Fig. 14-1. Composition of Khafjji asphaltene pyrolysis residue.

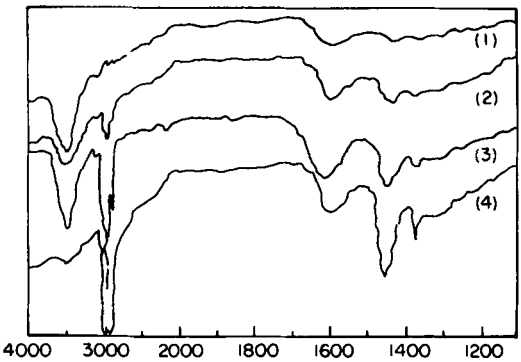

(1) COKE (450°C) (3) ASPHALTENES (400°C)

(2) COKE (400°C) (4) ORIGINAL ASPHALTENES

Fig. 14-2. Infrared spectra of residual fraction — coke and asphaltenes.

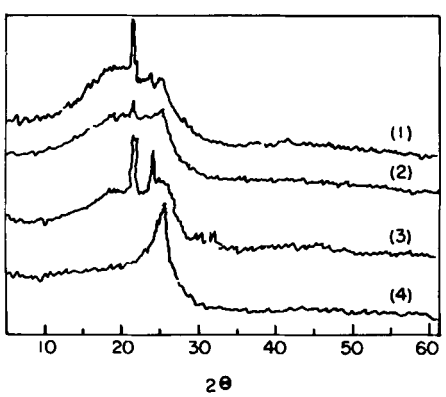

(1) ORIGINAL ASPHALTENES (3) COKE (350°C)

(2) ASPHALTENES (350°C) (4) COKE (400°C)

Fig. 14-3. X-ray diffraction patterns of coke and asphaltenes.

evidence that asphaltene molecules contain a variety of side chains varying in length from very short to surprisingly long.

Infrared spectra on the residue further proved that the alkyl side chains, which have absorption bands at near 2850–3000 cm^{-1}, 1460 cm^{-1}, and 1380 cm^{-1}, on the condensed aromatic ring sheets, are almost completely eliminated at 400°C. An absorption band centered at approximately 1600 cm^{-1} is assigned to aromatic carbon double bonding. Compared with the original asphaltenes, the 1600 cm^{-1} absorption band of asphaltene fraction from the pyrolysis residue is greater. This means that the aromatic content of such asphaltenes is increased by the cleavage

of side chains and dehydrogenation of the naphthenic portion in the unit sheets. In contrast to the case of asphaltenes, the height of 1600 cm^{-1} absorption band of coke decreases and disappears at 500°C. This suggests that the scission of most of the side chains results (1) in the delocalization of aromatic carbon double bonding and (2) in the formation of more stable aromatic ring resonance structure.

The X-ray diffraction patterns give similar results. The peak, observed at 2θ = 21.3° (d = 4.17 Å) and called the γ-band, associated with the spacing in the saturated portion of bitumen molecules. The peak over the range 2θ = 26.1° to 24.7° (d = 3.4 to 3.6 Å) is called (002)-spacing and represents the spacing between the layers of condensed aromatic ring sheets. Figure 14-3 shows that the γ-band in the X-ray diffraction pattern of coke obtained above 400°C disappears. Apparently, the side chains combining on the edges of the condensed aromatic sheets are entirely split (002). The sharp (002) spacing of coke obtained above 400°C suggests that the layer of the aromatic ring sheets approaches more closely and arranges more regularly by the cleavage of the side chains from the condensed aromatic sheets. Very little has appeared in published literature on the kinetics of asphaltene pyrolysis.

Magaril and Aksenova [6] proposed that the asphaltene thermal decomposition is a chain reaction of 1.5 order, i.e., $k = 4.4 \times 10^{-3} \exp(-35460/RT)$ ($mol^{-1/2}$ $cm^{1.5}$ s^{-1}). The asphaltenes used in the study were characterized by MW of 1000, carbon/hydrogen atom ratio of 1.01 and d^{20} of 1.20.

Asphaltene decomposition kinetics were also evaluated isothermally at 375°C, 400°C, and 450°C by Schucker [7]. The asphaltenes used were obtained from the Arab heavy vacuum residuum. A simple first-order kinetic model was fit to the weight loss versus time data by non-linear regression to obtain the thermal rate constant at each temperature (Fig. 14-4).

Further treatment of the rate data, using the Arrhenius equation, showed that the activation energy varies from about 17,500 cal/mol at lower temperatures, at which only 32% of the asphaltenes are cracked to volatiles, to 55,000 cal/mol at higher temperatures, at which almost 48% of the asphaltenes are converted to

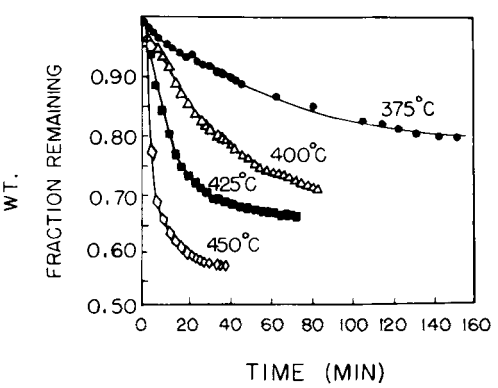

Fig. 14-4. Weight loss of asphaltenes during isothermal treatment.

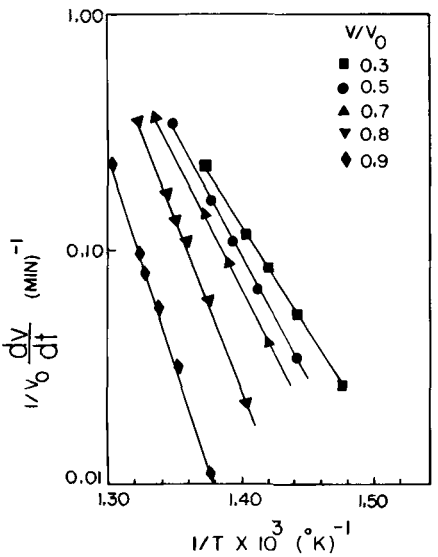

Fig. 14-5. Arrhenius plot for non-isothermal asphaltene decomposition. v = reaction velocity at time t, v_0 = initial reaction velocity.

volatiles. Thus, it seems that a distribution of activation energies for the asphaltene fraction results from isothermal kinetic analysis. Conducting the pyrolysis in a non-isothermal manner by increasing reaction temperature from 25° to 525°C at a fixed linear heating rate (β in °C/min), a narrow range of activation energies (42,000–55,000 cal/mol), was observed when β varied from 2 to 10°C/min. Simultaneous evaluation of data generated at different heating rates enabled Schucker [7] to propose a simple linear expression:

$$\ln \frac{1}{v_0}\frac{dv}{dT} = \ln k_0 + \ln\left(1 - \frac{v}{v_0}\right) - \frac{E}{RT}$$

An activation energy, therefore, is generated for every value of v/v_0 at which the derivatives are determined. The data and the fit of the model to five values of v/v_0 is shown in Fig. 14-5. Visually, it would appear that the slope would change as the reaction proceeds (i.e., v/v_0 increases). A plot of the activation energies obtained at eight different values of v/v_0 shows a variation in activation energy from about 42,000 to 80,000 cal/mol (Fig. 14-6).

There are several possible explanations for the observed behavior. First, there may be a distribution of bonding strengths in the asphaltenes leading to a distribution of activation energies for the reaction network. Alternatively, in the asphaltene molecule, there are two groups of bonds which need to be broken to produce volatile material. The first one comprises moderate-strength bonds (E = 40–50 kcal/mol) that are broken at lower temperatures, whereas the second, smaller group (E = 50–70 kcal/mol) of bonds are broken at higher temperatures, resulting in only incrementally greater conversions.

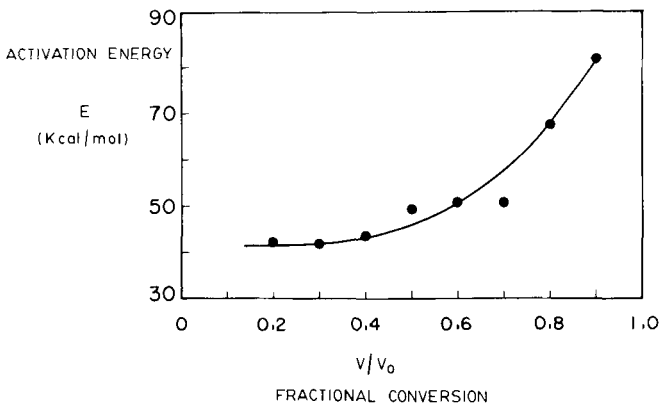

Fig. 14-6. Variation in activation energy with fractional conversion.

ASPHALTENE HYDROCONVERSION

Asphaltenes may be converted to distillate oils mainly by hydrogenation and hydrocracking, depending on the reaction conditions, and especially, the catalyst selected.

Asphaltene hydrogenation

Hydrogenation of asphaltenes from Japanese Akabira coal at 400° or 370°C under initial pressure of 9.8 to 10.4 MPa and using red-mud and sulfur catalyst was studied by Kanda et al. [8]. Liquid and solid products were extracted with benzene, after which benzene-solubles were extracted with hexane and separated into oil (soluble) and asphaltene (insoluble).

Analytical data indicate that in the remaining asphaltenes the H/C ratio and the total aromatic, naphthenic ring number per unit structure are nearly constant. The ring number per molecule and the number of average structure units per molecule (N) of the remaining asphaltenes, however, increase with conversion (Figs. 14-7 and 14-8). The number of aromatic rings per unit structure of oils decreases, but the number of naphthenic rings retains a constant value (Fig. 14-9). The change of mean molecular weight measured by VPO is shown in Fig. 14-10. In both the remaining asphaltenes and oils, the molecular weight increases with conversion. The structural parameters calculated from the results of ^{1}H NMR spectra show that the carbon aromaticity (f_a) of the oils decreases, and H_{au}/C_a and R (the degree of unsubstituted aromatic rings and the degree of aliphatic-chain substitution of the aromatic rings) increase with conversion (Fig. 14-11). These results suggest that under hydrogenation conditions, such asphaltene molecules are converted to oil mostly through the saturation of aromatic rings, decomposition of naphthenic rings, dehydroxylation, and breaking of heterorings. The smaller molecules tend to be converted more rapidly than larger

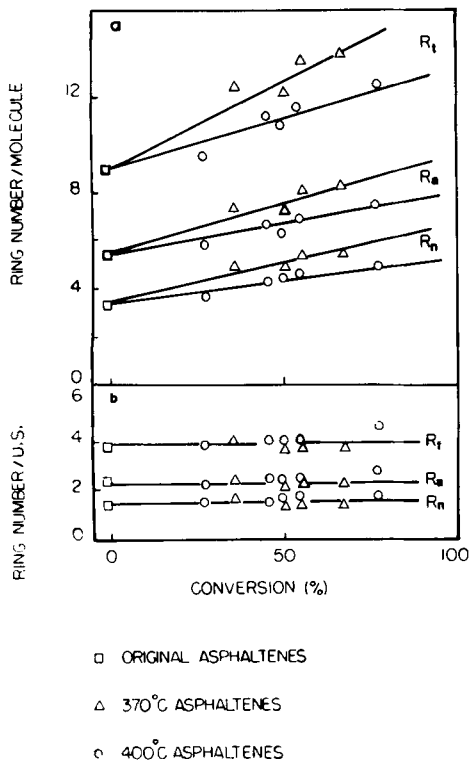

Fig. 14-7. (a) Total aromatic and naphthenic ring number per molecule of asphaltenes. (b) Total aromatic and naphthenic ring number per unit structure of asphaltenes.

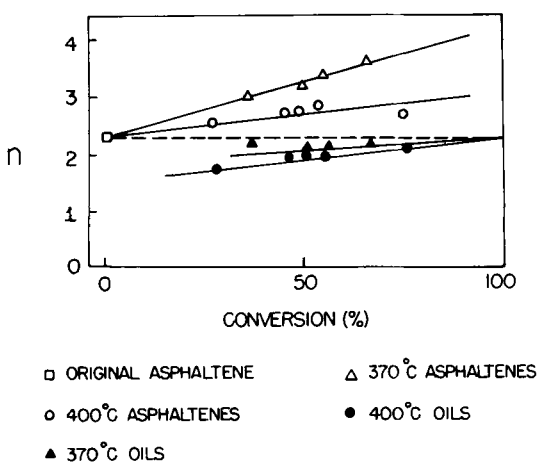

Fig. 14-8. Relationship between n-values of oils and asphaltenes and conversion (%).

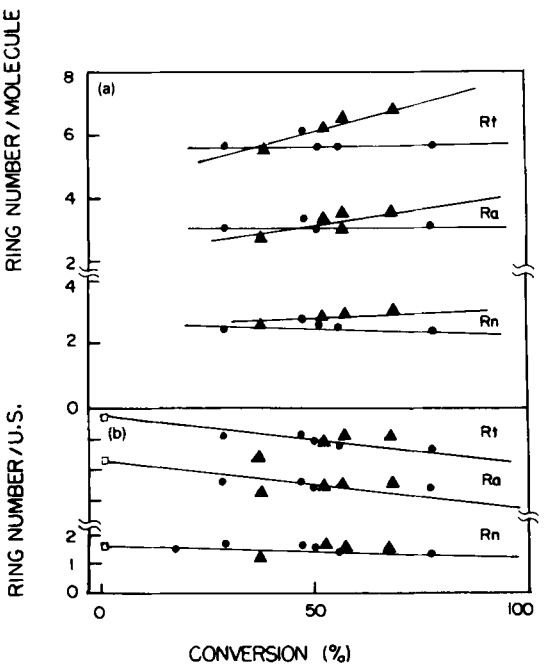

Fig. 14-9. Total, aromatic and naphthenic ring number per molecule of oils (a), and per unit structure of oils (b) vs. conversion.

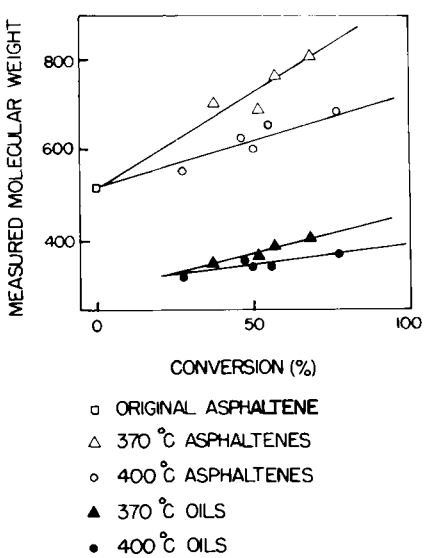

Fig. 14-10. Relationship between mean molecular weight of asphaltenes and oils (measured in $CHCl_3$ solution by VPO) and conversion (%).

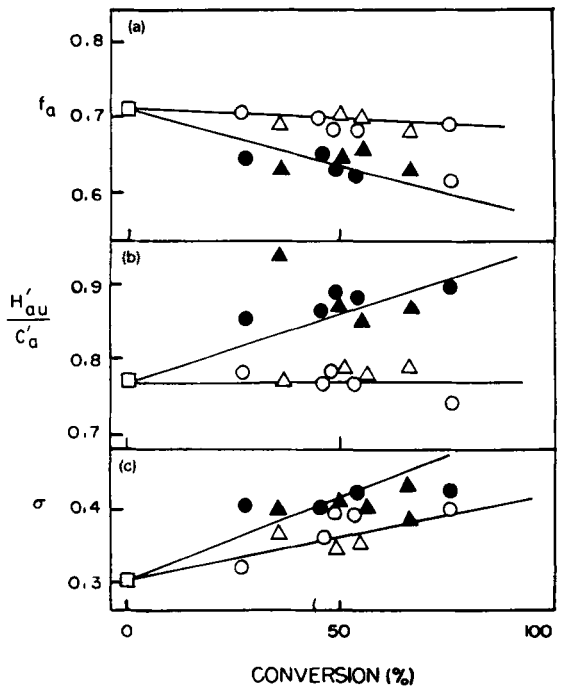

□ ORIGINAL ASPHALTENE △ 370°C ASPHALTENES

○ 400°C ASPHALTENES ▲ 370°C OILS

● 400°C OILS

Fig. 14-11. Structural parameters of asphaltenes and oils.

molecules, which convert at the later stage when they become sufficiently hydrogenated. The reaction takes place more severely at higher reaction temperatures.

Asphaltene hydrocracking

Studies on asphaltene hydrocracking of Khafjji vacuum residue, Athabasca bitumen, and Boscan crude indicate that during hydrocracking the hydrogenation and dealkylation of condensed polyaromatic rings are almost entirely suppressed. The main reactions are the destruction of asphaltene micelles caused by the removal of vanadium and the depolymerization of asphaltene molecules by removal of heteroatoms such as sulfur [9–13]. The latter is a partial rupture of weakly linked bonds between the polyaromatic rings. Contribution of these two reactions to the

asphaltene hydrocracking depends on the kind of feedstocks. For example, the destruction of asphaltene micelles is considered to be particularly pronounced in the asphaltenes having a high vanadium content, such as those in Boscan crude, whereas depolymerization is the principal cause of the changes in the asphaltenes produced from Athabasca bitumen, which has a low vanadium content. Reaction rates of larger asphaltene molecules are more rapid than those of smaller molecules. The number of unit sheets decreases without change in the structure of unit sheets.

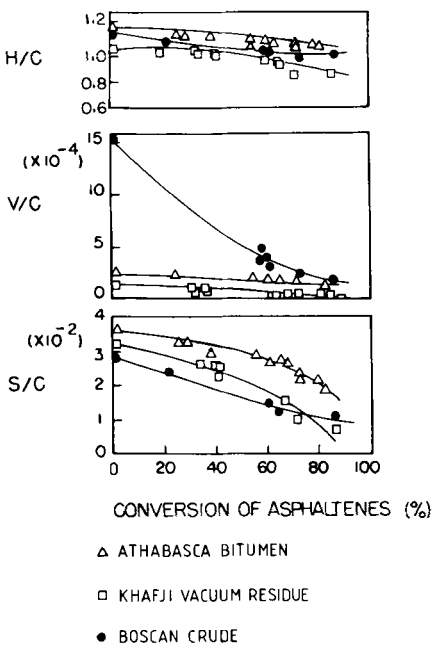

Fig. 14-12. H/C, V/C and S/C atoms ratios of asphaltenes.

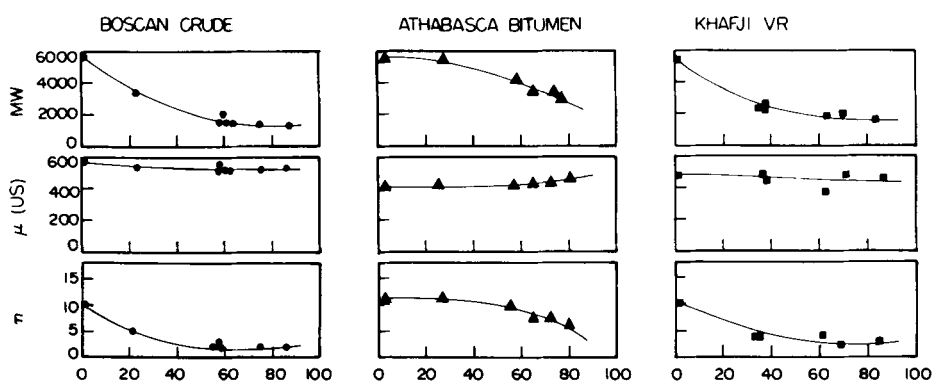

Fig. 14-13. Molecular weight, unit weight, and unit number per molecule of asphaltenes (by ^{1}H NMR).

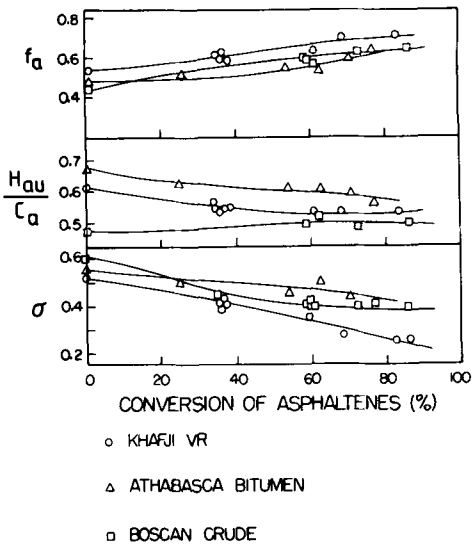

Fig. 14-14. Structural parameters of asphaltenes obtained from ^1H NMR spectra.

The analytical data which lead to the above conclusions are plotted in Figs. 14-12 to 14-14. Based on this data, a model of asphaltene cracking has been proposed (Fig. 14-15). It is established on the assumption that both the depolymerization and the destruction of micelles take place simultaneously during the decomposition of asphaltenes in ordinary heavy crude oils.

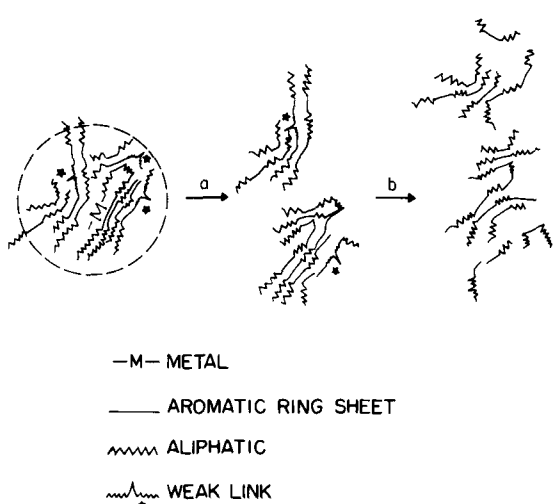

Fig. 14-15. Model of asphaltene cracking.

HYDRODESULFURIZATION OF HEAVY OILS: EFFECT OF ASPHALTENE CONTENT

The products of desulfurization of heavy petroleum fractions include diesel fuel, heating oils and residual fuel oils. Inasmuch as combustion of sulfur-containing fuel is the primary cause of SO_2 pollution of the atmosphere, the incentive is now strong for the production of fuels low in sulfur.

The amount of asphaltene content in the heavy feed oil has a large effect on the hydrodesulfurization reaction rate. In the case of atmospheric residues from various crude oils, the rate of desulfurization reaction is mostly dependent on the amount of asphaltene contained in the feed oil [25] (Fig. 14-16). The relation between the reaction rate constant (k_s) and the asphaltene content of the feed oil (C_{AO}) could be expressed approximately by the following equation:

$$\log k_s = -A_1 C_{AO} + B_1$$

where A_1 and B_1 are constants which depend on the catalyst and reaction conditions (Fig. 14-17). In the case of residues of various boiling ranges from the same crude oils, the above equation was inapplicable. Instead, the relation between the reaction rate constant (k_s) and the yield (Y) of residues (vol.% of crude) was expressed roughly by the following equation:

$$\log k_s = A_2 \log Y + B_2$$

where A_2 and B_2 are constants which depend on the kind of crude oil, reaction conditions, and catalyst used (Fig. 14-18).

When the amount of sulfur removed is less than 50% of the total, scarcely any asphaltenic sulfur is removed. In the range of 50–80% desulfurization, a decrease in the asphaltenic structure is not appreciable. When total sulfur removal exceeds 80%, the removal of asphaltenic sulfur is accompanied by the destruction of asphaltenic

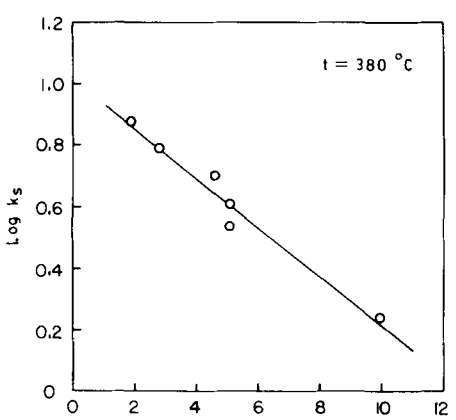

Fig. 14-16. Relation between reaction rate constant (k_s) and asphaltene content of feed oils.

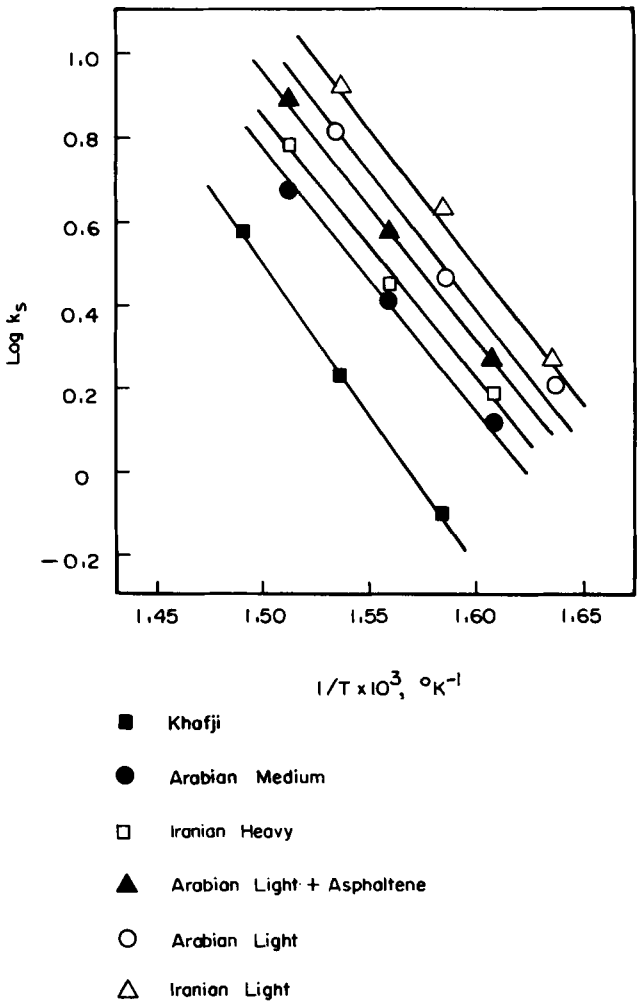

Fig. 14-17. Effect of the atmospheric residue from the various crude oils on reaction rate constant.

structure [14] (Figs. 14-19 and 14-20). Consequently, in order to produce fuel low in sulfur, the amount of asphaltenes necessary for conversion to lower-boiling fractions during heavy oil desulfurization must be as large as possible.

The reason the asphaltene content affects the reaction rate is not very clear. Considering the fact that the ratio of the asphaltenic sulfur content to the total sulfur content is not large (the average ratio is about 1 : 10), in addition to the existence of the difficult-to-remove sulfur compounds in the asphaltenes, the inhibiting effects of the asphaltenes and part of the resins could be the other causes, as previously mentioned.

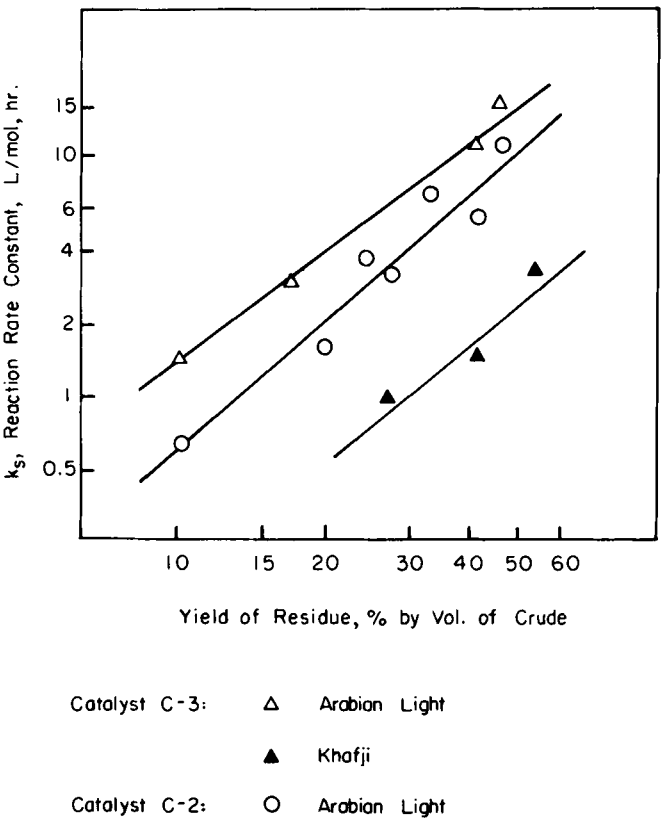

Fig. 14-18. Relation between reaction rate constant and yield of crude oils residue.

ASPHALTENE CONVERSION TO LOWER-BOILING PRODUCTS: IMPROVED PROCESSES FOR ASPHALTENE-CONTAINING HEAVY OILS

The residuum hydrodesulfurization process can be achieved by the direct, indirect, and intermediate methods. In order to produce fuel oil low in sulfur and to convert as large a quantity as possible of asphaltenes concentrated in the petroleum residue to lower-boiling point and more valuable products, the direct method is perhaps of greatest industrial interest at present time.

The catalysts used in the direct method are exposed to the more severe conditions. Deposition of coke and metal sulfides causes loss of catalyst activity by chemical modification of the surface and by physical blocking of the catalyst pores and fixed-bed interstices. Accumulation of the metal-containing deposits prevents regeneration of catalysts. This is why most of the efforts for process improvement are concentrated in searching for an active and stable catalyst.

The catalysts currently applied are formed from oxides of Co, Mo and other transition metals on an alumina or alumina-silica support. They are partially or

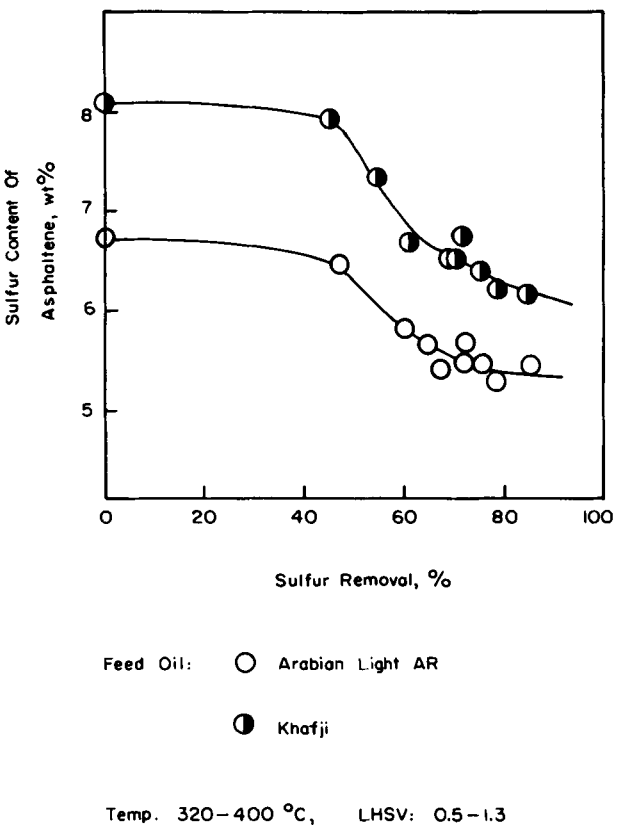

Fig. 14-19. Relation between sulfur content of asphaltenes and total sulfur removal.

completely sulfurized in operation. Molybdenum or tungsten appears to be the necessary constituent of a hydrodesulfurization catalyst, whereas neither cobalt nor nickel, if present alone, shows any significant activity. Inasmuch as combinations of Co (or Ni) and Mo (or W) are more active than Mo or W alone, Co and Ni are generally described as promoters. Data from the commercial units suggest that the activity of Mo–Ni is higher than Mo–Co, and that of Mo–Co is higher than Mo alone. The stability has a reverse order.

A representative fixed-bed process flow diagram is shown in Fig. 14-21. To avoid feed contamination with sodium chloride and corrosion products that will rapidly form deposits near the reactor entrance, a mesh basket containing loosely packed solids, which provide high interstitial capacity for deposited material, is placed after the feeding pump. A separate guard chamber operated as a swing reactor upstream of the main reactor, which served the same purpose. The guard-bed catalyst should have high demetallization activity and large interstitial volume so that it can accept a maximum amount of metal-containing deposits.

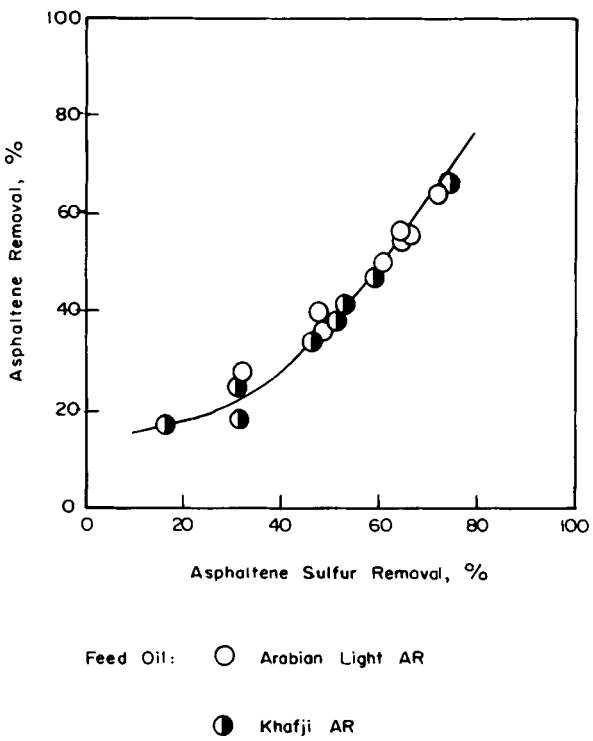

Fig. 14-20. Relation between total asphaltene removal and asphaltenic sulfur removal.

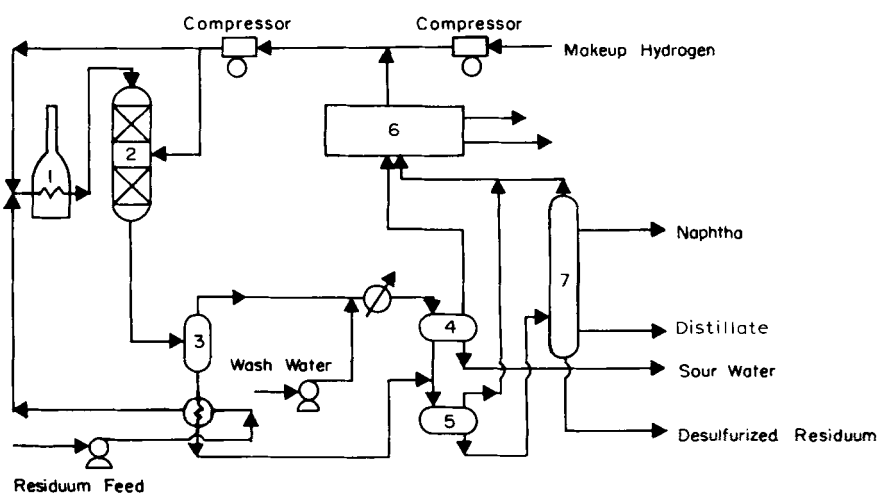

Fig. 14-21. Schematic diagram of a representative fixed-bed residuum hydrodesulfurization process. A guard-bed reactor may be placed upstream of the reactor. *1* = furnace; *2* = reactor; *3*, *4* = high-pressure separator; *5* = low-pressure separator; *6* = gas scrubbing H_2S recovery; *7* = fractionator.

TABLE 14-4

Approximate processing conditions in fixed-bed process for residue

Processing conditions	
Temperature (°C)	340–425
Pressure range (atm)	55–170
LHSV (volume feed/volume catalyst, h)	0.2–1
H_2 recycle rate (scf/bbl)	2000–10,000
Catalyst life (years)	0.5–1

TABLE 14-5

Elemental analysis and yields of hydrodesulfurization residuum (after Mosby et al. [15])

	Residuum feedstock	
	Khafji	West Texas sour crude oil
Element analysis:		
S (wt%)	4.30	3.65
N (wt%)	0.27	0.23
H (wt%)	11.01	11.08
C (wt%)	83.87	85.93
Ni (ppm)	32	37
V (ppm)	93	290
Sulfur content of product boiling at:		
$T > 343$°C (wt%)	1.0	1.0
Yields of products boiling at:		
$T < 182$°C (wt%)	6.35	5.12
$T = 182$–343°C (vol%)	9.3	5.7
$T > 343$°C (vol%)	91	94
H_2 consumption (scf/bbl)	580	420

Approximate processing conditions in a fixed-bed catalytic hydrodesulfurization are listed in Table 14-4, whereas the yields are presented in Table 14-5.

Three improved processes for efficient asphaltene conversion and desulfurization of asphaltene-containing heavy oils are described below.

Two-stage hydroconversion [17]

In designing a process, the following facts should be kept in mind: (1) sulfur contained in the asphaltene of a heavy oil is more difficult to remove than that contained in the distillable fraction; (2) most of the asphaltenic sulfur reduction results from conversion of the asphaltenes and not from desulfurization of the asphaltenes; (3) asphaltenes are converted at a very slow rate and very little change occurs in the remaining asphaltenes regardless of the level of overall residuum desulfurization; and (4) a catalyst with a relatively small average pore diameter

TABLE 14-6

Macropore volume characteristics of the first and second catalysts

	Macropore volume (% of total)	
	1st catalyst	2nd catalyst
Pore diameter range (Å):		
117– 200	86.1	23.9
200– 300	6.0	2.5
300– 500	3.5	4.6
500– 1000	1.4	6.5
1000– 1750	0.8	6.8
1750– 3500	–	9.3
3500–58000	2.2	46.4
Apparent bulk density (g/cm^3)	0.4–1.0	<0.4

can only accommodate a small fraction of the asphaltenes, causing most of the asphaltenes to bypass the catalyst and remain untouched. The proposed two-stage hydroconversion process consists of: (1) processing the asphaltene-containing heavy hydrocarbons with a catalyst, which reduces the sulfur in the distillable portion; and (2) processing the first reaction zone effluent with a second catalyst, which permits accelerated conversion and desulfurization of the asphaltenes.

Although the composition of the catalytic composites of two catalysts may be the same or different, their physical characteristics are different. The first catalyst constitutes less than 50% of the macropore volume, which is characterized by pore diameters greater than about 1000 Å. The second catalyst constitutes more than 50% of the macropore volume, which is characterized by pore diameters greater than about 1000 Å (Table 14-6).

The catalysts contain at least one metallic component from Groups VI-B and VIII of the Periodic Table combined with a porous carrier material. The Group VI-B components (Mo, W, or Cr) are utilized in an amount of about 4.0–30.0% by weight. The Group VIII metallic components are employed in amounts within the range of about 1.0–10.0% by weight, and the Fe, Co, and Ni are generally preferred. The preferred porous carrier material contains a composite of alumina and silica, containing approximately 10.0% to 90.0% silica by weight.

It was reported that more than 90% by weight of asphaltenes were converted to distillable fractions by using this process. The process may be conducted inversely, i.e., asphaltene conversion is achieved in the first stage by using the catalyst with larger average pore diameter and hydrocracking; additional asphaltene conversion occurs during the second stage [16].

Multistage hydrodesulfurization process

Multistage hydrodesulfurization process will convert a residual oil containing asphaltenes, metals, and sulfur to a substantially asphaltene-free oil without a

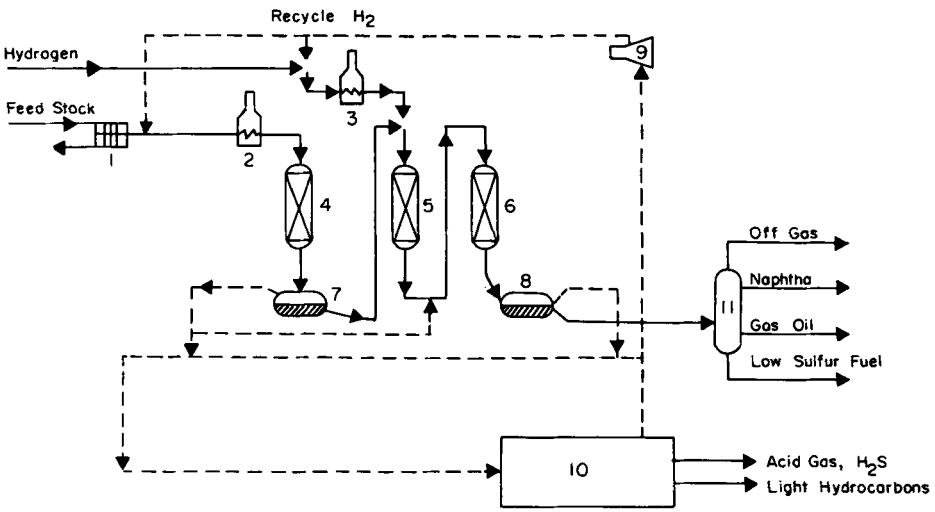

Fig. 14-22. Schematic flow diagram of a three-stage hydrodesulfurization process. *1* = filter; *2*, *3* = furnaces; *4*, *5*, *6* = reactors; *7*, *8* = flash chambers; *9* = compressor; *10* = recycle gas treatment.

distillation or solvent extraction step for removal of asphaltenes. The final stage effluent may be employed as the entire stream to a FCC (fluidized catalytic cracking) process (Fig. 14-22).

The catalysts comprise at least one metal from Group VIII and at least one metal from Group VI-B on alumina support, essentially free of silica. The hydrogenation metal composite is listed in Table 14-7.

The operating temperature is between 650° and 800°F. Increasing the temperature in each stage with increasing catalyst age compensates for catalyst activity aging loss. In the final stage, a lower hydrogen pressure (1300–1900 psi) than in the initial stage, which is up to 2300 psi, is maintained. The ratio of percent demetallization to percent desulfurization, therefore, is higher in the final stage than in the initial stage. The catalyst in the final stage comprises higher weight percents of Groups VI-B and VIII metals than those in the initial stage; consequently, the final stage produces a substantially asphaltene-free hydrodesulfurized effluent. The yield of boiling point

TABLE 14-7

Hydrogenation metal (wt%) on fresh catalyst

Stage	Metal (wt%)		
	Mo	Co	Ni
1st	3–16	0.3–0.6	0.2–2
2nd	4–18	0.5–7	0.3–3
3rd	6–26	0.7–9	0.4–4

fraction above the gasoline in the final stage effluent comprises more than 80% by volume (up to 98% by volume) of the feed. The feed may contain up to 10, 20 or even 25% by weight of the asphaltene content of the charge, whereas the effluent from the final stage is essentially free of asphaltenes.

Slurry process [18–24,26]

Another kind of reactor used commercially in residuum hydrodesulfurization is an ebullating-bed or slurry-bed reactor. The catalyst particles are held in suspension by the upward velocity of the liquid reactant, through which hydrogen flows concurrently. There are several advantages to this reactor design: (1) better heat and mass transfer than those in the fixed-bed process due to the vigorous stirring of feedstock, hydrogen, and catalyst particles; (2) decrease of the internal diffusion resistance and increase in the reactivity due to the use of small-particle or fine-powder catalyst; and (3) no excessive coke deposition upon catalyst surface during operation because of friction between the catalyst particles. Catalyst particles continuously enter and exit the reaction zone, and catalyst activity is maintained at a constant level. There are, however, some disadvantages: (1) the high degree of mixing of reactants in the direction of flow necessitates higher temperature or lower space velocities than those in a fixed-bed process to achieve the same conversion; (2) because of higher operating temperatures, undesired side reactions such as hydrocracking are more important, leading to higher hydrogen consumption; and (3) due to the high temperatures and pressures, there are complex problems of reactor stability and control.

The catalysts used comprise active hydrogenation metals from Groups V-B, VI-B and VIII, preferably catalytic vanadium sulfides. The utilization of active metals, which are deposited upon silica and/or alumina and are extremely corrosive, makes plant maintenance difficult and expensive. The unsupported catalysts used consist of finely divided particles colloidally dispersed within the charge stock. Usually, the unsupported vanadium sulfide catalyst is prepared in situ, and the concentration of solid particles ranges from about 10% to 25.0% of charge stock as the elemental metal. For example, the catalyst may be prepared by contacting vanadium oxide (V_2O_5) with ammonium sulfide to form an ammonium salt of the vanadium sulfide. The resulting ammonium salt of the vanadium sulfide is then thermally decomposed in a non-oxidizing atmosphere, and vanadium sulfide catalyst is recovered. An unsupported non-stoichiometric vanadium sulfide catalyst is usually prepared in situ. The fresh feed charge stock is an oxovanadate salt having the following structural formula:

$$[N(R)_4]VO(X)_5$$

where X is a cyano or thiocyano radical, and R is hydrogen or an alkyl group containing up to about 10 carbon atoms. On reacting the resulting mixture with hydrogen and hydrogen sulfide, the catalytic vanadium sulfide is produced in situ within the reaction zone. The precise atomic ratio of sulfur to vanadium in the catalytic non-stoichiometric vanadium sulfide is not accurately known, but it ranges from 0.8 : 1 to 1.8 : 1.

Typical operating conditions are as follow:

Temperature:	225–500°C
Pressure:	500–5000 psi
LHSV:	0.2–1.0
Hydrogen consumption:	5000–10,000 scf/bbl

The hydrogen contains from 1.0 mol% to about 20.0 mol% hydrogen sulfide, which maintains the catalyst as a sulfide. The presence of water in the process reduces the quantity of hydrogen sulfide as well as reduces the amount of hydrogen in circulation and reaction zone temperature.

The slurry process may be operated in two ways: cycling and non-cycling. Depending on the location of the hot oil pump, there are two cycling flow diagrams. In the "inner-cycling" flow diagram, the hot oil pump is placed inside or at the bottom of the reactor, whereas in the "outer-cycling" flow diagram the hot oil pump is placed outside or far from the reactor. Figure 14-23 shows a schematic flow diagram of an inner-cycling hydrogenation process. The H_2-oil ebullating-bed reactor, which is the first one in commercial operation, is shown in Fig. 14-24.

A non-cycling technology for residuum hydrogenation was developed by the Fushun Petroleum Institute of China. The process is characterized by its use of only the feed oil and hydrogen to fluidize the fine catalyst particles and by canceling the recycling of hot oil. More than 80% of particles used in the reactor should preferably range in diameter from 0.1 to 0.16 mm.

The slurry process may convert more than 90% by weight of asphaltene to distillable fraction and even produce asphaltene-free effluent.

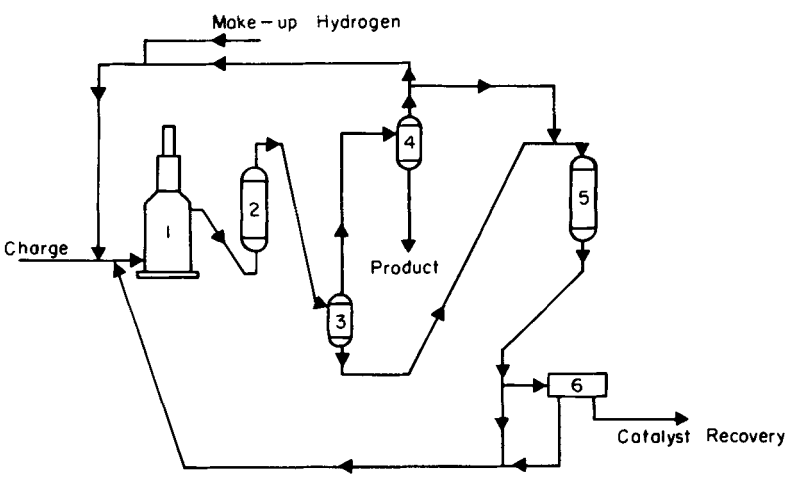

Fig. 14-23. Schematic flow diagram of an inner cycling residuum hydrogenation process. *1* = heater; *2* = reactor; *3* = hot separator; *4* = cold separator; *5* = reactor; *6* = catalyst separation.

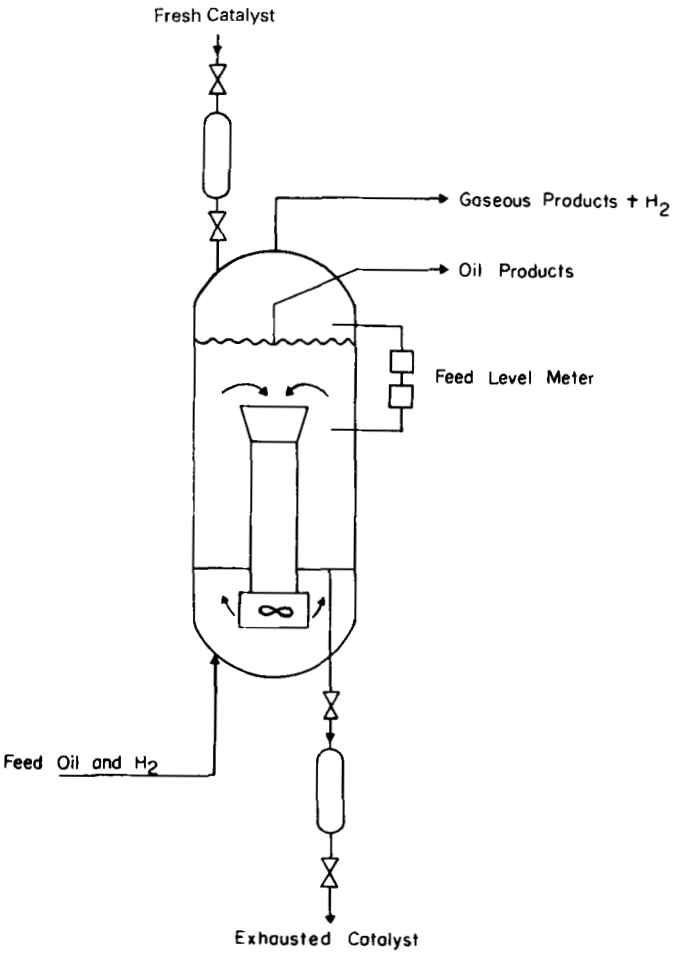

Fig. 14-24. H_2 ebullating-bed reactor.

REFERENCES

[1] Dickie, J.P. and Yen, T.F., Macrostructures of the asphaltene fractions by various instrumental methods. *Anal. Chem.*, 39: 1847–1852 (1967).

[2] Nakamura, M., Shiroto, Y. and Takahashi, H., Asphaltene cracking in catalytic hydrogenation treatment of heavy oils. *Nippon Kagaku Kaishi*, 6: 1037–1046 (1980).

[3] Nakajima, T., Ishikura, T., Asuka, H. and Yamakawa, I., Thermal cracking of asphaltenes fractionated from Khafjji asphalt. *Nippon Daigaku Seisankogakubu Hokoku*, 14(1): 119–126 (1981).

[4] Ignasiak, T.M. and Strausz, O.P., Reaction of Athabasca asphaltene with tetralin. *Fuel*, 57(10): 617–621, (1978).

[5] Moschopedis, S., Parkash, S. and Speight, J.G., Thermal decomposition of asphaltenes. *Fuel*, 55(7): 431–434 (1978).

[6] Magaril, R.Z. and Aksenova, E.I., Kinetics and mechanism of coking of cracking asphaltenes. *Khim. Tekhnol., Tr. Tyumen. Ind. Inst.*, 169–172 (1972).

[7] Schucker, R.C., Measurement dependent variations in asphaltene thermal cracking kinetics. *Symp. on Processing Heavy Oils and Residua, Am. Chem. Soc. Meet., Div. Pet. Chem.*, Seattle, Wash., March 20–25 (1983).

[8] Kanda, N., Itoh, H., Yokoyama, S. and Ouche, K., Mechanism of hydrogenation of coal-derived asphaltene. *Fuel*, 57(11) (1978).

[9] Takeuchi, C., Shiroto, Y. and Nakata, S., Asphaltene cracking in catalytic hydrotreating of heavy oils, 1. Processing of heavy oils by catalytic hydroprocessing and solvent deasphalting. *IEC, Process Des. Dev.*, 22: 236–242 (1983).

[10] Asaoka, S., Nakata S., Shiroto, Y. and Takeuchi, C., Asphaltene cracking in catalytic hydrotreating of heavy oils, 2. Study of changes in asphaltene structure during catalytic hydroprocessing. *IEC, Process Des. Dev.*, 22: 242–248. (1983).

[11] Takeuchi, C., Nakata, S., Fukui, Y. and Shiroto, Y., Asphaltene cracking in catalytic hydrotreating of heavy oils, 3. Characterization of products from catalytic hydroprocessing of Khafjji residue. *IEC, Process Des. Dev.*, 22: 248–257 (1983).

[12] Kurokawa, K. and Kondo, T., The reaction of asphaltene under mild hydrotreating conditions. *J. Jpn. Pet. Inst.*, 22(1) (1979).

[13] Wakabayashi, T., Koguchi, K., Nakayama, T. and Nakamura, E., Hydrocracking of oil sand bitumen. *Nippon Kagaku Kaishi*, 6: 1047–1053 (1980).

[14] Nomura, H., Sekido, Y. and Ohguchi, Y., Hydrodesulfurization reaction of residual oils. Part 2, Various side reactions in desulfurization reaction. *J. Jpn. Pet. Inst.*, 22(5): 296–302 (1979).

[15] Mosby, J.F., Hoekstra, G.B., Kleinhenz, T.A. and Sroka, J.M., Pilot plant proves resin process. *Hydrocarbon Process.*, 52(5): 93 (1973).

[16] O'Hara, M.J., *Catalytic Conversion of Asphaltene-containing Black Oil.* U.S. Patent 3: 640; 817 (1972).

[17] Gatsis, *J.G., Two-Stage Hydroconversion of Hydrocarbonaceous Black Oil.* U.S. Patent 3: 957; 622 (1976).

[18] Gatsis, J.G., *Hydrocarbon Hydrorefining Utilizing a Nonstochiometric Vanadium Sulfide Catalyst.* U.S. Patent 4: 194; 967 (1980).

[19] Gatsis, J.G. and Gleim, W.K.T., *Catalytic Slurry Process for Effecting the Conversion of a Hydrocarbonaceous Charge Stock Containing Asphaltenes, Metallic Contaminants, and Excessive Quantities of Sulfurous Compounds.* U.S. Patent 3: 622; 495 (1971).

[20] Gleim, W.K.T., *Catalytic Slurry Process for Converting Hydrocarbonaceous Black Oils with Hydrogen and Hydrogen Sulfide.* U.S. Patent 3: 619; 410 (1970).

[21] Gleim, W.K.T., *Catalytic Slurry Process for Hydrocarbonaceous Black Oil Conversion.* U.S. Patent 3: 675; 111 (1972).

[22] Hutchings, L.E., *Hydrorefining an Asphaltene-Containing Black Oil with Unsupported Vanadium Catalyst.* U.S. Patent 4: 139; 453 (1979).

[23] Rogers, E.S., *Catalytic Slurry Process for Converting a Hydrocarbonaceous Charge Stock Containing Hydrocarbon-Insoluble Asphaltenes.* U.S. Patent 3: 617; 503 (1971).

[24] Gleim, W.K.T., *Slurry Hydrorefining of Black Oil with Mixed Vanadium and Manganese Sulfides as Catalysts.* U.S. Patent 3: 694; 352 (1972).

[25] Hirotsugu, N., Sekido, Y. and Ohguchi, Y., Hydrodesulfurization reaction of residual oils. Part 1, Effect of reaction variables and feed oils on reaction rate. *J. Jpn. Pet. Inst.*, 22(5): 288–295 (1979).

[26] Stine, L.O. and Stolfa, F., *Catalytic Slurry Process for Effecting the Conversion of a Hydrocarbonaceous Charge Stock Containing Asphaltenes and Metallic Contaminants.* U.S. Patent 3: 622; 499 (1971).

This page intentionally left blank

Asphaltenes and Asphalts, 1. Developments in Petroleum Science, 40
edited by T.F. Yen and G.V. Chilingarian

Chapter 15

STUDIES OF ASPHALTENE DIFFUSION: IMPLICATIONS FOR ASPHALTENE STRUCTURE AND OPTIMAL UPGRADING REACTOR DESIGN

RAJEEV C. SANE, THEODORE T. TSOTSIS, IAN A. WEBSTER
and VIPPERLA S. RAVI-KUMAR

INTRODUCTION

The term asphaltene has been historically used to collectively describe the chemical components of a crude (and more specifically of a resid), which are generally more polar and larger in size. Since the earlier stages of the field of heavy-oil upgrading and hydroprocessing, asphaltenes have been defined as a solubility class of various components of a crude. Through the years, this definition attracted discussion and criticism (see, e.g., Bunger and Cogswell [1]). Because some of the asphaltene properties are dependent on their isolation techniques, the relevant question here is whether the asphaltenes produced by such isolation techniques bear any resemblance and similarity to compounds found in the original crude, and whether the asphaltenes themselves exist in the original crude rather than simply being an artifact of their separation process.

The debate whether the asphaltenes do even exist, and if they do, how one properly isolates and characterizes them, has continued for years and the historical details of the debate will not be dealt with here. Comprehensive descriptions can be found in a number of papers, see, e.g., papers by McKay et al. [2], Koots and Speight [3] and Wiehe [4]. The commonly held view today is that asphaltenes do exist and are found in the original resid. One, however, cannot uniquely characterize an asphaltene (and, in that manner, any other resid fraction) based on a single property alone like, for example, solubility. For petroleum-derived liquids and resids, two properties are needed to differentiate one resid fraction from the other. Which two properties one should use, however, still remains a matter of debate. In his pioneering paper, Long [5] first suggested that the composition of petroleum liquids can be represented in terms of a plot of molecular weight versus polarity. Long and Speight [6], furthermore, opted to use the solubility parameter as a measure of polarity, and the 5% and 95% points of the molecular weight distribution (as measured by gel permeation chromatography — GPC) as a measure of the molecular weight. Wiehe [4], on the other hand, used the number average molecular weight, as measured by vapor pressure osmometry (VPO), as a measure of molecular weight and the average hydrogen content as a measure of the molecular attraction.

Meanwhile, interest in the structure and polydispersity and the reactive and transport properties of asphaltenes has been steadily increasing among chemical

engineers and chemists working in the field of oil upgrading and hydroprocessing. Generally, the heavier the crude one deals with, the larger the percentage of asphaltenes one finds in it. The relative abundance of heavy crudes combined with the fluctuating supply of lighter crudes has made investigation of catalytic upgrading of tower bottoms of heavy crudes necessary. Because asphaltenes make up a major portion (up to 25%) of these crudes, their conversion to lighter fractions has become an important technical problem. The main obstacle in resid hydroprocessing is the presence of heteroatoms, such as sulfur, nitrogen, and metals (like nickel and vanadium), which poison the catalysts used for hydroprocessing. In terms of composition, asphaltenes contain a greater percentage of heteroatoms than all other fractions of a crude, and, therefore, present the greatest challenge during resid upgrading. Furthermore, most of the molecular components of an asphaltene are very large structures, with sizes approaching that of a typical catalyst pore. Hydroprocessing of asphaltenes involves a number of parallel and/or consecutive reactions like hydrodesulfurization, hydrodenitrogenation, hydrodemetallation, and cracking. Owing to the large size of most asphaltene entities, all these reactions occuring within the catalyst pellet, are diffusion-limited.

This being the case, it is unclear, from the standpoint of resid-upgrading reactor design, how important a role the knowledge of (and the debate on) detailed asphaltene chemistry really plays. The literature of asphaltene chemistry is voluminous. Considerably fewer studies, however, have dealt with the subject of asphaltene transport and diffusion through restricted porous catalysts and systems. The reasons for this are not readily evident. Certainly the chemical complexity of asphaltenes has been a contributing factor. Some of the earliest studies on the direct measurement of asphaltene diffusion were done by Thrash and Pildes [7] and Shimura et al. [8]. These studies on the diffusion of asphaltenes and residual oils were continued by Baltus and Anderson [9,10] and Baltus and coworkers [11–13]. For years now, asphaltene and resid upgrading reactor design has utilized the concept of asphaltenes being a single pseudo-molecular entity, to which one can assign a unique effective diffusivity and other effective transport properties. This concept, however, directly contradicts recent experimental evidence [14–17], which shows that one cannot assign a unique experimental diffusivity value to an asphaltene molecule. In fact, experiments show that the effective diffusivity of an asphaltene, as measured in a standard Wicke–Kallenbach cell using model porous membranes, can vary as a function of experimental time by as much as three orders of magnitude for the duration of an experimental run. The diffusivity, furthermore, is a strong function of temperature, pressure, and the catalyst pore size distribution.

These experimental findings and the fact that one cannot assign a unique experimental effective diffusivity to an asphaltene are not surprising to a number of researchers, who for the last few years have tried to address the fundamental engineering aspects of reaction and diffusion of asphaltenes in porous catalysts. Asphaltenes are far from being uniquely defined simple molecular entities. The work of this group has shed light on some of the unique aspects of the transport behavior of asphaltene molecules. Issues that have been or are being addressed include, but are not limited to, the effect of solvent on asphaltene diffusivity and the

effects of pore size, temperature and concentration. As a result of these studies, a picture of the asphaltene's structure is starting to emerge which, when completed, will hopefully be consistent with not only the transport and reaction data, but also the existing detailed chemical information about asphaltenes.

The authors view this paper as part of this process, i.e., as one of the first steps in the direction of developing a structural asphaltene model from transport data, which is consistent with the available reaction data as well as with what is known on the chemistry of asphaltenes. A simple conceptual model of the structure of an asphaltene is presented in this chapter. This model is not intended to be the final word on the subject of the structure of asphaltenes. Its purpose, instead, is to be one of the starting points in a debate, from which hopefully a complete model of the asphaltene structure will emerge. By design, therefore, the model does not concern itself with the detailed chemical structure but instead concentrates on a broad conceptual and macromolecular picture, an exercise quite similar to drawing a block diagram for a complex system. There are no mathematical equations or quantitative descriptions similar to those developed by Savage et al. [18] to simulate the chemistry of asphaltenes, or by Nortz et al. [13] and Sane and coworkers [14,16] to describe the transport properties. The model of the asphaltene structure, when completed, should, of course, include such a quantitative description, one which will most likely integrate the mathematical description of the asphaltene's chemistry with statistical models of its transport and reaction properties. To attempt to do so at this point is, however, premature.

The structural model presented here is in agreement with the experimental diffusivity data of the authors, as well as with the existing literature on asphaltene chemistry. In as much as the diffusivity data presented here is primarily for asphaltenes derived from a Hondo California crude, the model of asphaltene structure is strictly applicable to these asphaltenes. Asphaltenes derived from different crudes will differ significantly in chemical composition, reactivity, polydispersity, etc. The authors, however, believe that there are distinct similarities in the fundamental macromolecular structure of all asphaltenes and that the structural model presented here includes these distinct similarities.

WHAT IS KNOWN FROM THE LITERATURE ABOUT THE ASPHALTENE STRUCTURE

The scientific literature on the chemical composition and structure of asphaltenes is extensive. One of the earliest and most significant studies in the field is by Yen et al. [19] who used X-ray analysis of asphaltenes to determine structure. As a result of this study and a subsequent study by Dickie and Yen [20], Yen and coworkers proposed a model of the asphaltene's structure. This model has since then been disputed a number of times. Nevertheless, some of their original ideas have survived the test of time for thirty years. Yen and coworkers [19,20] suggested that asphaltenes are macromolecules but not in the traditional sense of large molecules, where all the various chemical elements like carbon, hydrogen, and heteroatoms are held together by strong chemical forces. Still, in their structural

asphaltene model, there are true large molecules involved. These molecules are condensed heterocyclic aromatic sheets with attached alkyl chains restricted to the plane of the sheet. Yen and coworkers perceive these sheets to be approximately 8.5–15 Å in diameter. They, furthermore, report these molecules to be capable of associating with each other in their third dimension in the presence of non-polar or slightly polar solvents to form stacked clusters about 16–20 Å in height. Such clusters consist of about five sheets (calculated from the experimental value of the interlayer distance), a number, which most likely will depend on the asphaltene type and the environment the asphaltene finds itself in. The nature of the forces causing the stacking, though not completely resolved, is believed to be both chemical, as in the case of covalent bonds between adjacent alkyl chains usually involving heteroatoms and paraffinic chains, and weak physical like van der Waals and hydrogen bonding. The most important conclusion arising from the work of Yen and coworkers is that such clustering does occur. This important observation has been verified a number of times since then. For example, Mieville et al. [21] observed that different GPC cuts of asphaltenes contain different numbers of clusters per molecule, and hence different molecular weights. But, the size of the unit cluster is essentially the same and relatively small (five aromatic and two naphthenic rings). Also, Speight and coworkers [22,23] clearly observed that the asphaltenes do associate in non-polar solvents and dissociate in polar solvents. Furthermore, it has been observed [24] that the concentration, temperature and aging affect the degree of association.

The association and clustering need not stop at the cluster (or particle) level. Molecular weight distribution studies have shown the presence of components of very large molecular weight (the exact limits of the molecular weight range are cause for disagreement and debate by several authors [22]). Dickie and Yen [20] observed the association of particles in electron micrographs to form micelles with diameters of the order of 100–300 Å. They also suggested that the clustering and association of the particles may be aided by the presence of various metals in an asphaltene. Again, as in the case for particles, the nature of the forces responsible for the formation of micelles is not clear, though they are believed to be primarily weak in nature (see, e.g., Pfeiffer and Saal [25] and Rao and Serrano [26] for a discussion on the colloidal nature and aggregation of micelles). Mieville et al. [21] observed a small peak in their GPC trace at very high molecular weights, probably due to micelle formation.

Where the metals are located in this structure and the role they play in the formation of particles and micelles has been a subject of many studies in the field. A number of general observations can be drawn from these studies. Most authors, for example, agree that two types of metals exist in an asphaltene, i.e., porphyrinic and non-porphyrinic. What proportion of these metals are porphyrinic and where they are located is, however, the subject of ongoing debate. Larson and Beuther [27] suggested that the porphyrinic metals are concentrated on the periphery of the asphaltene particles. According to them, nickel is located in the core of the micelle, whereas vanadium is concentrated on its external surface, a conclusion drawn primarily from the observation that nickel is more refractory in nature than vanadium. Sugihara et al. [28] claim that only a small fraction of the total nickel and

vanadium found in an asphaltene is of porphyrinic nature and is mainly concentrated on the periphery of the particle. They found vanadium to be predominantly in its 4+ valence state and nickel in its 2+ state. In agreement with Larson and Beuther (and other studies in this area), they found that nickel is significantly more refractory in nature than vanadium.

Fish et al. [29], in agreement with Sugihara et al. [28], also found the metals to be predominantly non-porphyrinic. Some vanadium (presumably porphyrinic in nature) was found in species of low molecular weight (compounds less than 400 daltons). They reported the nickel-containing components to be quite polar. Reynolds et al. [30] and later Mieville et al. [21] found all porphyrinic metals of a resid to be contained in the low-molecular-weight components. For example, almost all porphyrinic vanadium in crude was found in components of molecular weight less than 900 daltons [31]. Most non-porphyrinic components were contained in compounds of higher molecular weight although some lower-molecular-weight compounds were also present. Biggs et al. [32] found that most petroporphyrinic compounds are of smaller size compared to the non-porphyrinic metal compounds of an asphaltene. The non-porphyrinic compounds of an asphaltene seem to agglomerate with the aid of various polar components. Non-porphyrinic nickel and vanadium, according to Jacobs and Filby [33], are found in very similar pyrrole structures.

These, in the opinion of the authors, are some of the most representative studies in the voluminous literature on the subject of the chemical structure and composition of asphaltenes. There is a wealth of chemical information in these and other studies on the subject. The technical details are many and sometimes obscure, and not everybody agrees on them. Nevertheless, a consistent overall macromolecular picture is starting to emerge on the chemical structure and composition of asphaltenes. It is apparent that asphaltenes are not single, simple generic structures but rather a complex mixture of colloidal entities (micelles) of various sizes and shapes, consisting of assemblies of smaller particles, which in turn result from the clustering of lower-molecular-weight components, all in a state of dynamic exchange strongly affected by the presence of solvents, temperature, pressure and fluid mechanical conditions. The type and exact nature of forces resulting in the clustering of the lower-molecular-weight components are still being studied. Furthermore, the exact chemical composition of these compounds is still not clear and is the subject of ongoing investigations [19]. One would expect such micellular structures, consisting of colloidal aggregates of the primary particles, to be highly sensitive to their environment, i.e., whether the environment is polar or non-polar, the temperature and pressure, the presence of surfactants, etc. This is a picture which is consistent with what is known about asphaltenes. Obviously, this picture of the structure of an asphaltene molecule does not as yet have universal acceptance. Studies, based on the chemical analysis of asphaltenes, exist that claim that asphaltenes have a carbon- or sulfur-based polymeric structure [34,35] (though it has been reported that the basis for the chemical analysis might be in error [36,37]). The authors believe that the picture of an asphaltene as described above, i.e., a dynamic system in a constant state of interchange is a structure that is consistent with both the available chemical information and recent experimental investigations on the diffusivity and

transport of asphaltenes through model porous membranes. A brief overview of these experimental studies is found in the next section.

EXPERIMENTAL STUDIES OF ASPHALTENE DIFFUSIVITY

The authors have experimentally measured the diffusion of asphaltenes across model porous membranes. Further details (beyond those given here) about the experimental system and techniques can be found in a series of recent publications by them [14–17]. The asphaltenes used were *n*-pentane (or *n*-heptane) insolubles extracted from Hondo crude, a California Outer Continental Shelf oil, furnished by UNOCAL. The diffusion cell (see Fig. 15-1) was a Wicke–Kallenbach-type apparatus consisting of two well-mixed compartments (half-cells). During experiments of asphaltene diffusion, the half-cells are separated by a polycarbonate membrane containing straight, parallel, non-intersecting, cylindrical pores (supplied by Nuclepore Corp., Pleasanton, Calif.) The membrane pore size varied between 100 and 4000 Å. For the experiments reported here, the temperature was maintained at 45°C.

The experimental plan is outlined in Fig. 15-2. The first experiment was conducted with a 100 Å membrane. The authors started with a 5 wt% solution of *n*-pentane-insoluble asphaltene in xylenes, which was loaded in one of the half-cells, hereafter referred to as the high-concentration side (HCS). Pure xylenes were loaded in the other half-cell referred to as the low concentration side (LCS). The asphaltenes were allowed to diffuse through the membrane for a predetermined period of time. During the experiment, samples were withdrawn from the LCS and analyzed for sulfur, nickel and vanadium concentrations by X-ray fluorescence (XRF), and for molecular weight distributions by size exclusion chromatography (SEC). After the first experiment ended, the second experiment was initiated with a 150 Å membrane. Again, pure xylenes were loaded in the LCS. In this experiment, however, the HCS was filled with the asphaltene solution remaining in the HCS at the end of the first experiment with the 100 Å membrane. Further experiments were done with the 300 Å and 4000 Å membranes, in that order, starting again with pure xylenes in the LCSs and the HCSs containing the HCS solution carried over from the preceding experiment.

RESULTS AND DISCUSSION

The data collected from the diffusion experiments, depicting sulfur, vanadium and nickel concentrations in the LCS as a function of run time are plotted in Figs. 15-3 to 15-5. The initial sulfur, vanadium and nickel concentrations in the HCS are 4110.0, 49.5 and 21.6 ppm respectively. Figure 15-6 shows a scaled-up view of nickel and vanadium data for the 100 Å membrane at low times. For a semi-quantitative assessment of the data, the initial slopes for various elemental species for the different pore sizes were calculated from the concentration versus time curves, and have been plotted relative to the values for the 100 Å experiment (Fig. 15-7). Figures

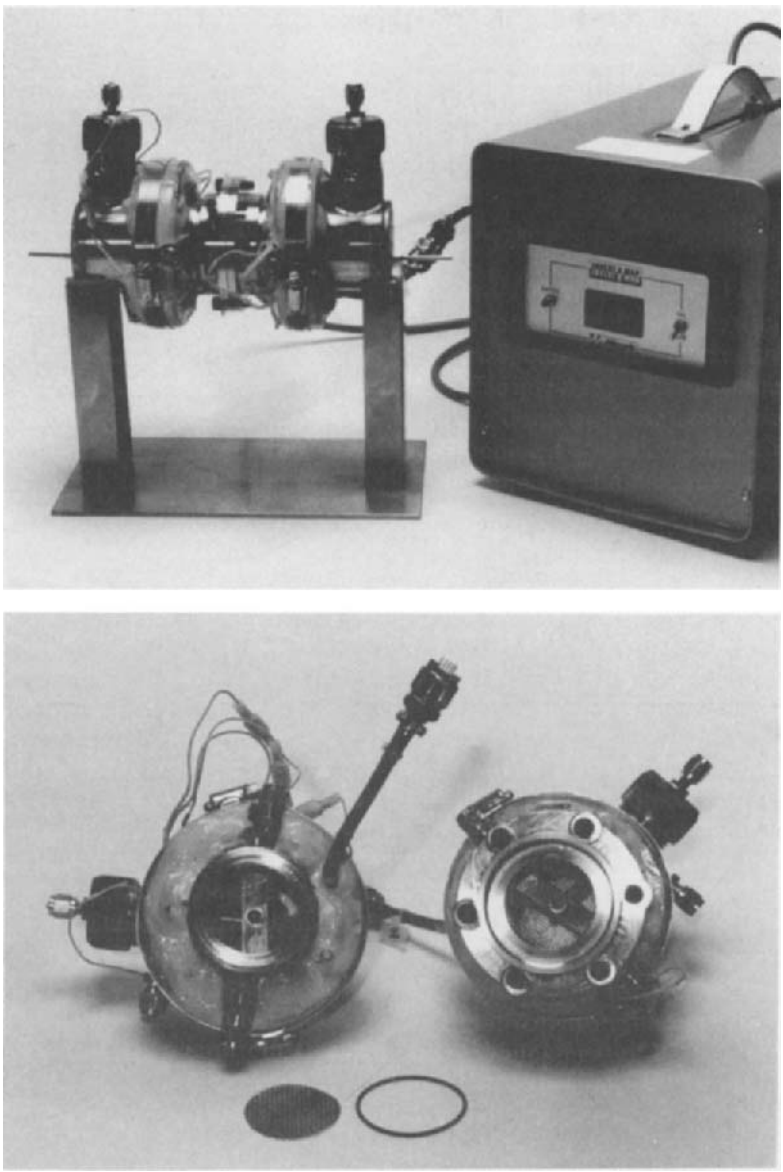

Fig. 15-1. The diffusion cell.

15-8 and 15-9 show typical SEC analyses of the LCS samples at various experimental times for two different pore sizes. The authors have drawn the following conclusions from these experimental data.

(1) Figures 15-8 and 15-9 show typical SEC data of LCS samples withdrawn at different run time. The polydisperse nature of asphaltenes is clear from these

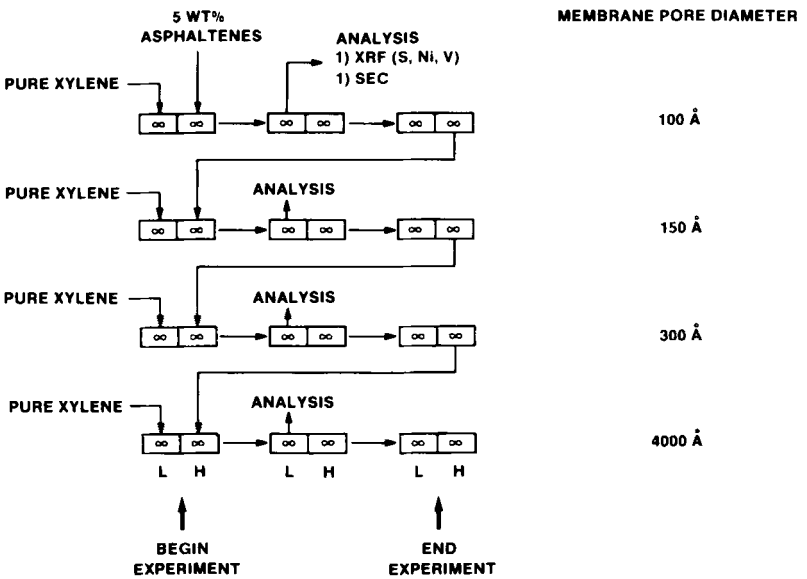

Fig. 15-2. Experimental plan.

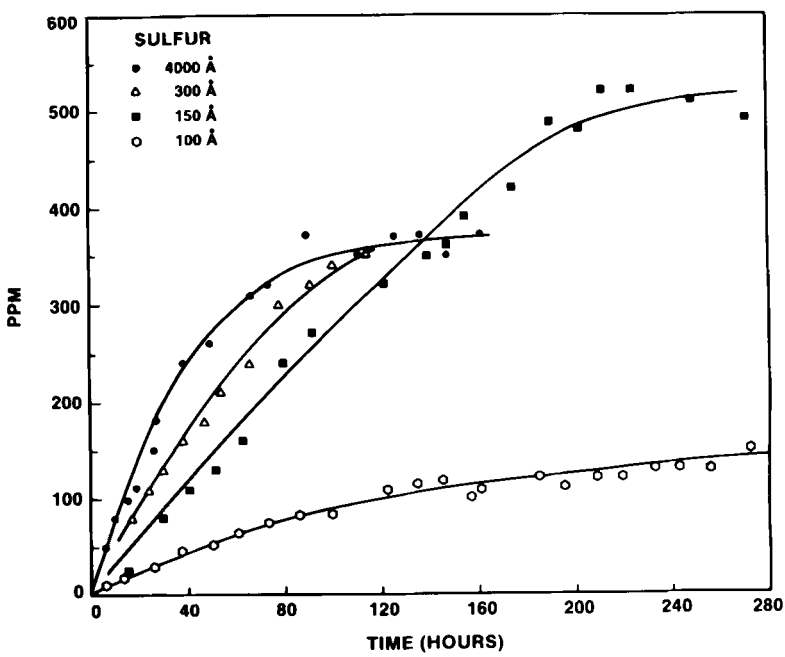

Fig. 15-3. Low side concentrations vs. run time: sulfur.

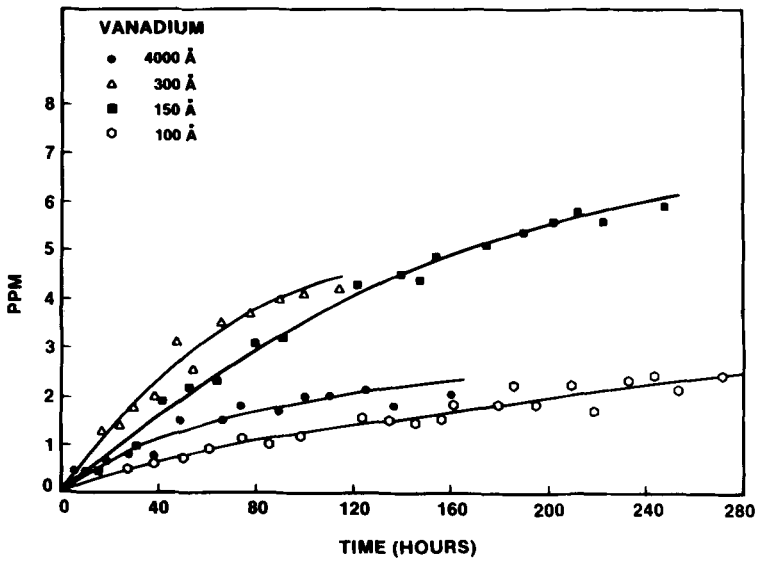

Fig. 15-4. Low side concentrations vs. run time: vanadium.

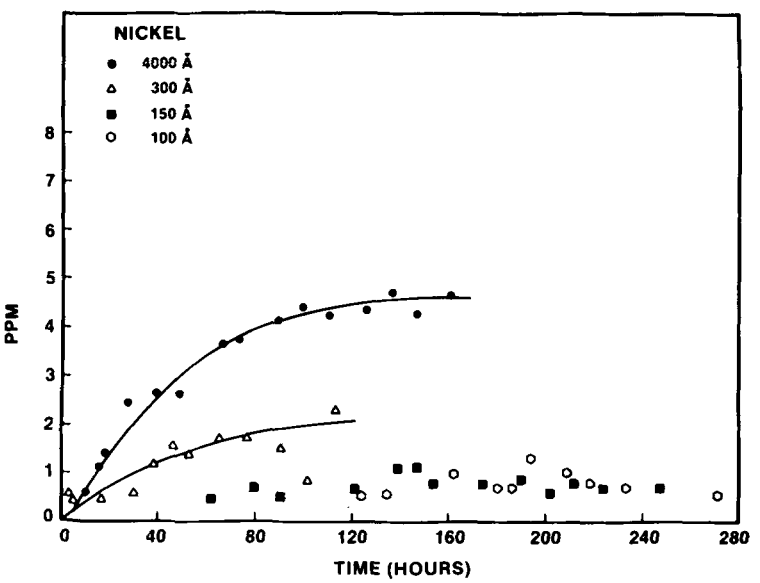

Fig. 15-5. Low side concentrations vs. run time: nickel.

figures. Asphaltenes are not simple and uniquely defined molecules but rather consist of a whole range of molecular components of various sizes. The components of smaller size diffuse faster than the components of larger size and, as a result, the molecular weight distribution of the asphaltene in the LCS at smaller times is

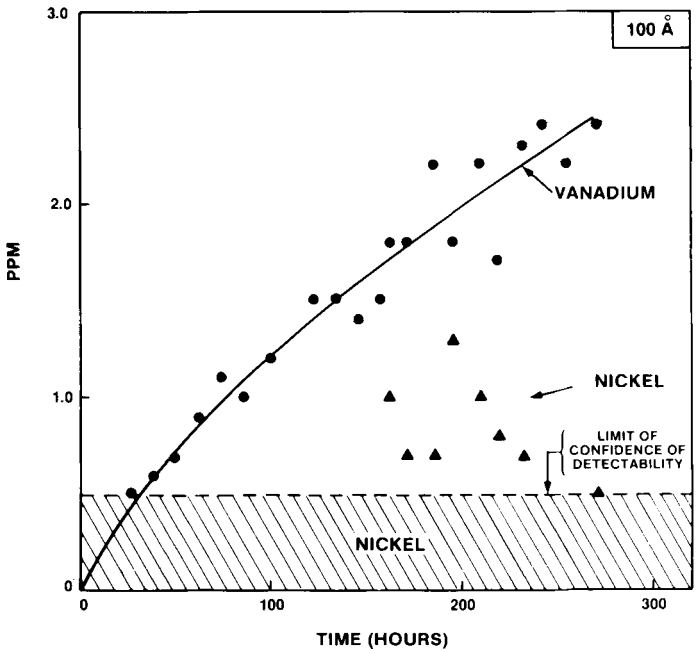

Fig. 15-6. Low side concentrations vs. run time: 100 Å pore size membrane.

skewed towards the lower molecular weights. At larger times, the molecular weight distribution of the asphaltene in the LCS approaches that of the asphaltenes initially loaded in the HCS. Clearly, this is an oversimplified picture of how asphaltenes diffuse through porous membranes. In fact, this mechanism of asphaltene transport, although indicative of the polydisperse nature of asphaltenes, is not inconsistent with the model of an asphaltene structure, which portrays asphaltenes as regular polymeric molecules. Any polydisperse polymer would diffuse in a similar fashion as indicated in Figs. 15-8 and 15-9. To realize that asphaltenes diffuse in a uniquely different fashion, one has to examine Figs. 15-8 and 15-9 in combination with Figs. 15-3 to 15-5. For example Fig. 15-5, clearly shows that there are components in the initial asphaltene that are larger than 150 Å. In fact, out of the total nickel species diffused throughout the whole series of experiments, only approximately 20% penetrate in the time allotted through the 100 and 150 Å membranes. How could it then be possible that the asphaltene at large times in Fig. 15-9 closely resemble the asphaltene initially loaded in the HCS? The only asphaltene structure capable of describing the data in Fig. 15-9 is the one previously described by the authors, namely:

> "the asphaltenes are not simple generic species but rather complex mixtures consisting of micelles of various sizes and shapes, of unformed micelles, of small particles and of high and low molecular weight chemical entities and attached alkyl chains, all in a state of dynamic exchange strongly affected by the presence of solvents, temperature, pressure, and fluid mechanical conditions".

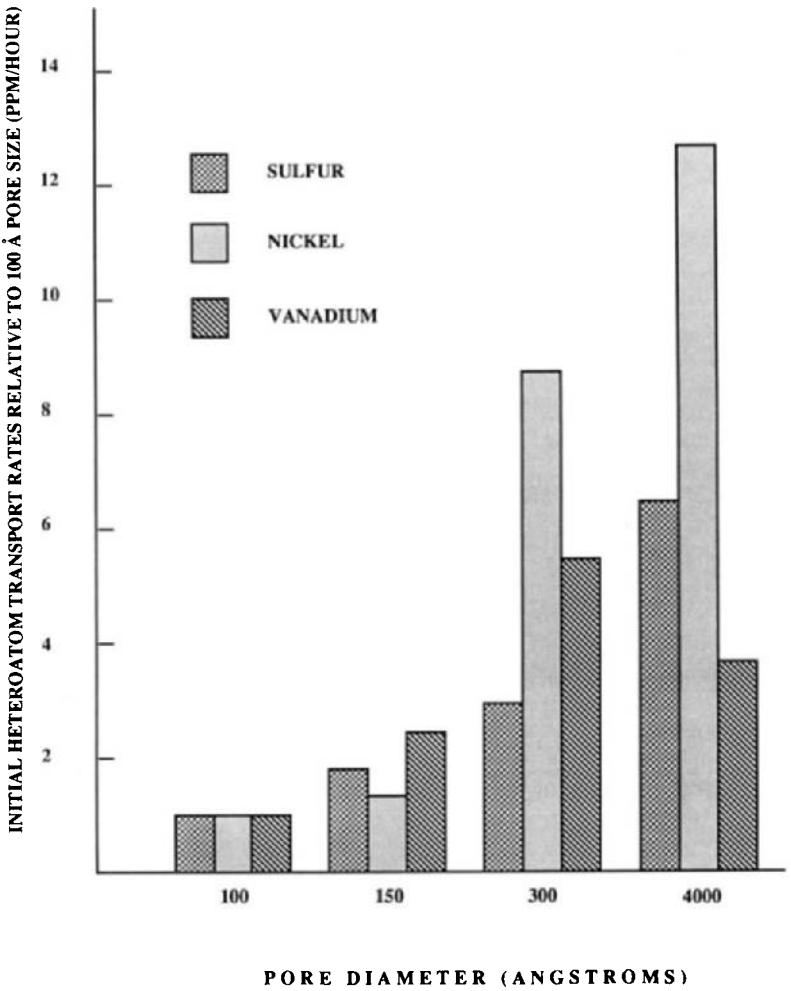

Fig. 15-7. Relative initial heteroatom transport rates across membranes.

Only a dynamic association–dissociation process can explain the fact that the large components of the asphaltenes, with nominal sizes larger than the diameter of the pore find their way from the HCS to the LCS.

The data in Figs. 15-8 and 15-9 also have some significant engineering implications. If one is to consider an asphaltene as a solubility class and then define a unique effective diffusivity D_e, the effective diffusivity will vary by an order of magnitude through the experiment.

(2) Nickel seems clearly to be concentrated in species with sizes above 150 Å (see Fig. 15-5). In fact, as mentioned above, less than 20% of all nickel diffused permeates through the 100 and 150 Å membranes. This is in agreement with the observations of Larson and Beuther [27] and Sugihara et al. [28], as well as with

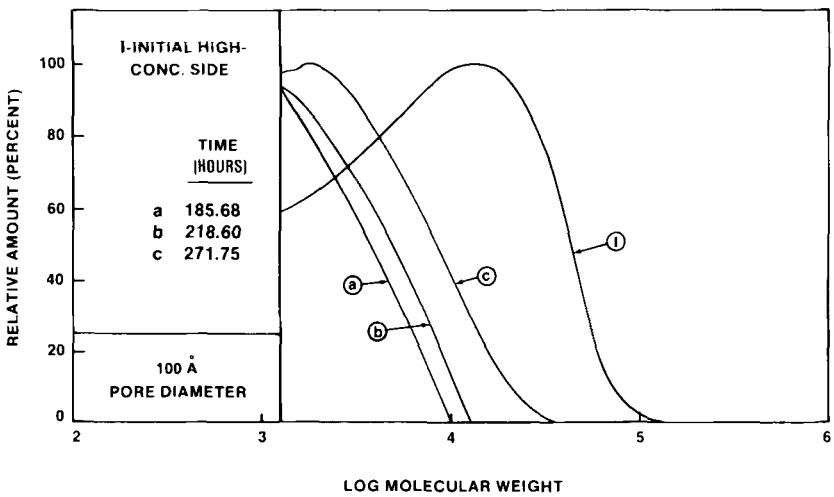

Fig. 15-8. SEC analysis of LCS samples: pore size 100 Å.

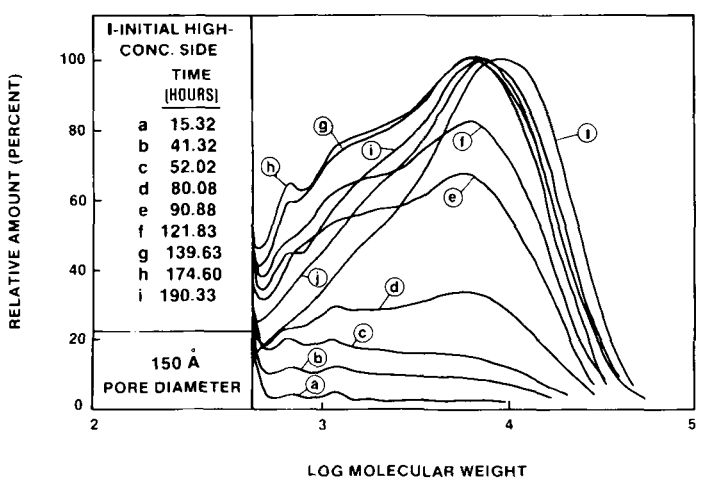

Fig. 15-9. SEC analysis of LCS samples: pore size 150 Å.

several investigators who found nickel particularly difficult to remove. In fact, the conclusion of Larson and Beuther [27] and Dickie and Yen [20] that nickel is most likely concentrated in the polar core of the micelle seems to be correct.

(3) Vanadium on the other hand, seems to be concentrated in components of less than 300 Å in size. In fact, more than 50% of vanadium penetrates through the 100 and 150 Å pores. This again is in agreement with the observations of Larson and Beuther [27] and Sugihara et al. [28], who found vanadium much easier to remove than nickel. It is also in agreement with the results of Fish et al. [29] and Reynolds et al. [30], who found vanadium in the lower-molecular-weight components of the

asphaltene. Over 50% of the sulfur appears to be contained in components of less than 150 Å, although significant amounts of sulfur are also contained in all sizes of asphaltene components. This generally agrees with the work of Hausler and Carlson [38], who found the distribution of sulfur throughout the various size components of asphaltenes to be very broad.

Implications of the asphaltene model for reactor design

A more detailed description of the findings of the present study of asphaltene diffusivity through model porous membranes can be found elsewhere [16,17]. The experimental results presented here show that the picture arising from transport investigations is completely consistent with the overall macroscopic picture of the structure of an asphaltene derived from chemical studies. Assuming that this model of the structure of an asphaltene is correct, the question then is, what are its implications for resid-upgrading reactor design? In the opinion of the authors, the implications are many and significant. Traditionally, resid-upgrading reactor design has utilized the concept of overall effective transport properties for asphaltenes and other resid fractions. In view of the existing chemical information on asphaltenes, the practice has been characterized as simplistic, but of some engineering utility. The authors believe that the practice is wrong, and can lead to significantly erroneous conclusions. One cannot define and should not define an effective diffusivity of an asphaltene. First of all, such an effective property cannot be measured. In the Wicke–Kallenbach diffusion experiments described here, the so-called "effective diffusivity" of an asphaltene molecule can vary by up to two orders of magnitude throughout a single experimental run. Diffusivities measured by uptake experiments will certainly be different and both types of measurements may give values which bear no relevance to transport under reactive conditions.

Is the previously stated concept of an asphaltene (that of a *complex mixture with its components being in a state of dynamic exchange*) significant for resid-upgrading catalyst design? The authors believe that it is, because it offers plausible explanations to what is happening during resid upgrading. Most of the nickel, for example, found in an asphaltene should not even be penetrating the structure of a typical upgrading catalyst, if it was not for the concept of "*dynamic exchange*" between the various asphaltene components (see Figs. 15-3 to 15-5).

The other plausible reason, why typical upgrading catalysts can process the heteroatoms found in a resid, is that the structure of an asphaltene represented by the above model, although valid at low temperatures, will not survive the higher upgrading temperature and pressure conditions, i.e., the micelles and even the particles will break apart. Superficially, this explanation is in contrast with experimental data (see, e.g., Wiehe [4], Savage and Klein [39] and Sane et al. [17]), which show that treatment at upgrading conditions of asphaltenes does not destroy their structure completely. Instead, it results in the incomplete conversion of asphaltenes to both lower-molecular-weight resid fractions like volatiles, saturates, aromatics, and resins, and to higher-molecular-weight components like coke. These data are open to interpretation, however, because the collection and analysis of the products take

place at lower temperatures and in view of the fact that the asphaltenes are being viewed as "*complex mixtures in a state of dynamic interexchange*". On the other hand, if one is to assume that the asphaltene's structure does not survive treatment at upgrading conditions, what, then, is the purpose of studying such structures? The issue here appears to be one of rates. Even if one is to assume that at elevated temperatures and pressures "micelles" and even "particles" break down, the question to be answered is, at which rate does this breakdown process occur? Contrary to laboratory reactors, where most of the studies of asphaltene chemical structure have taken place, most industrial reactors are continuous systems. The state of the asphaltene "molecule", therefore, does not only depend on the temperature, pressure, and solvent but also on the reactor's residence time. It is, therefore, very important to have a correct concept of the asphaltene's structure, and, through careful experimentation, one can then decide, whether or not such a concept has any practical implications at realistic upgrading conditions.

CONCLUSIONS

The authors have stated in the introduction that what they hoped to accomplish by the writing of this chapter is to trigger a debate, from which hopefully a complete model of the asphaltene's structure will emerge. The model of the asphaltene's structure used here is simply a broad conceptual macromolecular description of the structure of an asphaltene, which has been shown to be consistent not only with the literature on the detailed chemistry of asphaltenes but also, for the first time, with diffusivity measurements of asphaltenes in model porous membranes. Where one goes from here is not clear. The work of Klein and coworkers [18], who are trying to instill some mathematical formalism in the vast knowledge about the chemical structure of asphaltenes, is certainly in the right direction. It is important, however, to couple such an approach with quantitative statistical descriptions of asphaltene transport through porous systems. A model of the asphaltene's structure must not only be consistent with the knowledge of its chemistry but also with its known transport properties. After all, one should always remember that most upgrading reactors operate under diffusion-limited conditions. The knowledge of its chemical structure is of little value, if the asphaltene is unable to enter the catalyst's porous structure.

ACKNOWLEDGEMENTS

Acknowledgment is made to the National Science Foundation for support of this work. The authors also wish to acknowledge the strong interaction and collaboration with Unocal Science and Technology Division, especially with Dr. Geoffrey E. Dolbear. I.A. Webster thanks the UNOCAL Corporation for permission to participate in this research.

REFERENCES

[1] Bunger, J.W. and Cogswell, D.E., Characteristics of tar sand bitumen asphaltenes as studied by conversion of bitumen by hydropyrolysis. In: J.W. Bunger and C.N. Li (Editors), *Chemistry of Asphaltenes. ACS Adv. Chem. Ser.*, 195: 219 (1981).

[2] McKay, J.F., Amend, P.J., Cogswell, T.E., Harnsberger, P.M. Erikson, R.B. and Latham, D.R., Petroleum asphaltenes: Chemistry and composition. In: P.C. Uden and H.B. Jensen (Editors), *Analytical Chemistry of Liquid Fuel Sources. Tar Sands, Oil Shale, Coal, and Petroleum. Adv. Chem. Ser.*, 170: 128 (1977).

[3] Koots, J.A. and Speight, J.G., Relation of petroleum resins to asphaltenes. *Fuel*, 54: 179 (1975).

[4] Wiehe, I.A., A solvent-resid phase diagram for tracking resid conversion. *Ind. Eng. Chem. Res.*, 31: 530 (1992).

[5] Long, R.B., The concept of asphaltenes. In: J.W. Bunger and C.N. Li (Editors), *Chemistry of Asphaltenes. ACS Adv. Chem. Ser.*, 195: 17 (1981).

[6] Long, R.B. and Speight, J.G., Studies in petroleum composition. Development of a compositional "map" for various feedstocks. *Rev. Inst. Fr. Pét.*, 44: 205 (1989).

[7] Thrash, R.J. and Pildes, R.H., The diffusion of petroleum asphaltenes through well charaterized porous membranes. *Am. Chem. Soc., Div. Pet. Chem., Prepr.*, 26(2): 515 (1981).

[8] Shimura, M., Shiroto, Y. and Takeuchi, C., Effect of catalyst pore structure on hydrotreating of heavy oil. *Am. Chem. Soc. Meet., Div. Colloid Surf. Chem.*, Las Vegas, Nev. (1982).

[9] Baltus, R.E. and Anderson, J., Hindered diffusion of asphaltenes through microporous membranes. *Chem. Eng. Sci.*, 38(12): 1959 (1983).

[10] Baltus, R.E. and Anderson, J., Comparision of G.P.C. elution characteristics and diffusion coefficients of asphaltenes. *Fuel*, 63(4): 530 (1984).

[11] Baltus, R.E., Hindered diffusion of petroleum asphaltenes. In: S. Kaliaguine and A. Mahay (Editors), *Catalysis on the Energy Scene*. Elsevier, Amsterdam, p. 553 (1984).

[12] Kyriacou, K.C., Sivaramakrishna, V.V., Baltus, R.E. and Rahimi, P., Measurements of diffusion coefficients of oil residual fractions using porous membranes. *Fuel*, 67: 15 (1988).

[13] Nortz, R.L., Baltus, R.E. and Rahimi, P., Determination of the macroscopic structure of heavy oils by measuring hydrodynamic properties. *Ind. Eng. Chem. Res.*, 29(9): 1968 (1990).

[14] Sane, R.C., Webster, I.A. and Tsotsis, T.T., A study of asphaltene diffusion through unimodal porous membranes. In: J.W. Ward (Editor), *Catalysis. Proc. 10th North American Meeting of the Catalysis Society, May 1987, San Diego, California.* Elsevier, Amsterdam, pp. 705–716 (1988).

[15] Sane, R.C., Webster, I.A. and Tsotsis, T.T., Hondo asphaltene diffusion in microporous track-etched membranes. *Am. Chem. Soc., Div. Fuel Chem., Prepr.*, 33(3): 237 (1988).

[16] Sane, R.C., *Diffusion of Petroleum Asphaltenes in Porous Membranes.* Ph.D. Dissertation, University of Southern California, Los Angeles, Calif. (1991).

[17] Sane, R.C., Tsotsis, T.T., Webster, I.A. and Ravi-Kumar, V. S., Studies of asphaltene diffusion and structure and their implications for resid upgrading. *Chem. Eng. Sci.*, 47: 2683 (1992).

[18] Savage, P.E., Neurock, M. and Klein, M.T., Asphaltene reaction pathways: A chemical modeling analysis. *AIChE Spring Natl. Meet.*, New Orleans, La., March 6–10 (1988).

[19] Yen, T.F., Erdman, J.G. and Pollack, S.S., Investigation of the structure of petroleum asphaltenes by X-ray diffraction. *Anal. Chem.*, 33(11): 1587 (1961).

[20] Dickie, J.P. and Yen, T.F., Macrostructures of the asphaltic fractions by various instrumental methods. *Anal. Chem.*, 39(14): 1847 (1967).

[21] Mieville, R.L., Trauth, D.M. and Robinson, K.K., Asphaltene characterization and diffusion measurements. *Am. Chem. Soc., Div. Pet. Chem., Prepr.*, 34: 635 (1989).

[22] Speight, J.G., Wernick, D.L., Gould, K.A., Overfield, R.E., Rao, B.M.L. and Savage, D.W., Molecular weight and association of asphaltenes: A critical review. *Rev. Inst. Fr. Pét.*, 40: 51 (1985).

[23] Moschopedis, S.E., Fryer, J.F. and Speight, J.G., Investigation of asphaltene molecular weights. *Fuel*, 55: 227 (1976).

[24] Sheu, E.Y., Liang, K.S., Sinha, S.K. and Overfield, R.E., Polydispersity of asphaltenes in toluene. *Am. Chem. Soc., Div. Pet. Chem., Prepr.*, 35: 813 (1990).

[25] Pfeiffer, J.P. and Saal, R.N., Asphaltic bitumen as colloid system. *Phys. Chem.*, 44: 139 (1940).

[26] Rao, B.M.L. and Serrano, J.E., Viscometric study of aggregation interactions in heavy oil. *Fuel Sci. Technol. Int.*, 4(4): 483 (1986).
[27] Larson, O.A. and Beuther, H., Processing aspects of Va and Ni in crude oils. *Am. Chem. Soc., Div. Pet. Chem., Prepr.*, 11(2): 595 (1966).
[28] Sugihara, J.M., Branthaver, J.F., Wu, G.Y. and Weatherbee, C., Research on metal compounds in petroleum — Present and future. *Am. Chem. Soc., Div. Pet. Chem., Prepr.*, 15(2): C5 (1970).
[29] Fish, R.H., Komlenic, J.J. and Wines, B.K., Characterization and comparision of vanadyl and nickel compounds in heavy crude petroleums and asphaltenes by reverse-phase and size-exclusion liquid chromatography/graphite furnace atomic absorption spectroscopy. *Anal. Chem.*, 56(13): 2452 (1984).
[30] Reynolds, J.G., Biggs, W.R., Fetzer, J.C., Gallegos, E.J., Fish, R.H., Komlenic, J.J. and Wines, B.K., Molecular characterization of vanadyl and nickel non-porphyrin compounds in heavy crude petroleums and residua. *Collect. Colloq. Semin. (Inst. Fr. Pét.)*, 40: 53 (1984).
[31] Reynolds, J.G., Characterization of heavy residua by application of a D 2007 separation and electron paramagnetic resonance. *Liq. Fuels Technol.*, 3(1): 73 (1985).
[32] Biggs, W.R., Fetzer, J.C., Brown, R.J. and Reynolds, J.G., Characterization of vanadium compounds in selected crudes I. Porphyrin and non-porphyrin separation. *Liq. Fuels Technol.*, 3(4): 397 (1985).
[33] Jacobs, F.S. and Filby, R.N., Nickel and vanadium in chromatographic fractions of petroleum asphaltenes. *Am. Chem. Soc., Div. Pet. Chem., Prepr.*, 28(3): 758 (1983).
[34] Ignasiak, T., Kemp-Jones, A.V. and Strauss, O.P., The molecular structure of athabasca asphaltene. Cleavage of the carbon-sulfur bonds by radical ion electron transfer reactions. *J. Org. Chem.*, 42(2): 312 (1977).
[35] Suzuki, T., Itoh, M., Takegami, Y. and Watanabe, Y., Chemical structure of tar-sand bitumens by ^{13}C and ^{1}H NMR spectroscopic methods. *Fuel*, 61: 402 (1982).
[36] Holy, N.L., Reactions of the radical anions and dianions of aromatic hydrocarbons. *Chem. Rev.*, 74: 243 (1974).
[37] Speight, J.G. and Moschopedis, S.E., On the molecular nature of petroleum asphaltenes. In: J.W. Bunger and N.C. Li (Editors), *Chemistry of Asphaltenes. ACS Adv. Chem. Ser.*, 195: 1 (1981).
[38] Hausler, D.W. and Carlson, R.S., Online SEC-ICP: A new element specific molecular size tool for the petroleum industry. *Am. Chem. Soc., Div. Pet. Chem., Prepr.*, 30(1): 28 (1985).
[39] Savage, P.E. and Klein, M.T., Asphaltene reaction pathways, 3. Effect of reaction environment. *Energy Fuels*, 2: 619 (1988).

Asphaltenes and Asphalts, 1. Developments in Petroleum Science, 40
edited by T.F. Yen and G.V. Chilingarian

Chapter 16

POLYMER-MODIFIED BITUMEN *

CARLO GIAVARINI

INTRODUCTION — THE ROLE OF BITUMEN MODIFIERS

Bitumen plays a large part in determining many aspects of road performance. For many years, conventional bituminous materials performed satisfactorily. Today we are expecting more from asphalt pavement, and demands made upon roads increase year by year. Traffic grows every day and better performance is needed, including higher standards of safety and comfort. Moreover, maintenance work must be reduced both for practical and economic reasons; in fact, besides the maintenance-work cost, interruption of traffic flow during maintenance work is a considerable cost to society.

Special bituminous materials are also needed by the building industry for waterproofing, insulation, noise reducing, bridge decking, and for other uses. A wide range of modified bitumens now exists, which enable the engineer to meet this challenge.

For many years modified bitumens have been developed especially for industrial uses, adding fillers, fibers, rubber and polymers. Polymer-modified bitumens (PMBs) became commercial products with the creation of the "membranes", i.e., of reinforced bitumen sheets containing thermoplastic or elastomeric products widely used in Europe for impermeabilization [1–3].

Among the first polymeric materials to be used was a cheap, waxy material obtained as a waste by-product during polypropylene production: atactic polypropylene (APP) [4]. APP is no longer produced in many countries, due to the introduction of new, high-yield units for propylene polymerization.

In the last twenty years, a wide spectrum of modifying polymeric materials have been experimented with for bitumens used in road construction [5–8]. A detailed report on the state-of-art updated to 1982 was presented by Boutevin et al. [9] and Zenke [10,11].

One of the prime roles of a bitumen modifier is to increase the resistance to permanent deformation at relatively high temperatures, without adversely affecting the properties of the bitumen at low temperatures. This can be obtained either by increasing the elastic component of the bitumen, thus improving its flexibility, or by stiffening the bitumen, and so reducing the total viscoelastic response. Alternatively,

* As pointed out in the Introduction (Chapter 1), in the United States the term *asphalt* is used instead of *bitumen*.

it is possible to reach the same structural strength with a thinner layer of modified bitumen [12].

Ageing and adhesivity are two other characteristics of considerable importance which can be improved by a modifier.

Polymer-modified bitumens have a price higher than that of normal bitumens, and will surely not replace them in many areas of application where their use is sufficient.

Possible areas of application are: airports, busy motorways and city roads, special surfaces such as drainasphalt and thin layers, surface dressing for high traffic, slurry seals, bridges and tunnels, crossroads and parking areas for trucks, and renovation of concrete roads.

The so-called drainasphalts, rich in voids and permeable, are mainly used to prevent aquaplaning and to improve skid resistance: they are of interest also because of their noise-reducing effect.

Thin layers, having a thickness of 1.5 to 2.5 cm, are produced in most countries with modified bitumens. They are more homogeneous and durable, and are also applied on renovation or rutting.

Along with synthetic polymers, reclaimed rubber powder and waste polymeric products such as polyethylene and polypropylene are also being used in some countries [13–15].

TYPES OF POLYMERIC MODIFIERS

For a polymer to be effective, it must blend with the bitumen and improve resistance at high temperatures without making the bitumen too viscous at mixing temperatures or too brittle at low temperatures. If used in road asphalt, it should be capable of being processed by conventional equipment.

In any case, it must be available and cost-effective, being physically and chemically stable during storage, application, and service. Major problems are the solubility of polymer in bitumen and stability of the modified product.

The main groups of polymers used as bitumen modifiers are the following: (1) thermoplastic polymers, (2) natural and synthetic rubbers, (3) thermoplastic rubbers, and (4) thermosetting polymers.

In actual modified bitumens, mainly thermoplastic rubbers, as well as some thermoplastic polymers, are used. Natural and synthetic rubbers are hardly applied and thermosetting resins are used only for special applications.

The polymer portion ranges from about 2 to 10% by weight, the most used being around 5%. Processing viscosity and cost play a major role. Due to the low cost, waste polymeric products can reach percentages as high as 25%.

In some cases, two different polymers are added simultaneously, in order to confer to the modified bitumen the respective characteristics [16,17].

Let us now point out the differences between different types of polymers added to bitumens, and the influences affecting the preparation and use of the modified bitumens.

It is very important to remember that for each class of polymers there are different molecular weights, structures, viscosities, etc., and that in each case proper characteristics of the actual polymer should be studied for the use in PMBs.

Thermoplastic polymers

Thermoplastic polymers are characterized by softening on heating and hardening on cooling. Polyethylene (PE), atactic and isotactic polypropylene (APP, IPP), polyvinylchloride (PVC), polystyrene (PS), ethylene vinylacetate (EVA), and methylacrilate (EMA) are the main polymers of this group experimented as modifiers; PE, APP, EVA and EMA have been commercially applied.

Thermoplastic polymers associate at room temperature with bitumen, increasing its viscosity; however, they do not significantly confer any element of elastic deformation to bitumen, and can separate when heated.

The finer the polymer is distributed without losing its special structure or being completely dissolved, the more stable is the blend.

Polymonoolefin polymers do not contain double bonds and, therefore, have good thermal and aging resistance, but it is difficult to disperse them in the bitumen without segregation, unless low molecular weights are reached [2,18,19]. The performance is usually poor and it is necessary to add large quantities (5–10%), with the possibility of phase inversion and separation from the mixture.

PE and APP have been the subject of numerous researches and have found a number of industrial uses [1,6,7], but few road applications [20,21].

Dispersibility and stability appear to increase when crystallinity is decreased and chain ramification is increased, starting from the quasi-paraffinic chain of PE to its various homologues (Fig. 16-1) [2,9,18].

High-pressure, low-density PE, being more branched has a lower tendency to associate and separate than high-density PE.

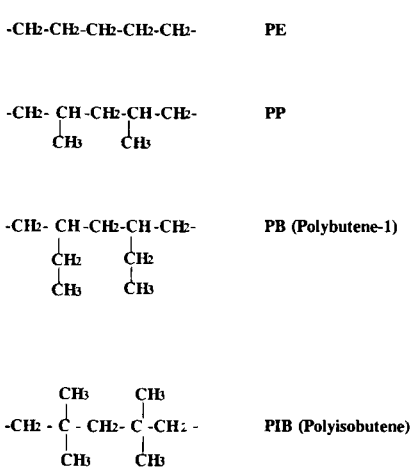

Fig. 16-1. Polyethylene and its homologues.

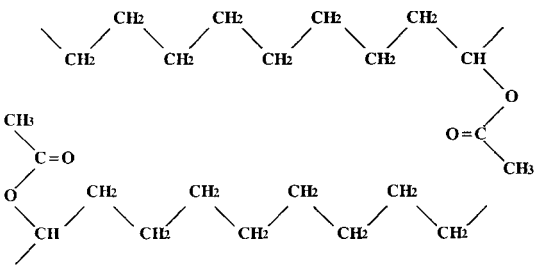

Fig. 16-2. Typical structure of EVA copolymers. The number of CH_2 groups in the crystalline region is much higher than represented.

The replacement of the lateral chains by benzene rings, as in PS or by chlorine, as in PVC, does not help dispersibility and homogeneity of PMB.

Especially important are some copolymers based on ethylene, such as ethylene–propylene copolymer (EMP), ethylene vinylacetate (EVA) and ethylene methyl-acrilate (EMA).

The larger side groups of EVA and EMA increase the resistance to separation, and improve performance. EVA and EMA introduce elements of adhesion, because of the polar groups, and of elastic deformation.

EVA copolymers have become very popular in this field. They are thermoplastic materials with a random structure whose properties are controlled by molecular weight and vinyl acetate content [22–24].

Vinyl acetate groups disrupt the closely packed arrangement of the polyethylene segments to give non-crystalline or amorphous regions (Fig. 16-2).

The thermal stability of EVA is significantly weaker than that of PE, but remains sufficient for the use in polymer-modified bitumens [25,26].

The presence of ethylene in polypropylene chains (EPM) reduces polymer crystallinity and improves compatibily.

Natural and synthetic rubbers

Natural rubber (NR) and synthetic rubbers such as polybutadiene, polyisoprene, butyl rubber, styrene–butadiene rubber (SBR), and polychloroprene have all been tested with bitumen.

NR is sensitive to decomposition and oxygen absorption. It has a molecular weight too high to be directly dissolved in the bitumen, and must be partially decomposed and mechanically homogenized. Natural and synthetic rubbers are better dispersed in the form of latex.

In general, synthetic rubbers made by polydiolefins, are easier to incorporate in bitumen than polymonoolefins, and confer characteristics of elasticity more evident than thermoplastic materials.

The double bonds contained in all chains can lead to a partial decomposition of the polymer chain by heating or in the presence of oxygen, and are the reaction points for cross-linking (vulcanization). "Vulcanizated" bitumen with improved duc-

tility and elasticity can be produced by adding sulfur and a catalyst to the bitumen–rubber mixture.

In the form of reclaimed tire crumb, rubber is directly used in vulcanized state. In order to be dispersed in the bitumen, it requires high temperatures and long digestion times [13,15,27]. If not partially de-vulcanized, it produces a heterogeneous binder with the rubber acting mainly as a flexible filler.

Thermoplastic rubbers

The thermoplastic elastomers used as bitumen modifiers are block copolymers of mono- and diolefins. The monoolefin is usually styrene, whereas the diolefin is butadiene or isoprene. They are synthesized in the SBS (or SIS) form, where S represents the polystyrene and B (I) the polybutadiene (polyisoprene).

These linear polymers show similar behavior to that of a crosslinked network, due to the fact that the polystyrene end-blocks aggregate into domains which at room temperature act as glassy network junctions for the elastic polybutadiene chains (Fig. 16-3). These materials, therefore, derive their strength and elasticity from a physical cross-linking of the molecules into a three-dimensional network. They become fluid and moldable at high temperature (>100°C), unlike the normal chemically crosslinked rubbers [28,29].

Polystyrene end-blocks give strength, whereas the polybutadiene mid-chains give the polymer its exceptional elasticy. The glassy polystyrenic domains are present in reasonable proportion, about 30 vol%, to provide reinforcement

SBS block copolymers are prepared not only in the linear form, but also in the form of a ramified copolymer with 3 or 4 threads parting from a central point (Fig. 16-4). Such "multi-armed" polymers are often referred to as star-shaped or radial SBS (rSBS)

All thermoplastic rubbers introduce into the bitumen strong elements of elastic deformation and allow stable dispersions to be achieved. Resistance to heat and to oxidation is lower than that of polyolefins due to the presence of double bonds in the main chain.

Different types of SBS copolymers, especially rSBS, have been used as bitumen modifiers in many countries under different trade names [4,10,12,28,30,31].

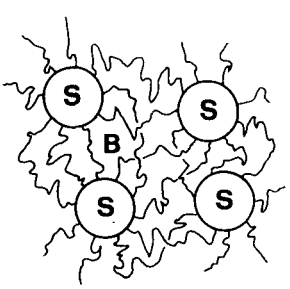

Fig. 16-3. Schematic structure of a SBS thermoplastic rubber. Average molecular weight is 10,000–15,000 for polystyrene (*S*) and 50,000–70,000 for polybutadiene (*B*).

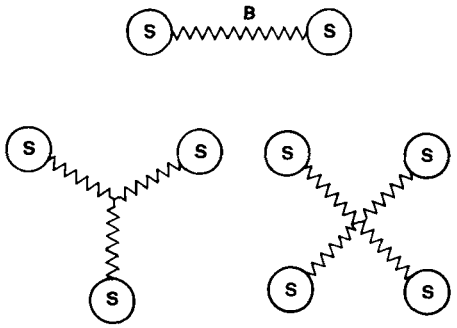

Fig. 16-4. Linear and radial SBS molecules.

Another thermoplastic elastomer experimented with in PMB preparation is EPDM (ethylene–propylene-diene), obtained by polymerizing a diene, usually ethyliolene norbornene, with the ethylene–propylene copolymer (EPR). The lateral olefinic groups, with double bonds and great volume, have higher capacity of dispersion and improved performance (elastic behavior), compared to PE and EPM copolymers [11,32].

The lateral double bond of the diene components creates the possibility of a subsequent reticulation in bitumen. Miscibility of EPDM with bitumen is not easy, and sometimes air blowing is applied to produce less unstable PMBs through formation of some crosslinking.

Ethylene–propylene rubbers (EPR) are thermoplastic rubbers containing some 50–60% ethylene, which are easily mixed with bitumen, providing that molecular weight and viscosity are properly chosen [18,19].

Interesting products are described containing a new class of heterophasic polyolefin copolymers [18,19] which show a behaviour similar to that of SBS polymers.

Table 16-1 shows the characteristics of a number of PMBs containing 6% of various polymers [18,19].

TABLE 16-1

Bitumens modified with 6% by weight of various polumers [18]

Polymer	R & B ASTM D-36 (°C)	Penetration ASTM D-5 (1/10 mm)	P.I.	Elastic recovery (%)	Stability R & B (°C)		Aging ASTM D-2872	
					upper	lower	% R & B	% pen
None	44	133	0.0	10	–	–	+9	−45
APP	47	145	1.3	10	55	45	–	–
LDPE	98	41	8.2	0	>100	52	+6	−18
EMA	63	61	2.1	45	65	63	+3	−13
EPDM	66	50	2.2	75	87	52	+3	−20
EPR	58	56	−1.0	75	60	50	+10	−30
SIS	66	82	3.6	85	54	52	−6	−20
SBS	98	72	7.5	95	>100	61	−34	−27

Thermosetting polymers

Once applied, thermosetting polymers do not soften when heated. They are not widely used in road paving, due to the high cost and special method of application; however, the properties they confer to the bitumen are quite good.

The best known products are based on epoxy resins [12,33,55]. They are applied by blending two components, one containing the resin and the other a hardener, which react chemically to form a strong three-dimensional structure.

Blended with bitumen in substantial amount, epoxy resins display the properties of modified thermosetting resins rather than those of bitumens. When the two components (resin and hardener) of a thermosetting resin are mixed, the usable life of the binder is limited.

The cured modified bitumen does not exhibit viscous flow and is very resistant to attack by chemicals, including solvents and fuels.

If the resin content is not too high, the bitumen softens and flows as temperature increases; but it is much less temperature-susceptible and virtually unaffected by temperature changes experienced on a road. Since its introduction in the sixties, epoxy asphalt has been used in a variety of special situations, including airport paving and bridge surfacing [33].

INFLUENCE OF BITUMEN CONSTITUTION

Major problems during preparation and use of PMB are homogenization of the polymer in bitumen and stability of the modified products. In other words, the polymer must be compatible with the bitumen and maintain such compatibility during storage and use. This is not an easy task to accomplish, because the two components of PMB have different chemical structure, and very different molecular masses, viscosities and densities.

The problem of compatibility is complicated by the existence of many types of bitumens whose differences not only depend on the composition of the original crude, but also on the production process [34]. In all cases there is a close connection between polymer type and bitumen composition, which allows satisfactory mixtures to be obtained. Very important is the content of bitumen components which act as solubilizers or swelling agents for the polymer. For example, in PMBs with high contents of APP (20–30%) the asphaltene-resin phase is finely dispersed in the swollen polymer, and the bitumen should be rich in saturates with high molecular weight [4]. A similar behavior is shown by other polyolefinic thermoplastic polymers.

On the other hand, the bitumen suitable for SBS blends should have a high aromatic and low asphaltene content. Tests on mixtures obtained from previously separated fractions and SBS showed definite incompatibility between polymer and asphaltenes, and good dispersion both for aromatics and resins [35]. Asphaltene content seems to be the most important chemical parameter also for EVA-modified bitumens [26].

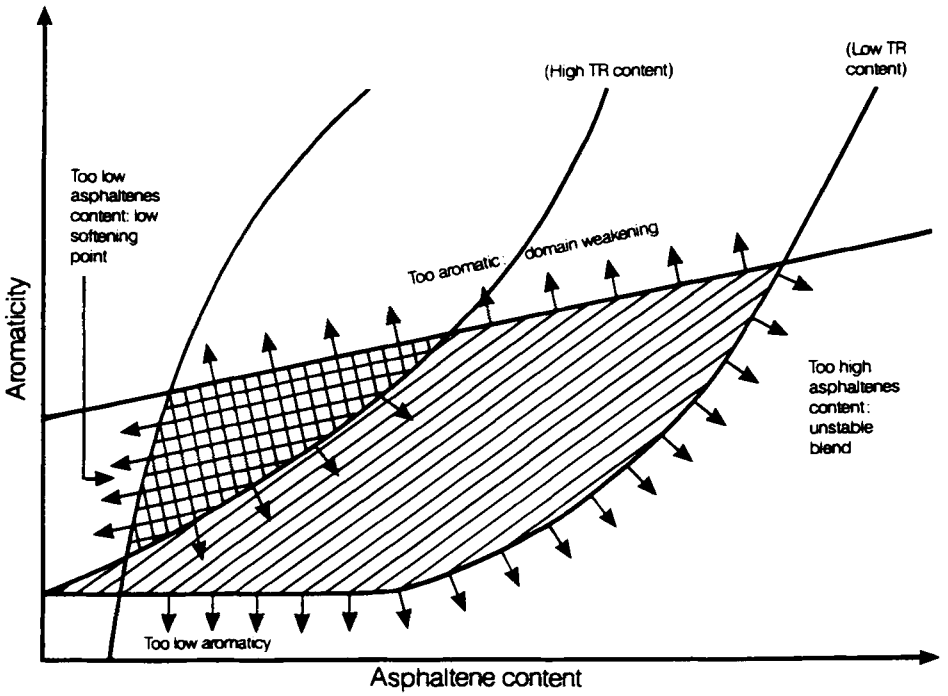

Fig. 16-5. Influence of bitumen composition on bitumen–SBS blends. (After Whiteoak [12].)

During the mixing step at high temperature, the aromatic components of the bitumen swell the polystyrene blocks of the SBS polymer, stretching the connecting polybutadiene chains. Cooling the mixture, the swollen polystyrene blocks cannot reach the initial position and the polybutadiene chains remain stretched, wrapping the bitumen components, which have not contributed to the polystyrene swelling. With bitumens having poor aromatic content, only the temperature is responsible for the block swelling, and the original structure is reached by cooling. In this case, no lattice is formed in the bitumen.

A number of authors [4,26,35,37–39] have studied the complex interrelationships between polymer and bitumen components, suggesting some graphic correlations (see Figs. 16-5 and 16-6, for example).

In conclusion, the main factors influencing compatibility and stability, besides the amount, structure and molecular weight of the polymer, are the following: (1) amount and molecular weight of the asphaltenes, (2) aromaticity of the maltene phase, and (3) storage temperature. Moreover, density and viscosity of both bitumen and polymer play an important role.

Bitumens obtained by thermal processes, such as visbreaking [40] contain free radicals which could react with the double bonds of some polymers [34]. In this case, it is more difficult to ascertain correlations for bitumen–polymer compatibility.

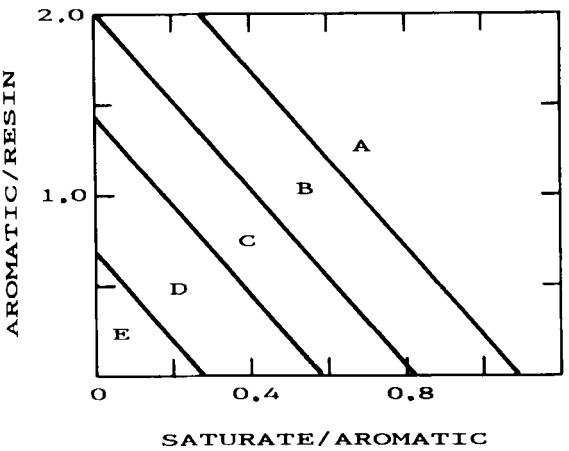

Fig. 16-6. Compatibility domains for bitumen–polymer mixture: *A*: Excellent mixes with 20% EP copolymer; *B*: good mixes with 10% EP and 10% APP; *C*: good mixes with 20% APP; *D*: satisfactory mixes with 10% SBS; *E*: bitumens with very high aromaticity. (After Costantinides et al. [36].)

In certain cases, special petroleum fractions are added to the bitumen in order to improve the compatibility. For SBS blends the technique of adding aromatic oils (e.g., furfural extracts) assumes that the aromatic and resin contents of the bitumen has to be sufficient for both asphaltene and rubber peptization [37,39]. Pyrolysis oils and fatty acid residues are also used as compatibilization agents [41].

MANUFACTURE OF THE POLYMER-MODIFIED BITUMENS

Different procedures have been developed to produce and process PMBs. Besides polymer and bitumen, a certain amount of energy is needed. The main factors influencing the dispersion rate are: (1) particle size of the polymer, (2) temperature, and (3) shear acting on the particles.

Mixing temperatures are usually in the range of 150–200°C or more; a number of mixers can be used (Fig. 16-7). It is claimed [43,12] that the most effective and economic system for dispersing SBS-like polymers in bitumen is the colloid mill (Fig. 16-8).

Mixing at high temperatures can be carried out in the presence of nitrogen in order to avoid oxidation of the polymer and of the bitumen or, on the contrary, can be helped by blowing air to improve compatibility, as in the case of EPDM.

Mixing time ranges from a few minutes to many hours. Optimum blending time is reached when the desired PMB properties of softening point, penetration and viscosity become constant due to good polymer dispersion, and before viscosity increase due to bitumen oxidation. Figure 16-9 shows an example of the evolution of viscosity and softening point for a thermoplastic polymer as a function of mixing time. Non-stable mixes must be continuously stirred before application.

Method	Mixer Design	Principle
Batch	Horizontal single shaft	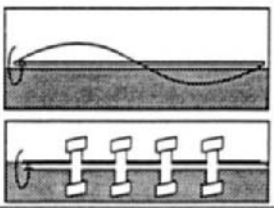
	Vertical single shaft	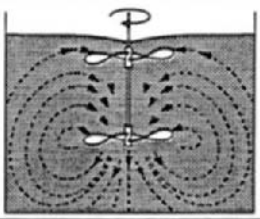
	Vertical Double shaft	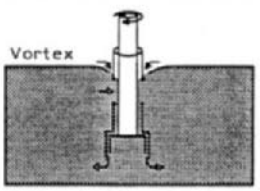
On line and systems	Rotor / Stator or Gear system	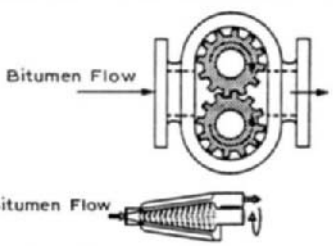

Fig. 16-7. Types of mixing equipment used to produce PMBs. (After Exxon [42].)

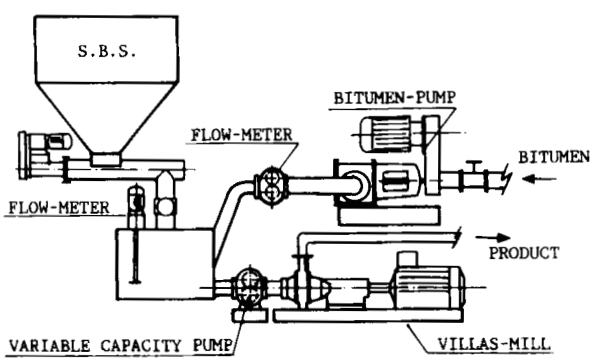

Fig. 16-8. On line blending of a thermoplastic rubber with a bitumen. (After Gerhard [43].)

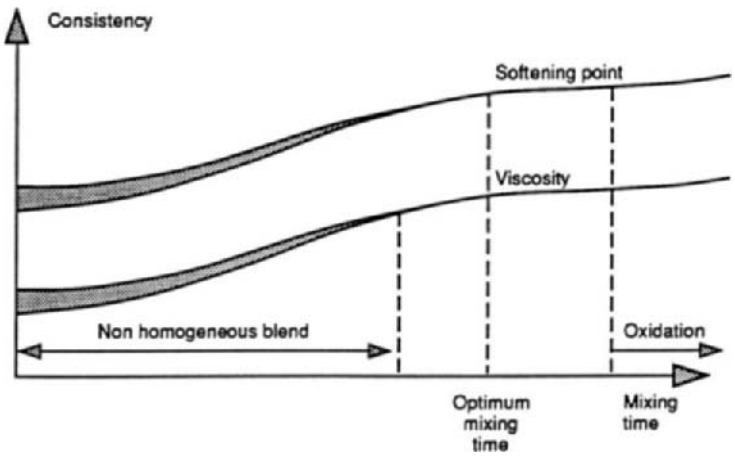

Fig. 16-9. Determination of optimum blending time for EVA–bitumen mixes. (After Exxon [42].)

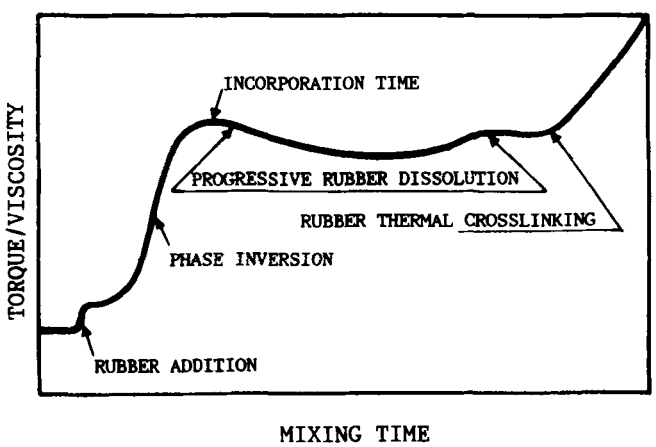

Fig. 16-10. Typical viscosity (torque)–time profile for bitumen–SBS mixes. (After Diani and Gargani [30].)

In the case of SBS mixes, the profile of the viscosity as a function of the mixing time, has the typical trend shown in Fig. 16-10. After rubber addition a viscosity (torque) increase is observed due to the progressive incorporation of rubber into the bitumen. In quite a short time, the rubber becomes the continuous phase of the mix and the bitumen acts as a plasticizer. Viscosity still increases and reaches a maximum followed by a decrease, probably due to the progressive swelling of polystyrene domains. The best properties of PMB correspond with the maximum. At very long times, a sudden and irregular increase takes place, due to thermal crosslinking of the polybutadiene [30].

Swelling and compatibilizing oils are sometimes added to improve mixability and stability of the final product [39,41].

Depending on the quantity of the added polymer and on its cost, sometimes PMBs are referred to as "hard" or "soft" mixes. PMBs are generally not produced by petroleum refineries owing to the special character of the production, but by special companies called "blenders", or by the road makers.

In the first case, the road maker uses hot ready-mixed products in its mixing plant. In the latter, the polymer is added in liquid (e.g., latex) or solid form (granules, powder, blocks, etc.) to the bitumen, either by modification of the bitumen prior to adding it to the asphalt mixing plant, or by adding the polymer directly into the asphalt mixing equipment.

The production of larger quantities at a central location (blender) offers a number of advantages in comparison with the modification at the mixing plant; however, the demand of thermostability and resistance to separation is higher. In any case, conventional equipment may be used to apply PMBs on the road.

PMBs can be produced, although less frequently, in the form of emulsions [44].

PROPERTIES OF POLYMER-MODIFIED BITUMENS

Microscopic structure

The properties of PMAS depend on the degree of dispersion of both polymeric and bituminous phases: the finer the dispersion of the polymer, the better is the mixture. Generally, coarse dispersions tend to separate and the polymer behaves as a filler. The first and most important test to be applied to a PMB should be the observation of its structure by reflection microscopy. The visualization technique is based on the use of the fluorescence by UV stimulating light [38,45]. The bituminous phase does not show any noticeable fluorescence, whereas the dispersed polymer produces a yellow-greenish fluorescence.

At the microscopic level, most PMBs exhibit a pronounced heterogeneity, so that they can be considered as biphasic mixtures. A distinction is made between PMBs whose continuous phase is a polymer matrix (in which bitumen globules are dispersed), and PMBs whose continuous phase is a bitumen matrix.

Depending on the type of polymer, a great variety of forms can be observed. The examination of a number of commercial products [45] showed that many of them were in the form of a dispersion, fine or coarse, of polymer globules in a continuous bituminous phase (Fig. 16-11).

Typical coarse dispersions are those made by adding a polymer to non-compatible or scarcely compatible bitumens. Fine dispersions can be obtained with polymers like EVA and some thermoplastic rubbers, providing that the bitumen is suitable and the mixing process is proper.

By increasing the polymer percentage and time of mixing, a phase inversion can be observed which causes a real modification of the structure of PMB and an important change of its properties.

For example, by mixing small percentages (1–2%) of SBS with a compatible bitumen, the microscope shows only a partial swelling of the dispersed polymer

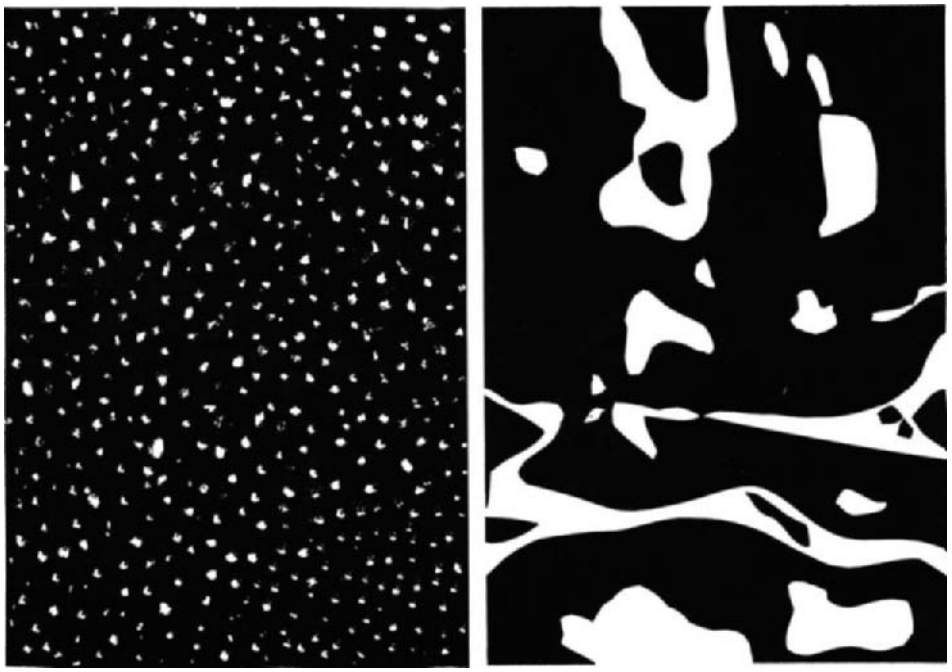

Fig. 16-11. Typical microscopic structure (250×) of polymers dispersed in bitumens. Left: Fine dispersion (1% SBS). Right: Coarse dispersion (4% SBS).

particles, with no interaction among them. By increasing the SBS content, a network (or sponge-like structure) is formed which includes the other bitumen particles not previously involved in polymer swelling (Fig. 16-12).

In general, the rheological properties of PMBs depend more on the properties of the continuous phase than on those of the dispersed phase. In fact, in PMB with polymeric matrix the rheological behavior of thermoplastic polymers such as PE is inferior to that of a thermoplastic rubber like SBS, which shows a "physical vulcanization". In PMBs with bitumen matrix, the polymer behaves as a plastic or elastic filler.

Bitumens poor in asphaltenes and rich in aromatics can dissolve certain polymers by hot mixing. A monophasic system is then obtained where the polymer is completely dissolved in the aromatic oils of the bitumen. The mechanical properties of such materials are usually poor.

Storage stability

An important feature for a wide application of PMBs is their storage stability. During storage at high temperatures, the polymer must not separate from the bitumen components and the PMB must not change its consistency too much. This is a minor concern for the manufacture of industrial products, such as

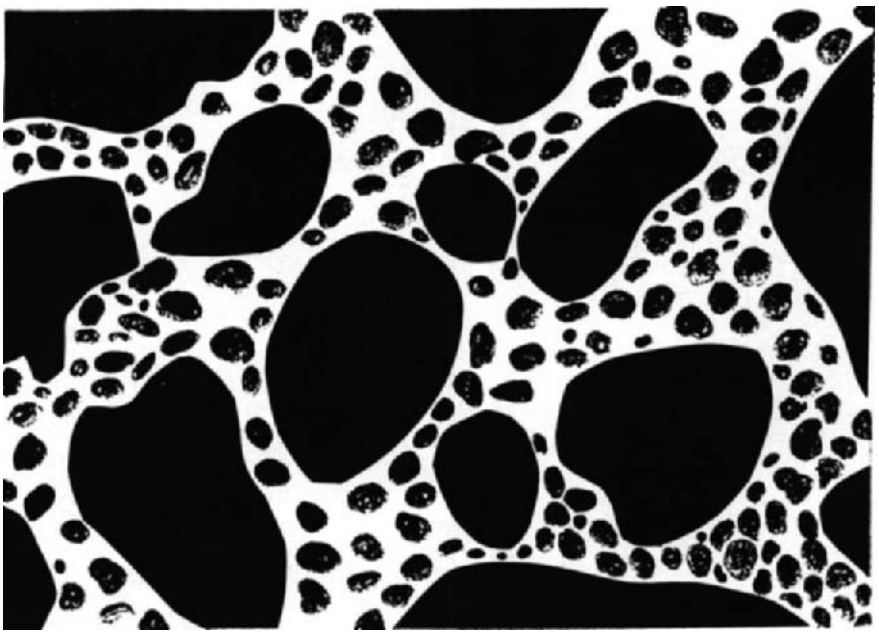

Fig. 16-12. Structure (250×) of a bitumen dispersed in a polymer (5% SBS).

the membranes, and for the mixes prepared just before application on the road.

There are a number of methods, more or less empirical, to measure the hot-storage stability. The binder can be kept in a vessel with three discharge arms along its length to enable the top, middle, and bottom thirds to be obtained separately. Penetration and softening point is then measured on the upper and bottom third [12].

Other methods use aluminum tubes, such as tooth-paste tubes, filled with the binder [46]. The closed tube is vertically stored for five days at high temperature (e.g., 160°C). After cooling, the aluminum is peeled off and the specimen is cut in three equal parts; top and bottom softening points are then measured. If the difference between the two parts is less than 2–3°C, the PMB is not stirred in the tank during storage and application.

Figure 16-13 shows typical differences between compatible and incompatible systems.

Rheological properties

Along with an increase in consistency, polymer modification changes the rheological properties considerably [47]. The effects of a modification depend on many factors and may vary considerably. Due to the complexity of the subject, one cannot generalize, and the quality of PMBs is not easily described by the conventional test methods.

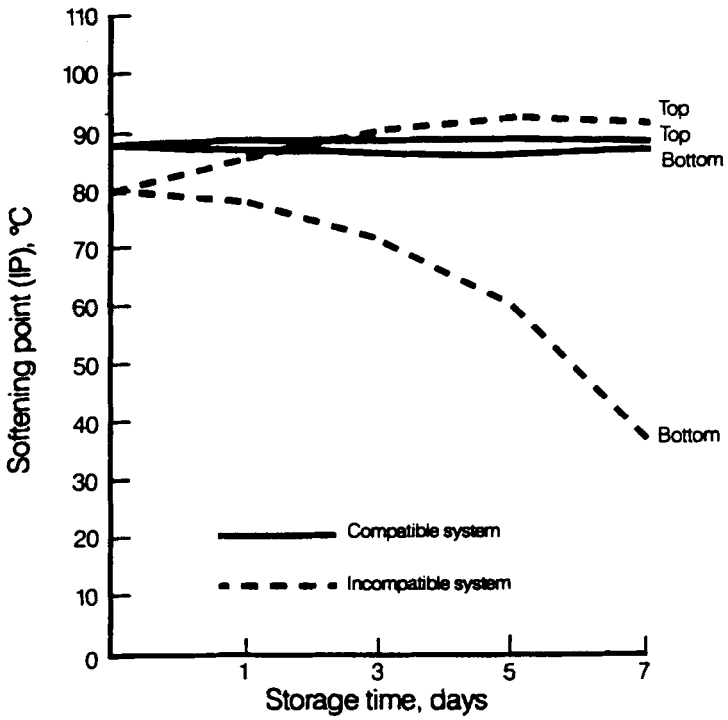

Fig. 16-13. Storage stability of compatible and incompatible PMBs. (After Whiteoak [12].)

All polymers, especially plastomers, increase the viscosity of the bitumens. The increase depends on type of polymer, molecular weight, and concentration. Among thermoplastic polymers, EVA is claimed to produce minimal viscosity changes compared to competitive products [23]. Typically, the addition of 5% EVA reduces the binder by one grade; thus:

200 pen + EVA ⟶ 100 pen
100 pen + EVA ⟶ 70 pen
70 pen + EVA ⟶ 50 pen

The range of plasticity is extended by thermoplastic polymers, with a reduction of temperature susceptibility. Generally, the breaking point does not rise, in comparison with the original bitumen, when the softening point increases sensibly. Figure 16-14 shows typical correlations between softening points of some polymer types and their concentration in the PMB.

A good PMB should have a relationship between viscosity and temperature of the type shown in Fig. 16-15. At high service temperature, e.g. 60°C, it should be significantly stiffer than the bitumen, in order to be more resistant to deformation. At low service temperature, e.g., below zero °C, it should be more flexible than the bitumen and, therefore, more resistant to cracking.

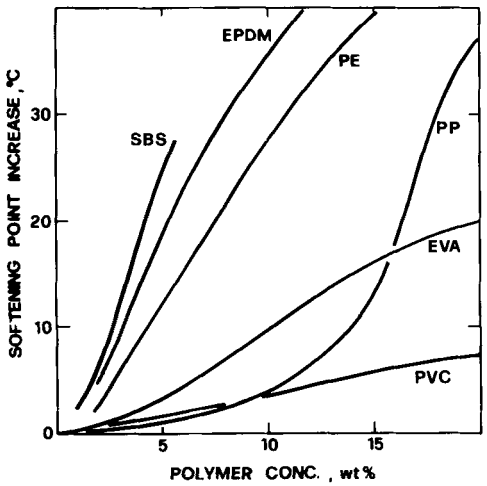

Fig. 16-14. Typical correlations between softening point of some polymer types and their concentration.

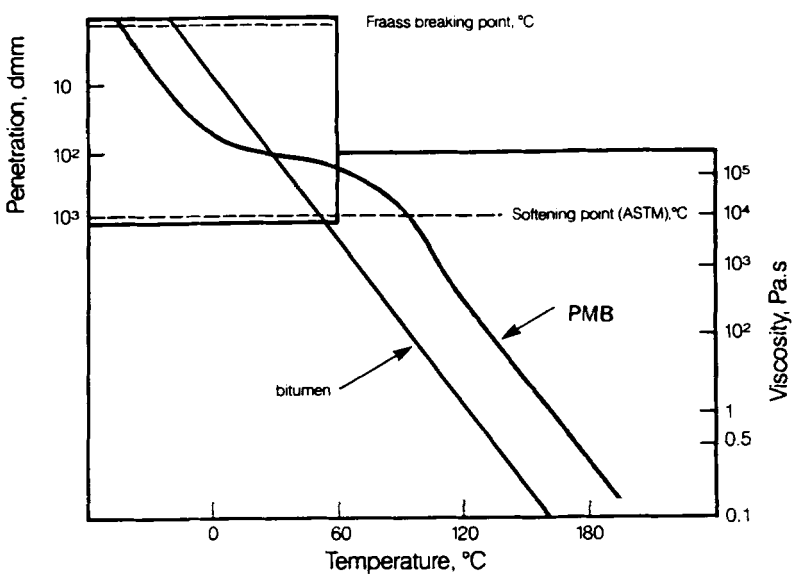

Fig. 16-15. Relationship between viscosity and temperature. (After Whiteoak [12].)

Thermoplastic rubbers, which form a three-dimensional structure in bitumen, greatly improve elasticity and give extra strength and ductility. Overemphasis of the elastic component within the standard viscoelastic model, however, may also have undesirable effects [48].

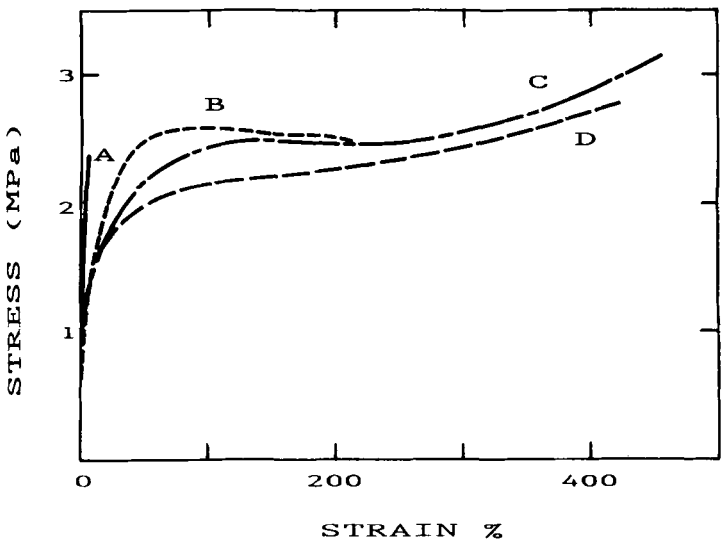

Fig. 16-16. Typical stress–strain curves (−10°C, 500 mm/min) of PMB with bituminous continuous phase (*A*); polymeric continuous phase, but coarse dispersion (*B*); polymeric continuous phase and fine dispersion (*C* and *D*). (After Brûlé and Brion [38].)

Other properties

In addition to the mentioned higher consistency and reduced temperature susceptibility, PMB may show special properties, such as elastic recovery, improved cohesion and adhesion, and different aging characteristics. With conventional test methods, these properties can only be incompletely registered.

The force–ductility test [49,50] and other modified ductility tests [32] have been proposed to discriminate between bitumens with different polymer additives and to measure the elastic recovery. Stress–strain tests are also applied, especially at low temperatures [38]. Figure 16-16 shows the difference between a PMB having a bitumen matrix and other PMBs with polymeric matrix.

The degree of improvement in deformation resistance has been demonstrated by wheel-tracking tests, whereas the degree of improvement in flexibility has been quantified by constant strain fatigue tests [12]. A good comparison is possible with wheel-tracking tests and dynamic tests.

A number of experiments have shown that many commercial modified binders have higher resistance to stripping [49], proving that cohesion and elastic behavior are not too strong [48].

Rheology and microstructure of aged PMBs have been studied by Lenoble [51]. It was observed that the creation of asphaltenes by aging can displace the microstructure of PMBs, and this change could have a significant impact on the rheological properties of the blend. For compatible systems, the aging phenomena increase the overall viscoelastic character and decrease the high-temperature susceptibility of

the binders. For non-compatible systems, the short-term aging is usually a further damaging factor for the performance of PMBs. A problem is whether PMBs can be re-used in the original or other applications (e.g., road asphalt recycling). With PMBs having stable structure and properties, and when the number of different classes of polymers used in PMBs is limited, this problem is easily solved.

PRODUCTS AND APPLICATIONS

A great number of PMBs and of polymers for the modification of bitumens are offered in the market. Along with the main petroleum and petrochemical companies, there are many medium and small companies which offer or use such materials. The products of the big companies are those of major importance. Most of such products are based on various SBS types; however, commercial products exist containing EVA, PE, SBR, EPDM and other polymers. Some companies, especially bitumen manufacturers, offer different types of PMBs for different purposes and climatic conditions. Petrochemical companies are increasingly interested in producing new and suitable polymers for PMBs, owing to the huge potential market for these products.

Industrial and road applications of PMBs are described in technical literature [6,7]. In France, experimental road sections have been set up since 1963, using bitumens modified with natural or synthetic rubbers; they were followed by other investigations and applications [52]. In the late eighties, some 8% of the bitumen used in France was PMB [53].

The Italian "Società Autostrade" started the experimental applications in 1972 on national motorways with a SBR-latex-modified bitumen and since then has laid out many miles of asphalt cement modified with various polymer types [21,54]. Applications are known in many other countries.

It appears that PMBs provide sound solutions to a number of technical problems related to road construction, and that most of them achieve this with minimal changes to established working practices. A lot of work has been done, but much is still left, to develop both the materials and the knowledge of their potential; not forgetting the economic aspects, which play an important role for the future development of PMBs.

ACKNOWLEDGEMENTS

The author wishes to thank Dr. U. Petrossi of Exxon Chemical for useful information.

REFERENCES

[1] *Proc., Bitumen Technol. Conf. (Progressi nella Tecnologia dei Bitumi)*. September–October, Milan, pp. 44–136 (1981).

[2] Matthieu, L. and Pagnini, D., Aging of polyalphaolefin modified bitumen for roofing membranes. *Proc. Int. Symp. on Roofing Technology*, Montreal, Que., pp. 459–466 (1991).
[3] *6th Int. Conf. Roofing and Waterproofing Worldwide*. London, May (1986).
[4] Costantinides, G., Lomi, C. and Schromek, N., Studio su mescole con APP. *Riv. Combust. ((Milan)*, 39(1): 1–14 (1985).
[5] *Proc., Int. Symp. on Chemistry of Bitumens*, Roma, June, Section G. Western Research Institute, Laramie, Wyo. (1991).
[6] *Proc. 3rd Eurobitume Symp.*, The Hague, September, Sect. IV, 1: 479–700 (1985).
[7] *Proc. 4th Eurobitume Symp.*, Madrid, October, Sect. I, 1: 25–327 (1989).
[8] *Rilem Seminar on Formulation, Control and Behaviour of Polymer Modified Bitumens either for Waterproofing or for Road Construction*. Dubrovnik, September (1988).
[9] Boutevin, B., Pietrasanta, Y. and Robin, J.J., Bitumen-polymer blends for coatings applied to roads and public constructions. *Progr. Org. Coatings*, 17: pp. 221–249 (1989).
[10] Zenke, G., *Verbesserung des Verformung swiderstandes durch polymermodifizierte Bitumen*. FA 7028, Bundesminister für Verkehr, Bonn (1982).
[11] Zenke, G., Polymermodifizierte Strassenbaubitumen im Spiegel von Literaturergebmissen. Versuch eines Resumees. *Die Asphaltstrasse*, Vols. 1, 4, 6 (1985).
[12] Whiteoak, D., *The Shell Bitumen Handbook*. Shell Bitumen UK, Surrey, pp. 149–168 (1990).
[13] Bednar, K., Mastic asphalt modified by scrap rubber. *4th Rilem Symp.*, Budapest, pp. 331–335 (1990).
[14] Beuse, P., Enrobés armées par déchets de matières plastiques. *Bull. Liaison Lab. Ponts et Chaussées*, 128 (1983).
[15] Sainton, A., Application of Flexochape asphalt–rubber binders to porous and very thin maintenance open-grade mixes. *3rd Eurobitume Symp.*, The Hague, 1: 630–634 (1985).
[16] Deligne, P. and Perdereau, P., Utilization of polymer modified bitumens. *3rd Eurobitume Symp.*, The Hague, 1: 579–583 (1985).
[17] Lesage, J. and Archinard, C., Le Routofiex. *3th Eurobitume Symp.*, The Hague, 1: 624–629 (1985).
[18] Braga, V., Giavarini, C. and Santarelli, M.L., Heterophasic polypropylene copolymers and ethylene–propylene rubbers as asphalt modifiers. *5th Eurobitume Symp.*, Stockholm, June (1993).
[19] Giavarini, C., Santarelli, M.L. and Braga, V., Engineering a new polyolefin copolymer for asphalt modification. *Chim. Ind.*, 75(4): 270–281 (1993).
[20] Nievelt, G., Ten years practical experience with the production of asphalt mixes with high stability. *3rd Eurobitume Symp.*, The Hague, 1: 480–483 (1985).
[21] Peroni, G. and Pallotta, S., L'Impiego nelle pavimentazioni di bitumi modificati con polimeri. *Riv. Autostrade*, 6: 34–45 (1983).
[22] Gilby, G.W., EVA copolymers as modifiers for bitumen binders. *Asphalt Technol.*, 36(6): 37–41 (1985).
[23] Woodside, A.R. and Peden, R.A., The use of EVA in bituminous mixes and surface dressing. *4th Eurobitume Symp.*, Madrid, 1: 219–223 (1989).
[24] Woolley, K.G., Polymer modified bitumen for extra value asphalt. *Asphalt Technol.*, 38 (9): 45–51 (1986).
[25] Eckmann, B. and Boussad, K., Polymer modified bitumen for road construction. *4th Eurobitume Symp.*, Madrid, 1: 145–148 (1989).
[26] Madella, A., Bourlot, F. and Brûlé B., Selection of asphalt cements for asphalt cement/EVA blends. *Paper G-9, Symp. on Chemistry of Bitumens*, Roma (1991).
[27] *Asphalt-Rubber Seminar*. October, Kansas City. Sponsored by Federal Highway Administration and Asphalt-Rubber Producers (1989).
[28] Bull, A.L. and Vonk, W.C., Thermoplastic rubber/bitumen blends for roof and road. *Shell Chemicals Tech. Manual*, TR 8: 15 (1984).
[29] *Encyclopedia of Polymer Science and Technology*. Interscience, New York, N.Y., 15: 508–530 (1971).
[30] Diani, E. and Gargani, L., Bitumen modification with SBS thermoplastic elastomers. *4th Eurobitume Symp.*, Madrid, 1: 276–279 (1989).
[31] Peffekoven, W., Experiences with Caribit in asphalt mixes. *3rd Eurobitume Symp.*, The Hague, 1: 537–541 (1985).

[32] Van Den Berg, F., Olexobit: a polymer modified bitumen. *3rd Eurobitume Symp.*, The Hague, 1: 664–667 (1985).
[33] Dinnen, A., Epoxy bitumen binders for critical road conditions. *2nd Eurobitume Symp.*, Cannes, 1: 294–296 (1981).
[34] Giavarini, C., De Filippis, P. and Del Manso, F., Relationship between the production process and chemical structure of bitumens. *Paper C-1, Symp. on Chemistry of Bitumens*, Roma (1991).
[35] Mancini, G., Del Manso, F. and Bocchi, L., Correlation between chemical type of bitumen fractions and their interactions with SBS copolymers. *Paper G-6, Symp. on Chemistry of Bitumens*, Roma (1991).
[36] Costantinides, G., Lomi, C. and Schromek, N., Mescole di bitumi con polimeri SBS. *Riv. Combust. (Milan)*, 41(6): 145–153 (1987).
[37] Bredael, P., Andriolo, P. and Killens, E., A structural study of the hot storage stability of SBS-modified bitumens. *Paper G-5, Symp. on Chemistry of Bitumens*, Roma (1991).
[38] Brûlé, B. and Brion, Y., Bitumen–polymer associations. *3rd Eurobitume Symp.*, The Hague, pp. 573–578 (1985).
[39] Lys, G. and Farges, C., Compatibilization des bitumes avec le SBS. *4th Eurobitume Symp.*, Madrid, 1: 141–143 (1989).
[40] Giavarini, C., Visbreaker and straight-run bitumens. *Fuel*, 63(11): 1515–1519 (1984).
[41] Jovanovic, J., Sokic, M., Smiljanic, M., Pap, I., Neumann, H.J. and Rahimian, I., The production of stable bitumen-polymer blends. *Paper G-3, Symp. on Chemistry of Bitumens*, Roma (1991).
[42] Exxon, *Polybilt, Datasheet appendix on Preblending, PB 003* (1989).
[43] Gerhard, D., Production process of SBS modified bitumen. *Rilem Seminar*, Dubrovnik, pp. 273–275 (1988).
[44] Marchal, J.L., Behaviour of polymer modified bitumen emulsions. *4th Eurobitume Symp.*, Madrid, 1: 158–161 (1989).
[45] Grimm, C., Application of microscopic methods in the field of polymer-bitumen binders. *4th Eurobitume Symp.*, Madrid, pp. 54–59 (1989).
[46] Breuer, J.U., Storage stability test. *Rilem Seminar*, Dubrovnik, p. 85 (1988).
[47] Neumann, H.J., Required properties and composition of polymer-bitumens either for waterproofing or road construction. *Rilem Seminar*, Dubrovnik, pp. 25–34 (1988).
[48] Lesage, J. and Groz, P.C., Should a road be elastic or plastic? *4th Eurobitume Symp.*, Madrid, 1: 171–175 (1989).
[49] Molenaar, J.M.M., Polymer modified bitumens. *Paper G-1, Symp. on Chemistry of Bitumens*, Roma (1991).
[50] Verburg, H.A. and Molenaar, J.M.M., Force-ductility test for specification of PMB. *Paper G-4, Symp. on Chemistry of Bitumens*, Roma (1991).
[51] Lenoble, C., Rheology and microstructure of aged polymers modified bitumens. *Paper G-2, Symp. on Chemistry of Bitumens*, Roma (1991).
[52] Brûlé, B., Brion, Y. and Tanguy, A., Paving asphalt polymer blends: relationships between composition, structure and properties. *Assoc. Asphalt Paving Technol.*, 57: 41–45 (1988).
[53] Bonomi, A., Methodologie de caractérization des liants modifiés. *Rilem Seminar*, Dubrovnik, pp. 119–133 (1988).
[54] Peroni, G. and Luminari, M., Esperienze della Società Autostrade. *AGIP Meet.*, Roma, April (1991).
[55] Giavarini, C., Bitumi modificati con resine epossidiche. *Riv. Combust. (Milan)*, 25 (9): 391–395 (1971).

Asphaltenes and Asphalts, 1. Developments in Petroleum Science, 40
edited by T.F. Yen and G.V. Chilingarian

Chapter 17

THERMODYNAMICS OF ASPHALT INTERMOLECULAR INTERACTIONS AND ASPHALT–AGGREGATE INTERACTIONS

E. KEITH ENSLEY

INTRODUCTION

The thermodynamics of materials can be approached via the macroscopic world or the microscopic world. The macroscopic approach examines energy changes in systems with no regard to molecular structure. For example, the approach would be to simply measure the changes in energy, enthalpy, entropy, and free energy with no concern to the microscopic world that brings about these changes. The microscopic approach is to examine molecular structure of a material and relate the structure to asphalt intermolecular interactions and asphalt–aggregate interactions or other phenomena and further relate these interactions to the physical and thermodynamic properties of these materials. Then, of course, there are bridges between the two. The most classical case would be statistical thermodynamics where the thermodynamic functions are related to the microscopic properties through partition functions. Another bridge that relates the microscopic to the macroscopic world is radial distribution functions as seen in fluid theories. Yet another bridge or partial bridge connecting the two worlds is the group contribution approach. The latter approach is to add functional properties of groups of atoms in a molecule to come up with approximate molecular physical and thermodynamic properties. All of these concepts and how they relate to asphalt structural properties and to asphalt–aggregate bonding are discussed here.

REVIEW OF THERMODYNAMICS OF THE MACROSCOPIC WORLD

The basic laws of thermodynamics and, thus the equations, require no knowledge about atomic or molecular structure of a material. The equations describing thermodynamic properties are based on conservation of energy and the impossibility of building a perpetual motion machine. Only much later did the relationship between entropy and randomness (Boltzmann's formula) lead to the bridge connecting thermodynamics and structure through the use of partition function. First, the writer concentrates on the original basic thermodynamic equations as discussed in a typical thermodynamic or physical chemistry text [1–3]. The first equation represents the conservation of energy:

$$\Delta U = q - w \tag{17-1}$$

where the energy change, ΔU, is equal to heat flow, q, minus work, w. The second equation represents a change in enthalpy:

$$\Delta H = \Delta U + \Delta(PV) \tag{17-2}$$

where the enthalpy change is equal to the energy change plus the change in the product of pressure, P and volume, V. The next equation which defines entropy mathematically represents the impossibility of constructing a perpetual motion machine:

$$\Delta S = \int \frac{\mathrm{d}q}{T} \tag{17-3}$$

where the entropy change, ΔS, is equal to the integral of energy flow divided by the temperature. This applies only for a reversible system. For an irreversible or spontaneous change, $\mathrm{d}S > \mathrm{d}q/T$. How far a system is from equilibrium can be represented by the change in free energy Eqs. 17-4 and 17-5:

$$\Delta A = \Delta U - T\Delta S \tag{17-4}$$

The Helmholtz free energy change, ΔA, is equal to the energy change ΔU minus the product of temperature T and entropy change ΔS (at a constant temperature). Similarly for the Gibbs free energy change:

$$\Delta G = \Delta H - T\Delta S \tag{17-5}$$

the Gibbs free energy change is equal to the enthalpy change minus the product of temperature and the entropy change (at a constant temperature). Several other useful thermodynamic relationships can be derived from the differential form of these equations (not restricted to constant temperature). One of these formulas is the equation of state for liquids:

$$\left(\frac{\partial U}{\partial V}\right)_{\mathrm{T}} = T\left(\frac{\partial P}{\partial T}\right)_{\mathrm{V}} - P \tag{17-6}$$

These thermodynamic equations represent the basis of the following discussion on macroscopic or classical thermodynamics of asphalt and asphalt–aggregate bonding.

THE COHESIVE ENERGY DENSITY: THE ENERGY THAT HOLDS ASPHALTS TOGETHER

The term on the left in Eq. 17-6 is referred to as the internal pressure term [4–6]. The internal pressure $(\partial U/\partial V)_{\mathrm{T}}$ is approximately equal to the cohesive energy density, $\Delta U/V_{\mathrm{m}}$, a term that in certain situations is easier to measure than $(\partial U/\partial V)_{\mathrm{T}}$. $\Delta U/V_{\mathrm{m}}$ is the energy required to evaporate one mole of a liquid with a molar volume of V_{m}. It is also the energy required to break all the intermolecular bonds in a liquid or solid and form a gas with negligible interactions. Hildebrand and Scott [6] related the cohesive energy density to many properties of liquids through the term they defined as the solubility parameter, δ, which they equated to the

TABLE 17-1

Cohesive energy densities and solubility parameters[a] of common liquids and polymers and other materials (Gardon [4], Barton [5])

Compound	Cohesive energy density $\Delta E/\Delta V$ (cal/cm^3)	δ (cal/cm^3)$^{1/2}$	δ (MPa)$^{1/2}$
Aliphatic hydrocarbons	44.8– 67.2	6.7 – 8.2	13.7–16.7
Aromatic hydrocarbons	75.7– 98.0	8.7 – 9.9	17.8–20.2
Perfluoro compounds	27.0– 65.6	5.2 – 8.1	10.6–16.3
Water	538.2	23.2	47.3
Alcohols	100.0–216.1	10.0 –14.7	20.4–30.0
Esters	62.4–114.5	7.9 –10.7	16.1–21.8
Amines	62.4–116.6	7.9 –10.8	16.1–22.0
Benzene	84.8	9.21	18.9
Polyethylene polymer	65.6– 68.9	8.1 – 8.3	16.5–16.9
Gilsonite	65.6– 86.5	8.1 – 9.3	16.5–19.0
Polystyrene	65.6–116.6	8.1 –10.8	16.5–22.0
Polyvinyl acetate	65.6– 86.5	8.1 – 9.3	16.5–19.0
Phenolic resins	86.7–187.7	9.31–13.7	19 –28
Amine resins	86.7–127.7	9.31–11.3	19 –23
Polystyrene	86.7	9.31	19 (moderate sol.)
Carbowax	86.7–216.1	9.31–14.7	19 –30
Poly methyl methacrylate	68.9–174.2	8.3 –13.2	17 –27 (moderate sol.)
Polycarbonate	86.7–106.1	9.31–10.3	19 –21
Nylon (6,6)	187.7–231.0	13.7 –15.2	28 –31

[a] Solubility parameters are given in two units because both units are used frequently in the discussion.

square root of the cohesive energy density:

$$\delta = (\Delta U/V_m)^{1/2} \tag{17-7}$$

Keeping with convention, δ^2 represents $\Delta U/V_m$ or the cohesive energy density. Applications of the solubility parameter to liquids and polymers are discussed by Barton [5]. Table 17-1 lists several solubility parameters, some of which have application to bituminous materials. These values are useful when interpreting the solubility of bituminous materials in various solvents and the solubility of polymers in bituminous materials. Several methods have been employed for determining solubility parameters or cohesive energy densities:

(1) Direct measurement of the heat of vaporization.

(2) Vapor pressure measurements and the application of the Clausius–Clapeyron or the Antoine equations [5,6].

(3 Boiling point measurements and the application of the Hildebrand–Scott relationship.

(4) Direct measurement of the internal pressure $(\partial U/\partial V)_P$.

(5) Direct measurement of the thermal pressure $(\partial P/\partial T)_V$.

(6) Polymer swelling measurements.

(7) Heats of mixing.

Internal pressure determinations, direct or indirect, and the heats of mixing offer the most promise for determining the solubility parameters and thus the cohesive energy densities of bituminous materials. Both methods are discussed in detail below.

Examination of the equation of state of liquids (Eq. 17-6) suggests that the internal pressure can be determined either by measuring $(\partial U/\partial V)_T$, the term on the left side of the equation, or the term on the right side, $T(\partial P/\partial T)_V - P$. A third but indirect method for measuring $(\partial U/\partial V)_T$ will also be discussed and applied to bituminous systems.

Calculation of internal pressure from $(\partial P/\partial T)_V$

Barton [5] discussed a piezometer for direct determination of $(\partial P/\partial T)_V$, the thermal pressure term. The equipment could easily be applied to asphalt in the molten state. A liquid is contained in a large bulb surrounded by a temperature controlled bath. As the temperature of the bath is increased, an increasing external pressure, P, is applied to a capillary exit from the bulk to maintain a constant volume. The internal pressure $(\partial U/\partial V)_T$ is the difference between $T(\partial P/\partial T)_V$ and P. This technique has not been applied to bituminous materials but should not present any major obstacle.

Calculation of internal pressure from $(\partial U/\partial V)_T$

Experimentally, it is easier to determine $(\partial U/\partial V)_T$ for an asphalt indirectly by measuring two differential changes rather than a single differential change seen above. $(\partial U/\partial V)_T$ can be written as a product of two terms that have been determined experimentally for bituminous materials:

$$\left(\frac{\partial U}{\partial V}\right)_T = \left(\frac{\partial U}{\partial P}\right)_T \left(\frac{\partial P}{\partial V}\right)_T \tag{17-8}$$

The rate of change of energy U with pressure change can easily be measured with the microcalorimeter shown in Fig. 17-1. The microcalorimeter shown in the figure was used to determine the change in energy of asphalt with pressure and has been described previously in the literature [7].

The microcalorimeter consists of two, 1400 electroplated silver-constantan thermopiles. Asphalt is contained in a thick-walled tube situated in the center of the thermopile. The other thermopile serves only as a blank. Mercury is used to transmit pressure from a Teledyne high-pressure pump to the asphalt. The equipment is capable of measuring changes in energies that occur within 10 psi increments. The value for $(\partial U/\partial P)_T$ is calculated from the slope of the line of the plot U versus P.

The reciprocal of $(\partial P/\partial V)_T$, or $(\partial V/\partial P)_T$, for a unit volume is the compressibility factor, β:

$$\beta = \frac{-1}{V}\left(\frac{\partial V}{\partial P}\right)_T = \left(\frac{-1}{V}\right)\left(\frac{\Delta V}{\Delta P}\right)_T \tag{17-9}$$

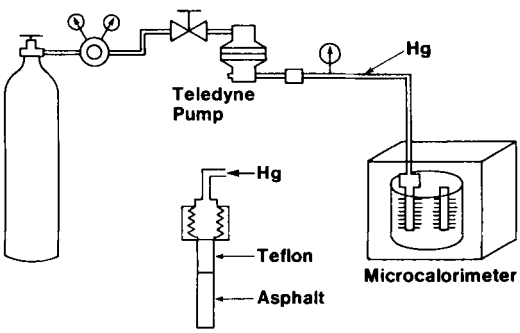

Fig. 17-1. Microcalorimeter and pressure system used to determine $(\partial E/\partial P)_T$ of asphalt. The microcalorimeter was also used to measure asphalt–aggregate bonding energies, asphalt intermolecular association and asphalt strain-energy curves.

(Equation 17-9 assumes a linear relationship between V and P over a selected temperature range.)

The compressibility factor can be measured directly from the slope of the curve obtained by plotting the volume of the material against the applied pressure. Mack [8] lists compressibility factors for six different asphalts over a temperature range of 25–90°C. A $(\Delta V/\Delta P)_T$ value for a cubic centimeter of material value was selected from the compressibility list and combined with a $(\Delta U/\Delta P)_T$ value from microcalorimetric data to obtain a cohesive energy term. Corresponding temperatures and similarities in asphalts were used to select required values. In a typical calculation, $(\Delta U/\Delta P)_T$ was found to be 0.00485 cal/atm for 1 gram of asphalt assuming a density 1 g/cm^3 and $\Delta P/\Delta V$ was found to be 23700 atm/cm^3. The product of $(\Delta U/\Delta P)_T$ and $(\Delta P/\Delta V)_T$ was calculated to be 480 J/cm^3 or 115 cal/cm^3, which is equal to the cohesive energy density. To compare cohesive energies with literature data, for example with polymers, the solubility parameter, δ, was calculated from the square root of the cohesive energy density. That is:

$$\delta = (480 \text{ J/cm}^3)^{1/2} = 22 \text{ (MPa)}^{1/2} = (115 \text{ cal/g})^{1/2}$$

It should be noted that J/cm^3 has the same numerical value as megapascals (MPa) or, as given by Eq. 17-6, energy per unit volume has the same units as pressure. The solubility parameter value of 22 $(\text{MPa})^{1/2}$ is similar to the solubility parameter of polymers which is important in asphalt–polymer interactions that are discussed later. A second technique that has been used to determine the compressibility factors is the measurement of sound velocity through asphalt. The velocity of sound, C, through an elastic medium is related to the bulk modulus and density as seen in Eq. 17-10 [2]:

$$C = \sqrt{E/\rho} \tag{17-10}$$

where E = bulk modulus = $V(\partial V/\partial P)_T^{-1}$ and ρ = density. The equipment for determining the compressibility factor by sound velocity is simpler than the equipment

required to measure compressibility, $-(1/V)(\partial V/\partial P)_T$, directly. This technique will probably find application to asphalt technology in the future. Cohesive energy densities are used to describe asphalt properties and asphalt modification, such as with polymers, in the subsequent discussions.

HEAT OF MIXING AS A MEASURE OF ASPHALT–POLYMER INTERACTIONS

Dissolution of a polymer occurs in two stages [9]. The solvent molecules first diffuse slowly into the polymer to produce a swollen gel. Sometimes this is all that occurs. If the solvent–polymer interactions are strong, the gel will gradually disintegrate into a true solution.

Because many polymers are amorphous and have certain characteristics similar to those of liquids, their solubility in asphalt are treated as liquid–liquid interactions. Heat of mixing is one example for measuring liquid–liquid interactions.

An equation for heat of mixing, ΔH_M, of component A with component B to form a mixture AB is shown below [4]:

$$\Delta H_M = \varepsilon_A + \varepsilon_B - 2\varepsilon_{AB} \tag{17-11}$$

where ε_A = the interaction energy of component A, for example an asphalt; ε_B = the interaction energy of component B, for example a polymer; and ε_{AB} = the interaction energy of the mixture AB. To a first approximation, interaction energies are proportional to cohesive energy densities.

If a large amount of energy is required to dissociate the molecules in material A and the molecules in material B, and if there is little interaction between the molecules in mixture AB, then the heat of mixing will be endothermic. Conversely, if the interaction between the molecules in mixture AB is greater than the interaction between the molecules in material A and the molecules in material B, then the heat of mixing will be exothermic. The heat of mixing can also be expressed in terms of measurable parameters as is given below in the Scratchard–Hildebrand equation [6]:

$$\Delta H_m = (X_i V_i + X_j V_j)(\delta_i - \delta_j)2\phi_i\phi_j \tag{17-12}$$

where X_i, X_j = the mole fractions of components i and j, V_i, V_j = the molar volumes of components i and j, δ_i, δ_j = the solubility parameters of components i and j, and ϕ_i, ϕ_j = the volume fractions of components i and j. As mentioned previously, the solubility parameter is equivalent to the square root of the cohesive energy density. This equivalence is discussed in more detail later.

The Scratchard–Hildebrand equation has been effectively applied to solvents with similar solubility parameters and solvents that are principally non-polar. To account for solvents that are polar, for example bituminous materials, Walker [10] modified the Scratchard–Hildebrand equation for heat of mixing to include interaction constant K. Walker's equation is shown below:

$$\Delta H = V_m \nu_B^2 \left[\varepsilon_A + \varepsilon_B - 2K(\varepsilon_A\varepsilon_B)^{1/2}\right] \tag{17-13}$$

where V_m = the molar volume of solvent, asphalt, ν_B = the volume fraction of polymer, K = an arbitrary constant, and the ε's the interaction energies defined previously. ΔH can be positive, zero, or negative depending upon whether K is less, equal to, or greater than one. If $K = 1$, then there is no special affinity for solvency. If $K < 1$, there is a lack of tendency for dissolution, whereas if $K > 1$, there is a tendency for dissolution. The interaction of polymers with asphalt produced both situations where $K > 1$ and $K < 1$.

Table 17-1 lists typical cohesive energy densities for polymers. High cohesive energy densities are the result of using solvents which have a strong hydrogen bonding capability. Asphalt would probably fall in the strong hydrogen bonding solvent category. Both the cohesive density of asphalt (discussed in prior section) and polymers are in the neighborhood of 360–440 MPa, or in terms of solubility parameters, δ = 19–21 $(MPa)^{1/2}$. Surprisingly, some of the cohesive energy densities of solvents are in the range of some polymers.

In Table 17-2, both negative and positive heats of mixing are seen. Two of the polymers, a polyethylene (LDPE) and a styrene–butadiene rubber (SBR-Latex), produce long-term endothermic curves, whereas two ethylene vinylacetate polymers (EVA) produce a more typical exothermic curve. If an enthalpy of mixing is endothermic, then the entropy of mixing must be positive for a spontaneous interaction and of such magnitude to overcome the positive enthalpy. The net result must produce a negative free energy change, a requirement for spontaneity [1] as discussed in the thermodynamic section (see Eq. 17-5). If materials such as solvent and solute have similar cohesive energy densities, then $\varepsilon_A + \varepsilon_B$ is similar in magnitude to $2(\varepsilon_A \varepsilon_B)^{1/2}$. If this holds, then K values determine whether the interaction is endothermic or exothermic. For a K value less than one, the interaction between solvent and solute tend to be endothermic and for a K value greater than one, the interaction tends to be exothermic. An exothermic interaction was observed for the interaction between ethylene vinylacetate and asphalt and an endothermic

TABLE 17-2

Heats of interaction between polymers and asphalt at 130°C

Asphalt	Additive	ΔH of interaction (mcal/g-2 hr)	Tail height (mcal/g)
AC-5	Dow (LDPE) 526[a]	+11,200	109
AR-1000	Dow (LDPE) 526	+11,800	113
AR-1000	SBR-Latex[b]	+16,800	153
AC-5	SBR-Latex	+16,000	103
AC-5	Elvax 150[c]	−1211	0.9
AR-1000	Elvax 150	−621	6.1
AC-5	EXO42	−480	2.0
AR-1000	EXO42	−680	2.1

[a] LDPE is a low-density polyethylene polymer.
[b] SBR is a styrene–butadiene rubber.
[c] Elvax and EXO42 are vinylacetate polymers.

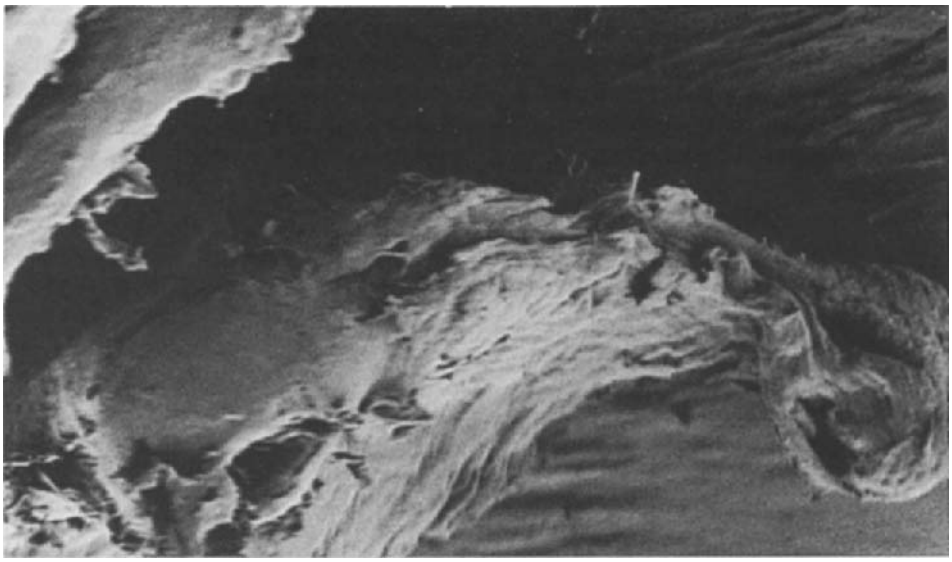

Fig. 17-2. Photomicrograph of low-density polyethylene (×140) — courtesy of Ethyl Corporation.

interaction was observed between polyethylene and the rubber polymers when they interacted with asphalt.

The polyethylene and styrene–butadiene polymers have K's less than 1 and are non-polar polymers. The vinylacetate polymers have K's that are greater than 1 and are polar polymers. The enthalpy values indicate that even though ΔH is positive, the entropy change is sufficient for the polymer and asphalt to interact and overcome the endothermic interaction. In effect, the polymer swells significantly so that the increase in randomness overcomes the decrease in intermolecular interactions.

A photomicrograph of low-density polyethylene is shown in Fig. 17-2 (courtesy of Ethyl Corporation). The possibility of asphalt interacting with polymers becomes even more apparent as the magnification of the polymer increases and its surface roughness becomes more obvious.

There is no sharp difference between swelling and dissolution. The extent to which a polymer interacts with an asphalt, whether by swelling, dissolution or a combination of the two, should have a large bearing on the final mix property of a polymer-modified asphalt.

The effect of polymer modification on viscosity susceptibility to temperature is discussed in a later section on viscosity as it relates to the change in the cohesive energy density.

HEAT OF MIXING OF RECYCLING AGENTS AND ANTISTRIP AGENTS

An area that needs more investigation in asphalt modification is the interaction of recycling agents and antistrip agents with asphalts. Both recycling agents and

antistrip agents are important in dissociating asphalt, allowing some of the "good bonding" asphalt molecules to become more available for bonding. The mixing of an antistrip agent with an asphalt is one example that has recently been investigated. An antistrip agent, CY-amine, was interacted with an oxidized California asphalt. The interaction was found to be exothermic and appears to continue for several hours. The observed negative enthalpy of mixing of the amine antistrip agent with the asphalt is probably due to the interaction between the nitrogen and oxygen functionality in the asphalt and the amine functionality in the antistrip agent, possibly through hydrogen bonding. The cohesive energy density ε_A for asphalt was found to be 115 cal/cm^3, as discussed previously. Although no direct data are available for ε_M, cohesive energy density of antistrip agent, it can be roughly calculated assuming that the antistrip is a mixture of long-chained amines. Data obtained from Barton [5] using an extrapolated curve of carbon number, for an amine compound, versus ε_M, shows $\varepsilon_M = 71$ cal/cm^3 in the region where the number of carbon atoms is 12–16. Using the ε_A values for asphalt shown above and ε_M value for a long-chained amine, the following combinations of cohesive energy densities seen in Eq. 17-13 were obtained:

$$\varepsilon_A + \varepsilon_M = 186 \qquad 2\sqrt{\varepsilon_A \varepsilon_M} = 181$$

As mentioned in the discussion for polymer interactions with asphalt, for ΔH in Eq. 17-13 to be exothermic, K must be greater than one if the sum $\varepsilon_A + \varepsilon_M$ and two times the square root of $\varepsilon_A \varepsilon_M$ are close in value. For an exothermic heat of mixing between the asphalt and the amine, K must be greater than 1.028 (i.e., 186/181). An exothermic increase is equivalent to an increase in K and the energy of interaction between the asphalt and the amine antistrip agent.

COHESIVE ENERGY DENSITIES AND DIPOLE INTERACTIONS

The dipole interactions discussed below enable a qualitative analysis of asphalt intermolecular and asphalt–aggregate interactions rather than a precise calculation of the interaction energies that could be used in Eq. 17-13. This is dictated by the molecular complexity of asphalt.

The three common interactions that govern asphalt physical and chemical properties, including the thermodynamic properties, are [2]: (1) permanent dipole (Keesome), (2) induced dipole (Debye), and (3) dispersion forces (London).

Permanent dipoles in asphalt arise from heterogeneity of the large asphalt molecules. (Typical asphalt composition based on both chemical analyses and solubility data are listed in Table 17-3 for three asphalts differing in asphaltene content.) Often, permanently polarized asphalt molecules can be further polarized either by surrounding polar molecules or by polar aggregate surfaces. An example of intermolecular interactions that would be a combination of permanent and induced polarization in asphalt is the interaction of a pyridinic nitrogen that has two unbonded electrons interacting with a hydrogen atom that is electron deficient. Interactions of this type and interactions of asphalt molecules with polar aggregate surfaces are

TABLE 17-3

Composition of three typical asphalts [a]

Asphalt composition	Asphalts [b] (%)		
	AAD	AAB	AAM
Asphaltenes	23	16	4
Polar aromatics	41	36	50
Naphthene aromatics	25	36	42
Saturates	9	11	2
Nitrogen	0.9	0.5	0.5
Sulfur	8.6	6.0	2.4
Oxygen	1-2	1-2	1-2

[a] Proposed functionalities that occur in the above fractions are seen in Fig. 17-3.
[b] These asphalts were included in the Strategic Highway Research Program.

both discussed later. Dispersion forces, or instantaneous localized dipole forces, are important forces in non-polar non-polarizable materials. For example, the non-polar paraffinic carbon types of asphalt molecules can interact with other paraffinic regions to form a bond without the presence of any permanent polarity in the molecule. Gardon [4] represented the fractional contribution of dispersion force and permanent and induced dipole forces in the following equation:

$$d + p + i = 1 \tag{17-14}$$

The product of fractional contributions and interaction energies for the interactions between component "A" and component "B" is seen below for each force:

Dispersion: $$d_A \varepsilon_A = \tfrac{3}{4} I_2 \alpha_A^2 \tag{17-15}$$

Permanent dipole: $$p_A \varepsilon_A = \tfrac{2}{3} kT \mu_A^4 \tag{17-16}$$

Induced dipole: $$i_A \varepsilon_A = 2\alpha_A \mu_A^2 \tag{17-17}$$

and

$$\varepsilon_{AB} = \tfrac{3}{2}\left(\frac{I_A I_B}{I_A + I_B}\right)\alpha_A \alpha_B + (\tfrac{2}{3}kT)\mu_A^2 \mu_B^2 + \alpha_B \mu_A^2 + \alpha_A \mu_B^2 \tag{17-18}$$

where: I is ionization potential, α is polarizability, k is Boltzmann constant, and μ is dipole moment. Equation 17-18 expresses the energy of interaction in terms of experimentally obtainable constants for pure materials A and B and the binary system AB.

A few productive qualitative statements can be made about asphalt interactions without resorting to actual calculations:

(1) Polynuclear aromatic compounds in asphalt are polarizable materials that greatly enhance the asphalt interaction energy, ε_{AB}.

(2) Saturate compounds in asphalt primarily interact through dispersion forces, which depend on ionization potentials and polarizability of the hydrocarbon entity.

(3) Oxidation with aging of asphalt mixes increases the polarity and polarizability of asphalt molecules, which greatly affect the asphalt interaction energy, ε_{AB}, and, consequently, the cohesive energy density. General observations of the interaction energy can be applied to pavement performance. For example, insufficient cohesive energy can lead to rutting at warm pavement temperatures, whereas high cohesive energies can lead to cracking at low pavement temperatures.

VISCOSITY AND COHESIVE ENERGY DENSITY OF ASPHALT

Viscosity measurements have been employed for many years as a technique for evaluating asphalts and predicting asphalt–aggregate performance. The original Newtonian viscosity has very little bearing on the asphalt flow properties at ambient temperatures and the relation of flow properties to performance. Originally, Newton defined viscosity through momentum transfer perpendicular to the direction of flow:

$$F/A = \eta(\partial V_x/\partial_y) \tag{17-19}$$

where F/A is the force per unit area between shear planes; V_x is the velocity component in the x direction, or direction of flow; $\partial V_x/\partial_y$ is the velocity gradient in the y direction, or direction perpendicular to flow; and η is proportionality constant or viscosity. Another way of expressing the viscosity is in terms of shear rate as given in Eq. 17-20, which applies the calculus principle that differentiation is independent of sequence:

$$F/A = \eta\dot{\gamma} \tag{17-20}$$

where $\dot{\gamma}$ = rate of shear or $[d(dx/dt)]/dy = [d(dx/dy)]/dt = \dot{\gamma}$.

A material is considered Newtonian if the viscosity η is independent of the rate of shear, $\dot{\gamma}$.

Momentum transfer may have very little effect on the flow properties of asphalt at pavement temperatures. The cohesive energy density or intermolecular interactions in asphalt is undoubtedly a greater contributor to viscous flow than momentum transfer at pavement temperatures.

The relationship between viscosity and cohesive energy is seen through equations that express viscosity as a function of temperature. Viscosity as a function of temperature has been expressed in a variety of equations [11]. One formula that has received a great deal of attention in asphalt viscosity measurements is the Andrade (also Arrhenius) exponential viscosity equation written below:

$$\eta = A\,e^{E/RT} \tag{17-21}$$

where η is the viscosity at temperature T, R is the gas constant, and A and E are constants usually determined from slopes and intercepts, respectively, of curves obtained from plotting $\log \eta$ versus $1/T$.

Andrade plots of log viscosity versus reciprocal temperature yield the viscosity energy of activation, E. A value of 54 kcal/mol was obtained on a typical AC-20

asphalt [12,13]. The relation between the viscosity activation energy and the cohesive energy density is given by the Eyring equation [14]. The Eyring concept of viscous flow is based on the premise that the activation energy of flow is principally due to moving molecules apart to form a hole for other molecules to move into. Heat of vaporization is also a function of the energy requirement for moving molecules apart. Or quoting Hershfelder et al. [15], "Since the bonds between neighboring molecules, which must be broken in order to make a hole, are the same as those which are broken in the process of vaporization, it follows that the energy required to form a hole (the size of the specific volume of a molecule) is the energy of vaporization, ΔU_{vap}." After several assumptions and grouping of constants, a simplified form of Eyring's equation can be written in terms of heat of vaporization, which is closely related to cohesive density or solubility parameter as mentioned previously. The reduced or simplified Eyring equation for Newtonian flow is:

$$\eta = B\, e^{\Delta U_{vap}/2.45RT} \tag{17-22}$$

where B contains a term for the number of molecules per unit volume; Planck's constant, ΔU_{vap}, is the heat of vaporization; and R is the gas constant. The cohesive energy density (Eq. 17-23a) is approximately equal to the heat of vaporization divided by the molar volume V_m. The RT term is the expansion work for one mole of liquid and is usually much less than the heat of vaporization:

$$\frac{\Delta U}{\Delta V} = \frac{\Delta U_{vap} - RT}{V_m} \simeq \frac{\Delta U_{vap}}{V_m} \tag{17-23a}$$

The viscosity is related exponentially to the cohesive energy density or the internal pressure $(\partial U/\partial V)_T$. It is interesting to compare the cohesive energy densities calculated from viscous flow to the cohesive energy density calculated from compressibility and microcalorimetric pressure data.

From viscous flow, the viscosity activation energy = 54 kcal/mol. Therefore, $\Delta U_{vap}/2.45 = 54$ or $\Delta U_{vap} = 132$ cal/g (or 132 cal/cm^3 for density equal to one) for molecular weight of 1000. From compressibility and microcalorimetric pressure data discussed previously:

$$\left(\frac{\partial U}{\partial V}\right)_T = \left(\frac{\partial U}{\partial P}\right)_T \left(\frac{\partial P}{\partial V}\right)_T \simeq \Delta U_{vap} = 115 \text{ cal/g} \tag{17-23b}$$

Again, $(\partial U/\partial V)_T \simeq \Delta U_{vap}/V_m$ was assumed. In conclusion, the similarity of the cohesive energy density calculated from the Andrade plot (132 cal/g) and the value calculated from Eq. 17-23b, implies that viscous flow in asphalt is principally due to intermolecular interactions and there is little contribution from momentum transfer.

Asphalt modification should affect the viscosity activation energy, which is equivalent to stating that asphalt modification affects the susceptibility of viscosity to temperature. The effects of modifying two asphalts with styrene–butadiene rubber are seen in Table 17-4. A reduction in viscosity temperature susceptibilities over two temperature ranges is noted [16]. A reduction was also reported by Khosla and Zahran [17].

TABLE 17-4

Viscosity temperature susceptibilities or viscosity activation energies obtained from log viscosity versus reciprocal of absolute temperature

Asphalt	Viscosity temperature susceptibility	
	−20° to 9°C	25° to 0°C
Original AR-1000	44.2	37.2
AR-1000 with SBR [a]	29.4	29.5
Original AC-5	42.9	31.4
AC-5 with SBR	31.3	27.3

[a] Styrene–butadiene polymer.

It was necessary to list two temperature ranges because $\log \eta$ versus reciprocal of the absolute temperature produced a curve that had different slopes when comparing the low-temperature range with the high-temperature range. Because the curve is not linear over a wide temperature range, the data represent three temperature susceptibilities.

(1) Low-temperature susceptibility, which is lower for the polymer-modified asphalt systems.

(2) High-temperature susceptibility, which is again lower for polymer-modified asphalt systems.

(3) A temperature susceptibility that bridges the two temperature ranges, which is much lower for modified-asphalt systems.

Barton [5] noted that the effect of temperature on cohesive energy densities can, for the most part, be neglected for moderate temperature changes, which may not hold for asphalt mixtures as observed in Table 17-4. Perhaps the temperature ranges in the table are significant if the asphalt and the modified asphalt are solid-like at the lower-temperature range and liquid-like at the higher-temperature range. The data show that the temperature susceptibilities are generally larger at lower temperatures, which is in agreement with typical equations that express the solubility parameters or the cohesive energy densities as a function of the temperature.

The lower-temperature susceptibilities of the polymer-modified systems would indicate that the addition of a polymer to an asphalt would mitigate rutting at high temperatures and cracking at low temperatures.

APPLICATION OF GROUP CONTRIBUTION TECHNIQUES TO THERMODYNAMIC AND PHYSICAL PROPERTIES OF ASPHALT

Calculation of macroscopic properties of materials such as viscosity, density, molar volume, etc., based upon microscopic or molecular structure is most applicable for relatively simple molecules. For relatively simple mixtures, the cohesive energies are calculated for each component and then the total properties of a mixture are calculated from contributions of each component.

TABLE 17-5

Group contributions to molar vaporization energy and molar volume [a]

Atom or group	ΔU (kJ/mol)	Molar volume (cm^3/mol)
$-CH_3$	4.71	33.5
$-CH_2-$	4.94	16.1
$\backslash C-H$ /	3.43	−1.0
–OH	29.8	10.0
$-NH_2$	12.6	19.2
–COOH	32.8	27.0
Phenyl	31.9	71.4
$-C(=O)-H$	21.4	22.3
–S–	14.1	12.0
$-S(=O)-$	39.1	–
$-C(=O)-$	17.4	10.8

[a] Barton [5], Fedors [18].

The technique can be applied to asphalt only in a qualitative way because of the difficulty in (1) separating asphalt into individual molecular species; and (2) lack of identification and amounts of the individual species.

Group contributions of asphalt functionalities are discussed for both cohesive energy density (or molar vaporization energy) and viscosity. As discussed previously [6], cohesive energy is approximately equal to molar vaporization energy. Group contributions of functional groups to molar vaporization reported by Barton [5] and Fedors [18] are listed in Table 17-5.

Data in Table 17-5 are useful when qualitatively analyzing how functionalities (Fig. 17-3) affect cohesive properties either in neat or oxidized asphalt [19]. For example, the $-CH_3$ group if oxidized in a pavement to COOH, increases its cohesive contribution from 4.71 to 32.8. Obviously, oxidation greatly affects the cohesive energy and, consequently, any property associated with it. Sulfide oxidation shows a similar increase but not quite as pronounced. Some groups might show a decrease in cohesive energy such as an –OH group going to a C=O (ketone or carboxylic acid) group.

The relation between cohesive energy density and viscosity, a property that influences pavement mix, was established in the previous section. Therefore, it is expected that viscosities can be calculated directly from viscosity functional group contributions. Reid et al. [20] discuss several techniques that have been employed to calculate viscosity from functional group contributions. These techniques are similar to the techniques employed in calculating functional group contribution to cohesive energy densities or molar vaporization energies. An example of the calculation of viscosity from functional group contributions is the method of Orrick and Erbar [20]. This method uses parameters A and B and group contributions by applying Eq. 17-24:

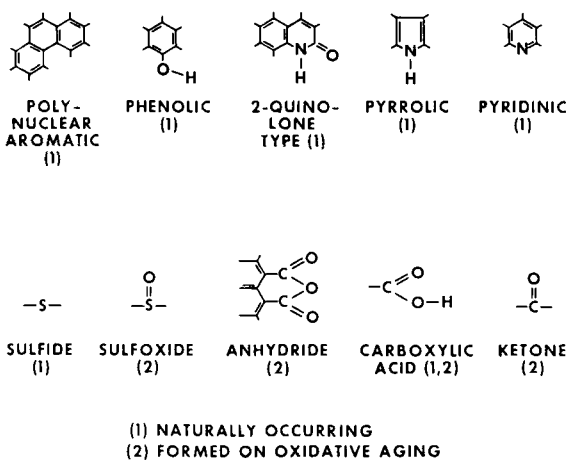

Fig. 17-3. Asphalt functionalities occurring in asphalt. (After Petersen [19].)

$$\ln\left(\frac{\eta}{\rho M}\right) = A + \frac{B}{T} \tag{17-24}$$

where η = viscosity, cP; ρ = density at 20°C, g/cm^3; M = molecular weight; and T = Kelvin degrees.

A few functionalities found in asphalt are listed in Table 17-6 along with corresponding parameters A and B. Unfortunately, parameters for sulfur and nitrogen functionalities have not been reported for this technique. The same polar constituents that contribute so greatly to the viscosity also contribute to the cohesive energy density, as would be expected, because the bulk viscosity is considered the principal contributor to viscosity and not the momentum transfer or shear viscosity.

Asphalt aging produces carboxylic acids, ketones, anhydrides, sulfoxides, and probably other oxygen groups that greatly enhance the viscosity of asphalt, as noted by the parametric values in Table 17-6.

TABLE 17-6

Orrich and Erbar[a] group contributions for viscosity parameters A and B

Group	A	B
C=C	0.24	−90
Aromatic	0	20
–OH	−3.00	1600
–C(=O)–O–O–	−1.00	420
–C(=O)–O–OH	−0.90	770

[a] Reid et al. [20].

There are other techniques for calculating macroscopic properties of materials from microscopic properties, but often the critical temperature of a material is required which limits their use for asphalt calculations.

TENSILE STRENGTH PROPERTIES OF ASPHALTS AND THERMODYNAMICS

It is important that asphalts have good tensile properties such that it stretches without breaking under a load and will spring back after the load has been removed. The tensile strength of asphalt has been related to the relaxation of asphalt under applied loads [21].

As might be expected, the ability of an asphalt to hold together, or possess a good tensile strength, is related to the cohesive energy density. Gardon [4] related the maximum tensile strength, T_{max}, for polymers to the cohesive energy density, δ^2, through the following equation:

$$T_{max} = 1.25 \times 10^7 \, \delta^2 \tag{17-25}$$

In the above relation, T_{max} is in units of dynes per square centimeter and δ^2 in units of calories per cubic centimeter. The maximum strength refers to the force per unit area just prior to breaking. However, it is difficult to determine the maximum tensile strength of asphalt just prior to breaking, because asphalt produces a thin thread, complicating cross-sectional measurements. Part of this difficulty in making the measurement might be overcome by stressing the asphalt at low temperatures and at a relatively fast rate. Both the cohesive energy density and the tensile strength increase with decreasing temperature.

Another way of relating strain and stress of a material with intermolecular energy is seen in the following experiment. The microcalorimeter discussed in a previous section was used in the writer's laboratories to measure the energy of elongation. For example, a rod is immersed in asphalt contained in a microcalorimeter cell at room temperature. A thin wire attached to the rod leading to the outside of the oven is pulled with a known force and the energy flow is detected. After a steady energy flow is obtained, the strain is held constant producing a decaying energy curve (see Fig. 17-4). When the curve reaches zero, the force is removed and an endothermic energy flow results. Although only a limited number of asphalts have been investigated using this technique, a few comments can be made about the exothermic curve produced while straining the asphalt and the endothermic curve produced during the stress removal:

(1) The more Hookean (more solid like) or more viscous the asphalt is, the steeper is the initial curve and the sharper is the initial peak.

(2) The less viscous the asphalts are, the lower and flatter the initial curves.

(3) The more viscous and more elastic the asphalts are, the greater the amounts of energies or the larger the secondary curves.

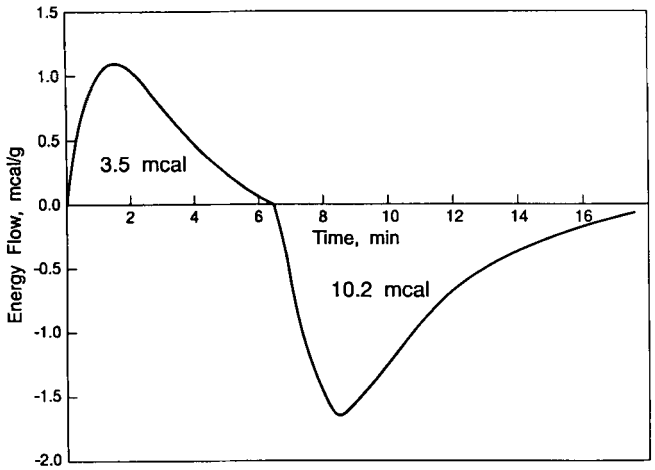

Fig. 17-4. Energy released when asphalt is strained to produce a steady energy flow (top of first peak); then strain is held constant (decay of first peak), followed by release of stress to produce bottom curve.

ENERGY OF ASSOCIATION IN ASPHALT

The energy that holds asphalt molecules together was previously defined as the cohesive energy density. This energy is due to forces such as dipoles, induced dipoles, and the London dispersion forces which can be determined using Eqs. 17-15 through 17-17. The energy of association as discussed in this section is also due to these forces, but is a measure of the difference in the association of molecules within the bulk asphalt, not the total cohesive energy.

In the initial stages of asphalt–aggregate bonding energy studies it was noted that several hours were required to reach thermal equilibrium within the asphalt [7]. An association–dissociation interaction was suspected as producing the slow approach to thermal equilibrium. The following data confirmed the association–dissociation concept. In Fig. 17-5 are seen two energy flow curves that result when asphalt previously heated to 250°C to promote intermolecular dissociation was allowed to reassociate in a microcalorimeter, at a temperature much lower than the dissociation temperature. Various association temperatures were investigated by Ensley [22]. From this, data plots were made (Fig. 17-6) of the fraction of energy released versus time. The data from the plots were used to obtain values for the parameters used in rate Eq. 17-26, which fit the experimental data very well. The derivation of the equation assumed a second-order rate and that the reaction or association did not go to completion or infinitely large associated species:

$$f = \beta\,[t/(t+\gamma)] \tag{17-26}$$

where: f = the fraction of the reaction that has occurred by time t, β = the ratio of monomers in dissociated state to the number of dipole-dipole bonds, and γ = 2 divided by the rate constant multiplied by the initial monomer concentration.

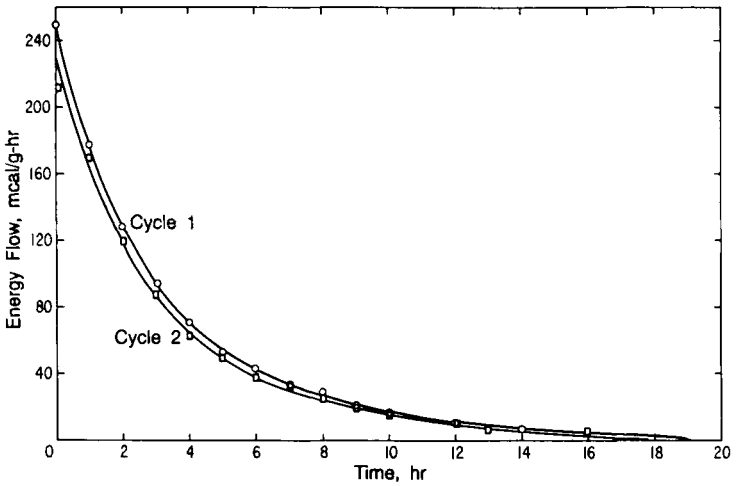

Fig. 17-5. Rate of energy released by time t vs. t for thermal cycling of asphalt sample.

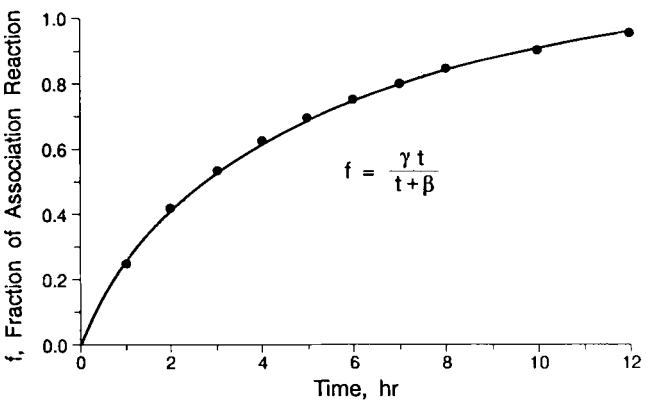

Fig. 17-6. The points represent experimental data. The solid line represents a plot of the equation with two parameters (γ, β).

Association energies, rate constants, activation energies and association numbers are presented in Table 17-7. The study indicated that thermal association–dissociation is reversible and association follows second order kinetics. Also the data supports the concept that the association in asphalt occurs through long chains of associated asphalt molecules and not by way of spherical micelles that has often been alluded to [8]. The magnitude of the activation energies of association (Table 17-7) are in the region for weak dipole–dipole and dipole–induced dipole bonding interactions, which are much lower than chemical bond breaking activation energies. The values for the heats of association are also very low supporting the weak interaction concept. Final support for the weak interaction concept is seen by examining the number of molecules in an associated species which is between 5 and

TABLE 17-7

Energies of association, rate constants, activation energies, and association numbers for three asphalts [a]

Asphalt	Temperature (°C)	Energies of association (kcal/mol)	Rate constant, k (l/mol-hr)	Activation energies (kcal/mol)	Association number
Idaho	190	0.25	1.04	14	7
	170	0.80	0.42	–	5
	160	1.25	0.26	–	6
	150	1.10	0.21	–	10
Gilsonite derivative	190	0.42	0.34	10	4
	170	0.91	0.24	–	4
	160	1.03	0.17	–	6
	150	1.14	0.14	–	6
B-3036	180	0.72	0.69	8	
	160	0.92	0.35	–	5
	150	1.12	0.30	–	10
	140	0.78	0.23	–	26

[a] Ensley [22].

26, depending on type of asphalt and temperature.

A similar type of association as discussed for asphalt molecular interactions can be now applied to asphalt–aggregate interactions.

THERMODYNAMICS OF THE ASPHALT–AGGREGATE BOND

The study of the asphalt–aggregate bond can be approached in two ways, either by studying the bond as it forms or by measuring the bond properties after it forms. The writer first discusses the mechanical methods used to study the asphalt–aggregate bond after the bond forms and then discusses one experimental technique that has been used to study the bond as it forms.

The effects of the interaction between asphalt and aggregate has commonly been investigated by scraping, peeling, or displacing asphalt from stone, typically by a mechanical method [8,23–25]. Majidzadek and Brovold [26] discussed the thermodynamics of the asphalt–aggregate bonding through contact angle measurements. Unfortunately for the experimentalists, but fortunately for the building of roads, the contact angle is near zero because of the strong tendency of asphalt to wet an aggregate surface. The Dupré contact angle equation (Eq. 17-27), as discussed by Majidzadek and Brovold, expresses the work of adhesion, W_A, in terms of the surface free energy, γ_L, of the asphalt and the contact angle θ:

$$W_A = \gamma_L(\cos\theta + 1) \tag{17-27}$$

γ_L is also called the surface tension, and for asphalt it is a more easily measured parameter than the contact angle. This equation implies that the strongest adhesion

is obtainable when θ is equal to zero:

$$W_A = 2\gamma_L \tag{17-28}$$

γ_L is usually in the range of 25–40 dynes/cm at 25°C. Thus the work of adhesion for the easily wetted aggregates is in the 50–80 dynes/cm range.

Contact angle measurements, water stripping, and scraping techniques are methods that measure the strength of the bond after the bond has formed. The following microcalorimetric technique follows the formation of the bond.

When a solid is wetted by a liquid, the solid-air interface is replaced by a solid–liquid interface. The energy change has been called the heat of immersion as previously discussed. In the initial studies of asphalt–aggregate interaction using a microcalorimeter, the energy released was called the "heat of immersion". More recently, it has been labeled "bonding energies" in order to relate the measurements to those in asphalt–aggregate mix design. This may not be precisely correct but highway engineers can relate to bonding energies better than to the heat of immersion.

A specially designed microcalorimeter [7], which was discussed previously, was used to measure the interaction between aggregate and molten asphalt. The aggregate was usually a selected mesh size (−35 +48 mesh). Bonding energy measurements were made between 130 and 150°C, a typical mix-plant temperature range.

The heat of immersion or bonding energy curve of an aggregate (−35 +48 mesh) bonding with an asphalt is shown in Fig. 17-7. Typically, there is a large initial

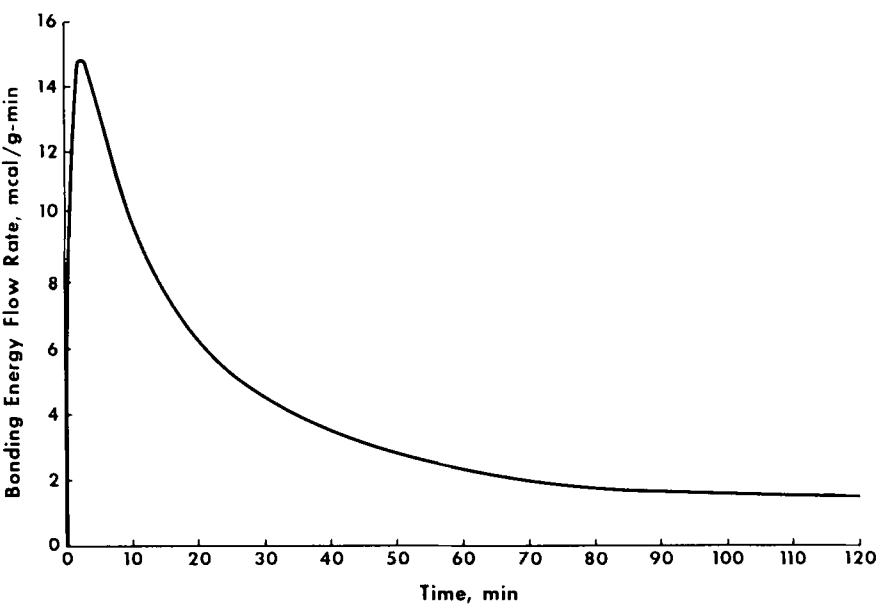

Fig. 17-7. Typical bonding energy curve showing the long-term interaction between a molten asphalt (150°C) and an aggregate (−35 +48 mesh).

TABLE 17-8

Bonding energies of neat and modified asphalt–aggregate systems

Aggregate	Surface area (m^2/g)	Aggregate modification	Asphalt	Asphalt modification	Bonding energy (mcal/g-2 hr)	Reference
Ottawa Sand	1.75	none	B-5684	none	443	[a]
Ottawa Sand	1.75	none	B-5679	none	90	–
RA-granite	0.10	none	AAM-1	none	69	[b]
RA-granite	0.10	Fe	AAM	none	280	–
RB-granite	0.83	none	AAM-1	none	333	–
RB-granite	0.83	none	AAM	AS-017 (5%)	624	–
RK-basalt	17.4	none	AAM-1	none	570	–
RJ-gravel	0.37	none	AAM-1	none	148	–
RJ-gravel	0.37	Fe	AAM	none	594	–
RJ-gravel	0.37	none	AAM	AS-017 (5%)[c]	737	–
RA-granite	0.10	Mg	AAM	none	123	–

[a] Taken from data supported by Federal Highway report and publication.
[b] Taken from final SHRP report.
[c] AS-017 refers to antistrip agent.

peak followed by a long tail. Part of the shape of the bonding curves is due to the initial strong asphalt–aggregate interaction followed by, what has been postulated, the formation of an interphase region. Thermal lag also influences the shape of the curve, which could partially be removed by deconvolution. The bonding energy curves reflect both the number of bonding sites and the bonding strength per site. The number of sites is closely related to the surface area. For standardization, most bonding energies have been reported for −35 +48 Tyler mesh size. Even though bonding energy data are in units of millicalories per gram per 2 hours, surface areas are recorted so that data can be reported in terms of energy per unit area.

Table 17-8 shows several bonding energies (2 hours) representative of neat and modified systems. The data in the table were extracted from various reports and papers [27,28] to represent the application of thermodynamic measurements to asphalt–aggregate interactions. For example, the Ottawa Sand aggregate was used to distinguish between tender and non-tender asphalts. A tender asphalt is an asphalt that ruts badly soon after construction and a non-tender asphalt is the one that does not show unusual rutting after construction. Non-tender asphalts had much higher bonding energies than the tender asphalts. Eight asphalts (only two are used as examples) were evaluated using Ottawa Sand as a standard aggregate.

The aggregates RA-granite, RB-granite, RK-basalt, and RJ-gravel reported in Table 17-8 are materials used in the Strategic Highway Research Program (SHRP). Both surface areas and aggregate composition were reported (only surface areas are reported here) because both of these aggregate properties influence bonding [27,28]. The bonding energy data and aggregate analyses indicate that iron, calcium, and magnesium are allegedly bonding promoters, whereas sodium and potassium could be deleterious, especially in the presence of water.

The effects of modifying an aggregate with iron and magnesium to enhance bonding energies are seen for RA-granite and RJ-gravel with AAM asphalt. The effect on bonding energies of the addition of an antistrip agent, AS-017, are also seen in Table 17-8.

Previously, it was proposed that asphalt bonding to an aggregate proceeded by orientation of the polar asphalt molecules at the aggregate surface [7,22,23, 29,28]. Quoting Barth, "Adsorption of polar asphaltenes by foreign surfaces takes place initially when such surfaces are first coated with molten asphalt (or oil-diluted bitumen); continued orientation of polarizable molecules continues from this stage onward, although more slowly due to high viscosity of the medium." Expanding on this concept, Ensley and Scholz [7] proposed that after a polar molecule becomes attached on the aggregate surface, the molecule becomes further polarized to produce a second bonding site. Evidence to support the formation of a multilayer or interphase region included flow-through-porous-media experiments and photomicrographs of the region near the aggregate surface.

The flow-through-porous-media (FTPM) technique consists of flowing filtered asphalt in a molten state through a column of aggregate (80–100 mesh). The rate of flow gradually decreases as the polar asphalt molecule build up on the aggregate surface. Analyses of the asphalt in the column indicate, in some systems, that molecules having carbonyl and sulfoxide functionalities concentrate slightly near the aggregate surface [27]. Photomicrographs [30] of a fractured region near the aggregate surface show perpendicular striations, indicating a perpendicular alignment in support of the molecular orientation concept.

OTHER APPROACHES TO THERMODYNAMICS OF ASPHALT AND ASPHALT–AGGREGATE INTERACTIONS

Mack [8] reviewed the possible applications of physical chemistry, including thermodynamics, to asphalt intermolecular interactions. He questioned the idea that asphalt molecules formed any sizable association in neat asphalt by intermolecular interactions. It had been reported that evaporation of solvent from solutions of asphalt produces clusters of asphaltenes. But when pictures of thin films of asphalt were obtained with an electron microscope, no such clusters were noted. Perhaps the aggregation of asphalt molecules following evaporation has incorrectly promoted a micelle concept. Asphalt is very ductile. Ductility implies that molecules can easily slip by one another so it is feasible that some of the flow properties of asphalt are due to asphalt structure consisting of linear chains of molecules loosely held together through dipole, induced dipole, and London dispersion forces. This concept may be closer to the actual molecular association that occurs in asphalt rather than association through micelles.

Will it ever be possible to calculate the properties of asphalt based upon molecular structure? This is doubtful because of the complexities of the asphalt molecules, variety of the molecules, and the asphalt composition variance. In an effort to understand the molecular structure of asphalt, it is of interest to discuss the differ-

ent molecular concepts and formula for liquid intermolecular interaction and in a qualitative way to apply it to the complex bituminous materials.

If one could calculate both the distribution of particles surrounding a selected particle and the associated interaction energy, then it would be possible to calculate most of the important properties of a fluid that would be of value. The total configurational energy, E, of a system of N molecules in volume V is given in Eq. 17-29 below in terms of the distribution $g(\nu)$ and the potential energy $\phi(\nu)$ of the molecules.

$$E = \frac{2\pi N^2}{V} \int_0^\infty \phi(\nu) g(\nu) \nu^2 \, d\nu \tag{17-29}$$

where ν = distance from representative molecule. Basically, the equation states that if one knows or can calculate the potential energy, $\phi(\nu)$, between any two molecules and simultaneously the distribution, $g(\nu)$, then one could calculate the total energy of a system. The calculation of these two interaction parameters have been approached by a variety of techniques. Labib and Malijevsky [31] presented nine different formulas representing the macroscopic properties in terms of the distribution functions and the interaction energy. These theories were compared through calculations of compressibility factors and internal energy calculations, the two factors mentioned previously that are important to the thermodynamics of an asphalt. Formulas of this nature apply only in a qualitative manner to bituminous materials because of the required assumptions necessary for the calculations. For example, $g(\nu)$ is difficult to determine mathematically even on simple ideal systems. It has, however, been determined experimentally by X-ray scattering techniques. Determination of $g(\nu)$, the particle distribution term, by X-ray scattering of thin asphalt films would be a real challenge.

The potential energy term, $\phi(\nu)$, can be expressed as a linear combination of a repulsion term and an attraction term:

$$\phi(\nu) = \phi_{\text{repulsion}} + \phi_{\text{attraction}}$$

Mies' equation is one example:

$$\phi(\nu) = A\nu^{-m} - B\nu^{-n} \tag{17-30}$$

where ν is the distance between molecular centers, A and B are constants, and m and n are integral constants that are usually in the 1 to 12 range. n and m are often determined experimentally. One experimental technique for evaluating these integers includes measuring the compressibility over a wide pressure range. The techniques used to determine compressibilities were discussed previously in the discussion of cohesive energies via compressibilities. The Hildebrand method has been used for calculating the constants A and B [2]. Data that are required include the molar volume at any temperature, the internal energy U which can be found through $(\partial U/\partial V)_T$ calculations, and again $g(\nu)$, the molecular or particle

distribution function. Application of this approach to bituminous materials offers a great challenge but is not impossible.

Another bridge between molecular properties and thermodynamic properties is through statistical thermodynamics. Mack [8] discussed the application of statistical thermodynamics to asphalt and its limitations. He noted that asphalt at ambient or low temperatures has properties of a disordered solid. He expressed the total partition function, Q, in terms of a momentum partition function and a configurational partition function.

The usual thermodynamic functions can be written in terms of the total partition function [2]:

Total energy: $$U = kT^2 \left(\frac{\mathrm{d}(\ln Q)}{\mathrm{d}T} \right)_{\mathrm{v}} \tag{17-31}$$

Free energy: $$A = -kT \ln Q \tag{17-32}$$

Entropy: $$S = k \left[\ln Q + T \left(\frac{\mathrm{d} \ln Q}{\mathrm{d}T} \right) \right] \tag{17-33}$$

The total partition function, Q, can be split into a contribution from momentum, rotation and oscillation. Momentum and rotation at low temperatures can probably be neglected for asphalt. The oscillatory contribution can be written as a sum of the potential energy of a particle in its equilibrium state and the potential energy due to displacement from the equilibrium position.

As usual, direct application to a complex material like asphalt is inherently difficult but a few comments are appropriate. For example, Mack expressed the energy of an oscillator in terms of the distance, a, between centers and through the use of the internal energy, U, as a function of the partition function, Q, and concluded $U = U(T) - \phi(a)$, where $U(T) = T(\partial U/\partial T) = C_{\mathrm{v}}T$, and $\phi(a)$ is the potential energy in the equilibrium position; C_{v} is the heat capacity at constant volume.

The energy of interaction term $\phi(a)$ was expressed in terms of an attraction term Ba^{-n} and a repulsion term Aa^{-m}:

$$\phi(a) = Aa^{-m} - Ba^{-n} \tag{17-34}$$

Saal [8] was able to show using asphalt compressibility data that:

$$n + m = 24 \tag{17-35}$$

The value for m, repulsive exponent, is usually in the range of 18, which means n is equal to 6, indicating a rather strong repulsive field. The other thermodynamic functions, Helmholtz free energy A and entropy S, can also be found in terms of the partition function, Q. However, it is always a matter of what approximations are necessary to achieve the end product for the values for U, S, and A, and then to decide if the final product is representative of the physical system. This will always be a challenge with complex bituminous materials.

SUMMARY

The complexity of bituminous materials fosters a continuation of research at both the microscopic and macroscopic level. At the microscopic level, separation of asphalts by chromatographic means followed by spectroscopic analyses has led to a better understanding of the functionalities in asphalt that contribute to the physical performance. Scientists will probably never separate asphalt into individual molecular components and identify the components, but they will get closer as instrumentation becomes more sophisticated.

In the meantime, the limited structural information can qualitatively be coupled with thermodynamic and rheological measurements for interpreting mix characteristics and, hopefully, it will be used for highway performance prediction.

ACKNOWLEDGEMENTS

Much of the work presented in this chapter is an accumulation of data obtained in the laboratories at Western Research Institute. The writer is grateful for data acquisition by several excellent technicians and young scientists including Mark Scott, Scott Smith, Steve Rickard, and Jane Tauer. Jane has given an added dimension in computer expertise. The writer also appreciates financial support by the Federal Highway Administration and more recently the Strategic Highway Research Program (SHRP). Without their support the work on asphalt would have been much more limited. And finally the writer would like to thank Jackie Greaser for typing and correcting errors in the manuscript.

REFERENCES

[1] Castellan, G.W., *Physical Chemistry*. Addison-Wesley, Reading, Mass., 717 pp. (1964).
[2] Moelwyn-Hughes, E.A., *Physical Chemistry*. Pergamon Press, New York, N.Y., 1334 pp. (1961).
[3] Lee, J.F., Sears, F.W. and Turcotte, D.L., *Statistical Thermodynamics*. Addison-Wesley, Reading, Mass., 374 pp. (1963).
[4] Gardon, J.L., Critical review of concepts common to cohesive energy density, surface tension, tensile strength, heat of mixing, interfacial tension, and butt joint strength. *J. Colloid Interface Sci.*, 39: 582–596 (1977).
[5] Barton, A.F.M., *Handbook of Solubility Parameters and Other Cohesion Parameters*. CRC Press, Boca Raton, Fla., 594 pp. (1983).
[6] Hildebrand, J.H. and Scott, R.L., *The Solubility of Nonelectrolytes*. Reinhold, New York, N.Y., 488 pp. (1950).
[7] Ensley, E.K. and Scholz, H.A., A study of asphalt–aggregate interactions by heats of immersion, *J. Inst. Pet.*, 58: 95–101 (1972).
[8] Mack, C., Physical chemistry, In: A. Hoiberg (Editor), *Bituminous Materials*. Interscience, New York, N.Y., 419 pp. (1964).
[9] Billmeyer, F.W., Jr., *Textbook of Polymer Science*, John Wiley and Sons, New York, N.Y., 578 pp. (1984).
[10] Walker, E.E., The solvent action of organic substances on polyacrylonitrile. *J. Appl. Chem.*, 2: 470–481 (1952).
[11] Brush, S.G., Theory of liquid viscosity. *Chem. Rev.*, 62: 513–536 (1962).

[12] Moavenzadeh, F. and Stander, R.R., Jr., Effect of aging on flow properties of asphalt. *Highway Res. Rec.*, 178: 1–29 (1967).
[13] Ensley, E.K., The influence of intermolecular interactions on viscosities at low temperatures: forced sphere and forced-cylinder viscometers, ASTM SPT 628. In: C.R. Marek (Editor), *Am. Soc. Test. Mater., Spec. Tech. Publ.*, 43: 43–55 (1977).
[14] Eyring, H., Viscosity, plasticity, and diffusion as examples of absolute reaction rates. *J. Chem. Phys.*, 4: 283–289 (1936).
[15] Hershfelder, J.O., Curtiss, C.F. and Bird, R.B., *Molecular Theory of Gases and Liquids*. John Wiley and Sons, New York, N.Y., 249 pp. (1954).
[16] Little, D.N., Button, J.W., White, R.M., Ensley, E.K., Kim, Y. and Ahmed, S.J., *Investigation of Asphalt Additives*. Federal Highway Administration, Washington, D.C., Report No. FHWA/RD-87/001, November (1986).
[17] Khosla, N.P. and Zahran, S.Z., A mechanistic evaluation of mixes containing conventional and polymer modified (styrelf) asphalts. *Proc. Assoc. Asphalt Paving Technol.*, 58: 20–30 (1989).
[18] Fedors, R.F., A simple model for the virtually crosslinked block polymers. *J. Polym. Sci.*, 26: 189–199 (1969).
[19] Petersen, J.C., *Quantitative Functional Group Analysis of Asphalts Using Differential Infrared Spectrometry and Selective Chemical Reactions — Theory and Application*. TRB Research Rec. 1096, Washington, D.C. (1986).
[20] Reid, R.C., Prausnitz, J.M. and Sherwood, T.K., *Properties of Gases and Liquids*. McGraw-Hill, New York, N.Y., p. 688 (1977).
[21] Anderson, D.I., Peterson, D.E. and Wiley, M., *Characteristics of Asphalts as Related to the Performance of Flexible Pavements*. Utah Project HPR State Study, Final Report No. 925B (1976).
[22] Ensley, E.K., A kinetic investigation of association in asphalt. *J. Colloid Interface Sci.*, 53: 452–460 (1975).
[23] Mack, C., Physical properties of asphalt in thin films. *Ind. Eng. Chem.*, 49: 422–427 (1957).
[24] Bikerman, J.J., Adhesion of asphalt to stone. *J. Mater.*, 1: 34–47 (1966).
[25] Mathews, D.H., Adhesion in bituminous road materials: A survey of present knowledge. *J. Inst. Petrol.*, 44: 423–432 (1958).
[26] Majidzadek, K. and Brovold, F.N., *State of the Art: Effect of Water on Bitumen-Aggregate Mixtures, Highway Research Board*, National Academy of Science, Washington, D.C., Special Report 98, (1968).
[27] Curtis, C.W., *Final Report: Fundamental Properties of Asphalt–Aggregate Interaction Including Adhesion and Adsorption-SHRP-A003B*. Strategic Highway Research Program, National Research Council, Washington, D.C. (1991).
[28] Ensley, E.K., Petersen, J.C. and Robertson, R.E., Asphalt–aggregate bonding energy measurements by microcalorimetric methods. *Thermochim. Acta*, 77: 95–107 (1989).
[29] Barth, E.J., *Asphalt Science and Technology*. Gordon and Breach, New York, N.Y., 700 pp. (1962).
[30] Ensley, E.K., Multilayer adsorption with molecular orientation of asphalt on mineral aggregate and other substrates. *J. Appl. Chem. Biotechnol.*, 25: 671–676 (1975).
[31] Labib, S. and Malijevsky, A., Test of simple fluid theories. *Collect. Czech. Chem. Commun.*, 48: 347–357 (1983).

Asphaltenes and Asphalts, 1. Developments in Petroleum Science, 40
edited by T.F. Yen and G.V. Chilingarian

Chapter 18

RELATIONSHIPS AMONG COMPOSITION, STRUCTURE, AND PROPERTIES OF ROAD ASPHALTS

BERNARD BRÛLÉ, GUY RAMOND and CHRISTIAN SUCH

INTRODUCTION

Reviewed is the past and ongoing research conducted at France's Laboratoire Central des Ponts et Chaussées (LCPC) (Public Works Central Laboratory) in the area of asphalt cements. The investigations cover the development of methods for characterizing the physicochemical and rheological properties of such materials, and the establishment of relationships between their composition, colloidal structure, and practical properties. For physicochemical characterization, the research makes use of such techniques as high-pressure liquid chromatography (HPLC), gel permeation chromatography (GPC), and differential scanning calorimetry (DSC). The rheological behavior of materials is studied by the peeling technique, viscoelastisimetry, and viscosimetry on thin films (with specially designed apparatus). Theoretical studies have led to the proposal of a new rheological behavior model better suited to experimental results than conventional models, characterized by its analogy with the laws of chemical kinetics, and allowing the calculation of a structural parameter as well as a parameter dependent on energy per unit volume dissipated and having activation energy characteristics. The foregoing assessment brings out the effectiveness of the facilities set up by the LCPC, and it is important to note that the new characterization methods indicate that asphalt cements with the same specifications have substantially different physicochemical compositions and rheological behaviors. Among the most important results, it is demonstrated that GPC made it possible to characterize the equilibrium of the colloidal structure of asphalt cement and to obtain information on the ability of asphaltenes to interact to form a more or less developed network responsible for the gel character of the rheological behavior noted. It is also demonstrated that information obtained by GPC on the interaction of asphaltene micelles is closely correlated with certain observed characteristics of rheological behavior.

The Laboratoire Cental des Ponts et Chaussées has long been engaged in research in the area of hydrocarbon binders. Regarding asphalt cements and asphaltic concretes, the observation during the past ten years of a certain number of disorders related, undoubtedly, to the increase in traffic and to its aggressive action (in France, axle loads of 13 metric tons are authorized) but not entirely explained by these factors, has emphasized the need for research on the relationships between composition and properties.

For asphalt cements, the research has a twofold objective:

(1) To acquire knowledge on the chemical composition of binders in the generic sense of the term, their microscopic and colloidal structure, and their rheological and practical properties, as well as on the evolution of these properties during mixing and weathering in situ.

(2) To establish experimental relationships between composition, structure, and properties and to determine the evolution of these relationships after mixing and weathering.

PHYSICOCHEMICAL CHARACTERIZATION OF ASPHALT CEMENTS

The study of the relationships between composition and properties calls for the use of reliable and fast means of characterization. In this area, the research of the LCPC associated with regional research laboratories involves the use of modern methods of liquid chromatography (HPLC and GPC), as well as thermal methods (essentially DSC).

High-pressure liquid chromatography

The HPLC technique was used initially for the characterization of asphalt cements and of the fractions composing them [1]. The study of operating parameters led to the choice of the following conditions:

(1) Packing = grafted silica C-18.
(2) Solvent A = chloroform–methanol–water: 50 : 40 : 10 (by volume).
(3) Solvent B = chloroform–methanol: 85 : 15 (by volume).
(4) Programming:
    Initial solvent = 80% of Solvent A.
    Final solvent = 100% of Solvent B.
    Gradient = No. 4 of Waters M 660 programmer.
    Programming time = 10 min.
    Flow rate = 2 ml/min.
    Detection = ultraviolet at 280 nm.

Programming is begun 2 minutes after injection. As an example, the chromatograms for a road asphalt cement obtained from a residue of blown and acidified Safaniya crude, its maltenes, and its asphaltenes are shown in Fig. 18-1.

The results of this research show that liquid chromatography with reverse phase polarity, on a C-18 grafted silica column, can be used for characterizing asphalt cements and their fractions through the use of a suitable solvent mixture (chloroform–methanol–water). Under these conditions, the chromatograms are clearly differentiated from one fraction to another. On the other hand, unlike what is generally observed with this type of support, the order of elution is not related directly to polarity because the low-polarity fractions are eluted before the higher-polarity fractions (maltenes, for example, are eluted before asphaltenes). It is thus difficult to compare elution volume and polarity. The injection of fractions having the

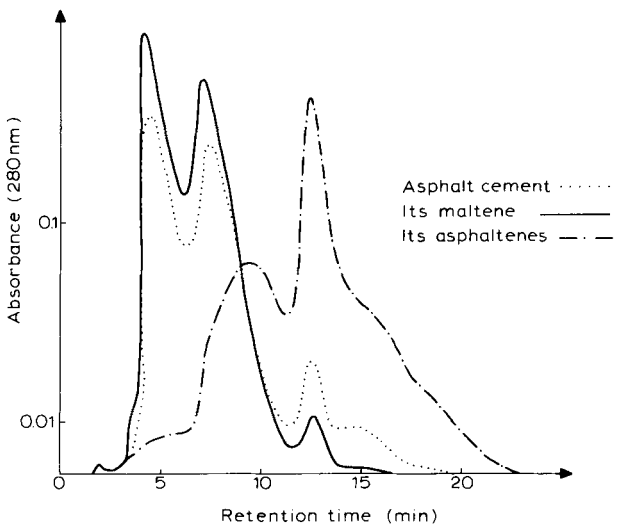

Fig. 18-1. HPLC chromatograms.

same polarity but different molecular weights (for example, aromatic fractions of maltenes and asphaltenes) and chloroform extracts show that the separation process is governed essentially by the solubility in chloroform.

During a later phase, the possibilities of applying HPLC to the fast determination of the generic composition of road asphalt cements was examined (it will be recalled that the generic composition is defined by the amount of saturated oils, aromatic oils, resins, and asphaltenes [2]). The technique adopted consists of eliminating the asphaltenes with *n*-heptane and then injecting the maltenes on a NH_2 grafted microsilica column [3]. The saturated oils are eluted at the dead volume and detected by differential refractometry, whereas the aromatic oils, slightly retained, are detected in ultraviolet. Resins, highly absorbed, are eluted by solvent backflushing. Figure 18-2 shows the type of chromatogram obtained. In this figure, column: μNH_2; solvent: heptane; flow rate: 2 ml/min; quantity injected: 160 μg; and BF: solvent backflush.

A comparison of the results of the fractionation of many samples of asphalt cements, conducted by using traditional methods, with those obtained by HPLC leads to the following conclusions:

(1) It is possible to characterize in a few minutes a solution of maltenes in heptane. There is a slight correlation between the HPLC results and the aromatic oil content, and a strong correlation between the HPLC data and the resin content. There is also a strong correlation between the HPLC results and the sum of the aromatic oil and resin contents.

(2) Correlation coefficients are clearly improved if they are calculated for a series of samples belonging to the same specification range.

(3) Unfortunately, it is difficult to control the reproducibility over a relatively long time period.

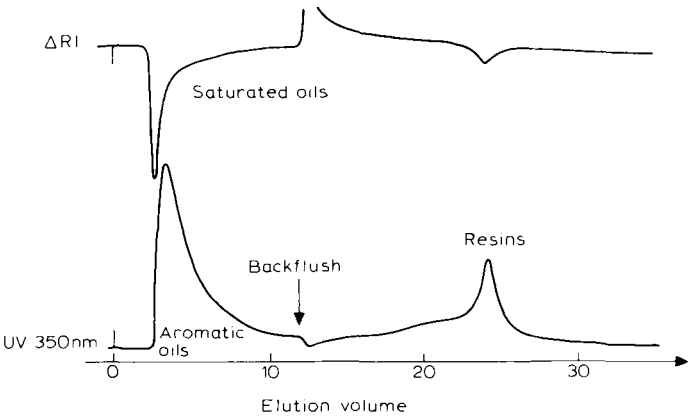

Fig. 18-2. HPLC chromatograms of maltenes of a 40–50 asphalt cement.

Gel permeation chromatography

The research activity of the LCPC within the area of GPC was much more extensive than in that of HPLC.

Initially, a simple qualitative characterization of asphaltenes [4] and asphalt cements [5] was sought, and the utility of a comparison between GPC and HPLC was examined [6,7]. Then, the attempt to use the technique in a more efficient manner for the determination of molecular weight distribution curves led to the observation of the colloidal behavior of asphalt cement solutions [8]. The purely analytical aspect was pursued along the following lines: (a) the correction of detector response, and (b) the experimental determination of a calibration curve for specific molecular weight, M. The equation in relation to traditional polystyrene standards is as follows [9]:

$$\log M \text{ (asphalt cement)} = 3.21 - 1.04X + 0.331X^2$$

where X is $\log M$ (polystyrene). The use of GPC, however, was especially important in the comparison of the colloidal structure of the binder and colloidal behavior of the solution.

The more recent work shows that, under well-chosen conditions, GPC makes it possible to obtain an image of the composition of the medium, in the colloidal sense of the term (intermicellar phase and dispersed phase distribution), and to assess the interaction properties of micelles within the colloidal system [10]. Conventional GPC (on a set of several columns with usual particle size ranging from 37 to 75 μm on very diluted solutions) leads to molecular weight distributions that are not greatly differentiated. In this case, neither the asphalt cement production method (straight-run distillation or semiblowing) nor the degree of weathering (natural or artificial) has a significant effect on the shape of the chromatograms. The GPC technique operates sufficiently slowly so that the dissociation has time to develop and the chromatograms obtained are close to those of ideal solutions.

A fast method is thus proposed, the conditions of which are as follows:

(1) Columns: dual columns of μStyragel of 10^3 and 10^4 Å, 30 cm long.
(2) Solvent: freshly distilled tetrahydrofuran.
(3) Injected quantity: 1 mg (10 μl of 10% solution).
(4) Flow rate: 3.5 ml/min.
(5) Detection: ultraviolet at 350 nm.

Under these conditions, it was possible to demonstrate that straight-run asphalt cements and especially their asphaltenes have bimodal distributions, whereas blowing always results in the appearance, more or less accentuated, of a third population being located toward the large molecular sizes. This is shown in Fig. 18-3, which give the chromatograms of blown and unblown road asphalt cements (Fig. 18-3a) and of asphaltenes extracted from these asphalt cements (Fig. 18-3b).

Systematic study of the influence of operating conditions on the image of molecular size distribution as obtained by GPC (and comparison between results obtained on μStyragel and on traditional Styragel) leads to the following conclusion: the entities eluted at the level of the third population (toward 1000 Å) and, to a lesser degree, at the level of the second population (220 Å) correspond to dissociable entities, because their apparent content decreases with the injected solution concentration [8].

The chromatograms of the asphaltenes of 40–50 asphalt cements before and after Rolling Thin Film Oven Test (RTFOT) are shown in Fig. 18-4 (under normalized conditions at 163°C). The signal height for a mass of about 100,000 gives the first idea of the interaction properties of the asphaltenes.

GPC examination of unfractionated asphalt cements indicates that it is not essential to isolate the asphaltenes in order to have information on intermicellar interactions, but the evaluation in this case is much less precise (Fig. 18-5). It is

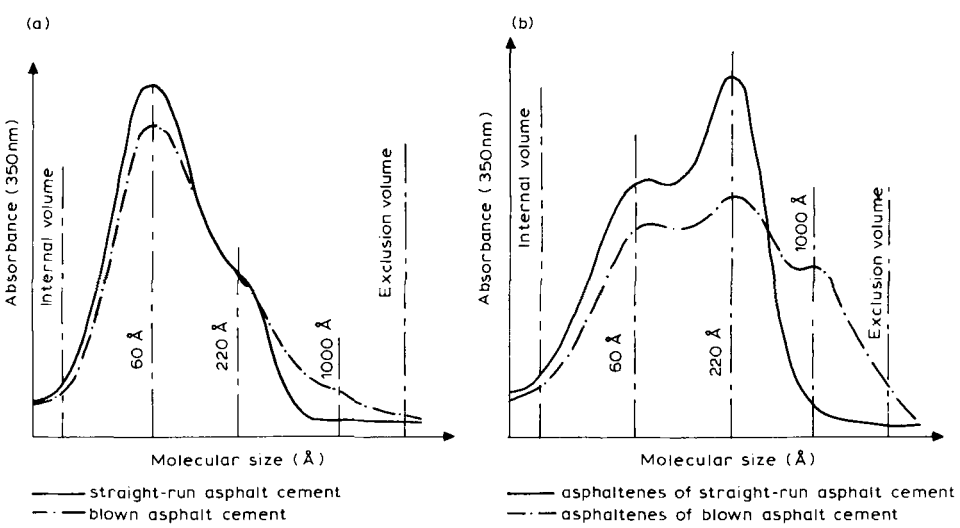

Fig. 18-3. Chromatograms of asphalt cements and asphaltenes.

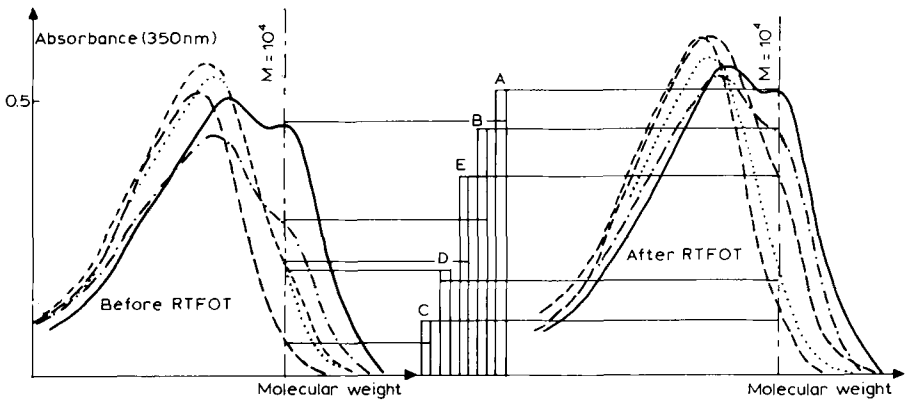

Fig. 18-4. GPC chromatograms of asphaltenes before and after RTFOT.

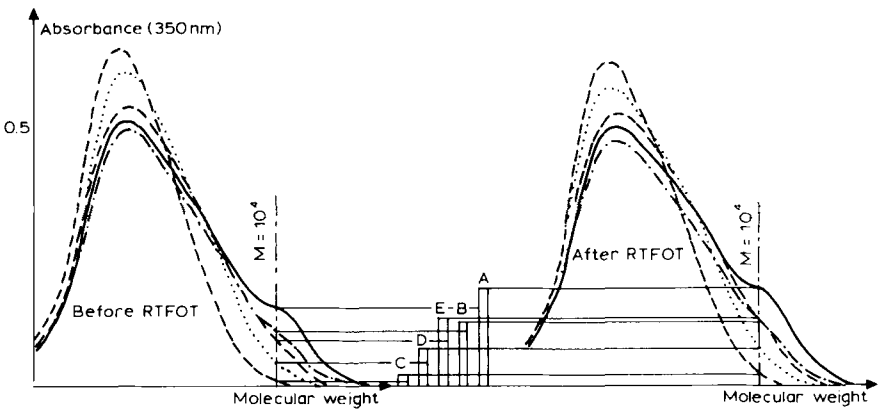

Fig. 18-5. GPC chromatograms of asphalt cements before and after RTFOT.

important to note that the information obtained on asphalt cements is not rigorously equivalent to that obtained on asphaltenes, because to isolate the latter, it was necessary to destroy the colloidal equilibrium of the system.

Because the entities eluted at the level of a mass of about 100,000 correspond to aggregates in the process of dissociation, it was decided to highlight the display of this intermicellar interaction property.

To accomplish this, the authors varied two parameters: the number of columns and the packing porosity. By eliminating one of the two columns, the elution time was divided by two, thereby limiting the dissociation. Moreover, by deliberately reducing the efficiency of the system in the range of large masses, the latter were obliged to group within a narrow range of elution volumes (in this instance, practically the exclusion volume if only the column of 1000 Å porosity is maintained).

With these new conditions of ultra-fast GPC, which differ from usual conditions only by the elimination of the 100,000 Å porosity column, the chromatograms shown

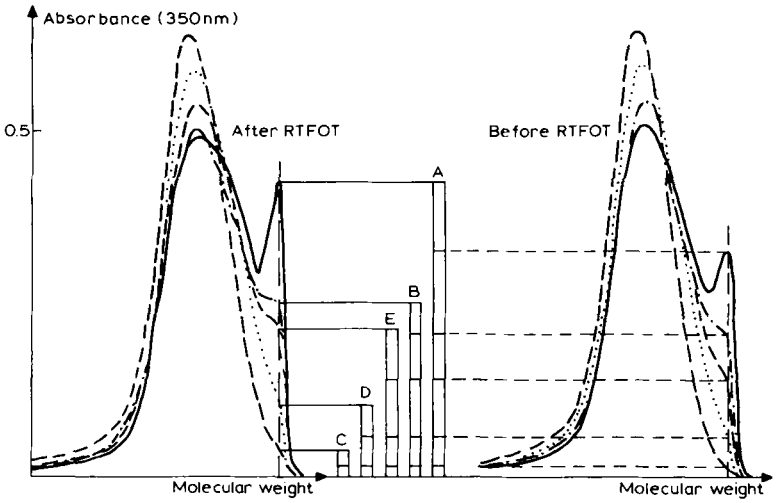

Fig. 18-6. Chromatograms of asphalt cements before and after RTFOT under ultra-fast GPC conditions.

in Fig. 18-6 are obtained. Under these conditions, the display of what shall be called the interaction index is obtained on unfractionated asphalt cement in a few minutes and in a satisfactory manner. For comparison, and arbitrarily, the interaction index will be marked as being the height of the signal at the exclusion volume for the ultraviolet detector. It is obvious that under these conditions the interaction index varies with all the operating parameters so that the comparisons can be only relative on a series of samples examined under rigorously identical conditions.

It is thus confirmed that ultra-fast GPC is a method of choice for the qualitative characterization of the complex equilibrium existing within the asphalt cement among:

Molecules $\rightleftharpoons$ micelles $\rightleftharpoons$ aggregates.

In such a diagram, the molecules (first population) are representative of the intermicellar phase; the micelles (second population with a mass of about 10,000) are representative of the soltype dispersed phase; and the interaction peak (entities with a mass exceeding 100,000) is an image of the fraction of the dispersed phase giving the binder its gel character. It is essential to note that there is no relationship between the interaction index and the consistency of the asphalt cement as it can be evaluated by penetrability measurement, for example. (Similarly, there is no relationship between the interaction index and the asphaltene content.)

Differential scanning calorimetry

Examples of the application of DSC to the characterization of road asphalt cements are relatively few, and the research was oriented by the desire to use

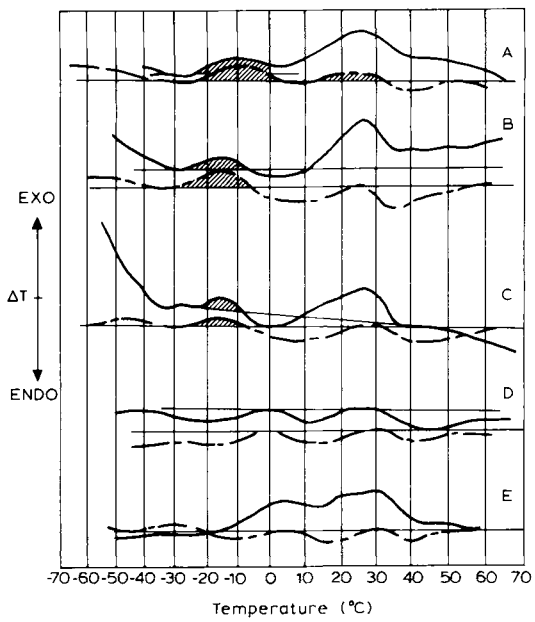

Fig. 18-7. Thermograms of five 40–50 asphalt cements: A, B, C, D, E.

the method to investigate phase transformation kinetics and molecular association aptitude [11].

In Fig. 18-7, the DSC curves of five 40–50 asphalt cements are grouped under helium and oxygen examined between −80°C and +80°C.

Under helium, the existence of exothermic transformations (of the crystallization type) are noted between approximately −30°C and 0°C and endothermic ones (of the fusion type) between approximately −5°C and +65°C. Their number and intensity are different for all the asphalt cements examined.

To better understand the origin of these transformations, Sample A was fractionated into its four generic groups. The thermograms of the fractions are shown in Fig. 18-8.

It can be observed that only the saturated and aromatic derivatives exhibit transformation waves. However, in a mixture in a ratio equivalent to that existing within the unfractionated asphalt cement, these two derivatives yield a thermogram very different from that of the original asphalt cement (Fig. 18-9).

Under oxygen, with the exception of one asphalt cement (Sample D) for which the DSC curve is little different from that obtained under helium, all of the thermograms are characterized by the existence of one or more exothermic waves between −30°C and +60°C.

The exothermic transformation domains at low temperatures (between −20°C and +5°C, −25°C and −8°C, and −30°C and −8°C, respectively, for asphalt cements A, B, and C) have the same range and comparable intensities. Changing the

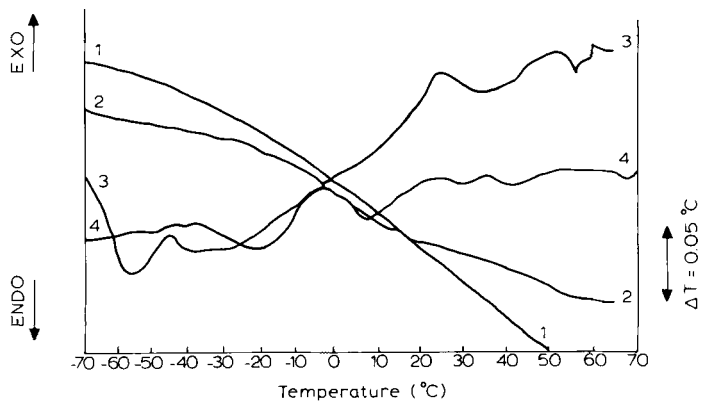

Fig. 18-8. Thermograms of fractions of asphalt cement A under helium (*1* = asphaltenes, *2* = resins, *3* = saturated, and *4* = aromatic).

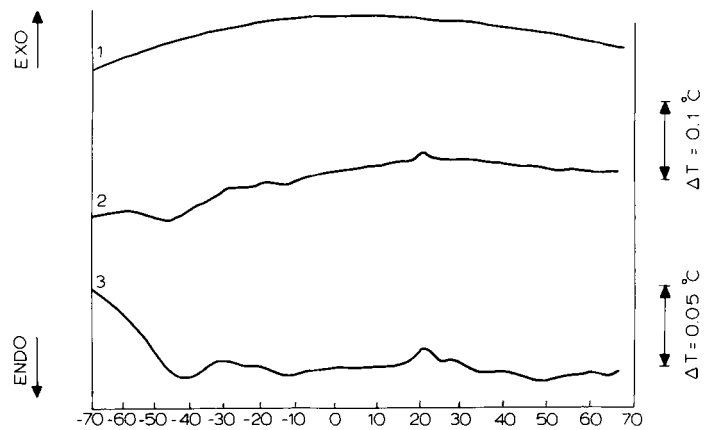

Fig. 18-9. Thermograms of mixture (1/1) of saturated and aromatic derivatives of asphalt cement A (*1* = derivative, *2* = uncorrected curve, and *3* = corrected curve).

scanning gas does not affect the constituents responsible for the crystallization delay.

On the other hand, at positive temperature, the physiognomy of the thermograms is completely different. The oxygen of the scanning gas appears to disturb substantially the equilibria of the phases and their transformation kinetics.

As in the preceding case, the repeatability of the test can be obtained only after the sample is allowed to rest for a few hours (24 hours). In addition, a return to helium gas after testing under oxygen makes it possible to obtain the same endothermic and exothermic waves again, meaning that under the operating conditions adopted there were no irreversible chemical reactions (oxidation).

The movements observed on these asphalt cements in an oxygen medium could thus be caused by oxygen interference on the aromatic sheets of the products. The

aromatic rings are electron acceptors, and the greater the delocalization, the stabler the compound formed.

CHARACTERIZATION OF RHEOLOGICAL BEHAVIOR

Research activity in this area is being pursued along two lines:

(1) The adaptation of existing instrumentation (such as the viscoelastisimeter) and the development of new facilities (peeling, sliding plate viscosimeter for ultra-thin film investigations or very small deformation cone-plane viscosimeter), allowing the experimental characterization of rheological behavior.

(2) The adaptation of non-linear viscoelastic behavior models to experimental results.

Experimental characterization

Peeling

To evaluate the cohesion of asphalt cements, a method frequently used in the field of polymers was chosen: peeling, which consists of measuring the force required to cause the failure of a film of binder under given speed and temperature conditions [12].

In practice, an angle of 90° is most often used, and the failure is obtained by imposing a separation speed and measuring the force generated. The failure may occur in the binder and the cohesion is then measured, or it may occur in the interface, making it possible to evaluate the overall adhesion.

Because peeling resistance depends on the width of the peeling front, it has been expressed by a parameter defined by the formula $\gamma = F/G$, F being the measured force and G the width of the peeling front. This may be represented as a function of speed in the form of isotherms in log-log coordinates (Fig. 18-10). In this form, it is possible to plot a master curve because of the horizontal shift defined by a translation factor, a_T, similar to the Williams–Landel–Ferry (WLF) parameter [13, p. 216].

In a study conducted on 12 binders it was demonstrated that [14]:

(1) On all of the asphalt cements tested, the peeling master curves have a parabolic shape in a representation giving a correspondence between the logarithm of the peeling force and the logarithm of the speed; this curve shape corresponds to the data of the literature. At low speed, the peeling force is small, increases with the increase in speed, goes through a maximum, and then drops. As a rule, when cracking propagates in an asphalt cement, the maximum force corresponds approximately to the beginning of the slip–stick phenomenon (case of brittle fracture in which the cracking speed is higher than the advancing speed: the force increases; the system stores energy, which is dissipated causing a sudden advance of the crack; and it is necessary to wait for the strip to tension again).

(2) The plotting of master curves leads to the adoption of different figures for the value of the constants C_1 and C_2 of the WLF law, depending on the asphalt cements.

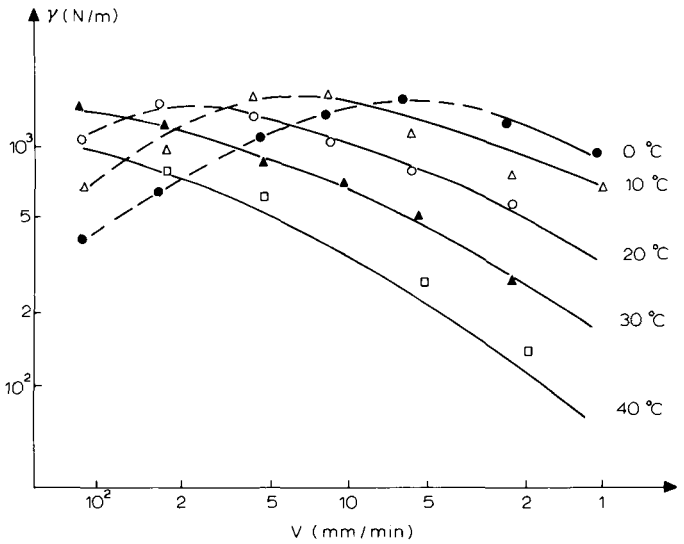

Fig. 18-10. Isothermal curves of peeling force.

(3) As the peeling fracture energy is related to the complex modulus and hence to the relaxation time spectrum, which can be assimilated with a log-normal curve, it is not surprising that the general shape of the master curves leads to a mathematical formula of the log-normal type [15].

(4) There is a good correlation between the speed giving the maximum force and the Fraass brittleness temperature.

In a second series of tests, an attempt was made to specify the relationship between the peeling resistance and the complex modulus. Figure 18-11 shows, for two asphalt cements (H and I), the variations of the loss modulus E_2 as a function of frequency (master curve at 10°C) and those of the peeling force as a function of traction speed, under the same temperature conditions.

Within the range of temperatures and speeds (or frequencies) tested, it is possible to assimilate them as a first approximation with a log-normal curve arc. This simplification is not absolutely rigorous, but allows them to be characterized more conveniently by two parameters: the median and the average peak widths ($\log f_m$ and σ_f for the loss modulus, and $\log V_m$ and σ_v for peeling).

In Table 18-1, the calculated values of the medians and the average widths of the loss-modulus and peeling curves are grouped for the six asphalt cements investigated, along with their conventional characteristics: (a) The parameters σ_v of the peeling curves represent about 50% of those of the complex modulus curves σ_f, and (b) the smaller the medians of E_2, the smaller the medians of the peeling curves.

The application of Grosch's formula ($V_m = \lambda_m f_m$) would thus give, for the parameter λ_m (defined as the average distance between two consecutive molecules), values on the order of 10^{-8} m for the asphalt cements G, H, I, and K, and on the order of 10^{-9} for the less sensitive asphalt cements F and J [16, p. 21]. The

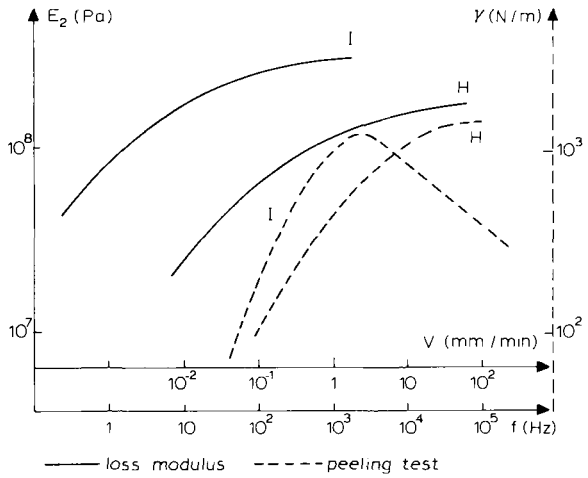

Fig. 18-11. Comparison of master curves of loss modulus as a function of frequency, and of the peeling resistance as a function of traction speed.

TABLE 18-1

Comparison between peeling and complex modulus for six asphalt cements

	Pen_{25} (0.1 mm)	R & B (°C)	PI (Pen.)	log f_m (Hz)	σ_f	log V_m (mm/min.)	σ_v	σ_v/σ_f	λ_m (10^{-9} m)
F	88	54	1.2	≃7	≃2.5	≃2.6	≃1.3	0.52	0.01
G	88	46	−1.1	4.1	1.6	1.3	0.9	0.56	0.26
H	82	48	0.1	5.1	2.1	1.8	1.25	0.60	0.083
I	82	44	−1.7	3.0	1.5	0.5	0.8	0.53	0.53
J	38	60	1.1	5.5	2.5	1.3	1.3	0.52	0.01
K	54	53	−0.3	4.0	1.9	0.65	1.2	0.63	0.7

parameter λ_m decreases as the penetration index (PI) increases, which was expected because an increase in molecular interlacing is accompanied by a decrease in thermal susceptibility.

Consequently, the peeling test appears to allow, with relatively simple equipment and operating procedures, a good discrimination of the binders from the viewpoint of cohesion and brittleness. Because the peeling force depends on the viscoelastic properties and in particular on the complex modulus, it may indirectly provide valuable qualitative information on the rheological behavior of the products tested.

This test can provide valuable information on the relationship between the energy restitution rate and the cracking speed, until a theoretical study would permit their direct calculation from the complex modulus. Carried out under slightly different conditions, this test could be used for testing overall adhesion on mineral supports with or without the presence of water.

Thin-film viscosimetry

Regarding thin-film viscosimetric experiments, the authors wanted to check whether the rheological behavior of asphalt cements between two solid surfaces separated by a few microns was the same as in the case of greater thickness. It appeared of interest to investigate the creeping of thin films to determine the behavior of the binder located at the interface. For this purpose it was necessary to design and build equipment specifically suited to this problem [18].

Thus a creep apparatus was designed based on the principle of simple shearing between two sliding parallel planes. The load is applied and the relative displacement of one of the planes as a function of time is measured. This original prototype is distinguished by the following:

(1) The imposed thickness of the examined film; a gluing bench makes it possible to obtain a rectangular film with an area of 18 cm^2 and a few micrometers thick (approximately 10 μm).

(2) The range of the authorized loads (1 to 10,000 g), which was obtainable by adequate dimensioning and a sliding system design that cancels all of the undesired movements.

(3) The loading system, which allows loading and unloading without disturbing the asphalt cement film, and tensioning is almost instantaneous.

(4) Finally, depending on the thickness chosen, the range of measurable speeds is between 10^{-4} and 10 μm/s and the corresponding gradients range from 10^{-6} to 1 s^{-1}.

The first experiments conducted were aimed at verifying and specifying the performance of this equipment. It was thus possible to obtain homogeneous asphalt cement films with a constant thickness (± 0.5 μm) and a minimum value of 6.5 μm for road asphalt cements of the 60 to 70 class, that is, having an average viscosity of 10^6 to 10^7 Pa s at 20°C. The deviation sensitivity tests under a light load demonstrated that, in the presence of an asphalt cement film more than 50 μm thick, the balance of the beam should be obtained within less than 500 mg to avoid any significant creep in the specimens (a few micrometers in 2 or 3 hours). The dynamic range of the possible loads is thus wide.

The minimum displacement speed depends on the system for regulating the temperature, which causes viscosity fluctuations. The tolerable fluctuation has been estimated within the limit of 1/10 of a degree. The curves determined for the smallest loads (between 1 and 5 g) and for the transducer used show that the steady flow established during the first instants remains stable throughout the test (about 18 hours). These speeds are on the order of 10^{-4} μm/s. On the other hand, the highest speeds measurable are deliberately limited to 10 μm/s for practical recording reasons.

Theoretical aspect: adaptation of non-linear viscoelastic behavior models to experimental results

It has been shown, based on cone-plane viscosimetry experiments on model asphalt cements (in which the maltenes have been replaced by tetraline), that the

equations governing the kinetics of the process are not linear and are similar to those that govern the advance of chemical reactions [18]. It will be recalled that in chemical kinetics, during a reaction, the variation in the concentration $|A|$ of the reagents follows a law of the type $d|A|/dt = k|A|^n$, where $d|A|/dt$ is the time derivative of A concentration, k is related to the activation energy, and n is related to the order of the reaction.

It is thus possible to transpose to rheology the two basic notions of activation energy and order. The application of these principles makes it possible to differentiate, by their orders, the behavior of asphaltenes extracted respectively from a straightrun asphalt and from a blown asphalt.

The continuation of experimentation by studying the evolution of shearing stress with time at a constant shearing rate followed by relaxation tests leads to curves that all have the shape shown in Fig. 18-12 [19].

It is noted that the stress increases regularly with time up to a maximum value that corresponds to a steady flow of the material and that depends on both the shearing rate and temperature. The representation in bilogarithmic coordinates of σ_{max} as a function of $\dot{\varepsilon}$ gives a line with an excellent correlation ($r^2 \geq 0.999$) for different temperatures. Figure 18-13 shows the lines obtained for 20°C, 40.5°C, and 60°C. Further, it has been noted that the experimental relaxation curves all confirm, with a good correlation, an equation of the type

$$d\sigma/dt = -k\sigma^n$$

Several experiments were carried out for different deformation values (after relaxation) and it was observed that the results were independent of these values. This led to the adoption of rheological model of the Maxwell–Norton type [20]. It is governed by the differential equation

$$\dot{\varepsilon} = J\dot{\sigma} + \alpha\sigma^n$$

The values of the parameters α and n were determined from the line ($\log \sigma_{max} -$

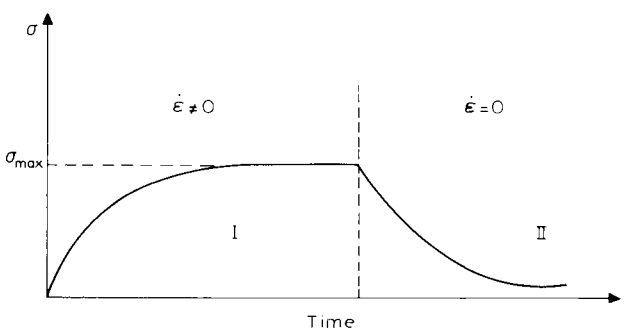

Fig. 18-12. Typical curves of isothermal evolution of stresses (*I* = test at constant shearing rate, and *II* = relaxation test).

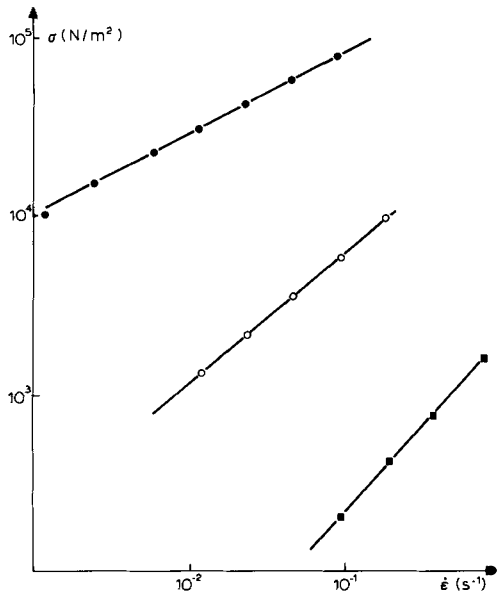

Fig. 18-13. σ_{max}–$\dot{\varepsilon}$ curves at three temperatures (● = 20°C, ○ = 40.5°C, and □ = 60°C).

TABLE 18-2

Numerical values of different parameters as a function of temperature

Parameter	Temperature (°C)				
	20	30	40.5	49	60
n	2.28	1.47	1.415	1.12	1.05
J (MKS)	8.5×10^{-4}	9.0×10^{-4}	9.5×10^{-3}	1.4×10^{-1}	1.3×10^{-1}
α (MKS)	6.56×10^{-13}	6.18×10^{-8}	4.85×10^{-7}	3.92×10^{-5}	3.90×10^{-4}

$\log \dot{\varepsilon}$) and the value of J from the relaxation curves. These values are given in Table 18-2 for different temperatures. The relative errors are estimated at about 5% for α and n, and 10–15% for J, at 20°C. These errors are smaller for high temperatures.

The rheological model is of great interest for two reasons. First, it allows, for relaxation investigations, an analogy with models that are well known in chemical kinetics (see previous discussion). Second, it is easily applicable to the case of multiaxial stresses because of the generalized Norton–Hoff law, which lends itself readily to numerical calculation (by finite elements, for example) [21]. In the model, n is a structural coefficient that reveals the importance of the spatial distribution of intermicellar interactions: the higher the value of this coefficient, the larger is the order because the material will then have the properties of a gel. On the other

hand, the closer the order to the unity, the more numerous and dispersed will be the asphaltene micelles without any strong interactions between them. The coefficient α is a function of the energy per unit volume dissipated and has the characteristics of an activation energy.

RELATIONSHIPS BETWEEN COMPOSITION, STRUCTURE, AND PROPERTIES

Review of colloidal structure of asphalt cements

The comparison of composition criteria, in the chemical sense of the term, with rheological behavior properties necessarily requires a schematic but realistic description of the colloidal structure of asphalt cements for proper understanding of the relationships.

In conventional diagrams, it is generally assumed that asphalt cements are colloidal systems made up of a suspension of asphaltene micelles peptized by resins in an oily medium. Concerning the macrostructure of asphaltenes, research conducted by Yen [22] has led to the proposal of the model shown in Fig. 18-14 for the asphaltene micelle. In this model, the overall cohesion of the micelle is provided by interactions between the π electrons of the pericondensed polynuclear aromatic sheets.

The Yen model, however, is not limited to the formation of micelles. It also offers the possibility of creating complex edifices formed by the association of several micelles into real aggregates, as shown in Fig. 18-15. The formation of these aggregates is considered to be related to intermolecular interactions, the nature of which is not indicated.

It is easily understood that one of the key parameters governing such a colloidal structure equilibrium is the chemical composition of its constituents. It is also easily observed that any modification in this equilibrium (notably, under the action of a temperature variation) leads to a modification in rheological behavior.

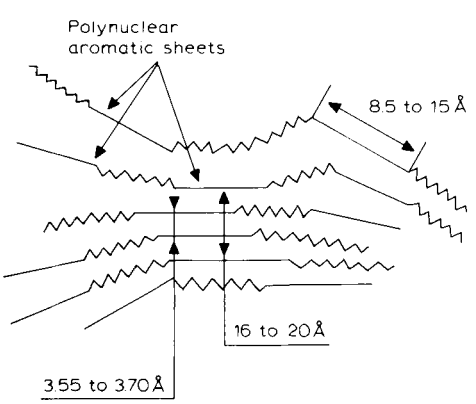

Fig. 18-14. Section of an asphaltene micelle model according to Yen [22].

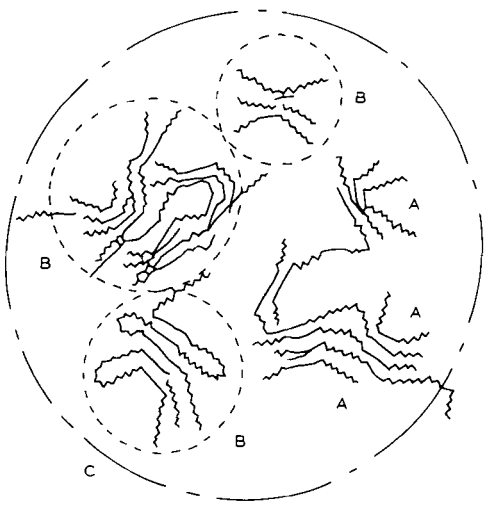

Fig. 18-15. Macrostructure of asphaltenes according to Yen [22] (*A* = molecule, *B* = micelle, and *C* = aggregate).

Comparison of composition and structure

Many authors have attempted to characterize the stability of the colloidal state of asphalt cements at ordinary temperature on the basis of chemical analysis in generic groups. Gaestel et al. [23], for example, have defined a colloidal instability index as the ratio of the sum of the amounts of asphaltenes and flocculants (saturated oils) to the sum of the amounts of peptizer (resins) and solvents (aromatic oils):

$$I_c = (\text{Asphaltenes} + \text{saturated oils})/(\text{resins} + \text{aromatic oils})$$

The higher the ratio, the more will be the asphalt cement of the gel type and the lower will be its colloidal stability. Gaestel et al. also noted that all the properties of the binder (softening point, ductility, embrittlement temperature, thermal susceptibility, elastic recovery, shearing susceptibility, etc.) vary significantly with the colloidal instability index and hence with composition.

These different investigations represent a major contribution to the understanding of relationships between composition and properties. It may be noted, however, that they take into account only the amount of asphaltenes without taking into account their quality. In fact post-research works have shown that asphaltenes derived from straight-run asphalts are different from those derived from blown asphalts.

Because of the arbitrary nature of the fractionation into generic groups and the lack of methods allowing direct observation of the colloidal structure of asphalt cements, it was considered of interest to develop a fast and reproducible analytical technique making it possible to work on the binder as is, without prior fractionation. This technique is GPC, discussed earlier in the chapter. Figure 18-16 shows the comparison that can be made between the structure of the binder characterized by

the equilibrium

$$\text{Oil} \rightleftharpoons \text{micelles} \rightleftharpoons \text{aggregates}$$

and the GPC chromatogram obtained in a few minutes under the previously proposed ultra-fast conditions. (It should be noted that, in this specific example, the asphalt cements A and B have practically the same asphaltene content, i.e., 15 and 15.2%, respectively, showing that the GPC interaction peak is independent of this content.)

The diagram presented (Fig. 18-16) offers two advantages, while complying with the models proposed in the past:

(1) It accounts for the results obtained with respect to the influence of the nature of asphaltenes on the viscosity of model asphalt cements and with regard to the application of GPC to the characterization of asphalt cements, and

(2) it introduces an additional property of the asphaltenes, namely, their ability to interact in order to yield a more or less complex network, responsible for the gel-type behavior.

The hypothesis set forth to explain the formation of aggregates specific to blowing (or weathering) is that the latter creates a certain number of active centers (polar functions) responsible for the intermicellar interactions (hydrogen bonding?). The more severe the blowing, the more numerous these interactions would be. It is hence easily observed that a straight-run asphalt cement is a colloidal system made up of individual micelles, hence of the sol type, as shown in the right part of Fig. 18-16. During blowing, not only does the asphaltene content increase but an

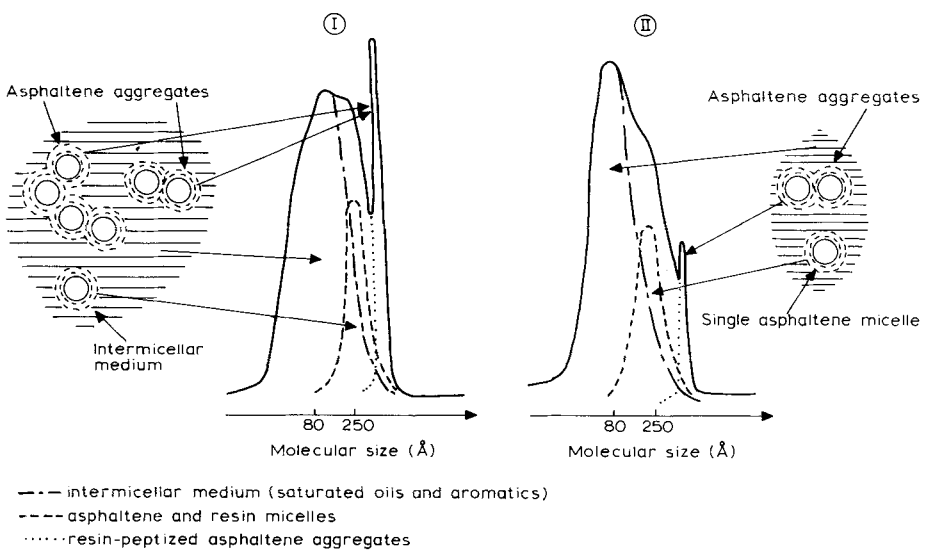

Fig. 18-16. GPC chromatograms (broken down into three populations) and colloidal structure of road asphalt cements (*I* = blown asphalt cement and *II* = straight-run asphalt cement).

increasing amount of micelles interacts to form aggregates that give the material an intermediate solgel structure with a viscoelastic behavior, the elastic component of which (or the structural viscosity) varies with the number of micelles engaged in the form of aggregates, and hence with the blowing rate. In the extreme case, for oxidized asphalt cements, the perfect gel structure is reached (left part of Fig. 18-16) in which the asphaltenes are organized in a three-dimensional network, giving the medium its elasticity.

This complement to the colloidal structural models already established makes it possible to state that one of the major parameters of the colloidal behavior is the interaction capability of the micelles, more than the asphaltene content. It thus accounts for the experimental results regarding a modification of the origin of asphaltenes in the model asphalt cements.

Discussion of relationships between composition, structure, and properties

It was seen previously that GPC makes it possible to obtain an image of the colloidal structure of asphalt cements (ratio of intermicellar and dispersed phases and, especially, quantitative information on sol $\rightleftharpoons$ gel equilibrium). Because the latter has a direct influence on rheological properties, it was logical to examine more closely the relationship that could be established between the characterization of asphalt cements by GPC and their rheological behavior. A first illustration of the relationship is shown in Fig. 18-17.

In Fig. 18-17, the chromatograms of four asphalt cements belonging to the same penetrability class (80–100) are compared with their parameter λ_m as it may be estimated by the interpretation of peeling curves. (λ_m is defined as the average distance between two constituent entities of the medium; in the case of gel systems, it corresponds to a distance between nodes) (see the section on "Experimental characterization").

Regarding the parameter n of the Maxwell–Norton model, it is interesting to compare the numerical values at 20°C of the interaction parameter evaluated by GPC for the five 40–50 asphalt cements shown in Fig. 18-6. As discussed previously, the Maxwell–Norton model is an order parameter defining the degree of medium organization (n is little different from unity for the sol system and increases with gel properties; see the section on Theoretical Aspect). If these asphalt cements are classified by increasing order of interaction index, the results obtained are those given in the following table [24]:

Sample	n
C	1.8
D	1.8
E	2.0
B	2.2
A	2.5

A more systematic study of 22 road asphalt cements of different origins (origin of crude and production process), including a certain number of naturally and

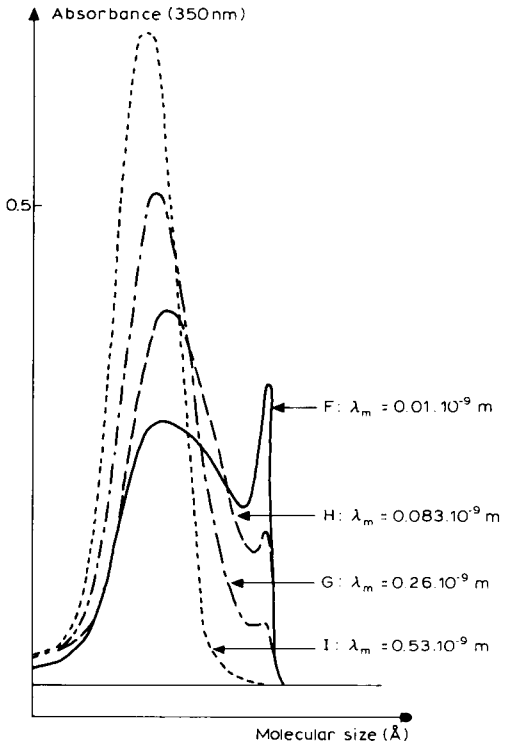

Fig. 18-17. Relationship between λ_m and the interaction index.

artificially weathered samples, indicated that the standard deviation of the relaxation spectrum (as it may be estimated by measuring the complex modulus at variable temperatures and frequencies) depends both on the amount of asphaltenes and on the intensity of their interactions [25]. A detailed statistical analysis has made it possible to determine the coefficients of a multiple regression with two variables and to select two models:

$$K\sigma = 2.08 + (0.899I/200) + 0.0348A$$

and

$$K\sigma = 2.305 + 0.0428[1 + (I/200)]A$$

where K = proportionally constant; σ = standard deviation of relaxation spectrum, I = GPC interaction index (height in mm of interaction peak under given operating conditions), and A = asphaltene content.

A correlation coefficient of 0.952 and a residual variance of 0.0208 are obtained using the first model, whereas with the second, the correlation coefficient is 0.944 and the residual variance is 0.0227.

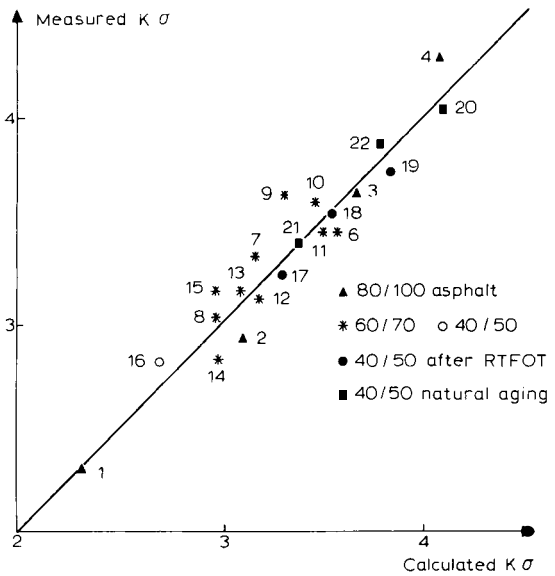

Fig. 18-18. Comparison of calculated and measured standard deviations.

Figure 18-18 allows a comparison of the values of $K\sigma$ measured and estimated on the basis of the first model. The results of this comparison, confirming the significance of interactions between the asphaltenes and showing their assessment by means of the interaction index, are already of significant practical value because they allow (a) an a priori classification of asphalt cements of a given category, and (b) follow-up of natural or artificial weathering by two simple tests that are rapid and that do not require much binder. Thus it is possible to limit the number of technological (or rheological) tests, which are clearly more difficult to carry out.

Ongoing, as yet unpublished, research in the area of the rheological behavior of ultra-thin films appears to be promising. It covers six 40–50 road asphalt cements of different origins, for which the viscosimetric behavior of films of different thickness ranges (6–8 μm; on the order of 25 μm; and on the order of 50 μm) has been investigated.

The results indicate the following:

(1) The viscosimetric behavior of the binder varies, for certain asphaltic cements, with the film thickness (Newtonian behavior for films of 50 and 25 μm becoming non-Newtonian for films of 6–8 μm).

(2) The apparent viscosity, for a given shearing rate, can be multiplied by a factor of more than 10 by simply decreasing the film thickness.

(3) Certain samples exhibit, in small thicknesses, a plastic flow threshold; it is to be noted that this flow threshold is observed only for asphalts exhibiting, in GPC, a clearly marked interaction peak, which is a new means of comparing composition and properties.

(4) Behavior depends on the recent thermal history of the sample, and the method permits the study of structural hardening.

SUMMARY

In this chapter, the facilities acquired by the LCPC road research laboratories in the area of physicochemical characterization (HPLC and GPC) and investigations on the rheological behavior of materials (peeling, viscoelastisimetry, viscosity of ultra-thin films) have been pointed out. It is important to note that these new characterization methods show that asphalt cements with the same specifications have substantially different chemical compositions and rheological behaviors. In the authors' view, emphasis should now be placed on the practical application of physicochemical methods such as GPC and also on the experimental relationships between the composition, structure, and properties of these materials.

Regarding the first point, it has been demonstrated that GPC enables a characterization of the complex colloidal equilibrium of asphalt cement:

Molecules (intermicellar phase) $\rightleftharpoons$ micelles $\rightleftharpoons$ aggregates

As the equilibrium is shifted to the right by blowing during manufacture and by low-temperature oxidation during in-situ weathering, GPC can be used to evaluate the blowing rate of new asphalt cements and the degree of evolution of in-situ weathered asphalt cements.

Regarding the second point, tests in progress indicate that the shifting of colloidal equilibrium to the right (as a result of blowing and weathering) is accompanied by an evolution of rheological properties from those of a sol system toward those of a gel system.

Research projects are concentrated essentially on the prediction of the behavior of materials during mixing and in-place weathering (experimental research on composition parameters capable of being associated with weathering susceptibility). Current investigations cover the relationship between the RTFOT and the evolution of properties during mixing for different types of asphalt cements, aggregates, and mixing plants. For the simulation of in-situ weathering, it appears to be important to look for an artificial weathering technique enabling the oxidation of asphalt cement at a temperature substantially lower than 160°C, which is the temperature of the RTFOT.

From the practical viewpoint, there is the problem of calibration of artificial weathering tests; a research program is under way for characterizing the evolution of well-selected binders on experimental road sections.

REFERENCES

[1] Zumer, M., Such, C. and Brûlé, B., Caractérisation d'un bitume (et de ses fractions) par chromatographie en phase liquide à polarité de phase inversée. *Analusis*, 9(4): 145–148 (1981).

[2] Brûlé, B. and Zumer, M., Application de la chromatographie liquide à hautes performances (CLHP) à la détermination rapide de la composition générique des bitumes. Rapp. Lab., Sér. Phys. Chim., PC-2, February (1984).
[3] Dark, W. and McGouch, R.R., Use of liquid chromatography in the characterization of asphalts. *J. Chromatogr. Sci.*, 16: 610–615 (1978).
[4] Brûlé, B., Application de la chromatographie sur gel perméable (GPC) à la caractérisation de fractions d'asphaltènes. *Bull. Liaison Lab. Ponts et Chaussées*, 85: 97–101 (1976).
[5] Brûlé, B., Caractérisation de produits bitumineux par chromatographie sur gel perméable. *Bull. Liaison Lab. Ponts et Chaussées, Spec. Vol.*, pp. 89–100 (1977).
[6] Such, C., Brûlé, B. and Baluja-Santos, C., Caractérisation d'un bitume routier par des méthodes chromatographiques (GPC et CLHP). *Bull. Liaison Lab. Ponts et Chaussées, Spec. Vol.*, pp. 101–108 (1977).
[7] Such, C., Brûlé, B. and Baluja-Santos, C., Characterization of a road asphalt by chromatographic techniques (GPC and HPLC). *Liq. Chromatogr.*, 2(3): 437–453 (1979).
[8] Brûlé, B., Contribution de la chromatographie sur gel perméable (GPC) à la caractérisation qualitative et quantitative des bitumes: Structure colloidale. *Lab. Ponts et Chaussées., Res. Rep.*, 76 (1978).
[9] Brûlé, B., Calibration curve for GPC analysis of asphalts. *Am. Chem. Soc., Fuel Div., Chromatography of Coal Derived Products*, Atlanta, April 1 (1981).
[10] Brûlé, B. and Migliori, G., Application de la chromatographie sur gel perméable (GPC) à la caracterérisation de bitumes routiers et de leur susceptibilité au vieillissement artificiel. *Bull. Liaison Lab. Ponts et Chaussées.*, 128: 107–120 (1983).
[11] Such, C., Bernard, A. and Poindefert, A., L'analyse thermique différentielle appliquée à l'étude de bitumes routiers. *J. Assoc. Fr. Calorimétrie et d'Analyse Thermique*. Geneva, III-2: 8–15 (1982).
[12] Pastor, M. and Ramond, G., Relations entre adhésion, cohésion et module complexe des bitumes. *Bull. Liaison Lab. Ponts et Chaussées*, 118: 47–52 (1982).
[13] Ferry, J.D., *Viscoelastic Properties of Polymers*. John Wiley and Sons, New York, N.Y., 482 pp. (1961).
[14] Ramond, G. and Pastor, M., Mesure de la cohésion des bitumes par pelage. *Cah. Groupe Fr. Rhéol.*, 5: 269–282 (1980).
[15] Jongepier, R. and Kuilman, B., Characteristics of the rheology of bitumens, *Proc., Assoc. Asphalt Paving Technol.*, 38: 98 (1969).
[16] Grosch, K.A., Relation between friction and viscoelastic properties of rubber. *Proc., R. Soc. London, Ser. A*, 274 (1963).
[17] Derkx, F., Campin, J. and Such, C., Appareillage pour l'étude de films bitumineux sous faible épaisseur. *Groupe Fr. Rhéol.*, December 2 (1983).
[18] Dron, R., Bestougeff, M. and Voinovitch, I.A., Contribution à l'étude des états structuraux des bitumes. *Lab. Ponts et Chaussées, Res. Rep.*, 75 (1978).
[19] Friaa, A. and Such, C., Un modèle rhéologique du type Maxwell–Norton pour le bitume routier. *C.R. Acad. Sci. Paris, Sér. B*, 197: 288 (1979).
[20] Norton, F.H., *The Creep of Steel at High Temperature*. McGraw-Hill, New York, N.Y., 130 pp. (1929).
[21] Friaa, A., *La loi de Norton–Hoff généralisée en plasticité et viscoélasticité.* Université P. et M. Curie, Paris (1979).
[22] Yen, T.F., Chemistry of asphaltenes. In: J.W. Burger (Editor), *Symp. Div. Pet. Chem., 178th Meet. Am. Chem. Soc., 1979. ACS Series*, 195: 39–51 (1981).
[23] Gaestel, C., Smadja, R. and Lamminan, K.A., Contribution à la connaissance des propriétés des bitumes routiers. *Rev. Gén. Routes et Aérodromes*, 466: 85–94 (1971).
[24] Such, C., Ramond, G. and Brûlé, B., Le comportement visqueux des bitumes en relation avec la distribution des tailles moléculaires. *Symp. Int. sur la Caractérisation des Huiles Lourdes et des Résidus Pétroliers*, Lyon, June (1984).
[25] Ramond, G., Pastor, M. and Brûlé, B., *Relations entre le Comportement Rhéologique des Bitumes Routiers et leur Caractérisation par Chromatographie sur Gel Perméable, Eurobitume,* La Haye, September (1985).

This page intentionally left blank

SUBJECT INDEX*

*Prepared by Dawood Momeni, George V. Chilingarian and T.F. Yen.

This page intentionally left blank